The Synthesis, Photochemistry & Electrochemistry of Dithienylethene Switches & their Organometallic Complexes

This Thesis is Presented for the Degree of Doctor of Philosophy

By

Emma Harvey B.Sc.

Under the Supervision of Dr. Mary Pryce

at

Dublin City University

School of Chemical Sciences

September 2011

__Declaration__

I hereby certify that this material, which I now submit for assessment on the programme of study leading to the award of Doctor of Philosophy is entirely my own work, that I have exercised reasonable care to ensure that the work is original, and does not to the best of my knowledge breach any law of copyright, and has not been taken from the work of others save and to the extent that such work has been cited and acknowledged within the text of my work.

Signed: _____   Student ID No.: <u>52316986</u>

Date: _____

Table of Contents

Chapter 2:   Synthesis   72

Co$_2$(CO)$_6$ Complexes

Co$_2$(CO)$_4$dppm Complexes

Chapter 3: Photochemistry of Thienyl-based Switches and their Cobalt Carbonyl Complexes

121

Clark, I. P.; George, M. W.; Greetham, G. M.; Harvey, E. C.; Long, C.; Manton, J. C.; Pryce, M. T. "Excited State Dynamics and Activation Parameters of Remarkably Slow Photoinduced CO Loss from (η^6-Benzene)Cr(CO)$_3$ in *n*-Heptane Solution: A DFT and Picosecond-Time-Resolved Infrared Study" *J. Phys. Chem. A.* **2010,** *114,* 11425–11431.

Clark, I. P.; George, M. W.; Greetham, G. M.; Harvey, E. C.; Long, C.; Manton, J. C.; Pryce, M. T. "Photochemistry of (η^6-Arene)Cr(CO)$_3$ (Arene = Methylbenzoate, Naphthalene, or Phenanthrene) in n-Heptane Solution: Population of Two Excited States Following 400 nm Excitation As Detected by Picosecond Time-Resolved Infrared Spectroscopy" *J. Phys. Chem. A.* **2011**, 115, 2985–2993.

<u>Dedication</u>

I would like to dedicate this thesis to my parents, Tommy and Patricia Harvey. I have been trying to put into words how grateful I am for all that they have done for me, but with so much to say, I fear that I will exceed my limited word-count for this thesis, so I'll leave it as this …………………………………...…………………………………………. …………..…………………………………..………………….. they're just brilliant!!

Abbreviations

$AlCl_3$ = aluminium chloride

$B(OBu)_3$ = tributyl borate

t-BuLi = tert-butyllithium

$CDCl_3$ = deuterated chloroform

$(CD_3)_2SO$ = deuterated dimethyl sulfoxide

$(CD_3)_2CO$ = deuterated acetone

C_5F_8 = Octaperfluorocyclopentene

CH_2Cl_2 = dichloromethane

$CHCl_3$ = chloroform

CH_3NO_2 = nitromethane

$Co_2(CO)_6$ = dicobalt hexacarbonyl

$Co_2(CO)_8$ = dicobalt octacarbonyl

$Co_2(CO)_4dppm$ = dicobalt tetracarbonyl bis(diphenylphosphino)methane

CS_2 = carbon disulphide

CuI = copper iodide

CV = cyclic voltammogram

DMF = N,N-dimethylformamide

Dmpm = bis(dimethylphosphino)methane

Dppf = bis(diphenylphosphino)ferrocene

Dppe = bis(diphenylphosphino)ethane

Dppm = bis(diphenylphosphino)methane

DTE = dithienylethene

Et_3N = triethylamine

IL = intraligand

IR = infra-red

$K_2(CO)_3$ = potassium carbonate

LMCT = ligand-to-metal-charge-transfer

$MgSO_4$ = magnesium sulphate

MLCT = metal-to-ligand-charge-transfer

Na$_2$(CO)$_3$ = sodium carbonate

NaOH = sodium hydroxide

Na$_2$CO$_3$ = sodium carbonate

Na$_2$SO$_4$ = sodium sulphate

NCS = N-chlorosuccinimide

Ni(dppp)Cl$_2$ = [1,3-bis(diphenylphosphino)propane]dichloronickel(II)

Ni(PPh$_3$)$_2$Cl$_2$ = bis(triphenylphosphine)nickel(II) dichloride

NIR = near infra-red

P((CH$_3$)$_3$Ph)$_3$ = Tris(2,4,6-trimethylphenyl)phosphine

Pd$_2$(dba)$_3$ = Tris(dibenzylideneacetone)dipalladium

Pd(dppf)Cl$_2$ = dichloro-[bis(diphenylphosphino)ferrocene] palladium

Pd(PPh$_3$)$_2$Cl$_2$ = dichloro-bis(triphenylphosphine) palladium

Pd(PPh$_3$)$_4$ = tetrakis-(triphenylphosphine)palladium

PPh$_3$ = triphenylphosphine

PSS = photostationary state

TBAI = tetrabutylammonium iodide

TBAPF$_6$ = tetrabutylammonium hexafluorophosphate

THF = tetrahydrofuran

TiCl$_4$ = titanium tetrachloride

TiCl$_3$ = titanium (III) chloride

Abstract

Chapter one presents a detailed literature survey on dithienylcyclopentene switches, describing their synthesis, properties and applications. The photochromic and electrochromic effects of functionalising such switching units with metal complexes, is then discussed. Finally, an introduction to cobalt carbonyl complexes is given, with an outline of the photochemical and electrochemical properties of such carbonyl complexes, as described in the literature.

Chapter two describes the synthetic procedures employed to prepare a number of dithienyl-perhydro- and perfluoro-cyclopentene switches, substituted with thienyl and ferrocenyl moieties. The methods used to generate their corresponding $Co_2(CO)_6$ and $Co_2(CO)_4dppm$ complexes are also described. ^{1}H, ^{13}C, ^{19}F and ^{31}P NMR techniques were employed to analyse the resulting products. Elemental analysis and infra-red spectroscopy were also utilised, where applicable, to further characterise the final pure compounds and the results are detailed in this chapter.

Chapter three describes the photochemical properties found for the thienyl-based dithienylcyclopentene switches and their corresponding cobalt carbonyl complexes. The photochromic properties of the thienyl-based switches were monitored in the UV-vis absorption spectra and the ^{1}H NMR spectra. Their thermal stability, fatigue resistance and fluorescent properties were also investigated. Furthermore, the effects of incorporating cobalt carbonyl moieties onto these thienyl-based switches, on their photocyclisation processes, are reported in this chapter.

Chapter four reports the photochromic behaviour of the ferrocenyl-based dithienylcyclopentene switches, as observed in the UV-vis and ^{1}H NMR. Investigations into the thermal stability, fatigue resistance and fluorescent properties of these switches were carried out. The effects on the photochromic properties of the ferrocenyl-based switches, following the introduction of $Co_2(CO)_6$ and $Co_2(CO)_4dppm$ moieties, are also described in this chapter.

Chapter five focuses on the electrochemical properties of the thienyl-based dithienylcyclopentene switches. Electrochemically induced cyclisation/ cycloreversion processes were investigated through cyclic voltammetry and UV-vis spectroelectrochemistry techniques. Similar experiments were carried out for the cobalt carbonyl derivatives in order to examine the effects of the presence of the metal carbonyls on the oxidative ring-closing/opening abilities of the thienyl-based switches. The effects of the oxidation processes on the cobalt carbonyl centres were also studied by monitoring the changes of the carbonyl stretches in the infra-red spectra.

Chapter six details the electrochemical behaviour of the ferrocenyl-based dithienylcyclopentene switches. The oxidative and reductive processes of these switches were monitored in the cyclic voltammograms and UV-vis spectra of these switches in order to investigate if ring-opening/closing can be induced by electrochemical means. Their $Co_2(CO)_6$ and $Co_2(CO)_4dppm$ complexes were also subjected to similar experiments in order to determine the effects of introducing such metal carbonyl complexes on the electrochemical switching behaviour of these ferrocenyl-based switches. IR spectroelectrochemical techniques were employed to examine the effects of oxidation processes on the cobalt carbonyl centres.

Chapter seven presents an overall conclusion of the results obtained, with an emphasis on a comparison between the effects of the thiophene substituents and the ferrocene units, and the prospects of future work in this area is discussed. All publications are presented in the appendix.

Introduction

Dithienylcyclopentene switches are compounds which can undergo structural changes from their open-ring to their closed-ring isomers, and vice versa, by photochemical and electrochemical means. The switching behaviour of such molecules induces changes in their electrical and optical properties such as: UV-vis absorption; luminescence; IR; and oxidative/reductive potentials. Such switches have applications towards the development of optoelectronic devices, in particular read/write memory devices with non-destructive read-out capabilities, due to their excellent fatigue resistance and thermal stability properties.

The basis of this thesis is to examine the effects of the central cyclopentene atoms (i.e. H *vs*. F), and the substituents attached to the thiophene units, on dithienylcyclopentene switches, on their photochemical and electrochemical properties. Furthermore, the influence of incorporating organometallic moieties, on the properties of the switches, is explored.

Dithienyl-perhydro-cyclopentene switches, and its perfluoro analogues, were appended with 3-ethynylthiophene and phenyl-3-ethynylthiophene moieties in order to investigate the effects of increasing the π-conjugation of the system on the cyclisation/cycloreversion processes, induced optically and electrically. The thermal stability and fatigue resistance of these switches were also analysed as such properties are highly important towards the development of practical applications. Their luminescent behaviour, in the open and closed-ring forms, was investigated as a possible non-destructive read-out method.

Incorporating organometallic complexes onto molecular switches can result in unique excited state reactivity, and hence significantly affect the photochromic and electrochromic properties of such switches. Ferrocene is an organometallic compound which is known for its excited state quenching ability, and its excellent electrochemical properties, due to its reversible oxidation process. Hence, the perhydro- and perfluoro-derivatives of the dithienylcyclopentene switches were substituted with ethynylferrocene and phenyl-ethynylferrocene moieties in order to examine, what was expected to be, the considerable influence of the ferrocene units on

the photochemical and electrochemical properties of the switches, in comparison to the properties found for the organic thienyl-based switches.

A number of transition metal complexes have been introduced onto molecular switching units in order to tune the properties of such systems. Cobalt carbonyl complexes are photochemically and electrochemically-active transition metal complexes, and to date, have not been integrated onto such switching systems. Hence, novel cobalt carbonyl compounds were synthesised by incorporating $Co_2(CO)_6$ moieties onto the alkynyl units on both sides of the thienyl-based, and ferrocenyl-based, dithienylcyclopentene switches described above, with the aim of investigating the influence of these metal carbonyl complexes on the photochemical and electrochemical ring opening/closing processes of these switches. Further to this, cobalt carbonyls exhibit sharp, intense bands in the CO region of the IR spectrum, hence, we extended our investigation to study the effects of the photochemical and electrochemical processes on the carbonyl IR bands, with the intention of examining IR spectroscopy as a possible non-destructive read-out method for data storage devices.

The introduction of electron-donating phosphine ligands onto cobalt carbonyl complexes increases the electron density on the Co-Co bond, thus stabilising these complexes. Hence, bis(diphenylphosphino)methane {dppm} ligands were substituted onto the $Co_2(CO)_6$ switches described above, generating the corresponding cobalt tetracarbonyl complexes {$Co_2(CO)_4dppm$}, with the intention of stabilising these metal complexes during photochemical and electrochemical processes. The influence of the $Co_2(CO)_4dppm$ complexes on the electro- and photo-cyclisation processes of the dithienylcyclopentene switches was investigated.

This thesis is divided into seven chapters. The synthetic methods and characterisation results of the dithienylcyclopentene switches, and their cobalt carbonyl complexes, are described in chapter two. The photochemical properties of the thienyl-based switches and metal complexes, and of the ferrocenyl-based switches and metal complexes, are discussed in chapters three and four respectively. Subsequently, chapters five and six detail the electrochemical properties of the thienyl and ferrocenyl-based systems, respectively. Finally, in chapter seven, an overall conclusion of the results, and the potential for future work in this area, is discussed. First and foremost, however, chapter one presents a detailed literature survey of dithienylcyclopentene switches,

and their corresponding organometallic complexes, followed by the photochemical and electrochemical properties of cobalt carbonyl complexes.

CHAPTER 1

Literature Survey

Chapter one presents a detailed literature survey of the synthetic methods employed to synthesise the perhydro- and perfluoro-derivatives of dithienylcyclopentene switches, and to further functionalise these switches with a variety of substituents.   The photochemical and electrochemical properties of these switches are described, with a comparison between the hydrogenated and fluorinated cyclopentene unit, followed by a description of how their switching properties can be utilised for a number of applications.   The effects of combining organometallic complexes and dithienylcyclopentene switches into the same system are described in detail, with a comprehensive review of the results reported in the literature.   Finally, the photochemical and electrochemical properties of cobalt carbonyl complexes are discussed.

1.1 Dithienylcyclopentene Switches

Photochromic molecular switches refer to compounds that can undergo reversible photo-induced transformation between two forms which have distinguishably different absorption spectra.[1,2] Following the photocyclisation process, after irradiation with light, the ring-opened form transforms to the ring-closed form. Apart from changes in the UV-vis spectra, other changes in various physical and chemical properties of the switch can result, such as, the refractive index, redox potential, polarity, fluorescence etc.[3,4,5] Photochromic switches are of much interest due to their reversibility, short response times, clean and tuneable energy input, and their ability to convert optical input into a number of useful output signals.[3] These properties can lead to a variety of applications in non-destructive optical data recording and storage,[1,3,6-9] molecular wires,[6,7] molecular switches,[6-9] filters[1,3] and polarisers.[1,3]

There are a number of different types of switches reported in the literature,[3,10] for example, spiropyrans, azobenzenes, fulgides and diarylethenes. Diarylethenes are one of the most promising switches for application as switching units, as they display excellent photochromic properties:[1,2,4,8-10] short response time, high quantum yields, excellent fatigue resistance, thermally irreversible, high reactivity in solid state, and large changes in the absorbance spectra between the two isomers. The most commonly used diaryethenes are diarylmaleic anhydrides, diarylmaleimides and diarylperfluorocyclopentenes.[1,6,7]

Diarylmaleic Anhydride   **Diarylmaleimide**   **Diarylperfluorocyclopentene**
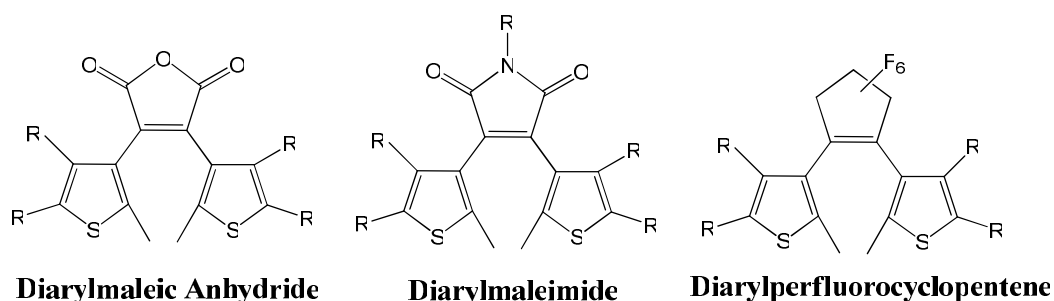
Figure 1.1: General structures of diarylmaleic anhydrides, diarylmaleimides and diarylperfluoro-cyclopentenes switches.

However, diarylmaleic anhydrides and diarylmaleimides are both sensitive to acidic conditions and have been found to degrade in the presence of air.[1,7] On the other hand, diarylperfluoro-cyclopentene switches have demonstrated photochromic stability in air, even at temperatures over 80ºC,[1,7] and therefore have attracted much attention in recent years, particularly those bearing two thiophene derived groups. Thus, the remainder of this review will focus on the synthesis, photochromic and electrochromic properties of dithienylcyclopentene type switches.

1.1.1 Synthesis

A number of methods have been reported for the synthesis of dithienylcyclopentene switches, and some of these are described briefly in the following section.

- **Dithienylper*fluoro*cyclopentene**

Method 1:
Irie et al[11] described the synthesis of dithienylperfluorocyclopentene by a lithiation reaction, followed by a double substitution reaction with octafluorocyclopentene (scheme 1.1).

- Firstly, they prepared 3,5-dibromo-2,4-dimethylthiophene (**1**), via a bromination reaction of 2,4-dimethylthiophene, by adding it to a solution of acetic acid, containing bromine, at 0ºC.

- This was followed by a lithiation reaction, where **1** was dissolved in ether and n-butyllithium was added at -60ºC. Water was subsequently added at room temperature to replace the lithium at the 5-position, thus yielding 3-bromo-2,4-dimethylthiophene (**2**).

- **2** was then subjected to another lithiation reaction, in THF. N-butyllithium was added at -60ºC, followed by perfluorocyclopentene at the same temperature, yielding 1,2-bis(2,4-dimethylthiophen-3-yl)perfluorocyclo-pentene (**3**).
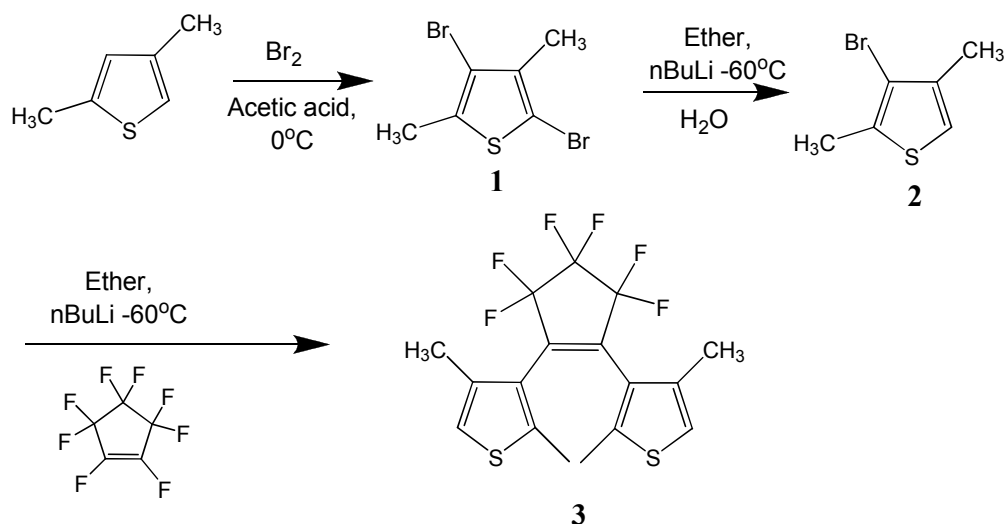
Scheme 1.1: Synthesis of 1,2-bis(2,4-dimethylthiophen-3-yl)perfluoro-cyclopentene (**3**).

Method 2:

Synthesis of dithienylperfluorocyclopentene by method 1 has a number of disadvantages:[6,7]

- The yields are moderate, as a large amount of the monosubstituted product is formed.

- Octaperfluorocyclopentene is difficult to work with as it is very volatile (bp. 26-28°C).

- Also, octafluorocyclopentene is very expensive and not readily available.

Therefore, Lucas et al[6] developed a different synthetic route with cheaper starting materials that are easier to handle and produce higher yields.

Firstly, they attempted a Friedel-Crafts acylation of 2-methyl-5-chlorothiophene with hexafluoroglutaryl dichloride and $AlCl_3$ in benzene or toluene, which has been described previously in the literature.[12] However, this reaction was not successful, which was probably due to the strongly electron-withdrawing fluorine atoms interfering with the formation of the acylium intermediate.

Their second approach was to generate diethyl hexafluoroglutarate, by a standard acid-catalysed esterification of hexafluoroglutaric acid,[13] in order to obtain the corresponding diketone (**6**) (illustrated in scheme 1.2).

A number of considerations had to be taken into account. Acylation must occur at the 3-position, however, 2- and 5-positions on the thiophene molecule are the most

reactive (positions 2 to 5 are illustrated in scheme 1.2 on compound **4**). Therefore, it is necessary to use only a thienyl group which is substituted at positions 2 and 5. It is also important to incorporate functionality in the final dithienylcyclopentene compound, in order for further derivatisation to be employed. The addition of a halogen group on the methyl thienyl compound can provide this function. However, it has been found that when bromothiophenes are employed, acylation occurs at the 2-position and the bromine substituent is shifted to the 3-position.[14] Iodine is known to react in a similar way therefore Lucas et al[6] used a chlorine substituent. 2-methyl-5-chlorothiophene (**4**) was synthesised by reacting 2-methylthiophene with N-chlorosuccinimide, in benzene and acetic acid.[6,7] To obtain the dithienyl-1,5-diketone (**6**), 5-chloro-2-methylthiophene underwent a bromination reaction at the 3-position, using Br$_2$ in chloroform, yielding 5-chloro-3-bromo-2-methylthiophene (**5**). Compound **5** was synthesised in order to ensure that the following lithiation reaction, in diethyl ether at -78ºC using n-BuLi, resulted in lithium/halogen exchange of the bromine at the 3-position, rather than at the chlorine in the 2-position. Once **5** was lithiated, diethyl hexafluoroglutarate was added to the reaction mixture at the same temperature, yielding 1,5-bis(5-chloro-2-methyl-3-thienyl)pentaflurodione (**6**). McMurry coupling followed, to achieve ring closure, by adding **6** to a solution of THF containing zinc and TiCl$_3$(THF)$_3$, at 40ºC. After purification by column chromatography, 1,5-bis(5-chloro-2-methyl-3-thienyl)cyclopentene (**7**) was obtained.[6]
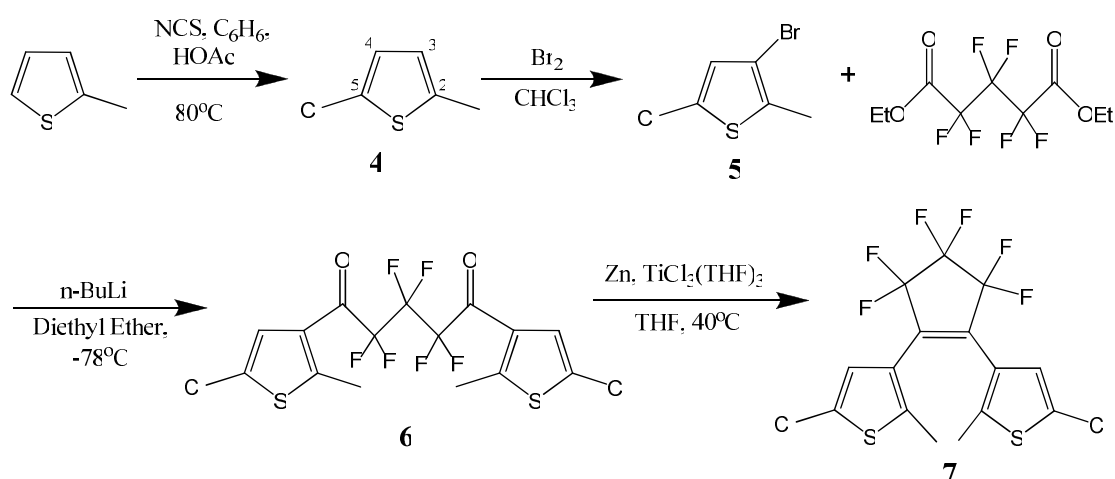
Scheme 1.2: Synthesis of 1,5-bis(5-chloro-2-methyl-3-thienyl)perfluorocyclopentene (**7**). Positions 2 to 5 on the thiophene molecular are illustrated on compound **4**.

- **Dithienylper*hydro*cyclopentene**

Due to the problems described above for the synthesis of dithienylperfluoro-cyclopentene, namely the expensive, volatile reagents required and the small scale reactions producing low yields, Lucas et al,[6,7] decided to synthesise a new class of diarylethenes, consisting of a perhydrocyclopentene structure bearing two thiophene groups. They reported the synthesis of dithienylper**hydro**cyclopentene by generating a 1,5-dithienyl-1,5-diketone group via a Friedel-Crafts acylation reaction, followed by a ring-closing step of the diketone, via a McMurry reaction, to form the central perhydrocyclopentene ring.

1,5-dithienyl-1,5-diketone can be synthesised by a Friedel-Crafts acylation of a methylated thienyl group to a 1,5-dinitrile, 1,5 diester or a 1,5-dicarboxylic dichloride, the latter being the preferred choice as it saves one step in the reaction process. Therefore, 2-methyl-5-chlorothiophene (**4**) was subjected to a Friedel-Crafts reaction with $AlCl_3$ and glutaryl dichloride, in CS_2 at 0°C, yielding 1,5-bis(5-chloro-2-methyl-3-thienyl)pentadione (**8**) (scheme 1.3).[6,7]

The final step to achieve the cyclopentene switch is ring closure via a McMurry reaction. Dechlorination of aromatic chlorides using Grignard reagents have been reported before,[15] therefore, **8** was refluxed in a solution of THF containing $TiCl_4$ and zinc (zinc is a milder reducing agent than Mg), and the desired 1,5-bis(5-chloro-2-methyl-3-thienyl)cyclopentene (**9**) was obtained (scheme 1.3).[6,7]
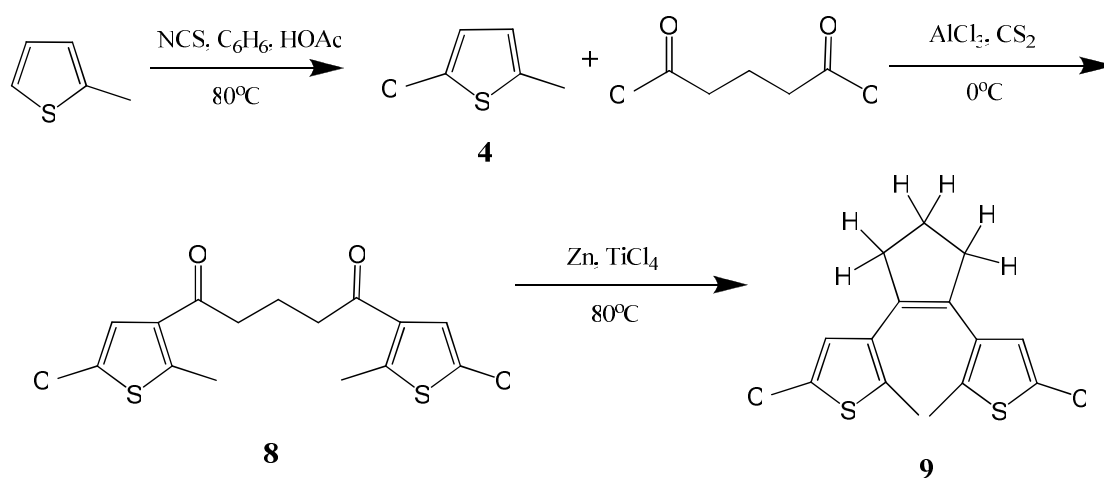
Scheme 1.3: Synthesis of 1,5-bis(5-chloro-2-methyl-3-thienyl)cyclopentene (**9**).

- **Functionalisation of Dithienylcyclopentenes**

The synthetic methods described above, by Lucas et al,[6, 7] focused on the generation of dithienylethene switches containing chlorine substituents. However, these methods can be varied slightly to generate 1,2-bis(2,5-dimethylthien-3-yl)cyclopentene or 1,2-bis(2-methylthien-3-yl)cyclopentene. The former merely requires the use of 2,5-dimethylthiophene in place of compound **4**, in schemes 3 and 4.[6,7] The latter can be obtained by using Mg, rather than zinc, in the final McMurry ring-closing reaction, as it is a stronger reducing agent, hence, resulting in dechlorination of the thienyl groups.[6,7] However, synthesising the dithienylcyclopentenes (perfluoro & perhydro), with chlorine atoms at the 5-poition of the thienyl groups, is the preferred method as it allows for functionalisation of the switches in a relatively easy manner by a variety of different reactions, as described below:

1) Lithiation Reactions

Compounds **7** and **9** can undergo a straightforward lithiation reaction, where chlorine/lithium exchange takes place at room temperature. Introduction of different reagents can yield a number of different functionalised products,[6] as illustrated in scheme 1.4, for example:
- Quenching the lithiation reaction with DMF, results in formation of the dialdehyde (**10**).[6,7]
- The addition of CO_2 to the lithiation reaction can form the diacid directly (**11**).[6]
- The addition of iodine to the doubly lithiated compound results in lithium/iodine exchange. This results in an iodine substituent at the 5-position on each thienyl group (**12**). Iodine is more reactive than chlorine, and so it can be employed in further reactions, such as Sonogashira reactions, to introduce a variety of substituents onto the switch.[16]
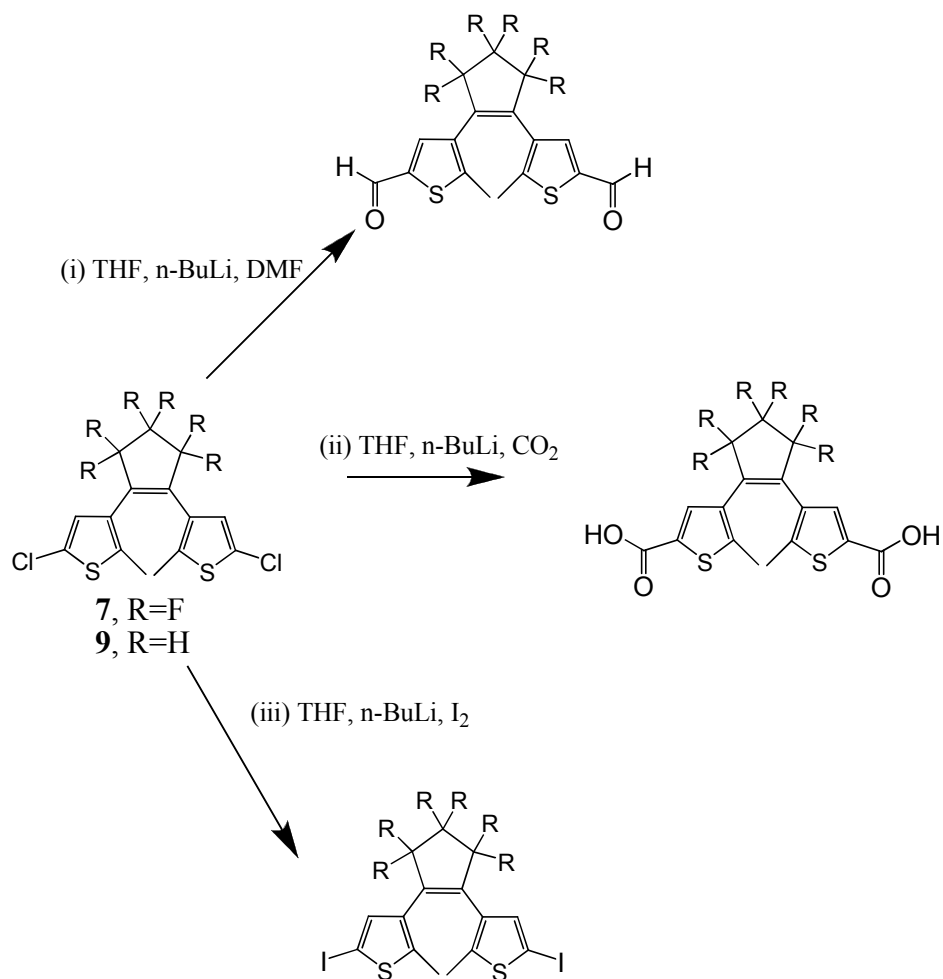
Scheme 1.4: Lithiation reactions of dithienylcyclopentene compounds to form: (i) dialdehyde derivative **10**, (ii) diacid derivative **11**, (iii) di-iodide derivative **12**.

2) Cross-Coupling Reactions

There is a lot of interest in increasing the aromatic character of the dithienyl-cyclopentene switches. There are a number of cross-coupling reactions that can be employed for this purpose, such as Negishi coupling, Kumada coupling, Suzuki coupling and Sonogashira coupling. Literature results using such methods are described below:

- *Negishi Coupling*

Irie at al[11] synthesised a benzene derivative of a dithienylperfluorocyclopentene switch by firstly substituting the thiophene molecule with a benzene ring, followed by synthesis of the diarylperfluorocyclopentene compound, as demonstrated in scheme

1.5.   A Negishi coupling reaction was used to generate the 5-thienyl-phenyl substituent.   2,4-dimethylthiophene and N,N,N'N'-tetramethylthiophene (TEMED) were dissolved in ether, and BuLi was added at ambient temperature, followed by the addition of zinc chloride.   After 4 hours of stirring this reaction mixture was added to a flask containing a THF solution of iodobenzene and Pd(PPh$_3$)$_4$, and the reaction was heated.   The resulting 2,4-dimethyl-5-phenylthiophene compound (**14**) was then iodinated, at the 3-position of the thiophene, by adding it to a solution of acetic acid, carbon tetrachloride, iodic acid and iodine.   The resulting 3-iodo-2,4-dimethyl-5-phenylthiophene compound (**15**) was then subjected to a lithiation reaction, followed by a double substitution reaction with octafluorocyclopentene, to produce 1,2-bis(2,4-dimethyl-5-phenylthiophen-3-yl)per-fluorocyclopentene (**16**).
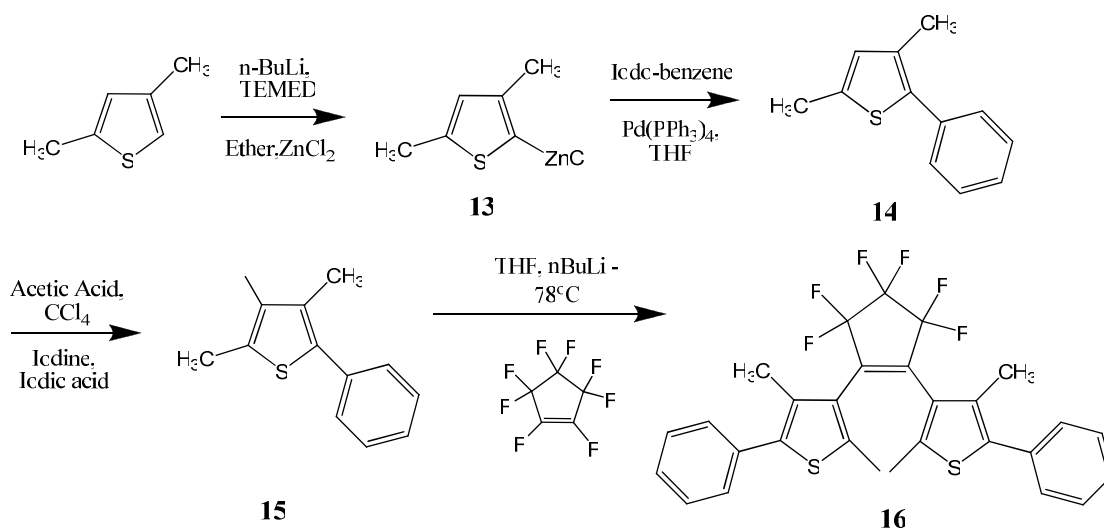
Scheme 1.5: Synthesis of 1,2-bis(2,4-dimethyl-5-phenylthiophen-3-yl)per-fluorocyclopentene (**16**) by a Negishi reaction.

-   *Kumada Coupling*

Lucas et al[6] attempted a Kumada coupling reaction where the substituent was coupled directly onto the dithienylcyclopentene compound.   1,5-bis(5-chloro-2-methyl-3-thienyl)perhydrocyclopentene (**9**) was reacted with 2-thienylmagnesium bromide (**17**) in diethyl ether, under reflux conditions, using Ni(dppp)Cl$_2$ as the catalyst.   This resulted in only a monosubstituted product (**18**).   Increasing the amount of catalyst did not improve the result, so a different catalyst [Ni(PPh$_3$)$_2$Cl$_2$], often employed in Kumada coupling reactions, was used.   The disubstituted compound was obtained, but only when a 1 equivalent amount of this catalyst was used.   As the percentage amount of the catalyst was decreased, the yield of the desired product decreased.   The problem

incurred here is most likely due to the lower reactivity of the chloride, in comparison to bromides or iodides.[6]   However, in the same year Peters et al[17] reported the successful disubstitution of 2-thiophene groups onto the dithienylperfluorocyclopentene switch (**20**). In contrast to Lucas' method, they substituted the chlorine atoms for bromine atoms on the diaryethene structure (**19**) first, used a different catalyst [Pd(dppf)Cl$_2$], and the reaction was carried out at 0ºC. Both of these reactions are illustrated in scheme 1.6 below:
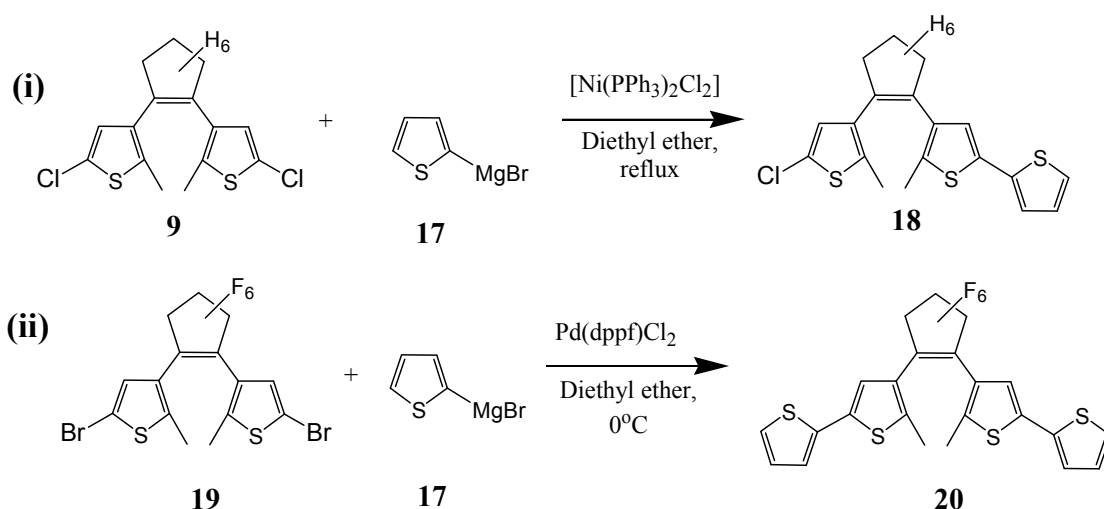
Scheme 1.6: Kumada Coupling: (i) Lucas' method[6]; (ii) Peters' method[17], where dppf = 1,1'-Bis-(diphenylphosphino)ferrocene.

- *Suzuki Coupling*

Tsivgoulis et al[18] reported the functionalisation of a diarylcyclopentene by varying the Suzuki coupling reaction conditions.   1,2-Bis-(2'-n-hexylthiophene-3'-yl)-perfluoro-cyclopentene (**21**) was converted into the boronic acid, by dissolving it in diethyl ether and adding n-butyllithium, followed by the addition of B(nOBu)$_3$.   The resulting boronic acid was kept in solution, as isolation can result in loss of boron, or the formation of anhydrides.   Therefore, it was added directly to a second reaction flask containing a solution of 2-bromothiophene, Pd(PPh$_3$)$_4$, ethylene glycol and aq. Na$_2$CO$_3$, in THF, under reflux.   This synthetic method was successful in yielding the desired 1,2-Bis-(2'-n-hexyl-5'-(thiophen-2-yl)- thiophene-3'-yl)-perfluorocyclopentene product (**22**).

Later this method was used by Lucas et al[6,19] in order to functionalise 1,5-bis(5-chloro-2-methyl-3-thienyl)perhydrocyclopentene (**9**) with two thiophene groups at the

15

5-position. Firstly they attempted a Suzuki coupling of the cyclopentene thienyl chloride compound with arylboronic acids, which was deemed unsuccessful. This was most likely due to the low reactivity of the chloro-thienyl bond, in comparison to aryl bromides and iodides, which are more commonly used in such a reaction. Therefore, instead of using the diarylcyclopentene compound as the aryl halide, they converted it into a boronic ester intermediate, and followed the same procedure as described by Tsivgoulis et al.[18]

21, R = C$_6$H$_{13}$ **22**, R = C$_6$H$_{13}$
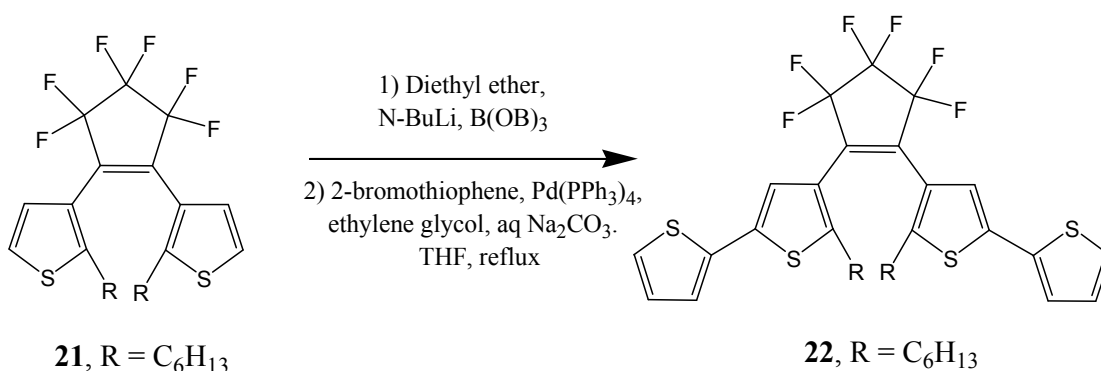
Scheme 1.7: The Suzuki Coupling method reported by Tsivgoulis et al.[18]

- *Sonogashira Coupling*

Launay et al[16] described the addition of two ethynylferrocene units to dithienyl-cyclopentene (perfluoro & perhydro) switches via a Sonogashira reaction. Before addition of the substituents, the two chlorine atoms present in 1,2-bis(1,5-bis(5-chloro-2-methyl-3-thienyl)cyclopentene (**9**) were replaced with iodine via a lithiation reaction described above in scheme 1.4. Then a Sonogashira reaction was employed to add ethynylferrocene substituents to the 5-poisiton of the thiophenes. Standard Sonogashira conditions were applied which involved adding ethynylferrocene to a mixture of THF, diisopropylamine, CuI and Pd(PPh$_3$)$_2$Cl$_2$. After stirring at room temperature for 72 hours, a low yield of the product was obtained, accompanied by a large amount of crude product which made the purification process very difficult. Therefore, a different method was employed which involved the generation of the catalyst in situ from Pd$_2$(dba)$_3$ with a bulky tris(2,4,6-trimethylphenyl)phosphine ligand and CuI. DMF and diisopropylethylamine were used as the solvents, and an excess of tetrabutylammonium iodide was also added. This new procedure allowed the reaction to start at -20°C, followed by stirring at room temperature, and the pure product was obtained successfully in a much higher yield (90%).[16]
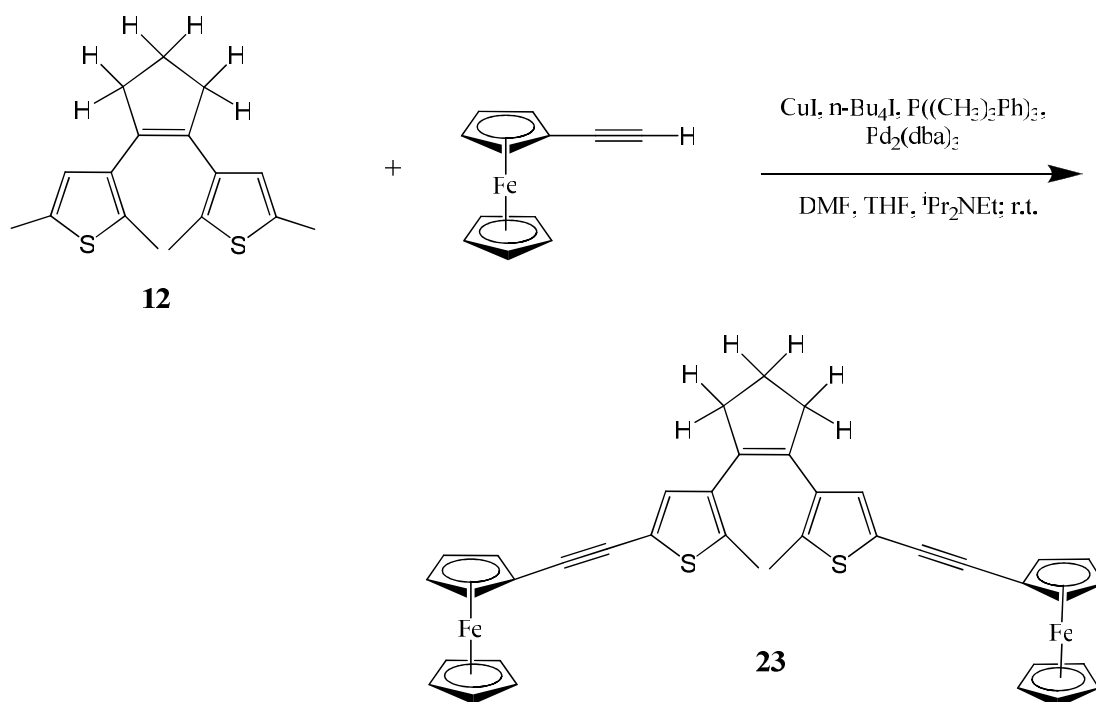
Scheme 1.8: The Sonogashira coupling method reported by Launay et al.[16]

1.1.2 Photochromism

Photochromism is a term used to describe light-induced reversible transformation of a molecule between two isomers.[10] In the case of diarylethene compounds, irradiation with UV light of the colourless open-ring isomer, results in photocyclyisation to form the coloured closed-ring isomer. This is a reversible process, with subsequent irradiation, with visible light, resulting in a cycloreversion process from the closed to the open form,[1] as illustrated in scheme 1.9.

Open-ring isomer   **Closed-ring isomer**
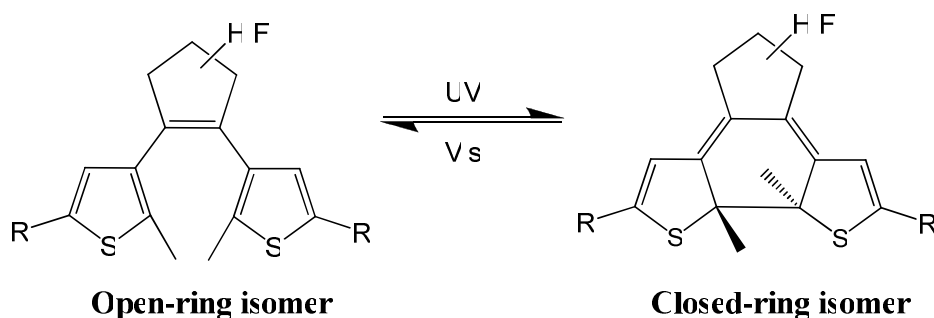
Scheme 1.9: Photochromic behaviour of dithienylcyclopentene switch. Irradiation with UV light results in ring-closure, whilst irradiation with visible light results in ring-opening.

The open-ring isomer is non-planar as free rotation is possible between the ethene moiety and the aryl group, and the π-electrons are localised in the two aryl groups.[2] Upon irradiation with UV light, photochemical conrotatory 6π-electrocyclisation of the 1,3,5-hexatriene moiety takes place, due to steric congestion, forming a cyclohexadiene structure.[2,20] Therefore, the closed isomer has a C_2-symmetrical helical structure, resulting in extension of the π-conjugation over the entire molecule.[3,9,20] This photoreaction takes place according to the Woodward-Hoffmann rule,[2] and results in changes in the physical and chemical properties between the two isomers, the most important of which are the changes in colour, and hence in their UV-vis spectra. Once the switch is exposed to visible light (λ > 420 nm) this photochemical process is reversed, and the open-ring isomer is regenerated.

- **Conformational Isomers**

The quantum yield obtained for the cyclisation process is largely dependent on the structure of the open-ring dithienylethene molecule. The open-ring form can exist as two conformational isomers:[1,2,4,9,10] a parallel conformation in which the two thienyl rings are in mirror symmetry, and an anti-parallel conformation with the rings in C_2 symmetry (scheme 1.10). These conformers exchange at room temperature and are present in almost equal amounts. The parallel conformers are photochemically inactive, as only the anti-parallel conformers can undergo photocyclisation, upon irradiation with UV light, according to the Woodward-Hoffmann rule. Therefore, the ratio of these two conformers defines the quantum yield obtained for the photocyclisation reaction, which is usually about 50% seen as the conformers generally exist in a 1:1 ratio.[1] However, replacing the inner substituents on the thienyl rings with larger molecules, such as isopropyl groups, or bridging the thiophene rings at the 2- and 4-positions, have been shown to increase the ratio of anti-parallel conformers, hence increasing the quantum yield for the photocyclisation reaction.[1,21]
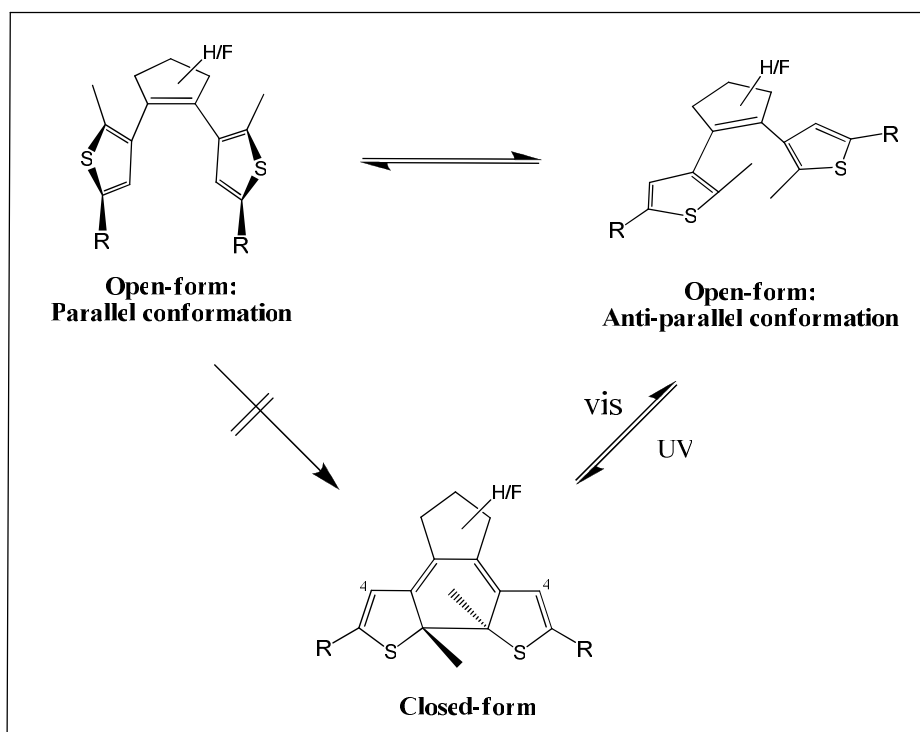
Scheme 1.10: Parallel and anti-parallel conformational isomers of open form dithienylethene switches. The parallel form is photochemically inactive. Only the anti-parallel conformers can undergo photocyclisation. Also, position 4 on the thiophene rings is illustrated here.

- **NMR**

The two conformations of the open-ring were distinguished by ^{1}H NMR theoretical studies, carried out by Nakamura et al.[8] The relative positions of the two thiophene moieties have a strong effect on the chemical shift of the methyl group protons attached at the 2-position. In the case of the anti-parallel conformer, the two methyl groups face the ring hence a high magnetic field is induced onto the methyl protons by the ring current, resulting in the presence of a peak at ~1.7 ppm in the ^{1}H NMR spectrum. In the case of the parallel conformer, this magnetic field affect is not applicable therefore the peak representing the methyl protons is shifted downfield to ~2.16 ppm.[8] However, for most diarylethene switches, the parallel and anti-parallel isomers fluxuate between each other on a very fast time-scale, hence, even at -90ºC, ^{1}H NMR analysis shows only one set of time-averaged signals.[22] There are exceptions where sterically demanding substituents are attached to the dithienylethene moiety, which hinders the rotation of the thienyl groups, resulting in two sets of ^{1}H NMR signals for the two open-ring conformers, as described previously by Irie et al.[11]

The photocyclisation reaction of the switches, from the open-ring to the closed-ring, can be detected by ^{1}H NMR. Ring-closure induces a chemical shift in the peaks representing the thiophene proton at the 4-position (scheme 1.10) and the methyl group protons. Due to the loss of their aromaticity, the thienyl protons are shifted upfield by about 0.4 - 0.8 ppm, but splitting or doubling of the peaks was not observed. The methyl protons are shifted downfield, but only very slightly (~0.03 - 0.27 ppm). These changes are characteristic of the C_2 symmetry of the closed form.[6,23]

- **Thermal Stability**

As mentioned previously, one of the main advantages of using diarylethene molecules as photo-switching units is their thermal stability.[1,2,4,8-10] Irie et al[24,25] explained the factors affecting the thermal stability properties of diarylethene switches, after theoretical studies were carried out. They reported that diarylethene derivatives bearing heterocyclic rings only undergo cyclisation and cycloreversion processes, between the open and closed forms, when irradiated with light and not when heat is applied. However, when phenyl rings are substituted in place of the heterocyclic rings, the cycloreversion process can be triggered by heat as well as light. This demonstrates that the closed form of the six-membered ring is much more unstable in comparison to the five-membered ring. To investigate this result further, they carried out theoretical calculations in order to examine the differences in energy between the ground-states of the open and closed ring isomers. A correlation diagram was constructed which suggested that the ground-state difference correlates with the energy barrier of the cycloreversion reaction i.e. the larger the ground-state energy difference between the open and closed forms, the smaller the reaction energy barrier for cycloreversion to occur. A large ground-state energy difference was calculated for the phenyl ring switch, with a correlating small reaction energy-barrier, therefore cycloreversion is expected to occur readily. However, the ground-state energy difference of the diarylethene moiety decreased when the phenyl groups were replaced by furyl groups, and further decreased when replaced with thienyl groups, accompanied by a growing increase in the reaction energy-barrier. Therefore, the closed-ring isomer of the thienyl group derivative is more stable than the open isomer, and a thermally induced cycloreversion reaction is not expected to occur readily.[24]

The differences in the thermal stability of these diarylethene derivatives can be explained in terms of the aromatic character of the substituent. The highly aromatic phenyl group produced the greatest ground-state energy difference. This energy difference decreased when five-membered rings, with lower aromatic character, replaced the phenyl groups, as a result of conjugated electron migration. Upon cyclisation to produce the closed-ring isomer, destabilisation occurs, due to the destruction of the aromatic ring, increasing the ground-state energy. Therefore, introducing aryl groups that have low aromatic stabilisation energy can increase the thermal stability of diarylethene switches.[24,25]

- **UV-vis Spectra**

The open-ring isomer is generally colourless, while the closed ring isomer can exhibit a number of different colours, such as yellow, red, blue etc., depending on the molecular structure of the diarylethene switch.[2,9] Therefore, the absorption bands of the open rings generally appear in the UV region at wavelengths between 240 nm and 350 nm approximately, whilst the strongly coloured closed isomers result in the appearance of new absorption bands in the visible region.

Non-zero absorption in the UV spectral region of the closed form indicates that both ring-closing and ring-opening takes place following photoexcitation. Therefore, in all cases a photostationary state (i.e. equilibrium situation) is achieved, which is determined by the quantum yields of ring opening/closing.[6,23] However, it can be assumed that the photostationary state represents the closed isomer as quantum yields recorded for diarylethenes showed that the cyclisation (ring-closing) is a more efficient process than the cycloreversion process (ring-opening).[6]

1.1.3 Electrochromism

In conjunction with their photochemical properties, diarylethene molecules can also undergo switching from the open to the closed form, and from the closed to the open form, by means of electrochemical oxidation/reduction processes. A combination of the photo- and electrochromic properties of these switches can be used for the development of non-destructible write-read-erase memory devices.[26,27,28] Therefore, investigations into the driving force and the tenability of their electrochemical processes has attracted much interest in recent years.

Oxidation of diarylethene compounds is followed by one of two possible reactions: oxidative cyclisation, involving transformation of the open-ring isomer to the closed-ring isomer, or oxidative cycloreversion, where the closed-ring isomer transforms to the open-ring isomer. This process is evident when comparison between the cyclic voltammograms of the open and closed forms, after a few redox cycles are performed, shows the presence of similar oxidation/reduction waves.[17] The reaction that takes place depends on the stability of the radical cations of the relative open and closed forms.[5,27] In other words, cyclisation reactions occur when the radical cations of the closed-ring isomers are more stable than the open-ring isomers but, when the radical cations of the open form are more stable than the closed form, an oxidative cycloreversion process takes place.[27,29,30]

- **Oxidation of the open-ring to the closed-ring**

According to data recorded in the literature,[5,17,26-28,30,31] oxidation of open-ring isomers of dithienylethene derivatives generally result in an irreversible oxidation process, at more anodic potentials than in the closed state. This is deemed to be characteristic of thiophene oxidation chemistry.[30] However, for some of these dithienylethene derivatives, a cyclisation reaction follows, producing the closed-ring isomer. This process is evident in the return cycle, after the initial irreversible oxidation peak, when two new reduction processes are observed at potentials coincident with those of the closed form. Browne et al[30] described the occurrence of an electrochemical cyclisation process of the open-ring isomer of compound **1H** upon oxidation. The

structure and the cyclic voltammograms of the open and closed-ring forms, of compound **1H**, are illustrated in figure 1.2. The first oxidation wave of the open-ring isomer **1Ho** takes place at a high potential, and represents an irreversible two-electron redox process, forming the dication radical **1Ho^{2+}**. Immediately following the formation of the open-ring radical dication (**1Ho^{2+}**), a cyclisation process takes place, forming the dication radical of the closed-isomer (**1Ho^{2+} → 1Hc^{2+}**).[26,28] The closed-ring dication radical is then reduced to its mono-cation radical (**1Hc^{2+} → 1Hc^{+}**), and finally to its neutral species (**1Hc^{+} → 1Hc**). This dication radical is stable enough to give rise to two characteristic reduction waves, and corresponding reversible oxidation waves.[26] The high stability of the cationic radical of the closed-ring isomer is due to the delocalisation of the positive charge along the conjugated system.[3,4,9,26]
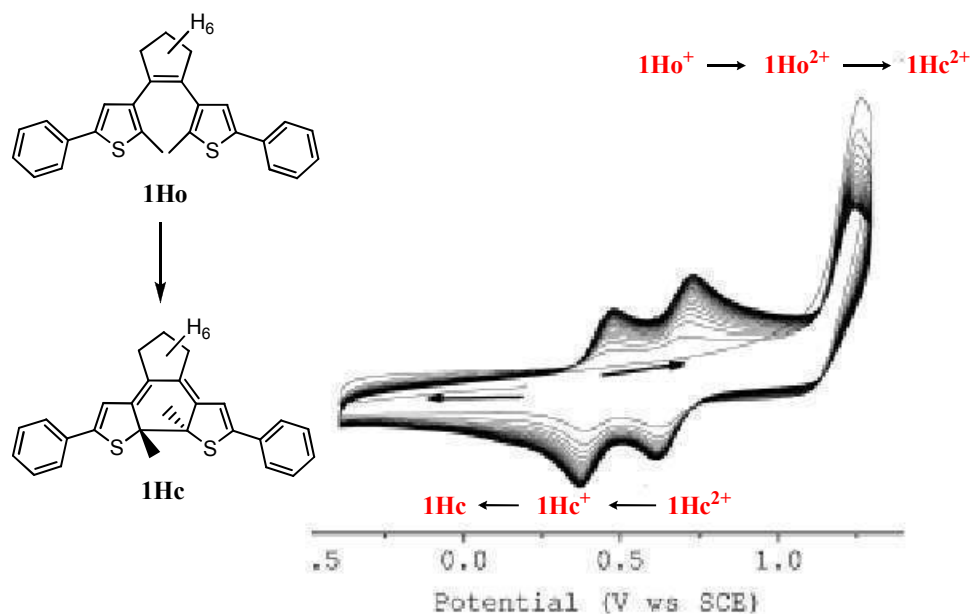
Figure 1.2: The cyclic voltammogram of compound **1H**, shown here, was obtained by Browne et al.[30] The CV shows the electrochemical ring-closing process of compound **1H**, upon oxidation of the open-ring isomer **1Ho**.

Colour changes in the electrochemical solution have been observed upon oxidative ring closure, and subsequent irradiation with visible light ($\lambda > 450$ nm) resulted in regeneration of the open-ring colour solution (usually clear).[5,27] Hence, the ability to electrochemically produce the closed-ring isomer, and photochemically produce the open-ring isomer, along with the clear difference in oxidation potentials between the open and closed forms, suggests that diarylethene derivatives have great potential for use as an electrochemical switch.[5]

- **Oxidation of the closed-ring to the open-ring**

Oxidation of dithienylethene closed-ring isomers generally leads to the presence of one or two reversible redox processes below ~0.8 V (which is demonstrated in figure 1). This reversible redox behaviour is not very obvious for open-ring isomers, which is probably due to the extended conjugated system obtained upon ring-closure, which helps to stabilise the electrochemically produced radical cations on the main backbone of the diarylethene unit.[3,4,9,26] However, some dithienylethene derivatives in their closed form can undergo a cycloreversion process, to produce their open-ring form, upon oxidation.[17,26,27,30,32]

Moriyama et al[27] described the occurrence of an electrochemical cycloreversion process of the closed-ring isomer of compound **2** upon oxidation. The structure and the cyclic voltammograms of the open and closed-ring forms, of compound **2**, are illustrated in figure 1.3 below.
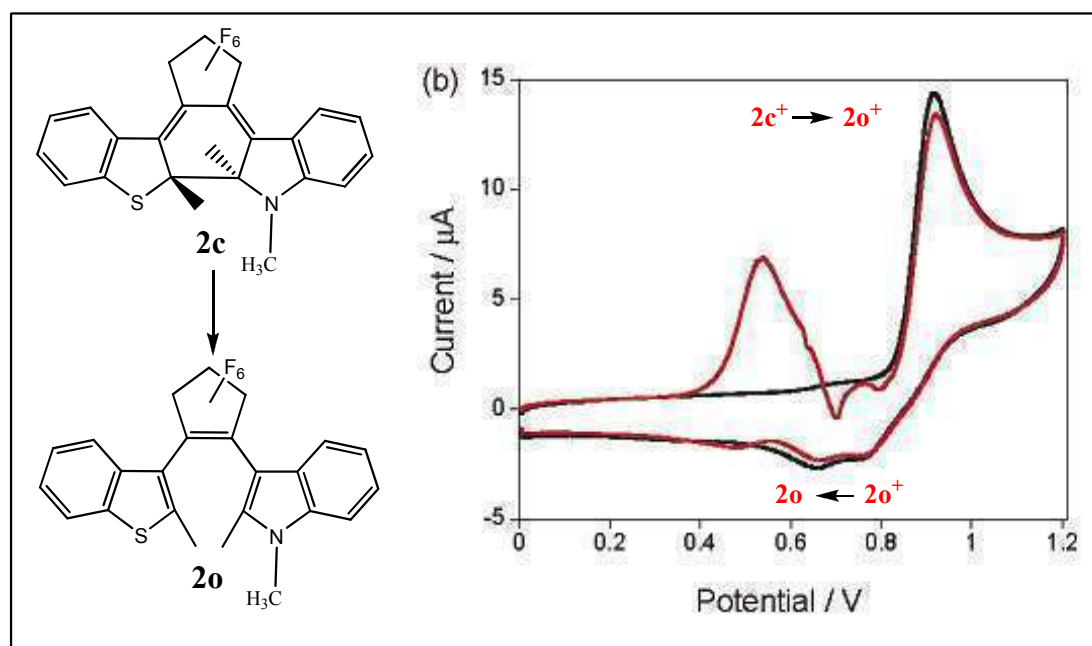
Figure 1.3: Illustrates the diarylethene structure of compound **2**, synthesised by Moriyama et al. Also shows the cyclic voltammograms of oxidation of the open-ring isomer **2o** (black) & oxidation of the closed ring isomer **2c** (red).[27]

During cyclic voltammetry experiments of the closed-ring isomer (**2c**), an irreversible oxidation peak at 0.92 V was observed, resulting in the loss of an electron, and the subsequent formation of the corresponding thermally unstable closed-ring radical cation (**2c**⁺). This radical cation quickly undergoes a cycloreversion reaction, forming

the radical cation of the open-ring isomer ($2c^+ \rightarrow 2o^+$). In general, dithienylethene open-ring isomers require a substantially more positive potential to undergo oxidation, in comparison to the closed-ring isomers. Hence, the open-ring radical cation ($2o^+$) removes an electron from another closed-ring molecule ($2c$), resulting in the neutral form of the open-ring isomer ($2o$), and regeneration of the original closed-ring radical cation ($2c^+$). This closed-ring radical ($2c^+$) then quickly undergoes cycloreversion to the open-ring isomer ($2o^+$), which removes an electron from another closed-ring molecule, and so on. Due to the fact that this oxidative cycloreversion process is a chain reaction, only a small amount of the closed-ring cation radical produced by electrochemical oxidation at the start is necessary, as the following oxidise/ring-open/reduce cycle will continue until the ring-closed form is completely converted to the ring-open form.[32]

1.1.4 Substituent Effects

Perfluorocyclopentene-based switches have been widely studied as switching units due to their thermal stability and fatigue resistance properties. However, as mentioned earlier, their problematic synthetic routes led Lucas et al to synthesise cyclopentene systems,[6,7] where the fluorine atoms were replaced by hydrogen atoms. A number of comparative tests were carried out to examine if the perhydrocyclopentene derivatives demonstrated the same important properties as the perfluorocyclopentene system,[6,23] and to study the effects of these alternative cyclopentene switches on their photochromic and electrochromic properties.[23,30,31]

- **Fatigue resistance/ thermal stability**

According to Irie,[25] the photostability of these switches is limited, and the main pathway for decomposition reactions to occur is from the excited state of the closed form. Studies show that the perhydro-based switch shows good fatigue resistance after a number of photocyclisation and photocycloreversion processes were carried out consecutively, however the photostability of the perfluoro-based molecules was found to be 2-3 times greater, in comparison.[6,23]

Thermal stability properties were investigated by heating the closed-ring perhydro- and perfluoro- derivatives at high temperatures (~80ºC to 100ºC) for prolonged periods of time eg. 14 hours. The closed-forms of the perhydrocyclopentene switches showed excellent thermal stability, however thermal conversion of the closed-ring form to the open-ring occurred before that observed for the perfluorocyclopentene derivatives. It should be noted that this thermal conversion process is clean, as no sign of decomposed product was evident.[6,7,23]

Overall, the perhydrocyclopentene-based switches show good fatigue resistance and thermal stability properties. However these properties are improved when perfluoro-derivatives are employed, therefore they are better suited for applications which are highly dependent on these properties, such as date storage.[23]

- **Switching processes**

One of the most interesting effects of substituting the fluorine atoms for hydrogen atoms on the cyclopentene structure of these switches is the changes observed in their electronic and redox properties. Incorporating different substituents onto the C5 position of thienyl rings can also have a significant effect on their photochemical and electrochemical processes. This is of great advantage as it allows for the generation of dithienylethene compounds with tuneable properties.

1) Photochemical properties

Feringa et al[23] reported the synthesis of the perfluoro- and perhydro- derivatives of 1,2-bis(2'-methyl-5'-phenylthien-3'-yl)cyclopentene. They further derivatised these compounds with methoxy and cyano substituents at the para position of the phenyl groups (see figure 1.4).

3H: R=H
3F: R=H
4H: R=OMe
4F: R=OMe
5H: R=CN
5F: R=CN
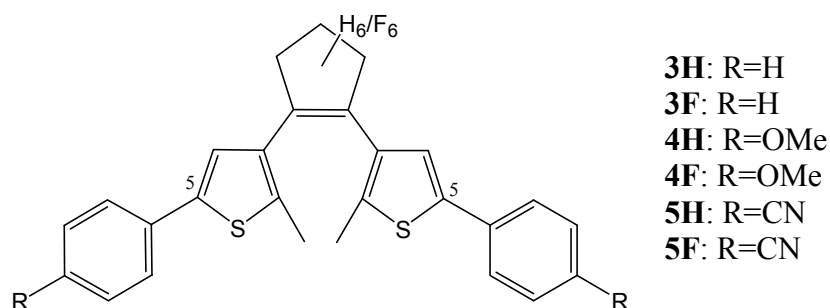
Figure 1.4: Perfluoro- and perhydro- derivatives of 1,2-bis(2'-methyl-5'-phenylthien-3'-yl)-cyclopentene, and their corresponding methoxy and cyano substituted derivatives.[23] Also, the C5 position on the thiophene rings is illustrated here.

The absorption peaks recorded in the UV-vis spectra of both the open and closed form of these compounds are listed in table 1.1 below. Comparison of the results obtained for the open-ring isomers of the perhydro- derivative (**3H**) and the perfluoro-derivative (**3F**) shows that there is quite a modest difference in the absorption bands recorded. However, upon ring-closure of **3H** and **3F**, a more pronounced difference between the new absorption peaks recorded in the visible region is observed, as is evidenced from the bathomochromic shift of 40 nm for the perfluorinated cyclopentene derivative. This is due to the electron-withdrawing effect of the fluorine atoms, in contrast to the electron donating ability of the hydrogen cyclopentene ring, on the switch.[23,30,31]

Table 1.1: Absorption spectroscopic data recorded (in hexane) for the open and closed ring isomers of the compounds shown in figure 1.4.[23]

Compound	R	λ_{max} Open	λ_{max} Closed
3H	H	277	529
3F	H	279	569
4H	OMe	279, 309	529
4F	OMe	290, 316	580
5H	CN	295, 332	570
5F	CN	271, 313	588

Substituting the para position of the phenyl groups, with electron-donating methoxy groups, barley affects the electronic properties of the perhydro-derivative (**4H**), whereas the λ_{max} of the perfluoro analogue (**4F**) is bathochromically shifted by 11 nm, both in the open and closed forms. The presence of the electron-withdrawing cyano groups, in place of the methoxy groups, has a more pronounced effect on both the perhydro and perfluoro switches. The λ_{max} of the open-ring isomer **5F** is blue-shifted by 8 nm, with respect to **3F**, whereas the open form of the perhydro-derivative **5H** is bathochromically shifted by 18 nm, in comparison to **3H**. An even greater influence of the cyano groups is found for the ring-closed isomers of **5F** and **5H**, as both are bathochromically shifted by 19 nm and 41 nm, respectively. The fact that altering the substituents on the phenyl groups induces significant changes in the electronic properties of these switches indicates good communication between the central cyclopentene unit and the phenyl substituents.[23,30,31]

2) *Electrochemical properties*

The switching behaviour of dithienylethene derivatives, induced by electrochemical means, is highly dependent on the central cyclopentene unit atoms (H *vs*. F), and the nature of the substituents at C5 of the methyl-2-thiophene rings. The substituents employed have been found to have a much greater influence on the electrochemical properties of dithienylethene switches, in comparison to their photochemical properties.[26,30,31]

Feringa et al[30,31] investigated the electrochemical properties of the compounds described in figure 1.4. The most obvious difference in the electrochemical properties

of the perhydro- and perfluorocyclopentene unit is the strong anodic shift, observed in the cyclic voltammogram of the perfluoro derivative (~200-800 mV), in comparison to the perhydro derivative, due to their electron-withdrawing and electron-donating abilities, respectively.[26,31] This anodic shift is evident in the oxidative potentials of these molecules listed in table 1.2.

Table 1.2: Oxidation potentials recorded for the open and closed ring isomers of compounds **3H**, **3F**, **4H** & **4F** illustrated in figure 1.4:[30] irr (irreversible); qr (quasi-irreversible); r (reversible).

Compound	R	E_{pa} (open)	E_{pa} (closed)
3H	H	1.16 (irr)	0.67, 0.43 (r)
3F	H	1.59 (irr)	0.85 (qr)
4H	OMe	0.99 (irr)	0.45, 0.32 (r)
4F	OMe	1.20 (irr)	0.67 (r)

The ability of the bridging cyclopentene moiety to stabilise various radical cationic species can be described as the driving force for either the ring-opening or ring-closing process to occur.[26,30,31] Therefore the central cyclopentene groups, although they are redox-inactive, significantly affect the switching properties of the diarylethene derivatives. Electron-donating moieties have been found to encourage oxidative ring-closure, where as electron-withdrawing groups favour ring-opening.[26,30,31]

In order for ring-closure to proceed following the oxidation process of the open-ring isomer, stabilisation of the radical cation through delocalisation of the charge is required. However, although delocalisation of the charge may increase the stability of the radical cation, the stability of the thienyl rings decreases due to loss of aromaticity. Therefore, the presence of the electron-donating perhydrocyclopentene group increases the electron density on the central alkene group. This helps to facilitate communication between the two thiophene rings, and hence, to further stabilise and increase the lifetime of the radical cation of the closed-ring isomer. Therefore, upon oxidation of the open-ring isomer, a cyclisation reaction from the open-ring form, to the closed-ring form, is thermodynamically allowed. When the perfluorocyclopentene derivatative is present, stabilisation of the radical cation of the ring-closed isomer by delocalisation of the charge is counteracted by the electron-withdrawing effect of the fluorine atoms, which decreases the electron density on the alkene group. Therefore,

ring-opening of the closed-ring cation, with localisation of the charge on the thiophene rings, results.[26,30,31] This phenomenon was reported by Feringa et al when they studied the electrochemical behaviour of the open- and closed-ring forms of compounds **3H** and **3F** (figure 1.4). They observed that oxidation of the open-ring isomer of **3H** resulted in a cyclisation process (**3Ho→3Hc**), whereas oxidation of the closed-ring isomer of **3F** resulted in a cycloreversion process (**3Fc→3Fo**).[30,31]

The nature (donor/acceptor) of the substituents at C5 of the thiophene rings can also have a significant effect on the direction of electrochromic switching of the dithienylethene rings.[26] Feringa et al[30,31] studied the electrochemical effects of introducing electron-donating methoxy groups onto the parent compounds **3H** and **3F** (figure 1.4). The oxidation potentials obtained for these derivatives (**4H**, **4F**) are listed in table 1.2. These results show clearly that the presence of the methoxy groups have decreased the first oxidation waves of **4H** and **4F** to lower potentials, in comparison to the parent compounds. This is a result of increased stability of the radical cations formed due to the electron-donating properties of the methoxy groups.

Also, interesting results were found for the electrochemical switching processes of these derivatives. A cyclisation process, upon oxidation of the open-ring isomer, to the closed-ring isomer occurred for the perhydrocyclopentene derivative **4H**, as expected. However, an oxidative cyclisation process was also observed for the open-ring isomer of the perfluorocyclopentene derivative **4F**, which is in contrast to the cycloreversion process observed for the parent compound **3F**. This result demonstrates the significant effect of incorporating the electron-donating methoxy group onto the switch. However, following spectroelectrochemical analysis of the oxidation process of **4F**, Feringa et al deduced that the effect on the switching direction of **4F** is not simply due to the electron-donating ability of the methoxy group, but in fact it is a result of an intramolecular electron-transfer process subsequent to initial oxidation of the methoxyphenyl groups.[30]

Overall, it is clear that the nature of the cyclopentene units, and the C5 thiophene substituents, on the dithienylethene derivatives, can have a profound affect on the switching processes of the compound. Hence, these switching molecules can be modified according to the desired properties, which is a great advantage for future applications.

1.1.5 Applications

The short response time, fatigue resistance and thermal stability of the switching behaviour of diarylethene compounds are promising features for application in molecular switches, molecular wires, single-molecule fluorescence and non-destructible high density data storage systems.[1,2,4,7,8,20,23] The switching behaviour of these compounds results in significant changes in the data obtained from the following analytical techniques: UV-vis spectroscopy, fluorescence spectroscopy, infra-red spectroscopy and oxidative electrochemistry. Some examples of how these diarylethene switches can be utilised in the design of such applications, using the analytical tools described, are presented here.

- **UV-vis**

The changes recorded in the UV-vis spectra, when ring-open diarylethene derivatives are transformed to the closed state following irradiation with UV light, can be used as the "read-out" event in memory media. Diarylethene compounds are a good choice for this application due to the large changes in the UV-vis spectra, and hence colour, observed upon switching processes. However, the absorption bands observed for the two photochromic states are the same absorption bands that induce the ring-opening/closing reactions. Therefore, sampling near these absorption bands induces cyclisation/cycloreversion processes of the photoactive compound, hence erasing the stored information.[1,2]

- **Fluorescence**

Some diarylethene molecules show strong fluorescence emission when they are in the open-ring form. However, upon irradiation with UV light, it has been recorded that the fluorescence intensity begins to decrease.[9,33,34] This suggests that the ring-closed isomers are fluorescently quenched. Therefore, the open-ring isomer can be described as being in the "ON" state, whilst the closed-ring isomer is in the "OFF" state. This difference in the fluorescence intensity of the open and closed forms is reversible, as once the closed form is irradiated with visible light, the open-form is regenerated, or

the "OFF" state is turned back "ON". The advantage of this process is that monochromatic visible irradiation can be used to induce the fluorescent behaviour, therefore limiting the occurrence of cyclisation/cycloreversion processes, hence minimising the destruction of the recorded information. Reversible changes in luminescence are of great interest due to their sensitivity, resolution and high contrast, making them very suitable for non-destructive optical read-out systems.[1,2]

- **Infra-Red**

Diarylethene molecules which display infra-red (IR) or near-field IR spectral changes between their open-ring and closed-ring isomers have also been reported.[1,8] These IR bands can be used as read-out light, with non-destructive properties, as their energy is too low to cause photochemical switching, High signal/noise ratio is desired so it is important that the open-ring isomer IR bands are well separated from the closed-ring isomer IR bands.

- **Electrochemistry/Photochemistry**

A combination of photochemical and electrochemical switching processes between the open and the closed diarylethene switches can be applied to data memory systems with a write/read/erase function. The information can be "written" by photo-chemically or electrochemically transforming the open-ring isomer to the closed isomer. Monitoring the first reversible oxidation of the closed form, at a potential where the open-form is electrochemically inert, allows for the information to be "read-out" in a non-destructive manner. The stored information can be then be erased by photochemically or electrochemically converting the closed-ring isomer back to the open-form.[28]

Photochemical or electrochemical switching of diarylethene molecules between the open and the closed forms can be used to control electrical conductivity in molecular wires. Upon ring-closure, the π-conjugated length of the system is increased, therefore increasing the conductivity of the system. This conductive effect can be controlled by reverting back to the open form.[4,6]

1.2 Dithienylcyclopentene Switches Substituted with Organometallic Complexes

Organometallic complexes are defined as compounds consisting of organic ligands bound to a transition metal. The bonding involved in such a complex results in new low-lying excited states, which can be populated by optical irradiation in the near-infrared, visible and ultraviolet region. Upon excitation, absorptions attributed to various excited states can be observed:[35,36]

- Intraligand (IL); the ligand has low-lying transitions involving orbitals which are centred on atoms not directly bonded to the metal, leading to absorptions similar to those of the free ligand.
- Metal to ligand charge transfer (MLCT); these transitions occur when the central metal atom or ion can act as a reducing agent, and if the attached ligands have orbitals with low enough energy to accept the electron i.e. when the metal acts as a donor group and the ligand acts as an acceptor group.
- Ligand to metal charge transfer (LMCT); these transitions occur when the ligand acts a donor group and the metal acts as an acceptor group.

Incorporating transition metals into organic ligands can result in unique excited-state reactivity and photochemical properties. For example, changes in electronic states can be controlled; facilitated intersystem crossing can be used to tune excited-state energetics, lifetimes, emissions and efficiencies; and intersystem crossing from the singlet excited state to the triplet state can result in the occurrence of processes such as electron and energy transfer.[37]

Photochromic switching molecules can be used in a variety of applications, as mentioned previously, due to their switching ability from open- to closed-ring isomers, with strong colour changes and extended π-conjugated systems taking place in the process.[1,2,8] Incorporating dithienylethene units and metal complexes into the same system can lead to a number of advantages, with regards to the properties and applications of both entities.

Using a dithienylethene switch as a bridging molecule between two metal complexes can enhance the performance of these complexes in a number of applications. Molecular photonic and electronic devices are based on the idea of manipulating electrons and photons at the molecular level. The molecules can function as wires, switches, diodes, transistors, and light-absorbing/emitting centres.[37] The advantage of using metal centres in such applications is the ability to tune the energy levels, excited state lifetimes and the redox properties of the system by changing the central metal atom.[38] The ability to transfer electrons intramolecularly between the two metal centres is important. By incorporating a photochromic switch as the bridging ligand between the two organometallic complexes, the electronic coupling between the two metallic centres is preserved, but more importantly the conductivity of the molecular wire can be controlled due to the change in π-conjugation of the system upon opening and closing of the ring. That is switching between the open-ring form and the closed-ring form can control the communication between the metals from the "ON" and "OFF" state, respectively.[38-44]

Attaching organometallic substituents onto the thiophene rings of dithienylethene compounds can significantly affect the photophysical and electrochemical properties of these photochromic molecules and tuning these properties can be achieved by changing the metal centres, leading to a number of advantages for the applications of dithienylethene switches.[42,45]

As mentioned previously, the dithienylethene structure can exist as two conformations in the open form: a parallel and an anti-parallel conformation. Only the anti-parallel conformer can undergo cyclisation reactions. These two conformers interconvert rapidly, so generally the quantum yield expected for the cyclised product is 0.5. However, it has been found that by incorporating bulky metal complexes onto the dithienylethene structure, the anti-parallel conformation is favoured, due to the steric repulsion between the substituents. Hence, the quantum yield for the cyclisation reaction increases as a result.[22,38,40,46,47]

One of the main applications for dithienylethene switches is the creation of an information storage system with non-destructible read-out properties. Stored information is readily lost during light driven read-out processes, as the light can electronically excite the photochromic switch. Non-destructive read-out processes, such as, locking the system in one state, or observing changes in electrochemical

properties, emission, or infra-red absorption are possible solutions. The photo- and electrochemical properties of metal complexes could be used to achieve this.[22, 38, 48] Incorporating metal complexes into dithienylethene switches can result in significant changes in the emission of the metal centre, or the electronic coupling between the two metal centres, upon photocyclisation processes. Changes in these properties can be utilised as non-destructive read-out functions.

Another possibility is for the metal complexes to function as photosensitisers for the photochromic process i.e. inducing the switching process through the triplet metal-to-ligand-charge transfer (^{3}MLCT) excited states, hence shifting the wavelength at which the cyclisation process can be triggered into the visible region.[22,38]

Although metal complexes can have a number of advantages on the photo- and electrochromic properties of the dithienylethene switch, they can also completely extinguish these properties.[38,39] If the electronic coupling between the photochromic core and the metal centres is too strong, the properties of the photochromic unit may change to such an extent that photoreactions can no longer occur. The coupling also depends on the nature of the spacer. If the conjugated spacer is extended too much, the redox groups and the additional conjugated parts can act as energy sinks, thereby suppressing the photochromic reactions. Therefore it is important to achieve a good balance of electronic interaction between the switching unit and the metal complexes. By using different spacers to connect the metal units to the photochromic core, the level of interaction in the system can be altered i.e. strongly or weakly interacting systems. Combinations of ethynyl units and aromatic groups have been reported as efficient electron transfer spacers, and therefore prevent a full electronic delocalization (upon excitation) on the system.[38,39]

1.2.1 Photochromic Properties

Incorporating dithienylethene switches and metal complexes into the same system can have a significant effect on the photocyclisation process, from the open to the closed-ring isomer, of the dithienylethene unit and on the emission properties of the metal complexes. The photochromic properties of such systems, and the effect of different metal centre substitutes, have been reported in the literature and some examples are discussed here.

- **Bipyridine Metal Complexes**
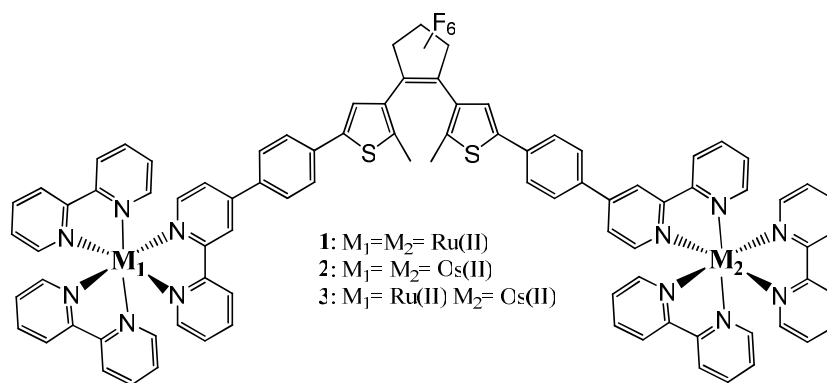
Figure 1.5: De Cola et al[38,43,47] reported the synthesis of a compound containing two metallated tris(bipyridine) substituents attached to 1,2bis(2-methylthiophene)-perfluorocyclopentene unit via a phenyl linker. The metal centres were substituted with bisruthenium (**1**), bisosmium (**2**), and ruthenium and osmium (**3**).

De Cola et al[38,43,47] reported the synthesis of three metal complexes containing two metallated tris(bipyridine) substituents attached to 1,2bis(2-methylthiophene)-perfluorocyclopentene unit via a phenyl linker. Compound **1** was substituted with homonuclear ruthenium metal centres, compound **2** was substituted with diosmium, and a third heteronuclear complex (**3)** was synthesised with two different metal centres, ruthenium and osmium. These complexes are represented in figure 1.5. Photochemical processes were carried out and some interesting results were obtained.

Upon UV irradiation of the Ru(II) complex **1** into the singlet state (^{1}IL), localised on the dithienylperfluorocyclopentene unit, photocyclisation of the switch occurred, evidenced by a colour change from yellow to green and the appearance of a new absorption peak at 614 nm in the UV-vis spectrum. Upon irradiation into the singlet metal-to-ligand charge transfer (^{1}MLCT) state at 458 nm, localized on the Ru(bpy)$_3$

part, the higher energy [1]IL state was not populated. Instead intersystem crossing took place to the triplet MLCT state ([3]MLCT), which was followed by energy transfer into the lower energy triplet state of the ligand ([3]IL), resulting in ring-closure of the photochromic unit.[38,47] This process is illustrated in the qualitative energetic scheme of the Ru(II) complex **1**, in scheme 1.11 below.   Almost identical, high quantum yields for the photocyclisation processes were obtained for both methods.[38,43] However, it was found that the quantum yield for the cyclisation reaction occurring from the [3]IL state significantly decreased in the presence of dioxygen, whereas cyclisaton reactions for the free ligand from the lowest [1]IL state were insensitive to oxygen quenching.   Also, the [3]MLCT and [3]IL states are close in energy, so equilibrium exists between them, resulting in a competition between the emissive and reactive processes.   Therefore, photocyclisation reactions from the triplet state take a few nanoseconds, where as reactions from the singlet state occur on the picosecond time scale.[38,47] Ring-opening was achieved slowly by irradiation with visible light in the region 600-750 unit. A shorter wavelength would overlap with the MLCT band at 458 nm and full photocyloreversion would not occur.[47]
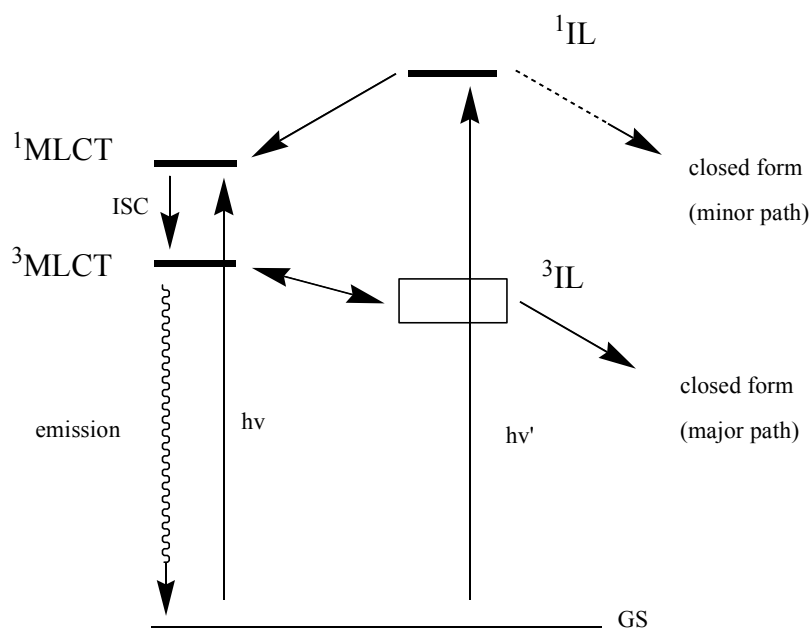
Scheme 1.11: Qualitative energetic scheme presented by De Cola et al[38] for the efficient sensitized photocyclisation of Ru(II) complex **1**.

In comparison to the Ru(II) complex **1**, the Os(II) complex **2** did not demonstrate such an efficient photocyclisation process. Due to the fact that the [1]MLCT state of the Os(II) complex is in a lower-lying energy compared to the Ru(II) one, irradiation into the [1]MLCT band did not result in energy transfer from the excited metal centre to the

photochromic unit, hence the photocyclisation reaction did not occur. Photoexcitation into the higher-energy ^{1}IL state of the dithienylethene moiety did result in the ring-closing process, with a new band at 550-700 nm in the absorption spectrum, but with a lower yield, in comparison to **1**, due to energy transfer into the lower-lying luminescent ^{3}MLCT state of the Os(II) complex **2**.[38,43,47] Photocycloreversion, of the closed form to the open form, also occurred for the Os(II) derivative after irradiation with visible light (>550 nm). However this was a slow process and some decomposition of the complex resulted.[43,47]

Upon excitation into the ^{1}IL and ^{1}MLCT states of the open form of the Ru(II) complex, efficient energy transfer occurred to the ^{3}MLCT state resulting in light emission at 619 nm. The intensity of the emission was found to be much lower compared to Ru(bpy)$_3$ complexes with no photochromic unit attached, due to the fact that either there is a direct pathway from the emissive state to the reactive state, or both reactions occur from the same state. It was also reported that the emissive properties were quenched upon photocyclisation to the ring closed form due to energy transfer to the photochromic unit excited states, which are at lower energy than the metal centre excited states in the closed form.[38,47]

Photoexcitation of the open-form Os(II) complex resulted in light emission at 730 nm, with an almost identical intensity to that obtained for an [Os(bpy)$_3$]$^{2+}$ complex without a photochromic unit attached. However, photocyclisation to the closed form quenched the emission of the Os(II) complex in a similar manner to the corresponding ruthenium complex.[38]

A heterodinuclear metal complex (**3**) containing Ru(II) and Os(II) was synthesised by De Cola et al in order to examine energy transfer processes between the two different metal centres, depending on the state of the photochromic unit (open or closed).[43] The excited states of the two metal centres differ in energy and so intramolecular processes between the Ru(II) complex, acting as the donor (or sensitiser), and the Os(II) complex, acting as the acceptor, were studied.[43,47]

The photocyclisation process was observed for this complex upon irradiation into the singlet state ^{1}IL of the photochromic unit at 334 nm in good yield (90%). Irradiation into the ^{1}MLCT state at 450 nm also resulted in ring closure, however the quantum yield was found to be only half of that obtained following irradiation at 334 nm.[43]

The absorption bands observed in the UV-vis for complex **3** were found to be average of the bands obtained for the bisruthenium (**1**) and bisosmium (**2**) complexes, which indicated that only weak interactions occur between the Ru(II) and Os(II) metal centres. A driving force for energy-transfer from the high-lying Ru(II) complex to the lower-lying Os(II) complex was induced by irradiation into the ^{1}MLCT band, resulting in light emission at two different wavelengths, 630 nm and 730 nm respectively.[43,47] The occurrence of an energy-transfer process was evident by the fact that the emission intensity of the Ru(II) complex largely decreased in comparison to the homodinuclear complex, whilst a major increase in the Os(II) emission intensity was observed.[43,47]

The state of the dithienylethene photochromic unit (open or closed) has a significant effect on the energy-transfer processes between the two metal centres on the complex. In the open-form, efficient energy-transfer was observed from the excited Ru(II) donor unit to the Os(II) acceptor unit. However, upon ring closure, the energy level of the photochromic unit drops significantly below the energy levels of the two metal centres, hence quenching the emissions. Therefore the closed switch acts as trap for both the excited metal complexes.[43,47]

This system is not applicable for an energy/information transfer system due to the fact that the excitation energy at 450 nm induces energy transfer as well as the ring-closing process, and because the closed switch influences both metal centres. It is important to be able to photochemically induce photocyclisation and energy-transfer processes in a separate manner.[47]
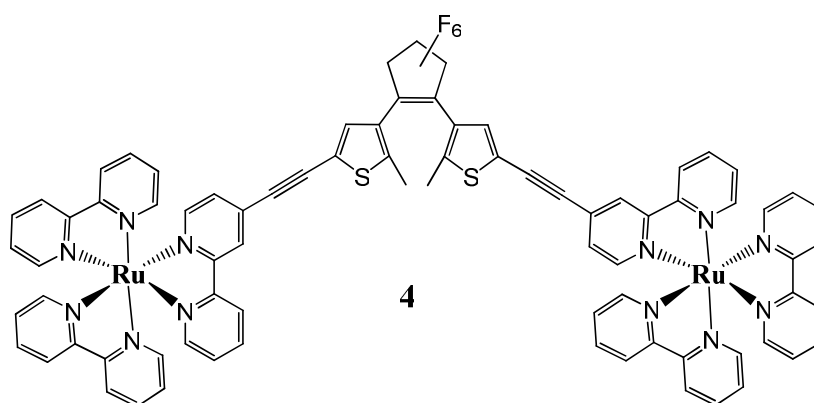
Figure 1.6: Ruthenium metal complex with a bridging photochromic unit (**4**) synthesised by Launay et al.[39]

Launay et al[39] investigated a similar system with bisruthenium metal centres. The only difference in the structure of complex **4** (figure 1.6), in comparison to complex **1** (figure 1.5), is that the phenyl spacer group was replaced by an ethynyl moiety. Photocyclisation upon UV irradiation, and photocycloreversion upon irradiation at $\lambda >$ 600 nm, were observed for this Ru(II) complex (**4**), which agreed with the results for complex **1**, reported by De Cola et al.[38] Irradiation into the [1]MLCT band was not reported by Launay and co-workers. The only difference observed in the absorbance spectrum of complex **4** was a bathochromic shift of the λ_{max} of the closed-ring isomer (670 nm), in comparison to that of complex **1** (619 nm). This is possibly due to the effect of the ethynyl linker employed in **4**, in comparison to the phenyl spacer unit in complex **1**.
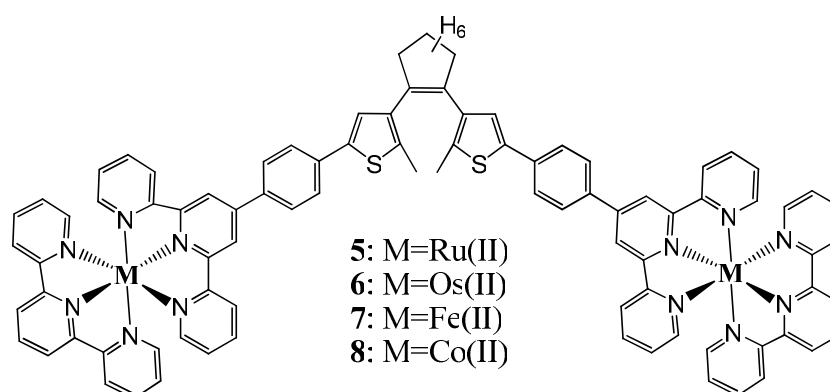
Figure 1.7: Abruna et al[42] synthesised four different metal complexes with a bridging photochromic unit. Complexes **5** to **8** were substituted with different metal centres: Ru(II), Os(II), Fe(II), and Co(II) respectively.

Abruna et al[42] also reported the photochromic properties of metal complexes similar to those studied by Launay[39] and De Cola[38,47]. However, two major structural differences were employed, as illustrated in figure 1.7: the per*fluoro*cyclopentene unit was replaced by a per*hydro*cyclopentene unit; and the metallated trisbipyridine complexes were substituted with metallated bisterpyridine groups. Four homonuclear derivatives were synthesised with different metal centres: bisruthenium (**5**), bisosmium (**6**), bisiron (**7**) and biscobalt (**8**) complexes. Upon UV irradiation into the excited state [1]IL of the photochromic unit, the photocyclisation reaction did not occur for the bisruthenium, bisosmium or bisiron complexes. Each of these complexes displayed an MLCT band in the visible region of the UV-vis spectrum and Abruna et

al deduced that possible quenching of the excited state [1]IL took place, preventing the occurrence of the cyclisation reaction. The biscobalt complex only displayed a very weak MLCT band in the UV-vis spectrum, and upon photoexcitation, ring-closure took place, although the photocycloreversion reaction, from the closed to the open form, was unsuccessful.

Abruna et al[41] performed further studies on dithienylcylopentene metal complex systems. This time they used a trisbipyridine metal complex in the centre of the system and attached three dithienylperhydrocyclopentene units via phenyl linkers (figure 1.8). Three different metal centre atoms were employed {Ru(II), Fe(II), Co(II)}, and the photochromic properties of the three derivatives were investigated.

9: M=Fe(II)
10: M=Co(II)
11: M=Ru(II)
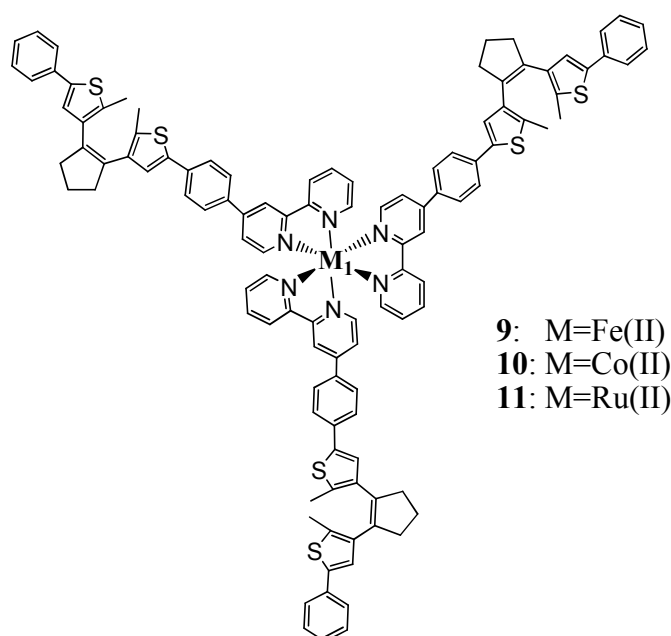
Figure 1.8: Abruna et al[41] synthesised a trisbipyridine metal complex with three photochromic units attached. Complexes **9**, **10** and **11** were substituted with different metal centres: Fe(II), Co(II) and Ru(II) respectively.

Irradiation of the Fe(II) complex, into the excited state [1]IL of the photochromic unit, resulted in ring-closure (~70%) after 8 hours, evidenced by a new broad absorption band between 440 and 700 nm present in the UV-vis spectrum.

Photocyclisation also occurred for the Co(II) complex upon irradiation into the singlet excited state of the photochromic unit, after 10 minutes. Almost all of the open form was converted to the closed form, indicating that all three dithienylcyclopentene units were photoactive. Upon irradiation with visible light (470 nm), only partial

photocycloreversion back to the open form occurred (~30%). The fast photocyclisation process for the cobalt complex (10 mins), compared to the slow process reported for the Fe(II) complex (8hrs), is due to the fact that the Co(II) complex has no intense MLCT band in the visible region. In contrast, the Fe(II) complex displays an MLCT band at 543 nm and upon irradiation, energy-transfer occurs from the photochromic unit to the low-energy [3]MLCT state.

The photocyclisation reaction of the Ru(II) complex was found to occur upon irradiation into the singlet excited state [1]IL of the dithienylethene units, and also upon irradiation into the [1]MLCT band at 470 nm. This is in contrast to the Fe complex, as photocyclisation could not be triggered through irradiation into the MLCT band (probably because of its low-energy [3]MLCT state). Analysis of the PSS reached for the ruthenium complex showed that only 67% of the open-form was converted to the closed form. The emission of the Ru(II) complex was completely quenched upon ring-closure due to intramolecular energy transfer from the [3]MLCT to the dithienylethene-centered triplet state [3]IL, which corresponds to the results reported for the Ru(II) complex **2** (figure 1.5) by De Cola at al.[38]

Overall, the results described from literature studies show that the photochromic properties of these systems are significantly influenced by the type of metal complex employed, the central metal atom used, and the spacer unit employed to attach the photochromic unit to the metal complex. A general pattern that emerged from these results is that Co(II) metal centres allow for efficient photocyclisation processes to occur from the [1]IL state; Ru(II) metal centres display ring-closing processes from irradiation into the [1]IL and the [1]MLCT states; Os(II) metal centres demonstrate photocyclisation processes from irradiation into the [1]IL but not from the [1]MLCT states; Fe(II) metal centres result in slow cyclisation processes from the [1]IL state only. Also observed was good cyclisation processes from metallated trisbipyridine complexes, but not from biterpyridine metal complexes, and substitution of a phenyl linker, by an ethynyl linker, resulted in absorption of the closed-ring isomer at lower energy. Emission processes for ruthenium and osmium complexes were observed for the open-ring isomers, but were quenched upon cyclisation to the closed-ring isomers.

- **Metal carbonyl and phosphine ligand complexes**
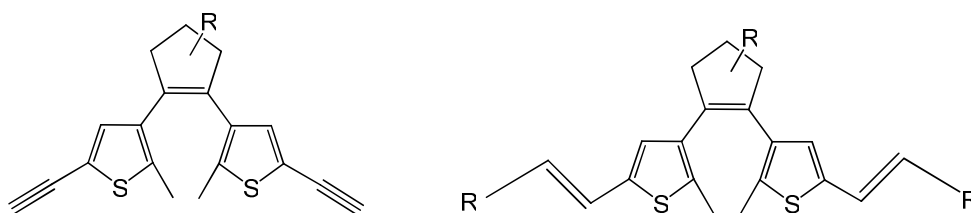
12H: R=H
12F: R=F

13H:R=H;R'= RuCl(CO)(PMe$_3$)$_3$
13F: R=F; R'= RuCl(CO)(PMe$_3$)$_3$
14H:R=H;R'= RuCl(CO)(PPh$_3$)$_2$Py
14F: R=F; R'= RuCl(CO)(PPh$_3$)$_2$Py
15H:R=H;R'= RuTp(CO)(PPh$_3$)$_2$
15F: R=F; R'= RuTp(CO)(PPh$_3$)$_2$
16H:R=H;R'= RuCl(CO)(PMP)
16F: R=F; R'= RuCl(CO)(PMP)

Figure 1.9: Liu et al[44] synthesised a number binuclear ruthenium vinyl complexes with dithienylethene units, with different ancillary ligands attached to the Ru metal (complexes **13** to **16**). The unmetallated compound **12** was used for comparison purposes.

As illustrated in figure 1.9, Liu et al[44] synthesised a series of ruthenium based metal complexes (**13-16**), with a bridging dithienylcyclopentene switch containing perhydro (**H**) and perfluoro (**F**) -cylopentene units, and different ancillary ligands were attached to the ruthenium metal centre. All of the binuclear ruthenium vinyl complexes underwent photo-cyclisation/cycloreversion processes. For the free ligand **12**, the quantum yield obtained for cyclisation of the perhydro complex was found to be higher than that of the perfluoro complex. However, upon attaching metal groups to the photochromic unit, the quantum yields of the perhydro complexes **13H-16H** decreased, whilst in the case of the perfluoro metal complexes **13F-16F,** the quantum yields for the ring-closing process increased. Also, the perhydro metal complexes turned a dark red colour, with new absorption peaks appearing in the region of 530-548 nm upon irradiation with UV light, whereas the perfluoro complexes turned a dark blue colour, with significant bathochromic shifting of their closed-ring absorption peaks to 622-642 nm, upon photocyclisation. It is also worth noting that the metal complexes reached the photostationary state more efficiently than the free ligand. In contrast, the photocycloreversion process, to the ring opened form, was much slower for the metal complexes than for the free ligand. This indicates that

metallation increases the stability of the ring-closed isomers. However, in the case of **13F**, ~40% of the complex had decomposed after 10 repeated cycles of the ring-opening/closing process, which was assigned to degradation of the CO ligands.

Overall, these results demonstrate the effects of the central switching unit and the metal ligands on the photochromic behaviour of these complexes with regards to the quantum yields, efficiencies and absorption spectra obtained.

17:M=Fe, L$_2$=(CO)$_2$, R=H
18:M=Ru, L$_2$=(CO)$_2$, R=H
19:M=Fe, L$_2$=(CO)(PPh$_3$), R=H
20:M=Ru, L$_2$=(CO)(PPh$_3$), R=H
21:M=Fe, L$_2$=dppe, R=Me

22
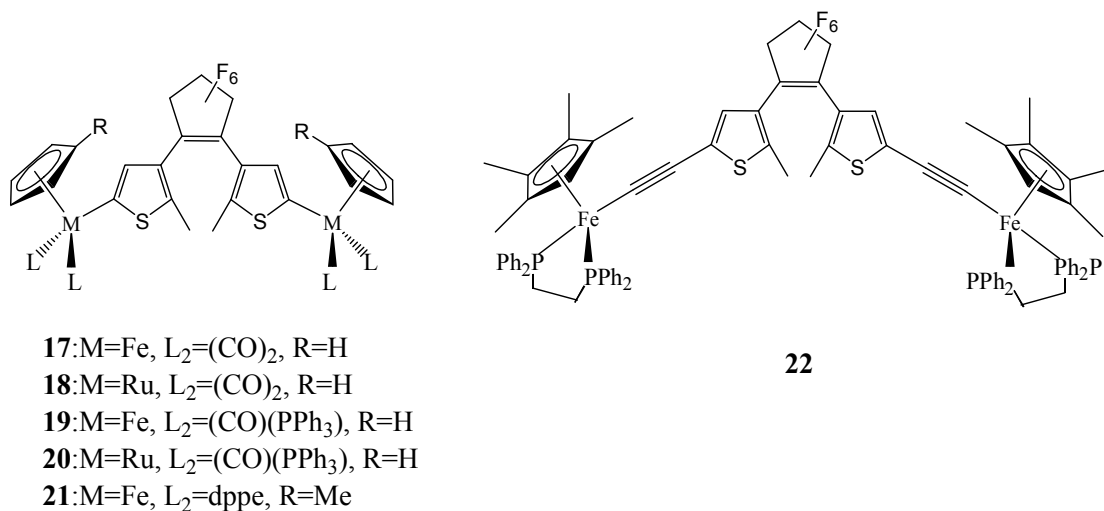
Figure 1.10: Akita et al[40, 46] synthesised a number of metal complexes with a bridging dithienylethene unit , with different metal centres and ancillary ligands (complexes **17** to **22**).

Akita et al[46] investigated the photochemical effects of attaching metal complexes, to a photochromic bridging unit, with different metal centres and ancillary ligands (figure 1.10). The photochemistry results showed that cyclisation processes occurred more efficiently for the ruthenium metal centred complexes, in comparison to the iron metal centred complexes. With regards to the ancillary ligands, it was found that the efficiency of the photocyclisation reaction was reduced upon introduction of phosphine ligands. In fact, the ring-closing process was completely inhibited for the Fe-dppe derivative (**21**). However, when the cyclopentadiene ring attached to the Fe core was replaced with a pentamethylcyclopentadiene ring, and an ethynyl spacing unit was incorporated between the photochromic unit and the Fe-dppe metal complex (**22**), photocyclisation/cycloreversion processes were observed.[40]

23

24
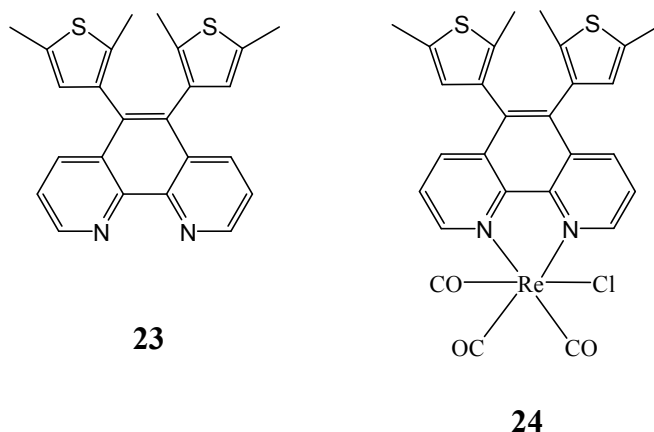
Figure 1.11: Yam et al[22] synthesised a rhenium(I) tricarbonyl diimine complex with a photochromic unit attached (**24**), and its corresponding free ligand (**23**).

Yam et al[22] described the photocyclisation processes of the free ligand **23** and metallated rhenium(I) tricarbonyl diimine complex **24**, illustrated in figure 1.11. Upon UV irradiation the open-form of the free ligand **23** cyclised to the closed form, with new absorption bands appearing at 510 and 540 nm. The metal complex **24** also underwent photocyclisation following UV irradiation into the singlet excited state (^{1}IL) of the photochromic unit, and the absorption bands of the closed form were red-shifted to 546 and 580 nm, in comparison to the free ligand, which was attributed to perturbation of the transitions by the metal centre in the metal complex. The quantum yields obtained for the ring-closing process were higher for the metal complex than the free ligand. A photocyclisation process was also observed for the metal complex upon irradiation into the ^{1}MLCT band at ~400 nm, with even higher quantum yields. Photocycloreversion, from the closed to the open forms, was observed for the free ligand and metal derivative, although, the quantum yields obtained for the ring-opening process were lower than the quantum yields obtained for the ring-closing process, for both compounds. In contrast to the cyclisation process, the quantum yields for the cycloreversion process were higher for the free ligand compared to the metal complex. These results indicate that the addition of the metal complex to the free ligand stabilised the ring-closed isomer. However subsequent thermal studies showed that the closed form of the free ligand was more stable to heat than the metal complex, suggesting that the closed form of the free ligand was more stable than that of the metal complex.

The emission spectra of the free ligand **23**, and metal complex **24**, changed significantly between the open-ring isomers and the closed-ring isomers. Upon

photoexcitation (λ_{exc} = 300 nm) of the free ligand in its open-form, an emission band was observed at 385 nm. However, following ring-closure, the emission band was red-shifted to 644 nm (λ_{exc} = 400 nm), which was attributed to the increase in the extent of π-conjugation in the closed-form. Photoexcitation of the ^{1}MLCT band of the metal complex (open form) at λ_{exc} = 400 nm resulted in an emission band at 595 nm, which was shifted to 620 nm in its closed form. The change in the emission origin, depending on the state of the photochromic unit (open or closed), can be assigned to the relative positions of the ^{1}MLCT and ^{1}IL excited states. In the open-form the MLCT state is lower lying than the ^{1}IL state, therefore energy transfer occurs from the ^{1}MLCT state to the ^{3}MLCT state, resulting in phosphorescence from the ^{3}MLCT state. However, in the closed-form, the ^{1}IL state is lower in energy than the ^{1}MLCT state, resulting in emission from the ^{1}IL state.
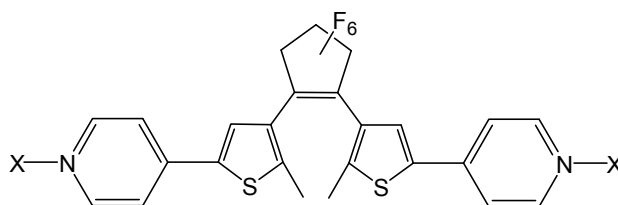
25: X is not present
26: X=W(CO)$_5$
27: X=Re(bpy)(CO)$_3$(CF$_3$SO$_3$)
28: X=[Ru(NH$_3$)$_5$](PF$_6$)$_2$

Figure 1.12: Lehn et al[48] synthesised a dithienylperfluorocyclopentene switch with pyridine groups attached to the thiophene units as the parent compound (**25**). The compound was derivatised with different metal complexes (**26-28**).

Lehn et al[48] reported that the tungsten and rhenium carbonyl complexes, **26** and **27** respectively (figure 1.12), displayed photocyclisation reactions upon UV irradiation at λ = 312 nm, and subsequent photocycloreversion processes following irradiation with visible light.

The closed form of the tungsten carbonyl complex **26** displayed a strong emission when excited in the region 200-400 nm, however much weaker fluorescence was observed for the open-ring isomers. In contrast, the rhenium complexes **27** displayed stronger emission when present in their open-form, than in their closed form isomers. This fluorescence discrimination between the open and the closed forms is triggered

upon photoexcitation at a wavelength that has low photochemical activity, thus, the state of the system (open or closed) is hardly affected. Therefore, these complexes show promising functions for use in optical data storage systems with non-destructive read-out properties.

Lehn et al[48] also reported the synthesis of a chemical locking system for use in non-destructive read-out applications. During attempts to photocyclise the open form of the ruthenium complex **28 (28o)** (figure 1.12) by irradiation with UV light, they observed only decomposition for the complex. Therefore, to obtain the closed-ring isomer of this complex (**28c**), they began with a photocyclisation reaction of the parent complex **25** (**25o** to **25c**), followed by addition of the ruthenium metal complex on the two pyridyl groups. Subsequent irradiation of **28c** with visible light ($\lambda > 600$ nm) did not result in photocycloreversion to the open form **28o**. Lehn et al concluded that the open and closed forms of complex **28** could not be photointerconverted and could only be prepared from their parent ligands **25o** and **25c**. Therefore, the parent ligand **25** could be used for storage information by interconversion between the open and closed forms by photochemical means. Upon complexation with Ru(II), yielding complex **28**, the stored information could be read-out in a non-destructive manner using visible light. Hence, generation of complex **28** can be deemed as chemically locking the stored information.

Overall, some interesting results were obtained for photochromic units attached to metal carbonyl and phosphine derivatives. In general, reports in the literature have shown that incorporation of the metal complexes onto the photochromic unit increased the efficiency of the photocyclisation process but decreased the efficiency of the ring-opening process. Therefore, metal complexes appear to stabilise the ring-closed form. Akita et al[40,46] demonstrated the effect of metal centres, ancillary ligands, and spacer units on the photochromic properties. They concluded that introducing an iron metal centre, in place of ruthenium, and phosphine ancillary ligands resulted in less efficient ring-closing processes. However, introduction of an ethynyl spacer unit was found to induce photochemical ring opening/closing processes to a compound that was unable to undergo either process previously. Attaching carbonyl ancillary ligands to two ruthenium metal centres, separated by a dithienylethene moiety (**13F**), was described by Liu et al[44] and decomposition resulted upon UV irradiation, due to the presence of

the CO ligand. This was probably due to the dissociation of CO molecules, which is known to take place upon irradiation. On the other hand, most of the complexes mentioned here contain CO ligands but no other decomposition reactions were reported in the literature.

In contrast to the results described above for the bipyridine metal complexes, the emission properties reported for these compounds were not quenched upon ring-closure. In fact Yam at el[22] and Lehn et al[48] observed fluorescence discrimination for a number of compounds that are good candidates for non-destructive read-out systems. Also, Lehn et al[48] reported a novel chemical locking system using a compound which does not undergo photochemical cyclisation or cycloreversion processes.

1.2.2 Electrochemical Properties

Incorporating organometallic moieties onto dithienylethene switches can influence the electrochromic properties of the switching unit. Thus, the electrochemical properties of bipyridine metal complexes, and metal carbonyl and phosphine ligand complexes, reported in the literature are described here.

- **Bipyridine Metal Complexes**

De Cola et al[38] performed electrochemical reduction experiments on the open and closed forms of the Ru(II) complex **1** (figure 1.5) and of the free unmetallated ligand. After reduction of the open form of the free ligand, and complex **1**, they concluded that electrochemical cyclisation to the closed forms did not occur. They failed to mention if a cycloreversion process occurred or not during their discussions of the electrochemical reductive processes of the closed form derivatives. In a separate publication, De Cola et al[43] reported the oxidative process of the open-form Ru(II)/Os(II) heteronuclear complex **3** (figure 1.5). Their discussion was based on the redox waves observed for the oxidation of the metal centres from the II to the III oxidation states. However, once again they failed to mention electrochemical cyclisation processes, and also no electrochemical analysis was described for the closed-ring forms.

Launay at al[39] investigated the electrochemical oxidation processes of the dinuclear Ru(II) complex **4** (figure 1.6) in the ring-closed and -open forms. Oxidation of the open-ring isomer resulted in a reversible oxidation process of the ruthenium metal centres from II-II to their fully oxidised forms III-III. Oxidation of the closed-ring isomer resulted in a photocycloreversion reaction from the closed to the open form, as evidenced by the loss in colour of the solution and the decrease of the absorption band at 670 nm, characteristic of the closed-ring form.

Abruna et al[42] investigated the electrochemical oxidation processes of the dinuclear metal complexes of Ru(II) (**5**), Os(II) (**6**), Fe(II) (**7**) and Co(II) (**8**), represented in figure 1.7. A reversible redox wave was observed for the ruthenium complex at 1.35 V, due to the oxidation of Ru(II) to Ru(III). Similar redox waves were observed for

the other central metal ions at 1.23 V ($Fe^{II/III}$), 0.99 V ($Os^{II/III}$) and 0.39 V ($Co^{II/III}$). Upon further investigation, electrochemical cyclisation processes were found to occur for the ring-open isomers of the ruthenium (**5**) and iron (**7**) complexes, following an irreversible oxidation process of the photochromic thienyl units at 1.22 V for both complexes. However, this process was not observed for the corresponding osmium and cobalt complexes. Abruna et al[42] suggested that the reason for this was that oxidation of the metal centres occurred before the oxidation of the thienyl rings, preventing electrochemical cyclisation.

Abruna et al[41] compared the electrochemical oxidation results of the Fe(II), Co(II) and Ru(II) trisbipyridine tris(dithienylcyclopentene) complexes **9**, **10** and **11** respectively (figure 1.8). The cyclic voltammogram of each complex displayed a reversible redox wave, corresponding to oxidation of the central metal ion from their II form to their III form, at +1.18 ($Fe^{II/III}$), +0.36 ($Co^{II/III}$), and +1.38 V ($Ru^{II/III}$). However, upon oxidation at potentials higher than their redox waves (1.25 V), cyclisation processes, from the open-ring to the closed-ring, occurred for all the complexes. The electrochemical process was also investigated for the free unmetallated ligand which also resulted in ring-closure upon oxidation at 1.22 V of the open-ring isomer. Therefore, incorporation of a metal centre didn't effect the electrochemical reactions of the compounds, just the potential value at which they occurred.

As mentioned in the previous section 1.1, electrochemical processes of dithienylethene units with a perfluorinated cyclopentene structure have generally resulted in cycloreversion processes, from the closed to the open-ring form, due to the electron-withdrawing effects of the fluorine atoms. Launay et al[39] reported an oxidative cycloreversion process for complex **4**, containing a perfluorinated cyclopentene unit, as expected. Therefore, it is clear that the metal complex attached didn't effect the direction of electrochemical switching for this complex. In light of this, further investigation into the electrochemical switching processes of the closed isomers of complexes **1**, **2** and **3**, reported by De Cola et al,[38,43] is required as oxidative ring-opening seems feasible following the results reported by Launay et al.[39] Abruna at al[41,42] reported the electrochemical processes of metal complexes containing perhydrocyclopentene units, represented in figures 1.7 and 1.8. The hydrogen atoms on the cyclopentene unit are expected to induce oxidative ring-closing processes due

to their electron-donating abilities. The results were as expected for the ruthenium based complexes, **5** and **11** and iron based complexes, **7** and **9**, which underwent oxidation cyclisation. This was not the case for the osmium (**6**) and cobalt (**8**) complexes, which did not undergo cyclisation reactions by electrochemical means. However, the cobalt trisbypridine complex (**10**), which had three separate dithienyl-perhydrocyclopentene units attached, did undergo an oxidation ring-closing process. Maybe this was due to the extra stability of the closed-ring radical cations provided by the three electron-donating photochromic units.

Overall, it seems that attaching bipyridine metal complexes to photochromic units does not have a pronounced effect on the direction of the electrochemical switching properties however it can prevent electrochemical switching altogether.

- **Metal carbonyl and phosphine ligand complexes**

Electrochemical methods can be employed to measure the extent of interaction between two metal termini separated by a dithienylethene unit. Liu et al[44] investigated the effect of the state of the photochromic unit (open or closed) on the communication between the two metal centres in complex **13F** (figure 1.9) by electrochemical means. In the open-ring form, oxidation led to one irreversible peak at 0.57 V attributed to a one-step 2-electron oxidative process of the two ruthenium centres from their II form to their III form, indicating a lack of communication between the metal centres. However, upon ring-closure via UV irradiation, two new reversible waves at lower potentials (0.02 V and 0.17 V) appeared upon oxidation. These waves were attributed to the oxidation of $Ru^{II,II}$ to $Ru^{II,III}$ and then to $Ru^{III,III}$, indicating that communication between the metal centres exists following ring-closure. Therefore, UV and visible light can be used to switch the communication between two metal centres between "ON" and "OFF".

The effect of the type of photochromic unit on the electronic properties of the metal centres was also reported here. Higher oxidative potentials, and a greater degree of separation between the oxidative waves, were observed for the perflourocyclopentene derivatives, due to the fact that the fluorine atoms help to facilitate stronger electronic communication between the two metal centres.

Liu et al[44] also reported that electrochemical oxidation, at potentials of 0.6 V and greater, led to cyclisation reactions for the perhydro and perfluoro metal complexes **13** to **16**. In general, it would be expected that the electron-withdrawing properties of the perfluorinated cyclopentene derivatives would lead to oxidative cycloreversion reactions however, this is not the case. This is a good example of how the metal complexes can significantly affect the properties of the dithienylethene unit.

Akita et al[46] investigated the cyclisation processes of the ruthenium and iron complexes by electrochemical means. Upon oxidation of the open-form of complexes **19**, **20** and **21** (figure 1.10) a cyclisation reaction took place, resulting in ring-closure. It should be highlighted that the iron complex **21** underwent oxidative cyclisation, but failed to cyclise by photochemical means. In the cases of the iron complexes **19** and **21**, photocycloreversion back to the open-form was not observed by photochemical or electrochemical means. Therefore, the closed structure can be firmly locked by electrochemical means.

These electrochemical results also demonstrated an increase in communication between the two terminal metal complexes from the open to the closed-ring isomers. Upon ring-closure, two well defined redox waves were observed, which are not present for the open-ring isomers. The central metal atom, and the electron-donating ability of the ancillary ligands, effects the separation between the two redox waves (i.e. the communication between the metal complexes). It was found that the ruthenium and phosphine derivatives resulted in greater degrees of separation compared to the iron and carbonyl derivatives respectively, with the Fe-dppe derivative **21** performing the best. Therefore, communication between the two metal centres can be controlled by electrochemical and photochemical stimuli.

With regards to the Fe-dppe complex containing the alkynyl spacer, and methylated cyclopentadiene ring (**22**: figure 1.10), Akita et al[40] did not observe oxidative ring-closure. However, an increase in communication between the two metal centres was observed. In the open form only one reversible redox wave was present in the cyclic voltammogram, whereas the electrochemistry of the closed-form demonstrated two well-separated redox waves, indicating an increase in communication between the metal complex termini due to extended π-conjugation in the closed-ring isomer. Therefore the communication property of the organometallic wire can be switched "ON" and "OFF" by UV and visible light in a reversible manner.

Overall, the literature studies of incorporating metal centred complexes, with carbonyl and phosphine ancillary ligands, onto a photochromic switching unit have given interesting electrochemical results. In general, the electrochemical results demonstrated an increase in communication between the two metal complex termini upon ring-closure, due to the increase in π-conjugation across the dithienylethene backbone. It was found that the type of dithienylethene switch, the central metal ion and the ancillary ligands employed also affected the communication properties. Perfluorinated cyclopentene units, in comparison to perhydrocyclopentene switches; ruthenium metal centres, in comparison to iron; and phosphine ancillary ligands, in comparison to CO, all facilitated communication between the two metal centres.

Electrochemical cyclisation reactions were observed for perhydrocyclopentene units, but also for their corresponding perfluorocyclopentene units by Liu et al.[44] Therefore, incorporating strongly-donating metal fragments can change the switching direction of dithienylethene units by oxidative processes.

Interestingly, some of the results described in the literature showed that the effect of the substituents on the photochromic properties were significantly different to the effects on the electrochemical properties, for the switches. For example, Akita et al[46] reported that the presence of phosphine ancillary ligands decreased the efficiency of the photocyclisation processes, but increased the communication between the two metal termini, as observed by electrochemical studies. Also, the Fe-dppe complex **21** (figure 1.10) did not undergo photochemical cyclisation but did undergo electrochemical ring-closure[46], however, its derivative complex **22** (figure 1.10), containing ethynyl linkers and a penta-substituted methyl cyclopentadiene ring, was found to cyclise by photochemical means but not by electrochemical means.[40]

1.3 Cobalt Carbonyl Complexes

Metal carbonyl complexes are one of the most photoreactive transition metal complexes.[49] They have been investigated for their use as carbon monoxide releasing molecules, which have applications as medicinal therapeutic agents towards combating a variety of diseases.[50-53]

Incorporating metal complexes and dithienylethene switches into the same system has demonstrated some interesting results. We have incorporated cobalt carbonyl complexes onto dithienylethene switches to investigate the effect of the photochemical and electrochemical properties of such systems, as detailed in chapters 3-6. Consequently, a brief discussion about the bonding, photochemical and electrochemical properties of cobalt carbonyl complexes, reported in the literature, is detailed here.

1.3.1 Bonding in Metal Carbonyls

- **Metal-Carbonyl Bonding**

The molecular orbitals present in a carbon monoxide (CO) orbital consist of a filled sigma (σ) orbital and two filled π-orbitals localised between the carbon and oxygen. Two lone-pairs are localised on the carbon and oxygen atoms, but are directed away from the molecule, and two π-antibonding (π^*) orbitals are present but are directed away from the CO internuclear region and are empty in the ground state.[35]

Upon bonding to a metal ion, carbon monoxide acts as a σ-donar, π-acceptor ligand, as represented in figure 1.13. The carbon monoxide donates electron density to the d, s and p-orbitals on the metal from the lone pair present on the carbon atom, in a σ-type bond. The CO molecule accepts electron-density from the metal, as the dπ electrons from the metal give rise to π back-bonding into the π^* orbital of the CO molecule.[35,36,36,49] Although the σ-bond is stronger, the π-bond weakens the carbon-oxygen bond to a greater extent as it directly populates the CO π-antibonding orbital.

Also, the ability of CO to accept electron-density from the metal results in stabilisation of the metal ion, especially those in low oxidation states.[35,49]
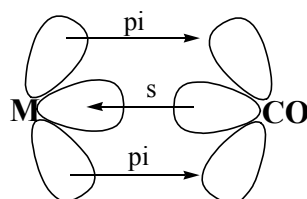
Figure 1.13: Represents the sigma (s) and π (pi) bonding orbitals involved in the bonding between a metal and a carbonyl group.

- **Metal-Alkyne Bonding**

Metal carbonyl complexes can be incorporated onto an organic compound through metal-alkyne bonds. Alkynes bond to metals in a perpendicular arrangement, with the C≡C bond perpendicular to the metal-alkyne bond. Alkynes posses a σ-bond and two π-bonds localised between the two carbon atoms, and two π^* orbitals on the two carbon atoms, directed away from the triple bond. Alkynes are considered to be σ-donor, π-acceptor ligands: alkynes donate electron density to metal atoms in a σ fashion, and accept electron density from the d-orbitals of the metal atoms into their π^* orbitals. However, their π-accepting ability is much less compared to CO ligands due to the low electronegativity of the carbons. The strength of these bonds can be affected by substituents attached to the alkyne. In general, electron-donating groups increase the σ-bonding but decrease the π-bonding. Electron-withdrawing groups have the opposite effect, and have been found to be more effective in increasing the overall strength of the metal-alkyne bond due to increased π back-bonding.[35,54]

Alkynes posses two π orbitals, located at right angles to one another which allow alkynes to bond to two metal atoms, in a bridging fashion (figure 1.14).[35,54]
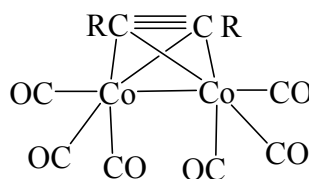
Figure 1.14: Represents the coordination of dicobalt hexacarbonyl [$Co_2(CO)_6$] onto an alkyne, in a bridging fashion.

1.3.2 Photochemistry

Photochemistry describes the reactions that take place following photoexcitation, with ultraviolet or visible light, into a higher excited state. Metal carbonyls are extremely photoreactive complexes. Due to the large degree of delocalisation of the central metal electrons into the CO ligands, these compounds are highly covalent and therefore electronic transitions can lead to significant changes in the bonding of such complexes.[35,49] An important photochemical reaction of metal carbonyl complexes is the loss of CO or L (ligand), followed by ligand substitution (Y), upon irradiation with light of specific wavelengths.[35,49]

$$M(CO)_n(L)_x \ + \ Y \ \xrightarrow{\ h\nu\ } \ M(CO)_{n-1}Y(L)_x \ + \ CO$$

$$M(CO)_n(L)_x \ + \ Y \ \xrightarrow{\ h\nu\ } \ M(CO)_n(L)_{x-1}Y \ + \ L$$
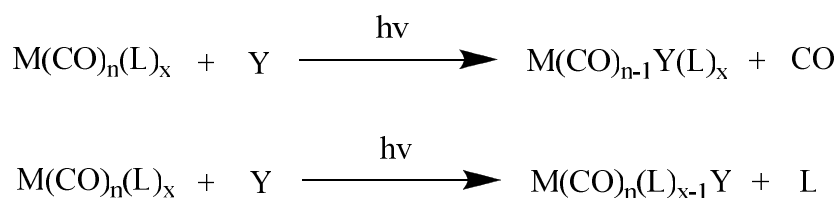
The substitution reaction quantum yield is dependent on the wavelength of light used for irradiation.[49] The entering ligands should be good π-acceptor ligands because the loss of CO, to yield stable low-valent complexes, requires substitution with ligands that are capable of stabilising the metal centre.[35,49] Some examples of efficient photochemical reactions of dicobalt hexacarbonyl complexes [$Co_2(CO)_6$] and the resulting photoproducts, reported in the literature, are described here.

Long et al[55] performed photochemical experiments on an alkynyl cobalt hexacarbonyl complex in order to investigate CO loss at a number of different wavelengths. Firstly they used a broadband lamp source with a cut-off filter of $\lambda_{exc} > 340$ nm. Upon photolysis of (μ_2-RC$_2$H)Co$_2$(CO)$_6$, in the presence of a trapping ligand L, (L=C$_5$H$_5$N or PPh$_3$), infra-red analysis showed that the cobalt pentacarbonyl complex was produced, followed by the cobalt tetracarbonyl complex after prolonged irradiation times, hence confirming that CO-loss can be achieved by photochemical methods. Similar results were obtained with a lower energy light-source $\lambda_{exc} > 400$ nm but longer photolysis times were required.

Subsequently, they investigated this photochemical process using monochromatic light. Irradiation with $\lambda_{exc} = 355$ nm did not result in CO-loss. Instead they found that

homolytic cleavage of the cobalt-cobalt bond occurred, followed by rapid recombination in an efficient manner. However, photolysis experiments carried out at $\lambda_{exc} = 532$ resulted in CO-loss and substitution with the trapping ligand PPh_3.

Therefore, the results published by Long et al demonstrate the effect of different excitation wavelengths on the photochemical reactions of cobalt hexacarbonyl complexes.

Ford et al[56] reported the formation of a number of photoproducts upon laser flash photolysis, with time resolved infra-red (TRIR) spectroscopy, of the cobalt hexacarbonyl complex, $Co_2(CO)_6(PMePh_2)_2$ (**A**). Following photolysis (with $\lambda_{irr} =$ 308–365 nm) two photochemical reactions were observed, resulting in the formation of two photoproducts, as represented in scheme 1.12:

1) The loss of a CO molecule resulting in formation of $Co_2(CO)_5(PMePh_2)_2$.
2) Photo-induced homolytic cleavage of the metal-metal bond to give the mononuclear metal-based radicals $^\bullet Co(CO)_3(PMePh_2)$.

These photoproducts became involved in further reactions, and the resulting products were dependent on the conditions of the experiment.

$$Co_2(CO)_6(L)_2 \xrightarrow{h\nu} Co_2(CO)_5(L)_2 \ + \ ^\bullet Co(CO)_3L$$
$$\textbf{A}$$
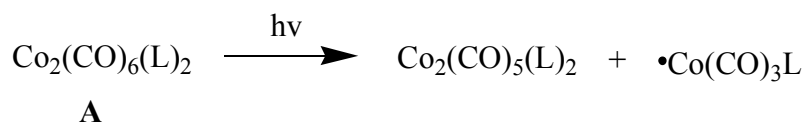
Scheme 1.12: When **A** was irradiated with light (L = $PMePh_2$), two photoproducts were initially generated by CO loss and homolytic bond-cleavage.

When $Co_2(CO)_5(PMePh_2)_2$ was photochemically formed, under an atmosphere of CO, it recombined with CO to regenerate the initial compound **A**. When the experiment was carried out in the presence of excess ligand ($PMePh_2$) under an Ar atmosphere, the $Co_2(CO)_5(PMePh_2)_2$ intermediate underwent a ligand substitution reaction, forming $Co_2(CO)_5(PMePh_2)_3$. These reactions are illustrated in scheme 1.13.

$$\textbf{(i)} \ \ Co_2(CO)_5(L)_2 \xrightarrow{+CO} Co_2(CO)_6(L)_2$$
$$\textbf{A}$$

$$\textbf{(ii)} \ \ Co_2(CO)_5(L)_2 \xrightarrow{+L} Co_2(CO)_5(L)_3$$
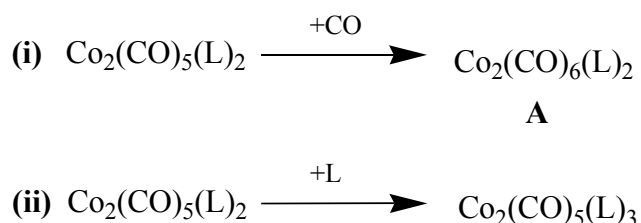
Scheme 1.13: $Co_2(CO)_5(L)_2$ undergoes further photochemical reactions: (i) under CO atmosphere; (ii) in the presence of excess ligand, where L = $PMePh_2$.

The radical photoproduct $^{\bullet}Co(CO)_3(PMePh_2)$ recombined to regenerate the initial complex **A**. However, this radical species also underwent a number of further reactions, yielding a variety of photoproducts, which were dependent on the reaction conditions, as illustrated in scheme 1.14:

- Under an atmosphere of CO, and in a solution of benzene, the $^{\bullet}Co(CO)_3(PMePh_2)$ radical produced a monocobalt tetracarbonyl species $[Co(CO)_4]$, accompanied by ligand dissociation. $Co(CO)_4$ underwent a combination reaction with the radical species, generating $Co_2(CO)_7(PMePh_2)$.

- Under an argon atmosphere and in the presence of excess ligand ($PMePh_2$), the radical species underwent ligand substitution to form $Co(CO)_2(PMePh_2)_2$, accompanied by CO loss. This new product reacted with the radical product, forming a third complex $Co_2(CO)_5(PMePh_2)_3$.

- When the solvent was changed from benzene to dichloroethane (DCE), under an atmosphere of argon, another reaction mechanism took place. Upon photolysis, the radical product extracted a chlorine from the chlorinated solvent to form a mononuclear product, $Co(CO)_3(PMePh_2)Cl$. It should be noted that in the presence of excess ligand, photosustitution pathways can also occur. Ford et al[56] reported such a result when a solution of **A** in DCE was photolysed at 365 nm, as demonstrated in scheme 1.14 below:

$$\textbf{(i)}\ [Co(CO)_3L]^{\bullet} \xrightarrow{+[Co(CO)_3L]^{\bullet}} Co_2(CO)_6(L)_2$$
$$\textbf{A}$$

$$\textbf{(ii)}\ [Co(CO)_3L]^{\bullet} \xrightarrow{+CO} Co(CO)_4 + L \xrightarrow{+[Co(CO)_3L]^{\bullet}} Co_2(CO)_7(L)$$

$$\textbf{(iii)}\ [Co(CO)_3L]^{\bullet} \xrightarrow{+L} Co(CO)_2(L)_2 + CO \xrightarrow{+[Co(CO)_3L]^{\bullet}} Co_2(CO)_5(L)_3$$

$$\textbf{(iv)}\ [Co(CO)_3L]^{\bullet} \xrightarrow{DCE} Co(CO)_3(L)Cl$$
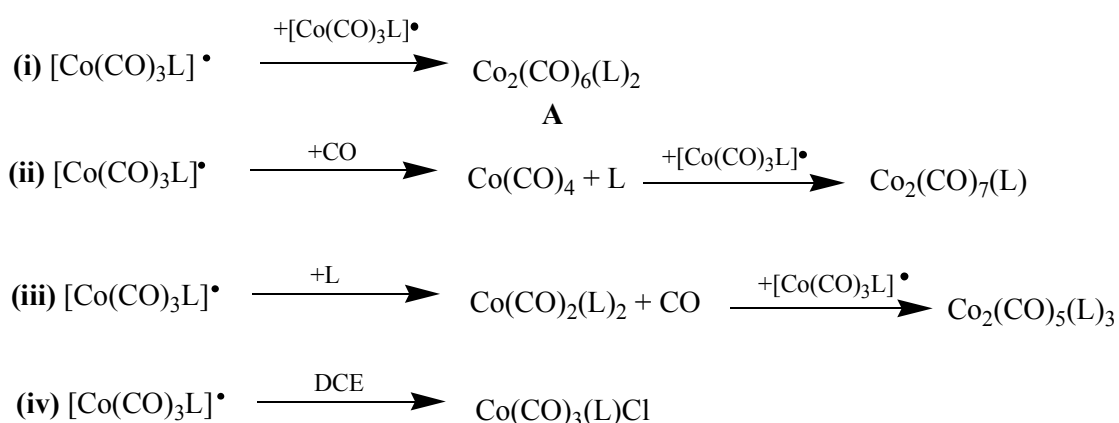
Scheme 1.14: The $Co_2(CO)_3(L)$ radical undergoes further photochemical reactions: (i) recombines to form the initial species **A**; (ii) under CO atmosphere produces $Co(CO)_4$ and $Co_2(CO)_7L$; (iii) in the presence of excess ligand produces $Co(CO)_2(L)_2$ and $Co_2(CO)_5(L)_3$; (iv) in dichloroethane (DCE) produces $Co(CO)_3(L)Cl$. $L=(PMePh_2)$ and reaction conditions (i) to (iii) were performed in benzene.

Overall, Ford et al[56] reported the photochemical loss of CO and homolytic cleavage of the cobalt-cobalt bond, upon irradiation of a dicobalt hexacarbonyl complex, corresponding to the results reported by Long et al.[55] Ford et al[56] also demonstrated the effect of the reaction conditions on the photochemistry of these complexes, such as, the presence of CO, excess ligand and chlorinated solvents.

1.3.3 Electrochemistry

- **Alkynyl Dicobalt Hexacarbonyl Complexes**

According to the literature, oxidation of alkynyl dicobalt hexacarbonyl complexes $(RC_2R'Co_2(CO)_6)$ generally results in an irreversible cathodic wave at room temperature, to form the radical cation $[RC_2R'Co_2(CO)_6]^{\bullet+}$.[57,58] Upon reductive processes, a one-electron reduction to the radical anion $[RC_2R'Co_2(CO)_6]^{\bullet-}$ is expected for strong π-acceptor CO ligands, followed by disintegration of the electrogenerated radical ion as a result of metal-metal bond cleavage.[57,59,60] Many disintegration substances are formed, however, severe fouling of the electrode occurs during the decomposition process making it difficult to fully investigate the decomposed products.[57,59,61] The only positively identified substances are as follows: $Co(CO)_4^-$, $RC_2R'Co(CO)_3$, free alkyne[59] and metallic Co. Subsequent anodic runs, after the primary 1-electron (1e) reduction process, can give rise to oxidation peaks due to the presence of some of these disintegration products. For example, $Co_2(CO)_4^-$ has been reported to appear at $E_{pc} = +0.12$ V[57,62] and $+0.25$ V[59] and $E_{1/2} = -0.08V$[61]. $RC_2R'Co(CO)_3$ has been recorded at -0.56 V or -0.83 V.[61]

Electronic Coupling

In a case where two (or more) cobalt carbonyl complexes are substituted onto the same system and separated by a bridging unit, electrochemical studies can be used to investigate the electronic coupling between the two metal centres.[58,63] The presence of one reduction/oxidation peak in the cyclic voltammogram of such a system indicates that no electronic coupling exists between the two metal termini. However, when two separate reduction/oxidation peaks are observed, communication between the two metal complexes, separated by a bridging unit, exists. The higher the degree of separation between the two peaks, the greater the interaction between the redox centres.[58] It has also been found that as the degree of electronic interactions increase, the redox process becomes energetically more favourable.[63]

The electrochemical properties of cobalt carbonyl complexes can be tuned by incorporating ligand substituents onto the metal complex, phosphine ligands being the most common, and considering the nature of the organic compounds attached to the alkynyl moiety. Also, the conditions of the experimental setup can also have a significant effect on the results obtained.

- **Phosphine Ligand Substituted $Co_2(CO)_4$ Complexes**

The introduction of an electron-donating phospine ligand onto the metal complex stabilises the complex by increasing the electron density on the Co-Co bond and hence increases the lifetime of the radical cations and anions. In comparison to the related $Co_2(CO)_6$ compound, the electron-rich core allows for easier oxidation at lower potentials, and increases the reversibility of the oxidative process. In contrast, higher negative potentials are required, in the range of 0.5 to 0.6V, for reduction to occur.[57,59,64]

The basicity of the phosphine ligand employed effects the potential values for reduction and oxidation.[57,63,64] A number of commonly employed phosphine ligands are listed in order of decreasing basicity value: dmpm > dppa > dppm.[62] The higher the electron donating ability (i.e. basicity) of the phosphine ligand, the easier the oxidation process (more positive $E_{1/2}(ox)$) and the harder the reduction process (more negative $E_{1/2}(red)$).

The phosphine ligand employed can also affect the stability of the oxidised/reduced species of these compounds. Such an effect was reported by Macazaga et al.[62] They synthesised two cobalt tetracarbonyl complexes with different phosphine ligand substituents, dppm and the more basic dmpm. The electrochemical results showed reversible waves in the case of the dppm substituted complex, but only quasi-reversible waves for the $Co_2(CO)_4$dmpm complex, at room temperature, indicating that the dppm substituent was better for stabilising the radical cation/anion. A similar result was also described by Marcos et al.[57] They reported the stabilisation effect, and hence complete redox reversibility, of incorporating a dppm ligand into a cobalt carbonyl structure, in comparison to the slightly more basic $[PPh_2Me]_2$ substituted derivative.

In the case of disubstituted cobalt carbonyl systems, phosphine ligand substituents have been found to affect the electronic coupling between the two metal centres. As mentioned previously, the greater the separation between the two reduction/oxidation peaks for such a complex, the greater the interaction between the two metal centres. Incorporating phosphine ligands can hinder or improve this interaction, depending on the substituent employed. Macazaga et al[62] reported that the more basic and less sterically demanding dmpm substituents in complex **2** (illustrated in figure 1.15), in comparison to the dppm substituents in complex **1**, decreased the electronic coupling interactions as they hindered efficient mixing between the filled metal fragments and polyne-based orbitals.
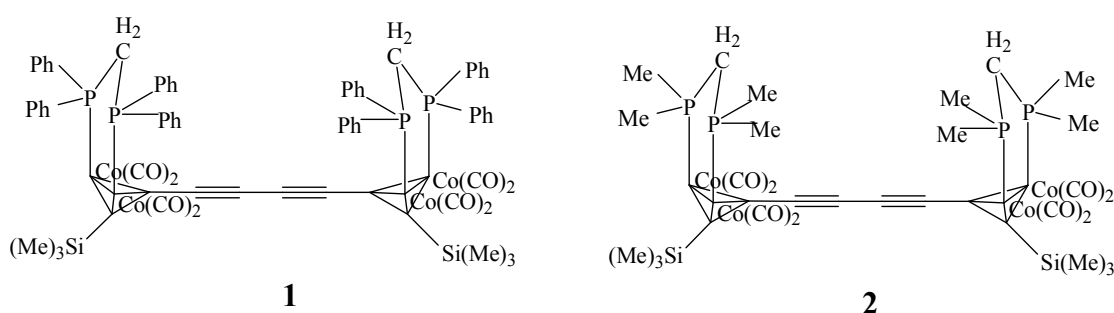
Figure 1.15: Macazaga et al[62] compared the electrochemistry of two disubstituted cobalt tetracarbonyl complexes containing different phosphine ligands: **1** bis(diphenylphosphino)methane [dppm]; and **2** bis(dimethylphosphino)methane [dmpm]. These complexes are illustrated here.

- **Alkynyl Substituents**

The redox properties of alkynyl cobalt carbonyl complexes such as $[RC\equiv CRCo_2(CO)_6]$ can be effected by the substituents directly attached (R), or in close proximity, to the alkynyl moiety. The steric bulk of the substituents (R), increase the lifetimes of the radical anions and therefore reversibility of the redox wave is more likely.[59,61] For example, if the capping-group of the alkynyl unit is the higher electron-donating subtituent $-SiMe_3$, compared to $-H$, the oxidation process is easier, whilst the reduction process is more difficult.[64] Also the chemical stability of the radical cations/anions formed is enhanced, and therefore the bulkier substituent $-SiMe_3$ increases the reversibility of the redox processes.[63]

- **Experimental Conditions**

Besides modifying the molecular structure of the cobalt carbonyl complexes, the experimental conditions employed can also have a significant effect on the electrochemical processes of such complexes:

Solvent

The solvent employed can influence the stability of the radical cations/anions, hence affecting the redox properties of the cobalt complexes. Macazaga and Medina et al[62,63] described slow decomposition reactions taking place when electrochemical experiments, with $Co_2(CO)_4L$ (where L = phosphine ligand) containing compounds, were carried out in dichloromethane. However, when dichloromethane was replaced by tetrahydrofuran, chemical reversibility in the reduction process was observed at room temperature.

Temperature

It has been demonstrated that electrochemical experiments run at lower temperature (-15ºC to -78ºC) can reduce the rate of, and also prevent, decomposition taking place, hence resulting in improved reversibility of the oxidation and reduction processes.[58,59,61,63]

Scan rate

As the scan rate increases, the time for decomposition reactions to take place decreases, resulting in more reversible oxidation and reduction processes.[61,62]

CO Atmosphere

Performing electrochemical experiments of a cobalt carbonyl complex $[(RC_2R')Co(CO)_6]$ under an atmosphere of CO can have a significant effect on the results obtained, as reported by Osella et al.[59] They reported that the radical $[(RC_2R')Co(CO)_3]^{\bullet}$ was easily produced in the presence of CO gas, which was readily reduced to $[(RC_2R')Co(CO)_3]^-$, and no longer participated in the redox cycle. Also, IR spectroelectrochemical experiments showed that the generation of $Co(CO)_4^-$ was increased, upon reduction, under a CO atmosphere. Therefore, in the presence of CO gas, the reversibility of the redox cycle decreased, and decomposition of the parent

complex increased, in comparison to experiments performed under an atmosphere of argon. Similar results were observed by Arewgoda et al,[61] who also reported the formation of $Co(CO)_4^-$ and $R_2C_2Co(CO)_3^-$.[61]

Overall, the literature report highlights how cobalt carbonyl moieties are highly photo- and electro-chemically active. Thus, we anticipated that incorporating such metal groups onto dithienylethene units may lead to some very interesting effects on the ability of the switches to undergo ring-closing/opening processes via photochemical and electrochemical means. The results obtained are described in the following chapters.

1.4 Bibliography

(1) Tian, H.; Yang, S. J. Recent Progresses on Diarylethene Based Photochromic Switches. *Chem. Soc. Rev.* **2004**, *33*, 85-97.

(2) Matsuda, K.; Irie, M. Diarylethene as a Photoswitching Unit. *J. Photochem. Photobiol. C.* **2004**, *5*, 169-182.

(3) Katsonis, N.; Lubomska, M.; Pollard, M. M.; Feringa, B. L.; Rudolf, P. Synthetic Light-Activated Molecular Switches and Motors on Surfaces. *Prog. Surf. Sci.* **2007**, *82*, 407-434.

(4) Zheng, C.; Pu, S.; Xu, J.; Luo, M.; Huang, D.; Shen, L. Synthesis and the Effect of Alkyl Chain Length on Optoelectronic Properties of Diarylethene Derivatives. *Tetrahedron* **2007**, *63*, 5437-5449.

(5) Xie, N.; Zeng, D. X.; Chen, Y. Electrochemical Switch Based on the Photoisomerization of a Diarylethene Derivative. *J. Electroanal. Chem.* **2007**, *609*, 27-30.

(6) Lucas, L. N.; de Jong, J. J. D.; van Esch, J. H.; Kellogg, R. M.; Feringa, B. L. Syntheses of Dithienylcyclopentene Optical Molecular Switches. *Eur. J. Org. Chem.* **2003**, 155-166.

(7) Lucas, L. N.; van Esch, J.; Kellogg, R. M.; Feringa, B. L. A New Class of Photochromic 1,2-Diarylethenes; Synthesis and Switching Properties of Bis(3-Thienyl)Cyclopentenes. *Chem. Commun.* **1998**, 2313-2314.

(8) Nakamura, S.; Yokojima, S.; Uchida, K.; Tsujioka, T.; Goldberg, A.; Murakami, A.; Shinoda, K.; Mikami, M.; Kobayashi, T.; Kobatake, S.; Matsuda, K.; Irie, M. Theoretical Investigation on Photochromic Diarylethene: A Short Review. *J. Photochem. Photobiol. A.* **2008**, *200*, 10-18.

(9) Yang, T.; Pu, S.; Fan, C.; Liu, G. Synthesis, Crystal Structure and Optoelectronic Properties of a New Unsymmetrical Photochromic Diarylethene. *Spectrochim. Acta A.* **2008**, *70*, 1065-1072.

(10) Kobatake, S.; Irie, M. Synthesis and Photochromic Reactivity of a Diarylethene Dimer Linked by a Phenyl Group. *Tetrahedron* **2003**, *59*, 8359-8364.

(11) Irie, M.; Sakemura, K.; Okinaka, M.; Uchida, K. Photochromism of Dithienylethenes with Electron-Donating Substituents. *J. Org. Chem.* **1995**, *60*, 8305-8309.

(12) Eapen, K. C.; Tamborski, C.; Psarras, T. Fluoro-Ketones. 3. Synthesis of Aryl Perfluoroalkylether Ketones by the Friedel-Crafts Acylation. *J. Fluorine Chem.* **1979**, *14*, 243-252.

(13) McBee, E.; Wiseman, P.; Bachman, G. Perfluoro Dibasic Acids and Derivatives. *Ind. Eng. Chem.* **1947**, *39*, 417.

(14) Arnold D.R., Hadjiantoniou. C. P. The Photochemical Reactivity of some Benzoylthiophene. 4. The Effect of an Adjacent Methyl Group on the Excited State Reactivity of 3-Benzoylthiophene. *Can. J. Chem.* **1978**, *56*, 1970.

(15) Hara, R.; Sato, K.; Sun, W. H.; Takahashi, T. Catalytic Dechlorination of Aromatic Chlorides using Grignard Reagents in the Presence of $(C_5H_5)_2TiCl_2$. *Chem. Commun.* **1999**, 845-846.

(16) Guirado, G.; Coudret, C.; Launay, J. P. Electrochemical Remote Control for Dithienylethene-Ferrocene Switches. *J. Phys. Chem. C.* **2007**, *111*, 2770-2776.

(17) Peters, A.; Branda, N. R. Electrochemically Induced Ring-Closing of Photochromic 1,2-Dithienylcyclopentenes. *Chem. Commun.* **2003**, 954-955.

(18) Tsivgoulis, G. M.; Lehn, J. M. Photoswitched and Functionalized Oligothiophenes: Synthesis and Photochemical and Electrochemical Properties. *Chem. Eur. J.* **1996**, *2*, 1399-1406.

(19) Lucas, L. N. Dithienylcyclopentene Optical Switches Towards Photoresponsive Supramolecular Materials. Ph.D. Thesis, Rijksuniversiteit Groningen, **2001**.

(20) Yokoyama, Y.; Kose, M. Reversible Control of Properties of Materials by Thermally Irreversible Photochromism. *J. Photochem. Photobiol. A.* **2004**, *166*, 9-18.

(21) Takeshita, M.; Nagai, M.; Yamato, T. A Photochromic Thiophenophan-1-ene. *Chem. Commun.* **2003**, 1496-1497.

(22) Yam, V. W. W.; Ko, C. C.; Zhu, N. Y. Photochromic and Luminescence Switching Properties of a Versatile Diarylethene-Containing 1,10-Phenanthroline Ligand and its Rhenium(I) Complex. *J. Am. Chem. Soc.* **2004**, *126*, 12734-12735.

(23) de Jong, J. J. D.; Lucas, L. N.; Hania, R.; Pugzlys, A.; Kellogg, R. M.; Feringa, B. L.; Duppen, K.; van Esch, J. H. Photochromic Properties of Perhydro- and Perfluorodithienylcyclopentene Molecular Switches. *Eur. J. Org. Chem.* **2003**, 1887-1893.

(24) Nakamura, S.; Irie, M. Thermally Irreversible Photochromic Systems. A Theoretical Study. *J. Org. Chem.* **1988**, *53*, 6136-6138.

(25) Irie, M. Photochromic Dithienylethenes for Molecular Photonics. *Phosphorus, Sulfur Silicon Relat. Elem.* **1997**, *120*, 95-106.

(26) Guirado, G.; Coudret, C.; Hliwa, M.; Launay, J. P. Understanding Electrochromic Processes Initiated by Dithienylcyclopentene Cation-Radicals. *J. Phys. Chem. B.* **2005**, *109*, 17445-17459.

(27) Moriyama, Y.; Matsuda, K.; Tanifuji, N.; Irie, S.; Irie, M. Electrochemical Cyclization/Cycloreversion Reactions of Diarylethenes. *Org. Lett.* **2005**, *7*, 3315-3318.

(28) Areephong, J.; Browne, W. R.; Katsonis, N.; Feringa, B. L. Photo- and Electro-chromism of Diarylethene Modified ITO Electrodes - Towards Molecular Based Read-Write-Erase Information Storage. *Chem. Commun.* **2006**, 3930-3932.

(29) Lee, J.; Kwon, T.; Kim, E. Electropolymerization of an EDOT-Modified Diarylethene. *Tetrahedron Lett.* **2007**, *48*, 249-254.

(30) Browne, W. R.; de Jong, J. J. D.; Kudernac, T.; Walko, M.; Lucas, L. N.; Uchida, K.; van Esch, J. H.; Feringa, B. L. Oxidative Electrochemical Switching in Dithienylcyclopentenes, Part 1: Effect of Electronic Perturbation on the Efficiency and Direction of Molecular Switching. *Chem. Eur. J.* **2005**, *11*, 6414-6429.

(31) Browne, W. R.; de Jong, J. J. D.; Kudernac, T.; Walko, M.; Lucas, L. N.; Uchida, K.; van Esch, J. H.; Feringa, B. L. Oxidative Electrochemical Switching in Dithienylcyclopentenes, Part 2: Effect of Substitution and Asymmetry on the Efficiency and Direction of Molecular Switching and Redox Stability. *Chem. Eur. J.* **2005**, *11*, 6430-6441.

(32) Peters, A.; Branda, N. R. Electrochromism in Photochromic Dithienylcyclopentenes. *J. Am. Chem. Soc.* **2003**, *125*, 3404-3405.

(33) Pu, S.; Liu, G.; Li, G.; Wang, R.; Yang, T. Synthesis, Crystal Structure and its Optical and Electrochemical Properties of a New Unsymmetrical Diarylethene. *J. Mol. Struct.* **2007**, *833*, 23-29.

(34) Xiao, S.; Yi, T.; Zhou, Y.; Zhao, Q.; Li, F.; Huang, C. Multi-State Molecular Switches Based on Dithienylperfluorocyclopentene and Imidazo [4,5-f] [1,10] Phenanthroline. *Tetrahedron* **2006**, *62*, 10072-10078.

(35) Geoffroy Gregory L., Wrighton Mark S. *Organometallic Photochemistry;* **1979**.

(36) Gray, H. B. *Chemical Bonds: An Introduction to Atomic and Molecular Structure;* **1994**.

(37) Otsuki, J.; Akasaka, T.; Araki, K. Molecular Switches for Electron and Energy Transfer Processes Based on Metal Complexes. *Coord. Chem. Rev.* **2008**, *252*, 32-56.

(38) Jukes, R. T. F.; Adamo, V.; Hartl, F.; Belser, P.; De Cola, L. Photochromic Dithienylethene Derivatives Containing Ru(II) Or Os(II) Metal Units. Sensitized Photocyclization from a Triplet State. *Inorg. Chem.* **2004**, *43*, 2779-2792.

(39) Fraysse, S.; Coudret, C.; Launay, J. P. Synthesis and Properties of Dinuclear Complexes with a Photochromic Bridge: An Intervalence Electron Transfer Switching "On" and "Off". *Eur. J. Inorg. Chem.* **2000**, 1581-1590.

(40) Tanaka, Y.; Inagaki, A.; Akita, M. A Photoswitchable Molecular Wire with the Dithienylethene (DTE) Linker, (dppe)(η^5-C$_5$Me$_5$)Fe-C≡C-DTE-C≡C-Fe(η^5-C$_5$Me$_5$)(dppe). *Chem. Commun.* **2007**, 1169-1171.

(41) Zhong, Y.; Vila, N.; Henderson, J. C.; Abruna, H. D. Transition-Metal Tris-Bipyridines Containing Three Dithienylcyclopentenes: Synthesis, Photochromic, and Electrochromic Properties. *Inorg. Chem.* **2009**, *48*, 7080-7085.

(42) Zhong, Y.; Vila, N.; Henderson, J. C.; Flores-Torres, S.; Abruna, H. D. Dinuclear Transition-Metal Terpyridine Complexes with a Dithienylcyclopentene Bridge Directed Toward Molecular Electronic Applications. *Inorg. Chem.* **2007**, *46*, 10470-10472.

(43) Jukes, R. T. F.; Adamo, V.; Hartl, F.; Belser, P.; De Cola, L. Electronic Energy Transfer in a Dinuclear Ru/Os Complex Containing a Photoresponsive Dithienylethene Derivative as Bridging Ligand. *Coord. Chem. Rev.* **2005**, *249*, 1327-1335.

(44) Lin, Y.; Yuan, J.; Hu, M.; Cheng, J.; Yin, J.; Jin, S.; Liu, S. H. Syntheses and Properties of Binuclear Ruthenium Vinyl Complexes with Dithienylethene Units as Multifunction Switches. *Organometallics* **2009**, *28*, 6402-6409.

(45) Hasegawa, Y.; Nakagawa, T.; Kawai, T. Recent Progress of Luminescent Metal Complexes with Photochromic Units. *Coord. Chem. Rev. , In Press, Corrected Proof.*

(46) Motoyama, K.; Koike, T.; Akita, M. Remarkable Switching Behavior of Bimodally Stimuli-Responsive Photochromic Dithienylethenes with Redox-Active Organometallic Attachments. *Chem. Commun.* **2008**, 5812-5814.

(47) Belser, P.; De Cola, L.; Hartl, F.; Adamo, V.; Bozic, B.; Chriqui, Y.; Iyer, V. M.; Jukes, R. T. F.; Kuhni, J.; Querol, M.; Roma, S.; Salluce, N. Photochromic Switches Incorporated in Bridging Ligands: A New Tool to Modulate Energy-Transfer Processes. *Adv. Funct. Mater.* **2006**, *16*, 195-208.

(48) Fernandez-Acebes, A.; Lehn, J. M. Optical Switching and Fluorescence Modulation Properties of Photochromic Metal Complexes Derived from Dithienylethene Ligands. *Chem. Eur. J.* **1999**, *5*, 3285-3292.

(49) Wrighton, M. Photochemistry of Metal-Carbonyls. *Chem. Rev.* **1974**, *74*, 401-430.

(50) Atkin, A. J.; Williams, S.; Sawle, P.; Motterlini, R.; Lynam, J. M.; Fairlamb, I. J. S. μ_2-Alkyne Dicobalt(0)hexacarbonyl Complexes as Carbon Monoxide-Releasing Molecules (CO-RMs): Probing the Release Mechanism. *Dalton Trans.* **2009**, 3653-3656.

(51) Kretschmer, R.; Gessner, G.; Gorls, H.; Heinemann, S. H.; Westerhausen, M. Dicarbonyl-bis(cysteamine)iron(II) A Light Induced Carbon Monoxide Releasing Molecule Based on Iron (CORM-S1). *J. Inorg. Biochem.* **2011**, *105*, 6-9.

(52) Zhang, W.; Atkin, A. J.; Thatcher, R. J.; Whitwood, A. C.; Fairlamb, I. J. S.; Lynam, J. M. Diversity and Design of Metal-Based Carbon Monoxide-Releasing Molecules (CO-RMs) in Aqueous Systems: Revealing the Essential Trends. *Dalton Trans.* **2009**, 4351-4358.

(53) Alberto, R.; Motterlini, R. Chemistry and Biological Activities of CO-Releasing Molecules (CORMs) and Transition Metal Complexes. *Dalton Trans.* **2007**, 1651-1660.

(54) Pettit, L.; Barnes, D. P *Complexes of Transition Metals: The Stability and Structures of Olefin and Acetylene Complexes of Transition Metals.* **1972**.

(55) M. Draper, S.; Long, C.; M. Myers, B. The Photochemistry of (μ_2-RC$_2$H)Co$_2$(CO)$_6$ Species (R=H or C$_6$H$_5$), Important Intermediates in the Pauson–Khand Reaction. *J. Organomet. Chem.* **1999**, *588*, 195-199.

(56) Marhenke, J.; Massick, S. M.; Ford, P. C. Time-Resolved Infrared Study of Reactive Species Produced by Flash Photolysis of the Hydroformylation Catalyst Precursor Co$_2$(CO)$_6$(PMePh$_2$)$_2$. *Inorg. Chim. Acta* **2007**, *360*, 825-836.

(57) Marcos, M. L.; Macazaga, M. J.; Medina, R. M.; Moreno, C.; Castro, J. A.; Gomez, J. L.; Delgado, S.; González-Velasco, J. Alkynyl Cobalt Complexes. An Electrochemical Study. *Inorg. Chim. Acta* **2001**, *312*, 249-255.

(58) Arnanz, A.; Marcos, M.; Moreno, C.; Farrar, D. H.; Lough, A. J.; Yu, J. O.; Delgado, S.; González-Velasco, J. Synthesis, Structures and Comparative Electrochemical Study of 2,5-Bis(trimethylsilylethynyl)thiophene Coordinated Cobalt Carbonyl Units. *J. Organomet. Chem.* **2004**, *689*, 3218-3231.

(59) Osella, D.; Fiedler, J. Reinvestigation of the Electrochemical-Behavior of the Co$_2$(Co)$_6$(Ethynylestradiol) Complex - Evidence of Efficient Recombination of the Electrogenerated Fragments. *Organometallics* **1992**, *11*, 3875-3878.

(60) Brooksby, P. A.; Duffy, N. W.; McQuillan, A. J.; Robinson, B. H.; Simpson, J. Infrared Spectroelectrochemistry of [Co$_3$(CPh)(CO)$_9$] in Methanol at a Platinum Electrode. *J. Chem. Soc., Dalton Trans.* **1998**, 2855-2860.

(61) Arewgoda, M.; Rieger, P. H.; Robinson, B. H.; Simpson, J.; Visco, S. J. Paramagnetic Organometallic Molecules .12. Electrochemical Studies of Reactions with Lewis-Bases Following Metal Metal Bond-Cleavage in R$_2$C$_2$Co$_2$(CO)$_6$ Radical-Anions. *J. Am. Chem. Soc.* **1982**, *104*, 5633-5640.

(62) Macazaga, M. J.; Marcos, M. L.; Moreno, C.; Benito-Lopez, F.; Gomez-González, J.; González-Velasco, J.; Medina, R. M. Syntheses, Structures and Comparative Electrochemical Study of π-Acetylene Complexes of Cobalt. *J. Organomet. Chem.* **2006**, *691*, 138-149.

(63) Medina, R. M.; Moreno, C.; Marcos, M. L.; Castro, J. A.; Benito, F.; Arnanz, A.; Delgado, S.; Gonzalez-Velasco, J.; Macazaga, M. J. Syntheses, Structures and Electrochemical Study of π-Acetylene Complexes of Cobalt. *Inorg. Chim. Acta* **2004**, *357*, 2069-2080.

(64) Arnanz, A.; Marcos, M.; Delgado, S.; González-Velasco, J.; Moreno, C. The Effect of Thiophene Ring Substitution Position on the Properties and Electrochemical Behaviour of Alkyne–dicobaltcarbonylthiophene Complexes. *J. Organomet. Chem.* **2008**, *693*, 3457-3470.

CHAPTER 2

Synthesis

*Chapter 2 describes the experimental procedures employed to synthesise the following perhydro- and perfluoro-dithienylcyclopentene switches: 1,2-Bis(5'-(3''-ethynylthiophene)-2'-methylthien-3'-yl)cyclopentene {**1H**}; 1,2-Bis(5'-(3''-ethynylthiophene)-2'-methylthien-3'-yl)perfluorocyclopentene {**1F**}; 1,2-Bis(5'-(4''-phenyl-3'''-ethynylthiophene)-2'-methylthien-3'-yl)-cyclopentene {**2H**}; 1,2-Bis(5'-(4''-phenyl-3'''-ethynylthiophene)-2'-methylthien-3'-yl)perfluorocyclopentene {**2F**}; 1,2-Bis(5'-ethynylferrocene -2'-methylthien-3'-yl)cyclopentene {**7H**}; 1,2-Bis(5'-ethynylferrocene-2'-methylthien-3'-yl)perfluorocyclopentene; {**7F**}, 1,2-Bis(5'-(4''-phenyl-ethynylferrocene)-2'-methylthien-3'-yl)cyclopentene {**8H**}; 1,2-Bis(5'-(4''-phenyl-ethynylferrocene)-2'-methylthien-3'-yl)perfluorocyclopentene {**8F**}. These switches were then coordinated with $Co_2(CO)_6$, and $Co_2(CO)_4dppm$. The products were characterised by ^1H, ^{13}C, ^{19}F and ^{31}P nmr spectroscopy and elemental analysis. The cobalt carbonyl complexes were further characterised by infra-red spectroscopy.*

2.1 Introduction

A number of synthetic methods used to synthesise dithienyl perhydro- and perfluoro-cyclopentene switches have been described in Chapter 1. The experimental procedures, detailed in section 2.3, to synthesise 1,2-Bis(5'-chloro-2'-methylthien-3'-yl)cyclopentene switches (with perhydro and perfluoro cyclopentene rings) were carried out following the same synthetic methods previously reported by Lucas et al.[1,2] These compounds were then further substituted with ethynylthiophene and ethynylferrocene moieties, using Sonogashira and Suzuki cross-coupling reactions, to produce compounds **1**, **2**, **7** and **8** (scheme 2.1). In light of this, a brief overview of Sonogashira and Suzuki reactions is given here.
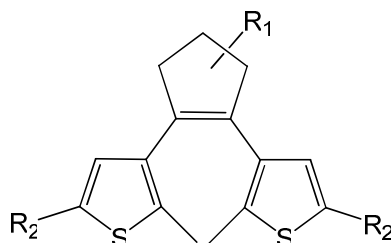
1H/F R$_1$=H/F R$_2$=ethyn th ophene
2H/F R$_1$=H/F R$_2$=4-pheny -3 -ethyny th ophene
7H/F R$_1$=H/F R$_2$=ethyn ferrocene
8H/F R$_1$=H/F R$_2$=4-pheny -ethyny ferrocene

Scheme 2.1: Represents the dithienylcyclopentene switches synthesised using Suzuki and Sonogashira cross-coupling reactions.

- **Suzuki Cross-Coupling Reactions**

The formation of carbon-carbon bonds can be achieved through cross-coupling reactions of organohalides and transition metal organometallic compounds.[3] Sonogashira and Suzuki reactions are among a number of commonly used cross-coupling reactions.[4] The majority of these coupling reactions proceed via three fundamental steps: oxidative addition, transmetalation and reductive elimination.[3,5,6]

Suzuki cross-coupling reactions (also known as Suzuki-Miyaura reactions) were first reported in 1979.[7] These types of reactions involve the formation of C-C bonds

through the palladium-catalysed cross-coupling of organic halides and triflates with organoboron derivatives, in the presence of a base.[4] Suzuki reactions have a number of advantages over other cross-coupling reactions[4,6] such as Kumada or Stille coupling, for example, the organoborane reagents are not toxic so the reaction is more environmentally friendly and the organoborane reagents are generally easy to prepare. The general mechanism of the Suzuki reaction[6,7] is illustrated in scheme 2.2, and is described as follows:

1) The palladium catalyst Pd^0 **A**, generated in-situ from the initial palladium catalyst added to the reaction, reacts with the organohalide (R-X), via oxidative addition, to form the organo-Pd^{II} species **B**.

2) The Pd^{II} complex **B** reacts with base to produce complex **C**.

3) The organoboron compound **D** does not readily undergo transmetalation with the organo-Pd^{II} complex **C** due to the low nucleophilicity of the organic group on the boron atom.[6] However, when the boron is activated with base, forming the boron-ate complex **E**, transmetalation is facilitated to produce the organo-Pd^{II} species **F**.

4) Reductive elimination occurs from the cis-isomer of complex **F**, forming the final compound **G**, and the Pd^0 catalyst **A** is regenerated.
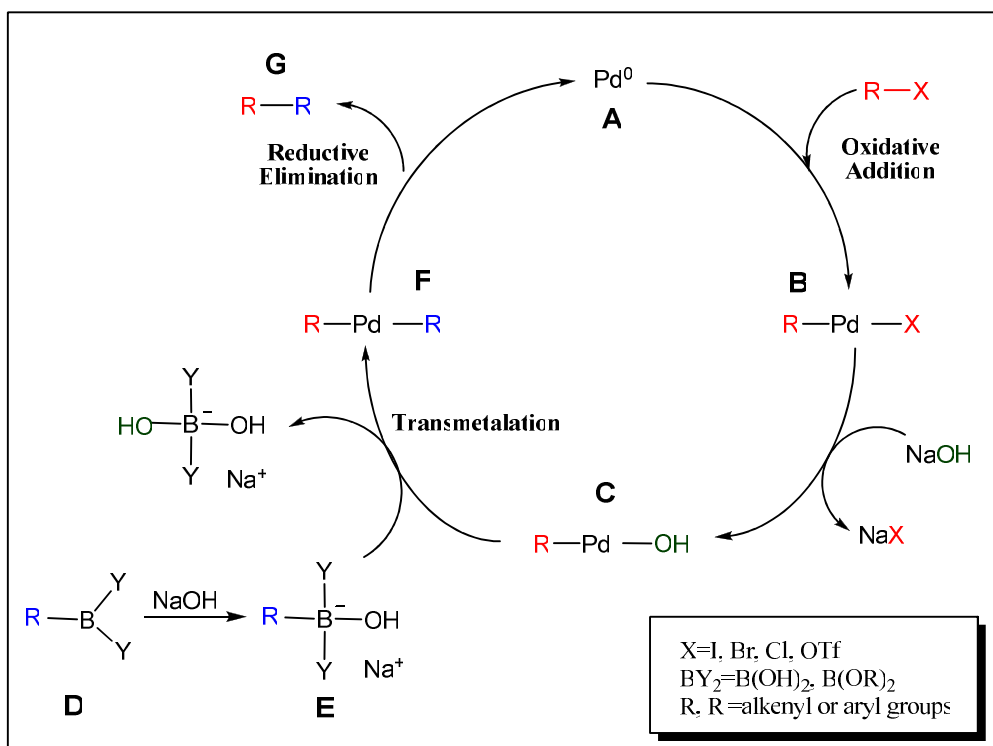
Scheme 2.2: Illustrates the general mechanism for the Suzuki cross-coupling reaction

74

The synthetic procedures detailed in section 2.3 describe the use of Suzuki cross-coupling reactions in order to substitute dithienylcyclopentene switches with bromobenezene substituents. The reaction conditions employed were the same as described previously by Feringa et al.[8]

- **Sonogashira Cross-Coupling Reactions**

Sonogashira-Hagihara coupling was discovered in 1975[9] (more commonly known as Sonogashira coupling), and involves the coupling of terminal alkynes with aryl and vinyl halides, in the presence of copper iodide (as a co-catalyst) and an amino base.[10-13] This reaction is believed to take place through two independent catalytic cycles,[10,11,14] as illustrated in scheme 2.3:
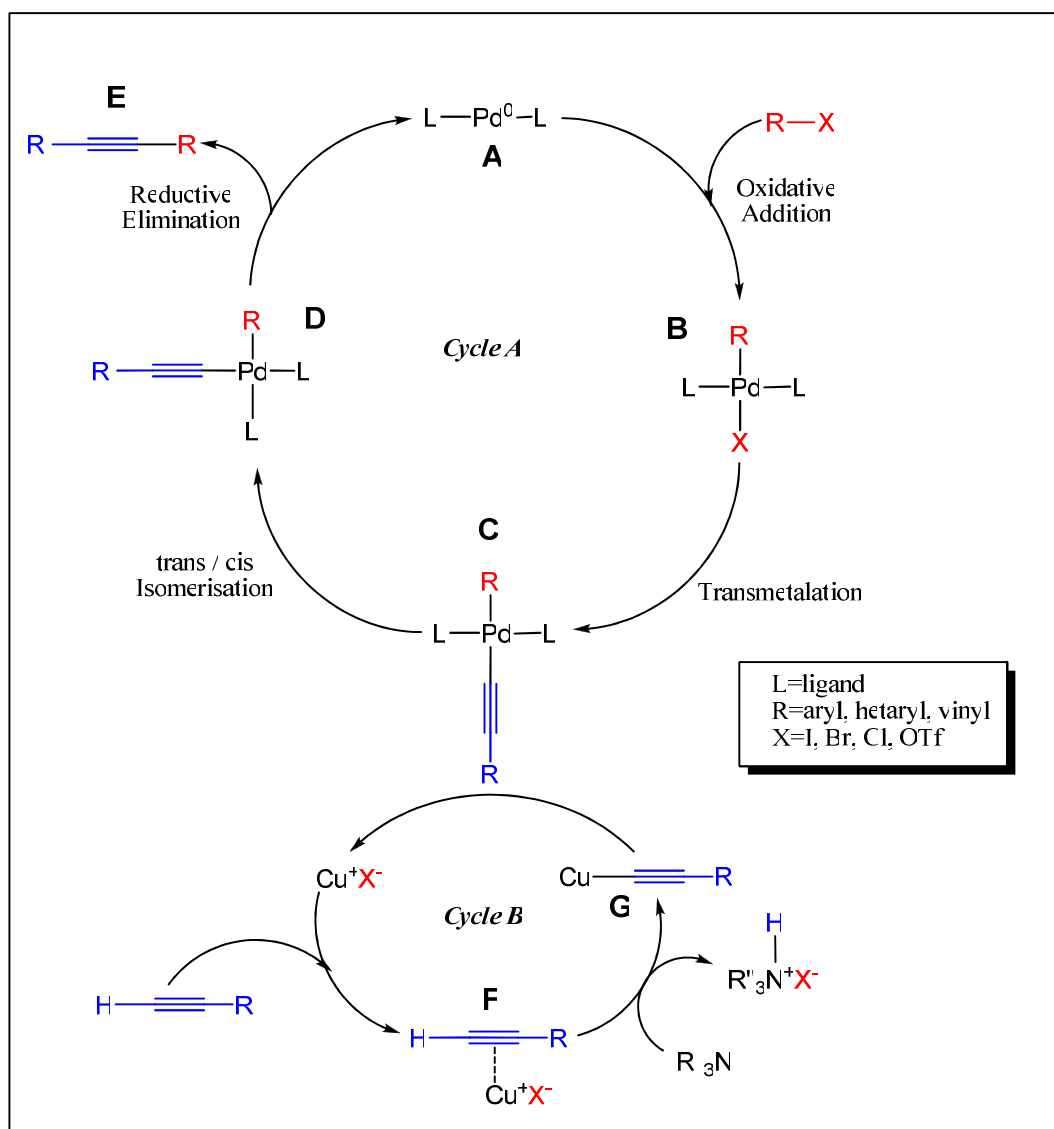
Scheme 2.3: Illustrates the general mechanism for the Sonogashira cross-coupling reaction.

Cycle A: The palladium cycle

1) The organohalide (R-X) undergoes oxidative addition to the palladium catalyst Pd^0L_2 **A**, generated from the initial palladium complex in-situ, to produce the Pd^{II} complex **B**.

2) The Pd^{II} complex **B** reacts with the copper acetylide **G** (produced in the copper cycle) through a rate-determining transmetalation step, generating complex **C** and expelling the copper halide CuX.

3) Trans/cis isomerisation takes place, converting the trans-oriented R and X to cis-orientation, giving complex **D**.

4) Reductive elimination of complex **D** results in the formation of the final coupled product **E**, along with regeneration of the Pd^0 catalyst.

Cycle B: The copper cycle

1) The base (usually an amine) deprotanates the terminal alkyne, resulting in the formation of a copper acetylide **G**, in the presence of the copper salt. However, it has been suggested that because the usually employed amines are not basic enough to deprotanate the alkyne, a π-alkyne Cu complex **F** could be involved in the cycle, making it easier for the base to abstract the more acidic alkyne proton.[10,14]

2) The copper acetylide **G** goes on to react with the Pd^{II} complex **B**, formed in the palladium cycle, producing complex **C** and the copper halide is regenerated.

The standard reaction procedures utilized for Sonogashira coupling reactions involve $Pd(PPh_3)_4$ as the palladium catalyst, copper iodide as the co-catalyst and triethylamine or diisopropylamine as the base. However, the success of the oxidative addition step is highly dependent on the organohalide involved.[3,10,15] For example, the barriers of oxidative addition of R-X increases in the order of R-I < R-Br < R-Cl. Also, if electron density is reduced on the R-X bond by the presence of electron-withdrawing groups, the rate of oxidative addition is increased, compared to those having electron-donating groups. Therefore, the reaction conditions and the reagents employed,[3,5,6,10] to achieve successful formation of a C-C bond, depend on the organohalide involved. Launay et al[16] reported the synthesis of dithienyl-perhydrocyclopentene switches with ethynyl ferrocene substituted onto both sides of the switch. Standard Sonogashira methods were employed initially [THF; diisopropylamine; CuI; $Pd((PPh_3)_2Cl_2)]$,

however the required product was accompanied by a large amount of di-1,4-ferrocenylbutadiyne, resulting in long and difficult purification processes to finally isolate the pure product with a 32% yield. Attaching ethynylferrocene onto the perfluorinated switch using the same reaction conditions proved even more difficult. In order to alleviate this problem, a different palladium catalyst was used, $Pd_2(dba)_3$, along with a trimethylphosphine ligand and tetrabutylammonium iodide, which drastically improved the yield (92%). Therefore, the latter reaction conditions, as described by Launay et al, were employed here for the purpose of attaching ethynylthiophene and ethynylferrocene substitutents onto the dithienylcyclopentene switches.

2.2 Experimental

2.2.1 Materials

All solvents used for synthesis were purchased from Sigma Aldrich, most of which were "ACS reagent" grade, at least: toluene, acetic acid, nitrosomethane, chloroform, hexane and heptane. For lithiation, Sonagashira and Suzuki reactions, all the solvents were anhydrous grade: n-butyllithium, tert-butyllithium, DMF and triethylamine. THF and diethyl ether were dried by refluxing over benzophenone ketyl and sodium, and distilled off freshly before use. All reactions were performed under nitrogen, N_2, which was supplied by Air Products Ltd, with the exception of the reactions employed to synthesise compounds **(i)**, **(ii)** and **(iv)**. All reagents were purchased from Sigma Aldrich and used without further purification: 2-methylthiophene, n-chlorosuccinimide, glutarylchloride, nitrosomethane, aluminium chloride, Zn-dust, titanium tetrachloride, bromine, iodine, copper iodide, n-tetrabutylammonium iodide, tris(2,4,6-triphenylphenyl)phosphine, tris(dibenzylideneacetone) dipalladium, 1-iodo-4-bromobenzene, 3-ethynylthiophene, ethynylferrocene, dicobalt octacarbonyl, bis(diphenylphosphino)methane, tributyl borate, 1,4-dibromobenzene, tetrakis-(triphenylphosphine)palladium and ethylene glycol. Octaperfluoro-cyclopentene was sourced from Rijksuniversiteit Groningen, Holland. Column chromatography was performed using neutral silica gel.

2.2.2 Equipment

All glassware used for synthesis was dried in an oven at ~150°C overnight. ^{1}H NMR spectra were recorded on a Bruker model AC 400 MHz spectrometer. ^{13}C and ^{31}P NMR spectra were recorded on a Bruker Avance III 600 ultrashield spectrometer (at 150 MHz and 242.9 MHz, respectively). ^{19}F NMR spectra were recorded on a Bruker model AC 400 MHz spectrometer (at 376.5 MHz). All NMR spectra were obtained in deuterated solvents: CDCl$_3$, (CD$_3$)$_2$SO or (CD$_3$)$_2$CO. Each spectrum was calibrated according to the deuterated solvent peak. The splitting patterns are designated as follows: s (singlet); d (doublet); dd (doublet of doublets); t (triplet); quintet; m

(multiplet) and br (broad). In the case of the ^{13}C NMR data, a quaternary carbon is denoted by "Cq". Infra-red spectroscopy was carried out on a Perkin Elmer "Spectrum GX" FT-IR spectrometer. For the IR data, "sh" denotes a shoulder band. Elemental analysis was carried out at Rijksuniversiteit Groningen, Holland.

2.3 Synthesis

Dithienylcyclopentene Switches

2.3.1   Synthesis of Dithienyl-per*hydro*cyclopentene Starting Material[1, 2]
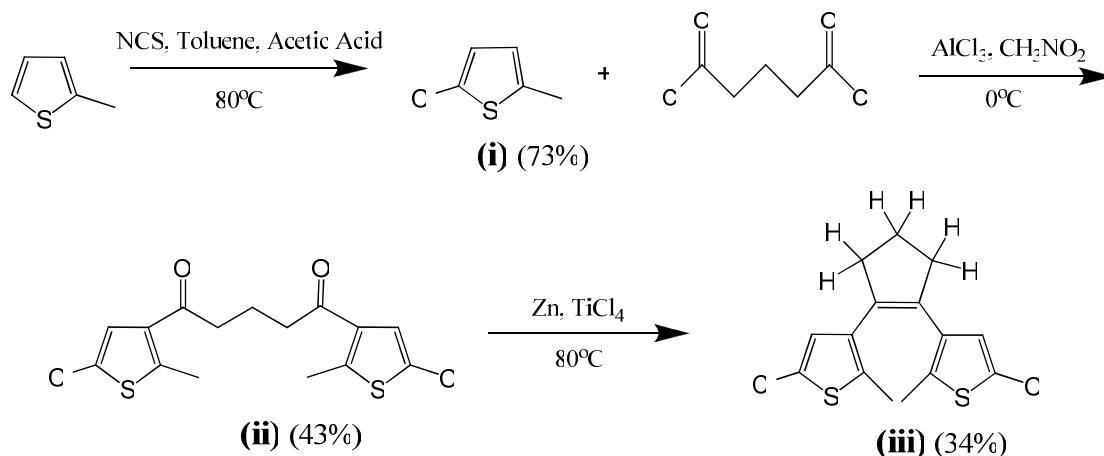
Scheme 2.4: Synthesis of dithienyl-perhydrocyclopentene **(iii)**

- *Synthesis of 5-Chloro-2-methylthiophene (i):*

Toluene (400 mL) and acetic acid (400 mL) were placed into a 2 L round-bottom flask. 2-Methylthiophene (100 mL, 1.03 mol) and N-chlorosuccinimide (152 g, 1.13 mol) were added, and the suspension was stirred at room temperature for 30 minutes, before refluxing for 1 hour. Once the mixture had cooled, a 3 M aq NaOH solution (300 mL) was added to the flask. The organic phase was subsequently washed with a 3 M aq NaOH solution (3 x 300 mL), dried over Na_2SO_4, filtered and the solvent was removed under vacuum to yield a pale yellow liquid. The product was purified by vacuum distillation (approx. 80°C), resulting in a colourless liquid (100 g, 73%).

^{1}H NMR (400 MHz, $CDCl_3$): δ = 2.31 (s, 3H, CH_3), 6.39-6.41 (m, 1H, thienyl-H3), 6.58 (d, J=2.2 Hz, 1H, thienyl-H4) ppm.

- *Synthesis of 1,5Bis(5'-chloro-2'-methylthien-3'-yl)pentadione (ii)*

A solution of 5-Chloro-2-methylthiophene (i) (32.3 mL, 0.3 mol) and glutarylchloride (25 g, 0.15 mmol), in nitromethane (300 mL), was cooled on ice. $AlCl_3$ (48 g, 0.36 mol) was added in portions to the solution, whilst stirring vigorously, and the reaction was stirred at room temperature for 2 hours. Ice-water was slowly added to the reaction mixture. The water layer was extracted with diethyl ether (3 x 150 mL) and then the combined organic phases were washed with water (1 x 100 mL), dried over Na_2SO_4, filtered and evaporated in vacuum to yield a brown tar (46.86 g, 43%). It was not necessary to purify this product for use in the next reaction. ^1H NMR (400 MHz, $CDCl_3$): δ = 1.98-2.12 (m, 2H, CH_2), 2.65 (s, 6 H, CH_3), 2.86 (t, J=6.8 Hz, 4H, CH_2), 7.19 (s, 2H-thienyl-H4) ppm.

- *Synthesis of 1,2-Bis(5'-chloro-2'-methylthien-3'-yl)cyclopentene (iii)*

THF (165 mL) and Zn-dust (8.25 g, 0.126 mol) were placed into an oven-dried three-neck round-bottom flask and stirred under nitrogen. $TiCl_4$ (20.46 mL, 95.04 mmol) was added very cautiously (by a separating funnel, fitted with a tap, connected to a neck of the flask) over a period of 30 to 60 minutes. The solution was refluxed for 45 minutes and a colour change from grey to dark green/blue was observed. The reaction mixture was cooled in an ice-bath before adding 1,5-Bis(5'-chloro-2'-methylthien-3'-yl)pentadione (ii) (23 g, 64 mmol) in portions, and then refluxed for a further 2 hours. 10% K_2CO_3 (150 mL) was added to quench the reaction. It was extracted with diethyl ether (4 x 50 mL), the combined organic layers were washed with H_2O (1 x 75 mL), dried over Na_2SO_4, filtered and the solvent was removed in vacuum. The dark brown/black crude product was purified with column chromatography, using silica and 100% pentane. The pure product was collected as the first fraction and was a light brown/cream coloured solid (7.18 g, 34%). ^1H NMR (400 MHz, $CDCl_3$): δ = 1.88 (s, 6H, CH_3), 2.01 (quintet, J=7.5 Hz, 2H, CH_2), 2.71 (t, J=7.5 Hz, 4H, CH_2), 6.57 (s, 2H, thienyl-H4) ppm. ^{13}C NMR (150 MHz, $CDCl_3$) δ = 14.31 (s, 2C, CH_3), 23.08 (s, 1C, CH_2), 38.47 (s, 2C, CH_2), 125.34 (s, 2C, Cq), 126.83 (s, 2C, CH), 133.44 (s, 2C, Cq), 134.58 (s, 2C, Cq), 134.98 (s, 2C, Cq) ppm.

2.3.2 Synthesis of Dithienyl-per*fluoro*cyclopentene Starting Material[2]
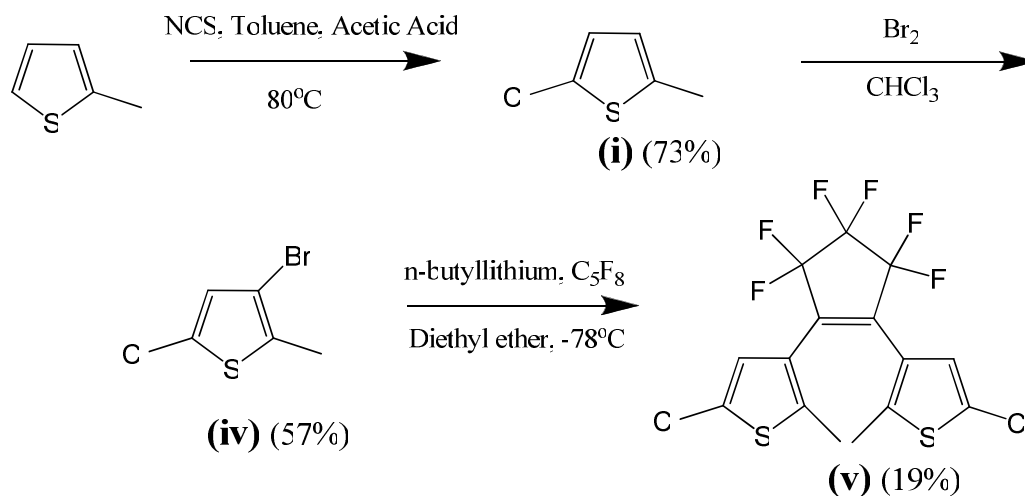
Scheme 2.5: Synthesis of dithienyl-perflurocyclopentene **(v)**

- *Synthesis of 5-chloro-2-methylthiophene (i):*

The reaction procedure used to synthesise 5-chloro-2-methylthiophene was described in section 2.3.1. The same batch of product was used for the synthesis of the perfluoro-cyclopentene switch.

- *Synthesis of 5-chloro-3-bromo-2-methylthiophene (iv)*

5-chloro-2-methylthiophene **(i)** (20 g, 151 mmol) was dissolved in $CHCl_3$ (150 mL) and cooled in an ice bath before a solution of bromine (8 mL, 156 mmol), in $CHCl_3$ (40 mL), was slowly added to the reaction flask. After the reaction mixture was stirred for 2 hours at room temperature, H_2O (300 mL) was added to the flask, and the water layer was subsequently extracted with CH_2Cl_2 (3 x 100 mL). The organic extracts were combined, dried over Na_2SO_4 and filtered. The solvent was evaporated, yielding an orange/brown oil which was purified by vacuum distillation, and a very pale yellow oil was obtained (18.06 g, 57%). ^1H NMR (400 MHz, $CDCl_3$): δ = 2.32 (s, 3H, CH_3), 6.73 (s, 1H, thienyl-H4) ppm.

- *Synthesis of 1,2-Bis(5'-chloro-2'-methylthien-3'-yl)perfluorocyclopentene (v)*

Distilled, dry diethyl ether (400 mL) and 5-chloro-3-bromo-2-methylthiophene (iv) (18.06 g, 85 mmol) were added to an oven-dried 1 L reaction flask, under nitrogen, and the solution was cooled to -78°C. n-Butyllithium (53.13 mL of 1.6 M solution in hexane, 85 mmol) was added to the flask and the solution was stirred at -78°C, under nitrogen, for 30 minutes. Octaperfluorocyclopentene (5.46 mL, 38.6 mmol) was quickly taken from the fridge via a syringe, and slowly added to the reaction flask. The reaction mixture was stirred for a further 4 hours at -78°C, then slowly allowed to warm to room temperature and left to stir overnight. The reaction was quenched with H_2O (250 mL) and extracted with diethyl ether (2 x 100 mL). The organic extracts were combined, dried over Na_2SO_4, filtered and the solvent was removed under vacuum. A dark orange/brown oil was obtained and was purified on a silica gel column, using 100% pentane. The second fraction was collected from the column and was further purified by recrystallisation in methanol and a small amount of CH_2Cl_2, yielding a creamy/yellow solid (7.14 g, 19%). ^1H NMR (400 MHz, $CDCl_3$): δ = 1.89 (s, 6H, CH_3), 6.88 (s, 2H, thienyl-H4) ppm. ^{13}C NMR (150 MHz, $CDCl_3$) δ = 14.29 (s, 2C, CH_3), 124.21 (s, 2C, Cq), 125.65 (s, 2C, CH), 128.18 (s, 2C, Cq), 140.67 (s, 2C, Cq) ppm (C-F resonances not located).

2.3.3 Synthesis of 1,2-Bis(5'-iodo-2'-methylthien-3'-yl)cyclopentene (vi)
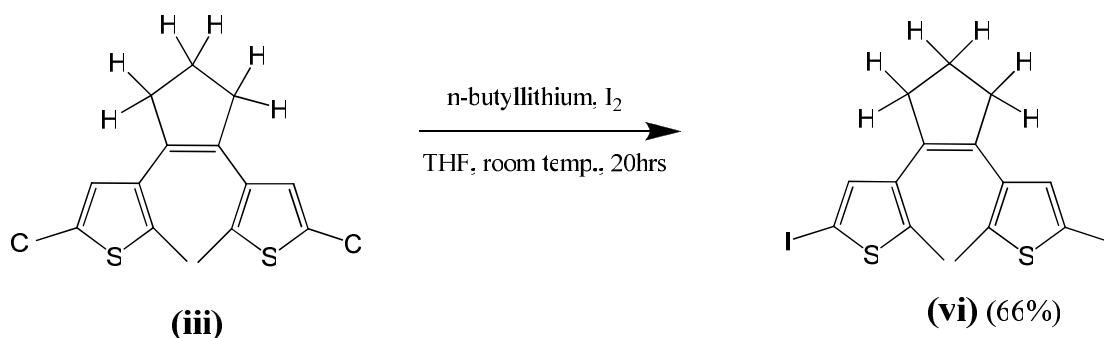
Scheme 2.6: Synthesis of 1,2-Bis(5'-iodo-2'-methylthien-3'-yl)cyclopentene **(vi)**

n-Butyllithium (4.75 mL of 1.6 M solution in hexane, 7.6 mmol) was added slowly to a solution of 1,2-Bis(5'-chloro-2'-methylthien-3'-yl)cyclopentene **(iii)** (1 g, 3.04 mmol) dissolved in dry, distilled THF (60 mL), and was stirred at room temperature under nitrogen. After 1 hour, Iodine (3.858 g, 15.2 mmol) dissolved in 20 mL of dry, distilled THF was added dropwise to the reaction mixture, and it was allowed to stir overnight under an inert atmosphere. The solution was quenched with water (50 mL) and extracted with dichloromethane (3 x 80 mL). The organic layers were combined, washed with a 50% aqueous solution of sodium thiosulphate pentahydrate (100 mL) to remove the excess iodine, washed with water (150 mL), dried over Na_2SO_4, filtered and dried under vacuum. The dark brown crude product was purified with column chromatography, using silica gel and 100% pentane, to yield a light brown solid (1.0283 g, 66%). ^{1}H NMR (400 MHz, $CDCl_3$): δ = 1.89 (s, 6H, CH_3), 2.02 (quintet, J=7.5 Hz, 2H, CH_2), 2.72 (t, J=7.5 Hz, 4H, CH_2), 6.89 (s, 2H, thienyl-H4) ppm.

2.3.4 Synthesis of 1,2-Bis(5'-iodo-2'-methylthien-3'-yl)perfluoro-cyclopentene (vii)
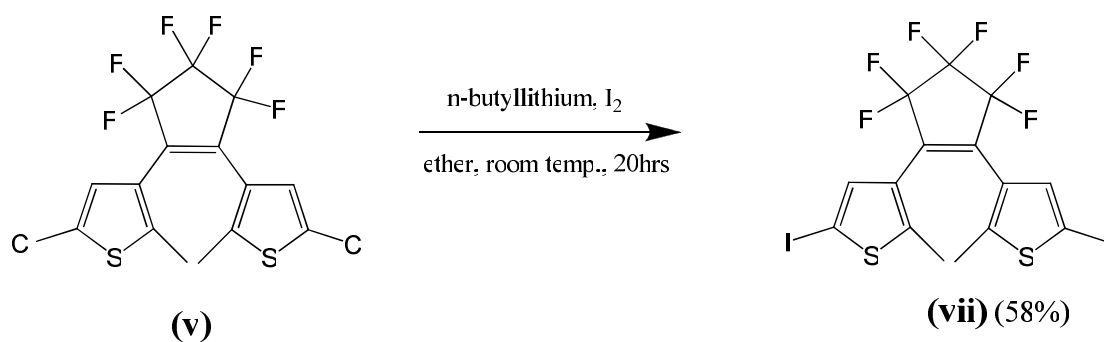
Scheme 2.7: Synthesis of 1,2-Bis(5'-iodo-2'-methylthien-3'-yl)perfluorocyclopentene **(vii)**

1,2-Bis(5'-chloro-2'-methylthien-3'-yl)perflourocyclopentene **(v)** (2 g, 4.57 mmol), n-butyllithium (7.15 mL of 1.6M solution in hexane, 11.4 mmol) and iodine (5.8 g, 22.9 mmol) were reacted together under the same reaction conditions as described for **(vi)**, with the exception that distilled, dry diethyl ether was used as the solvent instead of THF. The dark brown crude product was purified on a silica gel column, using 100% pentane, yielding a yellow/brown solid (1.6423 g, 58%). ^{1}H NMR (400 MHz, CDCl$_3$): δ = 1.88 (s, 6H, CH$_3$), 7.19 (s, 2H, thienyl-H4) ppm.

2.3.5 Synthesis of 1,2-Bis(5'-(3''-ethynylthiophene)-2'-methylthien-3'-yl)-cyclopentene {1H}
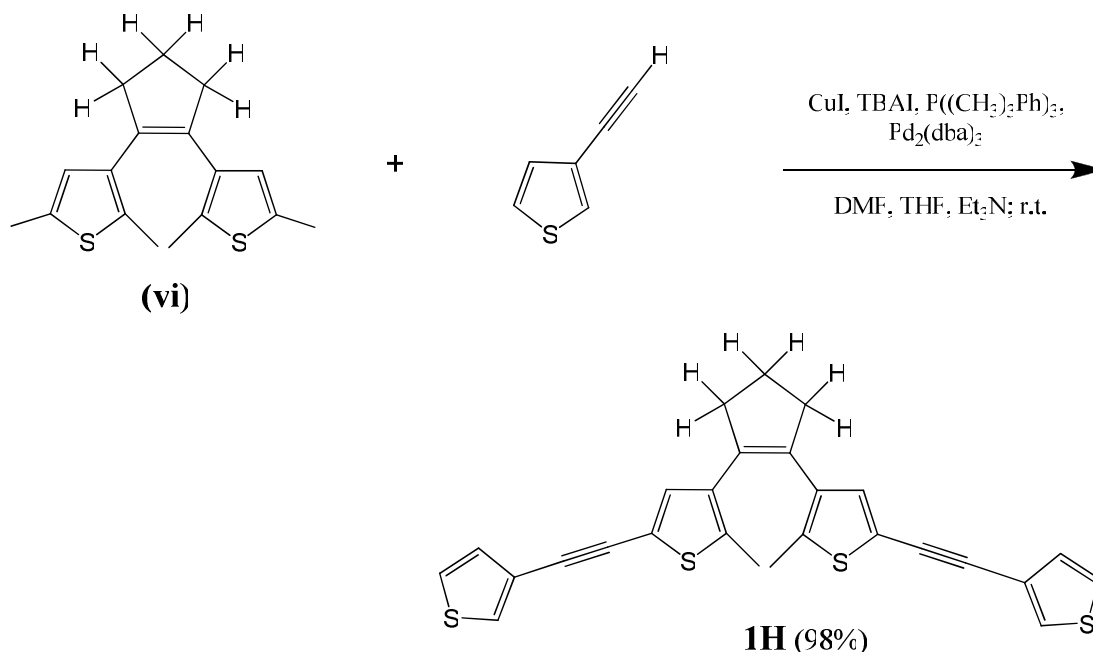
Scheme 2.8: Synthesis of 1,2-Bis(5'-(3''-ethynylthiophene)-2'-methylthien-3'-yl)cyclopentene {**1H**}

Anhydrous DMF (60 mL), anhydrous triethylamine (7 mL) and distilled, dry THF (7 mL) were added to an oven-dried round-bottomed flask. 1,2-Bis(5'-iodo-2'-methylthien-3'-yl)-cyclopentene **(vi)** (0.300 g, 0.586 mmol) was added to the flask, and after the solution was purged with nitrogen for 20 minutes**,** CuI (0.09 g, 0.473 mmol), tetra-butylammonium iodide (TBAI) (1.704 g, 4.613 mmol) and P((CH$_3$)$_3$Ph)$_3$ (0.18 g, 0.463 mmol), were also added to the reaction flask. The mixture was then freeze-evacuated three times, followed by the addition of Pd$_2$(dba)$_3$.CHCl$_3$ (0.035 g, 0.051 mmol) under nitrogen, and was left to stir for 5 minutes at room temperature. Subsequently, the flask was cooled to -20°C and 3-ethynylthiophene (0.127 ml, 1.29 mmol) was added. The solution was then allowed to warm up to room temperature and left to stir for 24 hours, under nitrogen. The reaction mixture was quenched with water, and the solvent was removed by vacuum distillation. The crude product was extracted three times with brine/dichloromethane, the organic extracts were combined, dried over MgSO$_4$ and filtered. The crude product was purified by column chromatography, using silica gel, and eluted with 100% hexane followed by a 9:1

mixture of hexane:CH_2Cl_2 respectively. The pure product was found to be the 4th band on the column, and a purple solid was obtained (0.2721 g, 98%). ^{1}H NMR (400 MHz, $(CD_3)_2SO$): δ = 1.89 (s, 6H, CH_3), 2.01 (quintet, J=7.5 Hz, 2H, CH_2), 2.77 (t, J=7.5 Hz, 4H, CH_2), 7.13 (s, 2H, thienyl-H4), 7.24 (dd, J=4.9 Hz, 1.2 Hz, 2H, ethynylthiophene-H5), 7.65 (dd, J=4.9 Hz, 3 Hz, 2H, ethynyl-thiophene-H4), 7.90 (dd, J=3 Hz, 1.2 Hz, 2H, ethynylthiophene-H2) ppm. ^{13}C NMR (150 MHz, $CDCl_3$) δ = 14.52 (s, 2C, CH_3), 23.02 (s, 1C, CH_2), 38.71 (s, 2C, CH_2), 82.54 (s, 2C, Cq), 87.78 (s, 2C, Cq), 119.18 (s, 2C, Cq), 122.26 (s, 2C, Cq), 125.50 (s, 2C, CH), 128.63 (s, 2C, CH), 129.85 (s, 2C, CH), 133.05 (s, 2C, CH), 134.63 (s, 2C, Cq), 135.87 (s, 2C, Cq), 137.16 (s, 2C, Cq) ppm. Anal. calc. for $C_{27}H_{20}S_4$ (%): C 68.60, H 4.26; found: C 67.59, H 4.36.

2.3.6 Synthesis of 1,2-Bis(5'-(3''-ethynylthiophene)-2'-methylthien-3'-yl)-perfluorocyclopentene {1F}
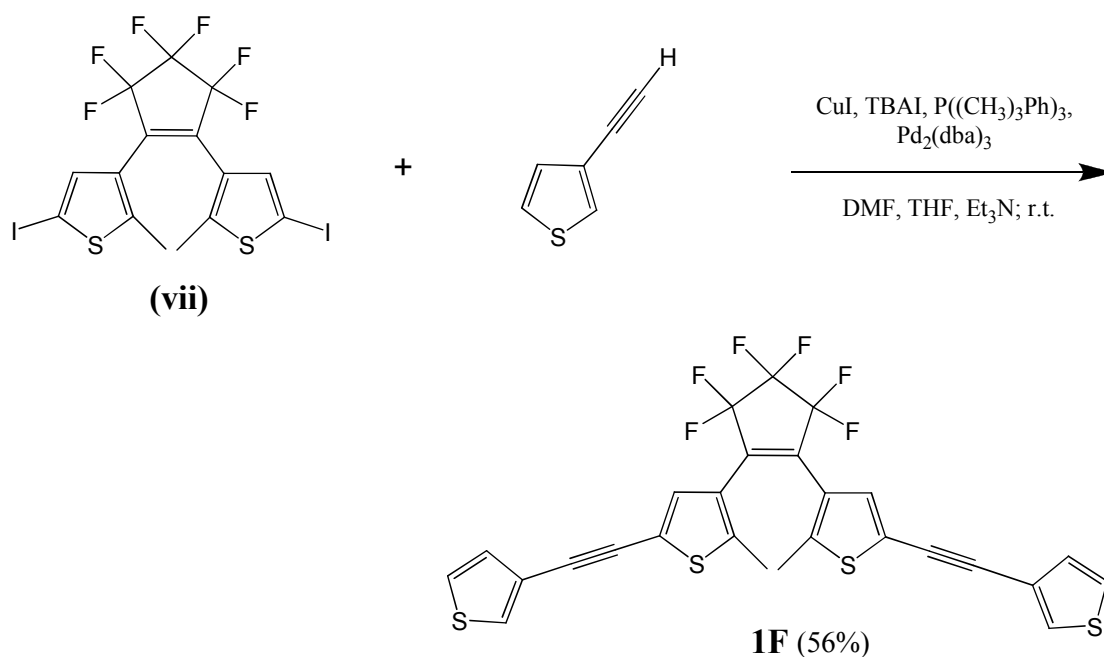
Scheme 2.9: Synthesis of 1,2-Bis(5'-(3''-ethynylthiophene)-2'-methylthien-3'-yl)perfluoro-cyclopentene (**1F**)

1,2-Bis(5'-iodo-2'-methylthien-3'-yl)perfluorocyclopentene (**vii**) (0.300 g, 0.484 mmol), CuI (0.075 g, 0.394 mmol), TBAI (1.42 g, 3.84 mmol) and $P((CH_3)_3Ph)_3$ (0.15 g, 0.386 mmol), $Pd_2(dba)_3.CHCl_3$ (0.044 g, 0.043 mmol), and 3-ethynylthiophene (0.104 mL, 1.06 mmol) were all dissolved in DMF (50 mL), THF (6 mL) and triethylamine (6 mL). The reaction was carried out using the same synthetic method as described for **1H**. Purification of the crude product was carried out on a silica gel column, using 100% hexane as the eluent, followed by a 9:1 mixture of hexane:CH_2Cl_2. The 4th band on the column was collected, and the pure product was obtained as a blue solid (0.1583 g, 56%). ^1H NMR (400 MHz, $(CD_3)_2SO$): δ = 1.97 (s, 6H, CH_3), 7.28 (dd, J=5 Hz, 1.2 Hz, 2H, ethynylthiophene-H5), 7.39 (s, 2H, thienyl-H4), 7.67 (dd, J=5 Hz, 3 Hz, 2H, ethynylthiophene-H4), 7.97 (dd, J=3 Hz, 1.2 Hz, 2H, ethynylthiophene-H2) ppm. ^{13}C NMR (150 MHz, $CDCl_3$) δ = 14.66 (s, 2C, CH_3), 81.11 (s, 2C, Cq), 89.33 (s, 2C, Cq), 121.60 (s, 2C, Cq), 121.95 (s, 2C, Cq), 124.93 (s, 2C, Cq), 125.80 (s, 2C, CH), 129.40 (s, 2C, CH), 129.75 (s, 2C, CH), 131.39 (s, 2C, CH), 143.25 (s, 2C, Cq) ppm (C-F resonances not located). ^{19}F NMR (376.5 MHz, $CDCl_3$) δ = -110.24 (t, J=5.2 Hz, 4F), -131.81 (quintet, J=5.2 Hz, 2F). Anal. calc. for $C_{27}H_{14}F_6S_4$ (%): C 55.85, H 2.43; found: C 55.51, H 2.25.

2.3.7 Synthesis of 1,2-Bis(5'-(4''-bromophenyl)-2'-methylthien-3'-yl)-cyclopentene (viii)[8]
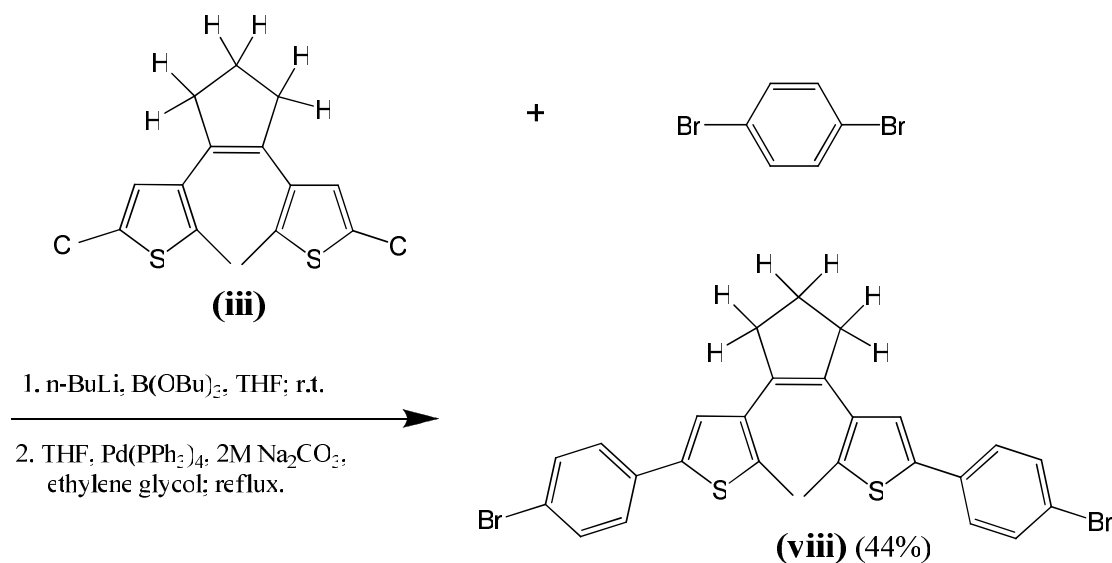
Scheme 2.10: Synthesis of 1,2-Bis(5'-(4''-bromophenyl)-2'-methylthien-3'-yl)-cyclopentene **(viii)**

An oven-dried flask was charged with a solution of 1,2-Bis(5'-chloro-2'-methylthien-3'-yl)cyclopentene **(iii)** (0.754 g, 2.29 mmol), in distilled, dry THF (80 mL), under an atmosphere of nitrogen. n-Butyllithium (3.6 mL of 1.6 M solution in hexane, 5.73 mmol) was added to the reaction flask, and after 1 hour of stirring, B(OBu)$_3$ (1.85 mL, 6.87 mmol) was added and the mixture was allowed to stir for a further 1 hour, in order to produce a boronic ester intermediate. In a separate 500 mL round-bottomed flask, a solution of 1,4-dibromobenzene (2.59 g, 9.16 mmol), dissolved in THF (200 mL), was purged with nitrogen. Pd(PPh$_3$)$_4$ (0.281 g, 0.252 mmol), 2M Na$_2$CO$_3$ (15 mL) and ethylene glycol (15 drops) were added to the flask, and purging was continued for 10 minutes. Then, the boronic ester intermediate was added dropwise, via a syringe, and the reaction was refluxed overnight, under an inert atmosphere. The mixture was extracted with water and diethyl ether, the organic layers were dried over MgSO$_4$, filtered and the solvent was removed. The crude product was purified on silica gel, and eluted with hexane, yielding a pale pink/purple solid (0.58 g, 44%). ^{1}H NMR (400 MHz, CDCl$_3$): δ = 1.99 (s, 6H, CH$_3$), 2.08 (quintet, J=7.5 Hz, 2H, CH$_2$), 2.83 (t, J=7.5 Hz, 4H, CH$_2$), 7.00 (s, 2H, thienyl-H4), 7.34 (d, J=8.5 Hz, 1.2 Hz, 4H, phenyl-H2,6), 7.44 (d, J=8.5 Hz, 3 Hz, 4H, phenyl-H3,5) ppm. ^{13}C NMR (150 MHz, CDCl$_3$) δ = 14.60 (s, 2C, CH$_3$), 23.17 (s, 1C, CH$_2$), 38.57 (s, 2C, CH$_2$), 120.84 (s, 2C, Cq), 124.55 (s, 2C, CH), 126.91 (s, 4C, CH), 132.00 (s, 4C, CH), 133.57 (s, 2C, Cq), 134.86 (s, 2C, Cq), 135.17 (s, 2C, Cq), 136.95 (s, 2C, Cq), 138.55 (s, 2C, Cq) ppm.

2.3.8 Synthesis of 1,2-Bis(5'-(4''-iodophenyl)-2'-methylthien-3'-yl)-cyclopentene (ix)
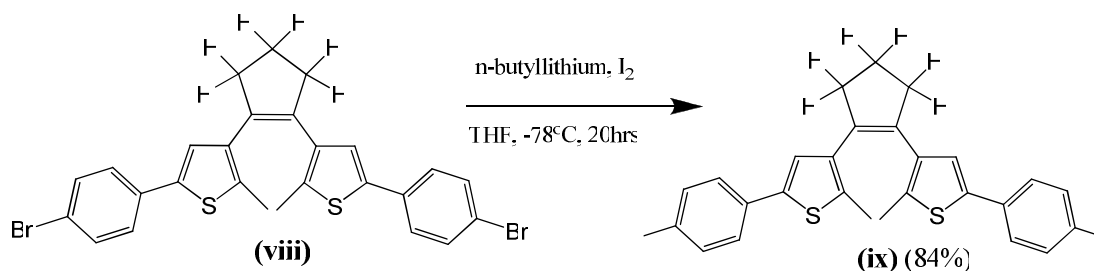
Scheme 2.11: Synthesis of 1,2-Bis(5'-(4''-iodophenyl)-2'-methylthien-3'-yl)cyclopentene **(ix)**

Distilled, dry THF (20 mL) was placed in a 50 mL oven-dried round-bottomed flask, and 1,2-bis(5'-(4''-bromophenyl)-2'-methylthien-3'-yl)-cyclopentene **(viii)** (0.4 g, 0.701 mmol) was added, under an atmosphere of nitrogen. The reaction flask was submerged in a bath of liquid nitrogen and acetone, and cooled to -78°C. tert-Butyllithium (1.03 mL of 1.7 M in hexane, 1.75 mmol) was added dropwise, via a syringe, and the solution was allowed to stir for 1 hour, under an inert atmosphere. In a separate 25 mL oven-dried flask, iodine (0.89 g, 3.51 mmol) was added to distilled, dry THF (10 mL), under N_2. The iodine solution was added dropwise, via a syringe, into the reaction flask, and the mixture was stirred for a further 1 hour at -78°C. Then the flask was allowed to warm-up to room temperature, and it was left stirring overnight under inert conditions. Water (20 mL) was added to the flask to quench the reaction, and it was extracted with dichloromethane (3 x 50 mL). The combined organic layers were washed with a 50% aqueous solution of sodium thiosulphate pentahydrate, in order to remove the excess iodine, washed with water, dried over $MgSO_4$ and filtered. The solvent was removed under reduced pressure, and the crude product was recrystallised in 4:1 methanol:CH_2Cl_2 and vacuum filtered, yielding a light purple-brown pure product (0.3921 g, 84%). ^{1}H NMR (400 MHz, CDCl$_3$) δ=1.98 (s, 6H, CH$_3$), 2.08 (quintet, J=7.5 Hz, 2H, CH$_2$), 2.83 (t, J=7.5 Hz, 4H, CH$_2$), 7.01 (s, 2H, thienyl-H4), 7.22 (d, J=8.5 Hz, 4H, phenyl-H2,6), 7.64 (d, J=8.5 Hz, 4H, phenyl-H3,5).

2.3.9 Synthesis of 1,2-Bis(5'-(4''-phenyl-3'''-ethynylthiophene)-2'-methylthien-3'-yl)-cyclopentene {2H}
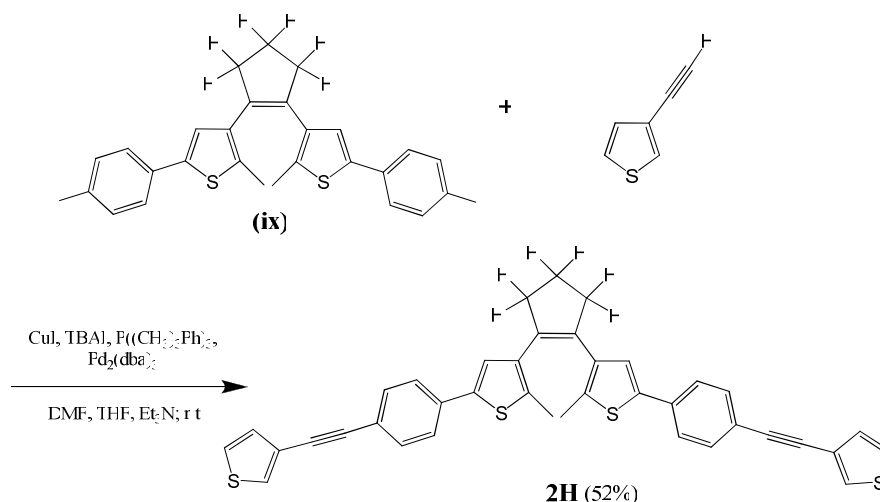
Scheme 2.12: Synthesis of 1,2-Bis(5'-(4''-phenyl-3'''-ethynylthiophene)-2'-methylthien-3'-yl)-cyclopentene {**2H**}

The same procedure described for **1H** was followed, starting from 1,2-Bis(5'-(4''-iodophenyl)-2'-methylthien-3'-yl)-cyclopentene (0.392 g, 0.59 mmol), CuI (0.09 g, 0.473 mmol), TBAI (1.704 g, 4.61 mmol), P((CH$_3$)$_3$Ph)$_3$ (0.18 g, 0.463 mmol), Pd$_2$(dba)$_3$.CHCl$_3$ (0.053 g, 0.051 mmol and 3-ethynylthiophene (0.145 mL, 1.475 mmol). Anhydrous DMF (60 mL), anhydrous triethylamine (7 mL) and distilled dry THF (7 mL) were used as the solvent mixture. The resulting crude product was purified by column chromatography. Silica gel was used as the stationary phase, and the pure product was eluted using 100% hexane, followed by 8:2 hexane:CH$_2$Cl$_2$, yielding a purple solid (0.191 g, 52%). ^{1}H NMR (400 MHz, (CD$_3$)$_2$SO): δ = 1.91 (s, 6H, CH$_3$), 2.05 (quintet, J=7.5 Hz, 2H, CH$_2$), 2.85 (t, J=7.5 Hz, 4H, CH$_2$), 7.27 (dd, J=5 Hz, 1.2 Hz, 2H, ethynylthiophene-H5), 7.41 (s, 2H, thienyl-H4), 7.51 (d, J=8.4 Hz, 4H, phenyl-H2,6), 7.60 (d, J=8.4 Hz, 4H, phenyl-H3,5), 7.66 (dd, J=5 Hz, 3 Hz, 2H, ethynylthiophene-H4), 7.90 (dd, J=3 Hz, 1.2 Hz, 2H, ethynylthiphene-H2) ppm. ^{13}C NMR (150 MHz, CDCl$_3$) δ = 14.67 (s, 2C, CH$_3$), 23.16 (s, 1C, CH$_2$), 38.64 (s, 2C, CH$_2$), 85.38 (s, 2C, Cq), 89.03 (s, 2C, Cq), 121.66 (s, 2C, Cq), 122.46 (s, 2C, Cq), 124.64 (s, 2C, CH), 125.15 (s, 4C, CH), 125.52 (s, 2C, CH), 128.70 (s, 2C, CH), 130.00 (s, 2C, CH), 132.07 (s, 4C, CH), 134.33 (s, 2C, Cq), 134.82 (s, 2C, Cq), 135.42 (s, 2C, Cq), 137.01 (s, 2C, Cq), 139.13 (s, 2C, Cq) ppm. Anal. calc. for C$_{39}$H$_{28}$S$_4$ (%): C 74.96, H 4.52; found: C 74.73, H 4.61.

2.3.10 Synthesis of 1,2-Bis(5'-(4''-phenyl-3'''-ethynylthiophene)-2'-methylthien-3'-yl)-perfluorocyclopentene {2F}

In order to attach benzene-ethynylthiophene substituents onto the perfluoro-cyclopentene switch, a different synthetic approach was employed, comparing to the method used for the perhydrocyclopentene switch, due to the limited amount of 1,2-Bis(5'-chloro-2'-methylthien-3'-yl)perflourocyclopentene **(v)** available.

- *Synthesis of 1-(3-thienylethynyl)-4-bromobenzene **(x)***
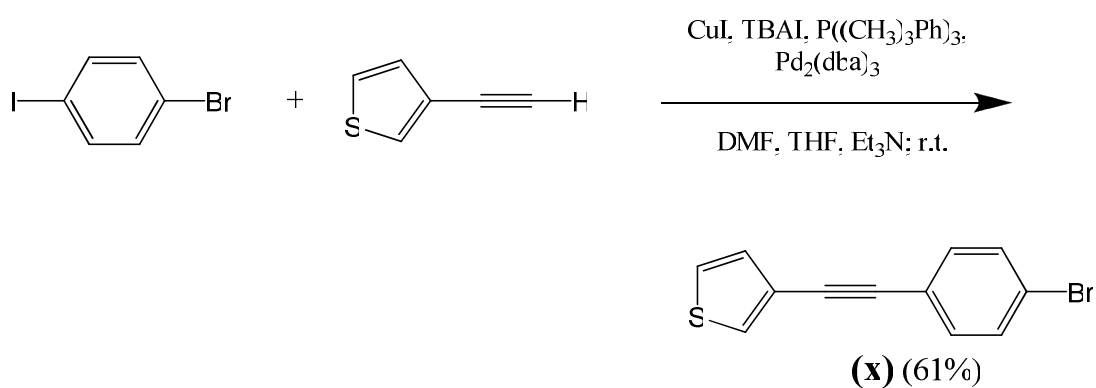
Scheme 2.13: Synthesis of 1-(3-thienylethynyl)-4-bromobenzene **(x)**

An oven-dried 250 mL round-bottomed flask was filled with anhydrous DMF (75 mL), anhydrous triethylamine (9 mL) and dry THF (9 mL). The solvent mixture was purged with nitrogen for 20 minutes, followed by addition of 1-iodo-4-bromobenzene (0.200 g, 0.707 mmol), CuI (0.113 g, 0.593 mmol), TBAI (2.13 g, 5.766 mmol) and P((CH$_3$)$_3$Ph)$_3$ (0.225 g, 0.579 mmol). The reaction mixture was freeze-evacuated three times. Then, Pd$_2$(dba)$_3$.CHCl$_3$ (0.066 g, 0.064 mmol) was added, and the reaction mixture was allowed to stir at room temperature for 5mins. The flask was cooled to -20°C and 3-ethynylthiophene (0.077 mL, 0.778 mmol) was added. The reaction mixture was then stirred for 24 hours at room temperature, under an inert atmosphere. Water was added to the flask in order to quench the reaction, and the solvent was removed by heating under vacuum, at a high temperature (~75°C). The resulting crude product was extracted with CH$_2$Cl$_2$ and brine. The organic extracts were combined, washed with water, dried over MgSO$_4$ and filtered. The solvent was removed, and the product was purified by column chromatography. Silica gel was

used as the stationary phase, and 100% hexane, followed by 8:2 hexane:CH_2Cl_2, was used as the mobile phase. A white solid was obtained (0.113 g, 61%). ^{1}H NMR (400 MHz, $(CD_3)_2CO$) δ = 7.24 (dd, J=5 Hz, 1.2 Hz, 1H, ethynylthiophene-H5), 7.47 (d, J=8.6 Hz, 2H, phenyl-H2,6), 7.57 (dd, J=5 Hz, 3 Hz, 1H, ethynylthiophene-H4), 7.60 (d, J=8.6 Hz, 2H, phenyl-H3,5), 7.77 (dd, J=3 Hz, 1.2 Hz, 1H, ethynylthiphene-H2) ppm. ^{13}C NMR (150 MHz, $CDCl_3$) δ = 85.75 (s, 1C, Cq), 87.90 (s, 1C, Cq), 121.79, (s, 1C, Cq), 122.10 (s, 1C, Cq), 122.34 (s, 1C, Cq), 125.67 (s, 1C, CH), 129.01 (s, 1C, CH), 129.97 (s, 1C, CH), 131.73 (s, 2C, CH), 133.06 (s, 2C, CH). Anal. calc. for $C_{12}H_7SBr$ (%): C 54.77, H 2.68; found: C 54.81, H 2.69.

- *Synthesis of 1,2-Bis(5'-(4''-phenyl-3'''-ethynylthiophene)-2'-methylthien-3'-yl)perfluorocyclopentene {2F}*
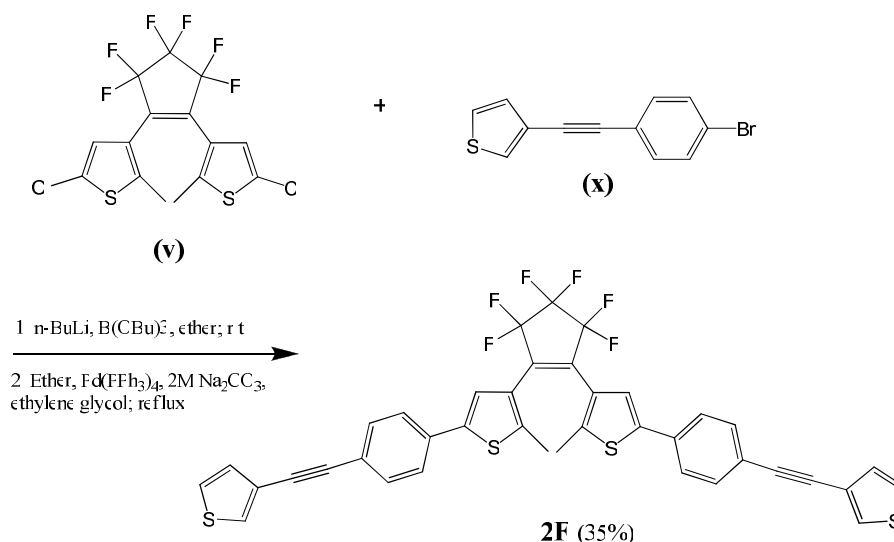
Scheme 2.14: Synthesis of 1,2-Bis(5'-(4''-phenyl-3'''-ethynylthiophene)-2'-methylthien-3'-yl)-perfluorocyclopentene {2F}

1,2-Bis(5'-chloro-2'-methylthien-3'-yl)perfluorocyclopentene **(v)** (0.1208 g, 0.276 mmol) was dissolved in distilled, dry diethyl ether (20 mL) in a 50 mL round-bottomed flask, under a nitrogen atmosphere. t-Butyllithium (0.41 mL of 1.7M solution in hexane, 0.69 mmol) was slowly added to the reaction flask. After 1 hour of stirring at room temperature, B(OBu)$_3$ 0.223 mL, 0.828 mmol) was added to the flask and the reaction mixture was stirred for a further 1 hour, forming a boronic ester intermediate. In a separate 100 mL flask, 1-(3-thienylethynyl)-4-bromobenzene (0.16 g, 0.608 mmol) was dissolved in distilled, dry diethyl ether (40 mL) and the solution

was purged with nitrogen for 20 minutes. Pd(PPh$_3$)$_4$ (0.0339 g, 0.03 mmol), 2M Na$_2$CO$_3$ (4 mL) and ethylene glycol (4 drops) were then added to the flask and purging was continued for a further 10 minutes. Subsequently, the boronic ester intermediate was removed from the 50 mL flask, via a syringe, and added directly to this reaction mixture. The solution was then refluxed overnight, under nitrogen. The mixture was extracted with water/diethyl ether, the organic layers were combined, dried over MgSO$_4$ and filtered. The solvent was removed under vacuum and the crude product was purified on a silica gel column, using 100% hexane, followed by a solvent mixture of 9:1 hexane:CH$_2$Cl$_2$. The 2nd blue band was collected from the column, and the pure product was obtained as a blue solid (0.07 g, 35%). ^{1}H NMR (400 MHz, (CD$_3$)$_2$SO): δ = 2.00 (s, 6H, CH$_3$), 7.29 (dd, J=5 Hz, 1.0 Hz, 2H, ethynylthiophene-H5), 7.57 (d, J=8.4 Hz, 4H, phenyl-H2,6), 7.62 (s, 2H, thienyl-H4), 7.67 (dd, J=5 Hz, 2.8 Hz, 2H, ethynylthiophene-H4), 7.70 (d, J=8.4 Hz, 4H, phenyl-H3,5), 7.93 (dd, J=2.8 Hz, 1.0 Hz, 2H, ethynylthiophene-H2) ppm. ^{13}C NMR (150 MHz, CDCl$_3$) δ = 14.21 (s, 2C, CH$_3$), 85.97 (s, 2C, Cq), 88.71 (s, 2C, Cq), 122.28 (s, 2C, Cq), 122.82 (s, 2C, CH), 122.96 (s, 2C, Cq), 125.50 (s, 4C, CH), 125.62 (s, 2C, CH), 126.16 (s, 2C, Cq), 128.96 (s, 2C, CH), 129.98 (s, 2C, CH), 132.25 (s, 4C, CH), 133.06 (s, 2C, Cq), 141.73 (s, 2C, Cq), 141.99 (s, 2C, Cq) ppm (C-F resonances not located). ^{19}F NMR (376.5 MHz, CDCl$_3$) δ = -110.01 (t, J=5.0 Hz, 4F), -131.83 (quintet, J=5.0 Hz, 2F). Anal. calc. for C$_{39}$H$_{22}$F$_6$S$_4$ (%): C 63.92, H 3.03; found: C 60.22, H 2.97.

2.3.11 Synthesis of 1,2-Bis(5'-ethynylferrocene-2'-methylthien-3'-yl)-cyclopentene {7H}[16]
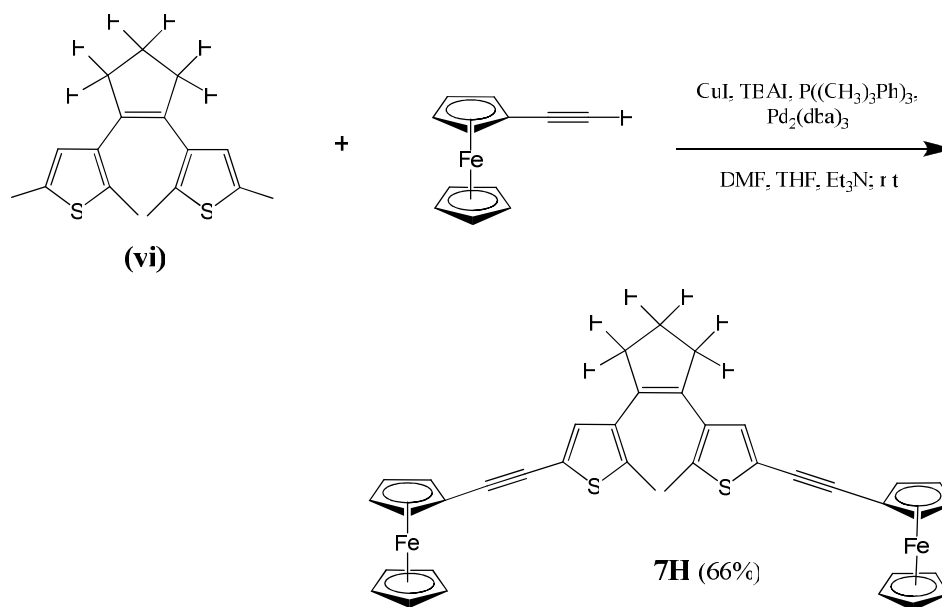
Scheme 2.15: Synthesis of 1,2-Bis(5'-ethynylferrocene-2'-methylthien-3'-yl)cyclopentene {**7H**}

A 100 ml oven-dried round-bottomed flask was filled with anhydrous DMF (40 mL), anhydrous triethylamine (5 mL) and distilled, dry THF (5 mL). 1,2-Bis(5'-iodo-2'-methylthien-3'-yl)-cyclopentene **(vi)** (0.200 g, 0.390 mmol) was dissolved in the solvent mixture, and the solution was purged with nitrogen for 20 minutes. Following the addition of CuI (0.06 g, 0.315 mmol), TBAI (1.136 g, 3.075 mmol) and $P((CH_3)_3Ph)_3$ (0.12 g, 0.309 mmol), the reaction mixture was freeze-evacuated three times. Under nitrogen, $Pd_2(dba)_3.CHCl_3$ (0.035 g, 0.034 mmol) was added to the flask, and the mixture was left to stir for 5 minutes, at room temperature. The reaction flask was cooled down to -20°C, ethynylferrocene (0.205 g, 0.975 mmol) was added, and the mixture was allowed to stir for 24 hrs at ambient temperature, under an inert atmosphere. The reaction was quenched with H_2O and the solvent was removed under reduced pressure, at a temperature of ~75°C. The crude product was extracted three times with brine/dichloromethane and the organic layers were washed with water, dried over $MgSO_4$ and filtered. After removal of the solvent, the crude product was purified on a silica gel column, using 100% hexane, followed by 8:2 hexane:CH_2Cl_2.

The 4th band on the column was collected, and the pure product was obtained as an orange solid (0.175 g, 66%). ^{1}H NMR (400 MHz, $(CD_3)_2SO$) δ = 1.88 (s, 6H, CH_3), 2.00 (quintet, J=7.3 Hz, 2H, CH_2), 2.77 (t, J=7.3 Hz, 4H, CH_2), 4.26 (s, 10H, Fc-Cp), 4.34 (t, J=1.8 Hz, 4H, Fc-H3,4), 4.56 (t, J=1.8 Hz, 4H, Fc-H2,5), 7.07 (s, 2H, thienyl-H4) ppm. ^{13}C NMR (150 MHz, $CDCl_3$) δ = 14.40 (s, 2C, CH_3), 22.99 (s, 1C, CH_2), 38.70 (s, 2C, CH_2), 67.50 (s, 2C, Cq), 70.49 (s, 4C, CH), 71.62 (s, 10C, CH), 72.22 (s, 4C, CH), 79.38 (s, 2C, Cq), 91.68 (s, 2C, Cq), 119.77 (s, 2C, Cq), 132.66 (s, 2C, CH), 134.51 (s, 2C, Cq), 135.60 (s, 2C, Cq), 136.70 (s, 2C, Cq) ppm. Anal. calc. for $C_{39}H_{32}S_2Fe_2$ (%): C 69.24, H 4.77; found: C 68.89, H 4.71.

2.3.12 Synthesis of 1,2-Bis(5'-ethynylferrocene-2'-methylthien-3'-yl)-perfluorocyclopentene {7F}[16]
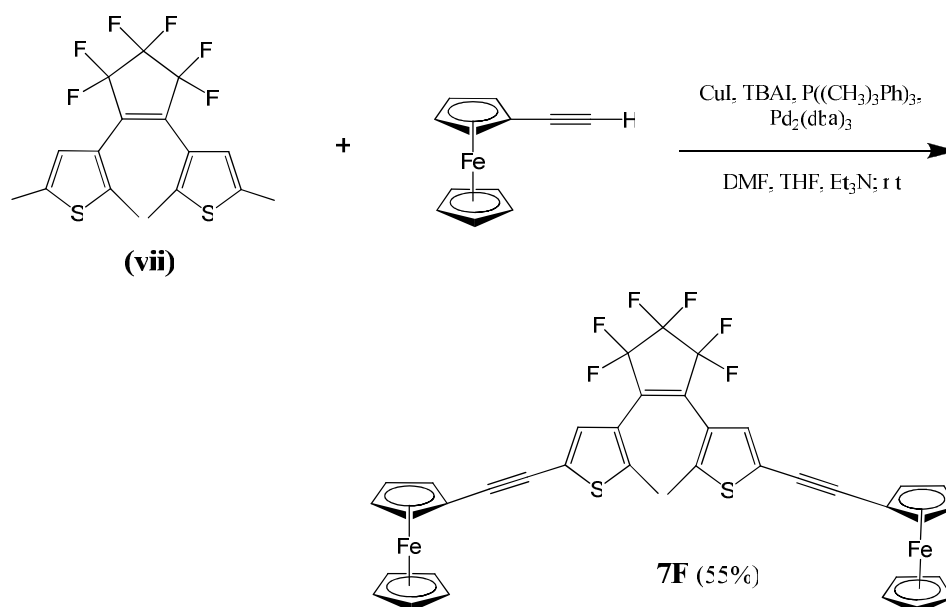
Scheme 2.16: Synthesis of 1,2-Bis(5'-ethynylferrocene-2'-methylthien-3'-yl)-perfluorocyclopentene {**7F**}

Anhydrous DMF (50 mL), anhydrous triethylamine (6 mL) and distilled, dry THF (6 mL), 1,2-Bis(5'-iodo-2'-methylthien-3'-yl)-perfluorocyclopentene **(vii)** (0.300 g, 0.484 mmol), CuI (0.075 g, 0.394 mmol), TBAI (1.42 g, 3.84 mmol), P((CH$_3$)$_3$Ph)$_3$ (0.15 g, 0.386 mmol), Pd$_2$(dba)$_3$.CHCl$_3$ (0.044 g, 0.043 mmol) and ethynylferrocene (0.224 g, 1.06 mmol) were all added to an oven-dried round-bottomed flask under the same reaction conditions as described for **7H**. Purification of the crude product was achieved by column chromatography, using silica gel, and eluted with a solvent mixture of 9:1, followed by 8:2, hexane:CH$_2$Cl$_2$. The 4th fraction of the column was collected and the pure product was obtained as an orange solid (0.21 g, 55%). ^{1}H NMR (400 MHz, (CD$_3$)$_2$SO) δ = 1.96 (s, 6H, CH$_3$), 4.28 (s, 10H, Fc-Cp), 4.37 (t, J=1.8 Hz, 4H, Fc-H3,4), 4.60 (t, J=1.8 Hz, 4H, Fc-2,5), 7.32 (s, 2H, thienyl-H4) ppm. ^{13}C NMR (150 MHz, CDCl$_3$) δ = 14.69 (s, 2C, CH$_3$), 64.63 (s, 2C, Cq), 69.57 (s, 4C, CH), 70.45 (s, 10C, CH), 71.74 (s, 4C, CH), 77.78 (s, 2C, Cq), 93.66 (s, 2C, Cq), 122.72 (s, 2C, Cq), 124.85 (s, 2C, Cq), 130.65 (s, 2C, CH), 142.66 (s, 2C, Cq) ppm (C-F resonances not located). ^{19}F NMR (376.5 MHz, CDCl$_3$) δ = -110.19 (t, J=4.9 Hz, 4F), -131.82 (quintet, J=4.9 Hz, 2F). Anal. calc. for C$_{39}$H$_{26}$F$_6$S$_2$Fe$_2$ (%): C 59.71, H 3.34; found: C 59.92, H 3.64.

2.3.13 Synthesis of 1,2-Bis(5'-(4''-phenyl-ethynylferrocene)-2'-methylthien-3'-yl)-cyclopentene {8H}
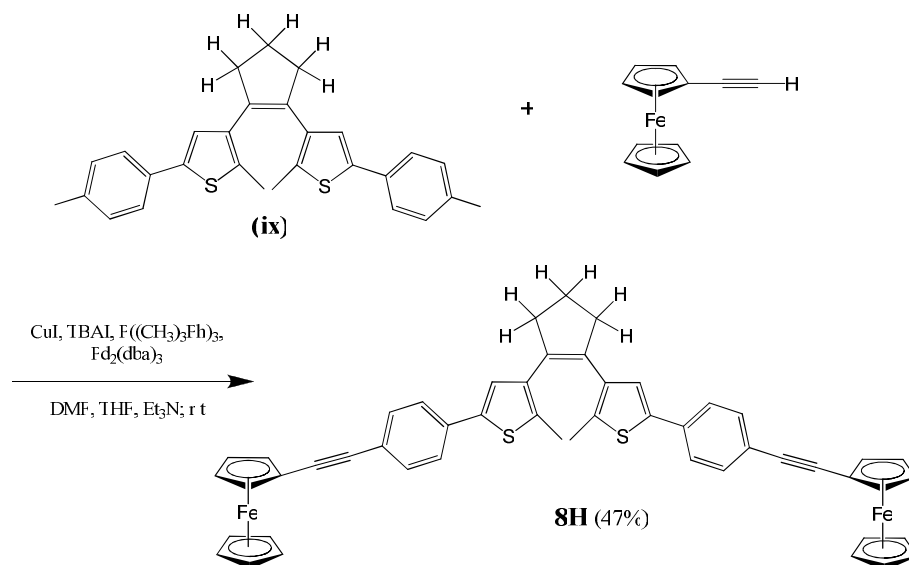
Scheme 2.17: Synthesis of 1,2-Bis(5'-(4''-phenyl-ethynylferrocene)-2'-methylthien-3'-yl)-cyclopentene {8H}

Using the same reaction method as described for **7H**, 1,2-Bis(5'-(4''-iodophenyl)-2'-methylthien-3'-yl)cyclopentene **(ix)** (0.300 g, 0.452 mmol) was dissolved in DMF (50 mL), THF (6 mL) and triethylamine (6 mL), followed by addition of CuI (0.75 g, 0.394 mmol), TBAI (1.42 g, 3.844 mmol), $P((CH_3)_3Ph)_3$ (0.15 g, 0.386 mmol), $Pd_2(dba)_3.CHCl_3$ (0.044 g, 0.043 mmol), and ethynylferrocene (0.2374 g, 1.13 mmol). The product was purified on a silica gel column, and eluted with a mixture of 9:1, followed by 8:2, hexane:CH_2Cl_2 respectively. The pure product was obtained as an orange solid (0.1747 g, 47%) and was found to be the 4th band collected from the column. ^1H NMR (400 Hz, $(CD_3)_2SO$) δ = 1.92 (s, 6H, CH_3), 2.05 (quintet, J=7.5 Hz, 2H, CH_2), 2.85 (t, J=7.5 Hz, 4H, CH_2), 4.27 (s, 10H, Fc-Cp), 4.35 (t, J=1.8 Hz, 4H, Fc-H3,4), 4.58 (t, J=1.8 Hz, 4H, Fc-H2,5), 7.39 (s, 2H, thienyl-H4), 7.46 (d, J=8.4 Hz, 4H, phenyl-H2,6), 7.55 (d, J=8.4 Hz, 4H, phenyl-H3,5) ppm. ^{13}C NMR (150 MHz, $CDCl_3$) δ = 14.64 (s, 2C, CH_3), 23.20 (s, 1C, CH_2), 38.64 (s, 2C, CH_2), 66.95 (s, 2C, Cq), 69.32 (s, 4C, CH), 70.46 (s, 10C, CH), 71.76 (s, 4C, CH), 85.96 (s, 2C, Cq), 89.32 (s, 2C, Cq), 122.48 (s, 2C, Cq), 124.51 (s, 2C, CH), 125.12 (s, 4C, CH), 131.95 (s, 4C, CH), 133.85 (s, 2C, Cq), 134.87 (s, 2C, Cq), 135.24 (s, 2C, Cq) 136.99 (s, 2C, Cq), 139.31 (s, 2C, Cq) ppm. Anal. calc. for $C_{51}H_{40}S_2Fe_2$ (%): C 73.92, H 4.86; found: C 72.20, H 4.90.

2.3.14 Synthesis of 1,2-Bis(5'-(4''-phenyl-ethynylferrocene)-2'-methylthien-3'yl)-perflourocyclopentene {8F}

A very limited amount of 1,2-Bis(5'-chloro-2'-methylthien-3'yl)perflouro-cyclopentene **(v)** was available. Therefore, an alternative synthetic approach, to the method used for the perhydrocyclopentene switch, was employed in order to attach benzene-ethynylferrocene onto the perfluorocyclopentene switch.

- *Synthesis of 1-(ferrocenylethynyl)-4-bromobenzene **(xi)***
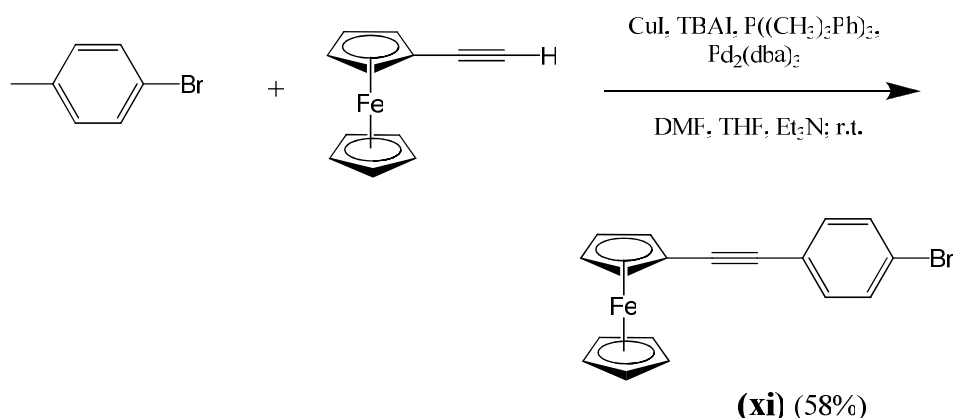
Scheme 2.18: Synthesis of 1-(3-ferrocenylethynyl)-4-bromobenzene **(xi)**

The same synthetic method was employed as described for **(x)**, starting with Anhydrous DMF (75 mL), anhydrous triethylamine (9 mL), distilled, dry THF (9 mL) and 1-iodo-4-bromobenzene (0.200 g, 0.707 mmol). Subsequently, CuI (0.113 g, 0.593 mmol), TBAI (2.13 g, 5.766 mmol) and P((CH$_3$)$_3$Ph)$_3$ (0.225 g, 0.579 mmol), Pd$_2$(dba)$_3$.CHCl$_3$ (0.066 g, 0.064 mmol) and ethynylferrocene (0.1638 g, 0.778 mmol) were all added to the reaction flask as described previously. Purification of the crude product was carried out by column chromatography, on silica gel, using 100% hexane, followed by 9:1, then 8:1 hexane:CH$_2$Cl$_2$, as the eluent, yielding an orange product (0.1508 g, 58%). ^{1}H NMR (400 MHz, (CD$_3$)$_2$CO) δ = 4.25 (s, 5H, Fc-Cp), 4.32 (t, J=1.8 Hz, 2H, Fc-H3,4), 4.52 (t, J=1.8 Hz, 2H, Fc-H2,5), 7.43 (d, J=8.6 Hz, 2H, phenyl-H2,6), 7.57 (d, J=8.6 Hz, 2H, phenyl-H3,5) ppm. ^{13}C NMR (150 MHz, CDCl$_3$) δ = 65.19 (s, 1C, Cq), 69.27 (s, 2C, CH), 70.29 (s, 5C, CH), 71.63 (s, 2C, CH), 84.73 (s, 1C, Cq), 89.74 (s, 1C, Cq), 121.73 (s, 1C, Cq), 122.91 (s, 1C, Cq), 131.52 (s, 2C, CH), 132.83 (s, 2C, CH). Anal. calc. for C$_{18}$H$_{13}$FeBr (%): C 59.13, H 3.58; found: C 59.04, H 3.68.

- *Synthesis of 1,2-Bis(5'-(4''-phenyl-ethynylferrocene)-2'-methylthien-3'-yl)-perfluorocyclopentene {8F}*
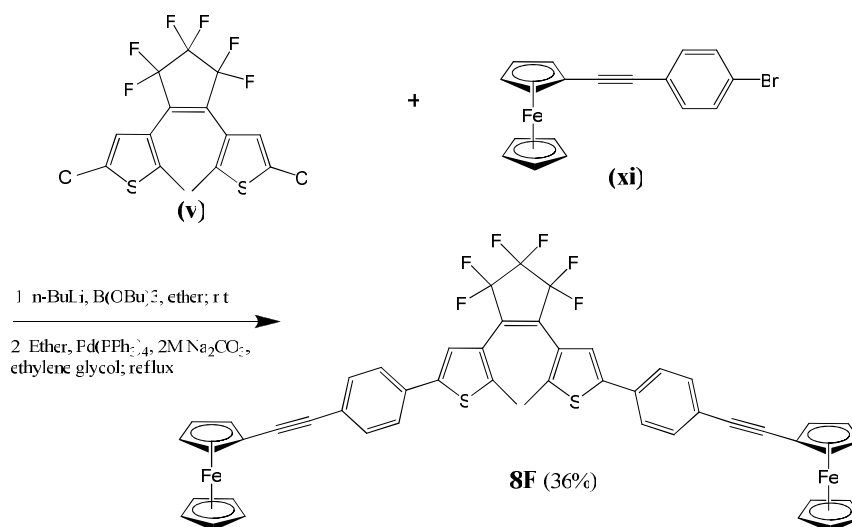
Scheme 2.19: Synthesis of 1,2-Bis(5'-(4''-phenyl-ethynylferrocene)-2'-methylthien-3'-yl)-perfluorocyclopentene {**8F**}

The same reaction procedure was followed as that described for **2F**. 1,2-Bis(5'-chloro-2'-methylthien-3'-yl)perfluorocyclopentene (**v**) (0.1469 g, 0.336 mmol), t-butyllithium (0.49 mL of 1.7M solution in hexane, 0.84 mmol) and B(OBu)$_3$ (0.232 mL, 1.01 mmol) were dissolved in diethyl ether (15 mL) and reacted to form a boronic ester intermediate. The boronic ester intermediate was added into a separate flask containing 1-(ferrocenylethynyl)-4-bromobenzene (0.2702 g, 0.74 mmol), Pd(PPh$_3$)$_4$ (0.0413 g, 0.037 mmol), 2M Na$_2$CO$_3$ (4 mL) and ethylene glycol (4 drops) in diethyl ether (40 mL). Following an overnight reflux, the crude product was worked-up and purified on a silica gel column, using a solvent mixture of 9:1, followed by 8:2, hexane:CH$_2$Cl$_2$. Fraction 4 was collected from the column, and the pure product was obtained as an orange solid (0.1147 g, 36%). ^{1}H NMR (400 MHz, (CD$_3$)$_2$SO) δ = 2.00 (s, 6H, CH$_3$), 4.28 (s, 10H, Fc-Cp), 4.36 (t, J=1.8 Hz, 4H, Fc-H3,4), 4.59 (t, J=1.8 Hz, 4H, Fc-H2,5), 7.51 (d, J=8.4 Hz, 4H, phenyl-H2,6), 7.60 (s, 2H, thienyl-H4), 7.66 (d, J=8.4 Hz, 4H, phenyl-H3,5) ppm. ^{13}C NMR (150 MHz, CDCl$_3$) δ = 14.79 (s, 2C, CH$_3$), 65.64 (s, 2C, Cq), 69.45 (s, 4C, CH), 70.51 (s, 10C, CH), 71.84 (s, 4C, CH), 85.63 (s, 2C, Cq), 90.07 (s, 2C, Cq), 122.77 (s, 2C, CH), 123.56 (s, 2C, Cq), 125.43 (s, 4C, CH), 126.11 (s, 2C, Cq), 132.08 (s, 4C, CH), 132.51 (s, 2C, Cq), 141.81 (s, 2C, Cq) 141.86 (s, 2C, Cq) ppm (C-F resonances not located). ^{19}F NMR (376.5 MHz, CDCl$_3$) δ = -109.96 (t, J=5.1 Hz, 4F), -131.78 (quintet, J=5.1 Hz, 2F). Anal. calc. for C$_{51}$H$_{34}$F$_6$S$_2$Fe$_2$ (%): C 65.40, H 3.66; found: C 63.16, H 3.67.

Co$_2$(CO)$_6$ Complexes

The Co$_2$(CO)$_6$ complexes were characterised by ^{1}H NMR, ^{19}F NMR, IR spectroscopy and elemental analysis. However, accurate ^{13}C NMR spectra could not be obtained due to the instability of the cobalt carbonyl complexes in deuterated chloroform over the time-scale of the ^{13}C NMR experiments (hours).

2.3.15 Synthesis of 1,2-Bis(5'-(3''-ethynylthiophene)-2'-methylthien-3'-yl)-cyclopentene [Co$_2$(CO)$_6$]$_2$ {3H}
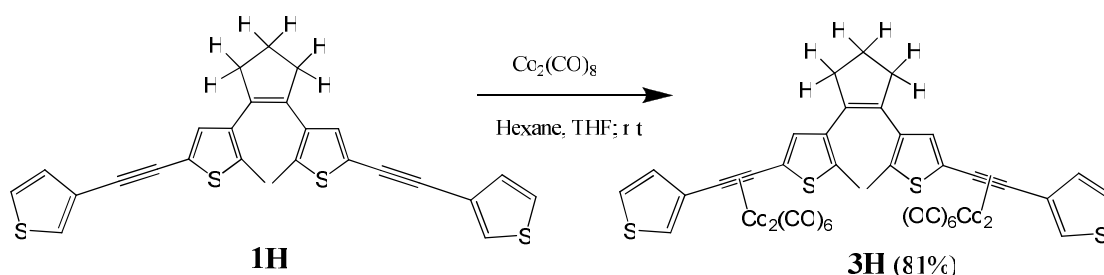
Scheme 2.20: Synthesis of 1,2-Bis(5'-(3''-ethynylthiophene)-2'-methylthien-3'-yl)-cyclopentene [Co$_2$(CO)$_6$]$_2$ {**3H**}

A 100 ml oven-dried round-bottomed flask was filled with a solution of 1,2-Bis(5'-(3''-ethynylthiophene)-2'-methylthien-3'-yl)-cyclopentene (**1H**) (0.08 g, 0.169 mmol), dissolved in hexane (20 mL) and dry THF (15 mL), and the solution was purged with nitrogen for 20 minutes. Co$_2$(CO)$_8$ (0.127 g, 0.372 mmol) was weighed out under nitrogen, and added to the flask. The reaction mixture was allowed to stir overnight at room temperature, under an inert atmosphere. The solvent was removed under reduced pressure, and the crude product was purified on silica gel, and eluted with 100% hexane, followed by 9:1 hexane:diethyl ether. A pure brown/black product was obtained (0.1432 g, 81%). ^{1}H NMR (400 MHz, (CD$_3$)$_2$CO): δ = 2.03 (s, 6H, CH$_3$), 2.07 (quintet, J=7.5 Hz, 2H, CH$_2$), 2.84 (t, J=7.5 Hz, 4H, CH$_2$), 7.25 (s, 2H, thienyl-H4), 7.36 (dd, J=5 Hz, 1.2 Hz, 2H, ethynylthiophene-H5), 7.62 (dd, J=5 Hz, 3 Hz, 2H, ethynyl-thiophene-H4), 7.82 (dd, J=3 Hz, 1.2 Hz, 2H, ethynylthiophene-H2) ppm. Anal. calc. for C$_{39}$H$_{20}$S$_4$O$_{12}$Co$_4$ (%): C 44.88, H 1.93; found: C 43.85, H 2.08. IR (THF, cm^{-1}) ν$_{CO}$ = 2089, 2055, 2025.

2.3.16 Synthesis of 1,2-Bis(5'-(3''-ethynylthiophene)-2'-methylthien-3'-yl)-perfluorocyclopentene [Co₂(CO)₆]₂ {3F}

Scheme 2.21: Synthesis of 1,2-Bis(5'-(3''-ethynylthiophene)-2'-methylthien-3'-yl)-perfluorocyclopentene [Co₂(CO)₆]₂ {**3F**}

1,2-Bis(5'-(3''-ethynylthiophene)-2'-methylthien-3'-yl)perfluorocyclopentene **(1F)** (0.16 g, 0.276 mmol) and $Co_2(CO)_8$ (0.207 g, 0.606 mmol) were reacted together in hexane (30 mL) and THF (20 mL), under the same conditions as described for **3H**. Purification of the crude product was achieved by column chromatography on silica gel, using 100% hexane as the eluent, yielding a dark brown/black solid (0.1564 g, 49%). ^{1}H NMR (400 MHz, $(CD_3)_2CO$): δ = 2.08 (s, 6H, CH_3), 7.36 (dd, J=5.1 Hz, 1.4 Hz, 2H, ethynylthiophene-H5), 7.51 (s, 2H, thienyl-H4), 7.65 (dd, J=5.1 Hz, 2.9 Hz, 2H, ethynylthiophene-H4), 7.84 (dd, J=2.9 Hz, 1.4 Hz, 2H, ethynylthiophene-H2) ppm. ^{19}F NMR (376.5 MHz, $CDCl_3$) δ = -110.06 (t, J=5.0 Hz, 4F), -131.79 (quintet, J=5.0 Hz, 2F). Anal. calc. for $C_{39}H_{14}F_6S_4O_{12}Co_4$ (%): C 40.68, H 1.23; found: C 39.76, H 1.33. IR (THF, cm^{-1}) ν_{CO} = 2092, 2058, 2029.

2.3.17 Synthesis of the closed-ring isomer of 1,2-Bis(5'-(3''-ethynylthiophene)-2'-methylthien-3'-yl)-perfluorocyclopentene [Co$_2$(CO)$_6$]$_2$ {3bF}

The closed-ring isomer **3bF** was synthesised in order to elucidate the photochemical and electrochemical results of the open-ring isomer **3F**, hence only a small amount of this compound was made. Therefore **3bF** was characterised by ^{1}H NMR and IR spectroscopy only. The ^{13}C NMR, ^{19}F NMR and elemental analysis data were not obtained for this compound.

Scheme 2.22: Synthesis of the closed-ring isomer of 1,2-Bis(5'-(3''-ethynylthiophene)-2'-methylthien-3'-yl)-perfluorocyclopentene [Co$_2$(CO)$_6$]$_2$ {3bF}

1,2-Bis(5'-(3''-ethynylthiophene)-2'-methylthien-3'-yl)perfluorocyclopentene **(1Fo)** (0.01 g, 0.017 mmol) was irradiated with UV light at 313 nm in deuterated acetone, and was monitored in the ^{1}H NMR until the open-ring isomer converted to the closed-ring isomer **(1Fc)**. The solvent was removed, and the closed-ring isomer **1Fc** was dissolved in a degassed solution of hexane (12 mL) and THF (3 mL) in the dark. Co$_2$(CO)$_8$ (0.15 g, 0.043 mmol) was added to the reaction flask, and the mixture was stirred overnight, under an inert atmosphere, in the dark. The crude product was purified on a silica gel column (covered with tin-foil), and eluted with 100% hexane, followed by 9:1 hexane:CH$_2$Cl$_2$. A dark blue product was obtained (0.009 g, 45%). ^{1}H NMR (400 MHz, (CD$_3$)$_2$CO): δ = 2.30 (s, 6H, CH$_3$), 6.67 (s, 2H, thienyl-H4), 7.36 (dd, J=5 Hz, 1.4 Hz, 2H, ethynylthiophene-H5), 7.65 (dd, J=5 Hz, 2.9 Hz, 2H, ethynylthiophene-H4), 7.87 (dd, J=2.9 Hz, 1.4 Hz, 2H, ethynylthiophene-H2) ppm. IR (THF, cm^{-1}) ν$_{CO}$ = 2094, 2063, 2035.

103

2.3.18 Synthesis of 1,2-Bis(5'-(4''-phenyl-3'''-ethynylthiophene)-2'-methylthien-3'-yl)cyclopentene [Co₂(CO)₆]₂ {4H}
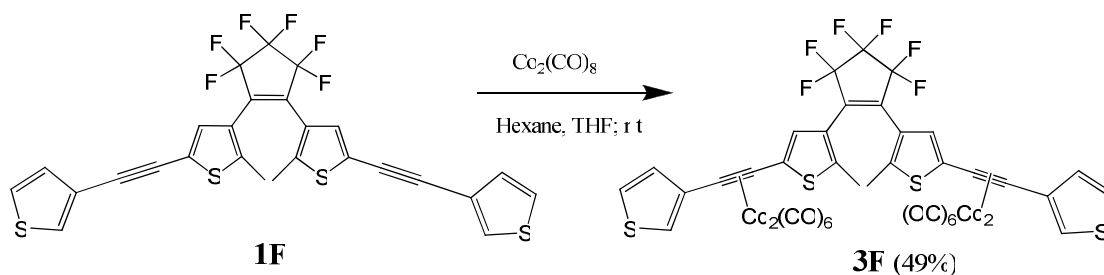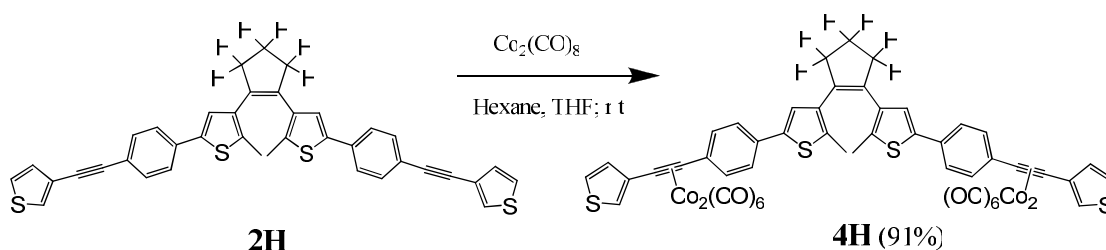

Scheme 2.23: Synthesis of 1,2-Bis(5'-(4''-phenyl-3'''-ethynylthiophene)-2'-methylthien-3'-yl)-cyclopentene [Co₂(CO)₆]₂ {**4H**}

Using the same procedure as described for **3H**, 1,2-Bis(5'-(4''-phenyl-3'''-ethynylthiophene)-2'-methylthien-3'-yl)-cyclopentene (**2H**) (0.100 g, 0.16 mmol) and Co₂(CO)₈ (0.121 g, 0.352 mmol) were reacted together. The crude product was purified on silica gel, with 100% hexane, followed by 9:1 hexane:diethyl ether, yielding a black solid as the pure product (0.174 g, 91%). ^{1}H NMR (400 MHz, (CD₃)₂CO): δ = 2.05 (s, 6H, CH₃), 2.09 (quintet, J=7.4 Hz, 2H, CH₂), 2.90 (t, J=7.4 Hz, 4H, CH₂), 7.35 (m, 4H, thienyl-H4 & ethynylthiophene-H5), 7.63-7.69 (m, 10H, ethynylthiophene-H4 & phenyl-H2,3,5,6), 7.80 (dd, 2H, J=3 Hz, 1.2 Hz, ethynylthiophene-H2) ppm. Anal. calc. for $C_{51}H_{28}S_4O_{12}Co_4$ (%): C 51.23, H 2.36; found: C 51.89, H 3.15. IR (THF, cm^{-1}) ν_{CO} = 2089, 2054, 2025.

2.3.19   Synthesis of the closed-ring isomer of 1,2-Bis(5'-(4''-phenyl-3'''-ethynyl-thiophene)-2'-methylthien-3'-yl)cyclopentene [Co₂(CO)₆]₂ {4bH}

In order to aid the analysis of the photochemical and electrochemical results of the open-ring isomer **4H**, a small amount of the closed-ring isomer **4bH** was synthesised, and the resulting compound was characterised by ^{1}H NMR and IR spectroscopy.
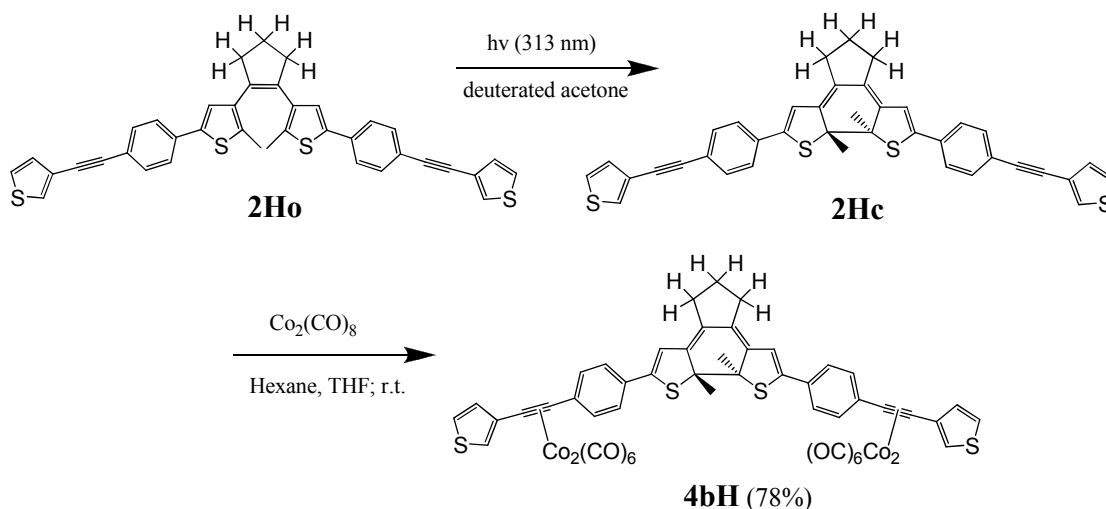
Scheme 2.24: Synthesis of the closed-ring isomer of 1,2-Bis(5'-(4''-phenyl-3'''-ethynylthiophene)-2'-methylthien-3'-yl)-cyclopentene [Co₂(CO)₆]₂ {**4bH**}

The open-ring isomer of 1,2-Bis(5'-(4''-phenyl-3'''-ethynylthiophene)-2'-methylthien-3'-yl)-cyclopentene (**2Ho)** (0.01 g, 0.016 mmol) was converted to the closed-ring isomer **4Hc** following irradiation with UV light (λ=313 nm) in deuterated acetone, whilst monitoring in the ^{1}H NMR. **4Hc** was reacted with Co₂(CO)₈ (0.014 g, 0.04 mmol), in a solvent mixture of hexane (12 mL) and THF (3 mL), following the same reaction procedure as described for **3bF**. Purification of the crude product was carried out on a silica gel column, and eluted with 100% hexane, followed by 9:1 hexane:CH₂Cl₂, yielding a dark purple product (0.015 g, 78%). ^{1}H NMR (400 MHz, (CD₃)₂CO): δ = 2.09 (s, 6H, CH₃), 2.12 (quintet, J=7.4 Hz, 2H, CH₂), 2.92 (t, J=7.4 Hz, 4H, CH₂), 6.82 (s, 2H, thienyl-H4), 7.35 (dd, J=5 Hz, 1.2 Hz, 2H, ethynylthiophene-H5), 7.65-7.72 (m, 10H, ethynylthiophene-H4 & phenyl-H2,3,5,6), 7.82 (dd, J=3 Hz, 1.2 Hz, 2H, ethynylthiophene-H2) ppm.   IR (THF, cm⁻¹) ν_{CO} = 2089, 2055, 2026.

2.3.20 Synthesis of 1,2-Bis(5'-(4''-phenyl-3'''-ethynylthiophene)-2'-methylthien-3'-yl)-perfluorocyclopentene [Co₂(CO)₆]₂ {4F}
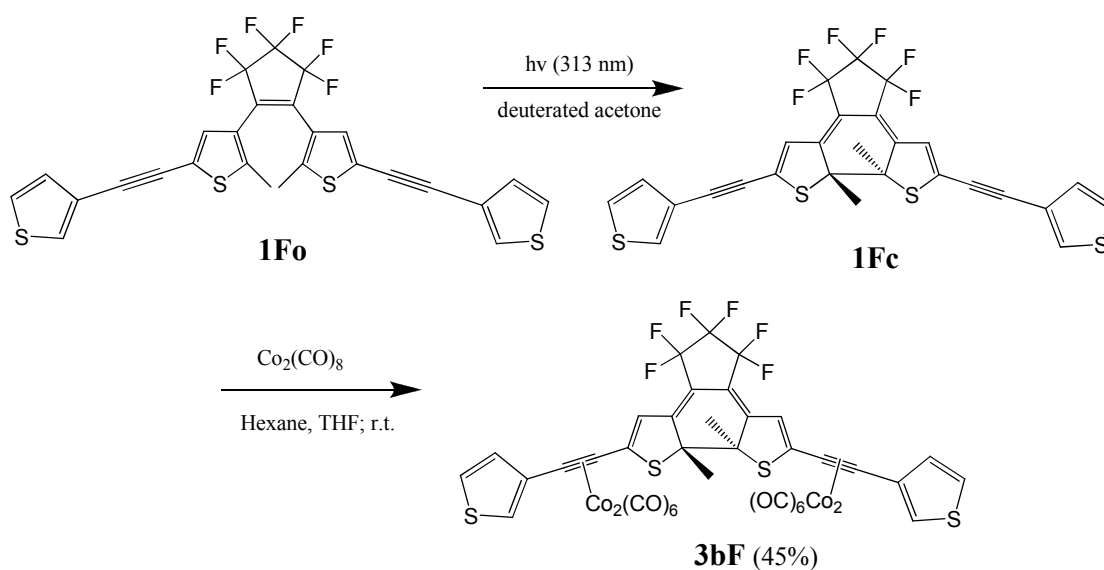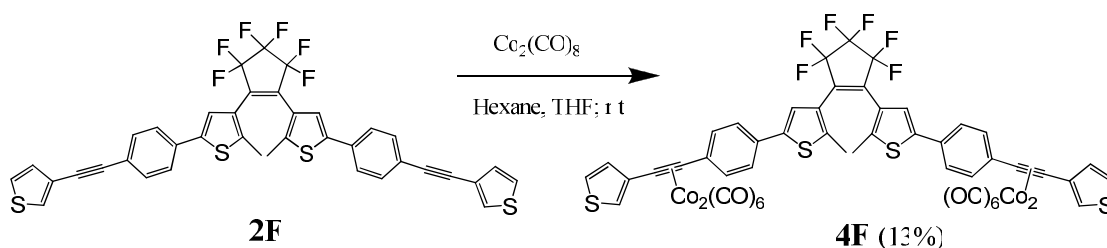

Scheme 2.25: Synthesis of 1,2-Bis(5'-(4''-phenyl-3'''-ethynylthiophene)-2'-methylthien-3'-yl)-perfluorocyclopentene [Co₂(CO)₆]₂ {**4F**}

1,2-Bis(5'-(4''-phenyl-3'''-ethynylthiophene)-2'-methylthien-3'-yl)perfluoro-cyclopentene (**2F**) (0.06 g, 0.082 mmol) and $Co_2(CO)_8$ (0.062 g, 0.180 mmol) were reacted together using the same method as described for **3H**. Column chromatography was used to purify the crude product, using silica gel and a solvent mixture of 9:1 hexane:CH_2Cl_2, yielding a dark brown/black solid (0.0137 g, 13%). ^{1}H NMR (400 MHz, $(CD_3)_2CO$): δ = 2.04 (s, 6H, CH_3), 7.35 (dd, J=5 Hz, 1.3 Hz, 2H, ethynylthiophene-H5), 7.61 (s, 2H, thienyl-H4), 7.65 (dd, J=5 Hz, 3 Hz, 2H, ethynylthiophene-H4), 7.73-7.78 (m, 8H, phenyl-H2,3,5,6), 7.82 (dd, J=3 Hz, 1.3 Hz, 2H, ethynylthiophene-H2) ppm. ^{19}F NMR (376.5 MHz, $CDCl_3$) δ = -110.04 (t, J=5.0 Hz, 4F), -131.81 (quintet, J=5.0 Hz, 2F). IR (THF, cm^{-1}) v_{CO} = 2090, 2055, 2026.

2.3.21 Synthesis of 1,2-Bis(5'-ethynylferrocene-2'-methylthien-3'-yl)-cyclopentene [Co$_2$(CO)$_6$]$_2$ {9H}
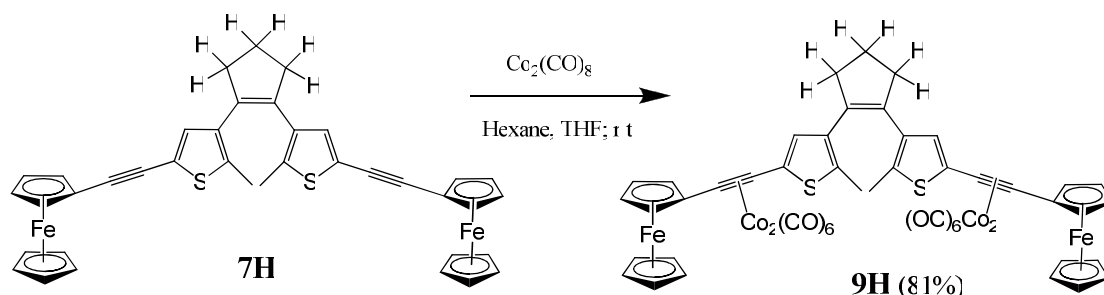
Scheme 2.26: Synthesis of 1,2-Bis(5'-ethynylferrocene-2'-methylthien-3'-yl)-cyclopentene [Co$_2$(CO)$_6$]$_2$ {**9H**}

Co$_2$(CO)$_8$ (0.112 g, 0.325 mmol) was added to a flask containing 1,2-Bis(5'-ethynylferrocene-2'-methylthien-3'-yl)-cyclopentene (**7H**) (0.100 g 0.148 mmol), dissolved in hexane (30 mL) and dry THF (20 mL), under the same reaction conditions as described for **3H**. The crude product was purified by column chromatography, on silica gel. 100% hexane was used as the mobile phase initially, and the polarity was increased to 9:1 hexane:diethyl ether, yielding a black solid (0.149 g, 81%). ^{1}H NMR (400 MHz, (CD$_3$)$_2$CO) δ = 2.08 (s, 6H, CH$_3$), 2.15 (quintet, J=7.3 Hz, 2H, CH$_2$), 2.95 (t, J=7.3 Hz, 4H, CH$_2$), 4.28 (s, 10H, Fc-Cp), 4.51 (t, J=1.8 Hz, 4H, Fc-H3,4), 4.575 (t, J=1.8 Hz, 4H, Fc-H2,5), 7.47 (s, 2H, thienyl-H4) ppm. Anal. calc. for C$_{51}$H$_{32}$S$_2$Fe$_2$O$_{12}$Co$_4$ (%): C 49.11, H 2.59; found: C 49.16, H 3.01. IR (THF, cm^{-1}) ν_{CO} = 2086, 2050, 2022.

2.3.22 Synthesis of 1,2-Bis(5'-ethynylferrocene-2'-methylthien-3'-yl)perfluoro-cyclopentene [Co₂(CO)₆]₂ {9F}
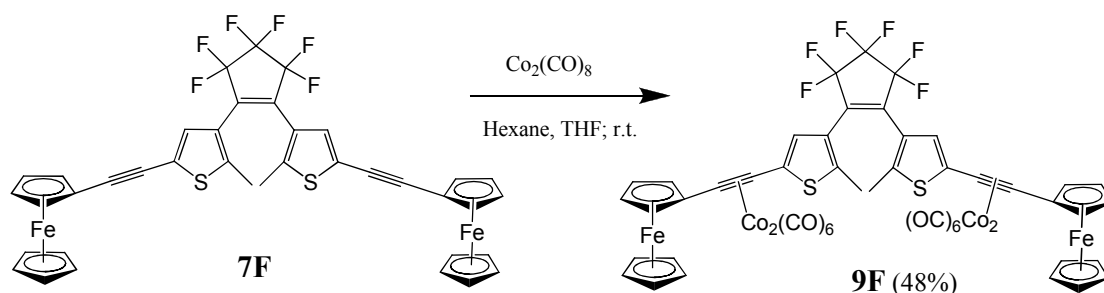
Scheme 2.27: Synthesis of 1,2-Bis(5'-ethynylferrocene-2'-methylthien-3'-yl)perfluoro-cyclopentene [Co₂(CO)₆]₂ {**9F**}

Using the same procedure as described for **3H**, 1,2-Bis(5'-ethynylferrocene-2'-methylthien-3'-yl)perfluorocyclopentene (**7F**) (0.1928 g, 0.246 mmol) was reacted with $Co_2(CO)_8$ (0.1848 g, 0.541 mmol), in hexane (40 mL) and dry THF (30 mL). The crude was purified on a silica gel column with 100% hexane, followed by 9:1 hexane:CH_2Cl_2, and a black solid was obtained (0.159 g, 48%). ^1H NMR (400 MHz, $(CD_3)_2CO$) δ = 2.14 (s, 6H, CH₃), 4.28 (s, 10H, Fc-Cp), 4.54 (t, J=1.5 Hz, 4H, Fc-H3,4), 4.58 (t, J=1.5 Hz, 4H, Fc-H2,5), 7.74 (s, 2H, thienyl-H4) ppm. ^{19}F NMR (376.5 MHz, $CDCl_3$) δ = -109.88 (t, J=5.0 Hz, 4F), -131.69 (quintet, J=5.0 Hz, 2F). Anal. calc. for $C_{51}H_{26}F_6S_2Fe_2O_{12}Co_4$ (%): C 45.20, H 1.93; found: C 46.57, H 2.16. IR (THF, cm⁻¹) ν_{CO} = 2089, 2053, 2026.

2.3.23 Synthesis of 1,2-Bis(5'-(4''-phenyl-ethynylferrocene)-2'-methylthien-3'-yl)-cyclopentene [Co$_2$(CO)$_6$]$_2$ {10H}
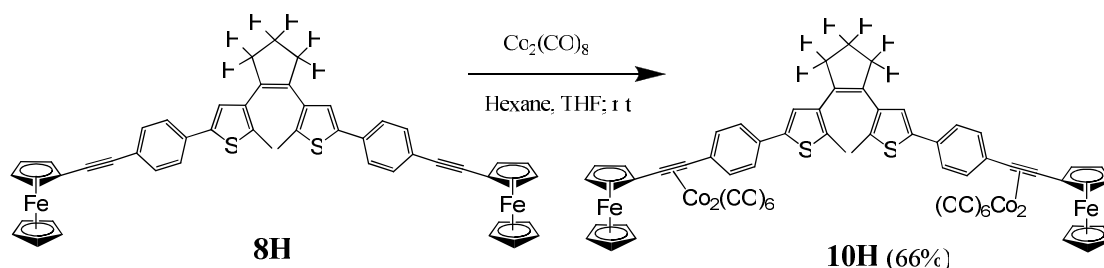
Scheme 2.28: Synthesis of 1,2-Bis(5'-(4''-phenyl-ethynylferrocene)-2'-methylthien-3'-yl)-cyclopentene [Co$_2$(CO)$_6$]$_2$ {**10H**}

1,2-Bis(5'-(4''-phenyl-ethynylferrocene)-2'-methylthien-3'-yl)-cyclopentene **(8H)** (0.085 g, 0.103 mmol) and Co$_2$(CO)$_8$ (0.0775 g, 0.227 mmol) were reacted together under the same conditions as described for **3H**. Column chromatography was used to purify the crude product, using silica gel and 100% hexane, followed by 9:1 hexane:CH$_2$Cl$_2$. The pure product was obtained as a black solid (0.0945 g, 66%). ^{1}H NMR (400 MHz, (CD$_3$)$_2$CO) δ = 2.07 (s, 6H, CH$_3$), 2.14 (quintet, J=7.4 Hz, 2H, CH$_2$), 2.91 (t, J=7.4 Hz, 4H, CH$_2$), 4.25 (s, 10H, Fc-Cp), 4.53 (t, J=1.8 Hz, 4H, Fc-H3,4), 4.59 (t, J=1.8 Hz, 4H, Fc-H2,5), 7.41 (s, 2H, thienyl-H4), 7.77 (d, J=8.4 Hz, 4H, phenyl-H2,6), 7.98 (d, J=8.4 Hz, 4H, phenyl-H3,5) ppm. Anal. calc. for C$_{63}$H$_{40}$S$_2$Fe$_2$O$_{12}$Co$_4$ (%): C 54.06, H 2.88; found: C 51.16, H 3.08. IR (THF, cm^{-1}) ν_{CO} = 2086, 2050, 2022.

2.3.24 Synthesis of 1,2-Bis(5'-(4''-phenyl-ethynylferrocene)-2'-methylthien-3'-yl)perfluorocyclopentene [Co$_2$(CO)$_6$]$_2$ {10F}

Scheme 2.29: Synthesis of 1,2-Bis(5'-(4''-phenyl-ethynylferrocene)-2'-methylthien-3'-yl)-perfluorocyclopentene [Co$_2$(CO)$_6$]$_2$ {**10F**}

The same procedure as described for **3H** was followed, starting with 1,2-Bis(5'-(4''-phenyl-ethynylferrocene)-2'-methylthien-3'-yl)perfluorocyclopentene (**8F**) (0.04 g 0.043 mmol) and Co$_2$(CO)$_8$ (0.032 g, 0.094 mmol). The crude product was purified on a silica gel column using 100% hexane, followed by 9:1 hexane:CH$_2$Cl$_2$, as the eluent and a black solid was obtained (0.059 g, 92%). ^{1}H NMR (400 MHz, (CD$_3$)$_2$CO) δ = 2.11 (s, 6H, CH$_3$), 4.26 (s, 10H, Fc-Cp), 4.54 (t, J=1.8 Hz, 4H, Fc-H3,4), 4.61 (t, J=1.8 Hz, 4H, Fc-H2,5), 7.67 (s, 2H, thienyl-H4), 7.88 (d, J=8.4 Hz, 4H, phenyl-H2,6), 8.04 (d, J=8.4 Hz, 4H, phenyl-H3,5) ppm. ^{19}F NMR (376.5 MHz, CDCl$_3$) δ = -110.02 (t, J=5.0 Hz, 4F), -131.74 (quintet, J=5.0 Hz, 2F). Anal. calc. for C$_{63}$H$_{34}$F$_6$S$_2$Fe$_2$O$_{12}$Co$_4$ (%): C 50.19, H 2.27; found: C 47.72, H 2.37. IR (THF, cm^{-1}) ν_{CO} = 2086, 2051, 2022.

2.3.25 Synthesis of the closed-ring isomer of 1,2-Bis(5'-(4''-phenyl-ethynyl-ferrocene)-2'-methylthien-3'-yl)perfluorocyclopentene [Co₂(CO)₆]₂ {10bF}

In order to elucidate the photochemical results obtained for the open-ring isomer **10F**, a small amount of its corresponding closed-ring isomer **10bF** was synthesised. Due to the limited amount of **10bF** available for further studies, this compound was characterised by ^{1}H NMR and IR spectroscopy only.
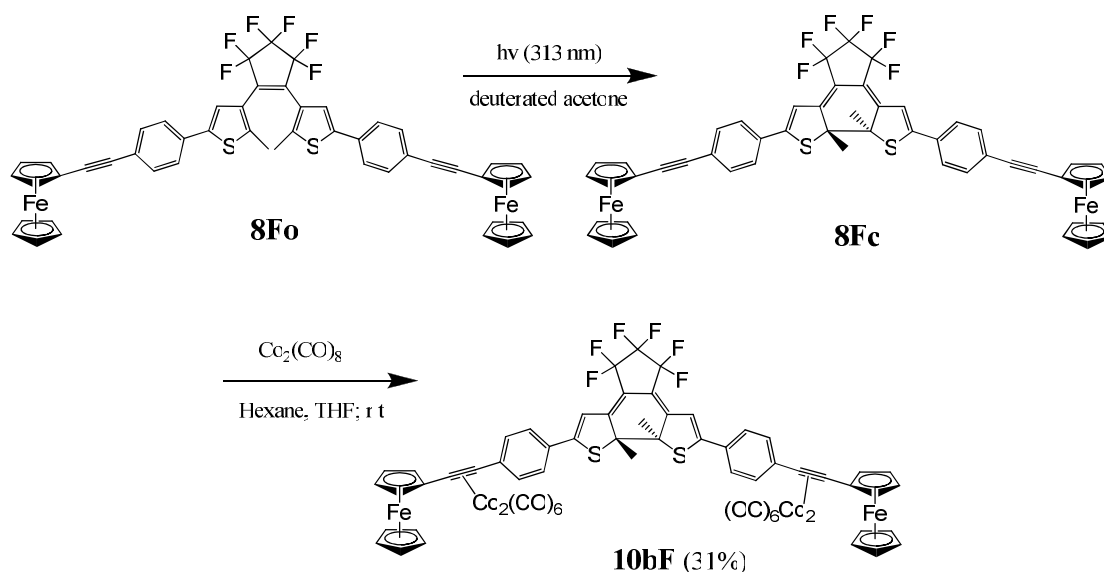
Scheme 2.30: Synthesis of the closed-ring isomer of 1,2-Bis(5'-(4''-phenyl-ethynylferrocene)-2'-methylthien-3'-yl)-perfluorocyclopentene [Co₂(CO)₆]₂ {**10bF**}.

1,2-Bis(5'-(4''-phenyl-ethynyl-ferrocene)-2'-methylthien-3'-yl)perfluorocyclopentene {**8F**} (0.01 g, 0.011 mmol) was irradiated with UV light at λ = 313 nm, in deuterated acetone, in order to induce cyclisation from the open-ring isomer {**8Fo**} to the closed-ring isomer {**8Fc**}. This process was followed using ^{1}H NMR spectroscopy. The corresponding Co₂(CO)₆ complex {**10bF**} was synthesised by reacting **8Fc** with Co₂(CO)₈ (0.009 g, 0.027 mmol), in a degassed solution of hexane (12 mL) and THF (3 mL), and the reaction mixture was stirred under N₂ overnight, in the dark. Purification of the crude product was carried out on a silica gel column, using 9:1 hexane:CH₂Cl₂, followed by 8:2 hexane:CH₂Cl₂, as the eluent. A dark blue product was obtained (0.005 g, 31%). ^{1}H NMR (400 MHz, (CD₃)₂CO) δ = 2.27 (s, 6H, CH₃), 4.27 (s, 10H, Fc-Cp), 4.56 (t, J=1.8 Hz, 4H, Fc-H3,4), 4.62 (t, J=1.8 Hz, 4H, Fc-H2,5), 7.09 (s, 2H, thienyl-H4), 7.97 (d, J=8.4 Hz, 4H, phenyl-H2,6), 8.10 (d, J=8.4 Hz, 4H, phenyl-H3,5) ppm. IR (THF, cm^{-1}) ν_{CO} = 2087, 2052, 2024.
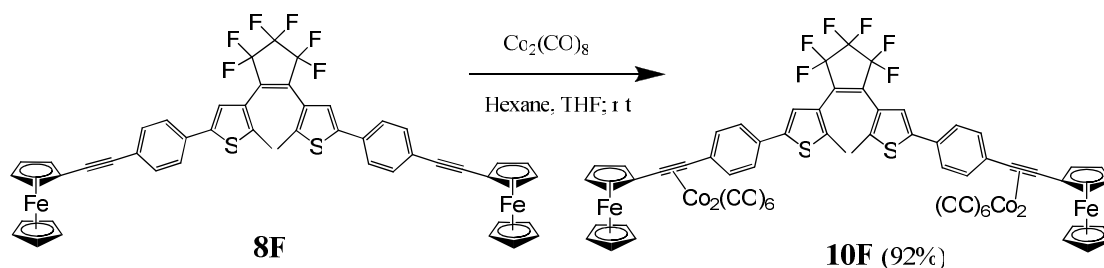
2.3.26 Synthesis of 1,2-Bis(5'-(3''-ethynylthiophene)-2'-methylthien-3'-yl)-cyclopentene [Co₂(CO)₄dppm]₂ {5H}
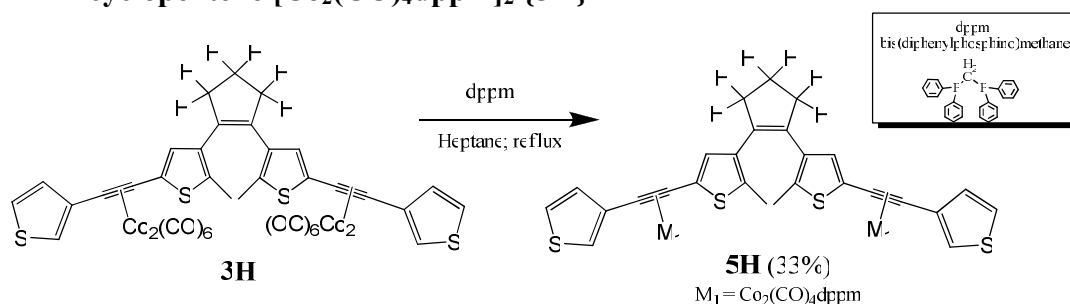
Scheme 2.31: Synthesis of 1,2-Bis(5'-(3''-ethynylthiophene)-2'-methylthien-3'-yl)-cyclopentene [Co₂(CO)₄dppm]₂ {**5H**}; and inset, the structure of bis(diphenylphosphino)methane

Bis(diphenylphosphino)methane {dppm} (0.101 g, 0.263 mmol) was added to heptane (65 mL) in an oven-dried round-bottomed flask and the solution was purged with nitrogen for 20 minutes. The reaction mixture was heated and, once the solution began to reflux, 1,2-Bis(5'-(3''-ethynylthiophene)-2'-methylthien-3'-yl)-cyclopentene [Co₂(CO)₆]₂ (**3H**) (0.1247 g, 0.119 mmol) was added to the flask. The solution was left to reflux for 40 minutes under an inert atmosphere. Once the flask had cooled, the solvent was removed under vacuum, and the product was purified by column chromatography. It was passed through a silica gel column, with a mobile phase consisting of 7:3 hexane:CH₂Cl₂, and the pure product was obtained as a pink/brown solid (0.0662 g, 33%). ^{1}H NMR (600 MHz, (CD₃)₂CO): δ = 1.84 (s, 6H, CH₃), 2.03 (quintet, J=7.5 Hz, 2H, CH₂), 2.67 (t, J=7.5 Hz, 4H, CH₂), 3.64 (t, J=10.6 Hz, 4H, dppm-CH₂), 6.82 (s, 2H, thienyl-H4), 7.15-7.44 (m, 46H, ethynylthiophene-H2,4,5 & phenyl-dppm) ppm. ^{13}C NMR (150 MHz, CDCl₃) δ = 14.38 (s, 2C, CH₃), 22.82 (s, 1C, CH₂), 34.36 (t, 2C, CH₂), 38.94 (s, 2C, CH₂), 83.19 (s, 2C, Cq), 88.12 (s, 2C, Cq), 121.24 (s, 2C, CH), 125.43 (s, 2C, CH), 127.80 (s, 2C, CH), 128.26 (m, 8C, CH), 128.36 (m, 8C, CH), 129.27 (s, 2C, CH), 129.51 (s, 4C, CH), 129.66 (s, 4C, CH), 131.50 (m, 8C, CH), 131.97 (m, 8C, CH), 134.38 (s, 2C, Cq), 134.44 (s, 2C, Cq), 136.19 (s, 2C, Cq), 136.44 (br, 4C, Cq), 136.97 (br, 4C, Cq), 142.17 (s, 2C, Cq), 143.16 (s, 2C, Cq), 204.43 (br, 4C, CO), 207.51 (br, 4C, CO) ppm. ^{31}P NMR (242.9 MHz, CDCl₃): δ = 37.37 (s, 4P) ppm. Anal. calc. for C₈₅H₆₄S₄O₈Co₄P₄ (%): C 60.04, H 3.79; found: C 56.03, H 3.94. IR (THF, cm^{-1}) ν$_{CO}$ = 2022, 1998, 1971, 1952 (sh).

2.3.27 Synthesis of 1,2-Bis(5'-(3''-ethynylthiophene)-2'-methylthien-3'-yl)-perflourocyclopentene [Co₂(CO)₄dppm]₂ {5F}
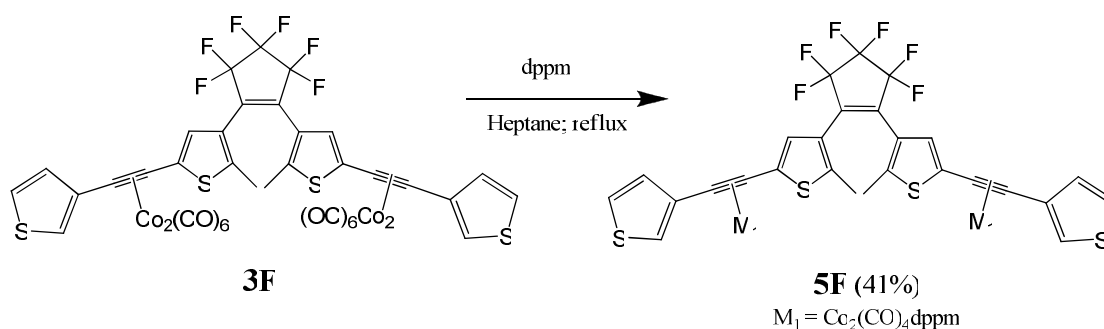
Scheme 2.32: Synthesis of 1,2-Bis(5'-(3''-ethynylthiophene)-2'-methylthien-3'-yl)-perfluorocyclopentene [Co₂(CO)₄dppm]₂ {**5F**}

Using the same procedure as described for **5H**, 1,2-Bis(5'-(3''-ethynylthiophene)-2'-methylthien-3'-yl)perflourocyclopentene [Co₂(CO)₆]₂ (**3F**) (0.1138 g, 0.099 mmol) and bis(diphenylphosphino)methane (0.0835 g, 0.217 mmol) were reacted together, and the crude product was purified on a silica gel column, with a solvent mixture of 7:3 hexane:CH₂Cl₂. A pink/brown solid was obtained (0.0734 g, 41%). ^{1}H NMR (400 MHz, (CD₃)₂CO): δ = 1.87 (s, 6H, CH₃), 3.58-3.75 (m, 4H, dppm-CH₂), 7.04 (s, 2H, thienyl-H4), 7.13-7.50 (m, 46H, ethynylthiophene-H2,4,5 & phenyl-dppm) ppm. ^{13}C NMR (150 MHz, CDCl₃) δ = 14.28 (s, 2C, CH₃), 34.29 (t, 2C, CH₂), 81.82 (s, 2C, Cq), 88.78 (s, 2C, Cq), 121.54 (s, 2C, CH), 124.89 (s, 2C, Cq), 125.62 (s, 2C, CH), 128.33 (m, 8C, CH), 128.43 (m, 8C, CH), 128.84 (s, 2C, CH), 129.06 (s, 2C, CH), 129.65 (s, 4C, CH), 129.77 (s, 4C, CH), 131.30 (m, 8C, CH), 131.96 (m, 8C, CH), 136.04 (br, 4C, Cq), 136.77 (br, 4C, Cq), 141.10 (s, 2C, Cq), 142.80 (s, 2C, Cq) 145.35 (s, 2C, Cq), 203.46 (br, 4C, CO), 204.81 (br, 4C, CO) ppm. ^{19}F NMR (376.5 MHz, CDCl₃) δ = -110.07 (t, J=5.3 Hz, 4F), -131.69 (quintet, J=5.3 Hz, 2F). ^{31}P NMR (242.9 MHz, CDCl₃): δ = 36.90 (s, 4P) ppm. Anal. calc. for C₈₅H₅₈F₆S₄O₈Co₄P₄ (%): C 56.46, H 3.23; found: C 56.98, H 3.49. IR (THF, cm^{-1}) ν_{CO} = 2025, 2000, 1974, 1954 (sh).

2.3.28 Synthesis of 1,2-Bis(5'-(4''-phenyl-3'''-ethynylthiophene)-2'-methylthien-3'-yl)-cyclopentene [Co$_2$(CO)$_4$dppm]$_2$ {6H}
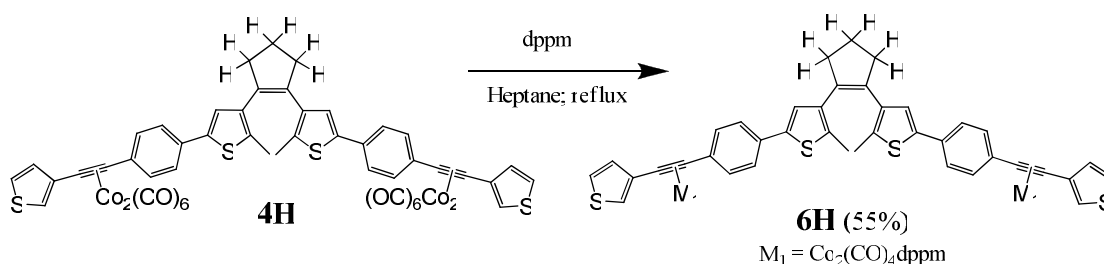
Scheme 2.33: Synthesis of 1,2-Bis(5'-(4''-phenyl-3'''-ethynylthiophene)-2'-methylthien-3'-yl)-cyclopentene [Co$_2$(CO)$_4$dppm]$_2$ {**6H**}

1,2-Bis(5'-(4''-phenyl-3'''-ethynylthiophene)-2'-methylthien-3'-yl)-cyclopentene [Co$_2$(CO)$_6$]$_2$ (**4H**) (0.113 g, 0.094 mmol) and bis(diphenylphosphino)methane (0.08 g, 0.208 mmol) were added to a reaction flask and refluxed in heptane (65 mL) under the same reaction conditions as described for **5H**. The crude product was purified by passing it through a silica gel column, using a solvent mixture of 7:3 hexane:CH$_2$Cl$_2$ as the eluent, yielding a pink-brown solid (0.096 g, 55%). ^{1}H NMR (400 MHz, (CD$_3$)$_2$CO): δ = 2.03 (s, 6H, CH$_3$), 2.09 (quintet, J=7.5 Hz, 2H, CH$_2$), 2.89 (t, J=7.5 Hz, 4H, CH$_2$), 3.58 (t, J=10.4 Hz, 4H, dppm-CH$_2$), 7.02 (s, 2H, thienyl-H4), 7.13-7.49 (m, 54H, phenyl-H2,3,5,6 & ethynylthiophene-H2,4,5 & phenyl-dppm) ppm. ^{13}C NMR (150 MHz, CDCl$_3$) δ = 14.72 (s, 2C, CH$_3$), 23.11 (s, 1C, CH$_2$), 34.34 (t, 2C, CH$_2$), 38.78 (s, 2C, CH$_2$), 87.58 (s, 2C, Cq), 94.06 (s, 2C, Cq), 121.11 (s, 2C, CH), 123.63 (s, 2C, CH), 125.41 (s, 4H, CH), 125.60 (s, 2C, CH), 128.25 (m, 8C, CH), 128.39 (m, 8C, CH), 129.30 (s, 2C, CH), 129.52 (s, 4C, CH), 129.65 (s, 4C, CH), 129.73 (s, 4C, CH), 131.40 (m, 8C, CH), 131.91 (m, 8C, CH), 132.27 (s, 2C, Cq), 134.28 (s, 2C, Cq), 134.69 (s, 2C, Cq), 136.03 (br, 4C, Cq), 136.92 (s, 2C, Cq), 137.10 (br, 4C, Cq), 140.11 (s, 2C, Cq), 142.03 (s, 2C, Cq), 143.28 (s, 2C, Cq), 204.25 (br, 4C, CO), 205.11 (br, 4C, CO) ppm. ^{31}P NMR (242.9 MHz, CDCl$_3$): δ = 36.92 (s, 4P) ppm. Anal. calc. for C$_{97}$H$_{72}$S$_4$O$_8$Co$_4$P$_4$ (%): C 62.89, H 3.92; found: C 62.15, H 4.08. IR (THF, cm^{-1}) ν$_{CO}$ = 2021, 1996, 1970, 1949 (sh).

*NOTE: The perfluorocyclopentene derivative of **6H** was not synthesised as there was not enough of the cobalt hexacarbonyl product (**5F**) available to carry out the synthesis.

2.3.29 Synthesis of 1,2-Bis(5'-ethynylferrocene-2'-methylthien-3'-yl)-cyclopentene [Co$_2$(CO)$_4$dppm]$_2$ {11H}

Scheme 2.34: Synthesis of 1,2-Bis(5'-ethynylferrocene-2'-methylthien-3'-yl)-cyclopentene [Co$_2$(CO)$_4$dppm]$_2$ {**11H**}

Following the same synthetic method as described for **5H**, 2-Bis(5'-ethynylferrocene-2'-methylthien-3'-yl)-cyclopentene [Co$_2$(CO)$_6$]$_2$ (**9H**) (0.100 g, 0.08 mmol) was reacted with bis(diphenylphosphino)methane (0.068 g, 0.176 mmol). The crude product was purified on a silica gel column, and was eluted with 100% hexane, followed by 9:1, and then 8:2, hexane:diethyl ether. The 3rd band was collected, and a dark pink/brown compound was obtained as the pure product (0.119 g, 78%). ^{1}H NMR (400 MHz, (CD$_3$)$_2$CO) δ = 2.09 (s, 6H, CH$_3$), 2.14 (quintet, J=7.5 Hz, 2H, CH$_2$), 2.78 (t, J=7.5 Hz, 4H, CH$_2$), 3.60-3.69 (m, 4H, CH$_2$-dppm), 4.10 (s, 10H, Fc-Cp), 4.35 (t, J=1.8 Hz, 4H, Fc-H3,4), 4.42 (t, J=1.8 Hz, 4H, Fc-H2,5), 7.01 (s, 2H, thienyl-H4), 7.16-7.43 (m, 40H, phenyl-dppm) ppm. ^{13}C NMR (150 MHz, CDCl$_3$) δ = 14.22 (s, 2C, CH$_3$), 22.47 (s, 1C, CH$_2$), 34.95 (t, 2C, CH$_2$), 39.53 (s, 2C, CH$_2$), 65.41 (s, 2C, Cq), 68.29 (s, 4C, CH), 69.50 (s, 10C, CH), 69.93 (s, 4C, CH), 85.46 (s, 2C, Cq), 90.17 (s, 2C, Cq), 127.57 (s, 2C, CH), 128.19 (m, 8C, CH), 128.28 (m, 8C, CH), 129.51 (s, 8C, CH), 131.67 (m, 8C, CH), 132.02 (m, 8C, CH), 134.10 (s, 2C, CH), 134.68 (s, 2C, CH), 136.05 (s, 2C, CH), 136.49 (br, 4C, Cq), 136.92 (br, 4C, Cq), 143.31 (s, 2C, Cq), 204.13 (br, 4C, CO), 205.12 (br, 4C, CO) ppm. ^{31}P NMR (242.9 MHz, CDCl$_3$) δ = 36.05 (s, 4P) ppm. Anal. calc. for C$_{97}$H$_{76}$S$_2$Fe$_2$O$_8$Co$_4$P$_4$ (%): C 61.18, H 4.02; found: C 61.35, H 4.25. IR (THF, cm^{-1}) ν_{CO} = 2019, 1994, 1968, 1949 (sh).

2.3.30 Synthesis of 1,2-Bis(5'-ethynylferrocene-2'-methylthien-3'-yl)perflouro-cyclopentene [Co$_2$(CO)$_4$dppm]$_2$ {11F}
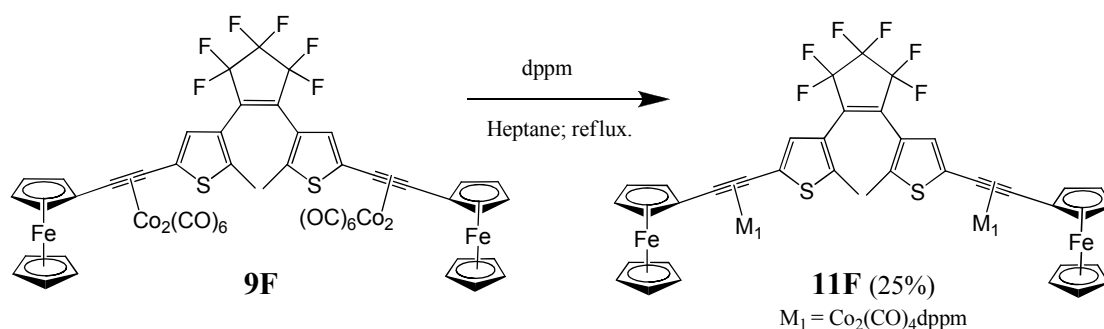
Scheme 2.35: Synthesis of 1,2-Bis(5'-ethynylferrocene-2'-methylthien-3'-yl)perfluoro-cyclopentene [Co$_2$(CO)$_4$dppm]$_2$ {**11F**}

1,2-Bis(5'-ethynylferrocene-2'-methylthien-3'-yl)perflouro-cyclopentene [Co$_2$(CO)$_6$]$_2$ (**9F**) (0.0814 g, 0.060 mmol) and bis(diphenylphosphino)methane (0.0508 g, 0.132 mmol) were refluxed in heptane (65 mL) under the same conditions as described for **5H**. Purification of the crude product was achieved by column chromatography, using a silica gel column and a solvent mixture of 7:3 hexane:CH$_2$Cl$_2$, yielding a dark pink/brown solid (0.03 g, 25%). ^{1}H NMR (400 MHz, (CD$_3$)$_2$CO) δ = 1.97 (s, 6H, CH$_3$), 3.60-3.78 (m, 4H, CH$_2$-dppm), 4.08 (s, 10H, Fc-Cp), 4.37 (t, J=1.8 Hz, 4H, Fc-H3,4), 4.42 (t, J=1.7 Hz, 4H, Fc-H2,5), 7.15-7.43 (m, 42H, thienyl-H4 & phenyl-dppm) ppm. ^{13}C NMR (150 MHz, CDCl$_3$) δ = 14.68 (s, 2C, CH$_3$), 34.26 (t, 2C, CH$_2$), 65.99 (s, 2C, Cq), 68.51 (s, 4C, CH), 69.43 (s, 10C, CH), 69.94 (s, 4C, CH), 82.18 (s, 2C, Cq), 89.67 (s, 2C, Cq), 124.72 (s, 2C, CH), 124.94 (s, 2C, Cq), 128.17 (m, 8C, CH), 128.43 (m, 8C, CH), 129.44 (s, 4C, CH), 129.76 (s, 4C, CH), 130.94 (m, 8C, CH), 132.37 (m, 8C, CH), 136.24 (br, 4C, Cq), 137.43 (br, 4C, Cq), 141.60 (s, 2C, Cq), 146.53 (s, 2C, Cq), 203.37 (br, 4C, CO), 205.76 (br, 4C, CO) ppm (C-F resonances not located). ^{19}F NMR (376.5 MHz, CDCl$_3$) δ = -109.76 (t, J=5.0 Hz, 4F), -131.63 (quintet, J=5.0 Hz, 2F). ^{31}P NMR (242.9 MHz, CDCl$_3$) δ = 35.47 (s, 4P) ppm. Anal. calc. for C$_{97}$H$_{70}$F$_6$S$_2$Fe$_2$O$_8$Co$_4$P$_4$ (%): C 57.90, H 3.51; found: C 55.79, H 3.76. IR (THF, cm^{-1}) ν_{CO} = 2021, 1996, 1970, 1951 (sh).

2.3.31 Synthesis of 1,2-Bis(5'-(4''-phenyl-ethynylferrocene)-2'-methylthien-3'-yl)cyclopentene [Co₂(CO)₄dppm]₂ {12H}
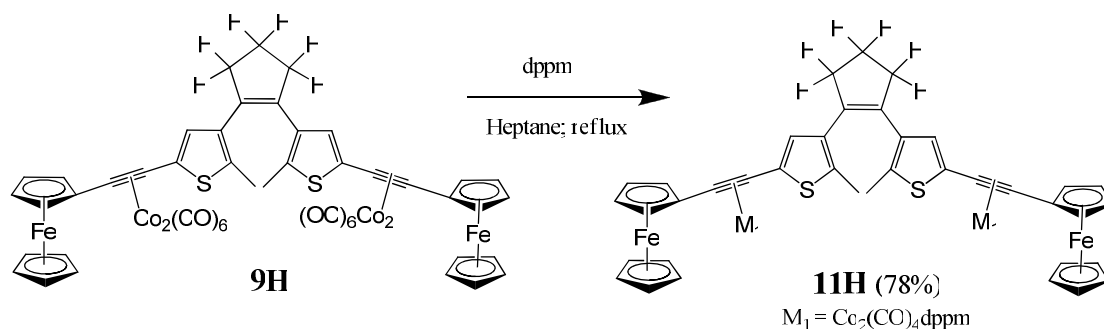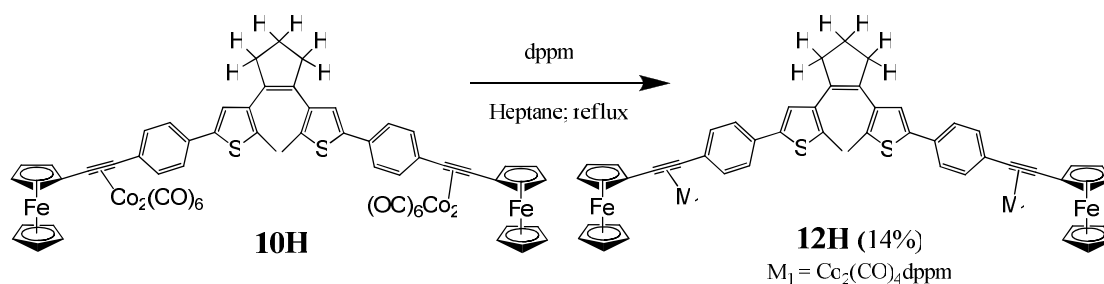

Scheme 2.36: Synthesis of 1,2-Bis(5'-(4''-phenyl-ethynylferrocene)-2'-methylthien-3'-yl)-cyclopentene [Co₂(CO)₄dppm]₂ {**12H**}

The same procedure as described for **5H** was followed, starting with 1,2-Bis(5'-(4''-phenyl-ethynylferrocene)-2'-methylthien-3'-yl)cyclopentene [Co₂(CO)₆]₂ (**10H**) (0.14 g, 0.100 mmol) and bis(diphenylphosphino)methane (0.0846 g, 0.220 mmol). The crude product was purified on a silica gel column, using a mixture of 7:3 hexane:CH₂Cl₂ as the eluent, and a dark pink/brown compound was obtained (0.029 g, 14%). ^{1}H NMR (400 MHz, (CD₃)₂CO) δ = 2.08 (s, 6H, CH₃), 2.15 (quintet, J=7.4 Hz, 2H, CH₂), 2.92 (t, J=7.4 Hz, 4H, CH₂), 3.55 (t, J=10.7 Hz, 4H, dppm-CH₂), 3.94 (s, 10H, Fc-Cp), 4.32 (s, 8H, Fc-H2,3,4,5), 7.14-7.34 (m, 42H, phenyl-dppm, thienyl-H4), 7.60 (d, J=8.1 Hz, 4H, phenyl-H2,6), 7.71 (d, J=8.1 Hz, 4H, phenyl-H3,5) ppm. ^{13}C NMR (150 MHz, CDCl₃) δ = 14.75 (s, 2C, CH₃), 23.19 (s, 1C, CH₂), 34.71 (t, 2C, CH₂), 38.84 (s, 2C, CH₂), 65.99 (s, 2C, Cq), 68.25 (s, 4C, CH), 69.33 (s, 10C, CH), 70.27 (s, 4C, CH), 84.33 (s, 2C, Cq), 90.19 (s, 2C, Cq), 123.66 (s, 2C, CH), 125.20 (s, 4C, CH), 128.24 (m, 16C, CH), 129.51 (s, 8C, CH), 130.33 (s, 4C, CH), 131.80 (m, 16C, CH), 132.09 (s, 2C, Cq), 134.30 (s, 2C, Cq), 134.75 (s, 2C, Cq), 136.71 (br, 8C, Cq), 137.01 (s, 2C, Cq), 140.23 (s, 2C, Cq), 142.98 (s, 2C, Cq), 204.84 (br, 4C, CO), 205.03 (br, 4C, CO) ppm. ^{31}P NMR (242.9 MHz, CDCl₃): δ = 36.28 (s, 4P) ppm. Anal. calc. for C₁₀₉H₈₄S₂Fe₂O₈Co₄P₄ (%): C 63.67, H 4.12; found: C 63.74, H 4.34. IR (THF, cm⁻¹) ν_{CO} = 2018, 1992, 1966, 1947 (sh).

2.3.32 Synthesis of 1,2-Bis(5'-(4''-phenyl-ethynylferrocene)-2'-methylthien-3'-yl)perfluorocyclopentene [Co$_2$(CO)$_4$dppm]$_2$ {12F}
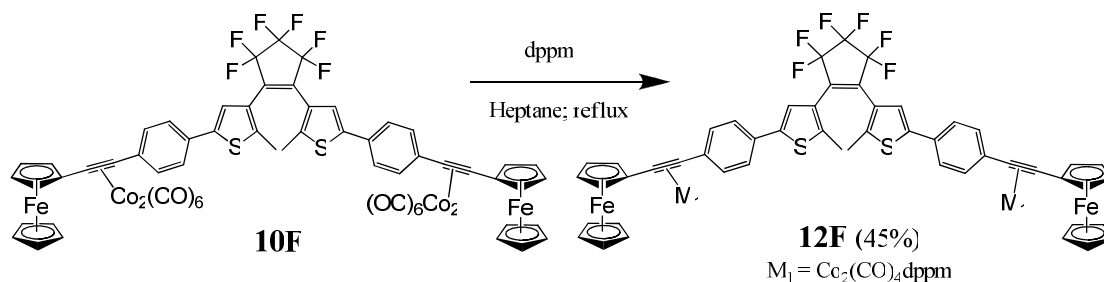
Scheme 2.37: Synthesis of 1,2-Bis(5'-(4''-phenyl-ethynylferrocene)-2'-methylthien-3'-yl)-cyclopentene [Co$_2$(CO)$_4$dppm]$_2$ {**12F**}

Under the same reaction conditions as described for **5H**, 1,2-Bis(5'-(4''-phenyl-ethynylferrocene)-2'-methylthien-3'-yl)perfluorocyclopentene [Co$_2$(CO)$_6$]$_2$ (**10F**) (0.055 g, 0.037 mmol) and bis(diphenylphosphino)methane (0.031 g, 0.081 mmol) were refluxed in heptane (65 mL). The crude product was passed through a silica gel column, using 8:2 hexane:diethyl ether, and the pure product was obtained as a dark pink/brown solid (0.036 g, 45%). ^{1}H NMR (400 MHz, (CD$_3$)$_2$CO) δ = 2.12 (s, 6H, CH$_3$), 3.29-3.41 (m, J=10.7 Hz, 4H, dppm-CH$_2$), 3.94 (s, 10H, Fc-Cp), 4.32-4.34 (m, 8H, Fc-H2,3,4,5), 7.14-7.34 (m, 40H, phenyl-dppm), 7.59 (s, 2H, thienyl-H4), 7.70 (d, J=8.3 Hz, 4H, phenyl-H2,6), 7.78 (d, J=8.1 Hz, 4H, phenyl-H3,5) ppm. ^{13}C NMR (150 MHz, CDCl$_3$) δ = 14.57 (s, 2C, CH$_3$), 34.57 (t, 2C, CH$_2$), 66.95 (s, 2C, Cq), 68.46 (s, 4C, CH), 69.50 (s, 10C, CH), 70.29 (s, 4C, CH), 83.71 (s, 2C, Cq), 89.36 (s, 2C, Cq), 121.90 (s, 2C, CH), 125.44 (s, 4C, CH), 126.16 (s, 2C, Cq), 128.24 (m, 16C, CH), 129.51 (s, 4C, CH), 129.59 (s, 4C, CH), 130.43 (s, 4C, CH), 130.75 (s, 2C, Cq), 131.81 (m, 16C, CH), 136.28 (br, 4C, Cq), 137.03 (br, 4C, Cq), 141.05 (s, 2C, Cq), 142.75 (s, 2C, Cq), 144.34 (s, 2C, Cq), 204.91 (br, 4C, CO), 205.15 (br, 4C, CO) ppm (C-F resonances not located). ^{19}F NMR (376.5 MHz, CDCl$_3$) δ = -109.88 (t, J=4.9 Hz, 4F), -131.77 (quintet, J=4.9 Hz, 2F). ^{31}P NMR (242.9 MHz, CDCl$_3$): δ = 36.26 (s, 4P) ppm. Anal. calc. for C$_{109}$H$_{78}$F$_6$S$_2$Fe$_2$O$_8$Co$_4$P$_4$ (%): C 60.49, H 3.63; found: C 54.96, H 4.06. IR (THF, cm^{-1}) ν_{CO} = 2019, 1993, 1966, 1947 (sh).

2.4 Bibliography

(1) Lucas, L. N.; de Jong, J. J. D.; van Esch, J. H.; Kellogg, R. M.; Feringa, B. L. Syntheses of Dithienylcyclopentene Optical Molecular Switches. *Eur. J. Org. Chem.* **2003**, 155-166.

(2) Lucas, L. N. Dithienylcyclopentene Optical Switches Towards Photoresponsive Supramolecular Materials. Ph.D. Thesis, Rijksuniversiteit Groningen, **2001**.

(3) Xue, L.; Lin, Z. Theoretical Aspects of Palladium-Catalysed Carbon-Carbon Cross-Coupling Reactions. *Chem. Soc. Rev.* **2010**, *39*, 1692-1705.

(4) Franzen, R.; Xu, Y. Review on Green Chemistry - Suzuki Cross Coupling in Aqueous Media. *Can. J. Chem.* **2005**, *83*, 266-272.

(5) Fleckenstein, C. A.; Plenio, H. Sterically Demanding Trialkylphosphines for Palladium-Catalyzed Cross Coupling Reactions - Alternatives to PtBu$_3$. *Chem. Soc. Rev.* **2010**, *39*, 694-711.

(6) Miyaura, N.; Suzuki, A. Palladium-Catalyzed Cross-Coupling Reactions of Organoboron Compounds. *Chem. Rev.* **1995**, *95*, 2457-2483.

(7) Narayanan, R. Recent Advances in Noble Metal Nanocatalysts for Suzuki and Heck Cross-Coupling Reactions. *Molecules* **2010**, *15*, 2124-2138.

(8) de Jong, J. J. D.; Lucas, L. N.; Hania, R.; Pugzlys, A.; Kellogg, R. M.; Feringa, B. L.; Duppen, K.; van Esch, J. H. Photochromic Properties of Perhydro- and Perfluorodithienylcyclopentene Molecular Switches. *Eur. J. Org. Chem.* **2003**, 1887-1893.

(9) Sonogashira, K.; Tohda, Y.; Hagihara, N. Convenient Synthesis of Acetylenes - Catalytic Substitutions of Acetylenic Hydrogen with Bromoalkenes, Iodoarenes, and Bromopyridines. *Tetrahedron Lett.* **1975**, 4467-4470.

(10) Chinchilla, R.; Najera, C. The Sonogashira Reaction: A Booming Methodology in Synthetic Organic Chemistry. *Chem. Rev.* **2007**, *107*, 874-922.

(11) Zhang, S.; Zhanga, M.; Shi, M. Pd/Cu Catalyzed Homo-Coupling Reactions of 2-Iodo-3-Iodomethyl-1,4-Diarylnaphthalene in the Presence of Arylacetylene. *Tetrahedron Lett.* **2007**, *48*, 8963-8966.

(12) Hundertmark, T.; Littke, A. F.; Buchwald, S. L.; Fu, G. C. Pd(PhCN)$_2$Cl$_2$/P(t-Bu)$_3$: A Versatile Catalyst for Sonogashira Reactions of Aryl Bromides at Room Temperature. *Org. Lett.* **2000**, *2*, 1729-1731.

(13) Batey, R. A.; Shen, M.; Lough, A. J. Carbamoyl-Substituted N-Heterocyclic Carbene Complexes of Palladium(II): Application to Sonogashira Cross-Coupling Reactions. *Org. Lett.* **2002**, *4*, 1411-1414.

(14) Sonogashira, K. Development of Pd-Cu Catalyzed Cross-Coupling of Terminal Acetylenes with Sp^2-Carbon Halides. *J. Organomet. Chem.* **2002**, *653*, 46-49.

(15) Negishi, E.; Anastasia, L. Palladium-Catalyzed Alkynylation. *Chem. Rev.* **2003**, *103*, 1979-2017.

(16) Guirado, G.; Coudret, C.; Launay, J. P. Electrochemical Remote Control for Dithienylethene-Ferrocene Switches. *J. Phys. Chem. C* **2007**, *111*, 2770-2776.

CHAPTER 3

Photochemistry of Thienyl-based Switches and their Cobalt Carbonyl Complexes

*Chapter 3 describes the photochromic behaviour of the perhydro- and perfluoro-switches, substituted with ethynylthiophene moieties: 1,2-Bis(5'-(3''-ethynylthiophene)-2'-methylthien-3'-yl)cyclopentene {**1H**}; 1,2-Bis(5'-(3''-ethynylthiophene)-2'-methylthien-3'-yl)perfluorocyclopentene {**1F**}; 1,2-Bis(5'-(4''-phenyl-3'''-ethynylthiophene)-2'-methylthien-3'-yl)-cyclopentene {**2H**}; 1,2-Bis(5'-(4''-phenyl-3'''-ethynylthiophene)-2'-methylthien-3'-yl)perfluorocyclopentene {**2F**}. Photocyclisation to the closed-ring isomers, and photocycloreversion to the open-ring isomers, was monitored by UV-vis absorption and ^{1}H NMR techniques. The fatigue resistance, thermal stability and fluorescence properties of these switches were also examined. The photochemical properties of the corresponding $Co_2(CO)_6$ complexes {**3H**, **3F**, **3bF**, **4H**, **4bH**, **4F**}, and $Co_2(CO)_4dppm$ complexes {**5H**, **5F**, **6H**} were investigated using UV-vis absorption and infra-red spectroscopy.*

3.1 Introduction

Photochromic molecules are of much interest due to their potential applications towards the development of various optoelectronic devices.[1,2] As discussed previously in chapter 1 of this report, dithienylcyclopentene switches are promising candidates for such applications due to their thermal stability and high fatigue resistance properties. Their luminescent properties are also of much interest as changes induced in their fluorescent behaviour, following photocyclisation, can be employed as a non-destructive readout method for use in such applications. In light of this, such properties of diarylethene switches have been well documented in the literature, and a brief summary of the results found are detailed here.

- **Fatigue Resistance**

Photostability is a very important property of dithienylcyclopentene switches. High fatigue resistant switches can undergo a number of colouring/bleaching cycles consecutively, without any sign of degradation of the switch. Literature studies have reported that a large number of diarylethene switches have high fatigue resistance, with no degradation recorded after hundreds, or even thousands, of colouring/bleaching cycles.[3-5] However, it is not always possible to monitor such a high number of cycles if an automatic setup is not available therefore some literature reports have described the results obtained after performing 5-10 consecutive cyclisation/cycloreversion cycles.[6-8] Such experiments can deduce if a switch has very low fatigue resistance, as significant degradation can be observed after a few switching cycles.

Lucas and de Jong et al reported the fatigue resistance of compounds **1-8**,[6,7,9] represented in figure 3.1. After five consecutive colouring/bleaching cycles they found that no degradation was observed for any of the compounds. Subsequent analysis by de Jong et al[6] revealed that the photostability of the perfluoro switch **1** was found to be 2-3 times higher then that of its perhydro-derivative **2**. They also found that attaching a dialdehyde group onto the 5-position of the thiophene rings on the dithienylcyclopentene switch, in place of the phenyl units, resulted in 8% degradation

of the switch after just one cycle, for both the perhydro and perfluoro analogues.[6,7,9] These results highlight that both various substituents on the thiophene rings, and the atoms on the cyclopentene ring, may effect the fatigue resistance properties of such switches. Increased photostability for the perfluorinated-derivatives was also reported by Branda et al.[10] Substitution of different groups onto the 2-positions of the thiophene units can also affect the photostability of such dithienylcyclopentene switches, as demonstrated by PU et al.[11] When methyl groups were attached to the 2 and 2'-positions of the thiophene rings, the switching molecule was found to degrade by 61% after 100 cycles, however, when replacing the methyl groups with n-propyl groups and hexyl groups, the percentage degradation decreased significantly to 16% and 32%, respectively, after 100 cycles. Hence the order of increasing photostability was found to be $CH_3 < n\text{-}C_6H_{13} < n\text{-}C_3H_7$, thus highlighting the fact that by changing the alkyl chain length of the substituent at the 2-position of the thienyl rings can significantly improve the fatigue resistance character of such compounds. Furthermore, Irie et al[12] demonstrated that the fatigue resistance of compound **1** (as illustrated in figure 3.1) was improved by substituting methyl groups at the 4 and 4' positions of the thiophene rings.
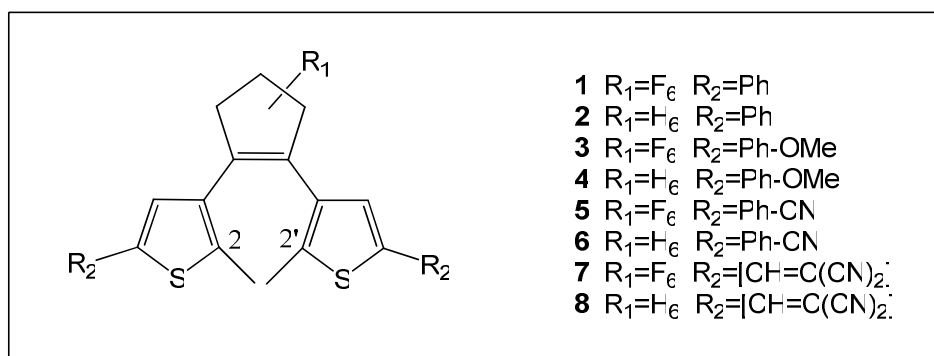
Figure 3.1: Represents structures of compounds **1-8** presented in the literature.[5-7,9,13,14] Also illustrated here are the 2 and 2' positions on the thiophene rings.

Supplementary studies were undertaken to investigate this phenomenon, and Irie et al[12] concluded that a decrease in the fatigue resistance properties of the dithienylcyclopentene switches is believed to be a consequence of the formation of a photochemical by-product during the photocyclisation/cycloreversion processes. Generation of this photochemically-induced by-product was later observed by Branda et al.[10] Irie et al found that the formation of this by-product occurs due to rearrangement of the thiophene rings, resulting in a condensed system with two six-

membered heterocyclic rings.[3,12] The molecular structure of this by-product is shown in scheme 3.1. This by-product forms from the closed-ring isomer, as is evidenced from the decrease in the yield of the open form during fatigue resistance experiments.[10,12] Generation of the by-product can be observed by following the changes in the UV-vis absorption spectra during irradiation. The absorption spectrum of the by-product is similar to that of the closed-ring isomer due to the similarities in the length of the π-conjugation system in both products.[10,12] Evidence of this by-product can also be observed in the aromatic region of the ^{1}H NMR spectrum.[10] The by-product appears to be photostable as it cannot undergo photobleaching back to the open-ring isomer.[10] Patel et al[15] performed theoretical calculations to predict the mechanism of the by-product formation and found two possible mechanisms based on diradical recoupling processes, which occur from the closed isomer.
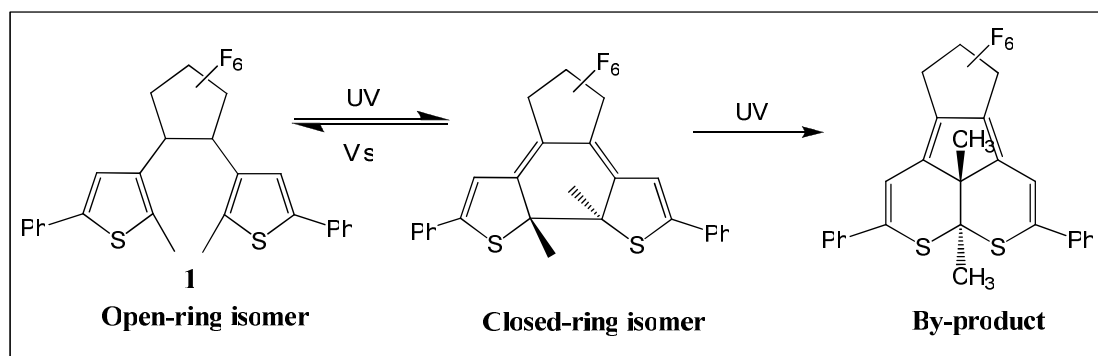
Scheme 3.1: Formation of the photostable by-product during UV irradiation processes, as reported by Irie at al.[12]

- **Thermal Stability**

The thermal stability of dithienylcyclopentene switches is measured by the rate of the thermally-induced cycloreversion process, from the closed to the open-ring isomer, or degradation processes if the case may be, at elevated temperatures. A number of literature papers[5-7,9,13,14] have reported the thermal stability properties of such dithienylethene switches, as represented in figure 3.1, and the results are summarised in table 3.1.

Table 3.1: The half-lives ($t_{1/2}$) of compounds **1-8**, at different temperatures, reported in the literature.

Compound	R_1	R_2	$t_{1/2}$ at 60°C	$t_{1/2}$ at 80°C	$t_{1/2}$ at 100°C
1[a][b][c]	F_6	Ph	-	-	-
2[a]	H_6	Ph	-	-	66 hrs
3[a][b][c]	F_6	Ph-OMe	-	-	-
4[a]	H_6	Ph-OMe	26 hrs	14 hrs	3 hrs
5[a][c]	F_6	Ph-CN	-	-	-
6[a]	H_6	Ph-CN	349 hrs	68 hrs	40 hrs
7[d]	F_6	CH=C(CN)$_2$	3.3 min	N/A	N/A
8[d]	H_6	CH=C(CN)$_2$	4.27 min	N/A	N/A

- (compound is stable) ; N/A (result at this temperature was not available)
[a] measured in toluene[6, 9]
[b] measured in decalin[5]
[c] measured in toluene[13]
[d] measured in benzene[7, 14]

The literature results presented here show that the perfluoro-derivatives **1**, **3** and **5** were found to be highly stable at elevated temperatures, with < 2% degradation observed after 14 hours at 100°C.[5,6,9,13] On the other hand, the corresponding perhydro-derivatives (**2**, **4** and **6**) were found to be less thermally stable in comparison.[6,9] This is not to say that in all cases the perfluoro-analogues are more stable then the perhydrocyclopentene switches, as demonstrated by the results obtained for compounds **7** and **8**, in which the presence of the strongly electron-withdrawing dicyanoethenyl groups greatly decreased the thermal stability of the switches, and to a greater extent for the perfluoro-derivative.[7,14] These results highlight the fact that the thermal stability of these switches is not only dependent on the cyclopentene ring substituents (H_6 *vs.* F_6), but also on the substituents attached to the thienyl moieties. Further evidence of this fact is realised by the results presented by Morimitsu et al.[16] In comparison to compound **1**, represented in figure 3.1, they found that introduction of bulky methoxy groups, at the 2 and 2' positions of the thiophene rings on the dithienylcyclopentene switch, resulted in thermal cycloreversion at temperatures above 70°C. The rates of the cycloreversion process were found to increase as the size of the substituent groups increased: MeO < EtO < i-PrO < cyclohexyloxy. It should be noted that the literature results presented here describe the occurrence of thermal conversion from the ring-closed to the ring-open

form. Thermal degradation processes were not observed for these switches presented in the literature.[5-7,9,13,14]

- **Fluorescence**

Photochemical switching between the open and closed forms can induce changes in the luminescent properties of diarylcyclopentene compounds. In general, the fluorescence of the open-ring isomers of these switches is quenched upon photocyclisation to the closed-ring isomers, however, the emission intensity initially recorded is recovered following photobleaching back to the open form. The extent of the fluorescence quenching is varied. Some closed-ring switches have been found to fluoresce, albeit at a much decreased intensity level relative to the corresponding open-ring isomer.[11,17-21] In other cases, photocyclisation can result in complete quenching of the florescence to the extent that the closed-form is determined to be non-emissive.[1,2,22,23] For example, Xiao et al[17] reported the fluorescence behaviour of two dithienylcyclopentene switches containing imidazo-phenanthroline moieties (**1.2H** and **2.2H**), as represented in figure 3.2.
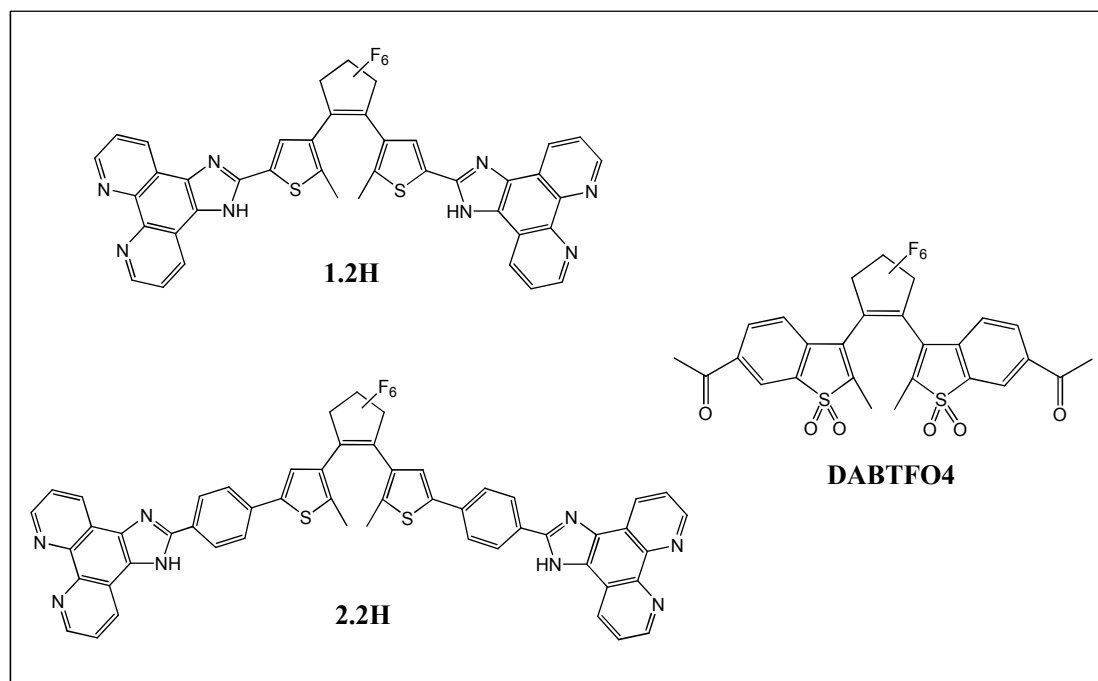
Figure 3.2: Illustrates the structures of the switches **1.2H** and **2.2H** described by Xiao et al,[17] and the switch **DABTFO4** described by Jeong et al.[24]

Both switches exhibited fluorescence in their open-ring forms. However, following UV irradiation, the fluorescence of **2.2H** was quenched to 7% of its original emission intensity recorded for the open isomer. On the other hand, the fluorescent intensity of **1.2H** only decreased to 54% of its original value, at its photostationary state. There have also been reports on some closed-ring isomers emitting fluorescence at the same intensity level, and even higher, than their corresponding open-ring isomers.[24-26] For example, Jeong et al[24] reported the fluorescent behaviour of a sulfone form of diacetyl diarylcyclopentene (**DABTFO4**), illustrated in figure 3.2, whereby the emission intensity was found to significantly increase upon photocyclisation from the open to the closed-ring isomer.

Literature reports indicated a trend in the fluorescent behaviour of the diarylethene derivatives, which correlated the photocyclisation quantum yield to the fluorescence quantum yield of these switches. In general, it was found that as the cyclisation quantum yield increased, the fluorescence quantum yield decreased.[2,11,17-19] This phenomenon was explained by Irie et al.[27] They took into account the lifetimes of the cyclisation reactions (picosecond time-scale) versus the fluorescent lifetimes (several hundred picoseconds) and derived two mechanisms to explain the possible correlation between the quantum yields and lifetimes of these two processes. The first mechanism is explained by the presence of the two conformations of the diarylethene switches, and the second involves competition in the excited state.

It is known that the open-ring form of diarylethene switches can exist as two conformational isomers: parallel and anti-parallel,[28] as represented in scheme 3.3. Only the anti-parallel conformers can undergo photocyclisation to the ring-closed form. Therefore, an increase in the ratio of anti-parallel conformations in the ground-state would result in an increase in the cyclisation quantum yield. Irie and co-workers[27] assigned the photo-inactive parallel conformers to be the cause of the fluorescence emission, as they are expected to have long lifetimes. Hence, an increase in the ratio of parallel conformers, in relation to anti-parallel conformers, would result in an increase in the fluorescence intensity and a decrease in the cyclisation quantum yield.

The second mechanism put forward by Irie et al[27] can be explained in terms of competition in the excited state. Cyclisation is induced following photoexcitation of the diarylethene molecules, however, when an excited molecule cannot enter the

cyclisation reaction channel, deactivation to the relaxed fluorescence state occurs resulting in the emission of fluorescence. Therefore, an increase in the cyclisation quantum yield results in a decrease in the number of unreacted excited molecules, and hence a decrease in the fluorescence intensity.
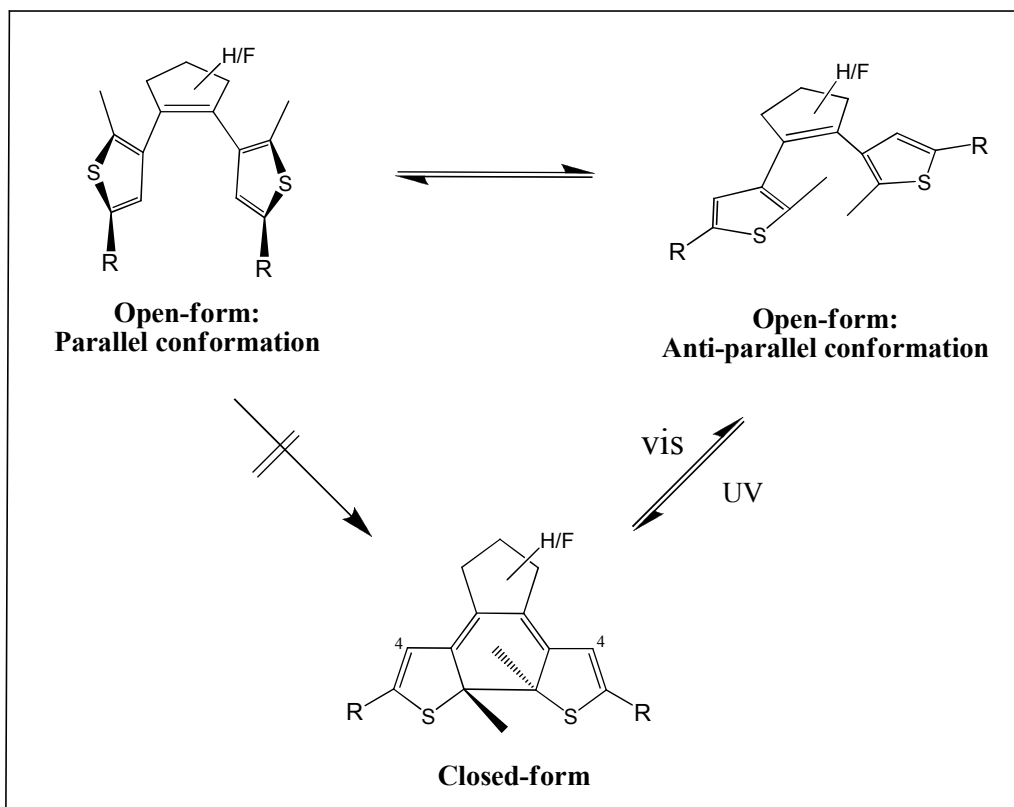
Scheme 3.2: Parallel and anti-parallel conformational isomers of open form dithienylethene switches. The parallel form is photochemically inactive. Only the anti-parallel conformers can undergo photocyclisation

Chapter 2 described the synthesis of dithienylcyclopentene switches substituted with ethynylthiophene moieties (**1H**, **1F**, **2H**, **2F**). This chapter provides a discussion of the results found following an investigation of their photochromic properties (as monitored in the UV-vis absorption and ^{1}H NMR spectra), along with their fatigue resistance, thermal stability and fluorescent properties. The synthesis of their corresponding $Co_2(CO)_6$ complexes (**3H**, **3F**, **3bF**, **4H**, **4bH**, **4F**) and $Co_2(CO)_4dppm$ complexes (**5H**, **5F**, **6H**) was also described in chapter 2. The photochemical properties of these complexes were investigated using UV-vis absorption and infra-red spectroscopy, and the effect of the metal carbonyls on the photochromic behaviour of these switches was determined. The structures of these compounds are illustrated in figure 3.3.
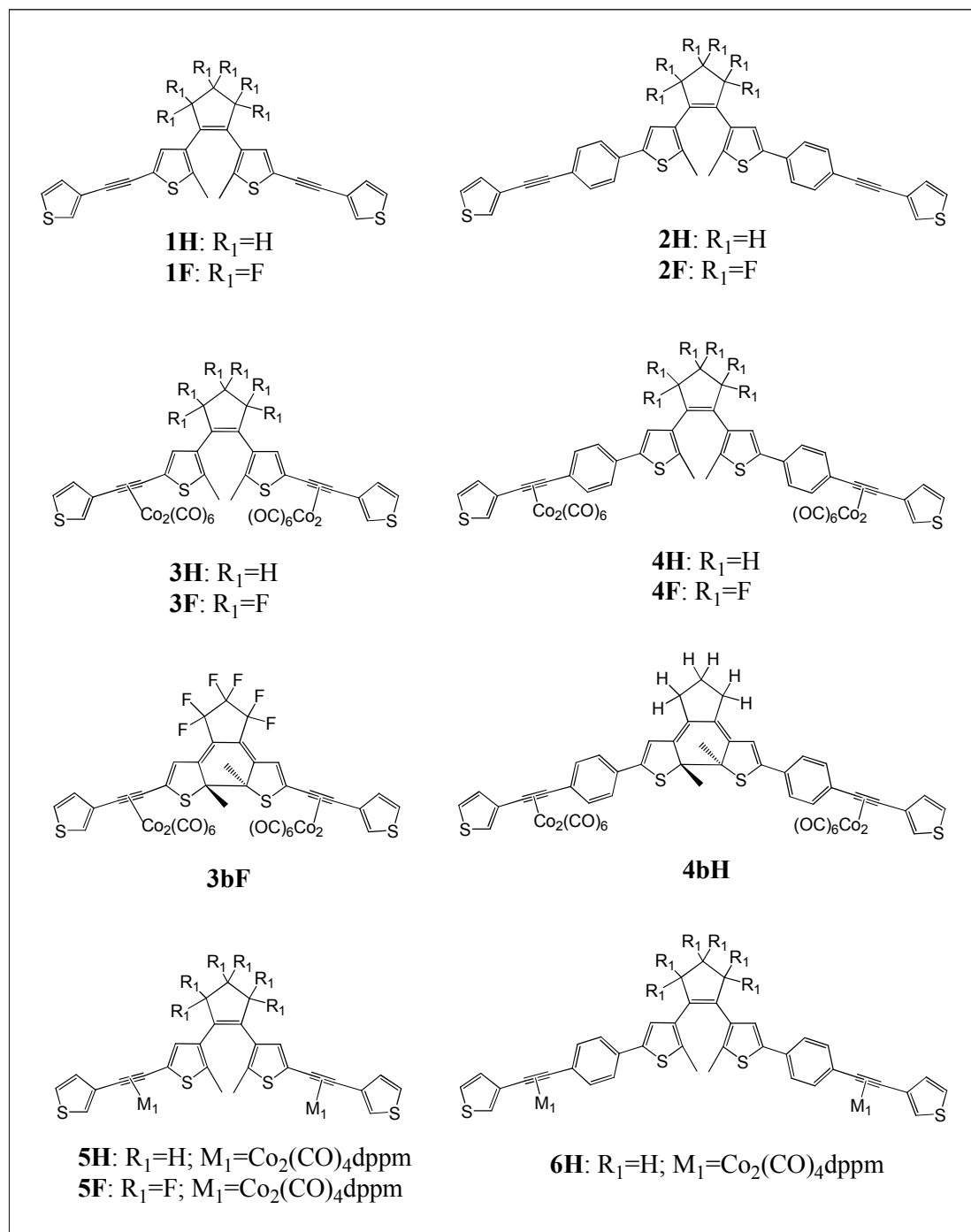
Figure 3.3: Illustrates the structures of the thienyl-based dithienylperhydro- and perfluoro-cylopentene switches **1H**, **1F**, **2H** and **2F** discussed in this chapter, and the corresponding $Co_2(CO)_6$ complexes {**3H**, **3F**, **3bF**, **4H**, **4bH**, **4F**} and $Co_2(CO)_4$dppm complexes {**5H**, **5F**, **6H**}.

3.2 Experimental

3.2.1 General Procedures

Photocyclisation/cycloreversion: Solutions of the compounds were made-up in THF at a concentration of 1.4×10^{-5} mol/L, placed in a 1 cm quartz cell, and purged with nitrogen. Ring-closing experiments were performed by irradiating the solution with monochromatic light at $\lambda = 313$ nm and recording the UV-vis absorption spectra at specific time intervals. Irradiation was carried out until the photostationary state of the compounds was achieved, or until no more changes were endured in the UV-vis spectra. Following this, ring-opening was induced by irradiation of the same solution with broadband visible light ($\lambda > 550$ nm) and the absorption spectra were recorded over time, until no further changes were observed in the spectra.

^{1}H NMR Studies: Solutions of these switches in deuterated acetone were irradiated with monochromatic light at 313 nm, under air, in a sealed NMR tube. The changes in the ^{1}H NMR spectra were observed over recorded irradiation time intervals.

Fatigue Resistance: Solutions of these switches, made-up in THF at a concentration of 1.4×10^{-5} mol/L, were purged with nitrogen gas and placed in a sealed 1 cm quartz cell. Cyclisation to the ring-closed isomer was induced by irradiation with a monochromatic light source at a wavelength of 313 nm, and cycloreversion back to the ring-open isomer was carried out using broadband filtered light > 550 nm. This process counted as one cycle, and the fatigue resistance properties were measured over five consecutive cycles.

Thermal Stability: The switches were irradiated with monochromatic light at $\lambda = 313$ nm, in a solution of toluene, until the photostationary state of the closed-ring isomer was reached, as monitored in the UV-vis absorption spectra. The stability of these switches at room temperature was measured by storing the solutions of the closed-switches under air in sealed glass vials, in the dark. After 10 weeks, the absorption spectra of these compounds were recorded and compared to the spectra measured initially. The stability of these switches was also measured at elevated temperatures (60°C, 80°C and 100°C) by placing non-degassed solutions of the closed-forms, in

toluene, on a temperature controlled heating mantel and measuring their absorption spectra at specific time intervals.

Fluorescence properties: The emission spectra of these compounds were recorded at room temperature in a solution of THF, at a concentration of 4 x 10^{-6} mol/L, in a 1 cm quartz cuvette. The samples were degassed with nitrogen. The ring-closed isomers were produced by irradiating the solutions at λ = 313 nm, until the photostationary state was observed in the UV-vis absorption spectra. Ring-opening was induced by irradiating with broadband light at λ > 550 nm.

Steady-state photolysis: Solutions of the cobalt carbonyl complexes were made-up in spectroscopic-grade THF, and purged with nitrogen for 20 minutes. The solutions were placed in a liquid IR cell, and irradiated with monochromatic light at two different wavelengths, 313 nm and 365 nm. The changes observed in the carbonyl stretches in the IR spectrum were recorded. These experiments were repeated in the presence of excess triphenylphosphine (PPh_3), which was used as a trapping ligand.

3.2.2 Materials

The solvents used for the analytical experiments, THF and toluene, were purchased from Sigma Aldrich, and were of spectroscopic grade. The deuterated acetone and triphenylphosphine were purchased from Sigma Aldrich. The solutions were degassed with nitrogen, which was supplied by Air Products Ltd.

3.2.3 Equipment

UV-visible spectra were recorded on a photodiode-array Agilent 8453 spectrometer, in a 1 cm quartz cell. Photochemical experiments were carried out in a 1 cm quartz cell, using a monochromatic 200W Hg lamp (Oriel Instruments, model no.: 68911) containing a 313 nm or 365 nm filter, and a broadband lamp (Oriel instruments, model no.: 68811) containing a λ > 550 nm filter. ^{1}H NMR spectra were recorded on a Bruker model AC 400 MHz spectrometer and the peaks were calibrated according to the deuterated solvent peak. Emission spectra were recorded in a 1 cm quartz cuvette, using a LS50B luminescence spectrophotometer. Infra-red spectra were recorded in a 0.1 mm sodium chloride liquid cell, on a Perkin Elmer "Spectrum GX" FT-IR spectrometer.

3.3 Results and Discussion

3.3.1 Photochromic Behaviour: UV-vis Absorption
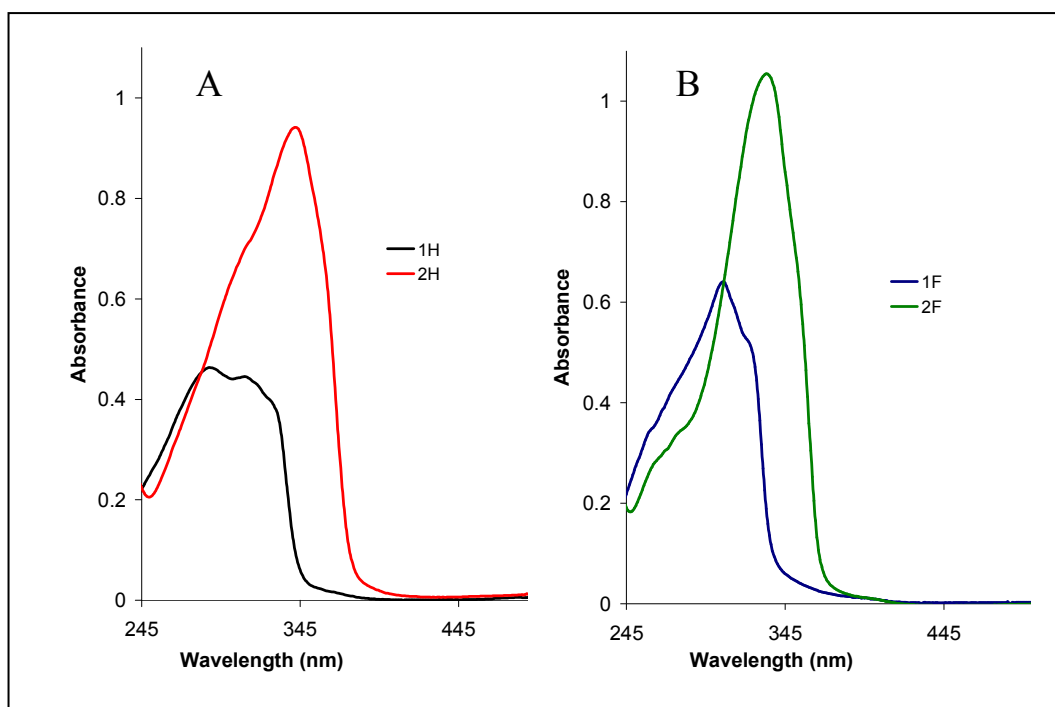
- **Open-ring isomer**

Figure 3.4: Absorption spectra of the open-ring isomers of compounds **1H/F** and **2H/F** in THF solution (c=1.4 x 10^{-5} mol/L). A: **1H** (black line), **2H** (red line); B: **1F** (blue line), **2F** (green line).

The UV-vis absorption spectra of the open-ring isomers of compounds **1H/F** and **2H/F** showed typical π-π* transitions in the near-UV region of the spectrum and no absorbance in the visible region. **1H** and **1F** displayed a broad absorbance band between 245 and 345 nm, with λ_{max} at 287 and 306 nm respectively. Extending the conjugation of these compounds, through the addition of a phenyl ring between the switching unit and the ethynylthiophene moieties, in **2H** and **2F**, resulted in both hyperchromic and bathochromic shifts (33 nm and 27 nm respectively) as highlighted in figure 3.4 and table 3.3.

- **Cyclisation**

Photocyclisation from the open-ring isomers of compounds **1H/F** and **2H/F**, to their corresponding closed-ring isomers, was induced by irradiating a degassed solution of the compound in THF, with UV light at λ = 313 nm, until no more changes were observed in their UV-vis absorption spectra i.e. until the photostationary state was reached. The absorption bands recorded in the UV-vis spectra, for the open and closed isomers of these switches, are summarised in table 3.3.

Table 3.3: UV-vis absorption data of the open-ring isomers, and closed-ring isomers (at the photostationary state (PSS)), of compounds **1H/F** and **2H/F**.

Compound[a]	Absorption Spectra in THF	
	Open-ring isomer	Closed-ring isomer (PSS)
	λ_{abs} [nm] (ε x 10^3 M^{-1} cm^{-1})	λ_{abs} [nm] (ε x 10^3 M^{-1} cm^{-1})[b]
1H	287 (29.6), 310 (28.3)	266 (sh), 317 (28.3), 360 (sh), **543** (14.8)
1F	259 (sh), 306 (43.9), 322 (sh)	262, 351 (27.0), 376 (sh), 397 (sh), **609** (18.2)
2H	305 (sh), 343 (69.0)	267 (sh), 329 (51.1), 382 (sh), **562** (29.1)
2F	262 (sh), 277 (sh), 333 (76.2)	276 (26.5), 362 (40.5), 395 (sh), **614** (23.3)

[a] The open-ring isomer, and the closed-ring isomer at the PSS (following irradiation at λ = 313nm), in THF.
[b] The extinction coefficients for the closed forms were determined at the photostationary state.
The λ_{max} in the visible region of the closed-ring isomers are highlighted in bold.
(sh) denote a shoulder band.

Irradiation of **1H**, in THF, with monochromatic light at 313 nm, resulted in photocyclisation of the switch from the open-ring isomer to the closed-ring isomer, as illustrated in scheme 3.3. This was evident from the change in the absorption spectrum, as there was a large increase in absorbance in the visible region, with a λ_{max} appearing at 543 nm (figure 3.5 and table 3.3), hence resulting in a colour change from colourless to purple. In the UV region, the band at 287 nm decreased significantly. The absorption band at 310 nm decreased slightly, and was red-shifted to 317 nm, with shoulders at 266 and 360 nm, however no isosbestic point was evident during this process. The photostationary state (PSS) was reached after 50 seconds of irradiation.

Figure 3.5: Absorption spectra of the cyclisation process from the open-ring isomers to the closed ring-isomers of compounds **1H** and **1F** in THF solution (c = 1.4 x 10^{-5} mol/L), following irradiation at 313 nm. A: **1H** (PSS reached after 50 seconds of irradiation); B: **1F** (PSS reached after 20 seconds of irradiation).

Upon irradiation of **1F** at λ = 313 nm, cyclisation to the closed form was evident from the appearance of an absorption band in the visible region, with a λ_{max} at 609 nm, and a colour change from colourless to blue. Dramatic changes were also observed in the UV region, as illustrated in figure 3.5, with a large bathochromic shift of the absorption band at 306 nm to 351 nm and shoulders at 376 and 397 nm, the appearance of a band at 262 nm, and an isosbestic point at 300 nm.
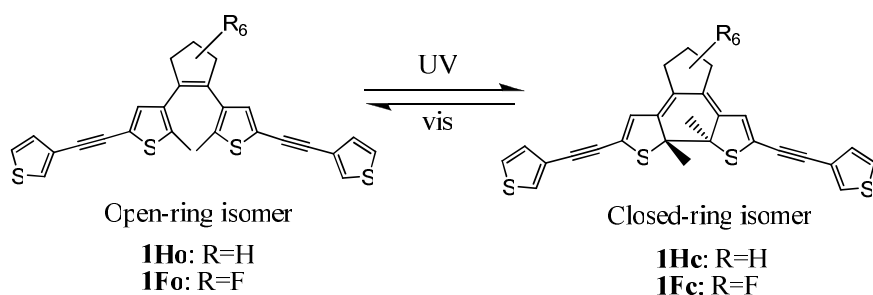
Scheme 3.3: Cyclisation from the open-ring isomer to the closed ring isomer, following irradiation at λ = 313 nm, of compounds **1H** (R=H) and **1F** (R=F).

Comparison of the results obtained show that there is a pronounced difference between the new absorption bands recorded for the ring-closed isomers of the perhydro- and perfluoro-derivatives. This is evident from the bathochromic shifts of the λ_{max} of **1Fc** in the UV region (34 nm) and visible region (66 nm), in comparison to **1Hc**, which can be assigned to the electron-withdrawing ability of the fluorine atoms in **1F**, in contrast to the electron donating ability of the hydrogen atoms in **1H**. It was also found that the photostationary state of the perfluoro-switch was reached after only 20 seconds of irradiation, less then half the time required for the perhydro-derivative (50 seconds).

When **2H** was irradiated at λ = 313 nm, the formation of the closed-ring isomer (scheme 3.4) resulted in the formation of a new band in the visible region of the UV-vis spectrum, with a λ_{max} at 562 nm, as shown in figure 3.6. The band at 343 nm decreased in absorption with a hypsochromic shift to 329 nm, upon cyclisation, along with the appearance of two shoulder bands at 267 and 382 nm and an isosbestic point at 370 nm. The photostationary state was reached after 30 seconds of irradiation and a colour change from colourless to purple was observed.
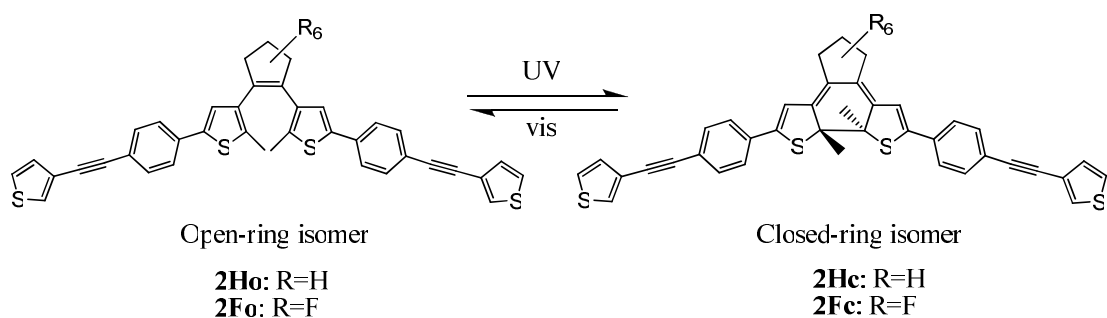
Scheme 3.4: Cyclisation from the open-ring isomer to the closed ring isomer, following irradiation at λ = 313 nm, of compounds **2H** (R=H) and **2F** (R=F).

Cyclisation of **2F** to the closed-form (scheme 3.4, figure 3.6), at $\lambda = 313$ nm, was evident by the appearance of a broad absorption band in the visible region of the UV-vis spectrum with λ_{max} at 614 nm, accompanied by a significant decrease in absorbance, and a bathochromic shift, of the band at 333 nm to 362 nm, and a shoulder at 395 nm. The appearance of an absorption band at 276 nm was also observed, along with two isosbestic points at 289 and 356 nm. This cyclisation process resulted in a colour change of the solution from colourless to blue, and the photostationary state was reached after 15 seconds.
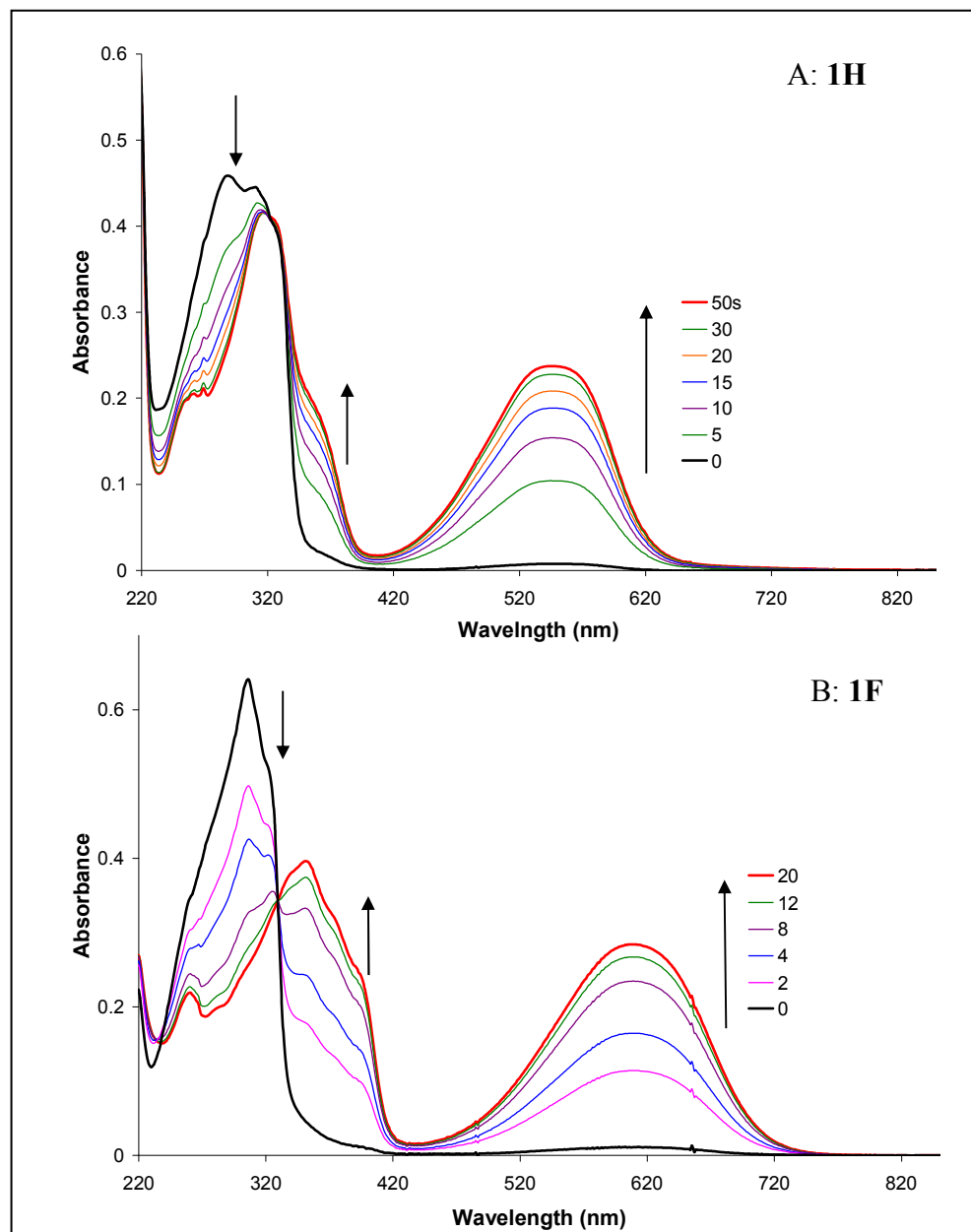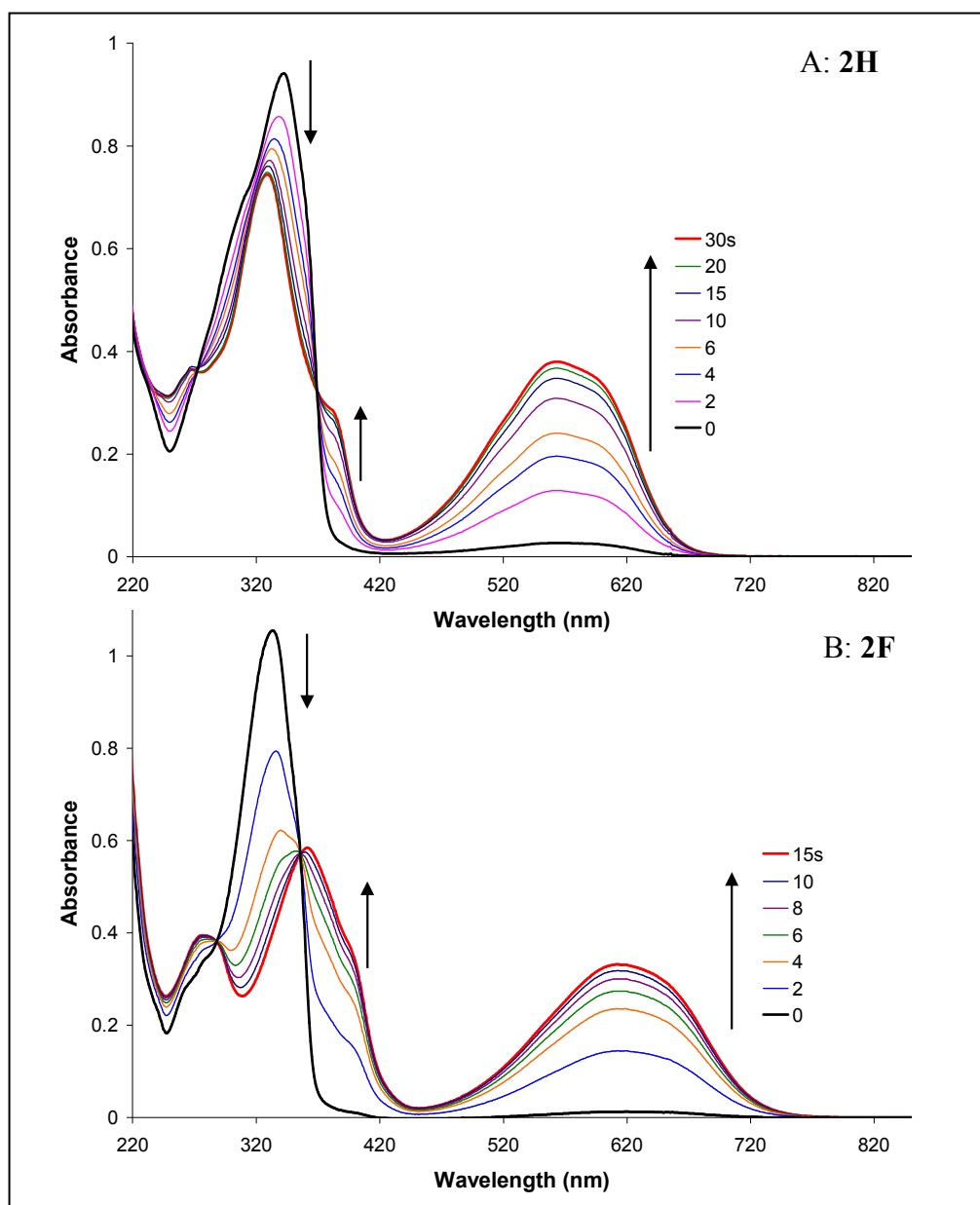

Figure 3.6: Absorption spectra of the cyclisation process from the open-ring isomers to the closed ring-isomers of compounds **2H** and **2F** in THF solution (c = 1.4 x 10^{-5} mol/L), following irradiation at λ = 313 nm. A: **2H** (PSS reached after 30 seconds of irradiation); B: **2F** (PSS reached after 15 seconds of irradiation).

Although the UV-vis absorption spectra of the open-ring isomers of **2H** and **2F** showed modest variations in their absorbance bands (table 3.3), the UV-vis spectra of the closed-ring isomers of the two derivatives showed marked differences. In comparison to the perhydro-derivative, a bathochromic shift of 33 nm was observed for the perfluoro-switch in the UV region, and 52 nm in the visible region. As mentioned for the perhydro and perfluoro-derivatives, **1H** and **1F** above, this is due to the effect of the electron-withdrawing ability of the fluorine atoms. Similarly, it took twice as long for the perhydro-switch **2H** to reach the photostationary state in comparison to the perfluoro-derivative **2F** (30 seconds and 15 seconds respectively).

When comparing the effects of extending the conjugation of the systems, similar results were found for both the perhydro- and perfluoro-derivatives in their closed-ring forms. The presence of the phenyl groups, between the switching unit and the ethynylthiophene moieties, resulted in a bathochromic shift for all the UV-vis absorbance bands. However, increasing the conjugation of the system had a more pronounced effect on the perhydro-derivatives, as the absorbance band in the visible region of the closed-ring isomer of **2H** was red-shifted by 19 nm, compared to that of **1H**, whereas a bathochromic shift of only 5 nm was observed for the closed-form of **2F**, in comparison to **1F**. Also, the time taken to reach the photostationary state, following irradiation, was significantly reduced for the extended perhydro-switch **2H** (30 seconds in comparison to 50 seconds for **1H**), and also reduced for the extended perfluoro-switch **2F**, but to a lesser extent (15 seconds in comparison to 20 seconds for **1F**).

- **Cycloreversion**

Cycloreversion processes from the closed-ring isomers back to the open-ring isomers were performed on each switch using broadband visible light ($\lambda > 550$ nm). The perfluoro-switches **1F** and **2F** returned fully to the open-ring forms after 90 and 180 seconds of irradiation with visible light, respectively, with absorbance bands in the visible region completely disappearing and the original absorbance bands in the UV region growing back. This process is illustrated for compound **2F** in figure 3.7. It is clear from these results that the efficiency of the cycloreversion process decreases when the π-conjugation of the system increases. A similar trend was recorded in the literature by Irie et al,[3] which has been attributed to a decrease in the anti-bonding nature in the singlet state of the central photogenerated carbon-carbon bond, with the extension of the π-conjugation.
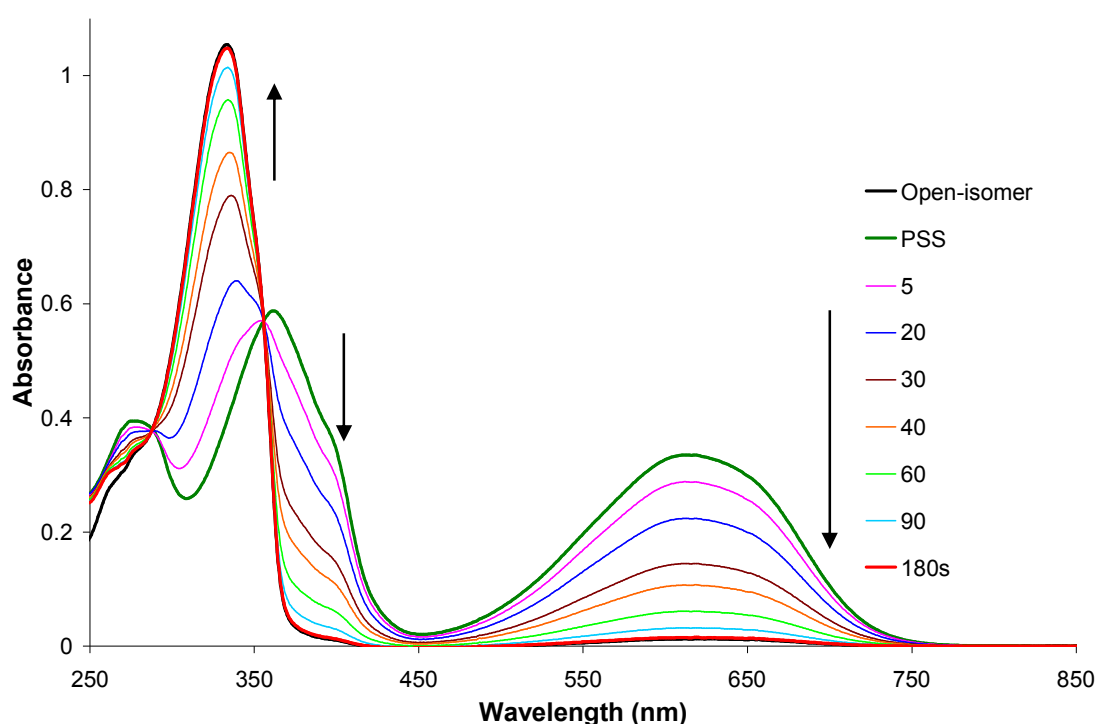
Figure 3.7: Absorption spectra of the cycloreversion process from the closed-ring isomer to the open-ring isomer of compound **2F,** in a solution of THF (C=1.4 x 10^{-5} mol/L), following irradiation with broadband light $\lambda > 550$ nm for 180 seconds (red line). The open-ring isomer recorded at the start of the experiment (before any irradiation takes place) is denoted by the black line. The PSS (green line) is the photostationary state of **2F** following irradiation with 313 nm light for 15 seconds.

The ring-opening process for the perhydro-derivative **2H** took 360 seconds to be complete, twice as long as its perfluoro-derivative **2F**, indicating that the presence of the fluorine atoms increases the efficiency of this process. In the case of compound **1H**, irradiation for 420 seconds results in cycloreversion back to the open-form, but not completely, as the presence of the band at 543 nm remains, even after prolonged irradiation at $\lambda > 550$ nm. Therefore the ring-closing/opening process is not fully reversible for **1H**. This will be discussed in more detail in the following sections.

3.3.2 Fatigue Resistance

The fatigue resistance properties of compounds **1H/F** and **2H/F** were investigated by performing five consecutive cyclisation/cycloreversion cycles in degassed solutions of THF, which is sufficient to determine whether or not these switches have very low fatigue resistance.

A solution of **1H**, in THF, was irradiated at 313 nm until the photostationary state was reached (50 seconds), followed by irradiation with visible light at $\lambda > 550$ nm (180 seconds), and the results were monitored in the UV-vis spectrum. The absorbance at 543 nm began to decrease after each colouring cycle, and began to increase after each bleaching cycle, as shown in figure 3.10.
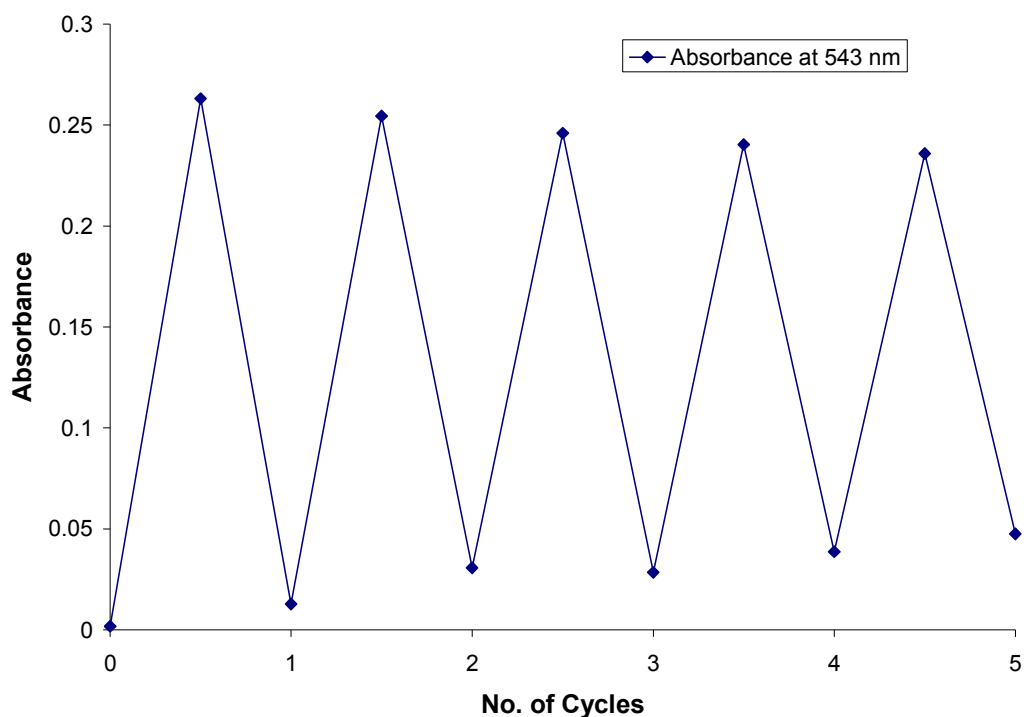
Figure 3.10: Fatigue resistance of **1H** in THF. The absorbance values of the open/closed forms were monitored at 543 nm over five colouring/bleaching cycles.

After five consecutive cycles it was found that approximately 10% of **1H** degraded during these photochemical processes. Such a result could possibly be due to the formation of a photochemical by-product following UV irradiation, which has been reported in previous literature studies,[3,10,12] and described in section 3.1. Further

investigations to confirm this theory were carried out using ^{1}H NMR spectroscopy, and the results are discussed in detail in the next section.

When similar experiments were carried out on the perfluoro-derivative, **1F**, it was found that 4% of the switch had degraded after five photocyclisation/cycloreversion reactions. This result shows a marked improvement in comparison to the result obtained for the perhydrocyclopentene analogue, signifying that the fluorine atoms help to stabilise the closed-ring isomer, and if not preventing, at least slowing down the rate of formation of the photo-induced by-product.

The colouring/bleaching cycles of **2H** were monitored at the λ_{max} of the closed ring-isomer at 562 nm. Approximately 1.5% of the switch degraded after five consecutive cycles. In comparison to the result obtained for **1H**, it is clear that extension of the conjugated system in **2H** facilitates the prevention of photodegradation, hence increasing the fatigue resistance of the switch.

Compound **2F** showed the highest fatigue resistance, with negligible degradation found after five cycles (figure 3.11). This is most likely due to the advantage of having the fluorine atoms centred on the cyclopentene ring, in comparison to its perhydro-derivative **2H**, combined with the extension of the π-conjugation of the switch, in comparison to **1F**.
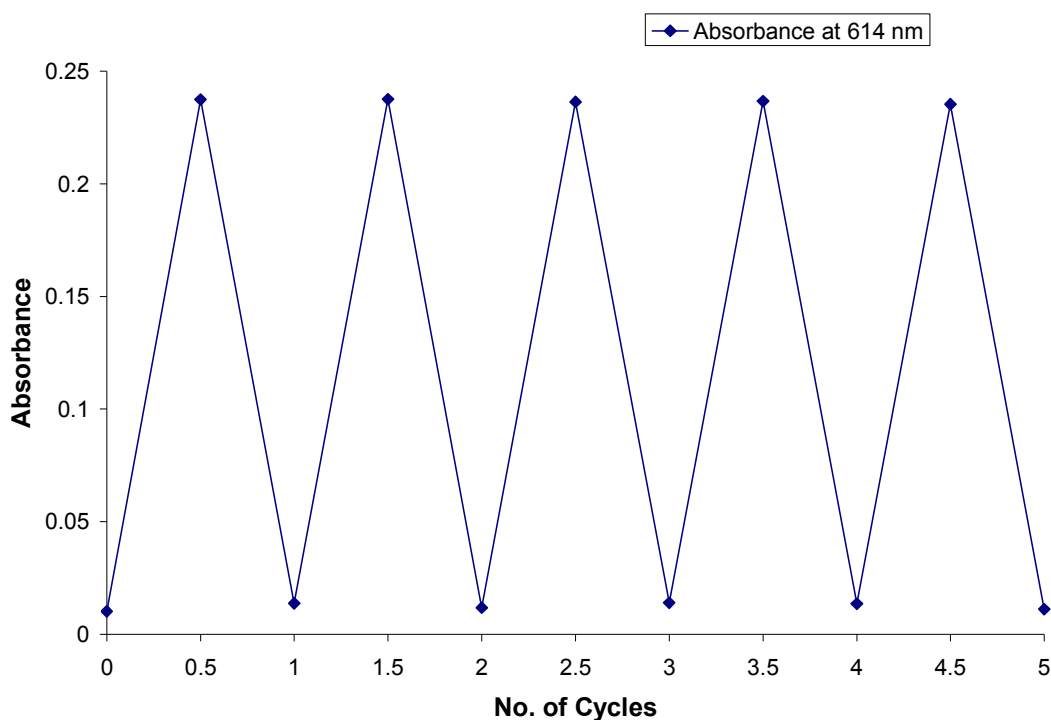
Figure 3.11: Fatigue resistance of **2F** in THF. The absorbance values of the open/closed forms were monitored at 614 nm over five colouring/bleaching cycles.

3.3.3 Photochromic Behaviour: ^{1}H NMR

Photoswitching between the closed and open forms of diarylcyclopentene compounds can be monitored in the ^{1}H NMR spectra, as described previously in chapter 1. Upon cyclisation to the closed-ring form, the proton at the 4-position of the thiophene ring on the dithienylcyclopentene unit (illustrated in scheme 3.5) undergoes an upfield chemical shift due to the loss of aromaticity. Although the other peaks present in the ^{1}H NMR spectrum are also effected upon UV irradiation, the chemical shift of this thiophene proton is the most dramatic, hence monitoring the relative integrals of the corresponding pairs of proton signals for the two isomers allows for the percentage conversion, from the open to the closed form, to be calculated to an approximate value.

Open-ring isomer   **Closed-ring isomer**
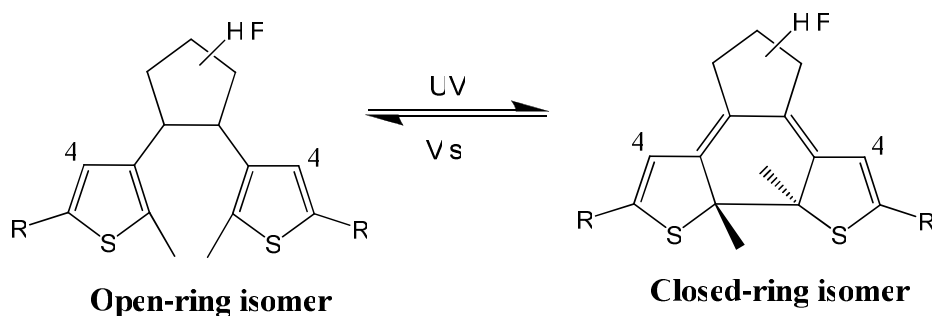
Scheme 3.5: Represents the structural change incurred on the dithienylcyclopentene unit upon ring-closure, and hence the loss of aromaticity of the thiophene rings. Also illustrated, the proton at the 4-position of the thienyl units.

The photocyclisation process was monitored by ^{1}H NMR for compounds **1H/F** and **2H/F** in deuterated acetone and the chemical shifts (in ppm), and the percentage conversion to the closed form, are denoted in tables 3.4 and 3.5 for these compounds.

Table 3.4: ^{1}H NMR chemical shift data (in ppm) of the proton at the 4-position of the dithienylcyclopentene thiophene ring (Th-H), for compounds **1F**, **2H** and **2F**, following irradiation at λ = 313 nm for 100 minutes, in deuterated acetone. Also, the estimated percentage conversion from the open to the closed-ring isomers.

Compound	δ Th-H open	δ Th-H closed	% Conversion
1F	7.36	6.59	> 95
2H	7.34	6.81	> 95
2F	7.60	7.04	> 95

The ^{1}H NMR spectrum of the open-ring isomer of **1F** exhibited a singlet peak at 7.36 ppm, representing the proton at the 4-position of the dithienylethene thiophene ring. Following irradiation with monochromatic light at λ = 313 nm, this peak started to decrease in intensity, with the appearance of a new singlet peak at 6.59 ppm correlating to the formation of the closed-ring isomer. After approximately 100 minutes of irradiation, the photostationary state was reached and the ratio of the peak intensity at 7.36 and 6.59 ppm was estimated to be 0:1, as shown in figure 3.8. This result indicates that the conversion of the open-ring isomer to the closed ring-isomer was greater than 95% for **1F**.
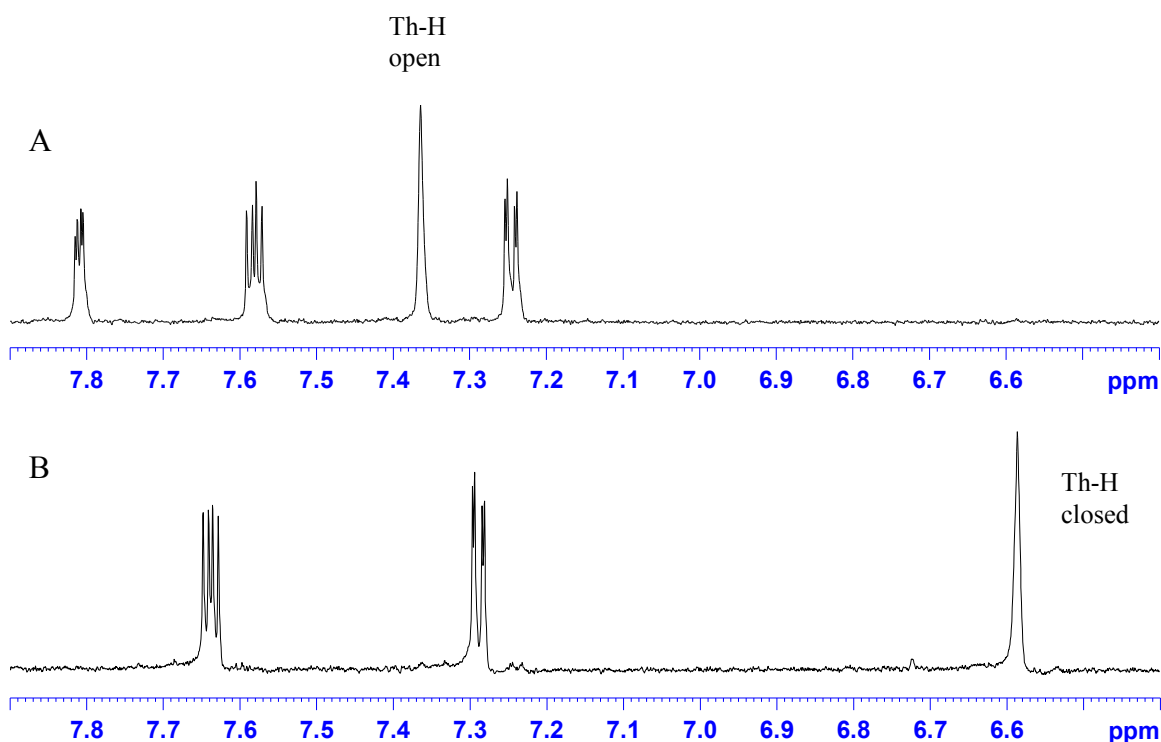
Figure 3.8: ^{1}H NMR spectral changes of **1F**, dissolved in deuterated acetone, upon irradiation at λ = 313 nm. A: open-ring isomer of **1F** before irradiation; B: closed-ring isomer of **1F** after 100 minutes of irradiation.

Similar results were obtained for compounds **2H** and **2F**, as detailed in table 3.4, as the conversion between the open and the closed forms at the photostationary state was also found to be greater than 95%.

In the case of compound **1H**, the ^{1}H NMR studies revealed that photocyclisation, to the closed form, was accompanied by the formation of a photochemical by-product, hence elucidating the low fatigue resistance found for **1H** in the previous section. The

spectral changes observed for **1H** are summarised in table 3.5, and the molecular structure of the by-product formed is illustrated in scheme 3.6.
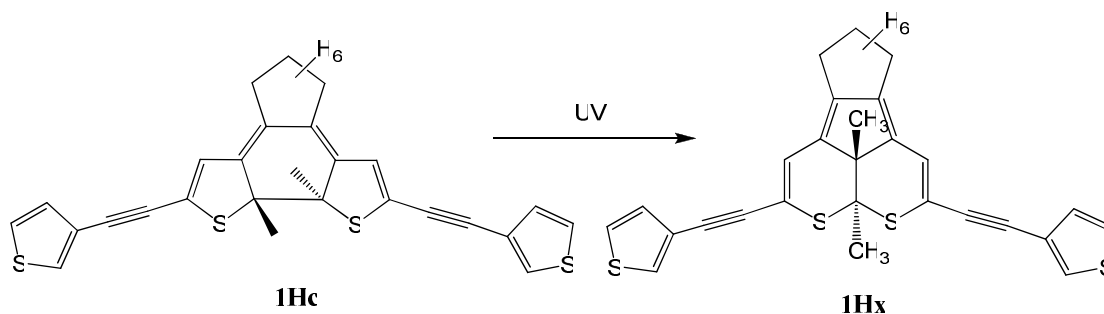
Scheme 3.6: Illustrates the by-product **1Hx** formed following continuous UV irradiation of the ring-closed isomer **1Hc**.

The peak representing the thiophene proton at the 4-position appeared at 7.06 ppm in the ^{1}H NMR spectrum of the open-ring isomer of **1H** (**1Ho**). Following UV irradiation for 30 minutes, a new peak was observed at 6.34 ppm, representing the formation of the closed-ring isomer **1Hc**, with the percentage conversion from the open to the closed form estimated to be 70%. After 60 minutes of irradiation the intensity of the peak at 6.37 ppm had increased, and the peak at 7.06 ppm had further decreased, however, a new peak was also observed at 6.53 ppm indicating that a photochemical by-product was forming (figure 3.9).

The ratio of the relative integrals for the three proton signals at 7.06, 6.53 and 6.37 ppm was found to be 0.13: 0.04: 1, respectively, after 60 minutes of irradiation. Hence the conversion of **1Ho** to **1Hc** at 6.37 ppm, and to the by-product (**1Hx**) at 6.53 ppm, was found to be 85% and 4% respectively (table 3.5). Further irradiation for 125 minutes resulted in an increase in the intensity of the peak at 6.53 ppm (11 % conversion to **1Hx**), whereas the peak at 6.37 ppm seemed to remain the same (85% conversion to **1Hc**). However, after 220 minutes of irradiation the peak at 6.37 ppm began to decrease (78% conversion to **1Hc**) whilst the peak at 6.53 ppm continued to increase (18 % conversion to **1Hx**). Interestingly, the intensity of the original peak at 7.06 ppm, relating to **1Ho**, did not change between the spectra recorded at 125 minutes and 220 minutes of irradiation, therefore signifying that the by-product is photochemically induced from the closed-ring isomer.
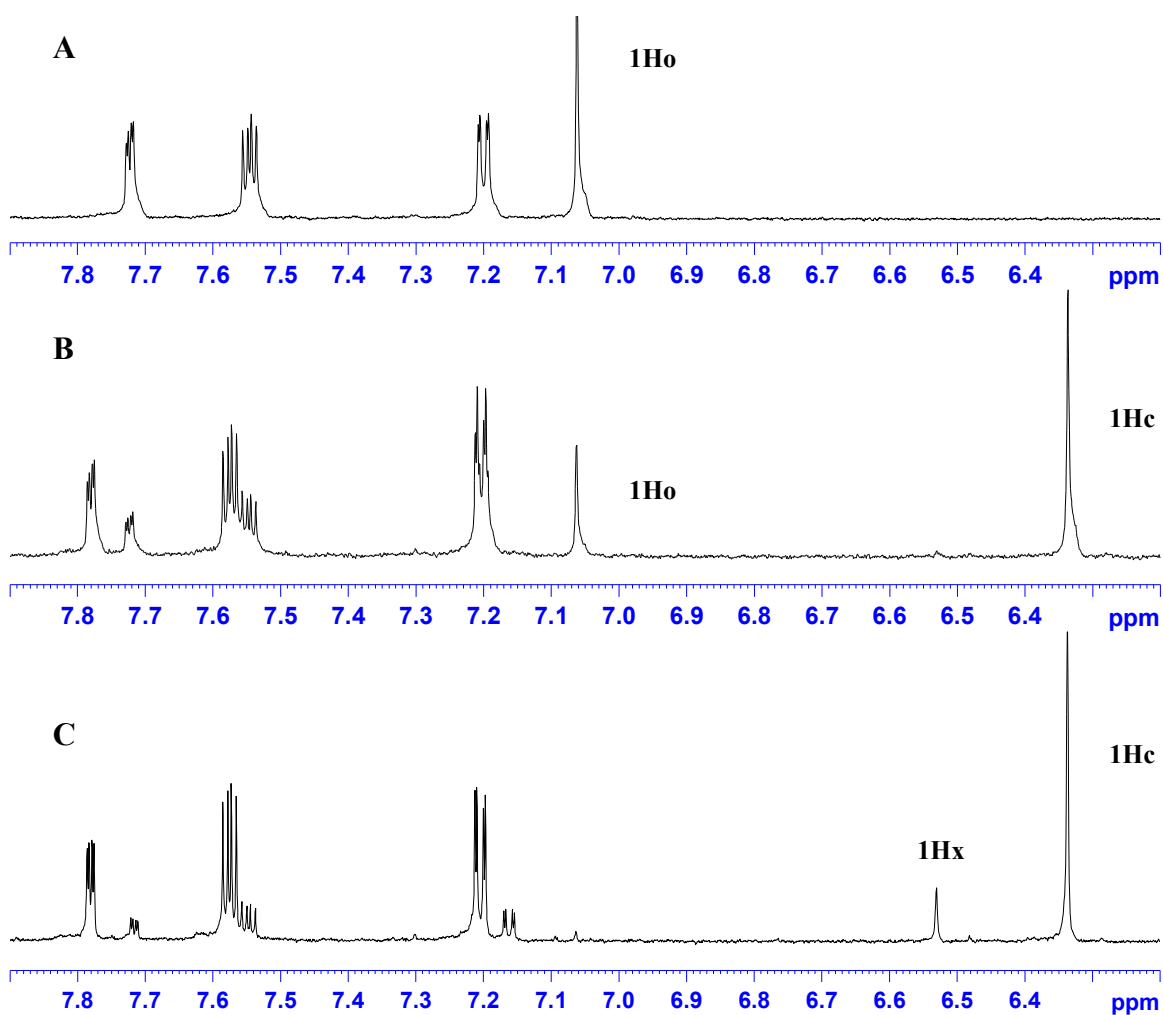
Figure 3.9: ^{1}H NMR spectral changes of **1H**, dissolved in deuterated acetone, upon irradiation at 313 nm. A: open-ring isomer **1Ho** before irradiation; B: new peak at 6.37 ppm due to formation of closed-ring isomer **1Hc** after 30 minutes of irradiation; C: new peak at 6.53 ppm due to formation of the by-product **1Hx** after 220 minutes of irradiation, also note that peak at 7.06 ppm representing open isomer barely visible;

Table 3.5: ^{1}H NMR chemical shift data (in ppm) of the thiophene-proton at the 4-position for compound **1H**, at different irradiation times ($\lambda = 313$ nm). Also, the estimated % conversion from the open-ring isomer to the closed-ring isomer, and to the by-product

Irradiation Time of **1H**	δ Th-H open	δ Th-H closed	Conversion (%)	δ Th-H by-product	Conversion (%)
30 min	7.06	6.34	70	-	-
60 min	7.06	6.34	85	6.53	4
125 min	7.06	6.34	85	6.53	11
220 min	7.06	6.34	78	6.53	18

.

145

3.3.4 Thermal Stability

The thermal stability of switches **1H/F** and **2H/F** were studied to investigate if the ring-closed isomers would undergo thermal cycloreversion back to their open-ring isomers. The switches were closed with UV light in a solution of toluene, and whilst heated to different temperatures under air, their absorbance spectra were recorded at different time intervals.

The closed switches were found to be thermally stable in the dark at room temperature, and after 10 weeks no changes were observed in their absorbance spectra. However, when the closed-switches were heated to 60°C, 80°C and 100°C the absorbance bands in the visible region, indicative of the closed-ring isomer, began to decrease over time. The rates of these thermal processes were measured at 60°C, 80°C and 100°C and the decay curves of the closed-isomers were plotted $\{ \ln([c]/[c]_0)$ *vs.* time$\}$, as illustrated in figure 3.12. The plots were found to be roughly linear, indicating first-order kinetics, hence the half-lives of the degrading switches were calculated from the equation $t_{1/2} = \ln 2/k$ (where the reaction rate k was the slope of the graphs). These results are summarised in table 3.6.
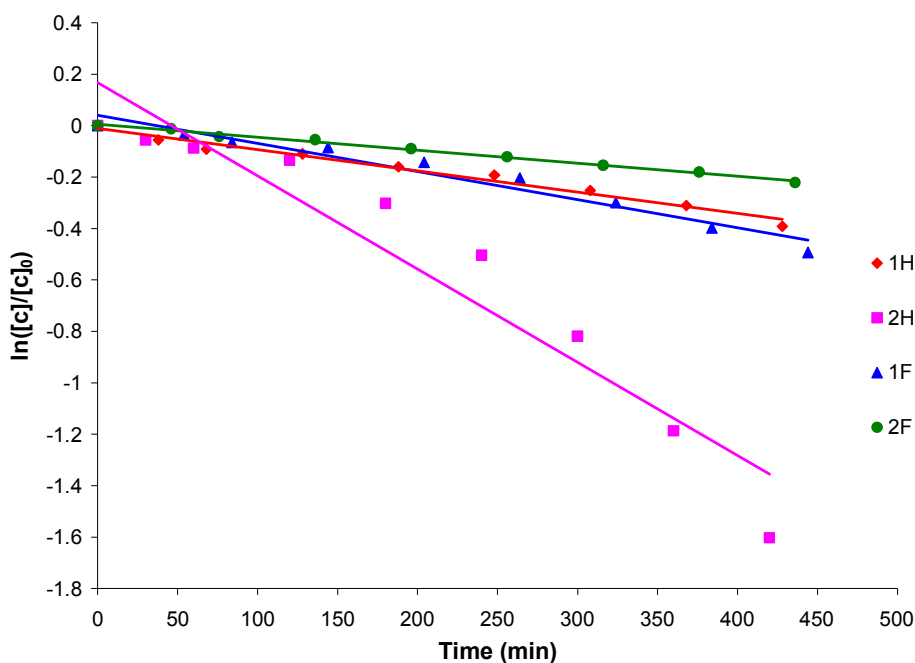
Figure 3.12: Thermal Stability of compounds **1H**, **2H**, **1F** and **2F** at 80°C for 7 hours.

After 70 hours at 60°C, **2F** showed no changes in the absorbance spectra, however under the same conditions, significant degradation of **1F** was observed, with the half-life calculated to be 147 hours. The perhydro-derivatives showed the opposite trend to their perfluoro analogues, where **1H** did result in degradation, with a half-life of 1155 hours, whilst **2H** was found to be the least stable at 60°C, with a half-life of 49.5 hours. The thermal stability of the closed-switches was also examined at 80°C (7 hours), and at 100°C (1-2 hours). The four switches showed increasing rates of degradation with increasing temperature, however, the decreasing order of stability was the same as that found for the experiments run at 60°C: **2F** > **1H** > **1F** > **2H**.

Table 3.6: Half lives of **1H/F** and **2H/F** in their closed-forms at 60°C, 80°C and 100°C, in toluene.

Compound	$t_{1/2}$ at 60°C (hr)	$t_{1/2}$ at 80°C (hr)	$t_{1/2}$ at 100°C (hr)
1H	1155	14	1.5
1F	147	10.5	1
2H	49.5	3	0.4
2F	No degradation	23	1

The order of stability of these compounds seems to suggest that the atoms in the cyclopentene ring and the substituents attached to the thiophene ring strongly affect the stability factors, almost to the same extent. The electron-withdrawing effect of the fluorines appear to heavily influence the more conjugated switches, with **2F** being the most stable and **2H** being the least stable. However, the absence of the phenyl linker between the switching unit and the ethynylthiophene moiety seems to have an interesting effect on the stability of the switches, with the perhydro-derivative performing better then the perfluoro-derivative.

In comparison to some thermal stability studies described in the literature,[5-7,9,13,14,16] as discussed in section 3.1, compounds **1H/F** and **2H/F** can be deemed to be reasonably thermally stable. However, although the absorption bands in the visible region of the UV-vis spectra, representing the closed forms, decreased during these thermal studies, the absorption bands in the UV region, representing the open form, did not re-emerge completely. Hence, contrary to the literature reports, these compounds appear to undergo degradation at these temperatures, in-conjunction with thermal cycloreversion processes, but further experiments would be necessary to confirm what thermal processes are taking place.

3.3.5 Fluorescence

The fluorescence behaviour of the switches was investigated at room temperature in THF (c = 4.0 x 10^{-6} mol/L), and the results are summarised in table 3.7. When **1H** was excited at the λ_{max} in the UV absorbance spectrum (287 and 310 nm) the intensity of the emission peak observed at 380 nm was so low (< 15) that the switch was regarded as non-fluorescent. A similar result was found for the perfluoro-derivative **1F** when excited at 306 nm (emission intensity < 10 at 470 nm). The corresponding ring-closed isomers were also found to be non-luminescent. The concentration of the solutions were altered in order to investigate whether the fluorescence intensity would increase with increasing concentration (1 x 10^{-5} and 2 x 10^{-5}), however no changes were observed.

Table 3.7: The fluorescent properties of diarylethenes **1H/F** and **2H/F**.

Compound	Excitation λ/nm	Emission λ/nm	
		Open-ring	Closed-ring
1H	287, 310	380*	380*
1F	306	470*	470*
2H	342	398	388
2F	333	384	384

* Indicates very weak fluorescence

However, upon the introduction of a π-conjugated system, through the presence of the phenyl moieties, fluorescence was observed for **2H**. Following excitation at 342 nm, an emission spectrum was recorded with a λ_{max} at 398 nm. However, excitation at 342 nm was found to induce ring-closing, and following irradiation of the solution at λ = 313 nm to produce the ring-closed isomer, a decrease in the emission intensity, and a blue-shift in the λ_{max} of the emission band to 388 nm, was observed. Once the photostationary state was reached, 50% of the emission intensity remained, as illustrated in figure 3.13. As described in section 3.1, it is typical for closed-ring isomers to cause a decrease in the emission intensity, and in many cases, the fluorescence is almost completely quenched upon cyclisation. Therefore, with reference to the theory put forward by Irie et al,[27] the emission intensity remaining for the closed form of **2H** may be a consequence of an incomplete cyclisation reaction and the existence of parallel conformations of **2H**. Cycloreversion back to the open-

ring isomer, following irradiation with visible light ($\lambda > 550$nm), reproduced the original emission spectra.
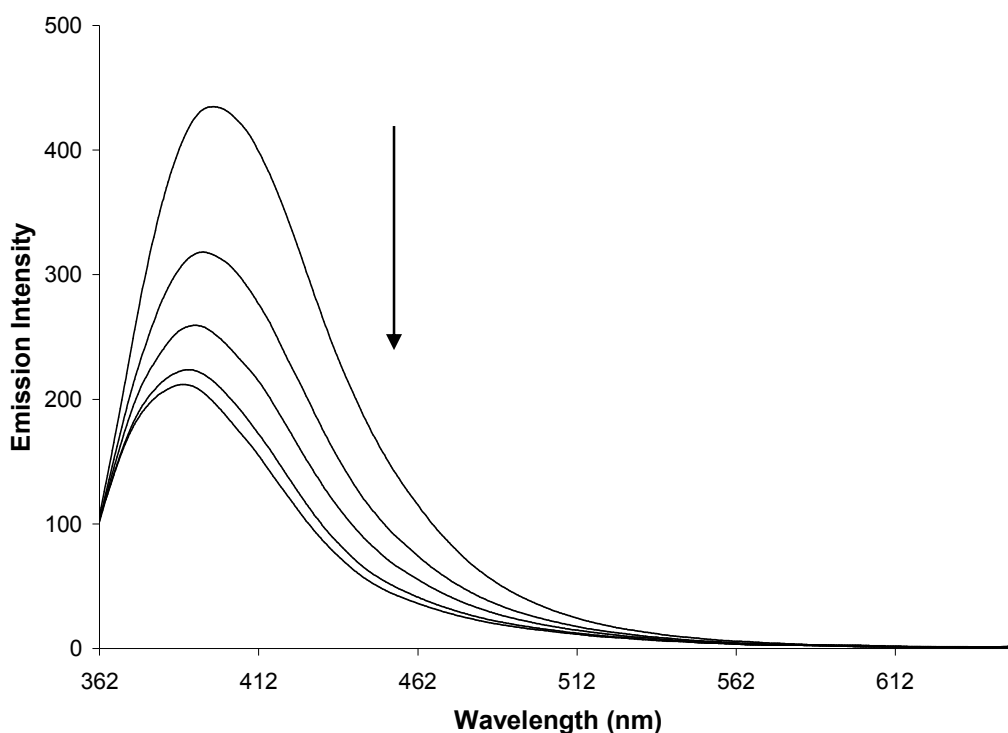
Figure 3.13: Emission spectral changes of **2H**, in THF (c = 4 x 10^{-6} mol/L), following irradiation at λ = 313 nm. The intensity of the emission decreased when the open-ring isomer cyclised to the closed-ring isomer, with 50% of the emission intensity remaining at the photostationary state.

In the case of **2F**, fluorescence was observed with a λ_{max} at 384 nm in the emission spectrum, following excitation at 333 nm. In comparison to the perhydro-derivative **2H**, the emission band of **2F** appeared at a similar wavelength, however, it was found to be approximately 30% less intense than the emission observed for **2H** at the same concentration (c = 4 x 10^{-6} mol/L). Excitation at 333 nm was found to induce ring-closing, as evidenced from a pale blue colour emerging in the solution. However, irradiation of **2F** at λ = 313 nm, forming the closed-ring isomer, did not result in a decrease in the emission intensity, as was found for the closed form of **2H**. Instead, the intensity of the emission marginally increased ($\sim$ 6%), as illustrated in figure 3.14. A significant increase in the emission intensity of such diarylethene switches, following cyclisation to the closed-form, has been reported on a few occasions.[24-26] However, in this case it is most likely due to an impurity in the solution of **2F**.
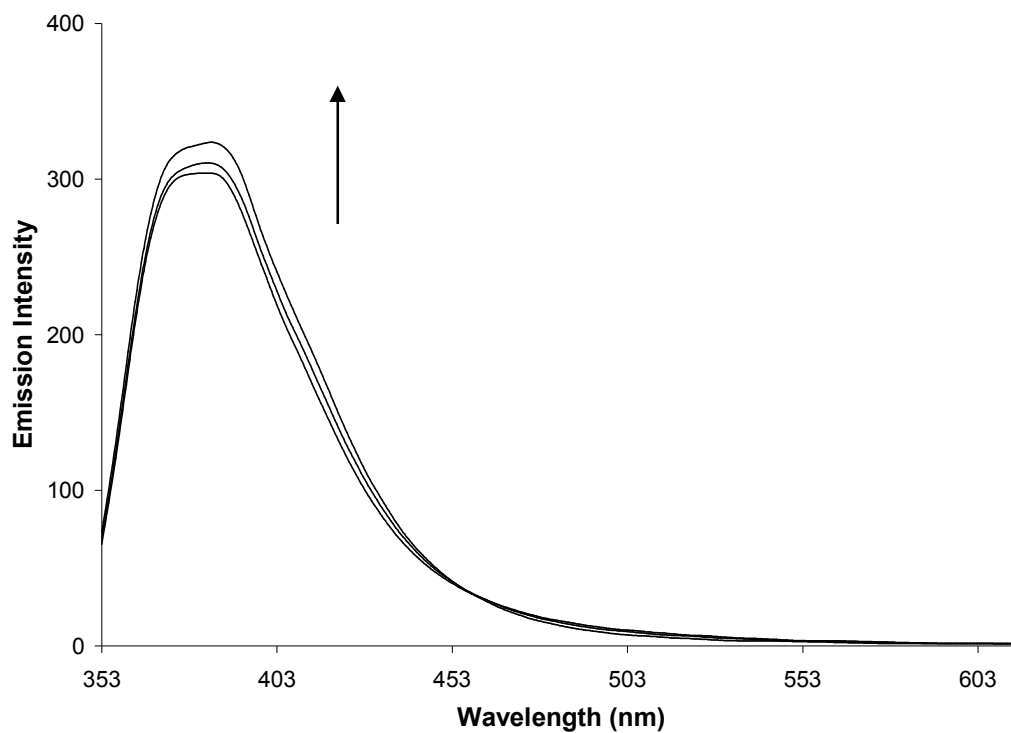
Figure 3.14: Emission spectral changes of **2F**, in THF (c = 4 x 10^{-6} mol/L), following irradiation at λ = 313 nm. The intensity of the emission increased slightly (~ 6%) when the open-ring isomer cyclised to the closed-ring isomer.

3.3.6 Cobalt Carbonyl Complexes: UV-vis Absorption Spectra
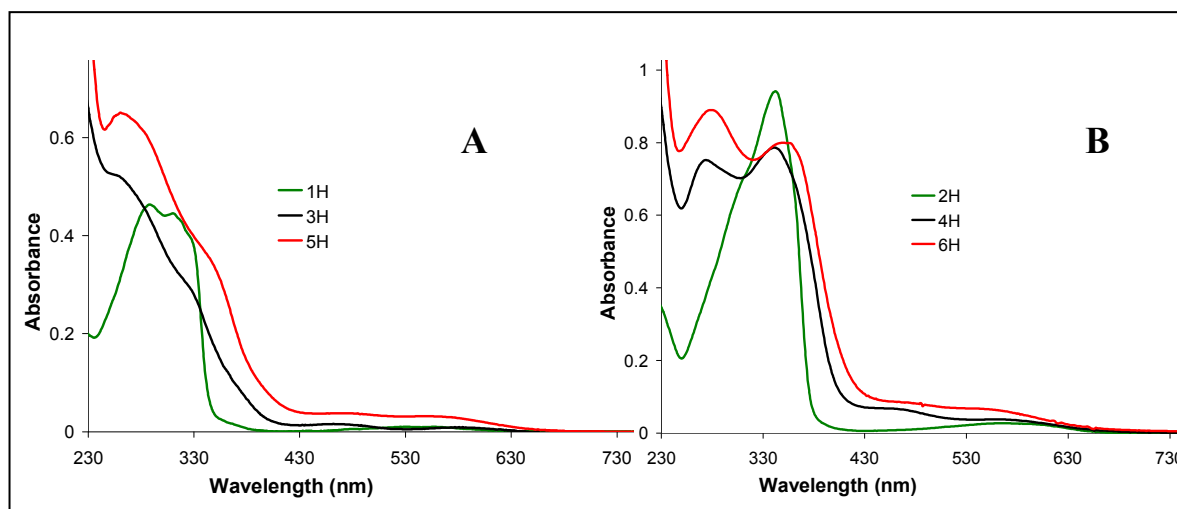
Figure 3.15: UV-vis absorption spectra of the open-ring isomers {**1H**, **2H**}, and their corresponding $Co_2(CO)_6$ complexes {**3H**, **4H**} and $Co_2(CO)_4dppm$ complexes {**5H, 6H**}, of the perhydro-cyclopentene compounds, in THF solution (c =1.4 x 10^{-5} mol/L). A: **1H** (green line), **3H** (black line), **5H** (red line); B: **2H** (green line), **4H** (black line), **6H** (red line).

The UV-vis absorption spectra of the $Co_2(CO)_6$ complexes {**3H/F**, **4H/F**} and the $Co_2(CO)_4dppm$ complexes {**5H/F**, **6H/F**} were recorded in THF. Incorporating cobalt metal complexes onto both sides of compounds **1H/F** and **2H/F** resulted in a significant change in the electronic absorption spectra of these switches, as illustrated for the perhydro-derivatives in figure 3.15. Attaching $Co_2(CO)_6$ onto compound **1H**, forming compound **3H**, resulted in a much broader absorbance in the UV region between 250 and 400 nm. The λ_{max} appeared at 252 nm, which is assigned to a ligand field "d-d" transition corresponding to the d orbitals on the cobalt atoms, and a shoulder appeared at 327 nm, which is due to the intraligand excited state. Low-lying metal-to-ligand charge-transfer (MLCT) bands were also observed in the visible region from 420 nm, extending to approximately 640 nm, with a λ_{max} appearing at 462 and 569 nm.

In the case of the extended π–conjugated analogue of **3H**, a ligand-field "d-d" transition and low-lying MLCT bands were also observed for **4H**, at 274 nm and in the region 430-680 nm, respectively. However, the intraligand band observed for **4H** at 341 nm was found to be far more prominent than that of **3H**, indicating that coordination of the $Co_2(CO)_6$ complexes involves relatively small perturbation of the electronic structure of the free ligand. This phenomenon is most likely due to the

presence of the phenyl moieties on either side of the switch, separating the switching unit and the alkynyl-bridged cobalt carbonyl units.

When the 1,2-bis(diphenylphosphino)methane {dppm} ligand was incorporated onto the cobalt carbonyl moieties, moderate changes were observed in the electronic absorption spectra for the complexes, with only a slight hyperchromic shift observed. Similar results were observed for the cobalt carbonyl complexes of the perfluoro-derivatives, and the results are summarised in table 3.8

Table 3.8: UV-vis absorption data for the open-ring isomers {**1H**, **1F**, **2H**, **2F**} and the corresponding $Co_2(CO)_6$ complexes {**3H**, **3F**, **4H**, **4F**} and $Co_2(CO)_4$dppm complexes {**5H**, **5F**, **6H**, **6F**}, in THF.

Absorption Spectra in THF					
Open-ring isomer λ_{abs} [nm] (ε x 10^3 M^{-1} cm^{-1})		$Co_2(CO)_6$ Complexes λ_{abs} [nm] (ε x 10^3 M^{-1} cm^{-1})		$Co_2(CO)_4$dppm Complexes λ_{abs} [nm] (ε x 10^3 M^{-1} cm^{-1})	
1H	287 (29.6), 310 (28.3)	**3H**	259 (50.8), 327 (27.4), 462 (3.6), 569 (2.1)	**5H**	260 (46.8), 348 (23.3), 474 (2.5), 555 (2.2)
1F	259 (24.3), 306 (43.9), 322 (35.3)	**3F**	275 (37.3), 326 (23.2), 452 (2.0), 555 (1.0)	**5F**	272(54.4), 340 (32.1), 474 (3.2), 555 (2.4)
2H	305 (46.5),343 (69.0)	**4H**	274 (51.2), 341 (53.0), 455 (4.7), 558 (2.4)	**6H**	279 (51.2), 351 (53.2), 474 (4.2), 555 (3.3)
2F	262 (22.4), 277 (25.3), 333 (76.2)	**4F**	274, 328, 450, 559		-

3.3.7 Photochromic Behaviour of Cobalt Carbonyl Complexes: Perhydro-Switches

The $Co_2(CO)_6$ (**3H** and **4H**) and the $Co_2(CO)_4$dppm (**5H** and **6H**) complexes of the perhydro-switches were irradiated with UV light, in a degassed solution of THF, in order to investigate the influence of the metal carbonyls on the switching behaviour of the dithienylcyclopentene units. These photochemical experiments were carried out using monochromatic light at 313 nm, and a lower energy wavelength at 365 nm, and the results observed in the UV-vis absorption spectra are summarised in table 3.9.

3H: M_1=$Co_2(CO)_6$
5H: M_1=$Co_2(CO)_4$dppm

4H: M_1=$Co_2(CO)_6$
6H: M_1=$Co_2(CO)_4$dppm
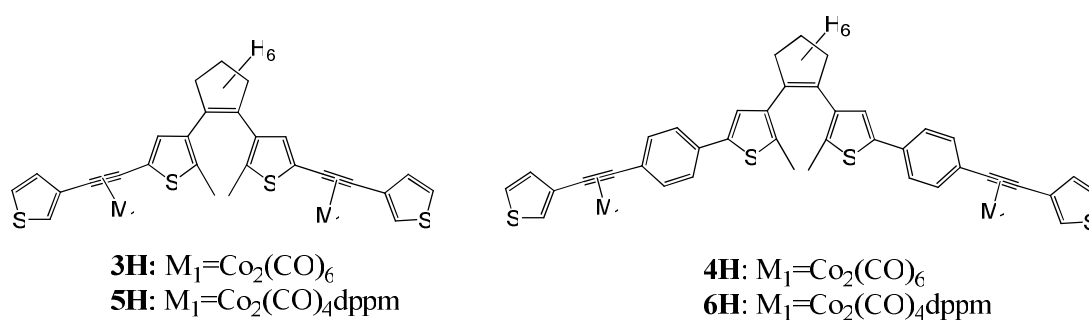
Figure 3.16: Illustrates the cobalt carbonyl complexes of the perhydro-switches (**3H**, **4H**, **5H**, **6H**).

Table 3.9: UV-vis absorption data of $Co_2(CO)_6$ complexes {**3H** and **4H**) and $Co_2(CO)_4$dppm complexes (**5H** and **6H**), in THF, in their open-ring forms and following irradiation at 313 nm and 365 nm.

Cobalt Carbonyl Complexes	Absorption Spectra in THF		
	Open-ring isomers λ_{abs} (nm)	313 nm Irradiation[a] λ_{abs} (nm)	365 nm Irradiation[a] λ_{abs} (nm)
3H	259, 327, 462, 569	259(↓), 327, 559(↑) {355}*	259(↓), 327, 462, 569 {391}*
5H	260, 348, 474, 555	260(↓), 348(↓), 474(↓), 555(↓) {400}*	260(↓), 348(↓), 474(↓), 555(↓) {400}*
4H	274, 341, 455, 558	274(↓), 311(↑), 341(↓), 561(↑) {393}*	274(↓), 311(↑), 341(↓), 561(↑) {393}*
6H	279, 351, 474, 555	279(↓), 351(↓), 563(↑) {370}*	279(↓), 351(↓), 563(↑) {417}*

[a] Decreasing absorbance (↓); Increasing absorbance (↑)
*{isosbestic points}

- **Irradiation of 3H and 5H**

When **3H** was irradiated with 313 nm light for 8 minutes, the solution changed from a pale yellow/brown to a pale purple colour. The band at 259 nm in the UV region of the absorption spectrum decreased significantly, whilst the absorption in the visible region increased (λ_{max} = 559 nm), with an isosbestic point present at 355 nm. This result indicates that cyclisation from the ring-open form to the ring-closed form occurred, as illustrated in figure 3.17.

Figure 3.17: UV-vis absorption spectrum of **3H**, in THF (c = 1.4 x 10^{-5} mol/L), following irradiation at λ = 313 nm for 8 minutes. The spectrum recorded at the start of the experiment (before irradiation) is denoted by the thick black line.

Cycloreversion back to the open-ring isomer was induced by irradiation with λ > 550 nm, which resulted in a decrease in the absorbance at 559 nm.   However, following 17 minutes of irradiation, the absorbance bands in the UV region did not return to the same value originally recorded, suggesting that **3H** underwent an irreversible photochemical process. This result is most likely a consequence of some cleavage of the $Co_2(CO)_6$ moieties.

To further examine the ring-closing process of **3H** the absorbance band in the visible region of **3H**, following λ_{irr} = 313 nm, was overlaid with the absorbance spectrum of the ring-closed isomer of the free ligand **1H**, as shown in figure 3.18. It is clear that

the molar absorptivity of the band in the visible, at the PSS of **1H**, is much greater then that of **3H**, indicating a significant decrease in the amount of the closed-ring formed for **3H**. It is also clear from this spectrum that the absorbance bands representing the closed-ring isomers have a similar shape, however, the λ_{max} was found to be bathochromically shifted for the $Co_2(CO)_6$ complex **3H**, in comparison to the free ligand **1H** (λ_{max} = 559 nm and 543 nm respectively). This suggests that the ring-closed isomer of the cobalt carbonyl complex was formed, although possibly some of the closed isomer of the free ligand, **1H**, was also present in the solution, at the PSS, due to cleavage of the metal carbonyl units.
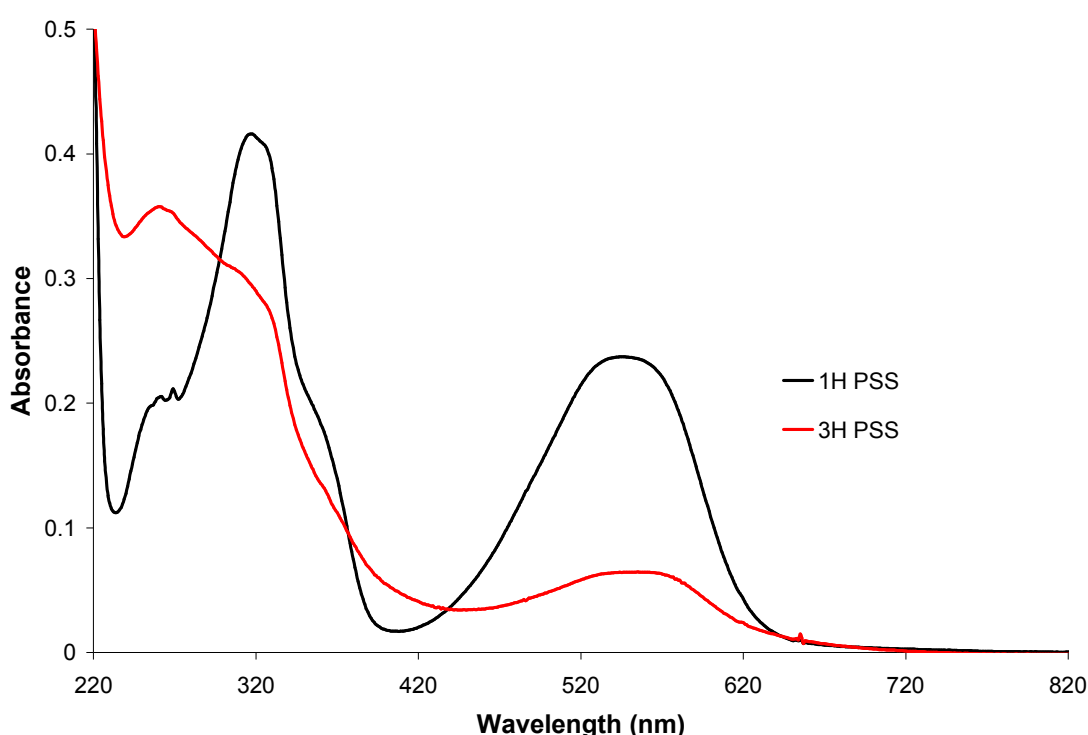
Figure 3.18: UV-vis absorption spectrum of **1H** (black line) and the corresponding $Co_2(CO)_6$ complex **3H** (red line), in THF (c = 1.4 x 10^{-5} mol/L), at the PSS following irradiation at λ = 313 nm.

A lower energy light source was used to induce cyclisation of **3H** in an attempt to reduce the decomposition processes of the cobalt carbonyl complexes. Therefore, **3H** was irradiated with λ = 365 nm, however cyclisation was not observed at this wavelength, with the absorption bands in the UV region decreasing, but no increase in the visible region. It should be noted that cyclisation of the free ligand, **1H**, did not occur at this wavelength either.

With the intention of introducing photochemical stability onto the cobalt switch, 1,2-bis(diphenylphosphino)methane {dppm} ligands were substituted onto the cobalt

hexacarbonyl complex **3H**, forming the tetracarbonyl complex **5H**. However, following irradiation at either 313 nm or 365 nm, no evidence was found for photocyclisation of **5H**, with decomposition of the complex evidenced by a decrease in the absorbance bands in the UV region.

- **Irradiation of 4H and 6H**

When **4H** was irradiated at 313 nm for 8 minutes, a colour change from yellow/brown to purple was observed. The appearance of a new absorption band in the visible region, with λ_{max} at 561 nm, indicated the presence of the ring-closed form in solution. The bands at 274 and 341 nm were found to decrease, with the appearance of a new band at 311 nm and an isosbestic point at 393 nm, as shown in figure 3.19.
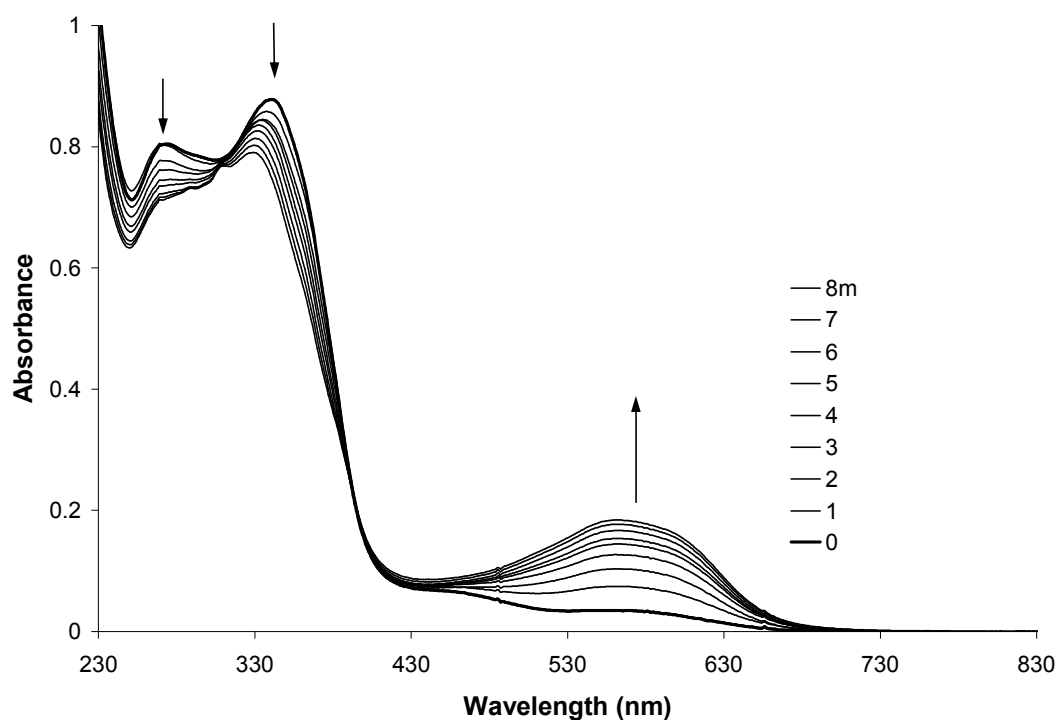
Figure 3.19: UV-vis absorption spectrum of **4H**, in THF (c = 1.4 x 10^{-5} mol/L), following irradiation with λ = 313 nm for 8 minutes. The spectrum recorded at the start of the experiment (before irradiation) is denoted by the thick black line.

Subsequent switching back to the ring-open form, following irradiation with $\lambda > 550$ nm, was evident from the decrease in the absorbance band in the visible region (figure 3.20). However, the bands at 274 and 341 nm did not recover substantially, but the new band at 311 nm continued to increase in absorbance, suggesting loss of the cobalt carbonyl moieties.

Irradiation with 365 nm light also induced ring-closing in **4H**, contrary to its less conjugated analogue **3H**, however it is worth mentioning that **2H** (the free ligand of **4H**) also undergoes cyclisation at 365 nm, unlike **1H** (the free ligand of **3H**). Unfortunately, the $Co_2(CO)_6$ complexes were not found to be photochemically stable at $\lambda_{irr} = 365$ nm, as the absorbance bands in the UV region did not return to their initial values.

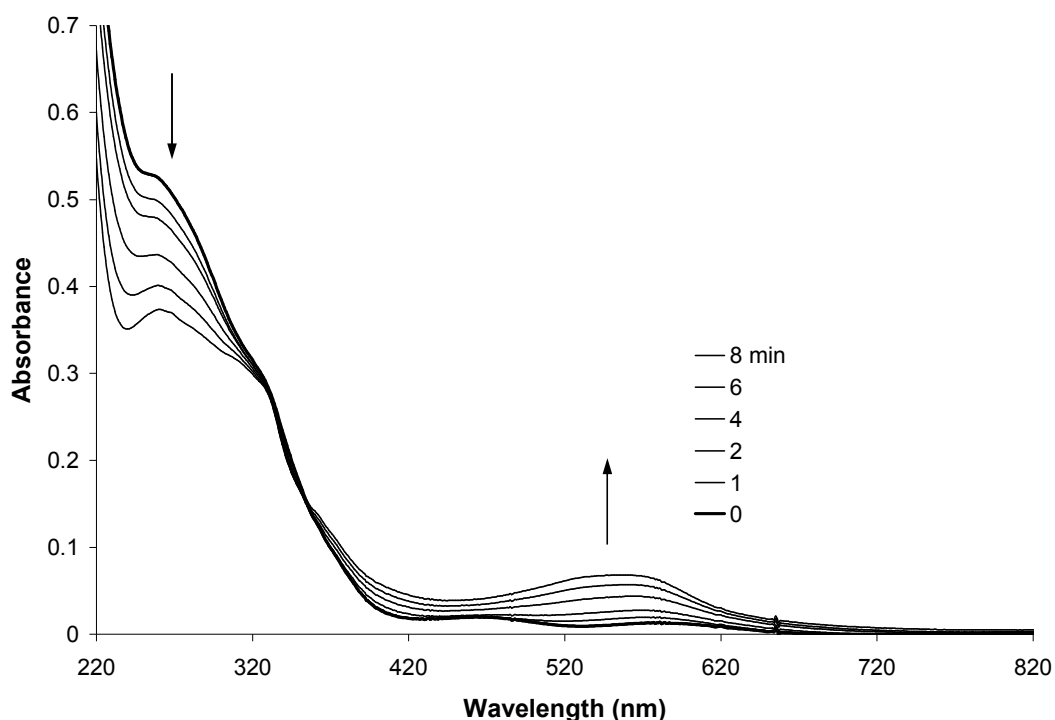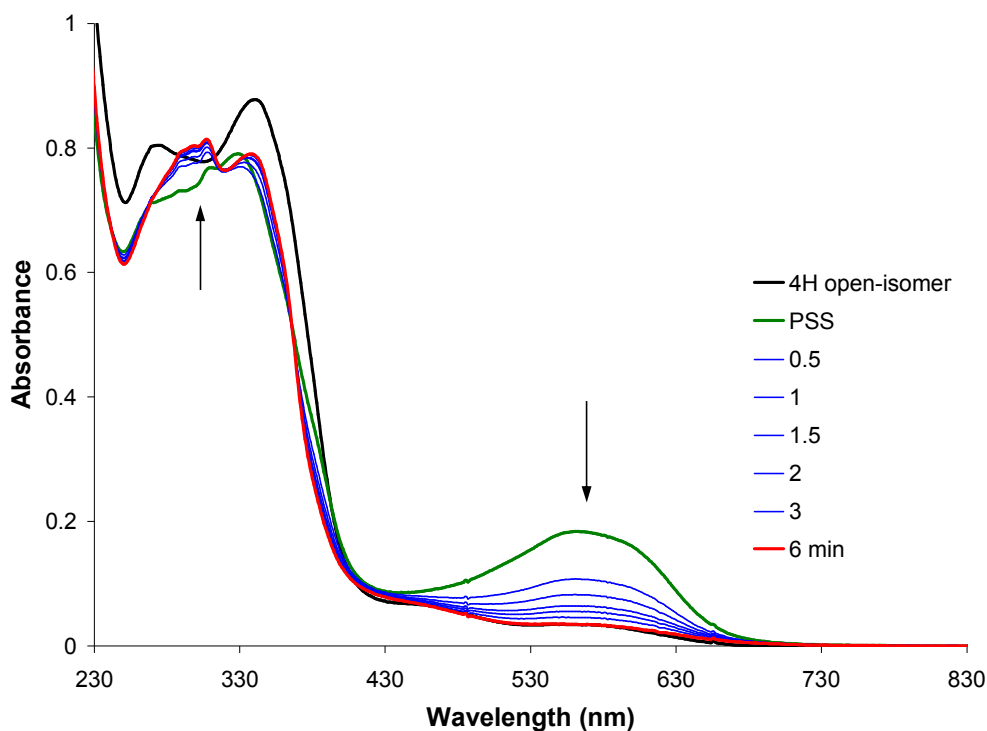**Figure 3.20:** UV-vis absorption spectrum of **4H**, in THF (c = 1.4 x 10^{-5} mol/L), following irradiation with $\lambda > 550$ nm for 6 minutes (red line); **4H** open-isomer before any irradiation (black line); **4H** at the PSS, following irradiation at $\lambda = 313$nm (green line).

The $Co_2(CO)_4$dppm complex **6H**, was found to undergo photocyclisation processes at both 313 nm and 365 nm, contrary to its less extended system **5H**, which was not found to undergo ring-closing at either wavelength. This could possibly be due to the presence of the phenyl moieties acting as spacer units between the central switching unit and the alkynyl cobalt carbonyl moieties. However, the presence of the dppm ligands on the cobalt centres was not found to stabilise the cobalt carbonyl moieties as originally intended, as although the band in the visible region decreased, the absorption bands in the UV region did not recover fully, following irradiation with visible light.

It was not clear if the ring-closed product of **4H** and **6H** was that of the cobalt carbonyl complex, or in fact the free ligand. In order to elucidate the results observed, the closed-ring isomer of **4H** was synthesised by converting the open-ring isomer of **2H** to the closed ring isomer (**2Hc**), followed by the addition of $Co_2(CO)_6$ complexes to produce **4bH**, as illustrated in scheme 3.7.
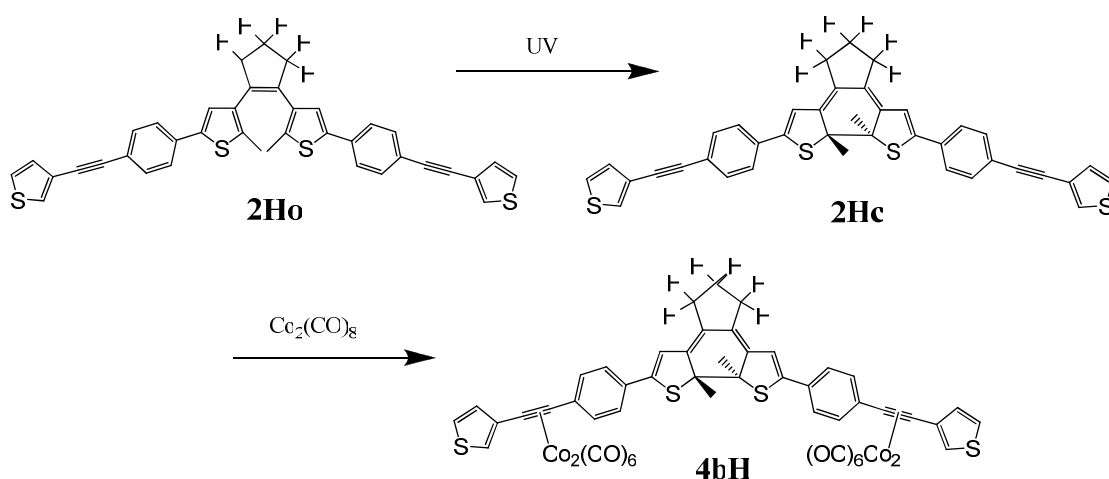
Scheme 3.7: Illustrates the formation of the ring-closed $Co_2(CO)_6$ complex **4bH**.

Figure 3.21 shows the UV-vis spectrum of the $Co_2(CO)_6$ complex **4H**, the $Co_2(CO)_4$dppm complex **6H** and the corresponding free ligand **2H**, following irradiation at $\lambda = 313$ nm, overlaid with the closed-ring $Co_2(CO)_6$ complex **4bH**. The λ_{max} of the closed-ring isomers of **4H** (561 nm) and **6H** (560 nm), were found to be almost identical to that of **2Hc** (562 nm), whereas the absorbance band of **4bH** in the visible region was found to be much broader in comparison, with a $\lambda_{max} = 584$ nm. Thus, UV irradiation of **4H** and **6H** appears to produce an absorption spectrum more similar to that of the closed-ring isomer of the free ligand, than the closed-ring isomer of the $Co_2(CO)_6$ complex **4bH**. Hence these results suggests that UV irradiation of **4H** and **6H** results in cleavage of the cobalt carbonyl units, and the resulting ring-closed isomer is the free ligand **2H**. Although, it is possible that some of the closed-form of the $Co_2(CO)_6$ and $Co_2(CO)_4$dppm complexes are also present in the solutions of **4H** and **6H**, following irradiation.
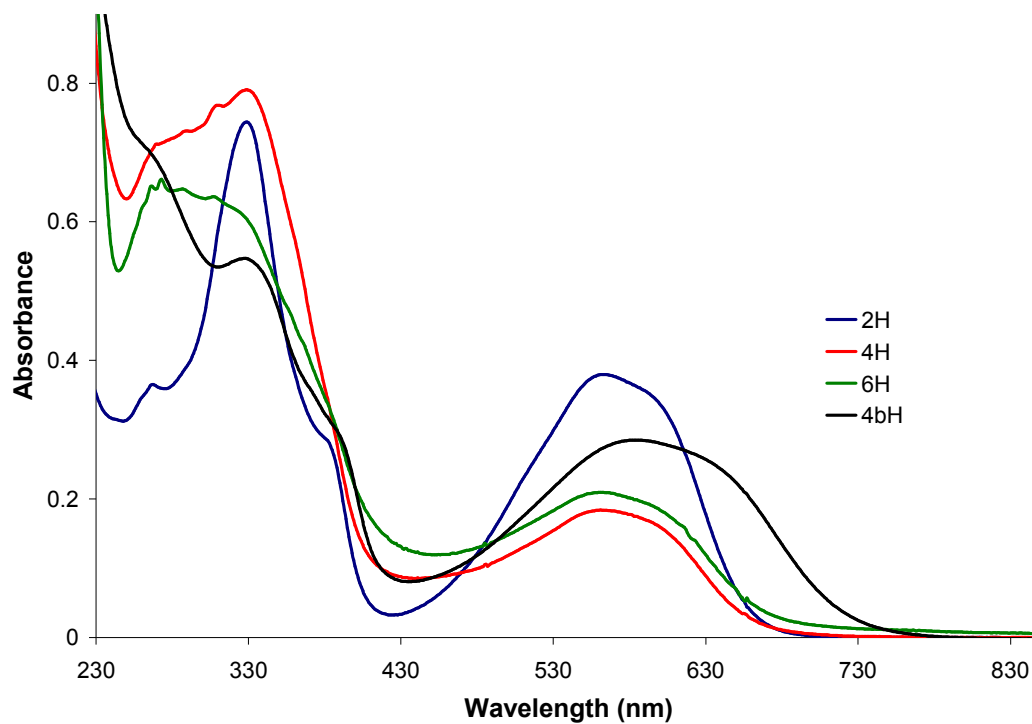
Figure 3.21: UV-vis absorption spectrum of the free ligand **2H** (blue line), the corresponding $Co_2(CO)_6$ complex **4H** (red line) and the $Co_2(CO)_4$dppm complex **6H** (green line), in THF, at the PSS following irradiation at $\lambda = 313$ nm, overlaid with the absorption spectrum of the ring-closed $Co_2(CO)_6$ complex **4bH** (black line).

3.3.8 Photochromic Behaviour of Cobalt Carbonyl Complexes: Perfluoro-Switches

The photochromic properties of the $Co_2(CO)_6$ (**3F** and **4F**) and $Co_2(CO)_4$dppm (**5F**) complexes of the perfluoro-switches were examined in order to investigate the influence of the metal carbonyls on the switching behaviour of the dithienylcyclopentene units. These photochemical experiments were carried by irradiating degassed solutions of these complexes, in THF, using monochromatic light at 313 nm and 365 nm, while monitoring the changes in the UV-vis absorption spectra. The results are summarised in table 3.10 and the structures of the perfluoro cobalt carbonyl complexes are illustrated in figure 3.22.

3F: M_1=$Co_2(CO)_6$
5F: M_1=$Co_2(CO)_4$dppm

4F: M_1=$Co_2(CO)_6$
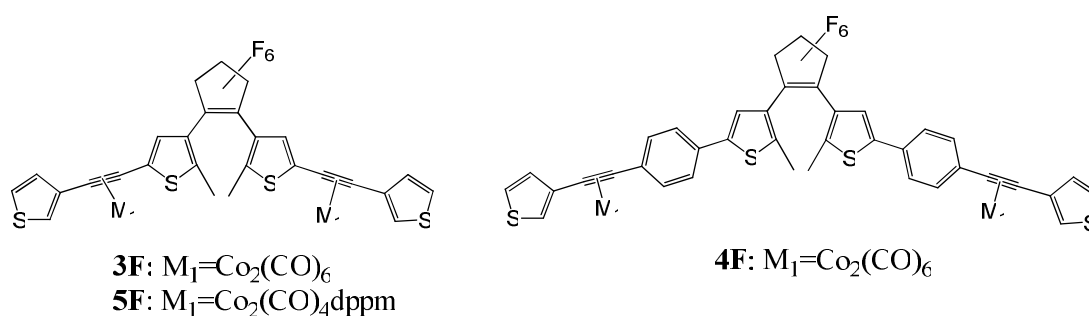
Figure 3.22: Illustrates the structures of the cobalt carbonyl perfluoro-switches (**3F**, **4F**, **5F**).

Table 3.10: UV-vis absorption data of $Co_2(CO)_6$ {**3F** and **4F**) and the $Co_2(CO)_4$dppm complex (**5F**), in THF, in their open-ring forms and following irradiation with monochromatic light at 313 nm and 365 nm.

Cobalt Carbonyl Complexes	Absorption Spectra in THF		
	Open-ring isomers λ_{abs} (nm)	313 nm Irradiation[a] λ_{abs} (nm)	365 nm Irradiation[a] λ_{abs} (nm)
3F	275, 326, 452, 555	275(↓), 326(↓), 603(↑) {345}*	275(↓), 326(↓), 452, 555 {358}*
5F	272, 340, 474, 555	272(↓), 340(↓), 474(↓), 555(↓) {402}*	272(↓), 340(↓), 474(↓), 555(↓) {428}*
4F	274, 328, 450, 559	274(↓), 328(↓), 619(↑) {366}*	274(↓), 328(↓), 619(↑) {366}*

[a] Decreasing absorbance (↓); Increasing absorbance (↑)
*{isosbestic points}

- **Irradiation of 3F and 5F**

Following irradiation of **3F** with $\lambda = 313$ nm, cyclisation to the ring-closed isomer was evident by an increase in the visible region of the absorption spectrum, with λ_{max} at 603 nm and a colour change from pale yellow/brown to light blue. The photostationary state was reached after 4 minutes of irradiation, and an isosbestic point was present at 345 nm. However the intensity of this absorption band was not as high as that recorded for the free ligand **1F**. Also noted, was a decrease in the band at 275 nm, and a moderate decrease in the intraligand band at 326 nm, as shown in figure 3.23.

Figure 3.23: UV-vis absorption spectrum of **3F**, in THF (c = 1.4 x 10^{-5} mol/L), following irradiation with $\lambda = 313$ nm for 4 minutes. The spectrum recorded at the start of the experiment (before irradiation) is denoted by the thick black line.

Following irradiation with $\lambda > 550$ nm for 6 minutes, the band at 603 nm decreased and the absorbance in the UV region ($\lambda_{max} = 275$ nm) increased, but only to about 40% of its original value, as shown in figure 3.24. As observed for its perhydro-derivative **3H**, it is clear that the closed-ring isomer for **3F** reverts back to the open-ring isomer, following irradiation with visible light (2 minutes), but the cobalt carbonyl complexes undergo an irreversible photochemical process during this colouring/bleaching process. Further evidence for cleavage of the metal carbonyl moieties is the

appearance of a shoulder at 306 nm following the cycloreversion process, which corresponds to the λ_{max} of the free ligand **1F**. However, it should be highlighted that following the ring-opening process, the absorbance bands in the UV region of **3F** recovered to a greater extent compared to **3H** (~40% *vs.* ~8% recovery of the initial absorbance values). This could possibly be an indication that the fluorine atoms have a stabilising effect on the $Co_2(CO)_6$ complex. Although, another contributing factor could be the decrease in radiation times required to reach the photostationary state (4 minutes for **3F** *vs.* 8 minutes for **3H**).
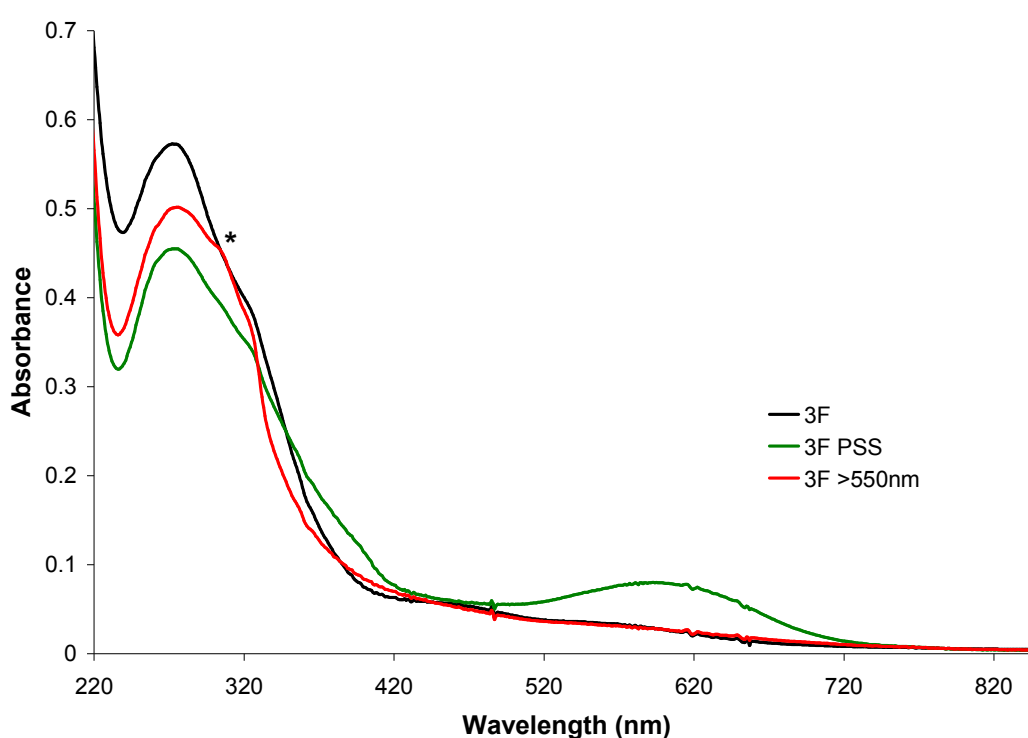
Figure 3.24: UV-vis absorption spectrum of **3F**, in THF (c = 1.4 x 10^{-5} mol/L), before irradiation (black line); at the PSS following irradiation with λ = 313 nm for 4 minutes (green line); following irradiation at λ > 550 nm (red line) where the band at 275 nm recovered to ~40% of its original value, and * indicates the shoulder at 306 nm, similar to that of the free ligand **1F**.

Irradiation of **3F** with 365 nm did not induce cyclisation, however decomposition of the $Co_2(CO)_6$ moieties was evident due to a decrease in the absorbance bands in the UV region. **1F** (the free ligand of **3F**), does undergo ring-closing at 365 nm, therefore the presence of the cobalt carbonyl complexes appear to inhibit the cyclisation process at this wavelength.

In the case of **5F**, incorporating dppm ligands onto the cobalt complex did not improve the stability of the metal carbonyl moieties. In fact, the presence of the

phosphine ligands inhibited the cyclisation processes at both 313 and 365 nm, with evidence of decomposition of the complex, due to a decrease in the absorbance bands in the UV region, at both irradiation wavelengths.

In an attempt to determine if the cyclised photoproduct of **3F** contained the cobalt carbonyl units, the closed-ring isomer of this complex was synthesised. The corresponding free ligand **1F** was irradiated with UV light, and complexed with $Co_2(CO)_6$ to produce **3bF**, as illustrated in scheme 3.8.
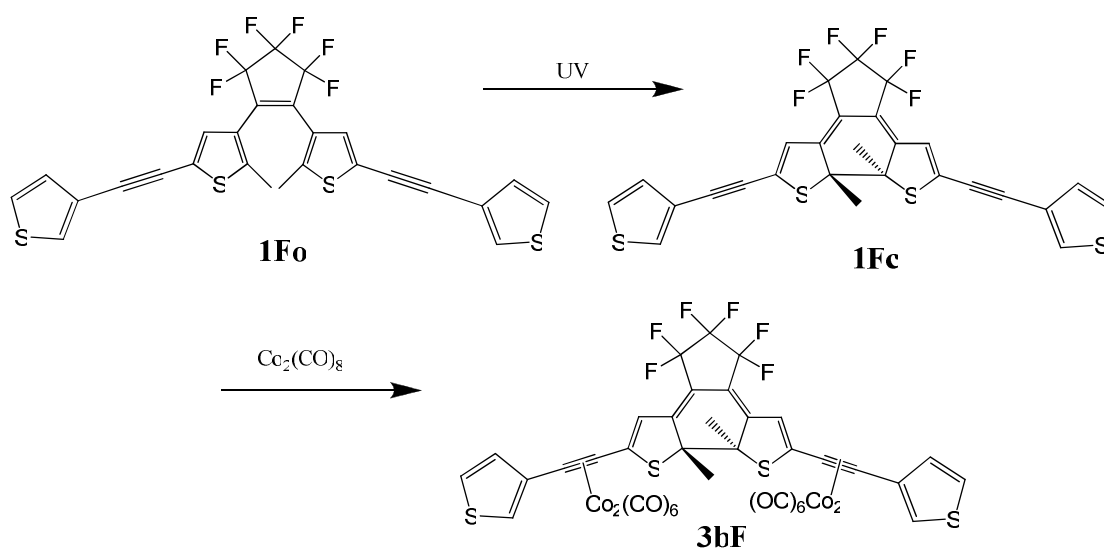
Scheme 3.8: Illustrates the formation of the ring-closed $Co_2(CO)_6$ complex **3bF**.

Figure 3.25 displays the absorption spectrum of the $Co_2(CO)_6$ complex **3F** and the corresponding free ligand **1F**, at the PSS following irradiation at 313 nm, overlaid with the UV-vis spectrum of the closed-ring isomer of the $Co_2(CO)_6$ complex **3bF**. It is clear from this spectrum that the absorbance band in the visible region at the PSS of **3F** (λ_{max} = 603 nm) is more similar to that of the free ligand **1F** (λ_{max} = 609 nm), as opposed to the closed-ring isomer **3bF** (λ_{max} = 661 nm). This result indicates that UV irradiation of **3F** results in cleavage of the $Co_2(CO)_6$ moieties from the switching unit, and that the absorbance band observed in the visible region of the UV-vis spectrum of **3F** is a consequence of the cyclisation of the free ligand **1F**. Although, it is possible that some of the closed-form of the $Co_2(CO)_6$ complex was also present in the solution of **3F** following irradiation.
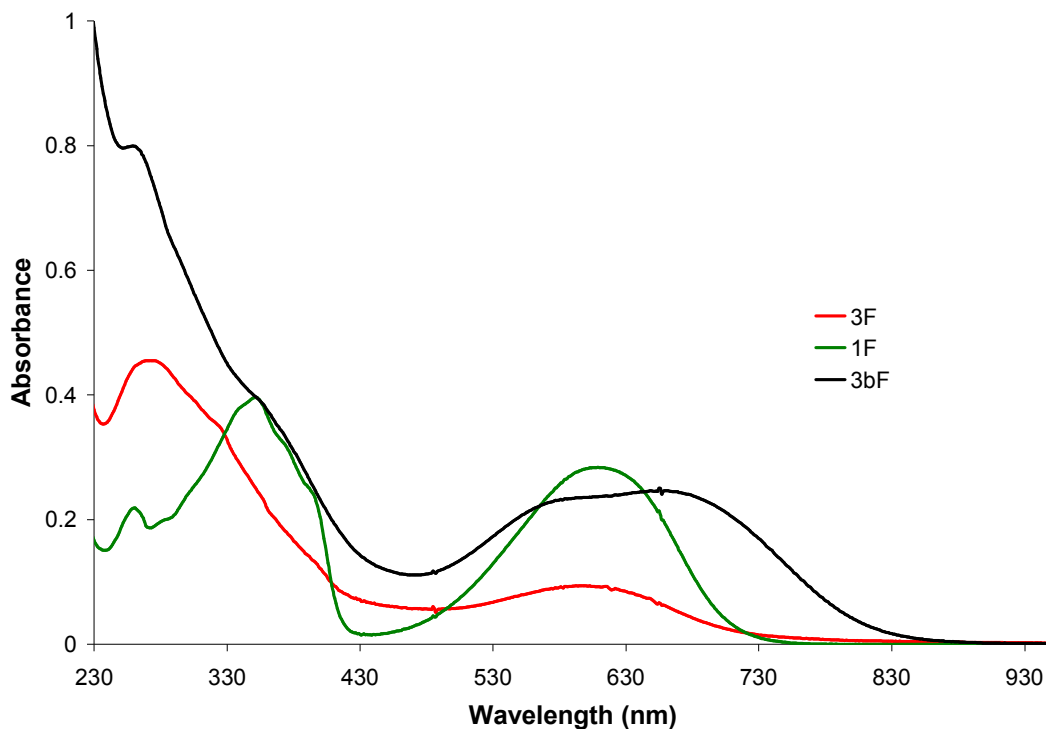
Figure 3.25: UV-vis absorption spectrum of the free ligand **1F** (green line), and the corresponding $Co_2(CO)_6$ complex **3F** (red line), in THF, at the PSS following irradiation at $\lambda = 313$ nm, overlaid with the absorption spectrum of the ring-closed $Co_2(CO)_6$ complex **3bF** (black line).

- **Irradiation of 4F**

The cyclisation process was also induced for **4F** following irradiation at $\lambda = 313$ nm, as evidenced by the colour change from yellow/brown to blue and the appearance of a broad absorption band in the visible region of the spectrum, with a λ_{max} at 619 nm. The photostationary state was reached after 2 minutes of irradiation, and the intensity of the absorbance band at 619 nm indicates that the percentage conversion from the open to the closed form is significantly less then the corresponding free ligand **2F**, but nevertheless, is greater then the other $Co_2(CO)_6$ complexes described here. A decrease in the bands at 274 and 328 nm was also observed, with an isosbestic point presented at 366 nm.

Photocycloreversion back to the open-form was achieved for this compound following irradiation at $\lambda > 550$ nm for 5 minutes. The absorbance bands in the UV region began to increase during this photobleaching process, with the bands at 274 nm and 328 nm almost completely returning to their original absorbance values, as illustrated in figure 3.27. This result suggests that during the photochromic cycle of **4F**, a small

amount of irreversible changes occurred for the metal carbonyl complex, however to a much lesser extent compared to the related $Co_2(CO)_6$ complexes, **3H**, **3F** and **4H**.
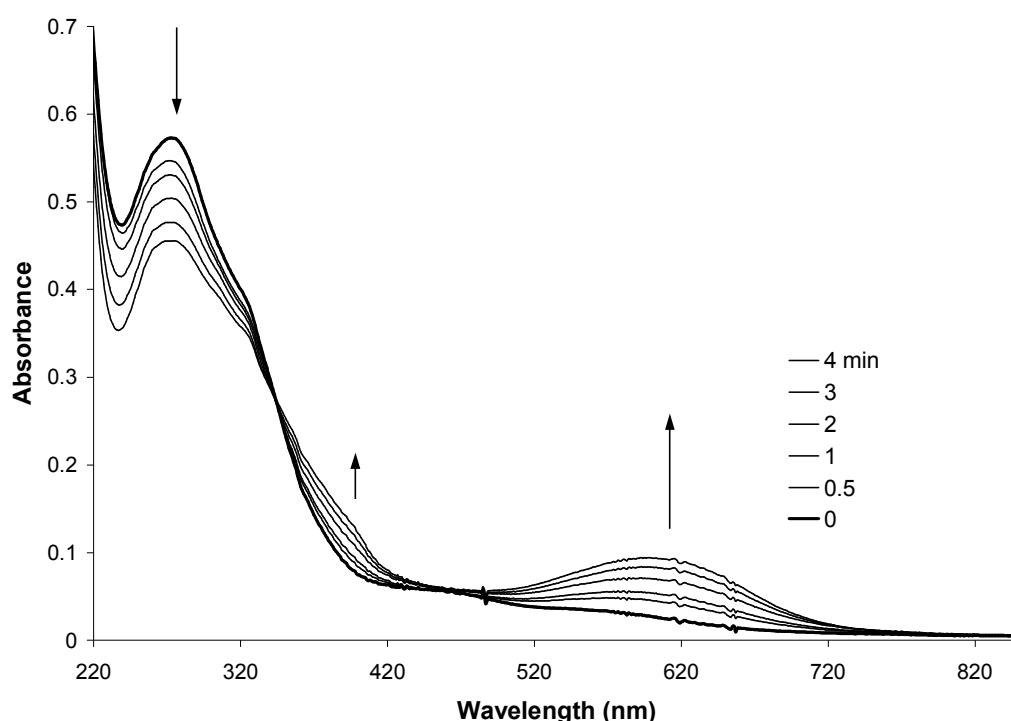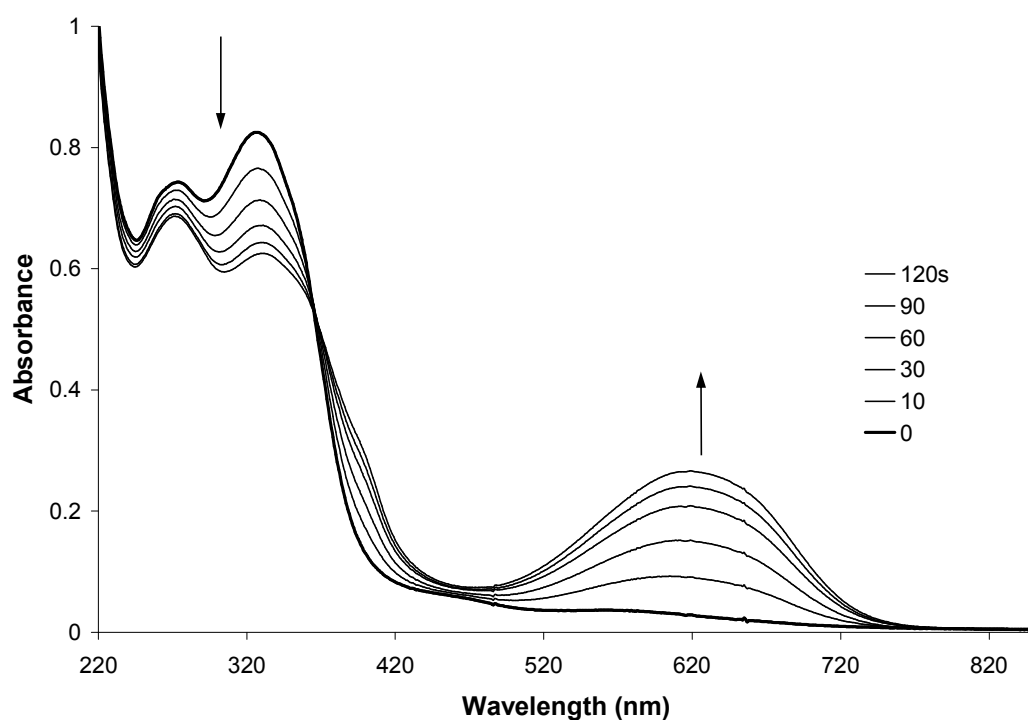

Figure 3.26: UV-vis absorption spectrum of **4F**, in THF (c = 1.4 x 10^{-5} mol/L), following irradiation with λ = 313 nm for 120 seconds. The spectrum recorded at the start of the experiment (before irradiation) is denoted by the thick black line.
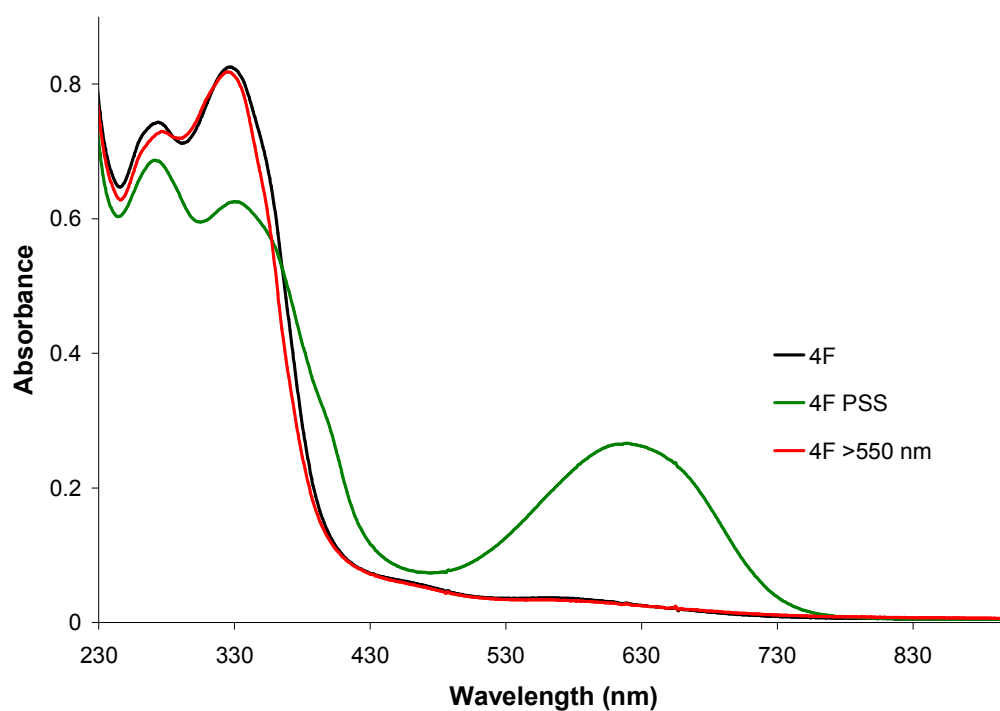
Figure 3.27: UV-vis absorption spectrum of the closed-ring isomer of **4F**, in THF (c = 1.4 x 10^{-5} mol/L): Open-ring isomer (black line); at the PSS following irradiation at 313 nm for 2 minutes (green line); following irradiation at > 550 nm for 5 minutes (red line).

Irradiation of **4F** with λ = 365 nm also induced formation of the closed-ring isomer, and the photostationary state was reached after 2.5 minutes of irradiation. Irradiating **4F** with this lower energy light source led to similar changes in the UV region as was described above for those performed at 313 nm. The effect of incorporating dppm ligands onto the $Co_2(CO)_6$ complexes of **4F** was not investigated due to the limited amount of **4F** to produce the tetracarbonyl complex.

Figure 3.28 displays a comparison between the UV-vis spectra of the $Co_2(CO)_6$ complex **4F**, and its corresponding free ligand **2F**, at the PSS following irradiation at 313 nm. Although the shape of the absorbance bands in the visible region are very similar, the λ$_{max}$ of **4F** (619 nm) is moderately bathochromically shifted by 5 nm in comparison to the free ligand **2F** (λ$_{max}$ = 614 nm), possibly suggesting that ring-closure of **4F** has occurred with the cobalt carbonyl complexes attached. More convincingly however, is the fact that the colouring/bleaching cycle appears to be much more reversible, due to the reforming of the bands in the visible region following the cycloreversion process. This result indicates that it is the $Co_2(CO)_6$ complexed switch that undergoes ring-closure.
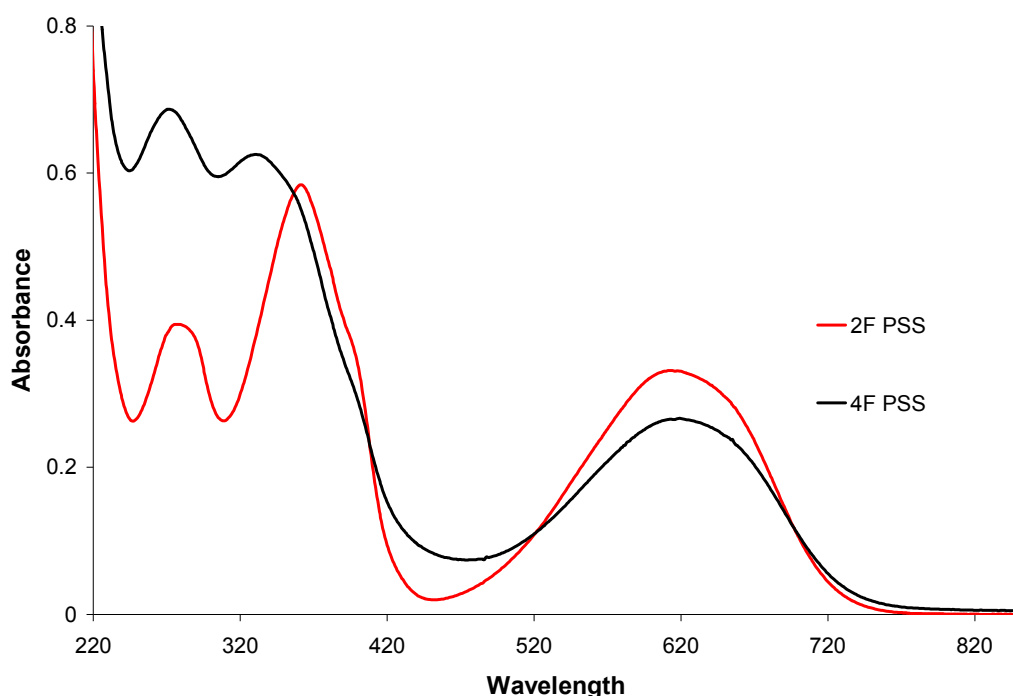
Figure 3.28: UV-vis absorption spectrum of the $Co_2(CO)_6$ complex **4F** (black line), and the corresponding free ligand **2F** (red line), in THF, at the PSS following irradiation at 313 nm.

3.3.9 Steady-State Photolysis: Infra-Red Spectra

In order to investigate the irreversible changes observed in the UV-vis spectrum following irradiation of the cobalt carbonyl thienyl-based switches, the photochemical behaviour of a number of the $Co_2(CO)_6$ and $Co_2(CO)_4$dppm complexed switches were monitored using infra-red spectroscopy.

Degassed solutions of **3H**, **4H**, **5H** and **6H** (figure 3.29) were prepared, in THF, and placed in an IR liquid cell. The solutions were irradiated at both 313 nm and 365 nm, and the changes in the carbonyl bands were monitored in the infra-red spectra. These experiments were also carried out in the presence of a trapping ligand, PPh_3, to trap any photoproducts produced. The resulting photoproducts were assigned according the results reported previously in the literature.[29-32]

3H: $M_1=Co_2(CO)_6$
5H: $M_1=Co_2(CO)_4$dppm

4H: $M_1=Co_2(CO)_6$
6H: $M_1=Co_2(CO)_4$dppm
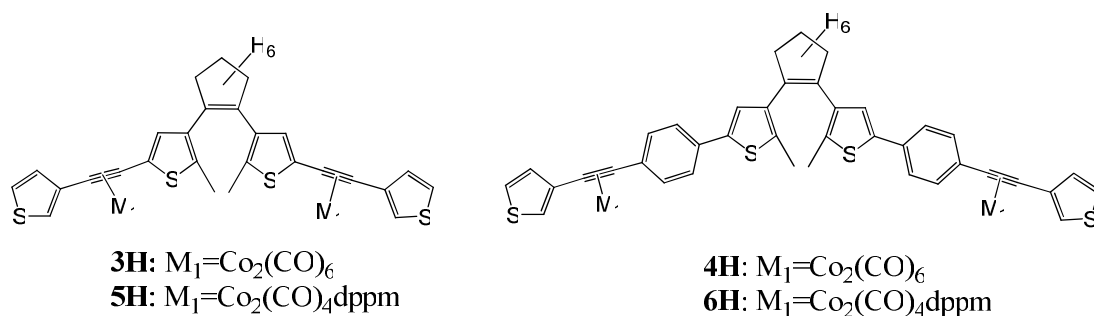
Figure 3.29: Illustrates the structures of the $Co_2(CO)_6$ {**3H**, **4H**} and the $Co_2(CO)_4$dppm complexes {**5H**, **6H**}.

- **Irradiation of 3H and 5H**

When a solution of **3H** was irradiated with 313 nm and 365 nm light, in THF, the $Co_2(CO)_6$ carbonyl bands, at 2089, 2054 and 2025 cm^{-1} in the IR, were found to decrease. After 10 minutes of irradiation the parent bands decreased by $\sim 10\%$, and after a further 40 minutes of irradiation by $\sim 20\%$. Although THF is considered to be a coordinating solvent, no new bands were observed in the IR spectrum, indicating degradation of the metal complex. In an attempt to trap intermediates, PPh_3 was added to a solution of **3H**, and irradiation was carried out at 313 nm and 365 nm.

Following irradiation at 365 nm for 10 minutes, the original $Co_2(CO)_6$ bands of **3H** (2089, 2054 and 2025 cm^{-1}) recorded at the start of the experiment, began to decrease.

However, new bands began to grow-in at 2061, 2010 and 1995 cm^{-1}, as illustrated in figure 3.30. This result indicates cleavage of a Co-CO bond, followed by substitution with PPh$_3$, thus forming the pentacarbonyl species (Switch)Co$_2$(CO)$_5$PPh$_3$. A band at 1960 cm^{-1}, attributable to the formation of the tetracarbonyl species, was also observed. When **3H** was irradiated at higher energy (λ = 313 nm) for 10 minutes, numerous new bands were observed in the IR spectrum, as shown in figure 3.30. The formation of the pentacarbonyl and tetracarbonyl species can be confirmed from reference to the literature:[29-31] (Switch)Co$_2$(CO)$_5$PPh$_3$ {2061, 2010, 1995 cm^{-1}}; (Switch)Co$_2$(CO)$_4$(PPh$_3$)$_2$ {1973, 1960 cm^{-1}}. However, two new bands were also observed at lower wavenumbers {1918 and 1885 cm^{-1}}. These bands are tentatively assigned to formation of the tricarbonyl and/or dicarbonyl species, following further substitution with the PPh$_3$ ligand.[32] From the results obtained following irradiation at both wavelengths, it was clear that the efficiency of the formation of the photoproducts of **3H** was greater at 313 nm, than at 365 nm.

Figure 3.30: The IR difference spectra of the Co$_2$(CO)$_6$ complex **3H**, in THF, following irradiation at 365 nm. (red line) and 313 nm (black line) for 10 minutes, in the presence of PPh$_3$. Negative bands indicate bleaching of the parent bands and the positive bands indicate formation of the photoproducts: (Switch)Co$_2$(CO)$_5$PPh$_3$ {*}; (Switch)Co$_2$(CO)$_4$(PPh$_3$)$_2$ {#}; (Switch)Co$_2$(CO)$_3$(PPh$_3$)$_3$ and/or (Switch)Co$_2$(CO)$_2$(PPh$_3$)$_4$ {o}.

When the $Co_2(CO)_4$dppm complex **5H** was irradiated at both 313 nm and 365 nm, in THF, a decrease in the parent bands at 2021, 1997 and 1969 cm^{-1} occurred, but no new bands were observed. Consequently, PPh_3 was added to the solution, and following irradiation at λ = 365 nm for 10 minutes, the parent bands decreased, and new bands appeared at 1989, 1951 and 1915 cm^{-1}, which can tentatively be assigned to the formation of the tricarbonyl species $(Switch)Co_2(CO)_3(dppm)(PPh_3)$. The same result was observed following irradiation at 313 nm, however, the intensities of the new bands were significantly increased relative to those observed at 365 nm, on the same timescale, as shown in figure 3.31.
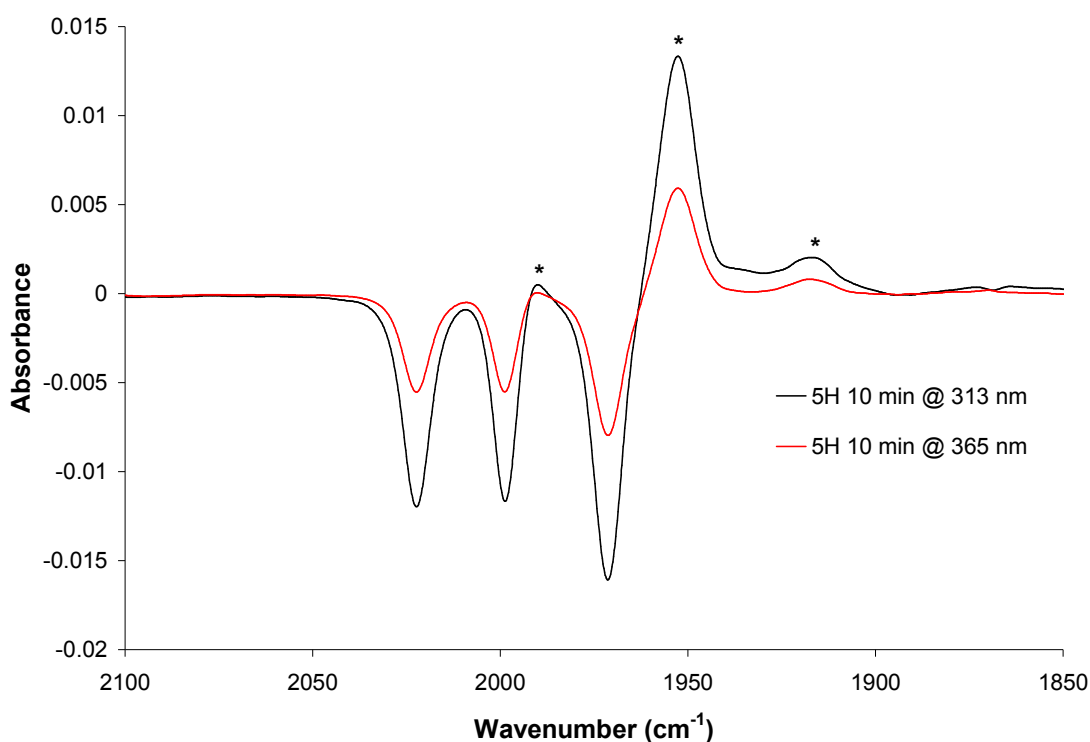
Figure 3.31: The IR difference spectra of the $Co_2(CO)_4$dppm complex **5H**, in THF, following irradiation at 313 nm (black line) and 365 nm (red line) for 10 minutes, in the presence of PPh_3. Negative bands indicate bleaching of the parent bands and the positive bands (marked *) indicate formation of the photoproduct, tentatively assigned as $(Switch)Co_2(CO)_3(dppm)(PPh_3)$.

- **IR Spectra of 4H and 6H**

Irradiation of the $Co_2(CO)_6$ complex **4H**, at 313 nm and 365 nm in THF, resulted in a decrease of the parent carbonyl bands at 2089, 2053 and 2025 cm^{-1} (by ~ 10% after 10 minutes of irradiation), with no new bands appearing, thus indicating that the cobalt carbonyl species undergoes photodegradation under these conditions. To aid the

analysis of this process, PPh$_3$ was added to the solution. Following 4 minutes of irradiation of **4H**, at 365 nm, bleaching of the parent bands resulted, in conjunction with the appearance of new bands at 2060, 2010 and 1995 cm^{-1}, signifying the formation of the pentacarbonyl species (Switch)Co$_2$(CO)$_5$PPh$_3$, and a band at 1962 cm^{-1} due to the generation of the tetracarbonyl species of **4H**, as shown in figure 3.32.
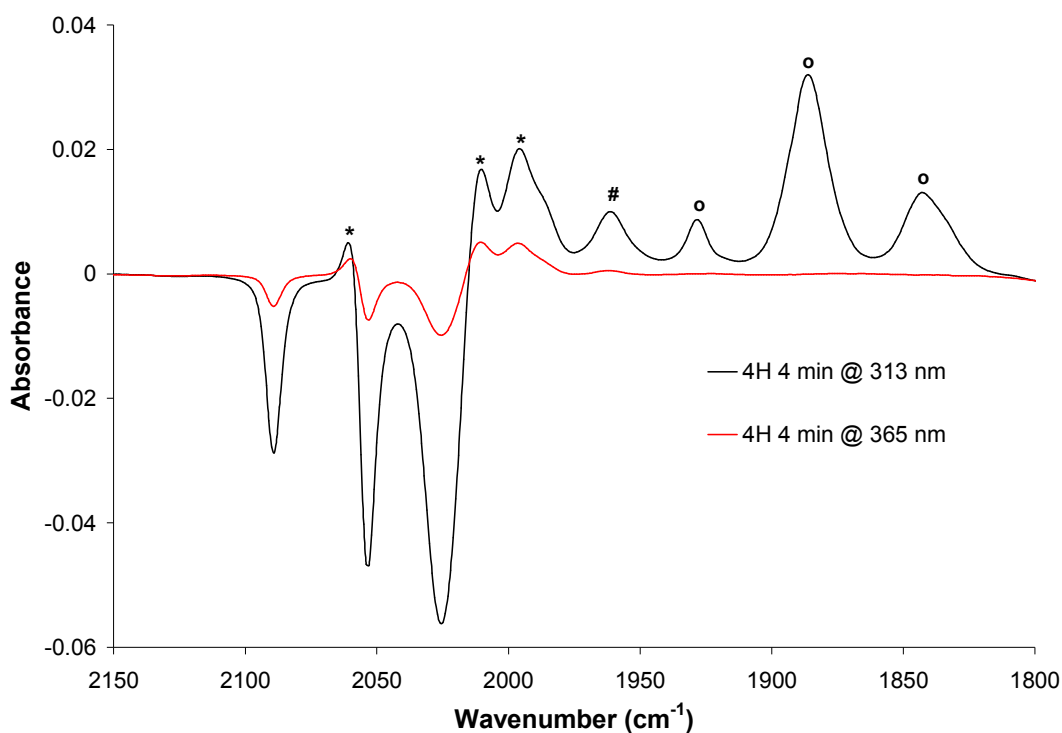
Figure 3.32: The IR difference spectra of the Co$_2$(CO)$_6$ complex **4H**, in THF, following irradiation at 365 nm. (red line) and 313 nm (black line) for 4 minutes, in the presence of PPh$_3$. Negative bands indicate bleaching of the parent bands and the positive bands indicate formation of the photoproducts: (Switch)Co$_2$(CO)$_5$PPh$_3$ {*}; (Switch)Co$_2$(CO)$_4$(PPh$_3$)$_2$ {#}; (Switch)Co$_2$(CO)$_3$(PPh$_3$)$_3$, (Switch)Co$_2$(CO)$_2$(PPh$_3$)$_4$ and/or (Switch)Co$_2$(CO)$_1$(PPh$_3$)$_5$ {o}.

When **4H** was irradiated at λ = 313 nm for 4 minutes, in the presence of PPh$_3$, photobleaching of the parent bands resulted, with the appearance of new bands at lower frequencies, associated with the formation of penta- and tetra-carbonyl species:[29-31] (Switch)Co$_2$(CO)$_5$PPh$_3$ {2060, 2010 and 1997 cm^{-1}} and (Switch)Co$_2$(CO)$_4$(PPh$_3$)$_2$ {1962 cm^{-1}}. At even lower wavenumbers, further bands appeared in the IR spectrum at 1927, 1885 and 1842 cm^{-1}. The assignment of these bands to specific photoproducts is more difficult. They are most likely a consequence of further substitution reactions with PPh$_3$, forming the tricarbonyl, dicarbonyl and/or monocarbonyl species,[32] however, further investigations are required to conclusively

assign these bands to specific carbonyl photoproducts. More importantly, by comparing the IR spectra obtained at 313 nm and 365 nm, as shown in figure 3.32, it was clear that photolysis at 313 nm induced CO loss at a much greater rate.

When the $Co_2(CO)_4dppm$ complex **6H** was irradiated with light at 313 nm and 365 nm, in THF, depletion of the parent carbonyl bands at 2020, 1996 and 1969 cm^{-1} was observed, however no new bands appeared, indicating decomposition of the cobalt carbonyl complex. The sample was irradiated with excess PPh_3 at $\lambda = 365$ nm, for 4 minutes, and bleaching of the parent carbonyl bands, along with the appearance of new bands at 1987, 1950 and 1914 cm^{-1}, was observed. These bands can tentatively be assigned to the formation of the tricarbonyl species (Switch)-$Co_2(CO)_3(dppm)(PPh_3)$.[32] Similar results were observed following irradiation of complex **6H** at higher energy ($\lambda = 313$ nm) for 4 minutes. However, the intensity of new bands were higher than those observed at 365 nm, as shown in figure 3.33, thus it appears that photolysis of the cobalt carbonyl moieties is more efficient at 313 nm.

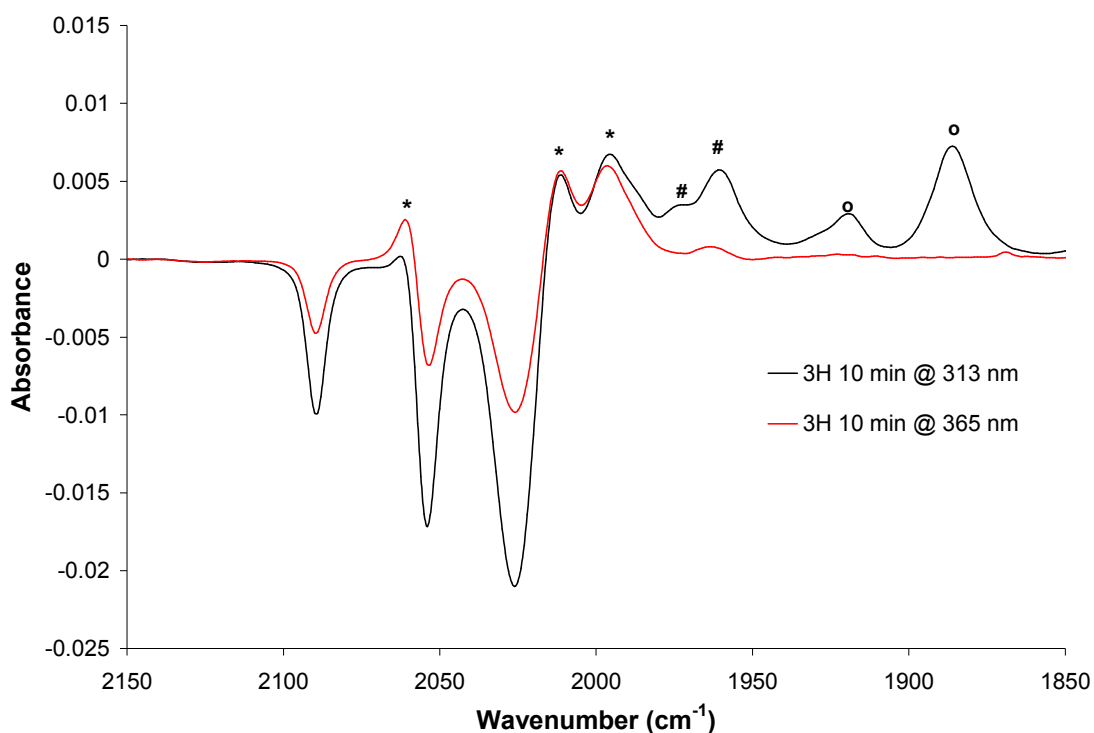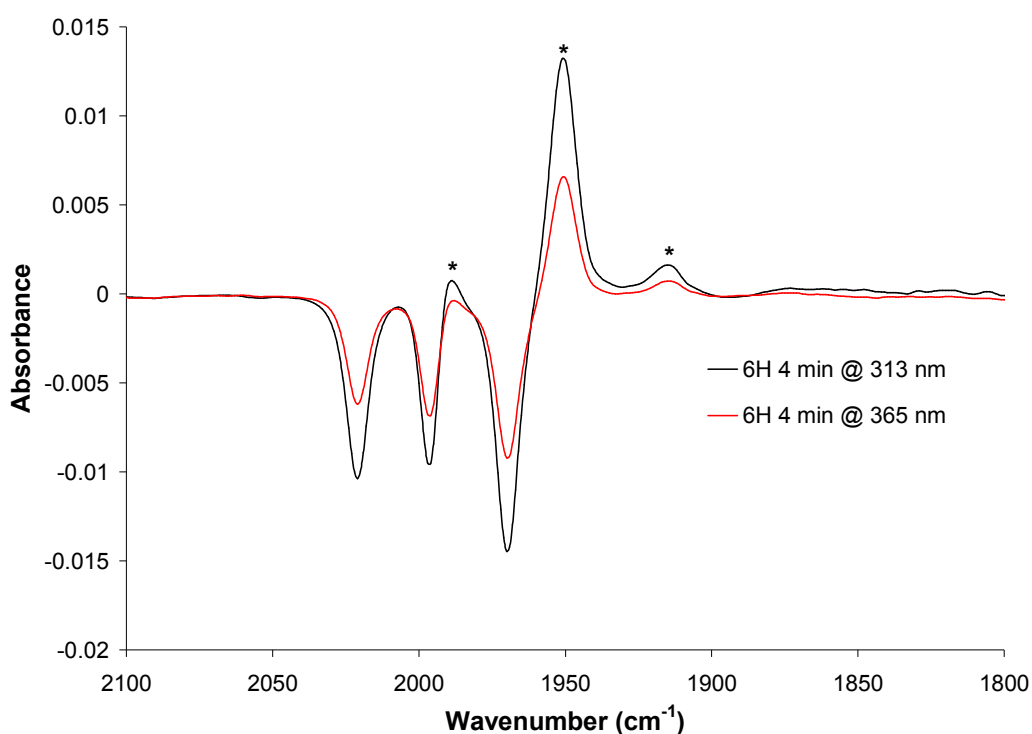**Figure 3.33:** The IR difference spectra of the $Co_2(CO)_4dppm$ complex **6H**, in THF, following irradiation at 313 nm (black line) and 365 nm (red line) for 10 minutes, in the presence of PPh_3. Negative bands indicate bleaching of the parent bands and the positive bands (marked *) indicate formation of the photoproduct, tentatively assigned as (Switch)$Co_2(CO)_3(dppm)(PPh_3)$.

171

From the steady-state photolysis experiments monitored in the IR, it can be concluded that the cobalt carbonyl complexes undergo photochemical Co-CO bond cleavage, which occurs more rapidly following irradiation at $\lambda = 313$ nm, in comparison to irradiation at lower energy (365 nm). Also, CO loss following photolysis of the $Co_2(CO)_4dppm$ complexes, appeared to be less efficient compared to the $Co_2(CO)_6$ complexes, thus highlighting the increased stability of the cobalt carbonyl moieties through the presence of the dppm ligand.

The cobalt carbonyl moieties on the more-conjugated derivatives, **4H** and **6H**, were found to undergo more efficient photoreactions compared to the shorter chain analogues, **3H** and **5H**. This phenomenon was particularly evident from the experiments of the $Co_2(CO)_6$ complexed switches performed at 313 nm. A number of photoproducts were formed following photolysis of **4H** on a shorter timescale (4 minutes) in comparison to **3H** (10 minutes), as evidenced by the more intense bands observed in the IR spectrum of **4H**, as illustrated in figure 3.34.
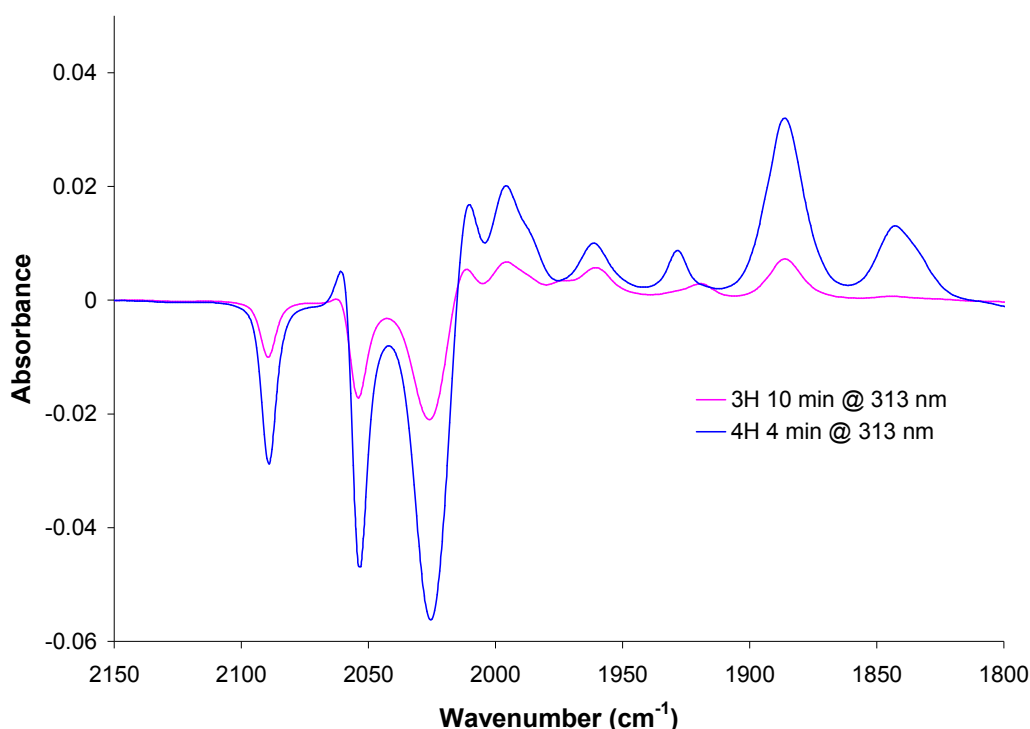
Figure 3.34: The IR difference spectra of the $Co_2(CO)_6$ complexes **3H** (pink line) and **4H** (blue line), in THF, following irradiation at 313 nm for 10 minutes and 4 minutes respectively, in the presence of PPh_3. Negative bands indicate bleaching of the parent bands and the positive bands indicate formation of the photoproducts.

Overall the steady state photolysis experiments have confirmed that CO loss occurs for these cobalt carbonyl moieties. The efficiency of this photochemical process appeared to be reduced by: 1) irradiation at lower energy ($\lambda = 365$ nm);   2) the presence of dppm ligands on the cobalt centre; 3) changes in the molecular structure of the complex i.e. in this case, reducing the length of the carbon chain. Therefore, it is clear that the stability of the cobalt carbonyl moieties can be tuned by a number of variants. In terms of the cyclisation processes described in the previous section, it can be deduced that as the switching unit undergoes a ring-closing process, the cobalt carbonyl units also undergo CO loss, followed by cleavage of the cobalt moieties from the alkynyl units.

3.3.10 Cycloreversion of the Closed-ring $Co_2(CO)_6$ Complexes

$Co_2(CO)_6$ complexes were incorporated onto the closed-ring isomers of **1F** and **2H**, producing the corresponding complexes **3bF** and **4bH** respectively, as illustrated in figure 3.35. These complexes were initially synthesised in order to aid the analysis of the cyclisation processes of the cobalt carbonyl complexes described in section 3.3.7 and 3.3.8. However, we later decided to investigate the cycloreversion processes of **3bF** and **4bH**, back to their open-forms, in order to examine if the presence of the $Co_2(CO)_6$ complexes would inhibit the ring-opening process, thus creating a chemical-locking system, which has been described previously in the literature for an organometallic switching complex.[25] Furthermore, we were interested to examine if cleavage of the cobalt carbonyl units would occur following irradiation at longer wavelengths.
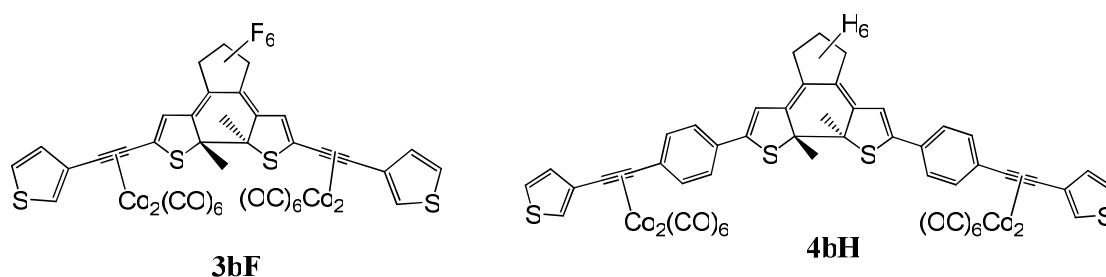
Figure 3.35: Illustrates the structures of the ring-closed $Co_2(CO)_6$ complexes **3bF** and **4bH**.
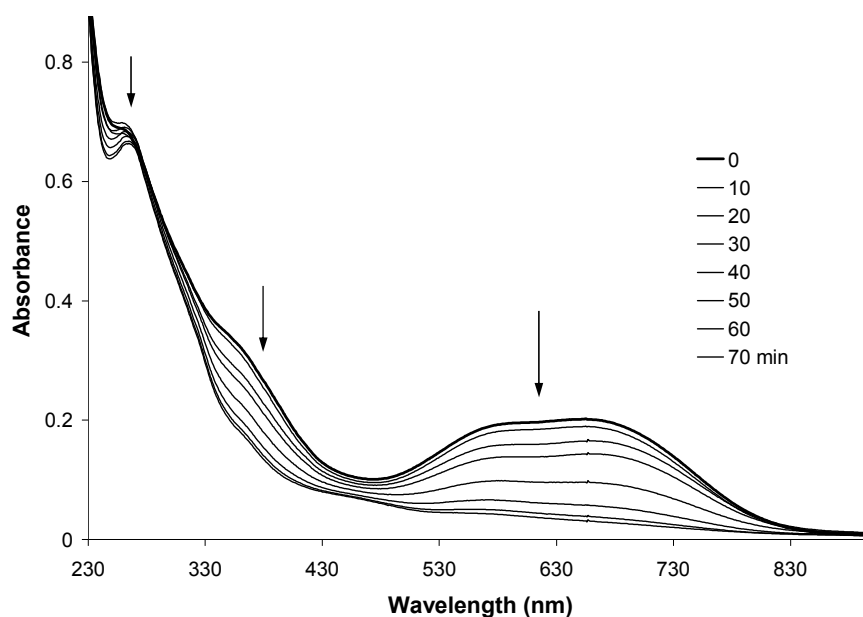
Figure 3.36: The UV-vis absorption spectrum of **3bF**, in THF, following irradiation at $\lambda > 650$ nm. The spectrum recorded at the start of the experiment (before irradiation) is denoted by the thick black line.

174

Cycloreversion of the ring-closed isomer **3bF** was induced by irradiation with broadband light, in THF, at $\lambda > 650$ nm and the results were monitored in the UV-vis absorption spectra, as shown in figure 3.36. Photobleaching back to the open-ring isomer was complete after 70 minutes of irradiation, as evidenced by the colour change from blue to colourless and the decrease in the absorption band in the visible region ($\lambda_{max} = 661$ nm). The shoulder at 365 nm also decreased in absorbance, however, the absorption band at 267 nm only decreased marginally from its original value. The fact that a large decrease was not observed in the UV region following irradiation at $\lambda > 650$ nm, contrary to the results obtained during the ring-closing process of **3F** at $\lambda = 313$ nm, indicates that the $Co_2(CO)_6$ complexes are significantly more stable under these irradiation conditions. It is clear from these results that the presence of the $Co_2(CO)_6$ complexes did not inhibit the ring-opening process, although the efficiency of the cycloreversion process for **3bF** (70 minutes) was dramatically reduced in comparison to that of the free ligand **1F** (1.5 minutes).
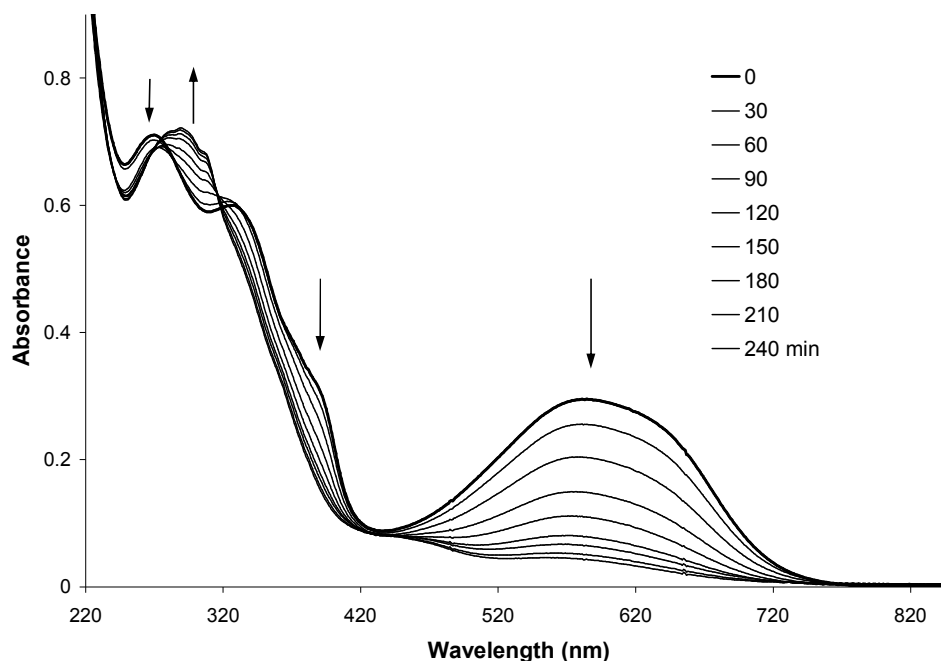
Figure 3.37: The UV-vis absorption spectrum of the cycloreversion process of **4bH** following irradiation at $\lambda > 650$ nm. The spectrum recorded at the start of the experiment (before irradiation) is denoted by the thick black line.

The closed-ring isomer **4bH** was also found to undergo cycloreversion back to the open-form, following irradiation at $\lambda > 650$ nm in THF, as evidenced from the colour change from purple to colourless, and the decrease of the absorption band in the visible region ($\lambda_{max} = 584$ nm), as shown in figure 3.37. However, the ring-opening

process took 240 minutes to be completed, therefore the presence of the $Co_2(CO)_6$ complexes considerably reduced the efficiency of the cycloreversion process in comparison to the corresponding free-switch **2H** (6 minutes). Also observed was a decrease in the bands at 274 and 328 nm, with a new band present at 293 nm. Figure 3.38 displays the UV-vis spectrum of **4bH** following irradiation with $\lambda > 650$ nm, overlaid with the corresponding open-ring isomer **4H** (synthesised previously); **4H** following irradiation at 313 nm and subsequent ring-opening at $\lambda > 550$ nm (named "**4H re-opened**"); and the open-ring isomer of the free-switch **2H**. It is clear from these spectra that some decomposition of **4bH** occurred during the cycloreversion process, as the resulting absorption band in the UV region is not comparable with that of the corresponding open-ring isomer **4H**. In fact the final spectrum recorded is somewhat similar to the absorption spectrum of "**4H re-opened**", which seems to suggest that similar decomposition processes may have occurred for **4bH** at $\lambda_{irr} > 650$ nm, as for **4H** following the colouring/bleaching cycle at 313 nm and > 550 nm respectively. However, there was no significant evidence that cleavage of the $Co_2(CO)_6$ moieties from **4bH** occurred, as an absorbance band at 343 nm, corresponding to the λ_{max} of the free-switch **2H**, was not observed.
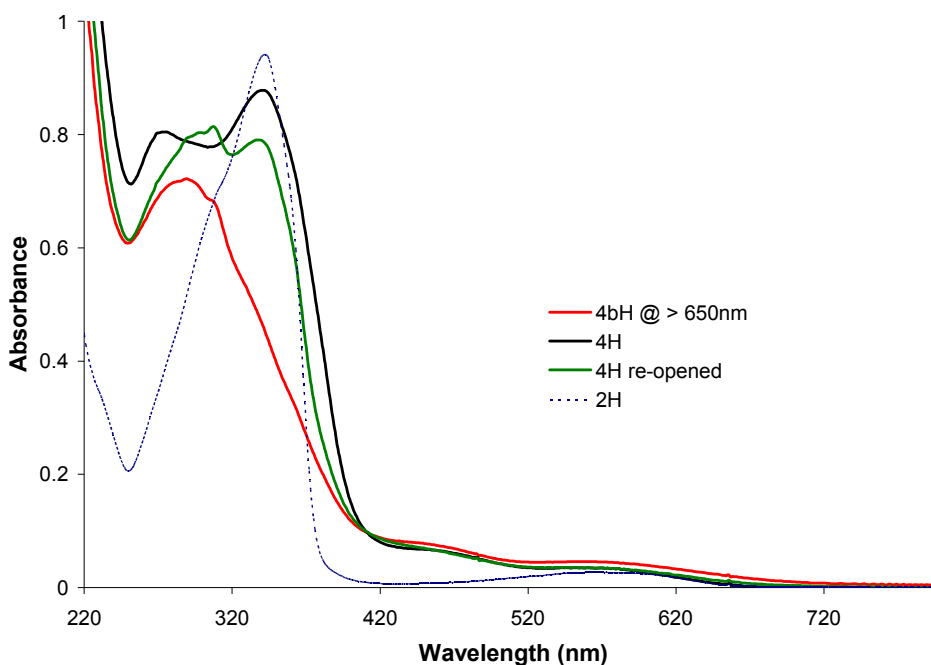
Figure 3.38: The UV-vis absorption spectrum, in THF, of: the cycloreversion process of **4bH** following irradiation at $\lambda > 650$ nm (red line); the open-ring isomer **4H** (black line); **4H** following ring-closing at 313 nm and subsequent ring-opening at $\lambda > 550$ nm ("**4H re-opened**" green line); the free-switch **2H** (--- blue line).

In order to elucidate the effects of the irradiation process at the $Co_2(CO)_6$ centre, a solution of **4bH** in THF, in the presence of a trapping ligand (PPh$_3$), was irradiated with broadband light at $\lambda > 650$ nm and the results were monitored in the IR. Following irradiation for a total of 360 minutes, the parent carbonyl bands at 2089, 2055 and 2025 cm^{-1} were found to decrease, as shown in figure 3.39. However, new bands began to grow-in at 2011 and 1996 cm^{-1}, indicative of the formation of the pentacarbonyl species, and a band at 1964 cm^{-1}, suggesting formation of the tetracarbonyl species. Thus, the IR results verify that CO loss occurs during the cycloreversion process of **4bH**.
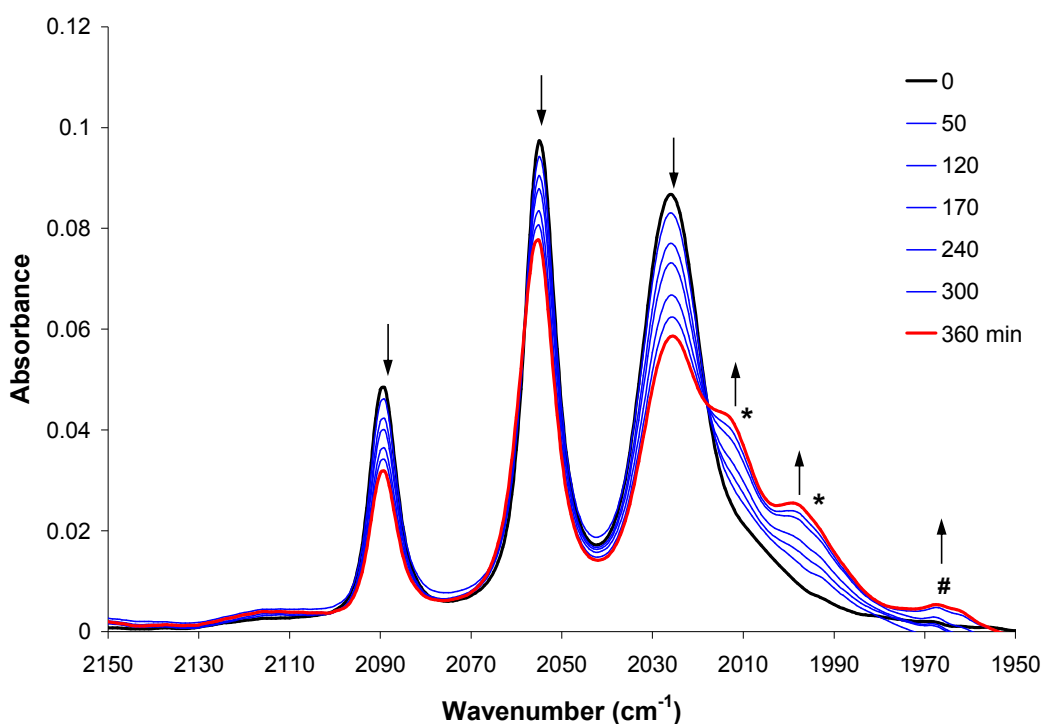
Figure 3.39: The IR absorption spectrum of **4bH**, in THF, following irradiation at $\lambda > 650$ nm, in the presence of PPh$_3$. The parent bands (black line) began to decrease, with new bands forming at lower frequency (blue lines). After 360 minutes (red line), new bands indicative of the pentacarbonyl species (*) and tetracarbonyl species (#) were present.

From the results obtained here, it was found that the cycloreversion process for **3bF** was more efficient compared to **4bH**. Although no trapping experiments with PPh$_3$ were carried out with **3bF**, it is possible that CO loss may also occur following irradiation with visible light, however, the UV-vis spectra indicated that the cobalt carbonyl complex **3bF** was more stable than **4bH**. Therefore, it is clear that the presence of the fluorine atoms on the cyclopentene ring, and/or the absence of the phenyl-ring spacers in **3bF**, significantly influenced the cycloreversion process and the stability of the $Co_2(CO)_6$ switch.

3.3.11 Fluorescence: Cobalt Carbonyl Complexes

The effect of complexation with cobalt carbonyl moieties, on the fluorescent properties of the switches **1H/F** and **2H/F**, was investigated. Solutions of the $Co_2(CO)_6$ complexes **3H/F** and **4H/F**, and the $Co_2(CO)_4dppm$ complexes **5H/F** and **6H**, were made-up in THF at a concentration of 4 x 10^{-6} mol/L, and the emission studies were performed at room temperature.

As discussed in section 3.3.5, the switches **1H** and **1F** were found to be non-emissive. As expected, the corresponding $Co_2(CO)_6$ and $Co_2(CO)_4dppm$ complexes, **3H/F** and **5H/F** respectively, were also found to be non-emissive under the same experimental conditions, and no changes were observed following photocyclisation to the ring-closed forms. Complexation with metal carbonyls has been described in the literature to quench the emission of luminescent compounds, and this phenomenon has been attributed to energy transfer.[30,33,34]

The more conjugated perfluoro-derivative, **2F**, was found to be fluorescent in both the open and closed-ring forms, however incorporating $Co_2(CO)_6$ onto the switch, giving **4F**, was found to quench the fluorescence. Photocyclisation to the ring-closed isomer was not found to induce fluorescence, hence indicating that irradiation at 313 nm did not result in cleavage of the $Co_2(CO)_6$ complex from the switching unit. This supports the results obtained during the colouring/bleaching processes monitored by UV-vis spectroscopy, as **4F** appeared to be the most stable during photolysis.

As described in section 3.4.5, the more conjugated perhydro-derivative, **2H**, was found to be fluorescent. When a solution of the corresponding $Co_2(CO)_6$ complex, **4H**, was excited into the intraligand band at 340 nm, an emission band appeared at 390 nm, albeit much weaker than the free ligand **2H**. The fact that the emission band appeared at approximately the same wavelength as that observed for the free switch **2H** (399 nm) indicates that fluorescence from the switching unit resulted, without significant contribution from the metal complex. Although, the intensity of the emission was significantly reduced (by ~93%) by introducing $Co_2(CO)_6$ moieties onto the switch. However, following irradiation of **4H** with UV light, to induce ring-

closing, the emission began to increase. Subsequent irradiation with broadband light λ > 550 nm, to induce cycloreversion back to the open form, resulted in a further increase in the emission intensity, and a shift in the λ_{max} from 391 to 399 nm, as illustrated in figure 3.40.
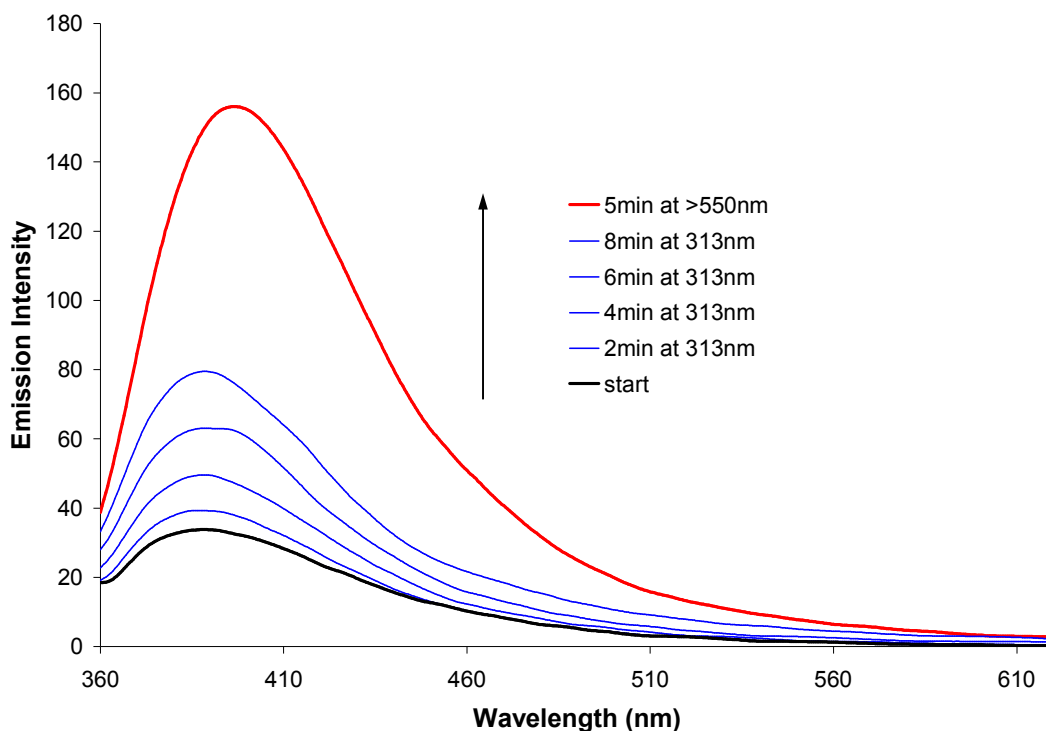
Figure 3.40: Emission spectrum of the $Co_2(CO)_6$ complex **4H**, in THF. Low emission intensity at the start (black line). Irradiation with light at 313 nm, to the ring-closed form, resulted in an increase in the emission intensity (blue lines). Subsequent irradiation with light > 550 nm to induce cycloreversion back to the open form resulted in further increase of the emission intensity (red line).

The change in the fluorescence spectra, following irradiation with light, suggests that cleavage of the $Co_2(CO)_6$ moiety occurs. This is in agreement with the result observed in the UV-vis spectra for **4H** (section 3.3.7), where loss of the cobalt carbonyl fragments was proposed.

Incorporating dppm onto the cobalt carbonyl switch, forming the $Co_2(CO)_4$dppm complex **6H**, completely quenched the fluorescence. Cyclisation to the closed form did not result in emission.

The closed-ring $Co_2(CO)_6$ complex **4bH** was found to have very weak fluorescence. However, following irradiation at λ > 650 nm, the fluorescence intensity was found to increase, as shown in figure 3.41. The emission spectrum recorded for **4bH**,

following visible light irradiation for 190 minutes, corresponds to the emission spectrum obtained for the corresponding open-ring isomer **4H**.   Thus, the cycloreversion process of **4bH**, to the open-ring form, induces changes in the emission spectrum.
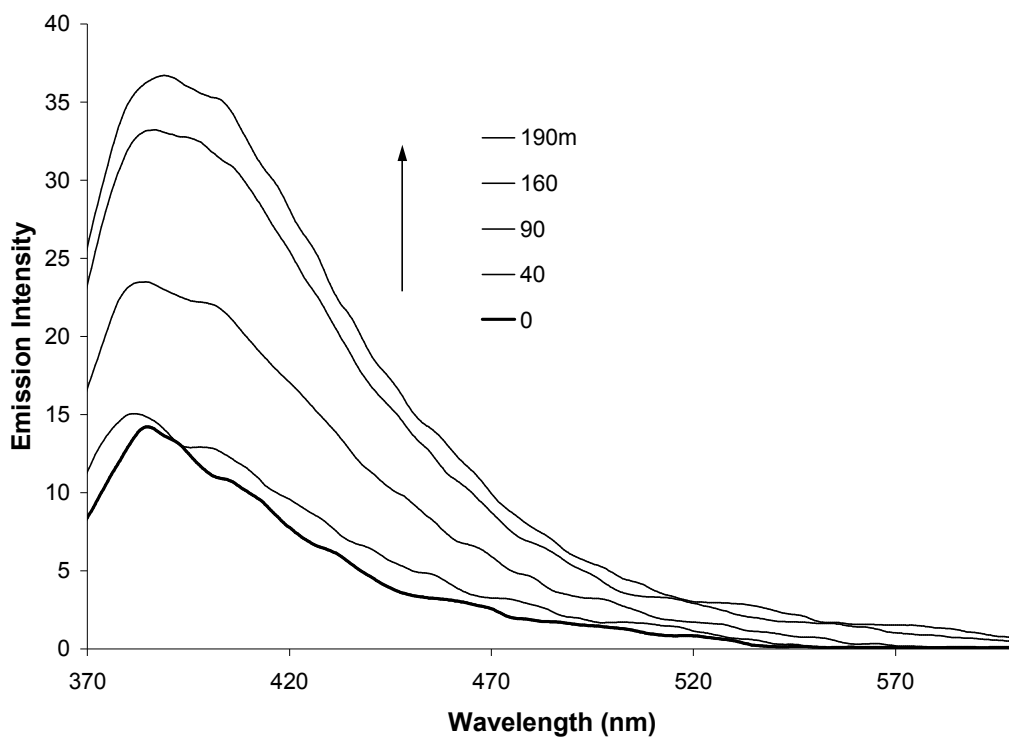
Figure 3.41: Emission spectrum of the $Co_2(CO)_6$ ring-closed complex **4bH**. Low emission intensity at the start (thick black line). Irradiation at $\lambda > 650$ nm for 190 minutes, to the ring-open form, resulted in an increase in the emission intensity.

3.4 Conclusion

Dithienyl-perhydro- and perfluoro-cyclopentene switches, with ethynylthiophene and phenyl-ethynylthiophene substituents, were synthesised. The effects of the atoms on the cyclopentene ring (H *vs.* F), and the substituents attached to the thienyl moieties of the switching unit, on the photochromic, fatigue resistance, thermal stability and fluorescent properties of the switch were investigated.

Photocyclisation processes were found to occur for the four switches (**1H**, **1F**, **2H**, **2F**), with new bands observed in the visible region of the UV-vis spectra (λ_{max} = 543, 609, 562 and 614 nm respectively), and their photostationary states were reached after 50, 30, 20 and 15 seconds respectively. These results show that the presence of fluorine atoms on the cyclopentene ring, and the extension of the π-conjugation of the system, through the addition of a phenyl-ring between the switching unit and the ethynylthiophene moieties, resulted in more efficient photocyclisation processes and shifted the absorbance bands in the visible region of the UV-vis spectra further into the red. The times taken for the cycloreversion processes to be completed for **1F**, **2F** and **2H** were recorded at 90, 180 and 360 seconds respectively, following irradiation with λ > 550 nm. These results showcase how the presence of the fluorine atoms improves the efficiency of the ring-opening process, whereas extending the π-conjugation of the system reduces the efficiency of this process. On the other hand, the closed-isomer of **1H** was not found to undergo complete cycloreversion back to the open-ring form. Analysis of the photochromic behaviour in the ^{1}H NMR spectrum of **1H** showed that a photostable by-product (**1Hx**) was produced during the photocyclisation process, and the results suggested that this by-product was formed from irradiation of the closed-ring isomer. Conversely, the proton NMR studies of the perfluorinated-derivatives (**1F** and **2F**) and **2H** showed that > 95% of the open-ring isomers were converted to the closed-ring isomers, following UV irradiation, with no evidence for the formation of a by-product.

The fatigue resistance experiments showed that the photostability of these switches was found to increase in the order of **1H** < **1F** < **2H** < **2F**, highlighting the stabilising effects of the fluorine atoms and the increased π-conjugation. The factors affecting the thermal stability, on the order hand, were not as straight forward. The trend

observed for the stability of these compounds, at elevated temperatures, was found to be **2H** > **1F** > **1H** > **2F**, in order of increasing stability. It is clear from these results that the thermal stability of these switches is affected by both the atoms present in the cyclopentene ring (H *vs*. F) and the substituents attached to the thiophene ring. Another observation from these experiments was that at elevated temperatures (60–100°C), the closed-ring switches underwent cycloreversion processes, in conjunction with degradation. It should be noted however, that the closed-ring isomers were stable at room temperature, over a ten week period.

The luminescent studies performed on these switches showed that compounds **1H** and **1F** were non-emissive, however an extension of the π-conjugated system resulted in fluorescence for the open-ring isomers of compounds **2H** and **2F**. Cyclisation to the closed-forms was found to quench the emission of **2H** by 51%, but had the opposite effect for the perfluorinated-derivative **2F**, as the emission intensity was found to increase marginally when converted to the closed-ring isomer.

Table 3.11: Irradiation times required for the free switches (**1H/F** and **2H/F**), and the corresponding $Co_2(CO)_6$ (**3H/F** and **4H/F**) and $Co_2(CO)_4$dppm complexes (**5H/F** and **6H**), to reach the photostationary state (PSS), following irradiation at 313 nm and 365 nm in THF.

Time to reach PPS of closed-ring isomer after irradiation							
Free Switches		$Co_2(CO)_6$ Complexes			$Co_2(CO)_4$dppm Complexes		
	Time at λ=313nm		Time at λ=313nm	Time at λ=365nm		Time at λ=313nm	Time at λ=365nm
1H	50 sec	**3H**	8 min	-	**5H**	-	-
1F	20 sec	**3F**	4 min	-	**5F**	-	-
2H	30 sec	**4H**	8 min	9 min	**6H**	25 min	35 min
2F	15 sec	**4F**	2 min	2.5 min			

(-) indicates no cyclisation occurred.

Coordination of cobalt carbonyl complexes onto compounds **1H/F** and **2H/F** was found to have a dramatic effect on the photochromic behaviour of the switches. Overall, the efficiencies of the photocyclisation processes for the $Co_2(CO)_6$ complexes (**3H/F** and **4H/F**) were significantly reduced in comparison to their corresponding free switches, following irradiation at λ = 313 nm. This hypothesis was evidenced by the time taken to reach the photostationary state (table 3.11) and the estimated decrease in the percentage conversion from the open to the closed form, following analysis of the

UV-vis spectra. This result may be attributed to a second irreversible photochemical process occurring for the cobalt carbonyl complexes during photocyclisation, involving cleavage of the cobalt carbonyl moieties from the switching unit. Evidence of this was observed in the UV-vis spectra of these complexes, whereby the absorbance bands in the UV region decreased during UV irradiation, and failed to re-emerge following irradiation with visible light. IR steady-state photolysis experiments verified that CO loss was occurring from the cobalt carbonyl complexes upon irradiation at $\lambda = 313$ nm. A lower energy light source ($\lambda = 365$ nm) was also used to induce cyclisation. The IR results showed a decrease in the rate of CO loss, in comparison to those observed at 313 nm. However, the lower energy light source was found to slightly increase the radiation times to form the closed-ring isomer for **4H** and **4F**, and in fact failed to induce any ring-closure for the less-conjugated derivatives **3H** and **3F**.

In an attempt to stabilise the photo-reactivity of the $Co_2(CO)_6$ switches, dppm ligands were incorporated onto the complexes, forming the corresponding tetracarbonyl $Co_2(CO)_4$dppm species, **5H**, **5F** and **6H**. Analysis of the UV-vis and IR spectra of **5H** and **5F**, during irradiation at 313 and 365 nm, showed photo-induced dissociation of CO from the complexes, but the cyclisation process was inhibited. However, photocyclisation to the closed form occurred for **6H**, in conjunction with CO loss, although, the efficiency of the ring-closing processes was found to decrease even further for **6H**, as evidenced from the results in table 3.11. The IR experiments indicated that dissociation of CO also occurred for the $Co_2(CO)_4$dppm moieties, following irradiation at both 313 and 365 nm, although at a slower rate compared to the results obtained for the $Co_2(CO)_6$ switches.

In an attempt to further help elucidate the results of the cyclisation processes of the cobalt carbonyl complexes, the closed-ring isomers of the $Co_2(CO)_6$ complexes **3F** and **4H** were synthesised, forming **3bF** and **4bF**. The UV-vis spectra of **3bF** and **4bH** displayed a band in the visible region which was bathochromically shifted by 52 nm and 22 nm, in comparison to the closed forms of the free ligands **1F** and **2H**, respectively. However, UV irradiation of the open-ring cobalt carbonyl complexes resulted in the appearance of absorbance bands in the visible region with λ_{max} values quite similar to the free ligand. Such a result suggests that some cleavage of the cobalt carbonyl groups occurred during irradiation, followed by cyclisation of the free ligand.

Incorporating cobalt carbonyl moieties onto **2F** and **2H** (i.e. **4F** and **4H** respectively) was found to quench the fluorescence of the switches. Subsequent UV irradiation of **4F**, forming the closed-ring, did not induce fluorescence. On the other hand, the emission intensity of **4H** increased following colouring/bleaching processes, indicating that some cleavage of the $Co_2(CO)_6$ moieties occurred, producing the free ligand **2H**. On the other hand, no fluorescence was observed for the corresponding $Co_2(CO)_4$dppm complex **6H**, even after UV irradiation, suggesting that photolytic cleavage of the cobalt carbonyl moieties did not occur for **6H**, which can be attributed to the stabilising effect of the dppm ligand.

Taking all of the results into account, it can be deduced that UV irradiation of the cobalt carbonyl complexes resulted in some of the following reactions: 1) cyclisation of the cobalt carbonyl switches, and 2) cleavage of the metal carbonyl groups, followed by cyclisation of the free ligand. Incorporating phenyl-rings between the switching unit and the alkynyl cobalt carbonyl moieties was found to favour the ring-closing process for the organometallic complex, with an increased amount of the open form converted to the closed form for **4H/F**, compared to the shorter chain analogues **3H/F**, as evidenced by the relative intensities of the bands in the visible region of the absorption spectra. Furthermore, the presence of fluorine atoms on the central cyclopentene ring was found to increase the stability of these complexes during irradiation, as evidenced by the increase in the UV region during the cycloreversion process. The IR studies showed that the cobalt carbonyl moieties were more stable towards UV irradiation by 1) the presence of electron-donating dppm ligands on the metal centre, and 2) the use of a lower energy light source (λ_{irr} = 365 nm). However, these parameters were not found to improve the cyclisation processes. Therefore, overall the results show that incorporating cobalt carbonyl groups onto dithienylethene switches have a significant effect on their photochromic properties. Although the reversibility of these systems is an issue, due to the tendency of the cobalt carbonyl moieties to undergo photo-decarbonylation, it is clear that these properties can be tuned by altering the substituents attached to the switching unit and the cobalt carbonyl groups, and the wavelength used to irradiate the samples.

The 'synthesised' closed-ring $Co_2(CO)_6$ complexes **3bF** and **4bF** were further investigated to establish if these complexes could undergo cycloreversion to their

corresponding open-ring forms. Both complexes were found to undergo ring-opening following irradiation at $\lambda > 650$ nm, after 70 and 240 minutes respectively. This result shows that the presence of the $Co_2(CO)_6$ moieties significantly reduced the efficiency of the cycloreversion processes, as the related free ligands **1F** and **2H** underwent ring-opening after just 1.5 and 6 minutes, respectively. Furthermore, the UV-vis results indicated that the cobalt carbonyl groups were quite stable during visible light irradiation for **3bF**, whereas evidence of irreversible photochemical reactions of the carbonyl moieties was observed for **4bH**, under these conditions. IR steady-state photolysis experiments, carried out for **4bH** in the presence of PPh_3, indicated that CO loss occurred during irradiation at $\lambda > 650$ nm. Therefore, the ability to manipulate the photochemical behaviour of these cobalt carbonyl switches, by altering the substituents attached to the dithienylethene unit, and the fact that the dissociation of CO takes place at low energy radiation ($\lambda > 650$ nm), suggests that closed-ring dithienylethene $Co_2(CO)_6$ complexes may be potential candidates towards the development of CO releasing molecules. Furthermore, the propensity for such dithienylethene switches to show fluorescence discrimination between the open and closed forms could be utilised as a fluorescent probe within the CORM, thus allowing the release of CO to be monitored in situ by an increase in fluorescence.

Overall, it can be concluded that the presence of fluorine atoms on the cyclopentene ring, and an extension of the π-conjugation of the system, improves the performance of such dithienylcyclopentene switches with regards to their photochromic, fatigue resistance and thermal stability properties. Hence, from the switches presented here, **2F** proved to be the most suitable candidate for the development of various optoelectronic properties. Although, the luminescent properties of **2F** are not ideal for its application towards a non-destructive readout method for memory media, as there is little difference in the emission properties in the open and closed forms.

Incorporating cobalt carbonyl complexes onto the switching units was not found to be advantageous with regards to the use of such compounds for applications towards optoelectronic properties, as the efficiency and reversibility of their photocyclisation processes was considerably reduced. However, the presence of these metal complexes has led to some very interesting results, and the dual photochemical processes occurring simultaneously could find use towards the development of carbon monoxide

releasing molecules,[35-37] as the CO release can be induced by a low energy light source, and detected by changes observed in the IR, UV-vis and luminescence spectra.

3.5 Bibliography

(1) Matsuda, K.; Irie, M. Diarylethene as a Photoswitching Unit. *J. Photochem. Photobiol. C.* **2004**, *5*, 169-182.

(2) Tian, H.; Yang, S. J. Recent Progresses on Diarylethene Based Photochromic Switches. *Chem. Soc. Rev.* **2004**, *33*, 85-97.

(3) Irie, M. Diarylethenes for Memories and Switches. *Chem. Rev.* **2000**, *100*, 1685-1716.

(4) Irie, M. Photochromic Dithienylethenes for Molecular Photonics. *Phosphorus, Sulfur Silicon Relat. Elem.* **1997**, *120*, 95-106.

(5) Uchida, K.; Matsuoka, T.; Kobatake, S.; Yamaguchi, T.; Irie, M. Substituent Effect on the Photochromic Reactivity of Bis(2-thienyl)perfluorocyclopentenes. *Tetrahedron* **2001**, *57*, 4559-4565.

(6) de Jong, J. J. D.; Lucas, L. N.; Hania, R.; Pugzlys, A.; Kellogg, R. M.; Feringa, B. L.; Duppen, K.; van Esch, J. H. Photochromic Properties of Perhydro- and Perfluorodithienylcyclopentene Molecular Switches. *Eur. J. Org. Chem.* **2003**, 1887-1893.

(7) Lucas, L. N.; de Jong, J. J. D.; van Esch, J. H.; Kellogg, R. M.; Feringa, B. L. Syntheses of Dithienylcyclopentene Optical Molecular Switches. *Eur. J. Org. Chem.* **2003**, 155-166.

(8) Xie, N.; Zeng, D. X.; Chen, Y. Electrochemical Switch Based on the Photoisomerization of a Diarylethene Derivative. *J. Electroanal. Chem.* **2007**, *609*, 27-30.

(9) Lucas, L. N. Dithienylcyclopentene Optical Switches Towards Photoresponsive Supramolecular Materials, Ph.D. Thesis, Rijksuniversiteit Groningen, **2001**.

(10) Peters, A.; Branda, N. R. Limited Photochromism in Covalently Linked Double 1,2-Dithienylethenes. *Adv. Mater. Opt. Electron.* **2000**, *10*, 245-249.

(11) Pu, S.; Li, M.; Fan, C.; Liu, G.; Shen, L. Synthesis and the Optoelectronic Properties of Diarylethene Derivatives having Benzothiophene and n-Alkyl Thiophene Units. *J. Mol. Struct.* **2009**, *919*, 100-111.

(12) Irie, M.; Lifka, T.; Uchida, K.; Kobatake, S.; Shindo, Y. Fatigue Resistant Properties of Photochromic Dithienylethenes: By-Product Formation. *Chem. Commun.* **1999**, 747-748.

(13) Irie, M.; Sakemura, K.; Okinaka, M.; Uchida, K. Photochromism of Dithienylethenes with Electron-Donating Substituents. *J. Org. Chem.* **1995**, *60*, 8305-8309.

(14) Lucas, L. N.; van Esch, J.; Kellogg, R. M.; Feringa, B. L. A New Class of Photochromic 1,2-Diarylethenes; Synthesis and Switching Properties of Bis(3-thienyl)cyclopentenes. *Chem. Commun.* **1998**, 2313-2314.

(15) Patel, P. D.; Mikhailov, I. A.; Belfield, K. D.; Masunov, A. E. Theoretical Study of Photochromic Compounds, Part 2: Thermal Mechanism for Byproduct Formation and Fatigue Resistance of Diarylethenes used as Data Storage Materials. *Int. J. Quantum Chem.* **2009**, *109*, 3711-3722.

(16) Morimitsu, K.; Shibata, K.; Kobatake, S.; Irie, M. Dithienylethenes with a Novel Photochromic Performance. *J. Org. Chem.* **2002**, *67*, 4574-4578.

(17) Xiao, S.; Yi, T.; Zhou, Y.; Zhao, Q.; Li, F.; Huang, C. Multi-State Molecular Switches Based on Dithienylperfluorocyclopentene and Imidazo [4,5-f] [1,10] Phenanthroline. *Tetrahedron* **2006**, *62*, 10072-10078.

(18) Yang, T.; Pu, S.; Fan, C.; Liu, G. Synthesis, Crystal Structure and Optoelectronic Properties of a New Unsymmetrical Photochromic Diarylethene. *Spectrochim. Acta A.* **2008**, *70*, 1065-1072.

(19) Pu, S.; Miao, W.; Cui, S.; Liu, G.; Liu, W. The Synthesis of Novel Photochromic Diarylethenes Bearing a Biphenyl Moiety and the Effects of Substitution on their Properties. *Dyes Pigments* **2010**, *87*, 257-267.

(20) Zheng, H.; Zhou, W.; Yuan, M.; Yin, X.; Zuo, Z.; Ouyang, C.; Liu, H.; Li, Y.; Zhu, D. Optic and Proton Dual-Control of the Fluorescence of Rhodamine Based on Photochromic Diarylethene: Mimicking the Performance of an Integrated Logic Gate. *Tetrahedron Lett.* **2009**, *50*, 1588-1592.

(21) Jukes, R. T. F.; Adamo, V.; Hartl, F.; Belser, P.; De Cola, L. Photochromic Dithienylethene Derivatives Containing Ru(II) or Os(II) Metal Units. Sensitized Photocyclization from a Triplet State. *Inorg. Chem.* **2004**, *43*, 2779-2792.

(22) Pu, S. Z.; Yang, T. S.; Li, G. Z.; Xu, J. K.; Chen, B. Substituent Position Effect on the Optoelectronic Properties of Photochromic Diarylethenes. *Tetrahedron Lett.* **2006**, *47*, 3167-3171.

(23) Pu, S.; Liu, G.; Li, G.; Wang, R.; Yang, T. Synthesis, Crystal Structure and its Optical and Electrochemical Properties of a New Unsymmetrical Diarylethene. *J. Mol. Struct.* **2007**, *833*, 23-29.

(24) Jeong, Y.; Yang, S. I.; Kim, E.; Ahn, K. Development of Highly Fluorescent Photochromic Material with High Fatigue Resistance. *Tetrahedron* **2006**, *62*, 5855-5861.

(25) Fernandez-Acebes, A.; Lehn, J. M. Optical Switching and Fluorescence Modulation Properties of Photochromic Metal Complexes Derived from Dithienylethene Ligands. *Chem. Eur. J.* **1999**, *5*, 3285-3292.

(26) Kim, M.; Kawai, T.; Irie, M. Fluorescence Modulation in Photochromic Amorphous Diarylethenes. *Opt. Mater.* **2003**, *21*, 271-274.

(27) Yagi, K.; Soong, C. F.; Irie, M. Synthesis of Fluorescent Diarylethenes having a 2,4,5-Triphenylimidazole Chromophore. *J. Org. Chem.* **2001**, *66*, 5419-5423.

(28) Kobatake, S.; Irie, M. Synthesis and Photochromic Reactivity of a Diarylethene Dimer Linked by a Phenyl Group. *Tetrahedron* **2003**, *59*, 8359-8364.

(29) M. Draper, S.; Long, C.; M. Myers, B. The Photochemistry of (μ_2-$RC_2H)Co_2(CO)_6$ Species (R=H or C_6H_5), Important Intermediates in the Pauson–Khand Reaction. *J. Organomet. Chem.* **1999**, *588*, 195-199.

(30) Coleman, A.; Pryce, M. T. Synthesis, Electrochemistry, and Photophysical Properties of a Series of Luminescent Pyrene-Thiophene Dyads and the Corresponding $Co_2(CO)_6$ Complexes. *Inorg. Chem.* **2008**, *47*, 10980-10990.

(31) Boyle, N. Novel Thienyl Dyes and Related Metal Carbonyl Complexes, Ph.D. Thesis, Dublin City University, **2011**.

(32) Chia, L. S.; Cullen, W. R.; Franklin, M.; Manning, A. R. Reactions of $(RC\equiv CR')Co_2(CO)_6$ Complexes with Monodentate and Bidentate Group 5 Ligands. *Inorg. Chem.* **1975**, *14*, 2521-2526.

(33) Shiotsuka, M.; Inui, Y.; Sekioka, Y.; Yamamoto, Y.; Onaka, S. Synthesis, Photochemistry, and Electrochemistry of Ruthenium(II) Polypyridyl Complexes Anchored by Dicobalt Carbonyl Units. *J. Organomet. Chem.* **2007**, *692*, 2441-2447.

(34) Wong, W. Y.; Choi, K. H.; Lin, Z. Y. Syntheses, Structures and Photophysical Properties of Metal Carbonyl Clusters with Dansyl and Acridone Luminophores. *Eur. J. Inorg. Chem.* **2002**, 2112-2120.

(35) Atkin, A. J.; Williams, S.; Sawle, P.; Motterlini, R.; Lynam, J. M.; Fairlamb, I. J. S. μ_2-Alkyne Dicobalt(0)hexacarbonyl Complexes as Carbon Monoxide-Releasing Molecules (CO-RMs): Probing the Release Mechanism. *Dalton Trans.* **2009**, 3653-3656.

(36) Kretschmer, R.; Gessner, G.; Gorls, H.; Heinemann, S. H.; Westerhausen, M. Dicarbonyl-bis(cysteamine)iron(II) A Light Induced Carbon Monoxide Releasing Molecule Based on Iron (CORM-S1). *J. Inorg. Biochem.* **2011**, *105*, 6-9.

(37) Zhang, W.; Atkin, A. J.; Thatcher, R. J.; Whitwood, A. C.; Fairlamb, I. J. S.; Lynam, J. M. Diversity and Design of Metal-Based Carbon Monoxide-Releasing Molecules (CO-RMs) in Aqueous Systems: Revealing the Essential Trends. *Dalton Trans.* **2009**, 4351-4358.

CHAPTER 4

Photochemistry of Ferrocenyl-based Switches and their Cobalt Carbonyl Complexes

*Chapter 4 describes the photochromic behaviour of the perhydro- and perfluoro-switches, substituted with ethynylferrocene moieties: 1,2-Bis(5'-ethynylferrocene-2'-methylthien-3'-yl)cyclopentene {**7H**}; 1,2-Bis(5'-ethynylferrocene-2'-methylthien-3'-yl)perfluorocyclopentene {**7F**}; 1,2-Bis(5'-(4''-phenyl-ethynylferrocene)-2'-methylthien-3'-yl)-cyclopentene {**8H**}; 1,2-Bis(5'-(4''-phenyl-ethynylferrocene)-2'-methylthien-3'-yl)per-fluorocyclopentene {**8F**}. Photoinduced ring-closing and ring-opening processes for these switches were monitored by UV-vis and ^1H NMR spectroscopy, and the fatigue resistance, thermal stability and fluorescence properties were also examined. The photochemical properties of the corresponding $Co_2(CO)_6$ {**9H**, **9F**, **10H**, **10F**, **10bF**}, and $Co_2(CO)_4dppm$ complexes {**11H**, **11F**, **12H**, **12F**} were investigated using UV-vis absorption and infra-red spectroscopy.*

4.1 Introduction

Ferrocene is an electron-donating group, which has been widely used in luminescent systems due to its photochemical stability.[1] Ferrocene has been described as a non-emissive molecule,[1,2] and in fact is known as an effective excited state quencher.[1,2] The quenching processes involved are believed to be due to energy transfer and/or electron transfer.[1-4] If the energy level of the excited singlet state, or triplet state, of ferrocene is lower than the energy levels of the excited molecule, then efficient energy transfer can take place. Therefore, the excited molecule (A*) can transfer energy from its higher energy level, to the lower energy level of the ferrocene molecule (Fc), which may then be followed by thermal relaxation of the excited state to the ground state:

$$A^* + Fc \ \rightarrow \ A + Fc^* \ \rightarrow \ A + Fc + \text{thermal energy}$$
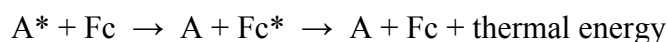
The occurrence of singlet-singlet energy transfer can be indicated by an overlap between the emission spectrum of the fluorescent molecule (A), and the ferrocene absorption spectrum.[1,3,5]

The electron transfer process is based on the fact that ferrocene acts as an electron donor, therefore the ferrocenium ion (Fc$^+$) is formed, followed by the recombination of the charges to restore both neutral species to the ground state, accompanied by an output of thermal energy:[1]

$$A^* + Fc \ \rightarrow \ A^- + Fc^+ \ \rightarrow \ A + Fc + \text{thermal energy}$$
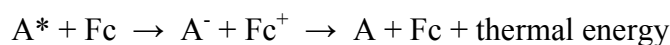
Some literature reports[6-8] have described the photochemical effects of incorporating ferrocene molecules onto photochromic switching units, the structures of which are illustrated in figure 4.1. Muratsugu et al[6] reported reversible photochromic properties of a dimethyldihydropyrene switch, disubstituted with ethynylferrocene (**DHP-1**), however the fluorescent properties of this switch was not accounted for. Sun et al[7] observed reversible photocyclisation/cycloreversion processes for a dithienylmaleimide switch, appended with two ethynylferrocene units (**TMF**), and described some very interesting results regarding the ability of this compound to

undergo luminescent switching. The open-ring form of **TMF** exhibited no or very weak fluorescence, which was attributed to the quenching effect of ferrocene via intramolecular electron transfer from ferrocene to dithienylmaleimide. However, following cyclisation to the closed-ring form, the fluorescence intensity was found to increase. The recovered emission was ascribed to the weakened intramolecular electron transfer process, and the fact that only a very small spectral overlap existed between the emission of the dithienylmaleimide and the absorption of the closed-isomer of **TMF**. In contrast, for the corresponding derivative **TM** (figure 4.1), with Br atoms in place of the ethynylferrocene moieties, the opposite luminescent properties were observed, with the fluorescence of the open-ring form decreasing upon ring-closing. This is a perfect example of how the photochemical properties of such switches can be tuned by incorporating organometallic complexes onto the switch.

Launay et al[8] described the cyclisation process, from the open to the closed-form, of a dithienylcyclopentene switch, substituted with ethynylferrocene units (**Fc-PCH-Fc**), and its perfluorinated-derivative (**Fc-PCF-Fc**), as illustrated in figure 4.1. However, no information was reported regarding the cycloreversion process, fluorescence or stability of these compounds.
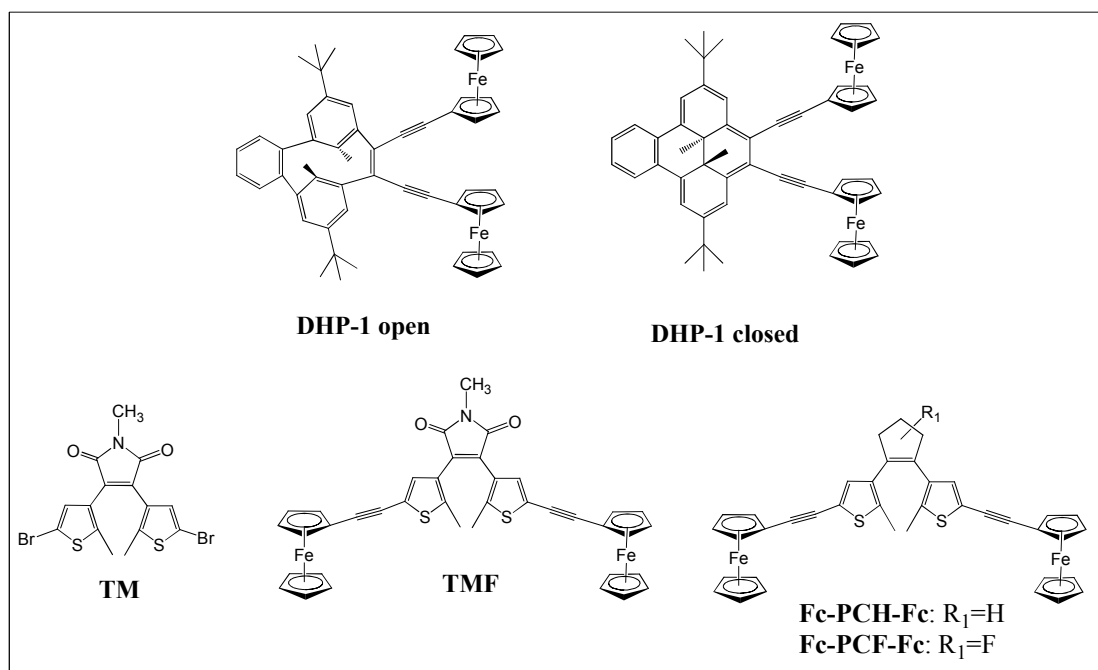
Figure 4.1: Structures of molecular switches, substituted with ethynylferrocene moieties, described in the literature: **DHP-1** open and **DHP-1** closed;[6] **TM** and **TMF**;[7] **Fc-PCH-Fc** and **Fc-PCF-Fc**.[8]

We synthesised the ethynylferrocene dithienyl-perhydro-cyclopentene switch (**7H**), and its perfluorinated-analogue (**7F**), reported previously by Launay et al,[8] as described in chapter 2. However, a more in-depth study of their photochemical properties, then previously described[8], was carried out and the results are detailed here. Their photochromic properties were monitored using UV-vis and ^{1}H NMR spectroscopy, and their fatigue resistance, thermal stability and fluorescent properties were examined. The effect of increasing the π-conjugation of the system, on these properties, was investigated by incorporating a phenyl ring between the switching unit and the ethynylferrocene moieties (**8H** and **8F**). Also, the corresponding $Co_2(CO)_6$ (**9H**, **9F**, **10H**, **10F**, **10bF**) and $Co_2(CO)_4$dppm complexes (**11H**, **11F**, **12H**, **12F**), of these ferrocene-based switches, were generated in order to study the effect of the cobalt carbonyl moieties on the switching behaviour of these molecules, and the results were monitored using UV-vis and infra-red spectra spectroscopy. The structures of these ferrocene-based switches are illustrated in figure 4.2.
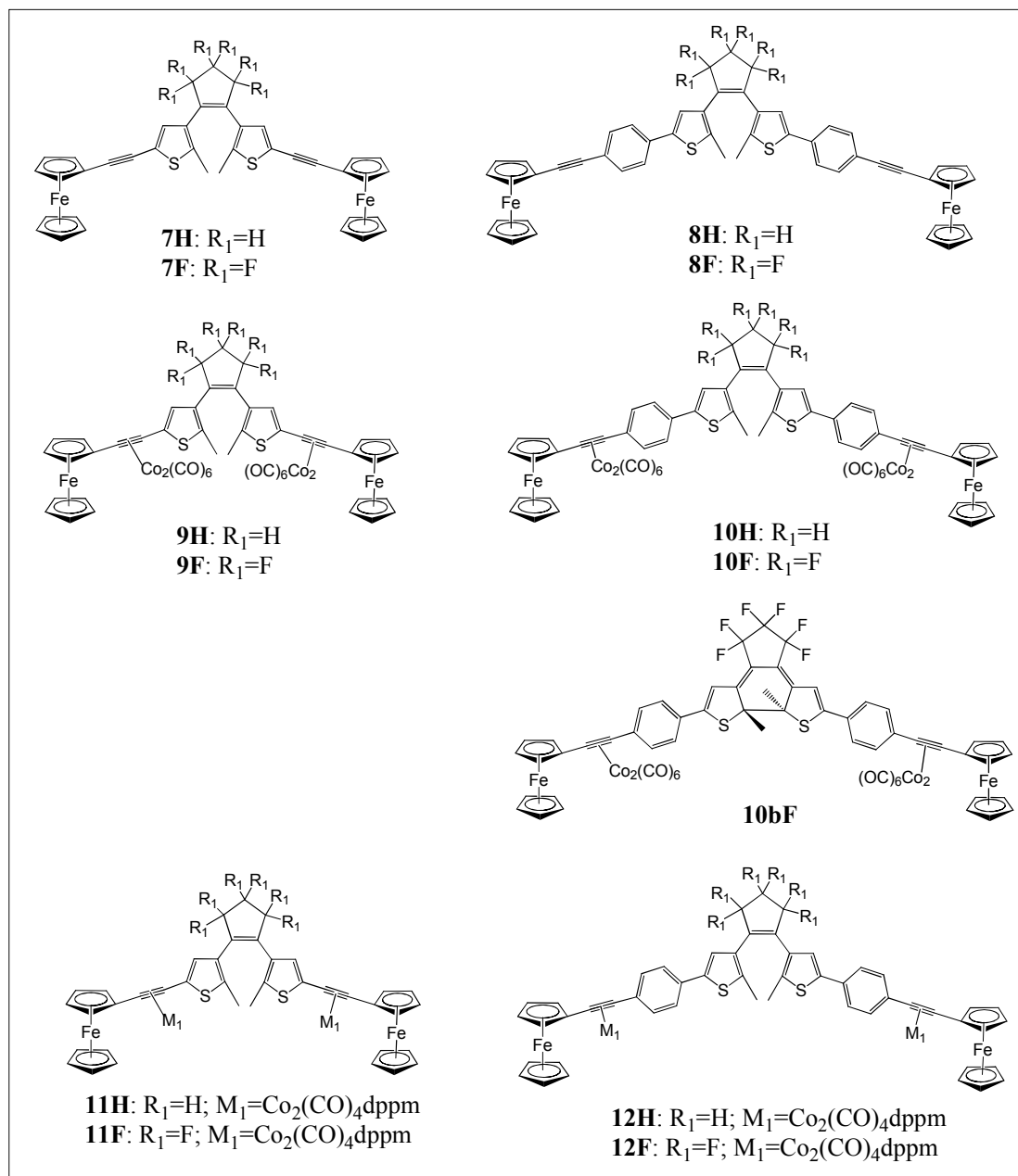
Figure 4.2: Illustrates the structures of the ferrocenyl-based dithienylperhydro- and perfluoro-cyclopentene switches **7H**, **7F**, **8H** and **8F** discussed in this chapter, and their corresponding $Co_2(CO)_6$ {**9H**, **9F**, **10H**, **10F, 10bF**} and $Co_2(CO)_4$dppm complexes {**11H**, **11F**, **12H**, **12F**}.

194

4.2 Experimental

4.2.1 General Procedures

Photocyclisation/cycloreversion: In a 1 cm quartz cuvette, 1.4 x 10^{-5} mol/L solutions of these compounds were made-up in THF and purged with nitrogen. The solutions were irradiated with monochromatic light at λ = 313 nm in order to induce ring-closing, whilst recording the UV-vis absorption spectra at specific time intervals. Irradiation was carried out until the photostationary states of the compounds were achieved, or until no more changes were endured in the UV-vis spectra. Following this, the same solutions were irradiated with broadband visible light (λ > 550 nm), in order to induce ring-opening, whilst recording the absorption spectra over time, until no further changes were observed in the spectra.

^{1}H NMR Studies: The switches were dissolved in deuterated acetone and placed in a sealed NMR tube. Compound **8H** was dissolved in deuterated benzene due to solubility issues in deuterated acetone. The samples were irradiated with monochromatic light at λ = 313 nm and the ^{1}H NMR spectra of the samples were recorded over time.

Fatigue Resistance: Solutions of these switches were made-up in THF (1.4 x 10^{-5} mol/L), purged with nitrogen and placed in a sealed 1 cm quartz cuvette. Cyclisation to the ring-closed isomer was induced by irradiation at λ = 313 nm, and cycloreversion back to the ring-open isomer was carried out using broadband filtered light with λ > 550 nm. This process counted as one cycle, and the fatigue resistance properties were measured over five consecutive cycles.

Thermal Stability: Solutions of the switches, in toluene, were irradiated with monochromatic light (λ = 313 nm) until the photostationary state of the closed ring isomer was reached, as monitored in the UV-vis absorption spectra. The stability of the closed switches was measured at room temperature by storing the solutions under air in sealed glass vials, in the dark. After 10 weeks, the UV-vis absorption spectra were recorded and compared to the spectra recorded initially. The stability of these switches at elevated temperatures was also measured at 60°C, 80°C and 100°C. Non-degassed solutions of the closed-forms, in toluene, were heated using a temperature

controlled heating mantel and their absorption spectra were recorded at specific time intervals.

Fluorescence properties: Solutions of the switches were made-up in THF, at a concentration of 4 x10^{-6} mol/L, placed in a 1 cm quartz cuvette and degassed with nitrogen. The emission spectra of these compounds were recorded at room temperature. The solutions were irradiated with UV light ($\lambda = 313$ nm) to produce the ring-closed isomers, followed by irradiation with visible light ($\lambda > 550$ nm) to revert back to the ring-open isomers.

Steady-state photolysis: Solutions of the cobalt carbonyl complexes, in THF, were purged with nitrogen for 20 minutes and placed in a liquid IR cell. The samples were irradiated with monochromatic light at two different wavelengths, 313 nm and 365 nm, and the changes observed in the carbonyl stretches in the IR spectrum were recorded. These experiments were repeated in the presence of excess triphenylphosphine (PPh$_3$), which was used as a trapping ligand.

4.2.2 Materials

The solvents used for the analytical experiments, THF and toluene, were purchased from Sigma Aldrich, and were of spectroscopic grade. The deuterated acetone, deuterated benzene and triphenylphosphine were purchased from Sigma Aldrich. The solutions were degassed with nitrogen, which was supplied by Air Products Ltd.

4.2.3 Equipment

UV-visible spectra were recorded on a photodiode-array Agilent 8453 spectrometer, in a 1 cm quartz cell. Photochemical experiments were carried out in a 1 cm quartz cell, using a monochromatic 200W Hg lamp (Oriel Instruments, model no.: 68911) containing a 313 nm or 365 nm filter, and a broadband lamp (Oriel instruments, model no.: 68811) containing a $\lambda > 550$ nm filter. ^{1}H NMR spectra were recorded on a Bruker model AC 400 MHz spectrometer and the peaks were calibrated according to the deuterated solvent peak. Emission spectra were recorded in a 1 cm quartz cuvette, using a LS50B luminescence spectrophotometer. Infra-red spectra were recorded in a 0.1 mm sodium chloride liquid cell, on a Perkin Elmer "Spectrum GX" FT-IR spectrometer.

4.3 Results and Discussion

4.3.1 Photochromic Behaviour: UV-vis Absorption
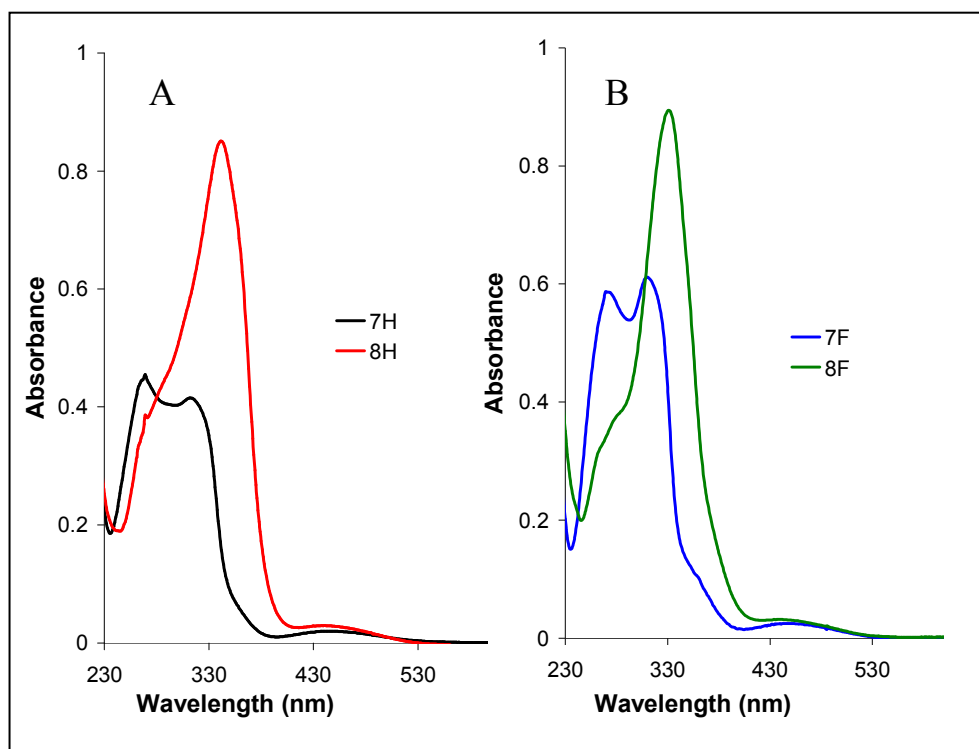
- **Open-ring isomer**

Figure 4.3: Absorption spectra of the open-ring isomers of compounds **7H/F** and **8H/F** in THF solution (c = 1.4 x 10^{-5} mol/L). A: **7H** (black line), **8H** (red line); B: **7F** (blue line), **8F** (green line).

Typical π-π* transitions were observed in the near UV region of the absorption spectra of the ferrocenyl-based dithienylcyclopentene switches **7H/F** and **8H/F**. A weak absorption band was also observed in the visible region for each of these switches, stretching from approximately 420 to 530 nm, and can be assigned as an MLCT band arising from the presence of the ferrocene moieties.[9,10] **7H** and **7F** show a broad absorption band between 245 and 380 nm, with two distinct λ_{max} at 270 and 312 nm, and at 270 and 310 nm, respectively. Introduction of a phenyl ring between the switching unit and the ethynylferrocene moieties for compounds **8H** and **8F** resulted in bathochromic and hypsochromic shifts of their absorbance bands in the UV region. The λ_{max} of **8H** and **8F** were bathochromically shifted by 29 nm and 21 nm, in

comparison to their corresponding compounds **7H** and **7F**, respectively, which can be attributed to the effects of the extension of the π-conjugation in these systems.

- **Cyclisation**

Compounds **7H/F** and **8H/F** underwent photocyclisation, from their open-ring isomers to their closed-ring isomers, following irradiation with UV light at 313 nm. This process was monitored using UV-vis absorption spectroscopy. Solutions of these compounds were prepared in THF and degassed with nitrogen. Irradiation was continued until the photostationary state (PSS) was reached i.e. until no more changes were observed in their UV-vis spectra, and the results are summarised in table 4.1.

Table 4.1: Absorption spectroscopy data of the open-ring isomers and at the photostationary state (PSS) of compounds **7H/F** and **8H/F**

Compound[a]	Absorption Spectra in THF	
	Open-ring isomer	Closed-ring isomer (PSS)
	λ_{abs} [nm] (ε x 10^3 M^{-1} cm^{-1})	λ_{abs} [nm] (ε x 10^3 M^{-1} cm^{-1})[b]
7H	265 (34.0), 312 (28.7), 445 (1.6)	275 (22.5), 314 (25.3), 362 (sh), **548** (15.8)
7F	269 (38.5), 310 (37.8), 354 (7.7) 441 (2.2)	273 (21.8), 318 (26.7), 354 (sh), **641** (21.1)
8H	277 (30.3), 341 (57.1), 441 (3.1)	266 (22.8), 323 (40.2), 384 (sh), **561** (17.5)
8F	281 (27.0), 331 (62.4), 442 (2.2)	273 (24.6), 356 (38.7), 399 (sh), **621** (25.4),

[a] The open-ring isomer, and the closed-ring isomer at the PSS (following irradiation at λ = 313nm), in THF.
[b] The extinction coefficients for the closed forms were determined at the photostationary state.
The λ_{max} in the visible region of the closed-ring isomers are highlighted in bold.
(sh) denotes a shoulder band.

Following irradiation at 313 nm in THF, **7H** underwent cyclisation from the open-ring form to the closed-ring form as illustrated in scheme 4.1. The absorption bands of the open-ring isomer at 265 and 312 nm in the UV-vis spectrum began to decrease and were red-shifted to 275 and 314 nm, as shown in figure 4.4, and a shoulder at 362 nm was observed. Generation of the closed form was evidenced by a new absorption band in the visible region (λ_{max} at 548 nm), and a colour change from pale yellow to purple. The photostationary state was reached after 35 minutes of irradiation, with an isosbestic point observed at 337 nm.

Figure 4.4: Absorption spectra of the cyclisation process from the open-ring isomers to the closed ring-isomers of compounds **7H** and **7F** in THF solution (c = 1.4 x 10^{-5} mol/L), following irradiation at λ_{irr} = 313 nm. A: **7H** (PSS reached after 35 minutes of irradiation); B: **7F** (PSS reached after 30 minutes of irradiation).

The changes in the UV-vis absorption spectrum of **7F** were monitored during irradiation at 313 nm. A new absorbance band appeared in the visible region with λ_{max} at 641 nm, and a colour change from pale yellow to blue was observed, verifying the occurrence of cyclisation from the open-ring isomer to the closed-ring isomer (scheme 4.1). During this process, the original absorbance bands of the open-ring isomer at 269 and 310 nm decreased and were bathochromically shifted to 273 and 318 nm, with a shoulder at 354 nm and an isosbestic point observed at 331 nm. The

photostationary state was reached after 30 minutes of irradiation, as illustrated in figure 4.4.
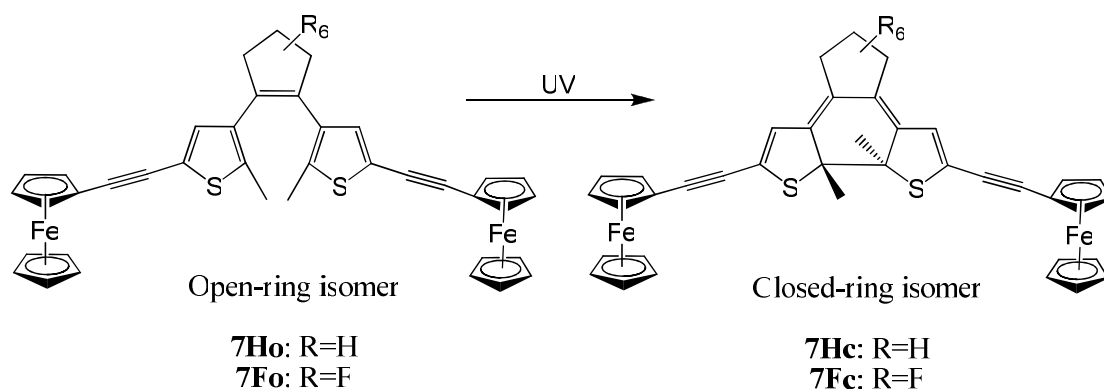
Scheme 4.1: Cyclisation from the open-ring to the closed ring isomer, following irradiation (λ = 313 nm) of compounds **7H** (R=H) and **7F** (R=F).

Comparison of the changes observed in the UV-vis spectra of the perhydro- and perfluoro-derivatives, **7H** and **7F** respectively, shows that similar changes were observed in the UV region of each switch following irradiation, as the absorbance bands of the open-ring forms decreased and were moderately red-shifted. However, a considerable difference in the absorbance band of the closed forms in the visible region was observed, with the λ_{max} of the perfluorinated switch **7F** bathochromically shifted by 93 nm relative to its perhydro-analogue **7H**. This result can be attributed to the effect of the electron-withdrawing ability of the fluorine atoms on the central switching unit of **7F**. It was also found that the photostationary state of **7H** was reached after 35 minutes of irradiation, whereas the PSS of **7F** was reached after 30 minutes.

Upon irradiation of **8H** at 313 nm, ring-closing from the open-form to the closed form (scheme 4.2) was evidenced from the appearance of a new band in the visible region of the absorption spectrum (λ_{max} = 561 nm) and a colour change from pale yellow to purple. Irradiation also led to changes in the UV region, as the absorbance band at 341 nm decreased and was blue-shifted to 323 nm, with a shoulder at 384 nm, as shown in figure 4.5. The photostationary state was reached after 40 minutes of irradiation, and an isosbestic point was observed at 374 nm.
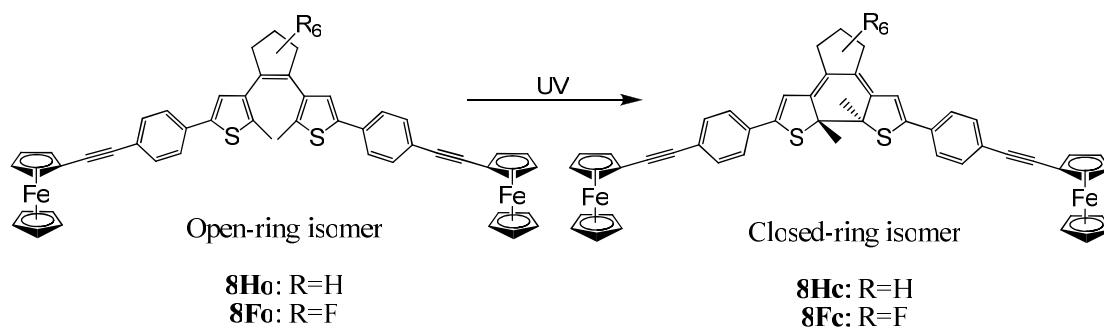
Scheme 4.2: Cyclisation from the open-ring to the closed ring isomer, following irradiation ($\lambda = 313$ nm) of compounds **8H** (R=H) and **8F** (R=F).

Cyclisation of the open-ring isomer to the closed-ring isomer of **8F**, as shown in scheme 4.2, occurred following irradiation ($\lambda = 313$ nm). Evidence of this process was observed in the UV-vis spectrum, as the absorbance band of the open-ring form at 331 nm decreased and was bathochromically shifted to 356 nm, with a shoulder at 399 nm, and the appearance of a new band in the visible region at 621 nm. In conjunction with these changes in the UV-vis spectrum, the solution changed from a pale yellow to a blue colour. An isosbestic point was observed at 354 nm, and the photostationary state was reached after 8 minutes of irradiation, as illustrated in figure 4.5.

The ring-closing process led to a number of different changes in the UV-vis spectra of **8H** in comparison to its perfluoro-analogue **8F**. Firstly the absorbance band in the UV region was blue-shifted by 18 nm for **8H**, but was red-shifted by 25 nm in the case of **8F**, following irradiation. Secondly, the λ_{max} of the absorbance band which appeared in the visible region of **8F** upon ring-closing was bathochromically shifted by 60 nm, relative to its perhydro-derivative **8H**. These differences can be assigned to the effects of the electron-withdrawing ability of the fluorine atoms in **8F**. Another major difference between these two switches is the time taken to reach the photostationary states i.e. 40 minutes for **8H** in comparison to 8 minutes for **8F**.
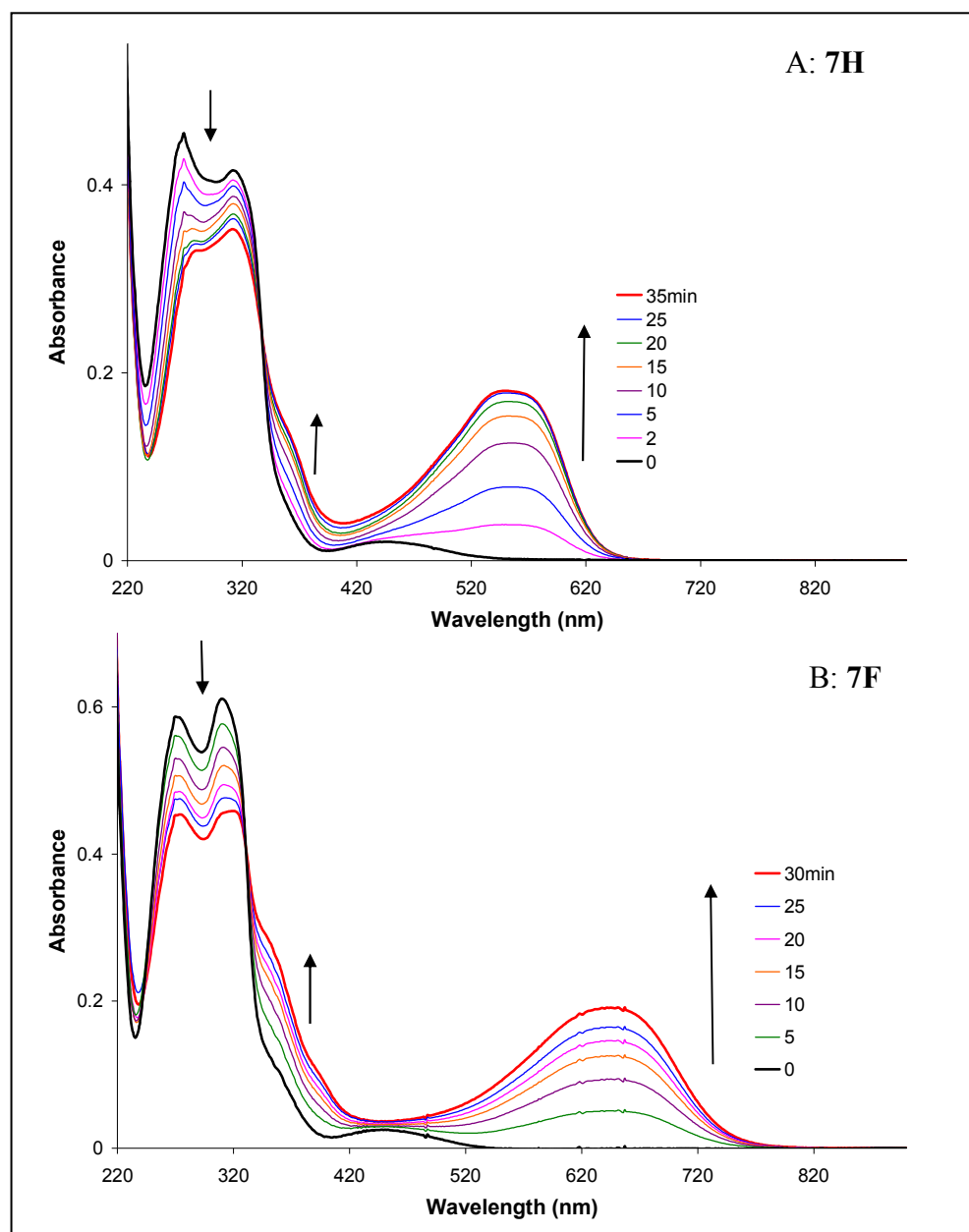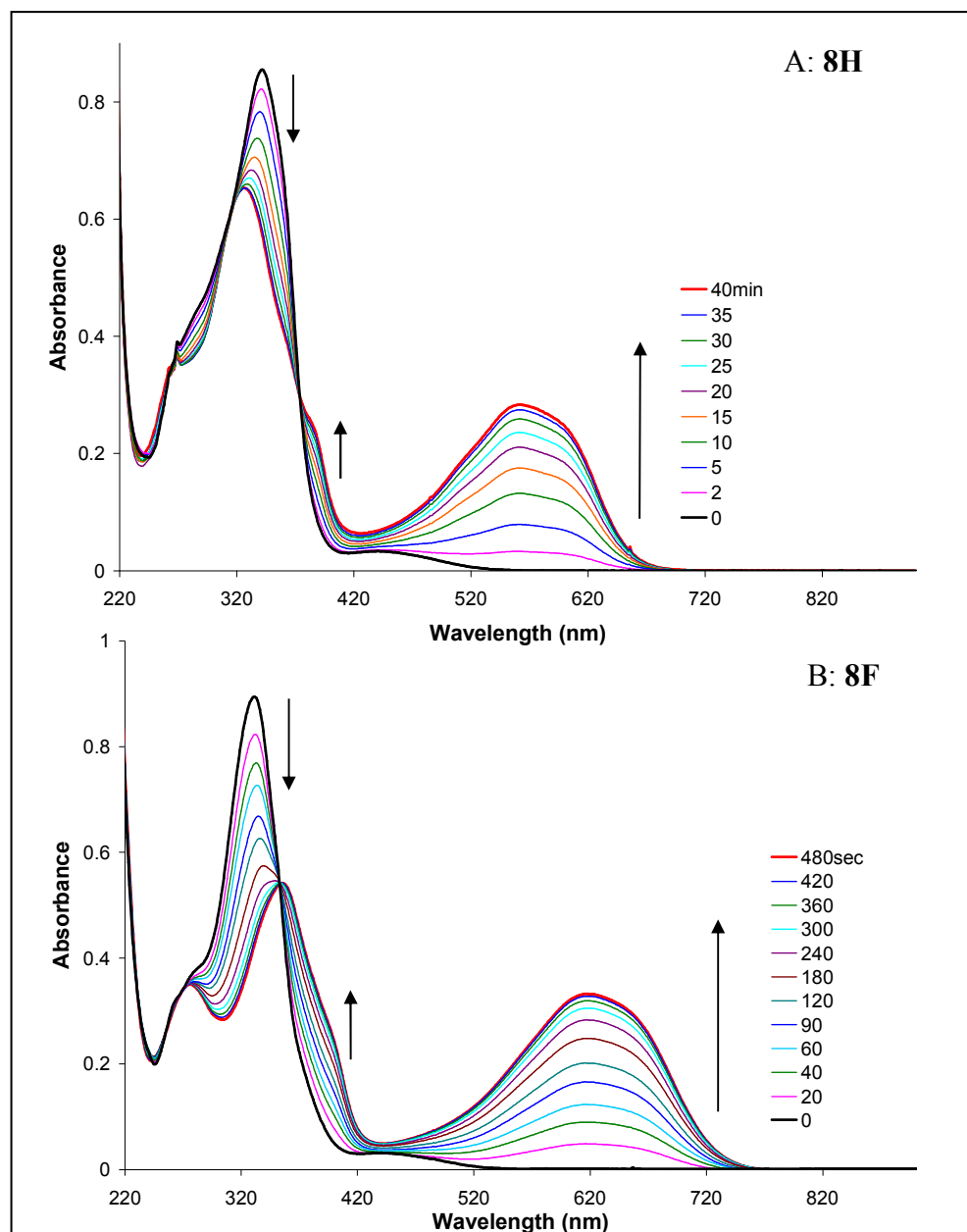
Figure 4.5: Absorption spectra of the cyclisation process from the open-ring isomers to the closed ring-isomers of compounds **8H** and **8F** in THF solution (c = 1.4 x 10^{-5} mol/L), following irradiation (λ = 313 nm). A: **8H**, PSS reached after 40 minutes of irradiation; B: **2F**, PSS reached after 480 seconds (i.e. 8 minutes) of irradiation.

When comparing the effects of extending the conjugation of the systems, by introducing phenyl-rings onto the molecular structure, as for compounds **8H** and **8F**, opposing results were found for the closed-forms of the perhydro-switches in comparison to their perfluoro-derivatives. In the case of the perhydro-derivatives, the absorbance band in the visible region of the closed-ring isomer of **8H** was found to be 13 nm further into the red, in comparison to its less conjugated derivative **7H**.

However, the irradiation time required to reach the photostationary state was increased for the more conjugated system **8H**, relative to **7H** (40 minutes versus 35 minutes respectively). Interestingly, the opposite results were found for the perfluorinated switches, as increasing the π-conjugation of the system in **8F** resulted in a blue-shift in the absorbance band in the visible region by 20 nm, in comparison to **7F**. Also, the irradiation times recorded to reach the PSS dramatically decreased for **8F** in comparison to its less conjugated derivative **7F** (8 minutes versus 30 minutes respectively).

- **Cycloreversion**

The closed-ring isomers of **7H/F** and **8H/F** were irradiated with broadband visible light ($\lambda > 550$ nm) in order to induce a cycloreversion process back to the open-forms. The perfluoro-switch **8F** underwent a complete cycloreversion process from its closed-ring isomer, back to its open-form, following 3 minutes of irradiation with visible light, as illustrated in figure 4.6. Its corresponding less-conjugated derivative **7F** was found to undergo cycloreversion back to its open-form after 7 minutes of irradiation, however, the UV-vis absorption spectrum did not return fully to that recorded at the beginning of the experiment.
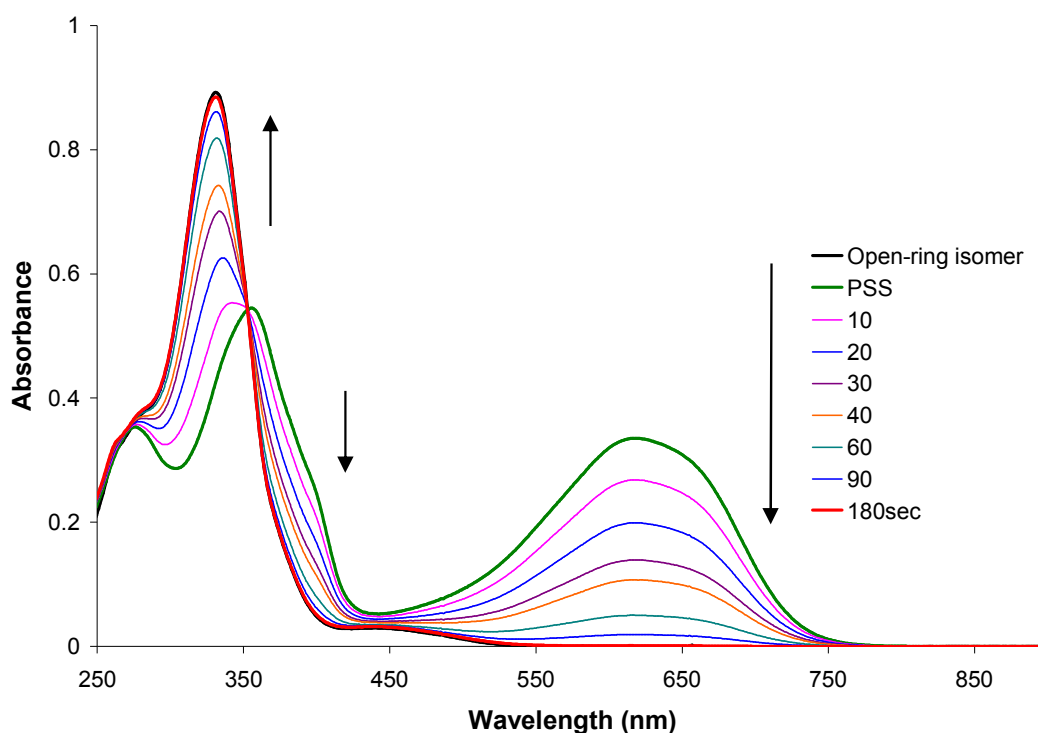
Figure 4.6: Absorption spectra of the cycloreversion process from the closed-ring isomer to the open-ring isomer of compound **8F,** in a solution of THF ($c = 1.4$ x 10^{-5} mol/L), following irradiation with broadband $\lambda > 550$ nm light for 180 seconds (red line). The open-ring isomer recorded at the start of the experiment (before any irradiation takes place) is denoted by the black line. The PSS (green line) is the photostationary state of **8F** following irradiation with 313 nm light for 8 minutes.

In the case of the perhydro-derivatives **7H** and **8H**, an incomplete cycloreversion process was observed for both switches. The closed-ring isomer of **8H** was found to revert back to its open-form, with a decrease in the absorbance band in the visible region, and the original bands observed in the UV region of the open-form growing back-in. However, after 7 minutes of irradiation, no more changes were observed and

the original spectrum of the open-ring isomer, recorded at the start of the experiment, was not obtained, as shown in figure 4.7.
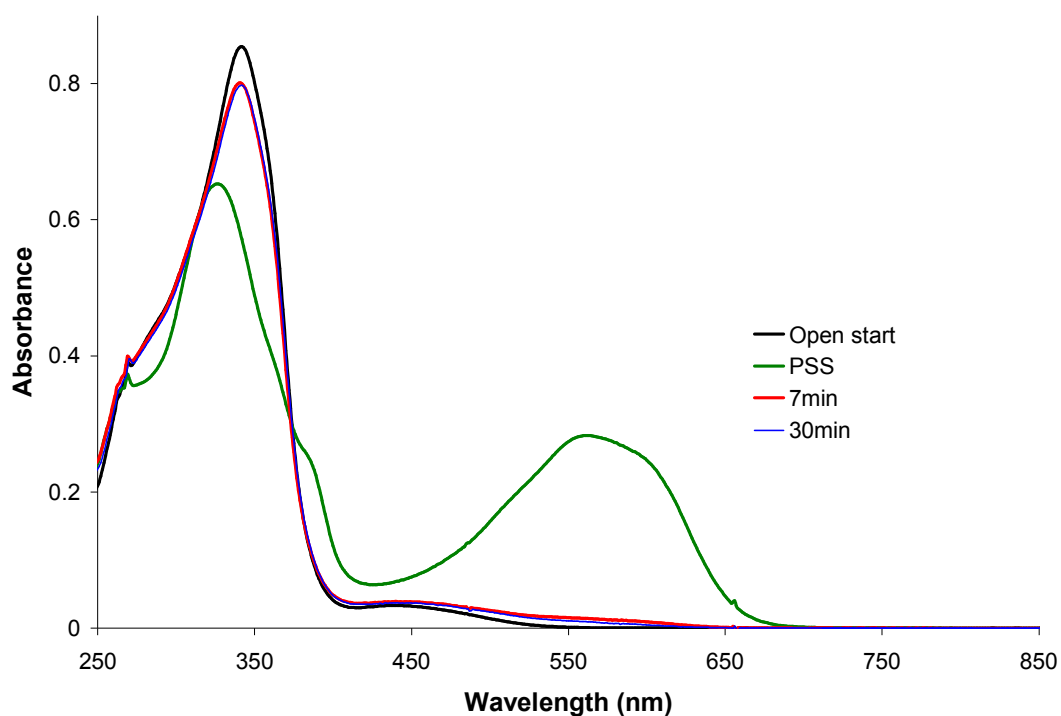
Figure 4.7: Absorption spectrum of **8H**, in THF (c = 1.4 x 10^{-5} mol/L): Open-ring isomer (black line); the photostationary state (PSS) following irradiation at 313 nm for 40minutes (green line); following irradiation at λ > 550 nm for 7 minutes (red line). Note no further changes observed even after 30 minutes of irradiation at λ > 550 nm (blue line)

Irradiation with visible light also induced cycloreversion of the closed-form of **7H**, back to its open-form, but at a considerably slower rate in comparison to its more conjugated analogue **8H**. After 45 minutes of irradiation, the absorbance band in the visible region at 548 nm decreased by approximately half of its absorbance value recorded at the PSS. The absorbance band in the UV region at 275 nm began to increase, but the band at 314 nm barely changed. These changes continued over time, but after a total of 270 minutes of irradiation (λ = 550 nm), no more changes were observed, and the original absorption spectrum of the open-ring isomer of **7H**, recorded at the start of the experiment, was not obtained. In fact approximately 20% of the absorbance at 548 nm remained, as illustrated in figure 4.8.
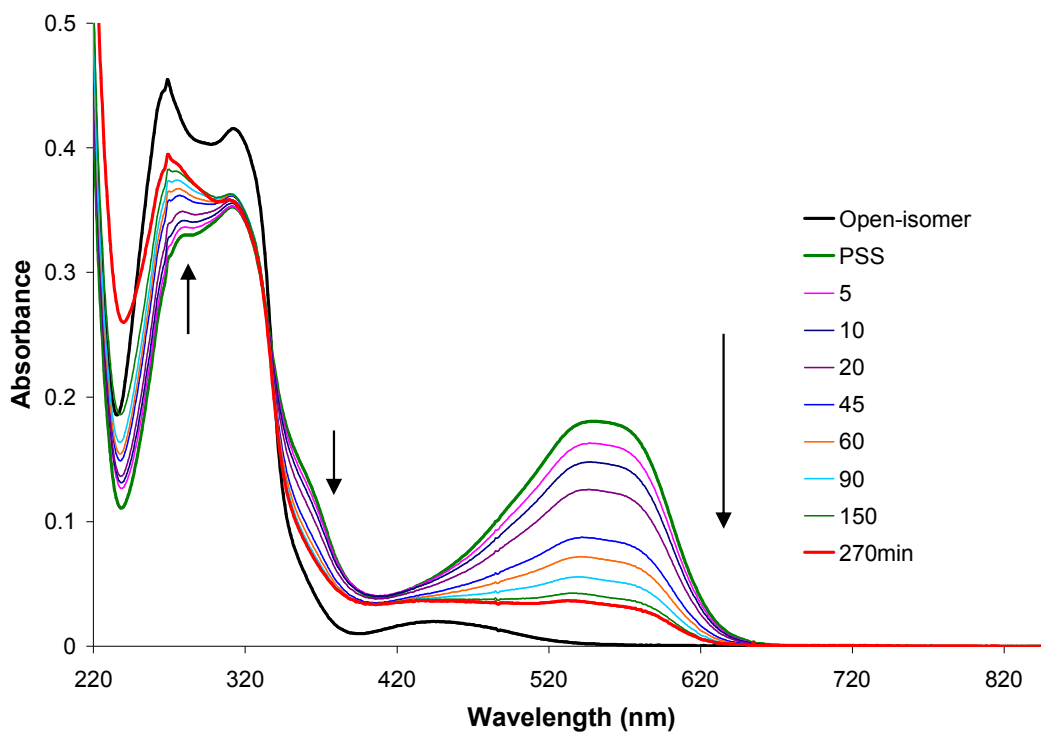
Figure 4.8: Absorption spectra of the cycloreversion process from the closed-ring isomer to the open-ring isomer of compound **7H,** in a solution of THF (c = 1.4 x 10^{-5} mol/L), following irradiation with broadband light $\lambda > 550$ nm for 270 minutes (red line). The open-ring isomer recorded at the start of the experiment (before any irradiation takes place) is denoted by the black line. The PSS (green line) is the photostationary state of **7H** following irradiation with 313 nm light for 35 minutes.

4.3.2 Fatigue Resistance

The fatigue resistance of compound **8F** was investigated by performing five consecutive cyclisation/cycloreversion cycles in a degassed solution of THF, whilst monitoring the absorbance at the λ_{max} (621 nm) of the band in the visible region in the UV-vis spectrum. The solution was irradiated with monochromatic light at 313 nm until the photostationary state was reached (8 minutes), followed by irradiation with visible light > 550 nm (2.5 minutes). This process was deemed as one cycle, and after five colouring/bleaching cycles it was determined that **8F** has a high fatigue resistance as less than 1% of **8F** had degraded, as demonstrated in figure 4.9. Such a result is comparable to high fatigue resistant dithienylethene switches described in the literature.[11-13]
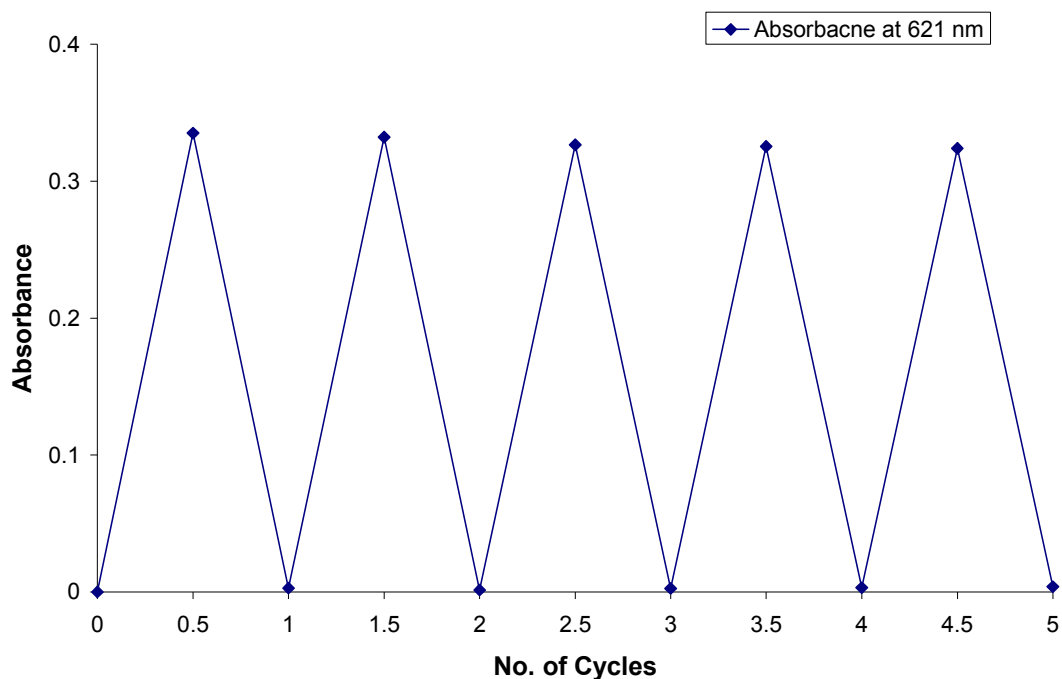
Figure 4.9: Fatigue resistance of **8F** in THF. The absorbance values of the open/closed forms were monitored at 621 nm over five colouring/bleaching cycles.

The fatigue resistance of **8H** was also investigated in the same manner as that described for **8F**. The colouring/bleaching cycles were monitored in the UV-vis spectrum at 562 nm, and after five consecutive cycles it was found that **8H** underwent significant decomposition during these photochemical processes, with a total of 50% degradation at the end of the experiment, as illustrated in figure 4.10. This result greatly contrasts to the high fatigue resistance found for its perfluoro-derivative **8F**,

thus highlighting the significant stabilising effect of the fluorine atoms on the switching unit.
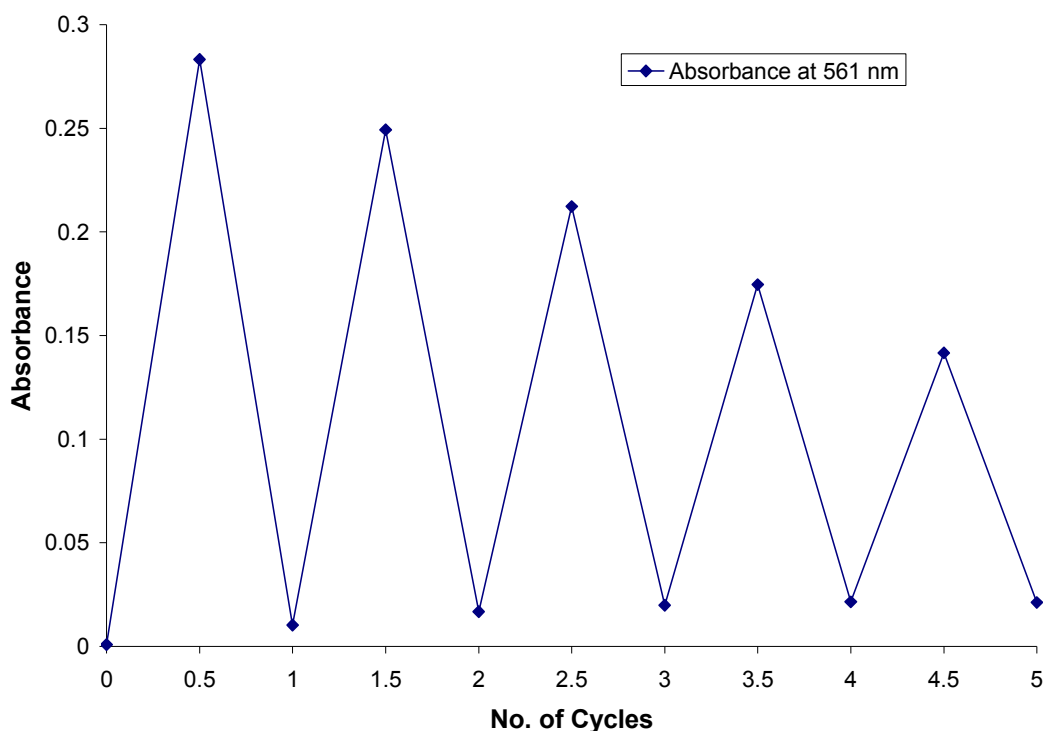
Figure 4.10: Fatigue resistance of **8H** in THF. The absorbance values of the open/closed forms were monitored at 561 nm over five colouring/bleaching cycles.

The fatigue resistance of the less conjugated ferrocenyl-based switches, **7H** and **7F**, were also investigated and both compounds were found to have very low fatigue resistance properties. **7F** was monitored in the UV-vis spectrum at 641 nm, and it was found that the first cycloreversion process, performed after ring-closing, did not completely reform the ring-open isomer, as approximately 4% of the absorbance at 614 nm remained. The subsequent cyclisation process did not return to the original absorbance recorded at 641 nm for the closed-ring isomer. Approximately 50% of **7F** had degraded after just one colouring/bleaching cycle.

In the case of the perhydro-derivative **7H**, the first bleaching process performed after ring-closing did not completely reform the open-ring isomer, as mentioned in the previous section, with ~20% of the absorbance at 548 nm remaining. The second colouring cycle revealed that ~30% of **7H** had decomposed. Although **7F** was found to degrade by ~50% after one colouring/bleaching cycle, suggesting that **7F** is less stable than **7H**, the fact that ~20% of the absorption remained in the visible region

following the first cycloreversion process of **7H**, indicates that **7H** is less photostable than **7F**.

Overall, it was found that the fatigue resistance of these ferrocenyl-based switches decreased in the order **8F** > **8H** > **7F** >**7H**. This trend highlights the fact that increasing the π-conjugation of the system and substituting fluorine atoms onto the cyclopentene unit, instead of hydrogen atoms, significantly improves the fatigue resistance of such switches. The most probable cause of the low fatigue resistance found for compounds **8H**, **7H** and **7F** is the generation of a photochemical by-product during the irradiation experiments, which has been reported previously in the literature.[14-16] Hence, the cyclisation processes of these switches were monitored by ^{1}H NMR spectroscopy, and the results are detailed in the following section.

4.3.3 Photochromic Behaviour: ^{1}H NMR

Photocyclisation from the open to the closed-ring isomers can be monitored by ^{1}H NMR, as described previously in chapter 1 and chapter 3. Hence, the ring-closing process was investigated in the ^{1}H NMR spectra for compounds **7H/F** and **8H/F**, in deuterated acetone, following irradiation with monochromatic light (λ = 313 nm). Table 4.2 details the chemical shifts (in ppm) of the proton at the 4-position of the thiophene ring on the dithienylcyclopentene unit of these switches, which is illustrated in scheme 4.3. The estimated percentage conversions to the closed-forms were also calculated for these compounds and are denoted in table 4.2.
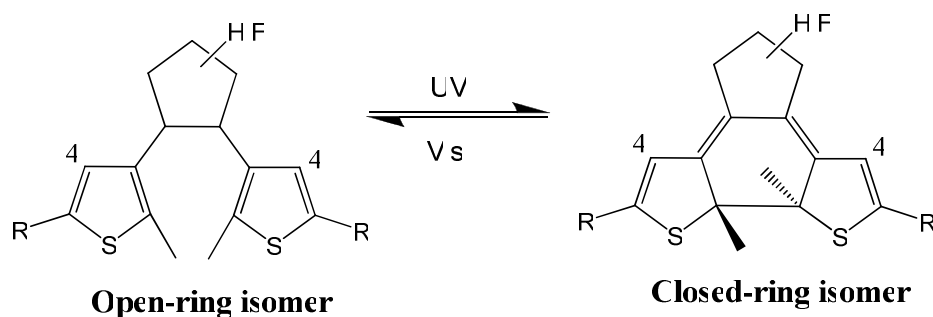
Scheme 4.3: Represents the structural change incurred on the dithienylcyclopentene unit upon ring-closure, and hence the loss of aromaticity of the thiophene rings. Also illustrates the proton at the 4-position of the thienyl units.

The proton at the 4-position of the thiophene ring on the main switching unit of compound **8F**, in its open-form, appeared as a singlet peak at 7.59 ppm in the ^{1}H NMR spectrum. Following irradiation with UV light at 313 nm, the intensity of this peak began to decrease and a new peak was found to appear at 7.03 ppm, which can be attributed to the formation of the ring-closed isomer. After 6 hours of irradiation, the ratio of the peaks at 7.59 and 7.03 ppm was found to be 0:1 respectively, as shown in figure 4.11. Hence, the percentage conversion from the open-ring isomer to the closed-ring isomer of **8F** was estimated to be > 95%.

Figure 4.11: ^{1}H NMR spectral changes of **8F**, dissolved in deuterated acetone, upon irradiation at $\lambda =$ 313 nm. A: open-ring isomer of **8F** before irradiation; B: closed-ring isomer of **8F** after 6 hours of irradiation.

In the case of the perhydro-derivative **8H**, which was dissolved in deuterated benzene due to low solubility in acetone, UV irradiation at 313 nm also resulted in the appearance of a new peak in the ^{1}H NMR spectrum. The initial peak at 7.05 ppm, representing the thiophene proton at the 4-position of the open-ring isomer, decreased and a new peak appeared at 6.26 ppm, representing the closed-ring isomer. After 29 hours of irradiation, the ratio of the peak intensities was found to be 0:1 respectively. This result suggests that the percentage conversion between the open and closed forms of **8H** was approximately > 95%. There was no evidence for the formation of a photostable by-product, as no further new peaks were observed in the ^{1}H NMR spectrum. However, noteworthy is the fact that the peaks present at the end of the experiment were not as sharp as those recorded at the start and the baseline was quite noisy, indicating that some decomposition of **8H** possibly occurred during the irradiation process. This theory could explain the results obtained previously for the fatigue resistance experiment, where approximately 50% of **8H** degraded following five consecutive colouring/bleaching cycles.

Table 4.2: ^{1}H NMR chemical shift data (in ppm) of the thiophene-proton at the 4-position of the dithienylcyclopentene thiophene ring (Th-H), for compounds **7H/F** and **8H/F** at different irradiation times (λ=313 nm). Also, the estimated percentage conversion from the open to the closed-ring isomers, and the by-products of compounds **7H** and **7F**.

Irradiation Time of **7H**	δ Th-H open	δ Th-H closed	Conversion (%)	δ Th-H by-product	Conversion (%)
6 hrs	7.01	6.26	25	-	-
21 hrs	7.01	6.26	36	6.47	11
Irradiation Time of **7F**	δ Th-H open	δ Th-H closed	Conversion (%)	δ Th-H by-product	Conversion (%)
6 hrs	7.30	6.49	10	-	-
21 hrs	7.30	6.49	35	6.63	3
40 hrs	7.30	6.49	51	6.63	8
Irradiation Time of **8H***	δ Th-H open	δ Th-H closed	Conversion (%)	δ Th-H by-product	Conversion (%)
29 hrs	7.05	6.26	>95	-	-
Irradiation Time of **8F**	δ Th-H open	δ Th-H closed	Conversion (%)	δ Th-H by-product	Conversion (%)
6 hrs	7.59	7.03	>95	-	-

(-) indicates that a peak due to the formation of a by-product was not present.
NMR spectra were recorded in deuterated acetone, with the exception of **8H**, which was recorded in deuterated benzene (denoted by *).

The ^{1}H NMR studies of **7F**, following exposure to UV light (λ = 313 nm), revealed that a photochemical by-product was formed, during the cyclisation process from the open to the closed-form, as illustrated in scheme 4.4. Such an occurrence has been described previously in the literature.[14-16]
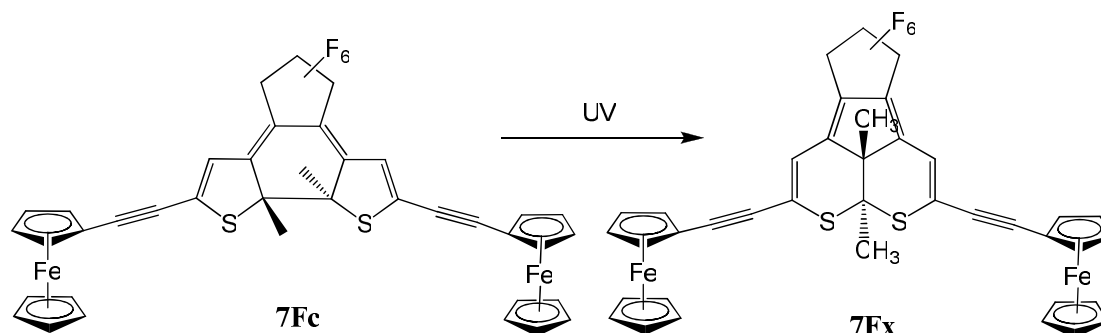
Scheme 4.4: Illustrates the by-product **7Fx** formed following continuous UV irradiation of the ring-closed isomer **7Fc**.

The open-ring isomer of **7F** exhibited a peak at 7.30 ppm in the ^{1}H NMR spectrum, representing the proton at the 4-position of the thiophene ring. Following UV irradiation for 6 hours, the intensity of the peak at 7.30 ppm began to decrease and a new peak at 6.49 ppm appeared, due to the formation of the closed-ring isomer (**7Fc**), as shown in figure 4.12. The percentage conversion from the open to the closed-form at this time was found to be ~ 10%. After 21 hours of irradiation, the peak at 6.49 ppm increased further and a new peak was observed at 6.63 ppm. The new peak at 6.63 ppm can be attributed to the formation of a photostable by-product (**7Fx**). The percentage conversion from the open to the closed-form (**7Fc**), and to the by-product (**7Fx**), was estimated as 35% and 3% respectively. The peaks at 6.49 ppm and 6.63 ppm further increased, and the initial peak at 7.03 ppm continued to decrease. After an additional 19 hours of irradiation, the percentage conversion to the closed-form (**7Fc**) and by-product (**7Fx**) was calculated as approximately 51% and 8% respectively.

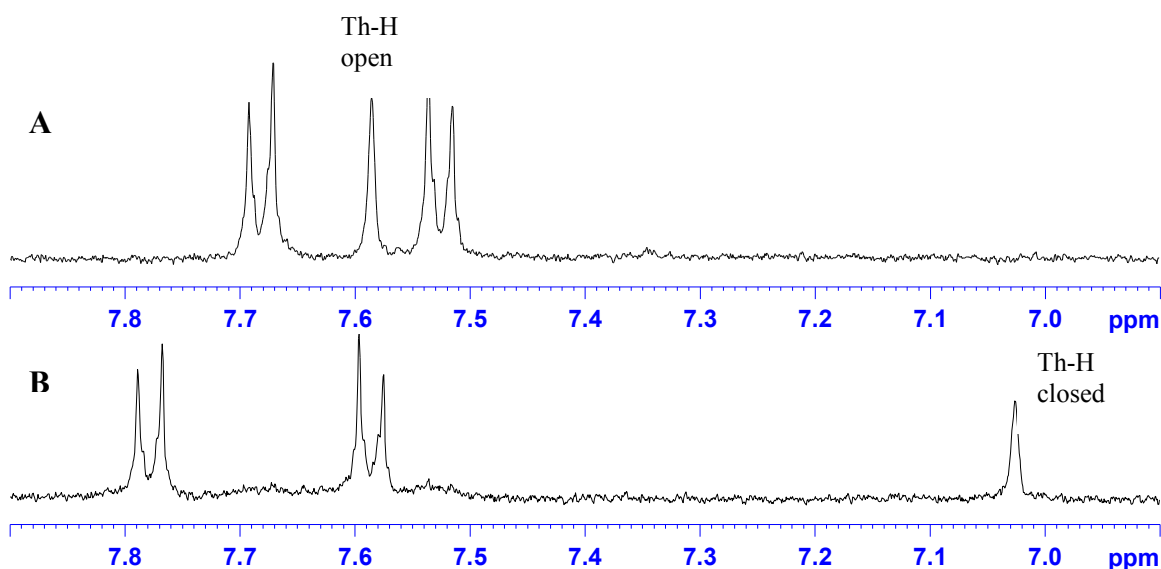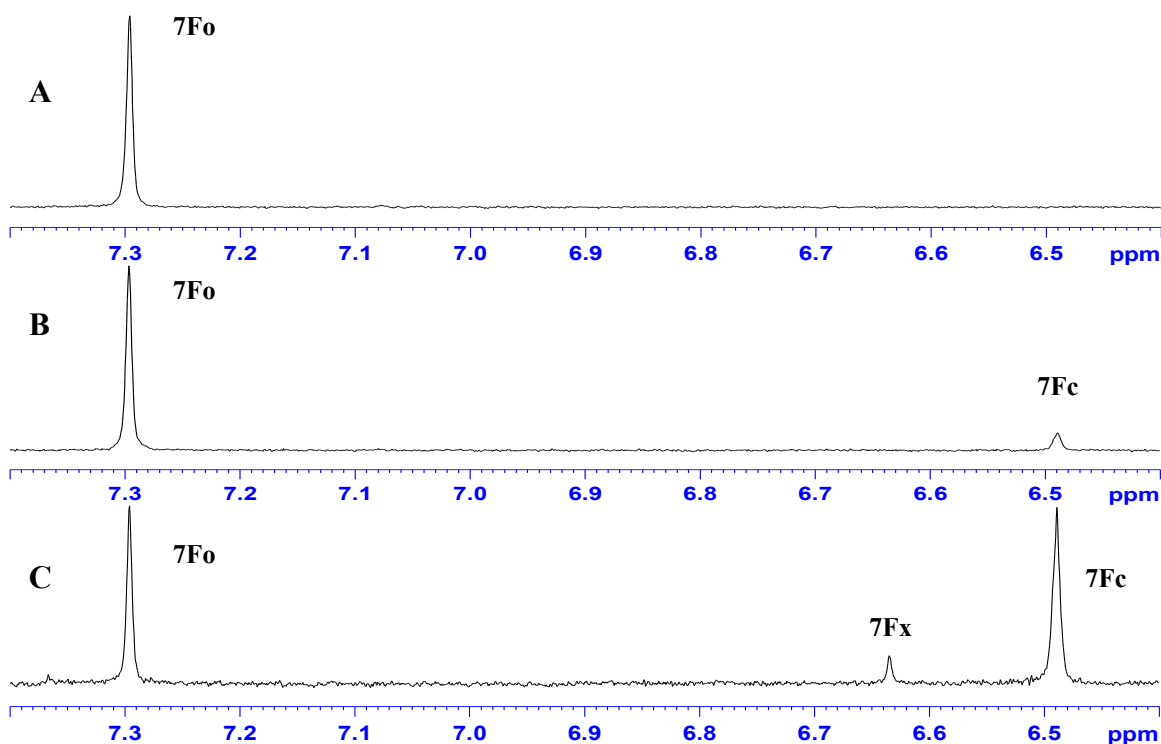**Figure 4.12:** ^{1}H NMR spectral changes of **7F**, dissolved in deuterated acetone, upon irradiation at λ = 313 nm. A: open-ring isomer **7Fo** before irradiation; B: new peak at 6.49 ppm due to formation of closed-ring isomer **7Fc** after 6 hours of irradiation; C: new peak at 6.63 ppm due to formation of the by-product **7Fx** after 40 hours of irradiation.

In the case of **7H**, the ^{1}H NMR monitored UV irradiation studies demonstrated the formation of a by-product for **7H** during the cyclisation process. The thienyl proton at the 4-position was found to appear at 7.01 ppm in the ^{1}H NMR spectrum of the open-ring isomer of **7H**. Following 6 hours of UV irradiation the intensity of this peak decreased, and a new peak was present at 6.26 ppm, which can be assigned to the formation of the closed-ring isomer (**7Hc**). The percentage conversion from the open to the closed form was estimated to be 25%. Continued irradiation for 15 hours led to further reduction of the peak at 7.01 ppm, with an increase in the peak at 6.26 ppm, attributed to the closed-isomer. However, in-conjunction with the formation of the closed-ring isomer, a photostable by-product was also generated, as evidenced by the appearance of a new peak at 6.47 ppm, the structure of which is illustrated in scheme 4.5. The relative integrals of the three peaks at 7.01, 6.47 and 6.26 ppm were calculated to be 1: 0.20: 0.67, respectively. Hence, after a total of 21 hours of UV irradiation, the percentage conversion from the open-form (**7Ho**) to the closed-form (**7Hc**), and to the by-product (**7Hx**), was approximately 36% and 11% respectively.
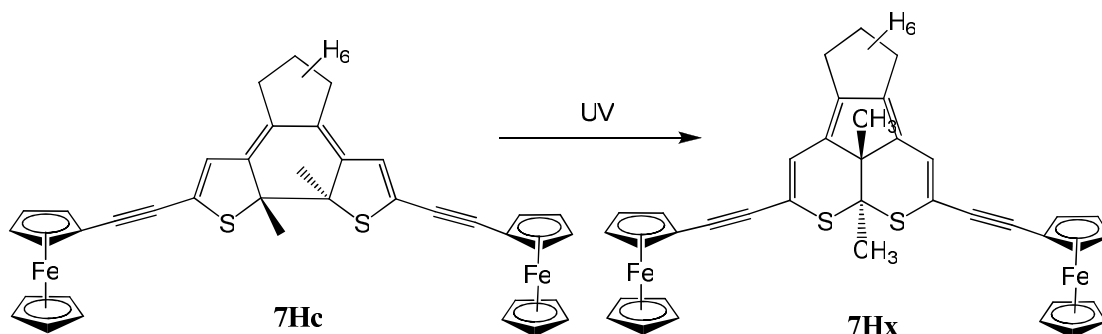
Scheme 4.5: Illustrates the by-product **7Hx** formed following continuous UV irradiation of the ring-closed isomer **7Hc**.

Overall, the ^{1}H NMR studies demonstrated that an extension of the π-conjugation of the system, in compounds **8H** and **8F**, increased the photo-stability of the compounds in their closed-forms, relative to their less-conjugated analogues **7H** and **7F**, as the generation of photochemical by-products were not found to occur for **8H** and **8F**. In the case of **8F**, this is in good agreement with the fatigue resistance experiments discussed in the previous section, as less than 1% of **8F** was found to degrade following five consecutive colouring/bleaching cycles. On the other hand, ~50% of **8H** decomposed during the same fatigue resistance experiments, however the ^{1}H NMR experiment did not show any evidence for the formation of a by-product. It is

possible that the formation of the by-product occurs but the amount produced is too low to be observed in the ^{1}H NMR spectrum. As mentioned previously, the ^{1}H NMR spectrum of **8H** was found to be very noisy at the end of the experiment. Therefore, another possibility is that **8H** undergoes some decomposition during such photochemical processes due to the long irradiation times required to induce ring-closure.

With regards to the by-products formed for **7H** and **7F**, during these photochemical processes, the results described here suggest that the by-product (**7Hx**), formed from **7H**, is much more readily produced in comparison to the by-product (**7Fx**) formed from its perfluoro-derivative **7F**. In the case of **7H** it was found that after 21 hours of irradiation, 36% of the open-ring had converted to the closed-ring, whilst 11% of the solution had converted to the by-product. On the other hand, after 21 hours of irradiation of **7F**, the percentage conversion of the open-ring isomer to the closed-ring isomer, and to the by-product, was found to be 35% and 3% respectively. This result suggests that more of the closed-form of **7F** is produced before the by-product is formed, in comparison to **7H**. These findings conform to the results of the cycloreversion and fatigue resistance studies discussed previously for these switches.

4.3.4 Thermal Stability

Solutions of **7H/F** and **8H/F**, in toluene, were irradiated with UV light in order to generate their ring-closed isomers, which were then stored in the dark at room temperature, and at elevated temperatures of 60, 80 and 100°C, under air. The thermal stabilities of these switches were studied by recording their absorbance spectra at different time intervals, at these temperatures, in order to investigate if thermal cycloreversion from the closed-ring to the open-ring forms would occur.

The ring-closed isomers of **7H/F** and **8H/F** were all found to be thermally stable at room temperature, with no changes observed in their absorbance spectra after ten weeks in the dark. Upon heating the closed-switches, to 60°C, 80°C and 100°C, the absorbance bands in the visible region of the UV-vis spectra began to decrease. The absorbance values at the λ_{max} in the visible region were monitored over time, and the decay curves of the closed-isomers were plotted $\{\ln([c]/[c]_0)$ vs. time$\}$, as illustrated in figure 4.9. The half-lives of the switches were calculated from the equation $t_{1/2}=\ln2/k$, as the plots were found to be roughly linear, indicating first-order kinetics, hence the slope of the graphs gave the reaction rate k. These results are detailed in table 4.3.
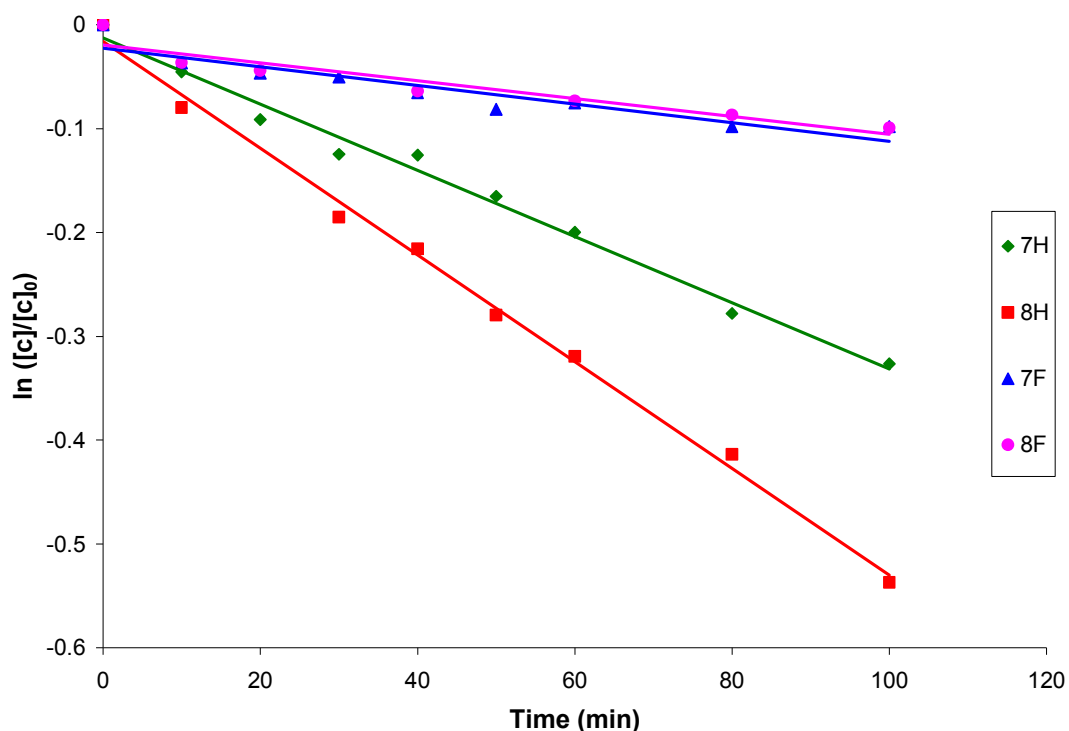
Figure 4.9: Thermal Stability of compounds **7H**, **8H**, **7F** and **8F** at 80°C for 1.5 hours.

The absorbance band in the visible region of the UV-vis spectrum of **7F** was found to steadily decrease over a period of 7 hours at 60°C, with its half-life calculated to be 128 hours. Its more conjugated derivative, **8F**, was found to behave in a similar manner under the same conditions, although slightly less stable, with a half-life of 115 hours. Conversely, the thermal stability of the perhydro-switches at 60°C was found to be considerably reduced in comparison to their fluorinated derivatives, with a half-life of 12 hours and 7 hours, calculated for compounds **7H** and **8H**, respectively. Although, a similar trend was observed for the perhydro-switches, as that found for their perfluoro-analogues, as extending the π-conjugation of the system marginally reduced the thermal stability of **8H**, in comparison to **7H**. The thermal stability of these switches was also investigated at higher temperatures of 80°C (1.5 hours) and 100°C (1 hour), and the results demonstrated that as the temperature increased, the half-lives decreased (table 4.3). At all three temperatures, the order of stability remained the same: **7F** > **8F** > **7H** > **8H**.

Table 4.3: Half lives of **7H/F** and **8H/F** in their closed-forms at 60°C, 80°C and 100°C in toluene.

Compound	$t_{1/2}$ at 60°C (hr)	$t_{1/2}$ at 80°C (hr)	$t_{1/2}$ at 100°C (hr)
7H	12	4	0.9
7F	128	17	6
8H	7	2	0.6
8F	115	14	4

Overall the results indicate that extending the π-conjugation of the system reduces the thermal stability of the switches, although to a moderate degree, as only a minor decrease was found for the half-lives calculated for **8H** and **8F**, in comparison to their less conjugated derivatives **7H** and **7F** respectively. A much more significant factor affecting the thermal stability properties were the central atoms located on the cyclopentene ring, as the presence of the fluorine atoms, in place of the hydrogen atoms, resulted in a considerable increase in the half-lives of these switches calculated at 60, 80 and 100°C. It is worth noting however, that the UV-vis spectra recorded during these experiments indicate that cycloreversion back to the open-form was accompanied by chemical degradation, under these conditions. Such chemical degradation has not been reported in the literature thus far, and only thermal cycloreversion processes have been discussed.[11,12,17-19] Further experiments are required to examine the thermal processes that are taking place.

4.3.5 Fluorescence

The fluorescence properties of **7H/F** and **8H/F** were investigated at room temperature, in THF. These ferrocenyl-based switches were not found to be luminescent, and subsequent generation of the closed-ring isomers did not induce emission. This phenomenon can be assigned to the quenching effect of the ferrocenyl moieties. As described in section 4.1, ferrocene is known as an excited state quencher, which can occur through energy transfer and/or electron transfer processes.[1-4]

4.3.6 Cobalt Carbonyl Complexes: UV-vis Absorption Spectra
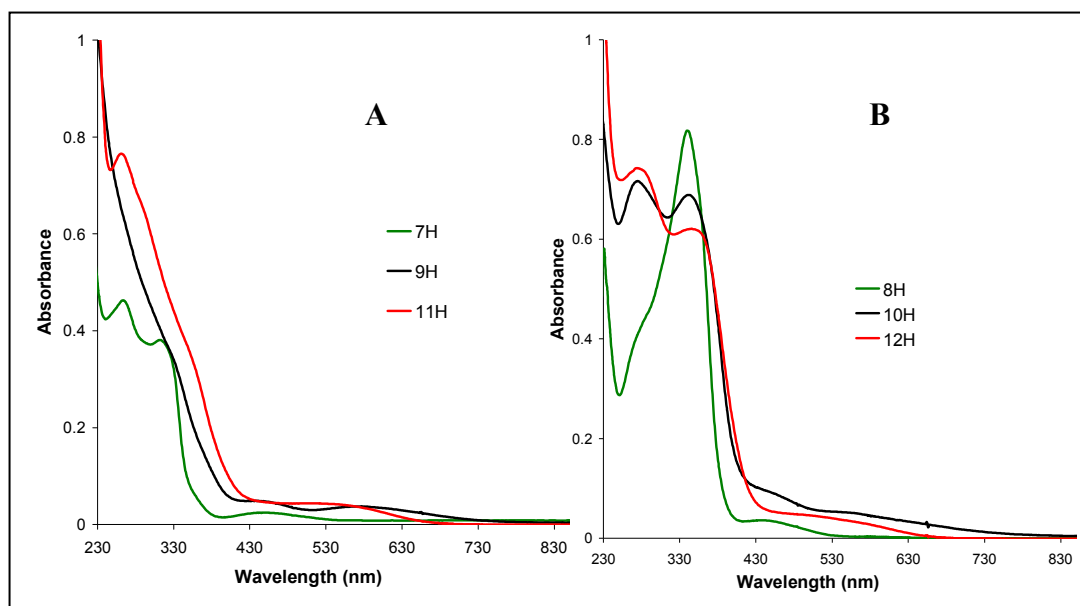
Figure 4.10: UV-vis absorption spectra of the open-ring isomers {**7H**, **8H**}, and their corresponding $Co_2(CO)_6$ {**9H**, **10H**} and $Co_2(CO)_4dppm$ complexes {**11H**, **12H**}, of the perhydro-cyclopentene compounds, in THF solution (c ≈ 1.4 x 10^{-5} mol/L). A: **7H** (green line), **9H** (black line), **11H** (red line); B: **8H** (green line), **10H** (black line), **12H** (red line).

The UV-vis absorption spectra of the $Co_2(CO)_6$ complexes {**9H/F**, **10H/F**} and the $Co_2(CO)_4dppm$ complexes {**11H/F**, **12H/F**} were recorded in THF. Significant changes were observed in the electronic spectra of the cobalt carbonyl complexes in comparison to their corresponding free ligands **7H/F** and **8H**/**F**, which is highlighted for the perhydro-derivatives in figure 4.10. Incorporating $Co_2(CO)_6$ complexes onto compound **7H**, forming compound **9H**, resulted in a much broader absorbance in the UV region, with a λ_{max} present at 262 nm, assigned to a ligand field "d-d" transition corresponding to the d orbitals on the cobalt atoms, and a shoulder at 328 nm, representing the intraligand excited state. In the visible region, a low-intensity, broad absorption band was observed from 420 to 750 nm, with λ_{max} at 445 and 570 nm. This band can be assigned to a metal-to-ligand charge transfer transition.

Similar results were found for the extended π–conjugated analogue **10H**, with a ligand-field "d-d" transition present at 276, and low-lying MLCT bands from 420 nm extending to 820 nm, with λ_{max} at 455 and 538 nm. In contrast to its less-conjugated derivative **9H** however, the intraligand band (λ = 342 nm) was found to be far more prominent for **10H**. This result suggests that addition of the $Co_2(CO)_6$ complexes

involves relatively small perturbation of the electronic structure of the free ligand **8H**, which is most likely due to the presence of the phenyl moieties on either side of the switch, separating the switching unit and the alkynyl-bridged cobalt carbonyl units.

In the case of the $Co_2(CO)_4$dppm complexes, only moderate changes were observed in the electronic spectra of the complexes in comparison to the hexacarbonyl derivatives, as highlighted in figure 4.10. Incorporating cobalt carbonyl complexes onto the perfluoro-switches resulted in similar changes in the absorption spectra as that described for the perhydro-analogues, and the results are summarised in table 4.4

Table 4.4: UV-vis absorption data for the open-ring isomers {**7H**, **7F**, **8H**, **8F**} and their corresponding $Co_2(CO)_6$ {**9H**, **9F**, **10H**, **10F**} and $Co_2(CO)_4$dppm complexes {**11H**, **11F**, **12H**, **12F**}, in THF.

Absorption Spectra in THF					
Open-ring isomer		$Co_2(CO)_6$ Complexes		$Co_2(CO)_4$dppm Complexes	
λ_{abs} [nm] ($\varepsilon \times 10^3$ M^{-1} cm^{-1})		λ_{abs} [nm] ($\varepsilon \times 10^3$ M^{-1} cm^{-1})		λ_{abs} [nm] ($\varepsilon \times 10^3$ M^{-1} cm^{-1})	
7H	265 (34.0), 312 (28.7), 445 (1.6)	**9H**	262 (46.7), 328 (27.8), 445 (4.3), 570 (3.0)	**11H**	262 (65.5), 291 (48.6), 351 (26.1), 511 (3.2)
7F	269 (38.5), 310 (37.8), 354 (7.7), 441 (2.2)	**9F**	270 (52.6), 327 (33.7), 438 (4.3), 555 (2.5)	**11F**	270 (64.5), 291 (54.2), 355 (28.3), 555 (3.1)
8H	277 (30.3), 341 (57.1), 441 (3.1)	**10H**	276 (48.1), 342 (45.0), 455 (4.7), 538 (2.5)	**12H**	276 (55.6), 347 (45.3), 490 (3.7)
8F	281 (27.0), 331 (62.4), 442 (2.2)	**10F**	276 (44.1), 340 (46.1), 445 (4.3), 555 (1.9)	**12F**	264, 286, 334, 490

4.3.7 Photochromic Behaviour of Cobalt Carbonyl Complexes: Perhydro-Switches

The perhydro ferrocenyl-based switches were substituted with $Co_2(CO)_6$ complexes {**9H** and **10H**} and $Co_2(CO)_4$dppm derivatives {**11H** and **12H**}, and the effects of the cobalt carbonyl complexes on the photochemical activity of the switches were investigated. The complexes were irradiated at two wavelengths: 313 nm and 365 nm, and the changes in the UV-vis absorption spectra were monitored. The results are summarised in table 4.5.

9H: M_1=$Co_2(CO)_6$
11H: M_1=$Co_2(CO)_4$dppm

10H: M_1=$Co_2(CO)_6$
12H: M_1=$Co_2(CO)_4$dppm
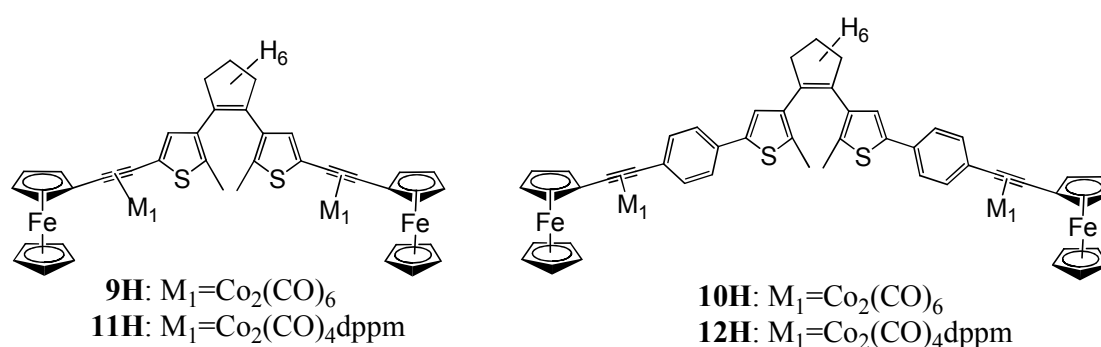
Scheme 4.7: Illustrates the cobalt carbonyl complexes of the perhydro-switches (**9H**, **10H**, **11H**, **12H**).

Table 4.5: UV-vis absorption data for the $Co_2(CO)_6$ {**9H** and **10H**) and $Co_2(CO)_4$dppm complexes (**11H** and **12H**), in THF, in their open-ring forms and following irradiation at 313 nm and 365 nm.

Cobalt Carbonyl Complexes	Absorption Spectra in THF		
	Open-ring isomers λ_{abs} (nm)	313 nm Irradiation[a] λ_{abs} (nm)	365 nm Irradiation[a] λ_{abs} (nm)
9H	262, 328, 445, 570	262(↓), 328(↓), 490-590(↑), {373}*	262(↓), 328(↓), 445(↑), 570(↓), {373}*
11H	262, 291, 351, 511	262(↓), 291(↓), 351(↓), 450(↑), {403}*	262(↓), 291(↓), 351(↓), 450(↑), {403}*
10H	276, 342, 455, 538	276(↓), 342(↓), 555(↑), {406}*	276(↓), 342(↓), 552(↑), {406}*
12H	276, 347, 490	276(↓), 347(↓), 555(↑), {422}*	276(↓), 347(↓), 552(↑), {422}*

[a] Decreasing absorbance (↓); Increasing absorbance (↑)
*{isosbestic points}

- **Irradiation of 9H and 11H**

When **9H** was irradiated at 313 nm for 60 minutes, the absorbance bands in the UV region of the spectrum at 262 and 328 nm began to decrease dramatically. A slight increase in the visible region between approximately 490 and 590 nm was also observed, with an isosbestic point at 373 nm, as illustrated in figure 4.10. However, longer irradiation times resulted in a decrease in the absorbance in the visible region. Comparing these results to those observed for the free ligand (**7H**) indicates that the presence of the $Co_2(CO)_6$ complexes inhibits the photocyclisation process for this switch. Subsequent irradiation with visible light ($\lambda > 550$ nm) did not reproduce the initial spectrum recorded at the start of the experiment. Thus, the changes observed in the UV-vis spectrum showed that there was little evidence of ring-closure for **9H**, and only decomposition of the cobalt carbonyl complex occurred. Similar results were obtained following irradiation at 365 nm.

1,2-Bis(diphenylphosphino)methane ligands were incorporated onto the cobalt carbonyl complexes, forming the $Co_2(CO)_4$dppm derivative **11H**, in an attempt to introduce stability. However, the same results were obtained as that found for **9H**, following UV irradiation at both 313 and 365 nm.
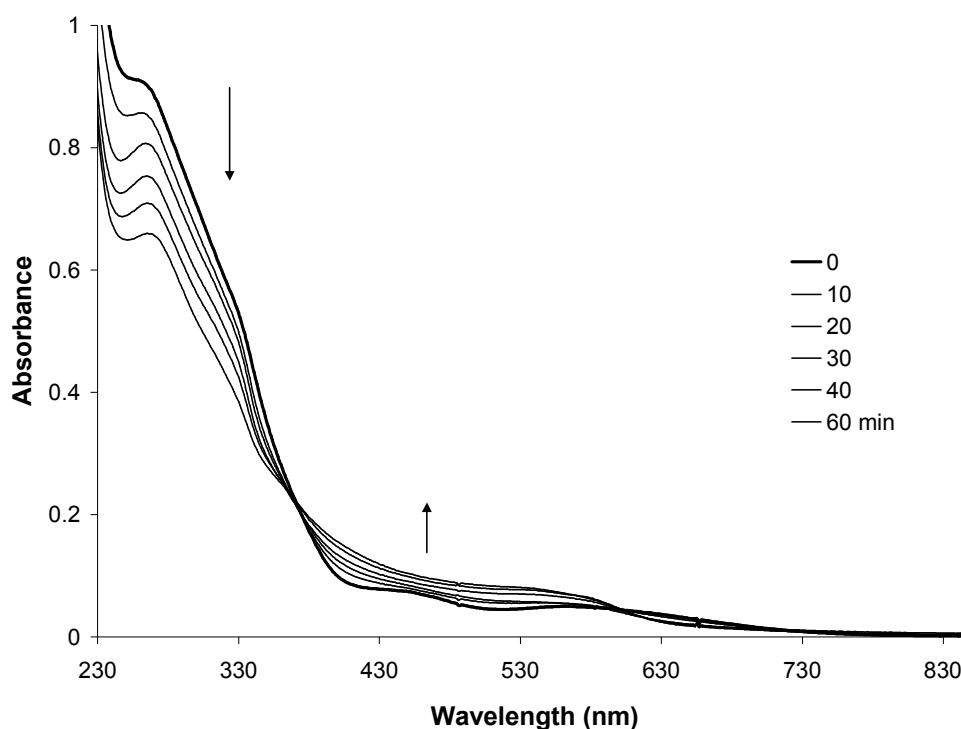
Figure 4.10: UV-vis absorption spectrum of **9H**, in THF, following irradiation at $\lambda = 313$ nm for 60 minutes. The spectrum recorded at the start of the experiment (before irradiation) is denoted by the thick black line.

- **Irradiation of 10H and 12H**

Irradiation of **10H** at λ = 313 nm resulted in a colour change from yellow/brown to purple and a new band was observed in the visible region of the UV-vis spectrum, with a λ_{max} at 555 nm. The changes observed in the UV-vis spectra indicate that photocyclisation to the closed-ring isomer occurred, and the photostationary state was reached after 45 minutes of irradiation. In-conjunction with these changes, a decrease in the absorbance bands in the UV region resulted, with a new band at 312 nm appearing and an isosbestic point at 406 nm, as shown in figure 4.11.
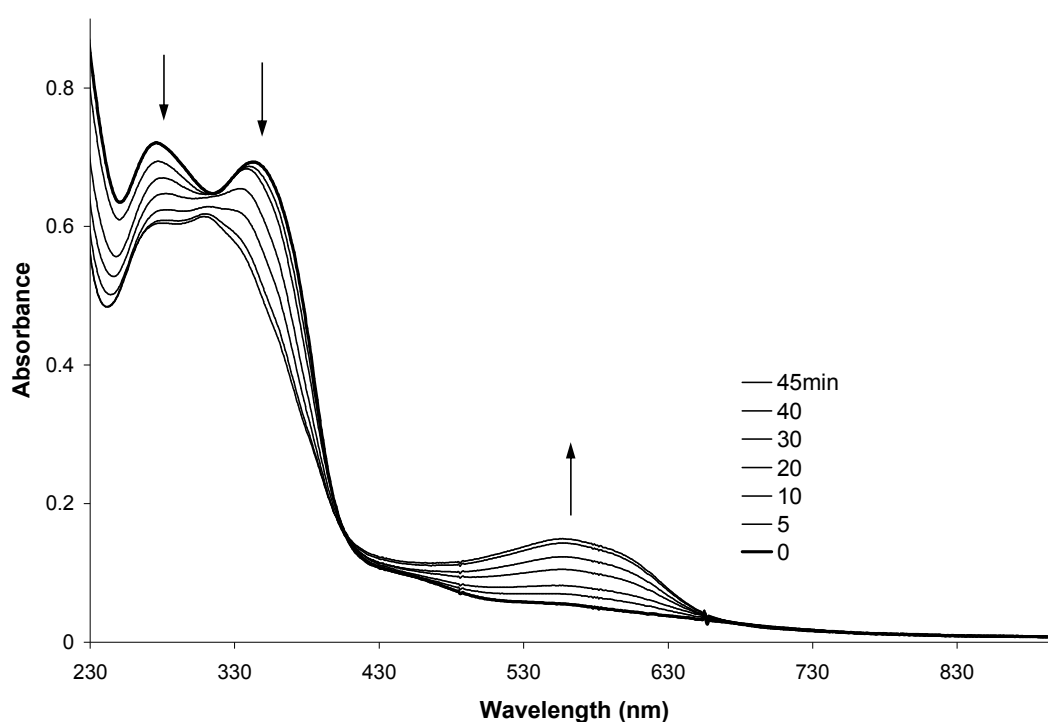
Figure 4.11: UV-vis absorption spectrum of **10H**, in THF, following irradiation at λ = 313 nm for 45 minutes. The spectrum recorded at the start of the experiment (before irradiation) is denoted by the thick black line.

Following irradiation with visible light, the band at 555 nm decreased due to subsequent ring-opening of the switch however, the bands in the UV region did not return to their original absorbance values, as shown in figure 4.12. These experimental results indicate that the $Co_2(CO)_6$ moieties underwent some decomposition during the irradiation processes. Similar results were found following irradiation of **10H** at 365 nm (for 55 minutes), with no sign of reduced degradation of the metal carbonyl complexes due to the use of a lower energy light source.
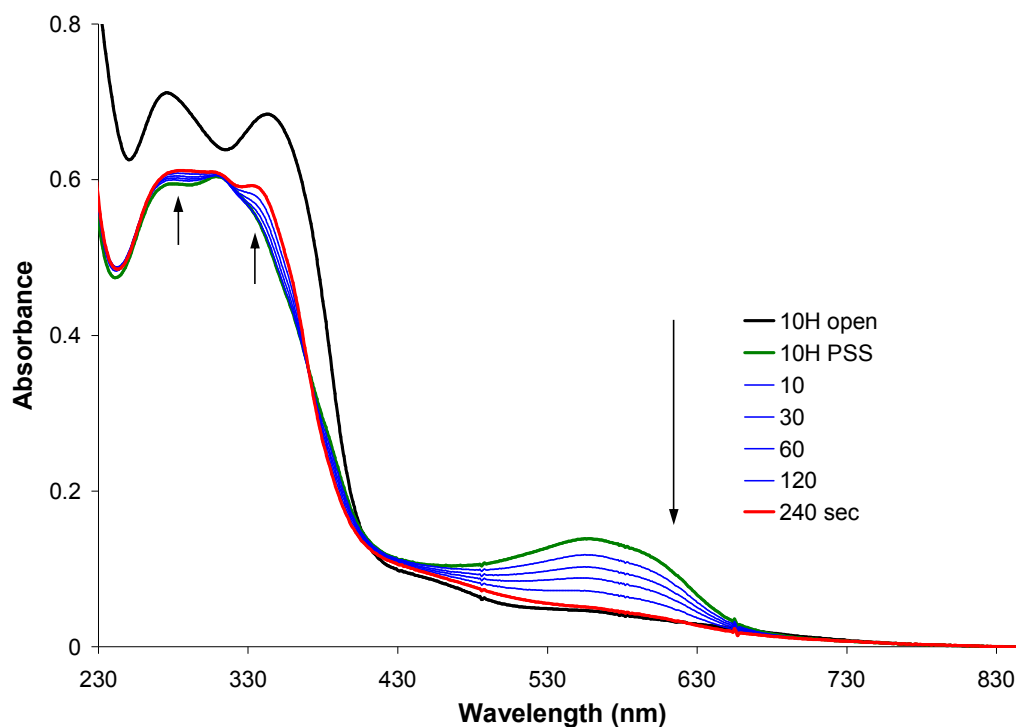
Figure 4.12: UV-vis absorption spectrum of **10H**, in THF (c = 1.4 x 10^{-5} mol/L): before irradiation (black line); at the PSS, following irradiation at λ = 313nm (green line); following irradiation with λ > 550 nm (blue lines); after 240 seconds at λ > 550 nm (red line).

Irradiation of the $Co_2(CO)_4$dppm derivative **12H**, at both 313 nm and 365 nm, was found to induce ring-closing, with a colour change from pale pink to purple and an absorbance band appearing in the visible region, with a λ_{max} at 552 nm. The dppm ligands were incorporated onto the cobalt carbonyl complexes in an attempt to stabilise the photochemical reactivity at the cobalt centre. However, **12H** was also found to undergo photodegradation with a decrease in the bands in the UV region, which did not return following the cycloreversion process. Also noted was a significant increase in the irradiation times required to reach the PSS of the band attributed to ring-closing at 552 nm, due to the presence of the dppm ligands, in comparison to the $Co_2(CO)_6$ analogue **10H** (100 minutes *vs*. 45 minutes respectively, at λ_{irr} = 313 nm). The corresponding free ligand switch, **8H**, reached the PSS after 40 minutes of irradiation.

The absorbance bands recorded in the visible region of the UV-vis spectrum, indicative of the closed-ring forms, at the PSS of the $Co_2(CO)_6$ complex (**10H**) and the $Co_2(CO)_4$dppm complex (**12H**), were found to have similar shapes and λ_{max} values to that of the free ligand (**8H**), as shown in figure 4.13 (λ_{max} = 561, 555 and 552 for **8H**,

10H and **12H** respectively). Also noted from figure 4.13, was that the intensity of the absorbance bands of the cobalt carbonyl complexes, in the visible region, were significantly lower in comparison to that of the free ligand, at the PSS.
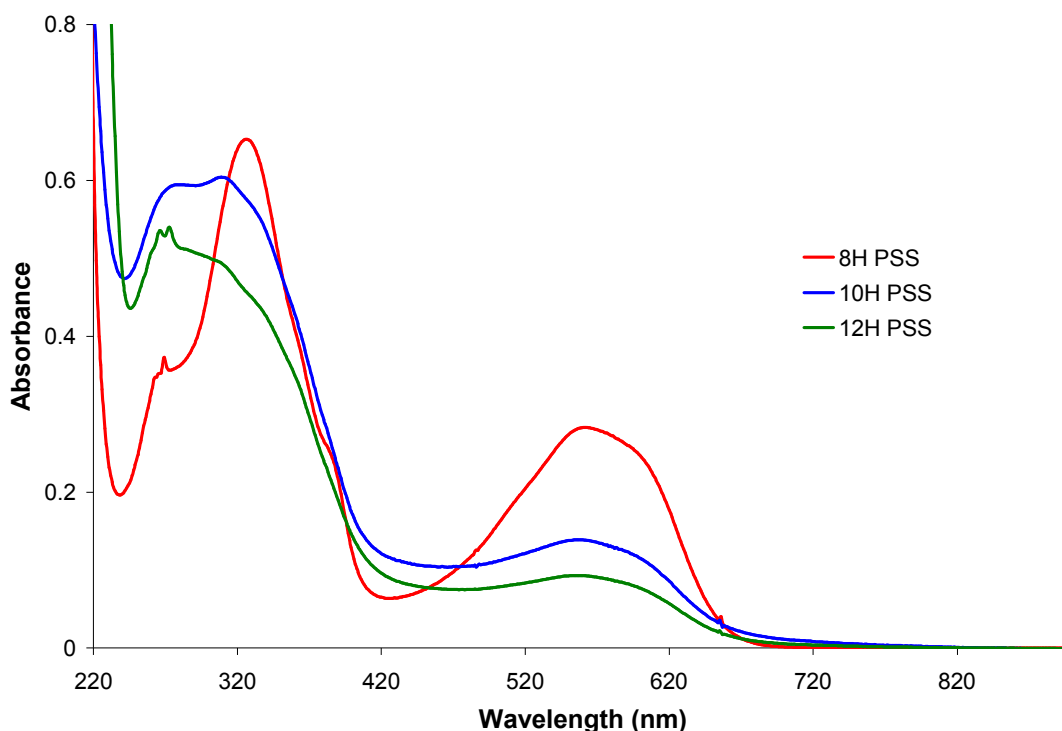
Figure 4.13: UV-vis absorption spectrum of the free ligand **8H** (red line), the corresponding $Co_2(CO)_6$ complex **10H** (blue line) and the $Co_2(CO)_4$dppm complex **12H** (green line), in THF, at the PSS following irradiation at $\lambda = 313$ nm.

Therefore, the results obtained from the irradiation experiments of the cobalt carbonyl complexes, **10H** and **12H**, suggest that cyclisation processes occur for these complexes, although the efficiency of this process was reduced in comparison to that of the free ligand switch **8H**. In addition, there appeared to be some degradation of the metal carbonyl moieties during the photochemical processes. Therefore, at the end of the experiment, it is possible that the solutions of **10H** and **12H** contained both the free ligand switch and the cobalt carbonyl complex switch. These results are in contrast to those observed for the shorter chain $Co_2(CO)_6$ and $Co_2(CO)_4$dppm derivatives (**9H** and **11H** respectively), in which case no cyclisation processes were observed. Thus, it appears that incorporating phenyl rings between the dithienylethene unit and the alkynyl cobalt carbonyl moieties allows for ring-closing to take place.

4.3.8 Photochromic Behaviour of Cobalt Carbonyl Complexes: Perfluoro-Switches

The photochemical properties of the fluorinated switches tethered to cobalt carbonyl units were also studied. Solutions of the $Co_2(CO)_6$ {**9F** and **10F**} and $Co_2(CO)_4$dppm {**11F** and **12F**} complexes, in THF, were irradiated at λ = 313 and 365 nm, and the changes observed in the UV-vis absorption spectra were monitored. The results are summarised in table 4.6 and the structures of these complexes are illustrated in scheme 4.8.

9F: $M_1=Co_2(CO)_6$
11F: $M_1=Co_2(CO)_4$dppm

10F: $M_1=Co_2(CO)_6$
12F: $M_1=Co_2(CO)_4$dppm
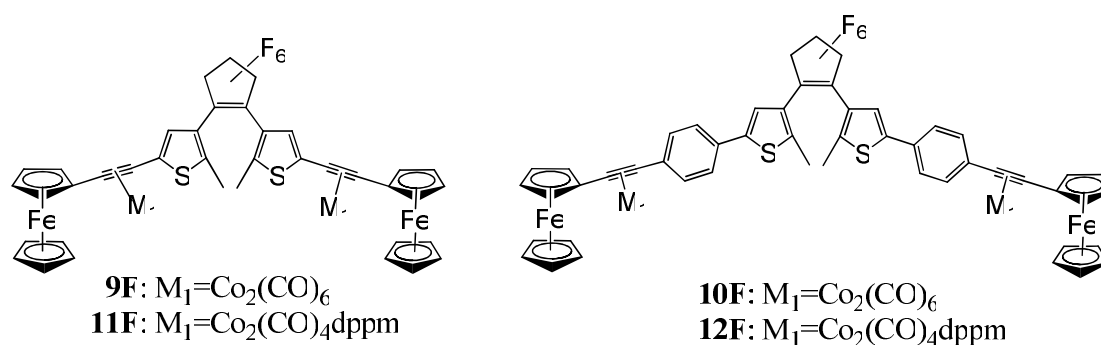
Scheme 4.8: Illustrates the cobalt carbonyl complexes of the perhydro-switches (**9H**, **10H**, **11H**, **12H**).

Table 4.6: UV-vis absorption data of the $Co_2(CO)_6$ {**9F** and **10F**} and $Co_2(CO)_4$dppm complexes (**11F** and **12F**), in THF, in their open-ring forms and following irradiation at 313 nm and 365 nm.

Cobalt Carbonyl Complexes	Absorption Spectra in THF		
	Open-ring isomers	313 nm Irradiation[a]	365 nm Irradiation[a]
	λ_{abs} (nm)	λ_{abs} (nm)	λ_{abs} (nm)
9F	270, 327, 438, 555	270(↓), 327(↓), 438 (↑), {379}*	270(↓), 327(↓), 438 (↑), {379}*
11F	270, 291, 355, 555	270(↓), 291(↓), 355(↓), 555(↓), {415}*	270(↓), 291(↓), 355(↓), 555(↓), {415}*
10F	276, 340, 445, 555	276(↓), 340(↓), 621(↑), {377}*	276(↓), 340(↓), 626(↑), {377}*
12F	264, 286, 334, 490	264(↓), 286(↓), 334(↓), 609(↑), {430}*	264(↓), 286(↓), 334(↓), 626(↑), {426}*

[a] Decreasing absorbance (↓); Increasing absorbance (↑)
*{isosbestic points}

- **Irradiation of 9F and 11F**

Irradiation of **9F**, at λ = 313 nm, resulted in a decrease in the bands in the UV region of the absorbance spectrum, at 270 and 327 nm, with a very small increase in the absorbance at 438 nm, and an isosbestic point at 379 nm (figure 4.14). However, even after 30 minutes of irradiation, there was no evidence for photocyclisation of **9F**, to the closed-ring isomer, in the visible region. The same result was found for the corresponding $Co_2(CO)_4$dppm complex **11F**. Irradiation of **9F** and **11F** at a lower energy wavelength (365 nm) also resulted in a decrease in the bands in the UV region, with no new band appearing in the visible region. Hence, it can be concluded that the presence of the $Co_2(CO)_6$ and $Co_2(CO)_4$dppm complexes inhibited the cyclisation process of this perfluoro-switch. The decrease in the UV region of the spectra suggests that some degradation of the complexes occurred. This result corresponds to the results obtained for the corresponding perhydro-derivatives **9H** and **11H**, as discussed in the previous section.
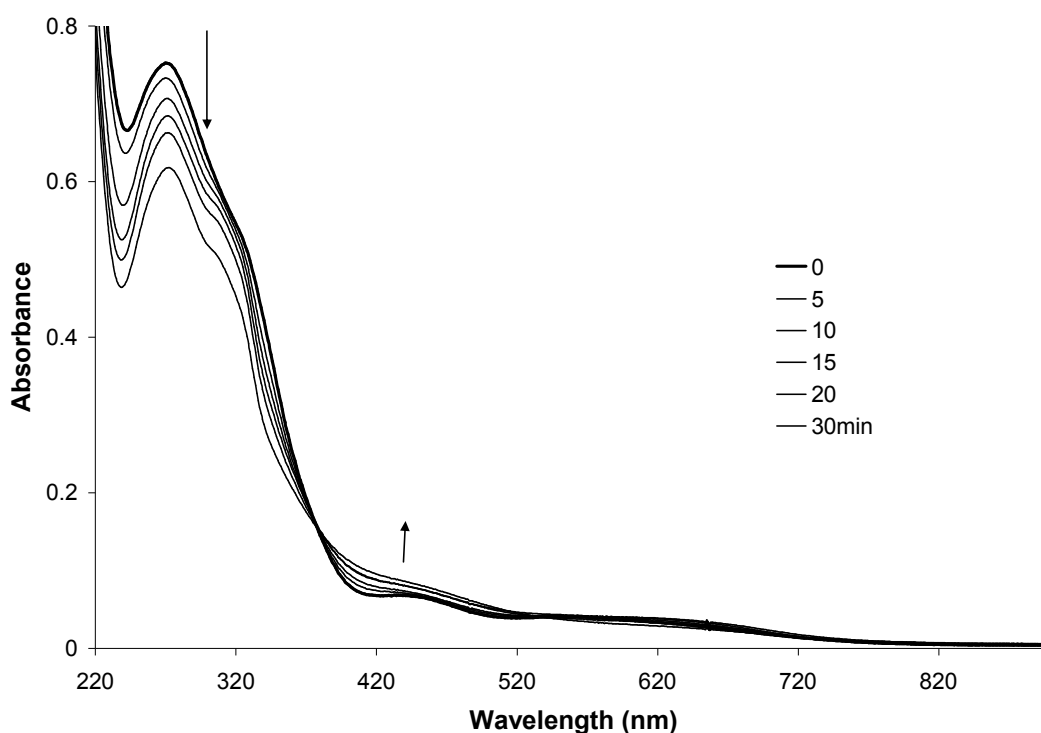
Figure 4.14: UV-vis absorption spectrum of **9F**, in THF, following irradiation at λ = 313 nm for 30 minutes. The spectrum recorded at the start of the experiment (before irradiation) is denoted by the thick black line.

- **Irradiation of 10F and 12F**

In contrast to the results observed for **9F**, the more conjugated analogue **10F** was found to undergo photocyclisation to the closed form following UV irradiation (λ = 313 nm). The absorbance bands in the UV region, at 276 and 340 nm, began to decrease, with an isosbestic point observed at 377 nm, and a new band appeared in the visible region (λ_{max} at 621 nm, figure 4.15). The photostationary state was reached after 16 minutes of irradiation, and a colour change from yellow/brown to blue/green was observed, indicative of the formation of the ring-closed isomer.
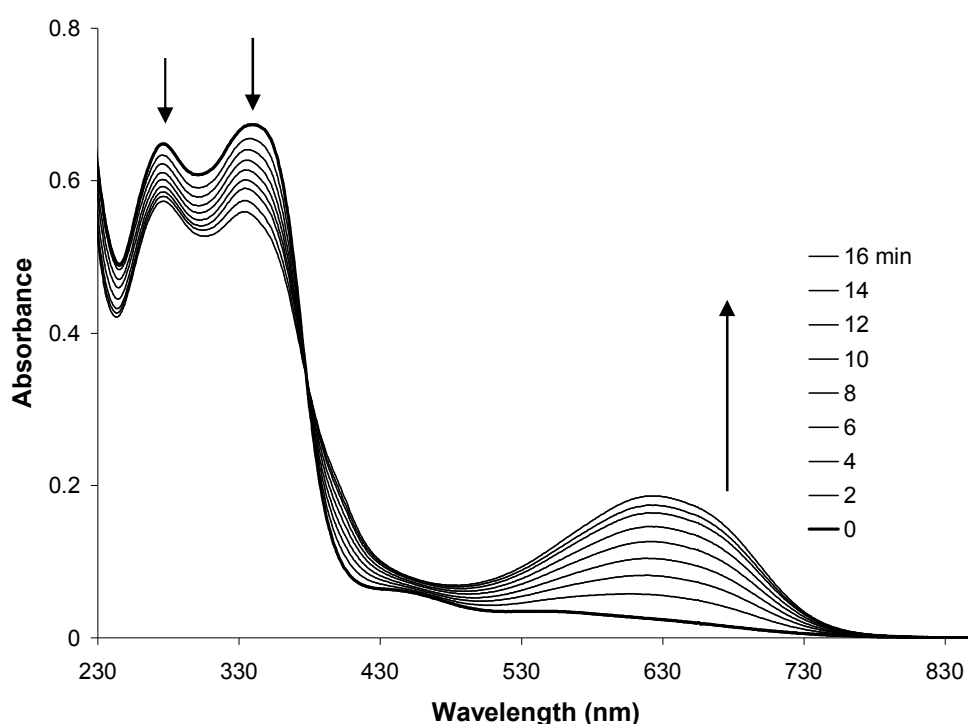
Figure 4.15: UV-vis absorption spectrum of **10F**, in THF, following irradiation at λ = 313 nm for 16 minutes. The spectrum recorded at the start of the experiment (before irradiation) is denoted by the thick black line.

Irradiation of **10F** at a lower energy (λ = 365 nm), also resulted in cyclisation to the ring-closed form. However, there were a few noticeable differences in the absorbance spectra recorded, in comparison to the changes observed following irradiation at 313 nm. Firstly, the intensity of the absorbance band in the visible region at the PSS was higher following irradiation at 365 nm, and the λ_{max} was red-shifted from 621 to 626 nm, in comparison to the results obtained at 313 nm. However, the PSS was reached only after 28 minutes of irradiation at 365 nm, almost twice the amount of time taken at 313 nm (16 minutes). Secondly, during irradiation at 365 nm, the intraligand band

at 340 nm decreased to a greater extent than the ligand-field band at 276 nm, as shown in figure 4.16, whereas both bands decreased to almost the same extent at 313 nm. These differences can be attributed to an increased amount of the closed-ring product formed following irradiation at 365 nm.
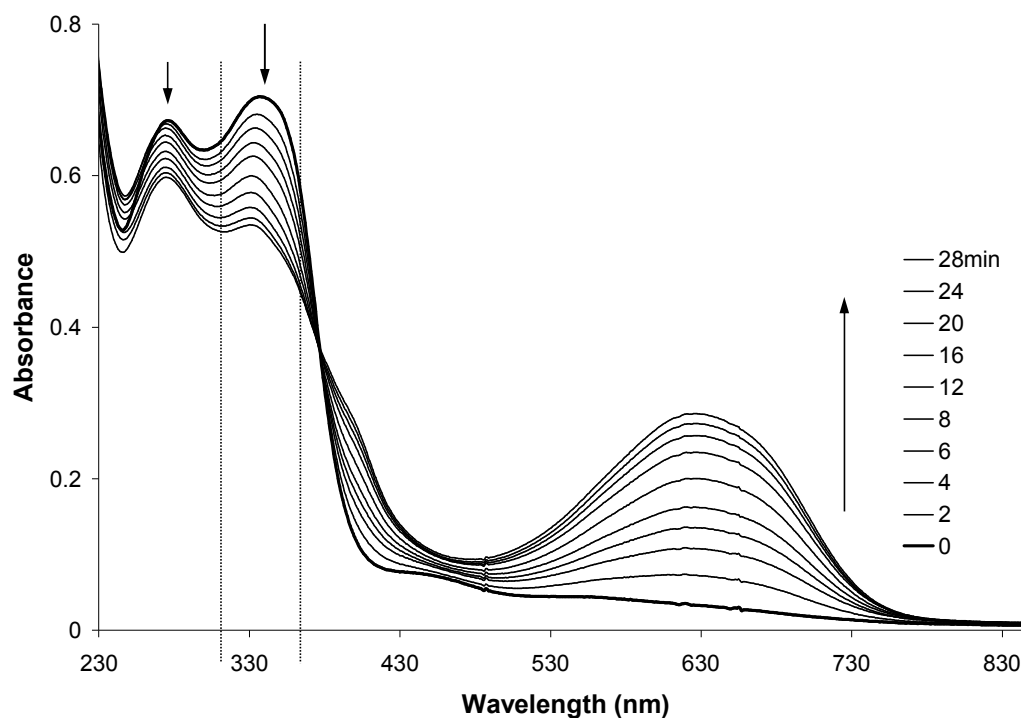
Figure 4.16: UV-vis absorption spectrum of **10F**, in THF, following irradiation at $\lambda = 365$ nm for 28 minutes. Also, two dotted lines intersecting the absorbance spectrum at 313 and 365 nm. The spectrum recorded at the start of the experiment (before irradiation) is denoted by the thick black line.

Following irradiation at 313 and 365 nm, subsequent cycloreversion processes were induced following irradiation with visible light at $\lambda > 550$ nm for 6 minutes, and the bands in the visible region of the UV-vis spectra were found to decrease accordingly. Interestingly, the bands in the UV region were also found to return towards their original absorbance values. The ligand-field band at 276 nm increased, but did not fully return to the initial value recorded, indicating loss of the $Co_2(CO)_6$ moieties during photolysis. The intra-ligand band at 340 nm also increased, but, was blue-shifted slightly to 331 nm, which is indicative of the λ_{max} of the open form of the free ligand (**8F**). This result suggests that photolysis of **10F** at 313 and 365 nm, resulted in some cleavage of the $Co_2(CO)_6$ moieties, hence giving rise to some of the free ligand. This process seemed to occur more readily following irradiation at 365 nm, as the

intraligand band at 340 nm increased to higher absorbance than that originally recorded, as illustrated in figure 4.17.
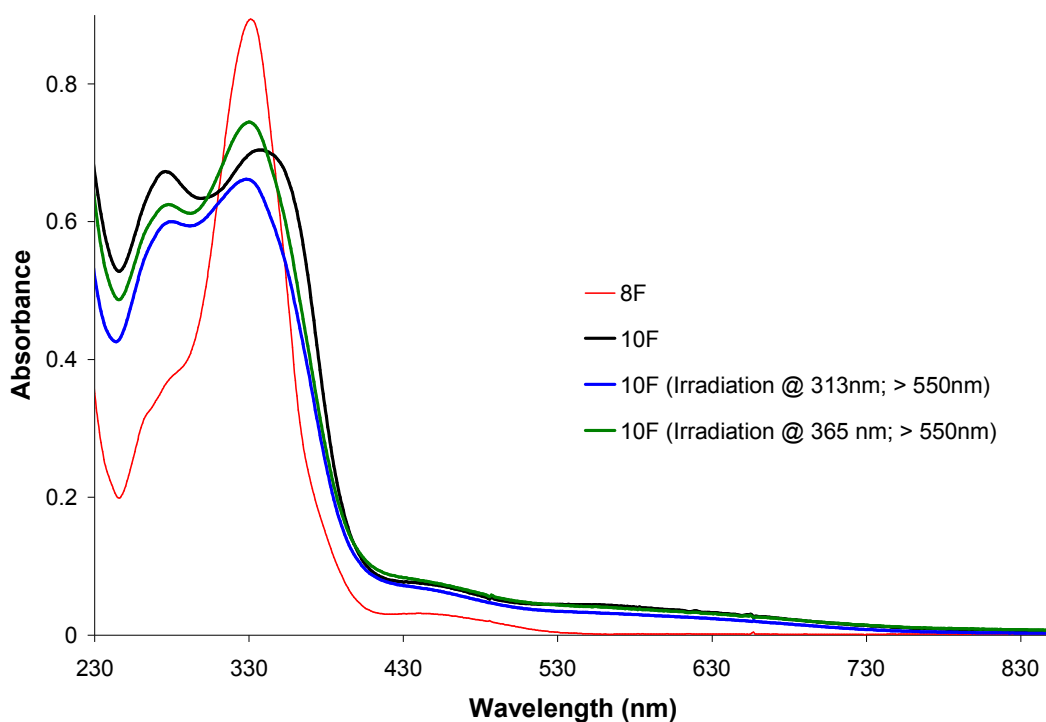
Figure 4.17: UV-vis absorption spectra, in THF, of: the free ligand **8F** (red line); the $Co_2(CO)_6$ complex **10F** (black line); **10F** following ring-closing at 313 nm and subsequent ring-opening at > 550 nm (blue line); **10F** following ring-closing at 365 nm and subsequent ring-opening at > 550 nm (green line).

Incorporating dppm ligands onto the $Co_2(CO)_6$ complexes of **10F**, forming the corresponding $Co_2(CO)_4$dppm complex **12F**, resulted in significant changes to the photochromic properties of the switch. Irradiation of **12F** at $\lambda = 313$ nm did induce cyclisation, with the appearance of a new band in the visible region of the spectrum ($\lambda_{max} = 609$ nm), but the amount of the closed-ring formed was considerably reduced in comparison to **10F**. Irradiation of **12F** at $\lambda = 365$ nm improved the yield of the ring-closed isomer, as evidenced by the intensity of the band in the visible region of the spectrum ($\lambda_{max} = 626$ nm). However, in comparison to the cyclisation process for **10F** ($Co_2(CO)_6$ analogue) the amount of the closed-ring formed remained less, as illustrated in figure 4.18. It should be noted that the presence of the dppm ligands also increased the irradiation times required to reach the photostationary state (20 minutes at 313 nm and 45 minutes at 365 nm).

Subsequent irradiation of **12F** with visible light resulted in a decrease in the band in the visible region as expected, however the bands in the UV region did not return to

their original absorbance values. In fact only a very small increase in the absorbance of the intraligand band at 334 nm was observed, and the band at 286 nm did not change during the ring-opening process. This result suggests that the $Co_2(CO)_4$dppm moieties underwent some photochemical degradation.

The $Co_2(CO)_6$ complex of the closed-ring isomer of **8F** was made (i.e. **10bF** as shown in scheme 4.9) in an attempt to elucidate whether or not the ring-closed products of **10F** and **12F** were that of the cobalt carbonyl complexes, or due to the cyclisation of the free ligand **8F** following photolytic cleavage of the metal carbonyl moieties.
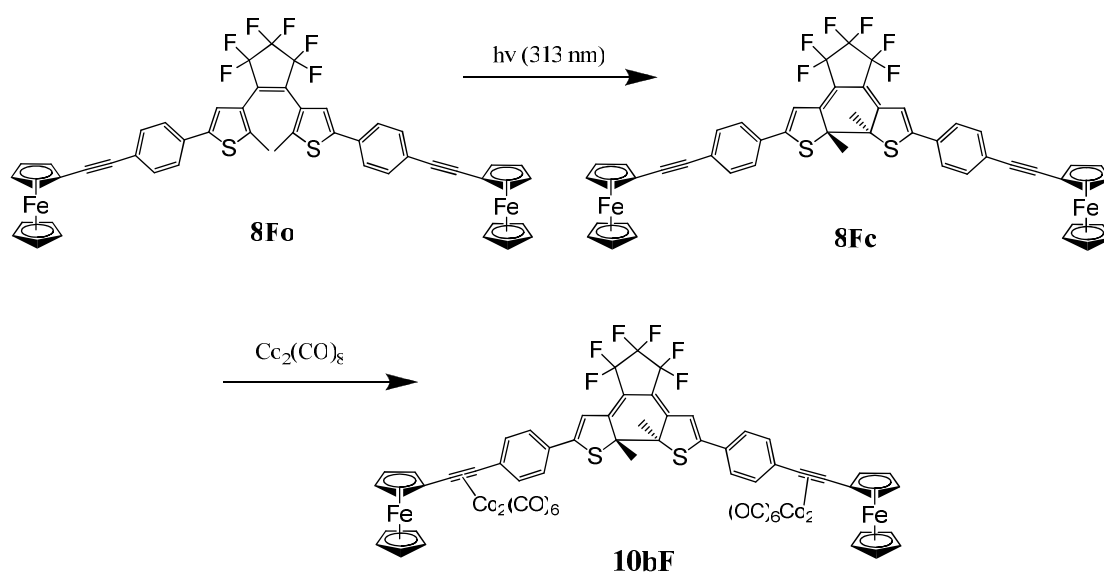
Scheme 4.9: Illustrates the formation of the ring-closed $Co_2(CO)_6$ complex **10bF**.

The UV-vis absorption spectrum of **10bF**, in THF, shows a broad absorption band in the visible region, with a λ_{max} at 631 nm. Figure 4.18 displays the absorption spectrum of **10bF** (black line), overlaid with the closed-ring isomer of the free ligand **8Fc** (red line), and the $Co_2(CO)_6$ and $Co_2(CO)_4$dppm complexes {**10F** and **12F** respectively}, following irradiation at both 365 and 313 nm. The λ_{max} of the absorbance bands in the visible region are presented in table 4.7 below. Although this spectrum does not unambiguously prove that the cobalt complexed switch cyclises, it does show that the absorbance bands of **10F** and **12F**, in the visible region have more of a resemblance to **10bF**, then the free ligand **8Fc**. Thus, this suggests that the cobalt carbonyl complexes cyclise with the metal carbonyls attached, albeit possibly with some cleavage of the cobalt carbonyl moieties, and at the end of the experiment the

solution contains a mixture of the cobalt carbonyl complexes and the free ligand. Furthermore, the UV-vis spectra highlight the reduction in the amount of the closed-ring isomer formed when irradiated at 313 nm, instead of 365 nm, and when dppm ligands are incorporated onto the switch.
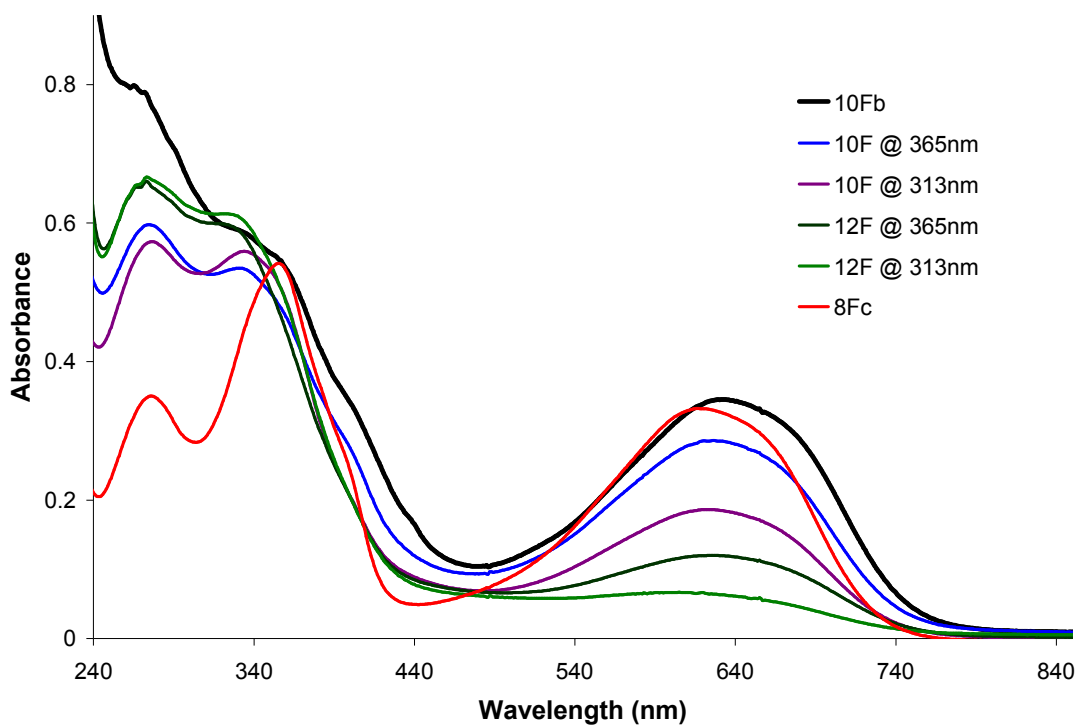
Figure 4.18: UV-vis absorption spectra, in THF, of: the closed-ring isomer of the free ligand **8Fc** (red line); the closed-ring isomer of the $Co_2(CO)_6$ complex **10bF** (black line); the $Co_2(CO)_6$ complex **10F** following irradiation at 365 nm (blue line) and 313 nm (purple line); and the $Co_2(CO)_4$dppm complex **12F** following irradiation at 365 nm (dark green line) and 313 nm (light green line).

Table 4.7: UV-vis absorption data of the λ_{max} the closed-isomer **8Fc**, and the $Co_2(CO)_6$ derivative, **10bF**, in THF. Also, the λ_{max} of the open-ring $Co_2(CO)_6$ {**10F**} and $Co_2(CO)_4$dppm {**12F**} complexes, following irradiation processes.

Cmpd	λ_{max} [nm]	Cmpd	λ_{max} [nm] (313 nm)[*]	λ_{max} [nm] (365 nm)[*]
8Fc	621	**10F**	621	626
10bF	631	**12F**	609	626

* indicates the wavelength at which the solution was irradiated

4.3.9 Steady-State Photolysis: Infra-Red Spectra

In order to examine the effects of irradiation processes on the $Co_2(CO)_6$ complexes, a solution of **10F**, in THF, was prepared in an IR liquid cell and the changes in the carbonyl bands were monitored in the infra-red spectrum following irradiation at 313 nm and 365 nm.   These experiments were also carried out in the presence of a trapping ligand, PPh_3, to trap any photodecarbonylation products.   The resulting photoproducts were assigned according the results reported previously in the literature.[20-23]
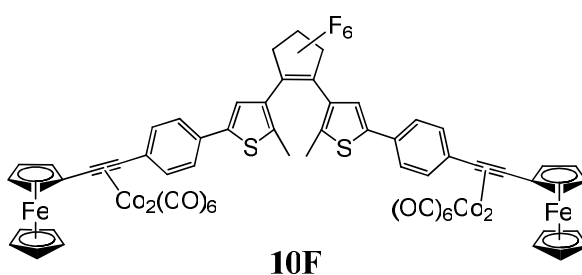
Figure 4.19: Illustrates the structure of the $Co_2(CO)_6$ complex **10F**.

Irradiation of **10F**, in THF, at 313 and 365 nm resulted in a decrease in the cobalt carbonyl bands at 2086, 2049 and 2022 cm^{-1} in the IR spectrum, with no new bands growing-in after 20 minutes of irradiation.   This result indicates that the $Co_2(CO)_6$ moieties undergo some decomposition.   In an attempt to "trap" intermediates in this photodecarbonylation process, an excess of triphenylphosphine (PPh_3) was added to the solution of **10F**.

When **10F** was photolysed at 365 nm for 5 minutes, the parent bands at 2086, 2049 and 2022 cm^{-1} began to decrease, with new bands appearing at 2057, 2006 and 1994 cm^{-1}.   This result indicates CO loss, followed by substitution of PPh_3, thus generating the corresponding pentacarbonyl species, $(Switch)Co_2(CO)_5PPh_3$ for **10F**.[20-22]   After 20 minutes of irradiation, bleaching of the parent bands continued, whilst the bands associated with the pentacarbonyl species continued to increase.   However, new bands appeared at 1982 and 1957 cm^{-1}, indicative of the formation of the tetracarbonyl species $(Switch)Co_2(CO)_4(PPh_3)_2$,[20-22] as shown in figure 4.20.
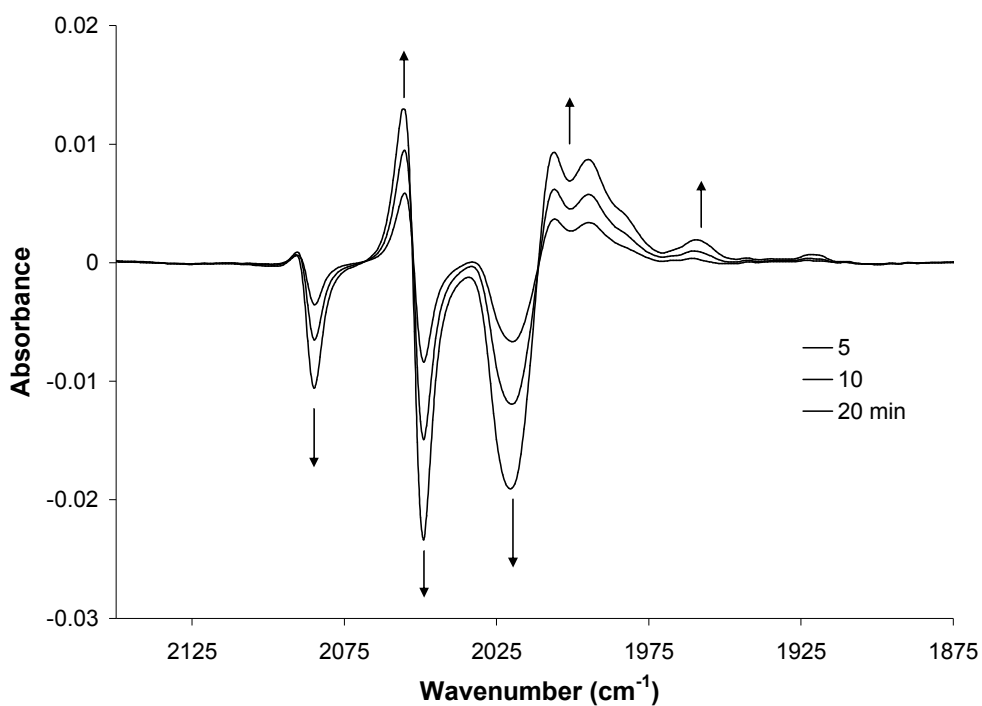
Figure 4.20: The IR difference spectra of the $Co_2(CO)_6$ complex **10F**, in THF, following irradiation at 365 nm for 20 minutes, in the presence of excess PPh_3. Negative bands indicate bleaching of the parent bands and the positive bands indicate formation of the PPh_3 substituted species.
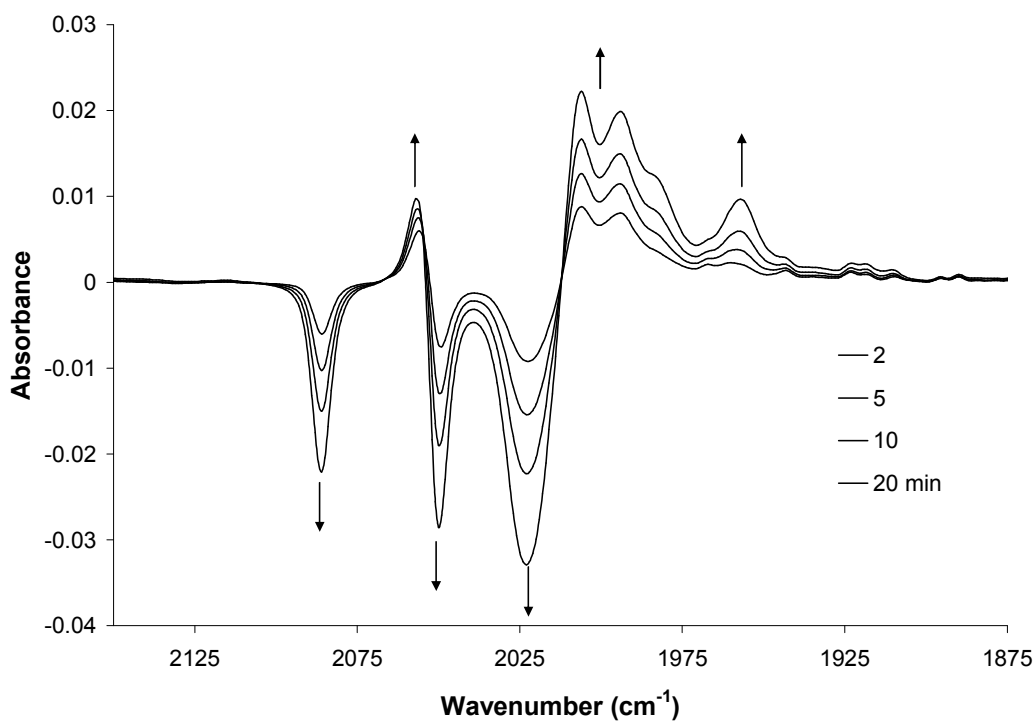
Figure 4.21: The IR difference spectra of the $Co_2(CO)_6$ complex **10F**, in THF, following irradiation at 313 nm for 20 minutes, in the presence of excess PPh_3. Negative bands indicate bleaching of the parent bands and the positive bands indicate formation of the substituted species.

Irradiation of **10F**, at 313 nm, also resulted in the loss of CO from the metal complex, followed by substitution with the PPh$_3$ ligands, as shown in figure 4.21. After 5 minutes of irradiation, the parent bands began to decrease and new bands appeared, which indicated the formation of the pentacarbonyl species (2057, 2006 and 1994cm^{-1}) and tetracarbonyl species (2082 and 1957 cm^{-1}) of **10F**. After another 15 minutes of irradiation, these bands continued to grow-in, as the parent bands continued to decrease. The IR spectra show that CO loss occurs more rapidly following irradiation at 313 nm, than at 365 nm.

4.3.10 Cycloreversion of the Closed-ring Co$_2$(CO)$_6$ Complex 10bF

Co$_2$(CO)$_6$ complexes were incorporated onto the closed-ring isomer of **8F**, producing the corresponding complex **10bF**, as illustrated in figure 4.22. The original purpose of synthesising this complex was to help in elucidating the photochemical results obtained for the cobalt carbonyl complexes discussed previously in section 4.3.8. However, the cycloreversion process was also investigated in order to determine the effects of the cobalt carbonyl units on this process, and on the other hand, the effects of visible light irradiation on the Co$_2$(CO)$_6$ moieties. The results are described here.
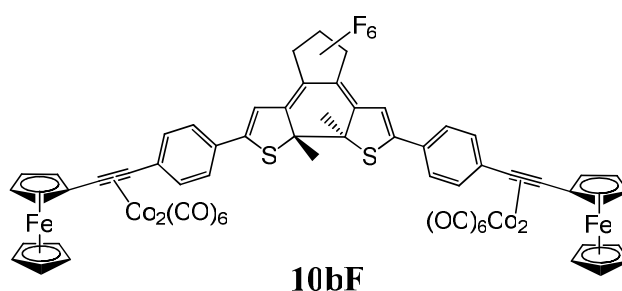
Figure 4.22: Illustrates the structure of the closed-ring Co$_2$(CO)$_6$ complex **10bF**.
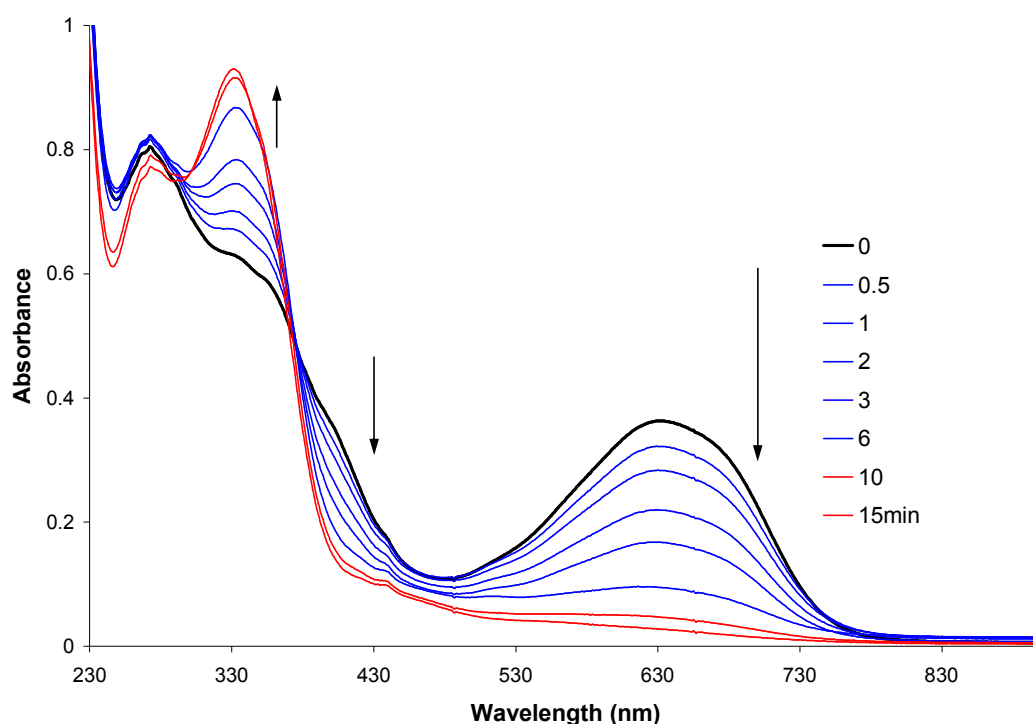
Figure 4.23: UV-vis absorption spectrum of the closed-ring isomer of the Co$_2$(CO)$_6$ complex **10bF** (black line), in THF, following irradiation at $\lambda > 650$ nm for 6 minutes (blue lines), and for 10 and 15 minutes (red lines).

The UV-vis absorption spectrum of **10bF**, in THF, displayed bands at 274, 337 and a shoulder at 357 nm in the UV region, and a broad absorption band in the visible region (λ_{max} at 631 nm). Irradiation with visible light at $\lambda > 650$ nm, for 6 minutes, resulted in a colour change from blue to colourless, along with a decrease in the absorption band in the visible region. In the UV region, the intraligand band at 375 nm increased, and an isosbestic point was observed at 375 nm. This result indicates that the closed-ring isomer underwent cycloreversion back to the open form. Longer irradiation times (after 10 and 15 minutes) resulted in a further decrease in the band at 631 nm. However, the intraligand band at 337 nm continued to increase and was slightly blue-shifted to 332 nm, the band at 274 nm began to decrease marginally, and a clean isosbestic point was no longer observed, as shown in figure 4.23. In comparison to the absorption spectrum of the open-ring isomer **10F**, this intraligand band had increased in absorption and was similar to the λ_{max} of the free ligand **8F**, as illustrated in figure 4.24. This indicates that irradiation at $\lambda > 650$ nm resulted in some cleavage of the $Co_2(CO)_6$ moieties from **10bF**, resulting in formation of some of the free ligand **8F**. Therefore, the solution of **10bF** at the end of the experiment (i.e. after 15 minutes at $\lambda_{irr} > 650$ nm) most likely contained a mixture of the open-ring $Co_2(CO)_6$ complex (**10F**) and the free ligand (**8F**).
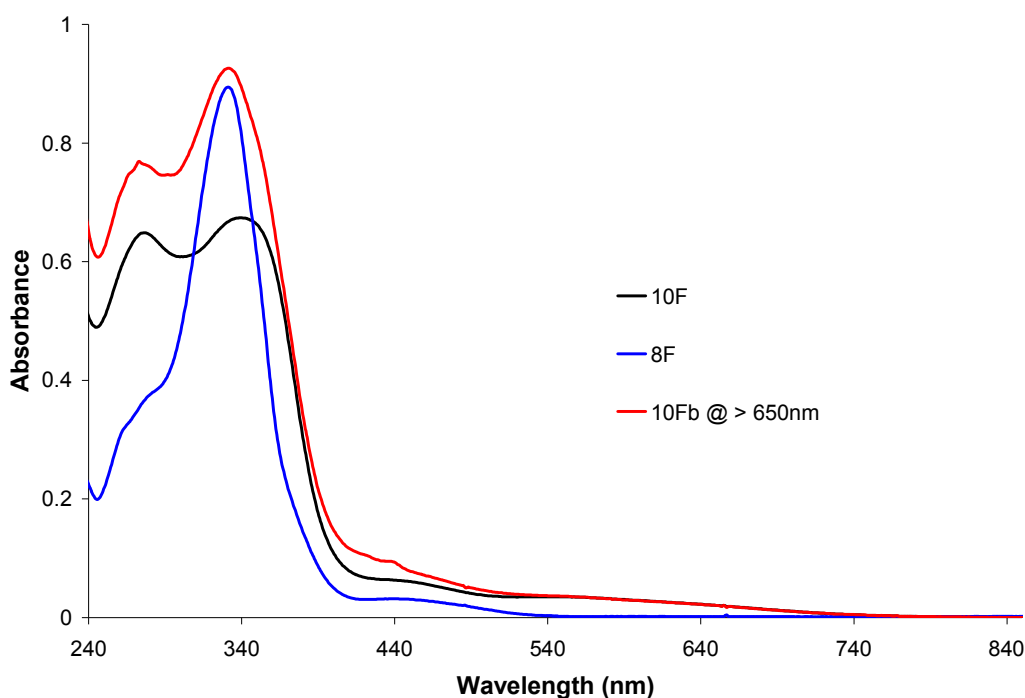
Figure 4.24: UV-vis absorption spectra, in THF, of: the closed-ring isomer of the $Co_2(CO)_6$ complex **10bF**, following irradiation at $\lambda > 650$ nm (red line); the open-ring isomer of the $Co_2(CO)_6$ complex **10F (**black line); and the open-ring isomer of the free ligand **8F** (blue line).

4.4 Conclusion

Ethynylferrocene and phenyl-ethynylferrocene moieties were substituted onto dithienyl-perhydro- and perfluoro-cyclopentene switches, generating switches **7H**, **7F**, **8H** and **8F**. Their photochromic, fatigue resistance, thermal stability and fluorescent properties were investigated, using absorption/emission and ^{1}H NMR spectroscopy as spectroscopic tools. The effects of the atoms located on the central cyclopentene ring, and the substituents attached to the switching unit, on these properties were determined.

The absorption spectra recorded for compounds **7H/F** and **8H/F**, following photocyclisation from the open-ring to the closed-ring isomers, showed that the λ_{max} of the absorbance bands were shifted further towards the red for the perfluorinated switches, in comparison to their perhydro-derivatives. An extension of the π-conjugation of the compounds, through the introduction of a phenyl ring between the ethynylferrocene moiety and the switching unit, resulted in a bathochromic shift of the λ_{max} of the absorbance band in the visible region for compound **8H**, relative to **7H**. Conversely, the opposite effect was observed for the perfluoro-derivatives, with the λ_{max} of the closed-form of **7F** appearing at the longest wavelength for the four switches, at 641 nm. Also noted was the time taken for each switch to reach the photostationary state following UV irradiation, with **7H**, **7F**, **8H** and **8F** taking 35, 30, 40 and 8 minutes respectively. In the case of the perhydro switches, it appears that the cyclisation process is marginally more efficient for the less conjugated switch **7H**, in comparison to **8H**, under the conditions used here. The presence of the fluorine atoms, on the central switching unit, seems to increase the efficiency of this process. However, once again, the opposite trend was found for the perfluoro-derivatives, with the cyclisation process of the more conjugated switch **8F** proving to be considerably more efficient then the other three switches. These results highlight how the substituents attached to the switching unit, together with the atoms present on the cyclopentene ring, strongly influence the cyclisation process, and the absorption spectra, of such switches.

The cycloreversion processes were found to be more efficient than the cyclisation processes for compounds **7F**, **8H** and **8F**, with the ring-open isomers reforming after

7, 7 and 3 minutes of irradiation with visible light, respectively. However, only **8F** was found to undergo a complete cycloreversion process, whereas **7F** and **8H** did not return fully to the original spectra recorded. In the case of **7H**, the cycloreversion process was considerably slower than the other three switches, and only after 4.5 hours of visible light irradiation were no more changes observed in the spectrum. At this point, ~20% of the absorbance at 548 nm was still remaining, therefore the cyclisation process of **7H** was found to be somewhat irreversible.

The fatigue resistance experiments determined that the photostability of these switches were found to decrease in the order: **8F** > **8H** > **7F** > **7H**. This result emphasises the stabilising effect of the fluorine atoms and, to a greater extent, the increased π-conjugation character, on the cyclisation/cycloreversion processes.

The ^{1}H NMR studies of the cyclisation processes of the ferrocenyl-based switches concluded that UV irradiation of **7F** and **7H** resulted in the formation of a photostable by-product in each case (**7Fx** and **7Hx**), whereas an estimated value of > 95% conversion from the open to the closed-ring isomer, with no evidence of by-product formation, was observed for **8H** and **8F**. These results clarify the poor fatigue resistance, and incomplete cycloreversion processes, described for **7F** and **7H**.

The thermal stability of the ferrocenyl-based switches was found to increase in the order: **8H** < **7H** < **8F** < **7F**. The half-lives calculated for the perfluorinated switches, **7F** and **8F** (at 60, 80 and 100°C), were very similar to each other, and the same was found for the perhydro-derivatives **7H** and **8H**. However, in both cases, the less conjugated switches, **7F** and **7H**, were found to be moderately more stable than their corresponding derivatives, **8F** and **8H**. On the other hand, the perfluorinated switches were found to be considerably more stable then their perhydro counterparts. Hence, the main influencing factor on the thermal stability of these switches was established to be the atoms located on the central cyclopentene ring i.e. F *vs.* H. However, it should be noted that a mixture of cycloreversion, in-conjunction with decomposition, was observed for these compounds when heated at elevated temperatures, but all four switches were found to be stable in the dark at room temperature.

Overall, it can be concluded that the photochromic, fatigue resistance and thermal stability properties were improved by extending the π-conjugation of the compounds, and substituting the cyclopentene ring with fluorine instead of hydrogen atoms. Thus, among the four ferrocenyl-based switches described here, **8F** was found to be the most

promising switch in terms of its potential for use in future applications. However, one of the main requirements of switching compounds is a fast response time. The fact that the photostationary state of the closed-ring isomer of **8F** was only reached after 8 minutes of UV irradiation, indicates that the response time on the molecular level may be too slow for a number of applications. Also, **8F** was deemed to be non-fluorescent at room temperature, therefore, other avenues would need to be explored in order to find an alternative non-destructive read-out method for **8F** to have potential use in memory media applications.

Incorporating cobalt carbonyl moieties onto **7H/F** and **8H/F** dramatically affected the photochromic behaviour of the switches. The presence of the $Co_2(CO)_6$ and $Co_2(CO)_4dppm$ moieties on the less-conjugated switches **9H/F** and **11H/F** inhibited photocyclisation of the switching units and decomposition of the cobalt carbonyl moieties was evident following UV irradiation. On the other hand, photocyclisation to the closed-ring isomers was observed for the more conjugated $Co_2(CO)_6$ derivatives **10H/F**, but was also accompanied by photochemical cleavage of the cobalt carbonyl units to some extent. Therefore, the ring-closed product formed at the photostationary state is believed to be a mixture of the closed-ring cobalt carbonyl complexes and that of the free ligand switch, in each case. Introducing dppm ligands onto the metal carbonyl units, producing the corresponding $Co_2(CO)_4dppm$ complexes **12H/F**, reduced the reversibility of the cyclisation process, with a decrease in the amount of the closed-ring formed, as evidenced by the relative intensities of the absorbance bands recorded at the PSS in the UV-vis spectra. Irradiation at 365 nm increased the amount of the closed-ring formed for the fluorinated derivatives, but not in the case of the perhydro switches. The results obtained indicated that the fluorinated complexes generated more of the ring-closed isomer, with an increase in the reversibility of the colouring/bleaching cycle, in comparison to the perhydro analogues. Investigations into the effects of irradiation at 313 and 365 nm on the $Co_2(CO)_6$ moieties were performed on **10F**, and the IR results obtained, in the presence of PPh_3, indicated that CO loss occurs under these conditions.

Table 4.8: Irradiation times required for the free switches (**7H/F** and **8H/F**), and their corresponding $Co_2(CO)_6$ (**9H/F** and **10H/F**) and $Co_2(CO)_4$dppm complexes (**11H/F** and **12H/F**), to reach the photostationary state (PSS), following irradiation at 313 nm and 365 nm in THF.

Time to reach PPS of closed-ring isomer after irradiation							
Free Switches		$Co_2(CO)_6$ Complexes			$Co_2(CO)_4$dppm Complexes		
	Time at λ=313nm		Time at λ=313nm	Time at λ=365nm		Time at λ=313nm	Time at λ=365nm
7H	35 min	**9H**	-	-	**11H**	-	-
7F	30 min	**9F**	-	-	**11F**	-	-
8H	40 min	**10H**	45 min	55 min	**12H**	100 min	130 min
8F	8 min	**10F**	16 min	28 min	**12F**	20 min	45 min

(-) indicates no cyclisation occurred.

In comparison to the free ligand switches **8H/F**, incorporating $Co_2(CO)_6$ {**10H/F**} and $Co_2(CO)_4$dppm groups {**12H/F**} onto the switch was found to bathochromically shift the λ_{max} of the absorbance band in the visible region, following photocyclisation processes. However, the efficiency of the ring-closing process for the cobalt carbonyl complexes was found to be reduced, with longer irradiation times required to reach the PSS (table 4.8). Furthermore, lower intensity absorbance bands were observed in the visible region at the PSS of the cobalt carbonyl complexes, relative to the free ligand switches, indicating a decrease in the amount of the closed-ring formed. The most problematic aspect is the photochemical decomposition reactions of the metal carbonyl groups. As mentioned previously, fatigue resistance properties are very important for such switching molecules in terms of their potential use in applications. Therefore, the irreversible nature of the photochemical processes of the cobalt carbonyl complexes described here is not ideal. However, the results have shown that the presence of the phenyl rings in **10H/F** and **12H/F**, acting as spacer groups between the switching unit and the alkynyl cobalt carbonyl moieties, allows cyclisation processes to occur. Furthermore, the presence of the fluorine atoms on the central cyclopentene unit influenced the cyclisation process, with more ring-closing occurring for the cobalt tethered complexes, and a more reversible cycloreversion process was observed, in comparison to the perhydro-derivatives. This highlights the ability to tune the properties of such cobalt carbonyl complexes by altering the substituents attached to the dithienylethene units. With further investigations into such complexes,

there is the potential to improve the photochromic properties to produce more "idealistic" switches towards the development of memory media devices.

On the other hand, the photochemical behaviour of the cobalt carbonyl moieties can be utilised towards the development of carbon monoxide releasing molecules (CORM's). The closed-ring isomer of the $Co_2(CO)_6$ complex **10F** was synthesised, forming **10bF**. The photocycloreversion process of **10bF** was examined following irradiation with visible light ($\lambda > 650$ nm). **10bF** was found to undergo ring-opening under these conditions however, the UV-vis results showed evidence for cleavage of the cobalt units. Although the photochemical behaviour of the $Co_2(CO)_6$ switch was not extensively investigated, there is potential for **10bF**, or a similar compound, to be applied towards the development of CORM's as a therapeutic agent.[24-26]

4.5 Bibliography

(1) Fery-Forgues, S.; Delavaux-Nicot, B. Ferrocene and Ferrocenyl Derivatives in Luminescent Systems. *J. Photochem. Photobiol. A.* **2000**, *132*, 137-159.

(2) Herkstroeter, W. G. Triplet Energies of Azulene, Beta-Carotene, and Ferrocene. *J. Am. Chem. Soc.* **1975**, *97*, 4161-4167.

(3) Martinez, R.; Ratera, I.; Tarraga, A.; Molina, P.; Veciana, J. A Simple and Robust Reversible Redox-Fluorescence Molecular Switch Based on a 1,4-Disubstituted Azine with Ferrocene and Pyrene Units. *Chem. Commun.* **2006**, 3809-3811.

(4) Bevilacqua, J. M.; Eisenberg, R. Quenching Studies of the Excited-State of (4,7-Diphenylphenanthroline)(1-(ethoxycarbonyl)-1-cyanoethylene-2,2-dithiolato)-platinum(II), Pt(Ph$_2$phen)(ecda), by Aromatic-Amines and Metallocenes and Determination of its Excited-State Reduction Potential. *Inorg. Chem.* **1994**, *33*, 1886-1890.

(5) Hasegawa, Y.; Nakagawa, T.; Kawai, T. Recent Progress of Luminescent Metal Complexes with Photochromic Units. *Coord. Chem. Rev.* **2010**, *254*, 2643-2651.

(6) Muratsugu, S.; Kume, S.; Nishihara, H. Redox-Assisted Ring Closing Reaction of the Photogenerated Cyclophanediene Form of Bis(ferrocenyl)dimethyldihydro-pyrene with Interferrocene Electronic Communication Switching. *J. Am. Chem. Soc.* **2008**, *130*, 7204-7205.

(7) Sun, L.; Tian, H. Dual-Controlled Dithienylmaleimide Switch Containing Ferrocene Units. *Tetrahedron Lett.* **2006**, *47*, 9227-9231.

(8) Guirado, G.; Coudret, C.; Launay, J. P. Electrochemical Remote Control for Dithienylethene-Ferrocene Switches. *J. Phys. Chem. C.* **2007**, *111*, 2770-2776.

(9) Thomas, K. R. J.; Lin, J. T.; Wen, Y. S. Synthesis, Spectroscopy and Structure of New Push-Pull Ferrocene Complexes Containing Heteroaromatic Rings (Thiophene and Furan) in the Conjugation Chain. *J. Organomet. Chem.* **1999**, *575*, 301-309.

(10) Vos, J. G.; Pryce, M. T. Photoinduced Rearrangements in Transition Metal Compounds. *Coord. Chem. Rev.* **2010**, *254*, 2519-2532.

(11) de Jong, J. J. D.; Lucas, L. N.; Hania, R.; Pugzlys, A.; Kellogg, R. M.; Feringa, B. L.; Duppen, K.; van Esch, J. H. Photochromic Properties of Perhydro- and Perfluorodithienylcyclopentene Molecular Switches. *Eur. J. Org. Chem.* **2003**, 1887-1893.

(12) Lucas, L. N.; de Jong, J. J. D.; van Esch, J. H.; Kellogg, R. M.; Feringa, B. L. Syntheses of Dithienylcyclopentene Optical Molecular Switches. *Eur. J. Org. Chem.* **2003**, 155-166.

(13) Xie, N.; Zeng, D. X.; Chen, Y. Electrochemical Switch Based on the Photoisomerization of a Diarylethene Derivative. *J. Electroanal. Chem.* **2007***, 609*, 27-30.

(14) Irie, M. Diarylethenes for Memories and Switches. *Chem. Rev.* **2000***, 100*, 1685-1716.

(15) Peters, A.; Branda, N. R. Limited Photochromism in Covalently Linked Double 1,2-Dithienylethenes. *Adv. Mater. Opt. Electron.* **2000***, 10*, 245-249.

(16) Irie, M.; Lifka, T.; Uchida, K.; Kobatake, S.; Shindo, Y. Fatigue Resistant Properties of Photochromic Dithienylethenes: By-Product Formation. *Chem. Commun.* **1999***, 747-748.

(17) Uchida, K.; Matsuoka, T.; Kobatake, S.; Yamaguchi, T.; Irie, M. Substituent Effect on the Photochromic Reactivity of Bis(2-thienyl)perfluorocyclopentenes. *Tetrahedron* **2001***, 57*, 4559-4565.

(18) Irie, M.; Sakemura, K.; Okinaka, M.; Uchida, K. Photochromism of Dithienylethenes with Electron-Donating Substituents. *J. Org. Chem.* **1995***, 60*, 8305-8309.

(19) Lucas, L. N.; van Esch, J.; Kellogg, R. M.; Feringa, B. L. A New Class of Photochromic 1,2-Diarylethenes; Synthesis and Switching Properties of Bis(3-thienyl)cyclopentenes. *Chem. Commun.* **1998**, 2313-2314.

(20) M. Draper, S.; Long, C.; M. Myers, B. The Photochemistry of (μ_2-RC$_2$H)Co$_2$(CO)$_6$ Species (R=H or C$_6$H$_5$), Important Intermediates in the Pauson–Khand Reaction. *J. Organomet. Chem.* **1999***, 588*, 195-199.

(21) Coleman, A.; Pryce, M. T. Synthesis, Electrochemistry, and Photophysical Properties of a Series of Luminescent Pyrene-Thiophene Dyads and the Corresponding Co$_2$(CO)$_6$ Complexes. *Inorg. Chem.* **2008***, 47*, 10980-10990.

(22) Boyle, N. Novel Thienyl Dyes and Related Metal Carbonyl Complexes, Ph.D. Thesis, Dublin City University, **2011**.

(23) Chia, L. S.; Cullen, W. R.; Franklin, M.; Manning, A. R. Reactions of (RC≡CR')Co$_2$(CO)$_6$ Complexes with Monodentate and Bidentate Group 5 Ligands. *Inorg. Chem.* **1975***, 14*, 2521-2526.

(24) Atkin, A. J.; Williams, S.; Sawle, P.; Motterlini, R.; Lynam, J. M.; Fairlamb, I. J. S. μ_2-Alkyne Dicobalt(0)hexacarbonyl Complexes as Carbon Monoxide-Releasing Molecules (CO-RMs): Probing the Release Mechanism. *Dalton Trans.* **2009**, 3653-3656.

(25) Kretschmer, R.; Gessner, G.; Gorls, H.; Heinemann, S. H.; Westerhausen, M. Dicarbonyl-bis(cysteamine)iron(II) A Light Induced Carbon Monoxide Releasing Molecule Based on Iron (CORM-S1). *J. Inorg. Biochem.* **2011***, 105*, 6-9.

(26) Zhang, W.; Atkin, A. J.; Thatcher, R. J.; Whitwood, A. C.; Fairlamb, I. J. S.; Lynam, J. M. Diversity and Design of Metal-Based Carbon Monoxide-Releasing Molecules (CO-RMs) in Aqueous Systems: Revealing the Essential Trends. *Dalton Trans.* **2009**, 4351-4358.

CHAPTER 5

Electrochemistry of Thienyl-based Switches and their Cobalt Carbonyl Complexes

*Chapter 5 describes the electrochromic behaviour of the perhydro- and perfluoro-switches, substituted with ethynylthiophene moieties: 1,2-Bis(5'-(3''-ethynylthiophene)-2'-methylthien-3'-yl)cyclopentene {**1H**}; 1,2-Bis(5'-(3''-ethynylthiophene)-2'-methylthien-3'-yl)perfluorocyclopentene {**1F**}; 1,2-Bis(5'-(4''-phenyl-3'''-ethynylthiophene)-2'-methylthien-3'-yl)-cyclopentene {**2H**}; 1,2-Bis(5'-(4''-phenyl-3'''-ethynylthiophene)-2'-methylthien-3'-yl)perfluorocyclopentene {**2F**}. The electrochemical properties of these switches were investigated using cyclic voltammetric and UV-vis/NIR spectroelectrochemical techniques. The electrochemical properties of the corresponding $Co_2(CO)_6$ complexes {**3H**, **3F**, **3bF**, **4H**, **4bH**, **4F**}, and $Co_2(CO)_4$dppm complexes {**5H**, **5F**, **6H**} were also examined, using similar techniques, in order to investigate the effects of incorporating cobalt carbonyl moieties onto the switches. IR spectroelectrochemical techniques were employed to explore the effects of the oxidation processes on the cobalt carbonyl moieties.*

5.1 Introduction

Dithienylcyclopentene (DTE) switches can undergo electrochemical cyclisation or cycloreversion processes, following oxidation of the DTE core, which usually occurs at high positive potentials ($\geq$ 1.0 V), which is typical of thiophene oxidation chemistry.[1] The driving force for the process that takes place, is dependent on the relative stability of the radical cations of the open and closed forms.[2,3] In general, it has been found that the central cyclopentene groups (i.e. H *vs.* F), and the substituents attached to the dithienylethene unit, greatly affect the oxidative processes, with electron-donating groups favouring ring-closure, and electron-withdrawing groups promoting the ring-opening process.[1,4,5] As described in chapter 1, oxidative ring opening/closing processes can be detected using cyclic voltammetry methods. However, UV-vis spectroelectrochemical methods have also been employed to follow the electrochemical ring opening/closing processes, and the cation radicals generated in situ, to support the results obtained by cyclic voltammetry, and to help elucidate the mechanisms involved in such electrochemical processes.[1,2,4-6] IR spectro-electrochemical techniques have also been utilised in order to analyse the effect of oxidative/ reductive processes, on specific moieties, in the molecular system.[7-9]

This chapter describes the electrochemical properties found for the thienyl-based dithienylcyclopentene switches (**1H**, **1F**, **2H**, **2F**), using cyclic voltammetric and UV-vis spectroelectrochemical techniques. The same methods were employed to investigate the effects of incorporating $Co_2(CO)_6$ moieties (**3H**, **3F**, **3bF**, **4H**, **4bH**, **4F**), and $Co_2(CO)_4$dppm moieties (**5H**, **5F**, **6H**) on the electrochromic properties of these switches. The consequence of the oxidation processes on the cobalt carbonyl complexes were examined through IR spectroelectrochemical techniques. The structures of thienyl-based switches, and their cobalt carbonyl complexes, are shown in figure 5.1.
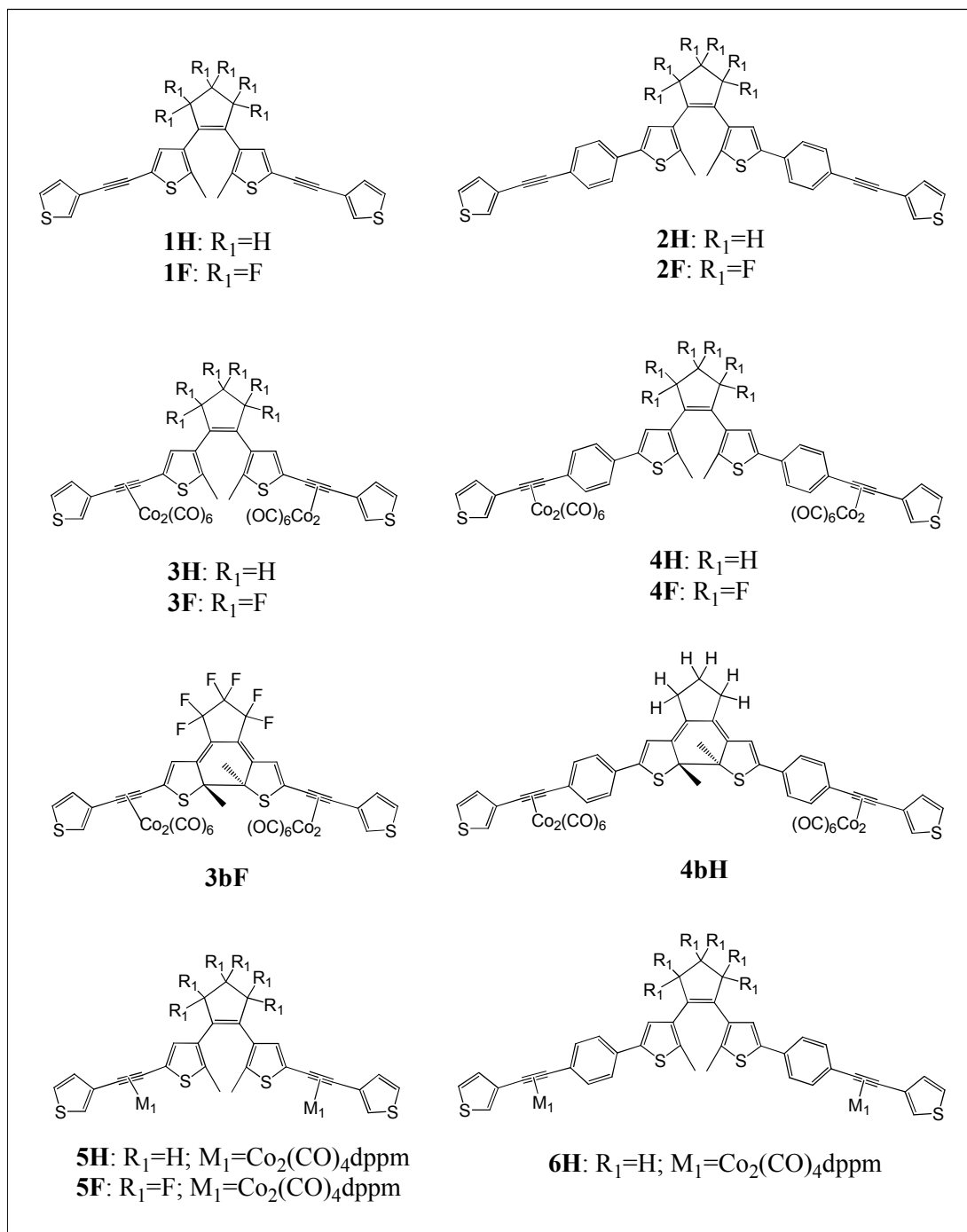
Figure 5.1: Illustrates the structures of the thienyl-based dithienylperhydro- and perfluoro-cylopentene switches **1H**, **1F**, **2H** and **2F** discussed in this chapter, and their corresponding $Co_2(CO)_6$ complexes {**3H**, **3F**, **3bF 4H**, **4bH**, **4F**} and $Co_2(CO)_4$dppm complexes {**5H**, **5F**, **6H**}.

5.2 Experimental

5.2.1 General Procedures

Cyclic Voltammetry: Cyclic voltammetry experiments were carried out in the dark, at room temperature, in a closed 10 ml two-neck round-bottomed flask. Solutions of the compound (~ 1 mmol) were made-up in spectroscopic grade dichloromethane, using tetrabutylammonium hexafluorophosphate (0.1 M) as the supporting electrolyte. The solutions were degassed with argon, and kept under an inert atmosphere throughout the experiment. A three-electrode system was set-up: glassy carbon was used as the working electrode, a platinum wire was employed as the counter electrode and a silver wire was used as the reference electrode. The cyclic voltammograms were obtained at a scan rate of 0.1 Vs^{-1}. The reference electrode was calibrated versus the decamethylferrocene redox couple (Fc^{*+}/Fc^*), which has a formal potential $E_{1/2}$ = - 0.07V versus SCE.[10]

UV-vis/NIR Spectroelectrochemistry: Spectroscopic grade dichloromethane was used as the solvent and 0.1 M tetrabutylammonium hexafluorophosphate [$TBAPF_6$] was used as the supporting electrolyte. The experiments were carried out, in the dark, using a platinum gauze mesh working electrode, in a custom-made quartz cuvette (2 mm path length) equipped with a solvent reservoir holding a silver wire reference electrode and platinum wire counter electrode (separated from the solution using a glass tube sleeve). The solutions were degassed with argon and kept under an inert atmosphere throughout the experiment. Bulk electrolysis was carried out over a variety of oxidation/reduction potentials, at room temperature, and UV-vis/NIR spectra were recorded until no further changes were observed. Subsequently, a potential of 0 V was applied to the system and spectra were recorded until changes in the spectra ceased. These experiments were typically carried out over a period of 20 to 40 minutes.

IR spectroelectrochemistry: Solutions of the cobalt carbonyl complexes were made-up in spectroscopic grade dichloromethane, containing tetrabutylammonium hexafluorophosphate (0.1 M) as the supporting electrolyte, and measured in an IR OTTLE cell. The cell contained a platinum gauze working electrode, a platinum

counter electrode, and a silver reference electrode. Bulk electrolysis was carried out at room temperature, over a variety of oxidation potentials and the changes in the IR spectra were recorded. Subsequently, a potential of 0 V was applied and the changes in the IR spectra were recorded.

Formation of the closed-ring isomers: The switches were dissolved in deuterated acetone and placed in a sealed NMR tube. With monitoring by ^{1}H NMR spectroscopy, the solutions were irradiated with monochromatic light, at 313 nm, until conversion from the open-ring to the closed-ring was complete, or before the photochemical by-products formed.

5.2.2 Materials

The dichloromethane was of spectroscopic grade and was purchased from Sigma Aldrich. The tetrabutylammonium hexafluorophosphate, decamethylferrocene and deuterated acetone were all purchased from Sigma Aldrich. The argon gas was supplied by BOC Ltd.

5.2.3 Equipment

Cyclic voltammetry and bulk electrolysis experiments were carried out using a CH Instruments Chi600a potentiostat. The electrodes used for the cyclic voltammetry experiments were a glassy carbon (working), silver wire (reference), and platinum wire (counter), all purchased from CH Instruments. UV-vis/NIR spectroelectrochemistry experiments were carried out on a Jasco V-670 spectrophotometer, in a custom-made quartz cuvette (2 mm path-length) equipped with a solvent reservoir, which was purchased from Starna Scientific. The electrodes employed were a platinum gauze mesh (working), a silver wire (reference) and a platinum wire (counter). Infra-red spectroelectrochemistry experiments were carried out on a Perkin Elmer "Spectrum 65" FT-IR spectrometer, using an electrochemical IR OTTEL cell purchased from IDEAS! UvA B.V. The IR cell contained a platinum gauze working electrode, a platinum counter electrode, and a silver reference electrode. Photochemical experiments were carried out using a 200W Hg lamp (Oriel Instruments, model no.: 68911) containing a 313 nm filter. ^{1}H NMR spectra were recorded on a Bruker model AC 400 MHz spectrometer.

5.3 Results and Discussion

5.3.1 Thienyl-based Switches: Cyclic Voltammetry

Electrochemical induced switching, of the thienyl-based switches **1H/F** and **2H/F**, was investigated by cyclic voltammetry. The open-ring isomers were irradiated with UV light (at 313 nm) in order to generate the closed-ring isomers. Cyclic voltammetry experiments were performed on both the open and closed forms, in 0.1 M solutions of $TBAPF_6/CH_2Cl_2$, at a scan rate of 0.1 Vs^{-1}. Decamethylferrocene was employed as a reference and the results are reported against the ferrocene redox couple Fc^{*+}/Fc^* ($E_{1/2}$ = -0.07 *vs.* SCE). The structures of the open and closed switches are illustrated in figure 5.2.
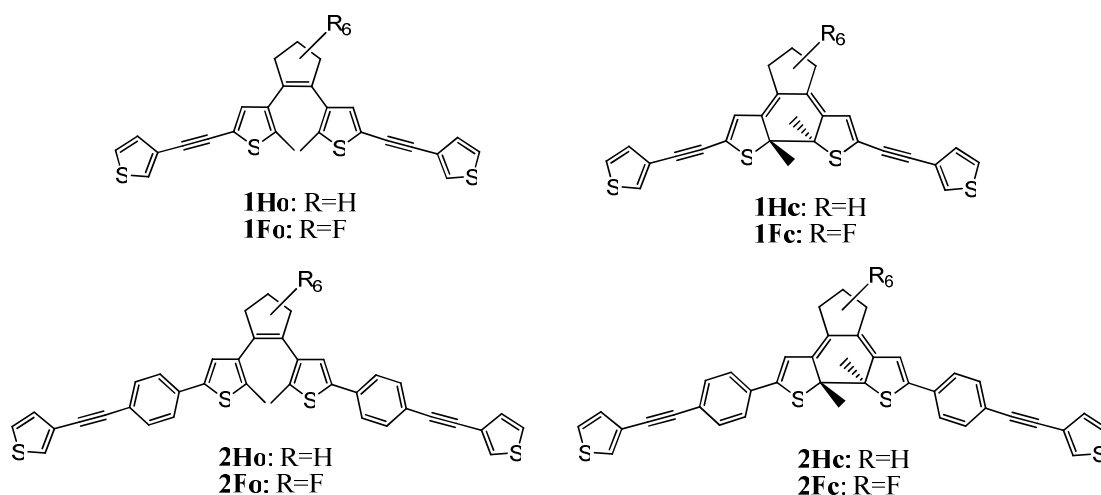
Figure 5.2: Illustrates the structures of the open and closed isomers of compounds **1H/F** and **2H/F**.

- **Reduction Process**

Reductive electrochemistry was carried out on the open and closed-ring isomers in the range from 0 to -2.0 V. The potential limit of the solvent (CH_2Cl_2) is -2.0 V, therefore experiments were not carried out at lower potential values. Within this potential range no reduction processes were observed for the open-ring isomer **1Fo**. However, the closed-ring derivative (**1Fc**) revealed two irreversible reduction waves at -1.1 V and -1.49 V (*vs.* SCE), as shown in figure 5.3, which can be attributed to the generation of the mono- (**1Fc⁻**) and di-anion (**1Fc²⁻**) species respectively. The fact that **1Fc** underwent reduction processes at > -2.0 V can be ascribed to the extension of the π-conjugation of the system in the closed-ring isomer, which reduces the HOMO-LUMO gap, hence allowing reduction processes to occur at less negative potentials.[11,12]
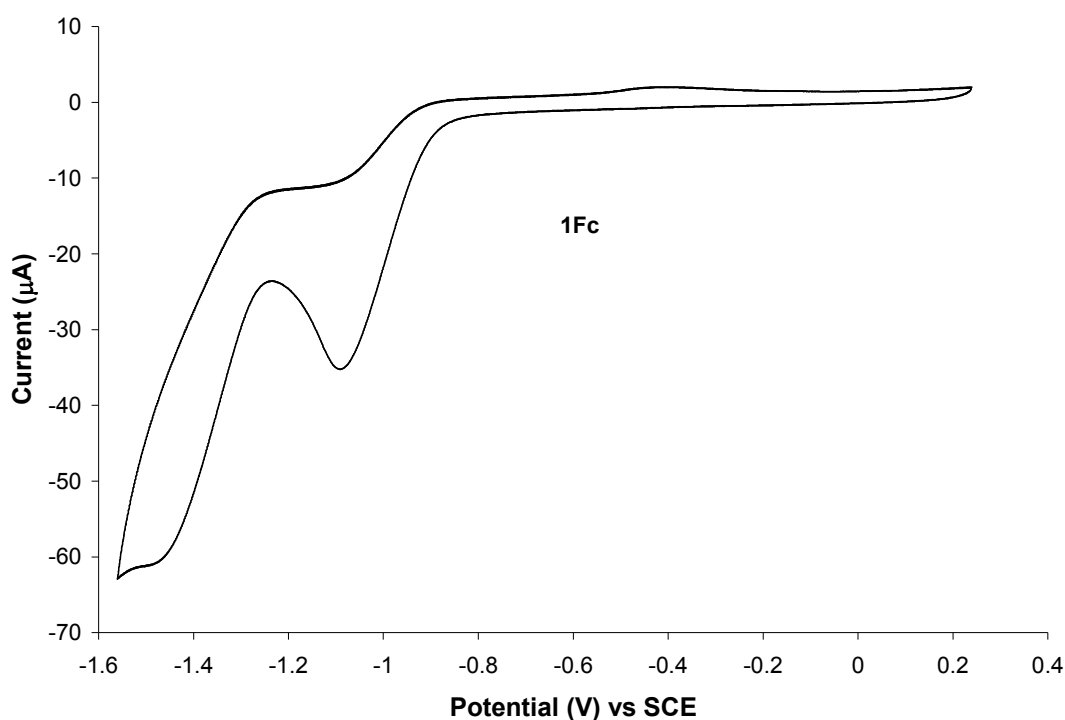
Figure 5.3 Cyclic voltammogram of the reduction process of **1Fc**, in 0.1 M TBAPF$_6$/CH$_2$Cl$_2$, at a scan rate of 0.1 Vs^{-1}.

Similar results were observed for **2F**. No reduction waves were observed for the open-ring isomer **2Fo** below the potential limit of the CH_2Cl_2 solvent, whereas the cyclic voltammogram (CV) of the closed-ring isomer **2Fc** displayed two irreversible reduction waves at -0.95 and -1.2 V (*vs.* SCE), representing the formation of the

monoanion (**2Fc⁻**) and dianion (**2Fc²⁻**) species respectively. Conversely, no reduction processes were observed for the open- or closed-ring isomers of the perhydro derivatives **1H** and **2H**, at potentials higher then -2.0 V. This can be attributed to the ability of the hexafluoro substituents to stabilise the LUMO (i.e. the first reduction process) to a greater extent then the hydrogen substituents[1,11,12], hence resulting in the occurrence of reduction processes of the perhydro analogues at more negative potentials, beyond the solvent range.

- **Oxidation Process**

The oxidation processes of the open and closed-ring isomers of **1H/F** and **2H/F** were examined in order to determine whether oxidative cyclisation or cycloreversion processes occurred for theses switches. The oxidation potentials observed in the CVs of these compounds are summarised in table 5.1.

Table 5.1: Redox properties of **1H/F** and **2H/F** in the open and closed forms.

	Cyclic Voltammetry Oxidation Potentials						
	Open-Ring Isomers				Closed-Ring Isomers		
	E_{pa} (V)	E_{pc} (V)	$E_{1/2}$ (V)		E_{pa} (V)	E_{pc} (V)	$E_{1/2}$ (V)
1Ho	0.65^{rc}	0.60^{rc}	0.63^{rc}	**1Hc**	0.65^{rc}	0.55^{rc}	0.60^{rc}
	0.95^{rc}	0.88^{rc}	0.92^{rc}		0.95^{rc}	0.85^{rc}	0.90^{rc}
	1.55^{a}	-	-				
2Ho	0.50^{rc}	0.42^{rc}	0.46^{rc}	**2Hc**	0.56^{rc}	0.42^{rc}	0.49^{rc}
	0.82^{rc}	0.75^{rc}	0.79^{rc}		0.88^{rc}	0.74^{rc}	0.81^{rc}
	1.23^{a}						
1Fo	1.71^{a}	-	-	**1Fc**	1.13^{b}	0.89^{b}	1.01
2Fo	0.99^{rc}	0.92^{rc}	0.96^{rc}	**2Fc**	1.04^{rc}	0.92^{rc}	0.98^{rc}
	1.11^{rc}	1.07^{rc}	1.09^{rc}		1.17^{rc}	1.07^{rc}	1.12^{rc}
	1.63^{a}						

All values listed are values of potential (V) *vs*. SCE, recorded in 0.1 M TBAPF₆/CH₂Cl₂. at 0.1 Vs⁻¹.
[a] indicates an irreversible oxidation process
[b] indicates a quasi-reversible oxidation process
[rc] indicates peaks assigned to ring-closed species

Electrochemical oxidation of **2Ho** resulted in an irreversible oxidation peak at 1.23 V (*vs*. SCE), as shown in figure 5.4. The returning sweep displayed two reduction waves at 0.75 and 0.42 V, and the subsequent oxidation sweep showed two new

corresponding oxidation waves at 0.50 and 0.82 V, which were not present before the oxidation occurred at 1.23 V. This result indicates that oxidative cyclisation from the open to the closed-ring isomer occurred, as described previously in the literature.[1,2,5,6] The large oxidation peak at 1.23 V represents the oxidation of the open-ring isomer **2Ho** to its radical dication **2Ho^{2+}**, which was immediately followed by cyclisation to form the closed-ring dication **2Hc^{2+}**. The dication radical was subsequently reduced to the monocation radical (**2Hc^{2+} → 2Hc$^+$**) and then to its neutral form (**2Hc$^+$ → 2Hc**), at 0.75 V and 0.42 V respectively. The stability of the closed form resulted in the oxidation waves observed in the subsequent anodic sweeps.
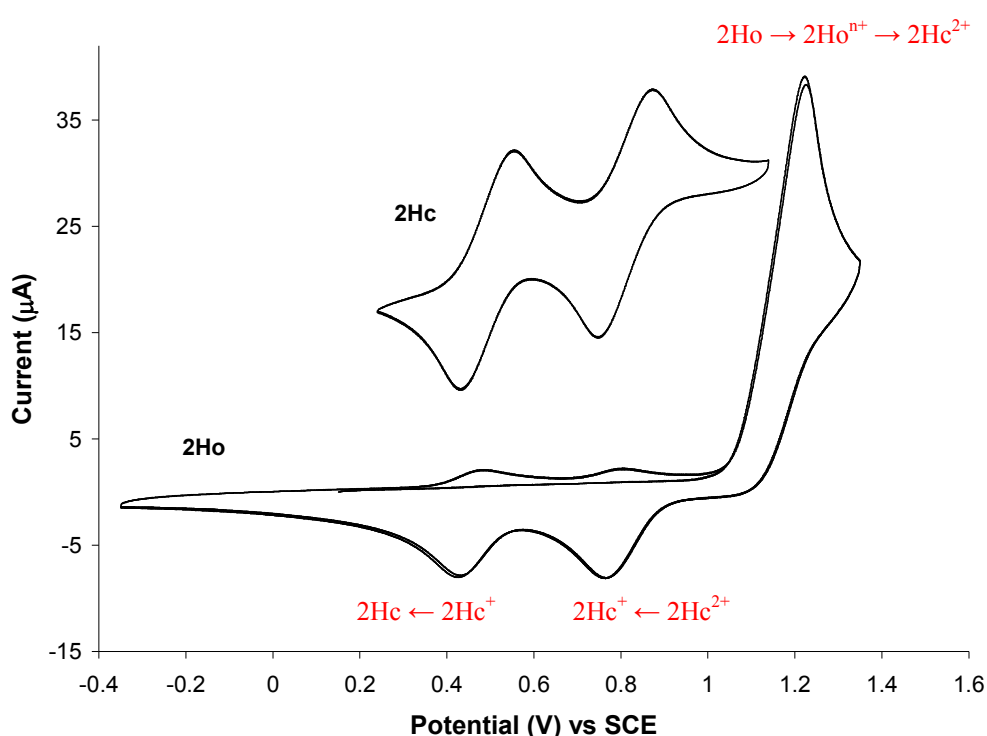
Figure 5.4 Cyclic voltammogram of **2Ho** (bottom) and **2Hc** (top), in 0.1 M TBAPF$_6$/CH$_2$Cl$_2$, at a scan rate of 0.1 Vs^{-1}. The CV of the closed form is offset along the coordinate for clarity.

Oxidation of the corresponding closed-ring isomer **2Hc** was manifested in two reversible waves at E$_{1/2}$ = 0.49 and 0.81 V, representing the formation of the monocation **2Hc$^+$** and dication species **2Hc^{2+}** respectively. These redox waves correspond to the two redox waves observed for **2Ho** following oxidation at 1.23 V, as shown in figure 5.4, hence confirming the oxidative cyclisation of **2Ho**.
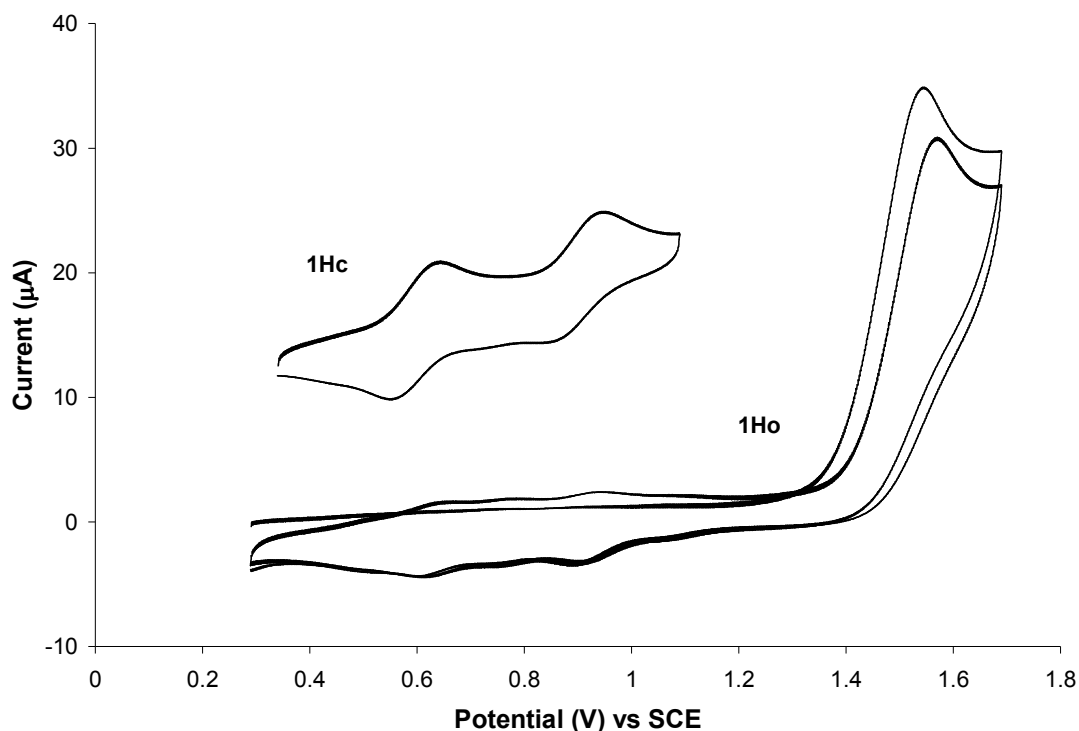
Figure 5.5 Cyclic voltammogram of **1Ho** (bottom) and **1Hc** (top), in 0.1 M TBAPF$_6$/ CH$_2$Cl$_2$, at a scan rate of 0.1 Vs^{-1}. The CV of the closed form is offset along the coordinate for clarity.

Evidence of oxidative ring-closing was also observed for the less conjugated derivative **1Ho**. An irreversible oxidation peak at 1.55 V (*vs.* SCE) was followed by two small reduction peaks at 0.60 and 0.88 V. The subsequent oxidation sweep displayed two new corresponding oxidation waves at 0.65 and 0.95 V, which were not present before oxidation occurred at 1.55 V. The CV of the closed-ring isomer **1Hc** displayed two oxidation waves at 0.65 and 0.95 V, and two corresponding reduction waves at 0.55 and 0.85 V respectively, typical of the generation of the monocation **1Hc$^+$** and dication **1Hc^{2+}** species, respectively. The similarities between the CVs of the open and closed-ring isomers of **1H** (figure 5.5) suggest that **1Ho** undergoes oxidative ring-closing in a similar fashion to that described for its more conjugated derivative **2Ho**. Hence the oxidation peak at 1.35 V can be assigned to the oxidation of the open-ring isomer **1Ho**, immediately followed by a cyclisation process, forming the closed-ring dication species **1Hc^{2+}**. Subsequent reduction to the monocation (**1Hc^{2+}** → **1Hc$^+$**) and neutral species (**1Hc$^+$** → **1Hc**) is denoted by the reduction peaks at 0.60 and 0.88 V respectively.

Also noted in the CVs of both **1Ho** and **1Hc**, was an unexpected third reduction peak at approximately 0.75 and 0.72 V, respectively. A corresponding oxidation peak was present at 0.78 V in the CV of **1Ho**, which was not observed for **1Hc**, although it could possibly be obscured by the oxidation peak at 0.65 V. This result suggests that oxidation of **1Hc** results in the generation of a new species, of unknown structure (assigned as **1Hy**). Similar electrochemically-produced by-products have been reported previously in the literature,[1,4] and its formation is believed to compete with that of the closed-form, although the structure, and mechanism by which it is formed, have yet to be elucidated.

In contrast to the perhydro analogue **1Ho**, the perfluoro-derivative **1Fo** was not found to undergo oxidative cyclisation. The similarities between the CVs of **1Fo** and **1Fc** indicate an oxidative cycloreversion process takes place for the closed-ring isomer **1Fc**.
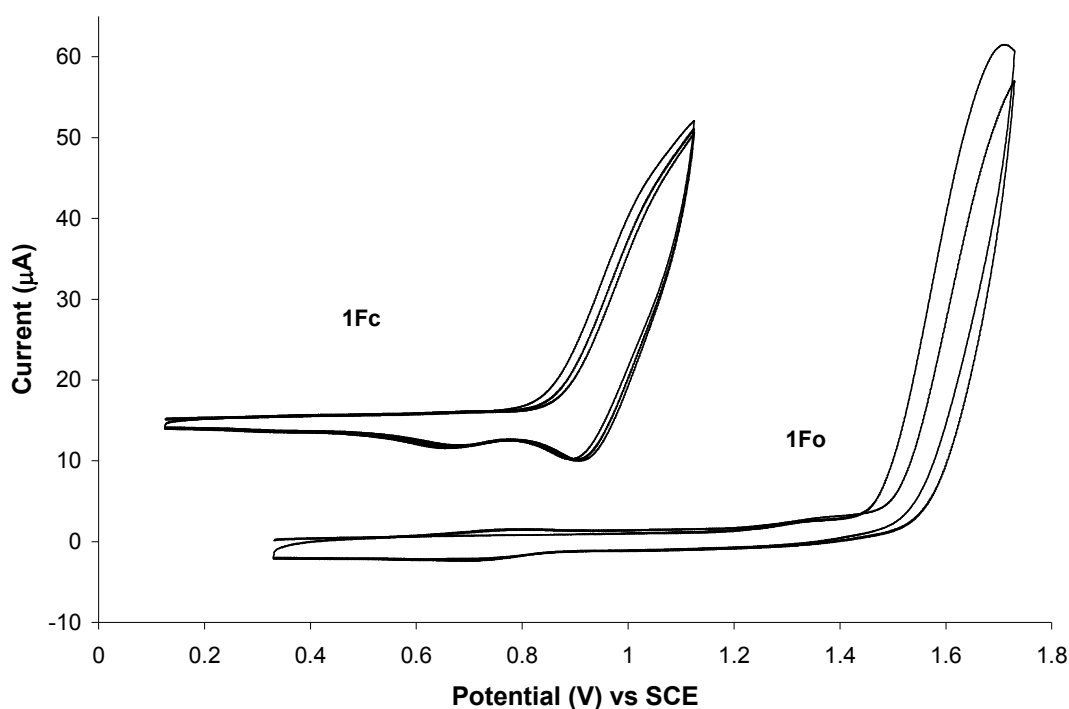
Figure 5.6 Cyclic voltammogram of **1Fo** (bottom) and **1Fc** (top), in 0.1 M TBAPF$_6$/CH$_2$Cl$_2$, at a scan rate of 0.1 Vs^{-1}. The CV of the closed form is offset along the coordinate for clarity.

Oxidation of the perfluoro analogue **1Fo** resulted in a large irreversible oxidation peak at 1.71 V (*vs.* SCE), as shown in figure 5.6, assigned to the formation of the dicationic species **1Fo^{2+}**. In the subsequent sweeps, redox waves indicative of the formation of

the mono- and di-cationic species of the closed-form were absent. However, a small reduction wave appeared at 0.72, and a corresponding oxidation peak at 0.82 V, as shown in figure 5.6. These peaks can tentatively be assigned to the generation of an unknown electrochemical species (assigned as **1Fy**), as already described for **1H**.

The CV of **1Fc** (figure 5.6) displayed similarities to that of the open-ring isomer **1Fo**, which indicated that **1Fc** underwent oxidative cycloreversion to the open-form. Such a process has been detailed in the literature, and is believed to involve a chain reaction mechanism.[2,13] An irreversible oxidation peak at 1.13 V was observed in the CV of **1Fc**, resulting in the formation of the thermally unstable closed-ring radical cation (**1Fc$^+$**), which rapidly undergoes a cycloreversion reaction, forming the radical cation of the open-ring isomer (**1Fc$^+$** → **1Fo$^+$**). As described already, the open-ring isomer **1Fo** undergoes oxidation at a much more positive potential (1.71 V), in comparison to the closed-ring isomer. Hence, the open-ring radical cation (**1Fo$^+$**) removes an electron from another closed-ring molecule (**1Fc**), resulting in the neutral form of the open-ring isomer (**1Fo**), and regeneration of the original closed-ring radical cation (**1Fc$^+$**). Subsequently, this closed-ring radical (**1Fc$^+$**) then quickly undergoes cycloreversion to the open-ring isomer (**1Fo$^+$**), which removes an electron from another closed-ring molecule, and so on, thus resulting in a chain reaction. The corresponding reduction peak, at E_{pc} = 0.89 V, can be ascribed to the reduction of a small amount of the closed-ring cation **1Fc$^+$**, which did not take part in the chain reaction. A second reduction peak was observed at 0.64 V, with a small corresponding anodic peak at 0.72 V. A similar redox process was observed in the literature reports, but was not assigned to any particular species.

In contrast to **1Fo**, its corresponding more conjugated derivative **2Fo** was found to undergo oxidative cyclisation to the closed-form, as illustrated in figure 5.7. The CV of the closed-ring isomer **2Fc** displayed two one-electron redox waves at $E_{1/2}$ = 0.98 and 1.12 V (*vs.* SCE), representing the formation of the monocation radical **2Fc$^+$**, and dication species **2Fc^{2+}**, respectively.

The CV of **2Fo** displayed a large irreversible peak at 1.63 V, representing a two-electron oxidation process of the open-ring isomer, rapidly followed by cyclisation to the closed-ring isomer, forming the dication radical **2Fc^{2+}**. In the returning sweep two new reduction waves were observed at 0.92 and 1.07 V, and their corresponding oxidation waves appeared at 0.99 and 1.11 V in the consecutive anodic sweep.

Therefore, the dication radical $\mathbf{2Fc^{2+}}$ was reduced to the monocation species $\mathbf{2Fc^+}$, and then to the neutral form $\mathbf{2Fc}$, at $E_{1/2}$ = 1.09 and 0.96 V respectively. These redox waves are in agreement with those observed in the CV of $\mathbf{2Fc}$, as illustrated in figure 5.7, hence verifying the occurrence of electrochemically induced ring-closure of $\mathbf{2Fo}$ to $\mathbf{2Fc}$.
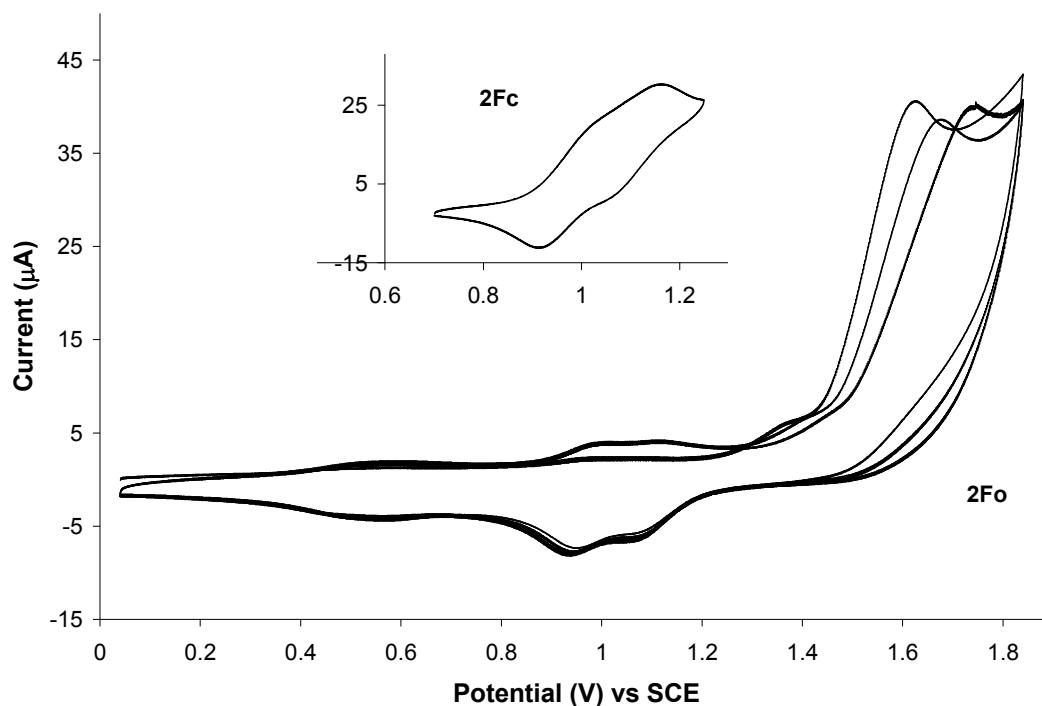
Figure 5.7 Cyclic voltammogram of $\mathbf{2Fo}$ in 0.1 M TBAPF$_6$/CH$_2$Cl$_2$, at a scan rate of 0.1 Vs^{-1}. Inset is the CV of the closed-ring isomer $\mathbf{2Fc}$.

A small reduction wave at 0.55 V, and a corresponding oxidation wave at 0.59 V was also observed in the CV of $\mathbf{2Fo}$, following oxidation at 1.63 V, although similar peaks were not observed in the CV of the closed form $\mathbf{2Fc}$. This indicates that the new redox waves are possibly a consequence of a rearrangement process of the dithienylethene switching unit during cyclisation processes, from the open to the closed form, resulting in a newly formed oxidative by-product (assigned as $\mathbf{2Fy}$), as described previously for $\mathbf{1H}$ and $\mathbf{1F}$.

The results described here demonstrate the significant effect the atoms on the central cyclopentene units (H *vs.* F) have on the redox properties of the switches. In the case of the less-conjugated derivative $\mathbf{1Fo}$ the oxidation process is anodically shifted by 160 mV in comparison to its perhydro analogue $\mathbf{1Ho}$. This can be ascribed to the

ability of **1Ho** to stabilise the HOMO (i.e. first oxidation process) to a greater extent due to the presence of the electron-donating hydrogen atoms on the central cyclopentene core. The effect of the hydrogen atoms can also be described as the driving force for the oxidative ring-closure observed for **1Ho**. In order for ring-closure to proceed, delocalisation of the charge is required in order to stabilise the radical cation, however the stability of the thienyl rings decreases due to loss of aromaticity. The presence of the electron-donating H atoms increases the electron density on the central alkene group, thus facilitating communication between the two thiophene rings. Hence, the stability of the radical cation of the closed-ring isomer is increased, and therefore oxidative cyclisation, from the open to the closed-ring form, is thermodynamically allowed. On the other hand, the electron-withdrawing fluorine atoms on **1Fo** have the opposite effect. Stabilisation of the radical cation of the ring-closed isomer, by delocalisation of the charge, is counteracted by the electron-withdrawing effect of the fluorine atoms, which decreases the electron density on the alkene group. Therefore, ring-opening of the closed-ring cation occurs, with localisation of the charge on the thiophene rings. Similar trends have been reported in the literature.[1,4,5,13,14]
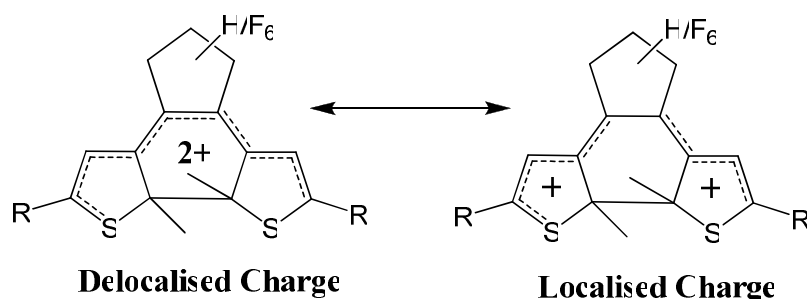
Scheme 5.1: Illustrates delocalised charge across the entire switching unit, and localised charge on the individual thiophene rings.

Extending π-conjugation within the switches, through the introduction of phenyl rings between the cyclopentene unit and the ethynylthiophene moieties, in the case of compounds **2H** and **2F**, was found to have significant effects on the redox properties of the switches. The first oxidation of **2Ho** was cathodically shifted by 400 mV in comparison to its perfluoro analogue **2Fo**, due to the stabilising effect of the hydrogen atoms on the HOMO, as previously described for **1Ho** and **1Fo**. The oxidation process of **2Ho** occurred at a less positive potential in comparison to its less-conjugated derivative **1Ho**, with a cathodic shift of 320 mV. A similar result was also

found for **2Fo**, with the oxidation process cathodically shifted by 80 mV relative to **1Fo**. More importantly, oxidation of **2Fo** resulted in a cyclisation process to the closed form. On the contrary, the closed-ring isomer of **1F** underwent an oxidative ring-opening process. These results suggest that the electron-rich phenyl groups contribute to the stabilisation of the cation radical following delocalisation of the charge, hence further stabilising the HOMO, and thus allowing oxidation to occur at lower potentials, relative to their less-conjugated derivatives **1H/1F**, and **2Fo** to undergo oxidative ring-closure.

The cyclic voltammetry results also revealed the formation of the unknown species **1Hy**, **1Fy** and **2Fy** following oxidation processes. Such oxidation species have been described previously by Browne et al.[1,4] They ascribed the formation of these species to a thermally activated rearrangement of the dication radical of the closed-ring isomers of similar switches. They found that such species could be inhibited by environmental control, such as the solvent or temperature employed, or by the introduction of electron-donating groups. Interestingly, the only switch described here which did not show any evidence for the formation of such an oxidative species was **2H**. With reference to the results described by Browne et al, this could possibly be due to the extra stability provided by the electron-donating ability of the hydrogen-atoms on the cyclopentene ring, together with the electron-rich phenyl groups.

5.3.2 Thienyl-based Switches: UV-vis/NIR Spectroelectrochemistry

The cyclic voltammetry experiments indicated that oxidative ring-closure occurred for **1H**, **2H** and **2F**, and oxidative ring-opening occurred for **1F**. UV-vis/NIR spectroelectrochemistry was carried out on the open and closed-ring isomers in order to further investigate the oxidation processes of these switches, and to ultimately confirm the results established from the cyclic voltammetry experiments. The results obtained in the UV-vis/NIR are summarised in table 5.2, and were assigned to the corresponding oxidation products from reference to results published in the literature.[1,2,6] The structures of the open and closed switches **1H/F** and **2H/F** are illustrated in figure 5.8.
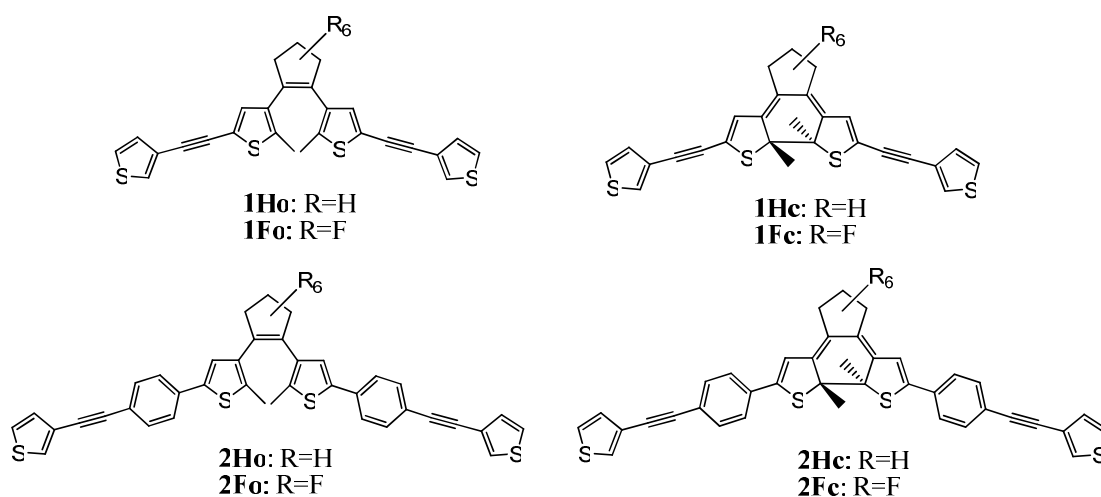
Figure 5.8: Illustrates the structures of the open and closed isomers of compounds **1H/F** and **2H/F**.

Table 5.2: UV-vis/NIR spectroelectrochemistry data for the open and closed-ring isomers of compounds **1H/F** and **2H/F**, following oxidation processes at varying potentials.

	Oxidation Potential	λ_{abs} (nm)		Oxidation Potential	λ_{abs} (nm)
1Ho	Start 1.3 V 1.6 V	290, 310 455, 566, 666 469, 575, 666, 867	**1Hc**	Start 0.6 V 0.9 V	318, 540 283, 405, 779, > 1100 448, 568, 674
2Ho	Start 1.4 V	334 471, 590(sh), 657	**2Hc**	Start 0.6 V 0.9 V	326, 560 442, 781, > 1030 467, 590(sh), 654
1Fo	Start 1.6 V	305 237, 345-700	**1Fc**	Start 1.2V	327, 608 242, 305, 442, 740-960
2Fo	Start 1.8 V	328 613, 780-1100	**2Fc**	Start 1.2 V	286, 353, 613 328, 810, 1457

The data was recorded in 0.1 M TBAPF$_6$/CH$_2$Cl$_2$ *vs.* Ag/Ag$^+$

Oxidation of **2Hc** was carried out at 0.60 V and 0.90 V (the potentials associated with the generation of the monocation **2Hc$^+$** and dication **2Hc^{2+}** species in the CV respectively), and the changes in the UV-vis/NIR spectra were recorded. Oxidation at 0.3 V, which was increased to 0.6 V, resulted in depletion of the **2Hc** absorption bands at 326 and 560 nm, in-conjunction with the formation of new bands at 442, 781 and > 1030 nm, as shown in figure 5.9. These bands can be assigned to the formation of the monocation radical **2Hc$^+$**. Increasing the oxidation potential to 0.9 V resulted in a decrease in the **2Hc$^+$** bands at 781 and > 1030 nm, with a concomitant formation of strong absorption bands at 467 and 654 nm, and a shoulder at 590 nm, assigned to the generation of the dication radical **2Hc^{2+}** (figure 5.10).

Subsequent reduction, at 0 V to -0.2 V, resulted in a decrease in the bands associated with the cation species, however the original spectrum of **2Hc** was not recovered. An increase in the absorption band in the UV region was observed, with λ_{max} at 337 nm, which lies between the λ_{max} of the closed-ring isomer **2Hc** and the open-ring isomer **2Ho** (λ_{max} = 326 and 344 nm respectively). Thus, the results indicate that the oxidation process of **2Hc** is not reversible, and in fact, ring-opening of **2Hc** occurs.
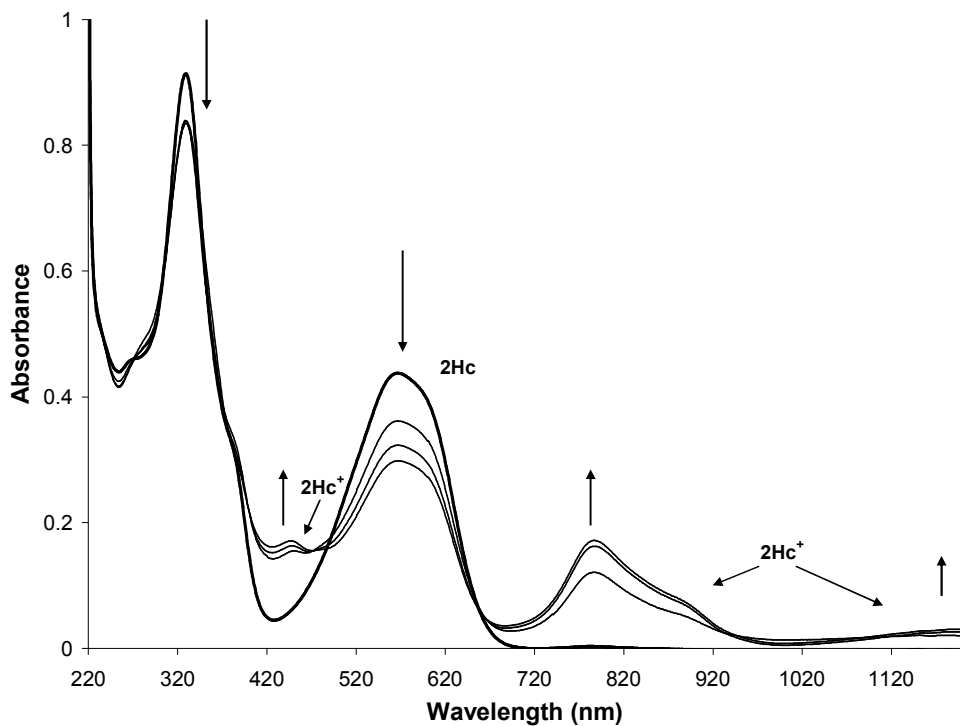
Figure 5.9: UV-vis/NIR spectrum of **2Hc**, showing oxidation of **2Hc** to **2Hc**[+] at 0.60V, in 0.1 M TBAPF$_6$/ CH$_2$Cl$_2$.
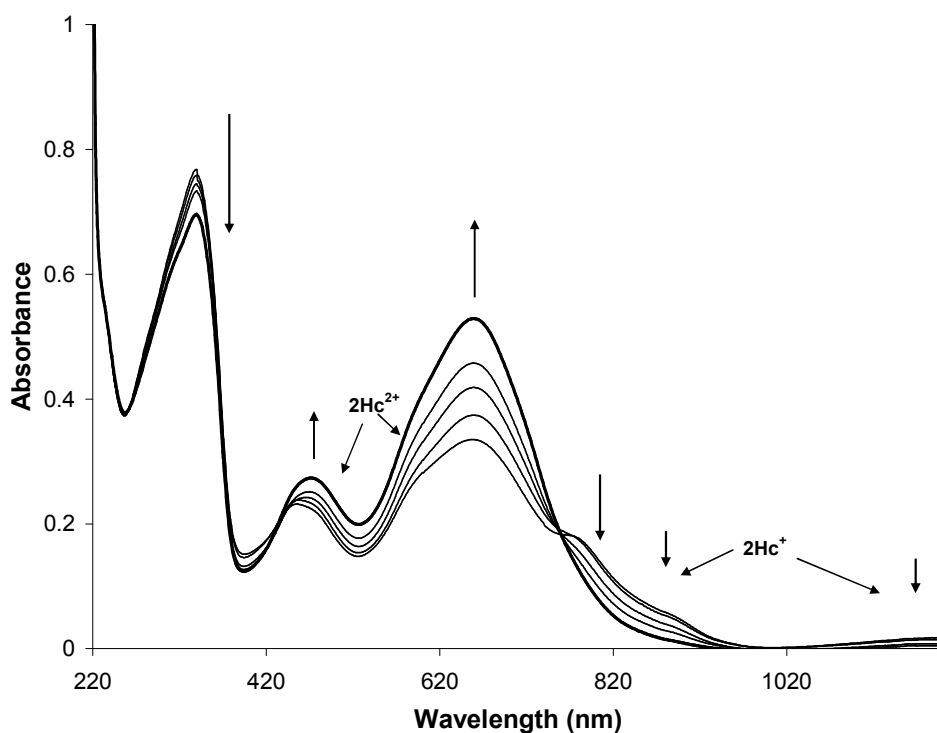
Figure 5.10: UV-vis/NIR spectrum of **2Hc**, showing oxidation of **2Hc+** to **2Hc**[2+] at 0.90V, in 0.1 M TBAPF$_6$/CH$_2$Cl$_2$.

When bulk electrolysis of the open-ring isomer **2Ho** was carried out, at a potential of 1.4 V, the absorption bands at 334 nm began to decrease, whilst strong absorption bands appeared in the UV-vis spectrum (figure 5.11) at 471 nm and 657 nm, with a shoulder at 590 nm. These bands correspond to the absorption bands recorded for the dication species of the closed form **2Hc^{2+}**. The absence of absorption features associated with the monocation species **2Hc^{+}** indicates that cyclisation of **1Ho** occurs following a two-electron oxidation process of the open-ring form, followed by cyclisation to the closed dication radical (**2Ho** → **2Ho^{2+}** → **2Hc^{2+}**).

Subsequent reduction at 0V (figure 5.12) resulted in a decrease in the bands at 475 and 657 nm, revealing the formation of bands at 445 and 781 nm, which are associated with the monocation species of the closed form **2Hc^{+}**, and a band at 563 nm, assigned to the neutral species of the closed-isomer **2Hc**. The presence of these bands is expected, as the reduction of **2Hc^{2+}** occurs in two separate one-electron reduction steps, firstly to the monocation **2Hc^{+}** and then to the neutral species **2Hc**, as shown in the CV of **2H**. Further reduction leads to the disappearance of the **2Hc^{+}** and **2Hc** bands, with an isosbestic point at 374 nm, and the band in the UV region at 337 nm increased. The final spectrum recorded did not resemble that of the closed-ring isomer **2Hc** as expected. Instead, a strong band was present at 337 nm, with weak absorptions at 449, 663 and 717 nm, allocated to some decomposition products. Therefore, the bulk oxidation of **2Ho** was not found to be fully reversible and did not result in the generation of the closed-ring isomer.
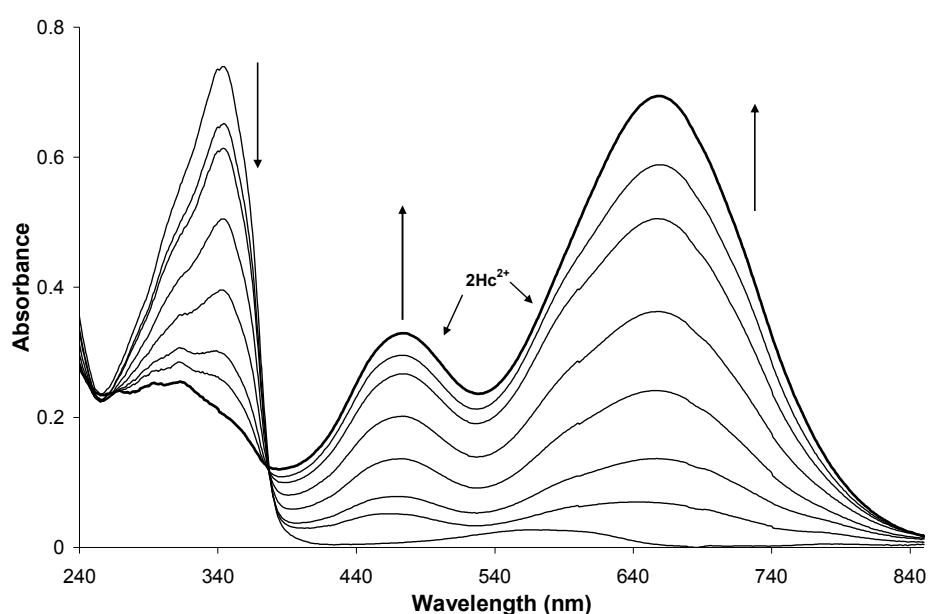
Figure 5.11: UV-vis spectrum of **2Ho**, showing oxidation of **2Ho** to **2Hc^{2+}** at 1.4 V, in 0.1 M TBAPF$_6$/CH$_2$Cl$_2$.
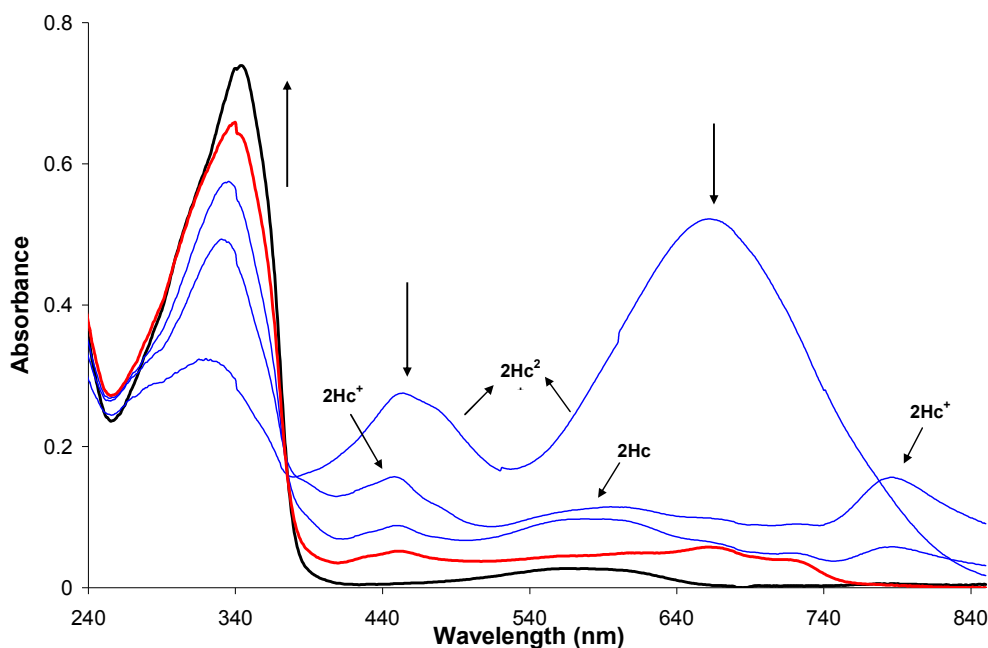
Figure 5.12: UV-vis spectra for **2Ho**, in 0.1 M TBAPF$_6$/CH$_2$Cl$_2$, showing the subsequent reduction of the oxidised species **2Hc^{2+}** at 0 V (blue lines). As the absorbance in the visible region decreased, bands associated with the monocation species **2Hc$^+$**, and neutral species **2Hc**, of the closed form became evident. The reduction process was not found to be fully reversible as the final spectrum recorded (red line) did not match the initial spectrum recorded (black line).

On oxidation of **1Hc**, from 0.2 to 0.6 V, the original bands in the absorption spectrum, at 318 and 540 nm, began to decrease. New bands appeared at 283, 405, 779 and > 1100 nm, as shown in figure 5.13, which can be assigned to the formation of the monocation radical **1Hc$^+$**. Increasing the oxidation potential to 0.9 V resulted in a decrease in the **1Hc$^+$** absorption bands, and the appearance of strong absorption bands at 448, 568 and 674 nm. Such changes can be ascribed to the formation of the dication species of the closed form **1Hc^{2+}**. Reduction at 0 V to -0.2 V, resulted in depletion of the **1Hc^{2+}** absorbance bands, however, the original spectrum recorded was not obtained. An increase in absorbance was observed at 283 nm, but the bands at 318 nm and 540 nm did not return, thus indicating that the oxidation process of **1Hc** is not reversible, and may result in ring-opening of **1Hc**.

Oxidation of the open-ring isomer **1Ho** at 1.3 V, resulted in a decrease in the initial absorbance bands at 290 and 310 nm, in concurrence with new bands appearing at 455, 566 and 666 nm. In comparison to the results obtained in the UV-vis/NIR spectrum of **1Hc**, these bands suggest that oxidation of **1Ho** results in the formation of **1Hc^{2+}**, without out the generation of **1Hc$^+$**, hence the cyclisation process occurs from the dication species of the open form: **1Ho** → **1Ho^{2+}** → **1Hc^{2+}**. The absence of a

strong absorption band at ~ 540 nm, following reduction processes at 0 V, showed that the cationic species of the closed-ring was not reduced to the neutral species of the closed form. Instead an overall decrease in the absorption bands in the visible region resulted, with an increase in the absorbance in the UV region. The original spectrum recorded at the start was not obtained, thereby indicating that some decomposition occurred during the bulk electrolysis experiments.
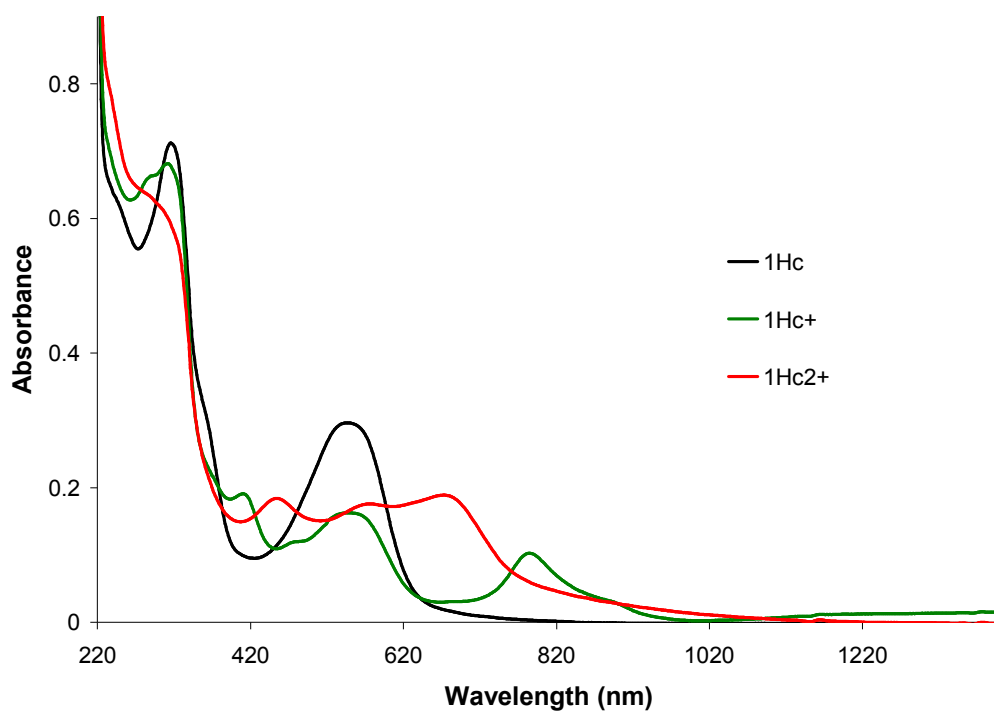
Figure 5.13: UV-vis/NIR spectrum of **1Hc** (black line) in 0.1 M TBAPF$_6$/CH$_2$Cl$_2$, following oxidation at: 0.6 V forming **1Hc$^+$** (green line); at 0.9 V forming **1Hc^{2+}** (red line).

The UV-vis/NIR spectroelectrochemistry data recorded for the closed-ring isomers of the perhydro switches **1Hc** and **2Hc**, have demonstrated the changes in the absorption spectra following oxidative formation of their relative monocation and dication species. Similar changes were observed in the UV-vis spectra of the corresponding open-ring isomers, **1Ho** and **2Ho**, respectively. Thus, these results, together with the results observed in the cyclic voltammograms, confirm that oxidative cyclisation processes occur for **1Ho** and **2Ho**. However, the CVs of the perhydro switches indicate reversible oxidation processes for the closed-ring isomers, and generation of the neutral species of the closed form, in the case of the open-ring isomers. Conversely, the bulk electrolysis oxidation experiments were not found to be fully reversible. In fact, the UV-vis spectra obtained, following subsequent reduction at 0 V, indicated ring-opening processes occurred in each case. Such a result can be

ascribed to the considerable increase in the timescale of the UV-vis spectroelectrochemistry experiments (minutes), in comparison to the cyclic voltammetry experiments (seconds). Therefore, within the timescale of the bulk electrolysis processes, regeneration of the neutral species of the closed form is circumvented by a ring-opening process of the cationic species and restoration of the open-ring isomer, along with some degradation of the switches under these electrochemical conditions.

In the case of the perfluoro-derivative **2Fo**, the cyclic voltammetry results indicated that oxidative cyclisation to the closed-ring isomer occurred. The oxidation processes for **2Fo** was investigated in the UV-vis/NIR spectrum, and following oxidation at 1.8 V, the initial absorbance band recorded at 328 nm began to decrease. A new band began to grow-in at 613 nm, which is similar to the absorbance band of the closed-ring isomer **2Fc**, hence confirming the occurrence of oxidative cyclisation. An increase in absorbance in the range 780-1100 nm was also observed, which can tentatively be assigned to the generation of the monocation species of the closed form, $2Fc^+$. The subsequent spectrums recorded showed a small increase at 613 nm, however the absorbance in the region 780-1100 nm began to decrease, and there was no evidence for the formation of the dication species $2Fc^{2+}$. This is in contrast to the results obtained for the perhydro-derivatives **1H** and **2H**, as there was little evidence for the formation of the cation radical species of **2Fc**. Subsequent reduction at 0V resulted in a decrease in the band at 613 nm, and the initial band at 328 nm did not return to its original intensity.

Oxidation of **2Fc** at 1.2 V resulted in a continual decrease in the absorbance band at 613 nm. On closer inspection, the first UV-vis/NIR spectrum recorded, at 1.2 V, displayed a low intensity increase in absorbance in the region 750 - 1620 nm, with two λ_{max} present at 810 and 1457 nm. Such spectral features can be attributed to the generation of the monocation $2Fc^+$ and dication $2Fc^{2+}$ species, however, they were found to decrease in intensity in the subsequent spectra recorded, as shown in figure 5.15. During the oxidation processes, an increase in the absorbance in the UV region was also observed, resulting in a single absorbance band at 328 nm, coincident with the absorbance band associated with the open-ring isomer **2Fo**. Subsequent reduction at 0 V, results in a further decrease at 613 nm, and increase at 328 nm. This result

indicates that oxidation of **2Fc** results in a cycloreversion process to the open-ring form.
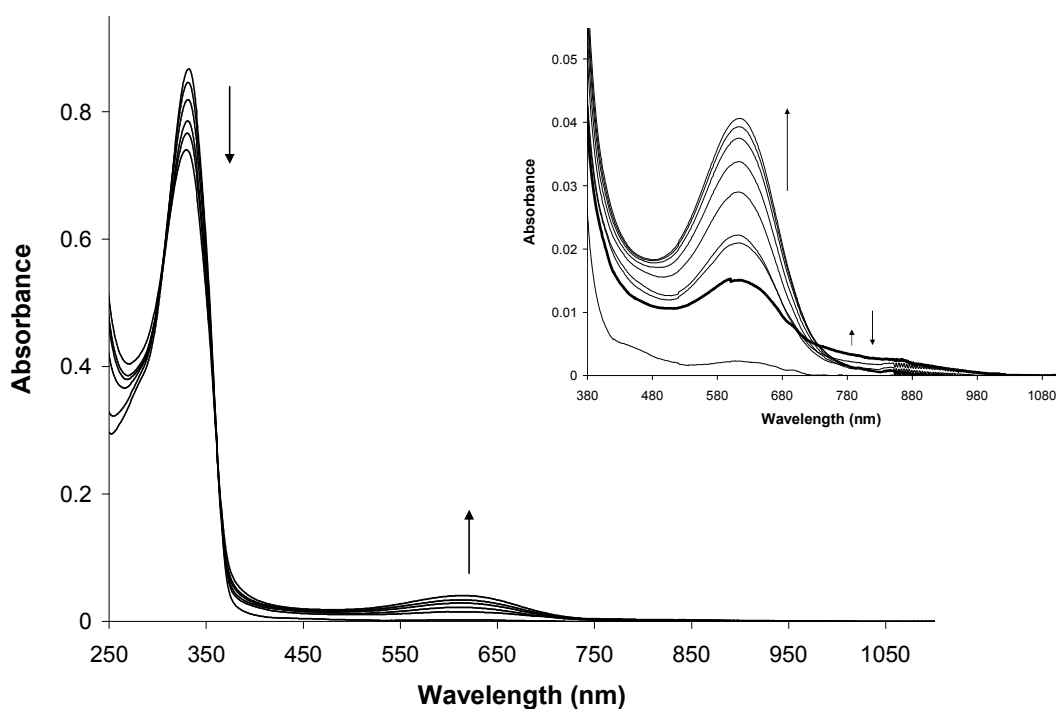
Figure 5.14: UV-vis/NIR spectrum of **2Fo,** in 0.1 M TBAPF$_6$/CH$_2$Cl$_2$, following oxidation at 1.8 V. Inset shows the same spectrum between 380 and 1100 nm, showing an increase in the absorbance band at 613 nm and at > 780 nm (thick black line).
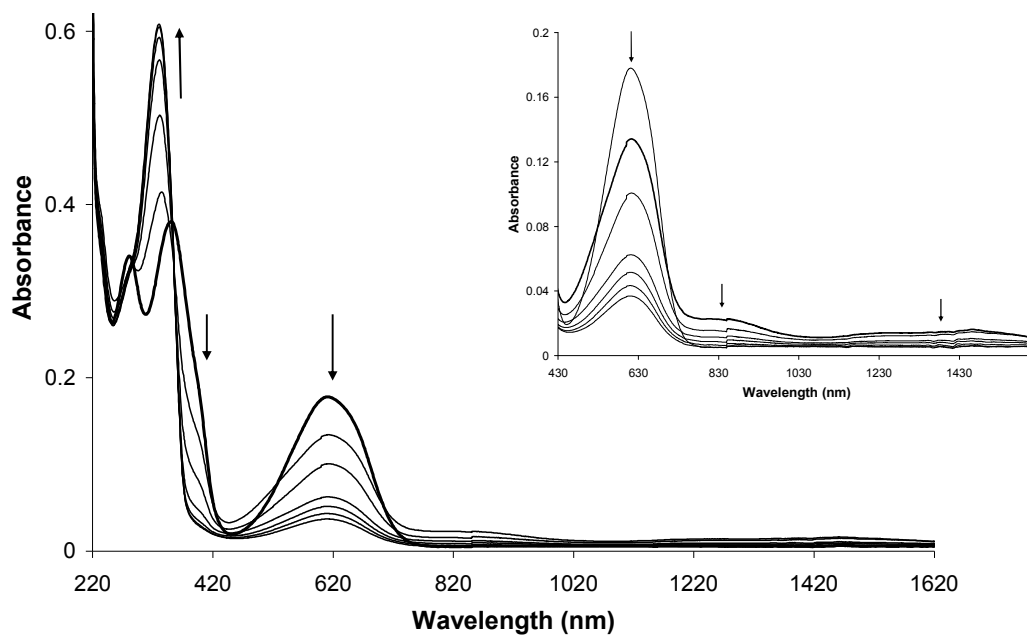
Figure 5.15: UV-vis/NIR spectrum of **2Fc,** in 0.1 M TBAPF$_6$/CH$_2$Cl$_2$, following oxidation at 1.2 V. Inset shows the same spectrum recorded between 430 and 1500 nm, showing a decrease in the absorbance band at 613 nm, and an initial low intensity absorption at 810 and 1457 nm (thick black line).

Overall, evidence of oxidative cyclisation was observed in the UV-vis/NIR spectra of **2Fo**, due to the appearance of an absorbance band at 613 nm, associated with the neutral form of the closed-ring isomer. The generation of some of the cationic species of the closed-ring was also observed in the spectra of **2Fo** and **2Fc**. However, in comparison to the results observed for the perhydro-derivatives, the formation of the closed-ring species was in low yield, and ring-opening processes were observed for both isomers at the end of the bulk electrolysis experiments. Such a result can be ascribed to the low stability of the closed-ring cationic species of **2F**, which in turn, is associated with the extent of electronic interaction existing between the two thiophene rings on the dithienylethene switch.[1]
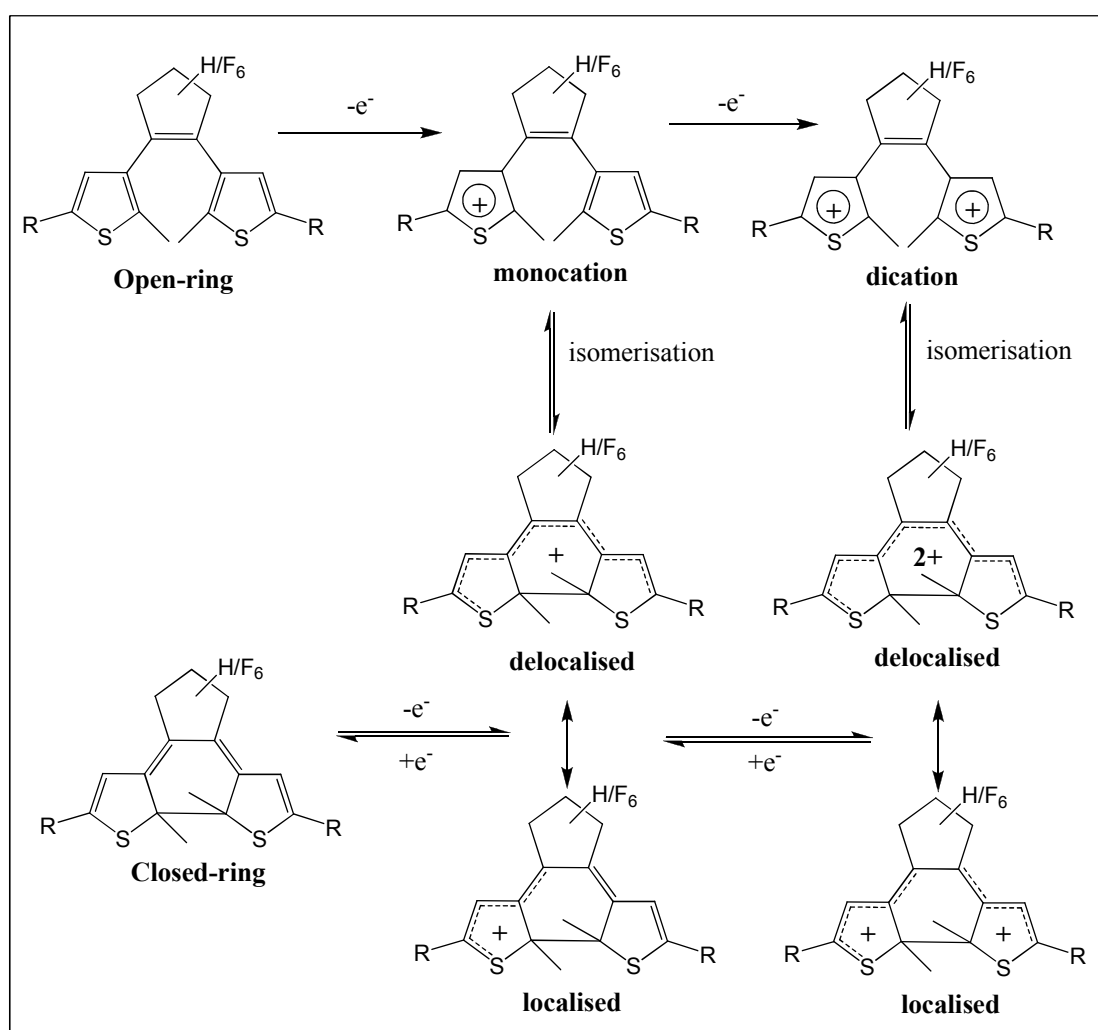
Scheme 5.2: General scheme representing the electrochemical processes of dithienylethene switches, as described by Browne et al.[1,4]

The extent of electronic communication between the thienyl units can be related to the separation between the redox waves of the monocation and dication species of the

closed form in the CV's (ΔE). The value of ΔE is considerably smaller for **2F** (*ca.* 140 mV), in comparison to the ΔE values found for the perhydro-derivatives, **1H** and **2H** (*ca.* 300 mV and 320 mV respectively). Browne et al[1,4] described a resonance structure, with delocalised charge over the entire dithienylethene unit, and localised charge on the two thiophene rings, as illustrated in scheme 5.2. The former is associated with ring-closing processes, and the later favours ring-opening processes, as described previously in section 5.3.1. The reduced stability of the oxidised species of **2F** is a consequence of the electron-withdrawing fluorine atoms on the central cyclopentene ring, which are poor at facilitating delocalisation of the charge, hence, communication between the two thiophene rings on the dithienylethene unit is decreased. Therefore, although **2F** does undergo oxidative cyclisation processes, within the timescale of the bulk electrolysis experiments, the equilibrium lies heavily on the localised side, hence oxidative cycloreversion occurs.

In the case of the perfluoro-derivative **1Fo**, the cyclic voltammetry results described an irreversible two-electron oxidation process to the dication radical **1Fo^{2+}**. The UV-vis/NIR spectroelectrochemistry experiments, performed on **1Fo** at 1.6 V, resulted in a decrease in the absorbance band at 305 nm, with a new concurrent band appearing at 237 nm, and a broad low intensity absorbance in the range 345 - 700 nm (figure 5.16). These changes can be assigned to the generation of the **1Fo^{2+}** species. As expected, there was no evidence for the ring-closed isomer **1Fc.** Subsequent reduction at 0V resulted in a decrease in the absorbance spectrum between 485 to 700 nm, however, the initial band at 305 nm did not return to the original intensity due to the irreversible nature of the oxidation process.

The similarities between the CV's of the open and closed isomers of **1F** indicated that **1Fc** underwent oxidative cycloreversion to the open form. The changes observed in the UV-vis/NIR spectrum of **1Fc**, following oxidation at 1.2 V, confirmed this result, as shown in figure 5.17. The absorbance band in the visible region at 608 nm, indicative of the closed-ring isomer, began to decrease, and a new band appeared in the UV region at 305 nm, corresponding to the absorbance band associated with the open-ring form. New bands also appeared at 242 and 442 nm, and a low intensity absorbance in the range 740-960 nm. These bands are tentatively assigned to the generation of the cationic species, of either the open or closed form of **1F** (i.e. **1Fo$^+$** or **1Fc$^+$**), or to decomposition products formed during the bulk electrolysis experiments.

However, these features cannot be exclusively designated to one particular species due to the presence of the band at 608 nm, which may mask further bands. Subsequent reduction at 0V resulted in a decrease in the bands in the visible region, and a further increase at 305 nm.
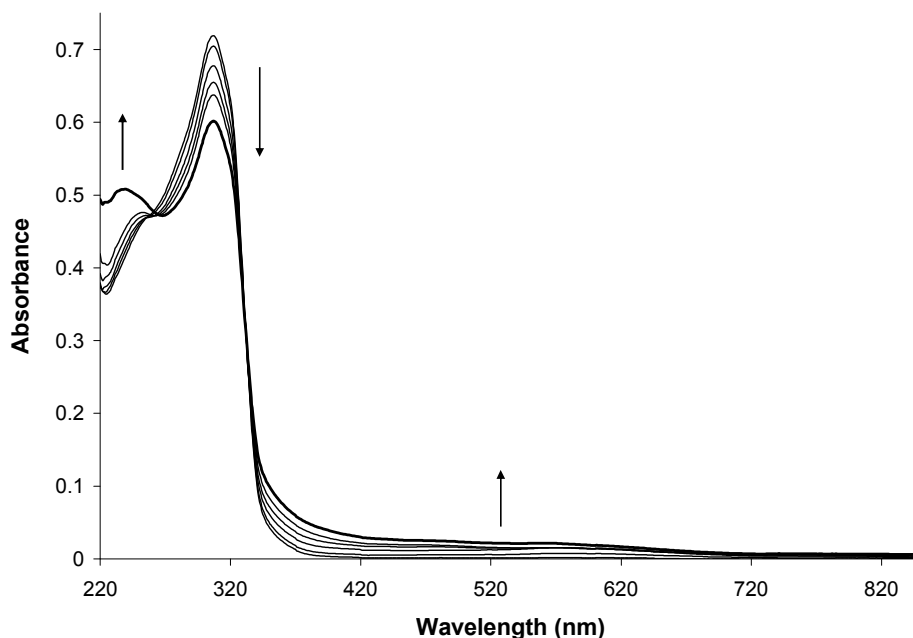
Figure 5.16: UV-vis spectrum of **1Fo** following oxidation at 1.6 V, in 0.1 M TBAPF$_6$/CH$_2$Cl$_2$.
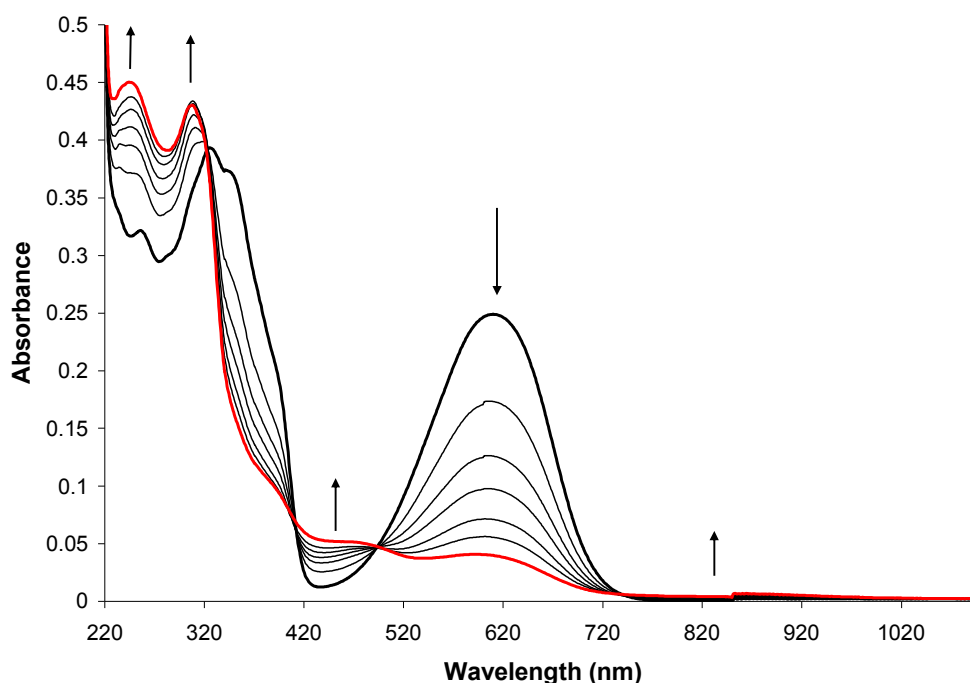
Figure 5.17: UV-vis spectrum of **1Fc**, following oxidation at 1.2 V, in 0.1 M TBAPF$_6$/CH$_2$Cl$_2$. The absorbance band at 608 nm, recorded in the initial spectrum (thick black line), decreases following oxidation at 1.2 V. The final spectrum recorded is denoted by the red line.

271

5.3.3 $Co_2(CO)_6$ Complexes: Cyclic Voltammetry

A number of literature reports have described the redox properties of alkynyl $Co_2(CO)_6$ complexes.[15-20] In this section, the electrochemical reductive and oxidative behaviour of the $Co_2(CO)_6$ complexes **3H/F** and **4H/F** are discussed. The presence of organometallic substituents on the dithienylethene switches have been reported to influence the electrochromic behaviour of such switches, by inhibiting or inducing oxidative cyclisation/cycloreversion processes.[21-23] Therefore, the oxidation processes of the $Co_2(CO)_6$ complexes **3H/F** and **4H/F** were investigated in order to examine the effects of the $Co_2(CO)_6$ moieties on the ability of the switches to undergo electrochemical ring-opening/closing isomerisation processes. The redox properties of the cobalt carbonyl complexes were examined using cyclic voltammetric techniques, in 0.1 M solutions of $TBAPF_6/CH_2Cl_2$, at room temperature, at a scan rate of 0.1 Vs^{-1}. The results were calibrated against the redox couple of decamethylferrocene $Fc*^+/Fc*$ ($E_{1/2}$ = -0.07 *vs.* SCE). The structures of the cobalt carbonyl complexes described here are illustrated in figure 5.18.
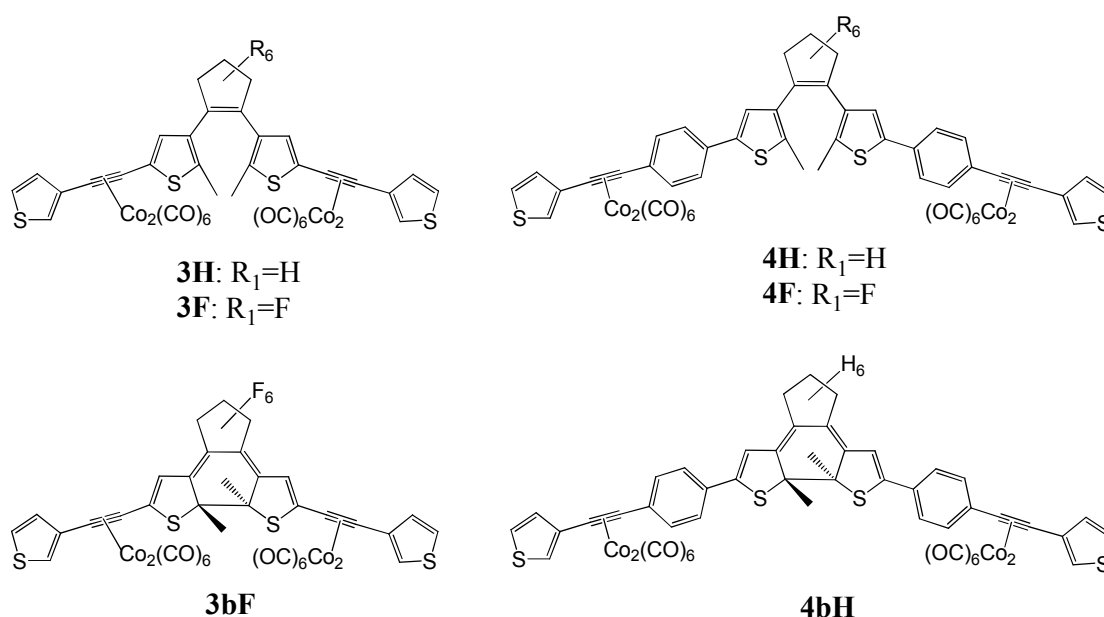
Figure 5.18: The structures of the open-ring $Co_2(CO)_6$ complexes **3H/F** and **4H/F**, and of the closed-ring $Co_2(CO)_6$ complexes **3bF** and **4bH**.

- **Reduction Process**

Alkynyl $Co_2(CO)_6$ complexes are known to undergo one-electron reduction processes, forming the radical anion $[RC_2R'Co_2(CO)_6]^{\bullet-}$, which subsequently undergoes decomposition as a result of metal-metal bond cleavage. Some of the decomposition products have been identified as $Co(CO)_4^-$, $RC_2R'Co(CO)_3$ and free alkyne.[15-19]

Our studies revealed similar results to those reported in the literature for the $Co_2(CO)_6$ complexes **3H**, **3F**, **4H** and **4F**. In each case, the cyclic voltammograms displayed a single bielectronic irreversible reduction peak, in the range of -1.09 V to -1.28 V *vs.* SCE (table 5.3), forming the corresponding dianions **3H^{2-}**, **3F^{2-}**, **4H^{2-}** and **4F^{2-}**. Hence, the reduction peak represents a one-step two-electron process, due to a one-electron reduction of each of the two $Co_2(CO)_6$ units. Following the formation of the radical anions, disintegration of the $Co_2(CO)_6$ units occurred for each complex, as evidenced by the appearance of new irreversible oxidation peaks in the subsequent anodic sweeps.

Table 5.3: The cyclic voltammetry results of the reduction processes of **3H/F**, **4H/F**, **3bF** and **4bH**.

Compound	E_{pc} (V)	E_{pa} (V)
3H	-1.28[a]	-0.83[a], -0.33[a], -0.22[a], -0.07[a]
4H	-1.20[a]	-0.63[a], -0.14[a]
4bH	-1.12[a]	-0.58[a], -0.08[a], +0.06[a]
3F	-1.09[a], -0.35	-0.57[a], +0.10[a]
3bF	-0.86[a], -1.01[b]	-0.90[b], +0.06[a]
4F	-1.12[a]	+0.06[a]

All values listed are values of potential (V) *vs.* SCE, recorded in 0.1 M TBAPF$_6$/CH$_2$Cl$_2$, at 0.1 Vs^{-1}.
[a] indicates an irreversible oxidation
[b] indicates a quasi-reversible oxidation

The perfluorinated switches (**3F** and **4F**) underwent reduction processes at less negative potentials in comparison to their corresponding perhydro analogues (**3H** and **4H**). This can be attributed to the electron-withdrawing ability of the fluorine atoms, which help to stabilise the radical anion. Therefore, the reduction process of **3F** occurred at the least negative potential (-1.09 V), while the perhydro-derivative **3H** occurred at the most negative potential (-1.28 V), as shown in figure 5.19. The phenyl groups in **4F** and **4H** separate the alkynyl cobalt carbonyl unit and the cyclopentene switch, hence the influence of the hydrogen and fluorine atoms was decreased. Thus,

the reduction of **4F** occurred at a lower potential (-1.12 V) when compared to **3F**, whereas **4H** was reduced at a higher potential (-1.20 V) relative to **3H**. There appeared to be a greater amount of decomposed products for the fluorinated complexes. This is evidenced by the relative intensities of the oxidation peaks attributed to the disintegration products, as illustrated for **3H** and **3F** in figure 5.19. The CV's of **3H** and **4H** displayed very small oxidation peaks, following the reduction process. On the other hand, the perfluoro-derivative **3F** resulted in a relatively intense oxidation peak at 0.10 V, with a corresponding reduction peak at -0.35 V, and another oxidation peak present at -0.57 V. These peaks are tentatively assigned to the formation of the $Co(CO)_4^-$ and $RC_2R'Co(CO)_3$ species, from reference to the literature.[15-17,19,24] An oxidation peak was observed at 0.06 V in the CV of **4F**, following the reduction process, which is also tentatively assigned to the formation of the $Co(CO)_4^-$ species.
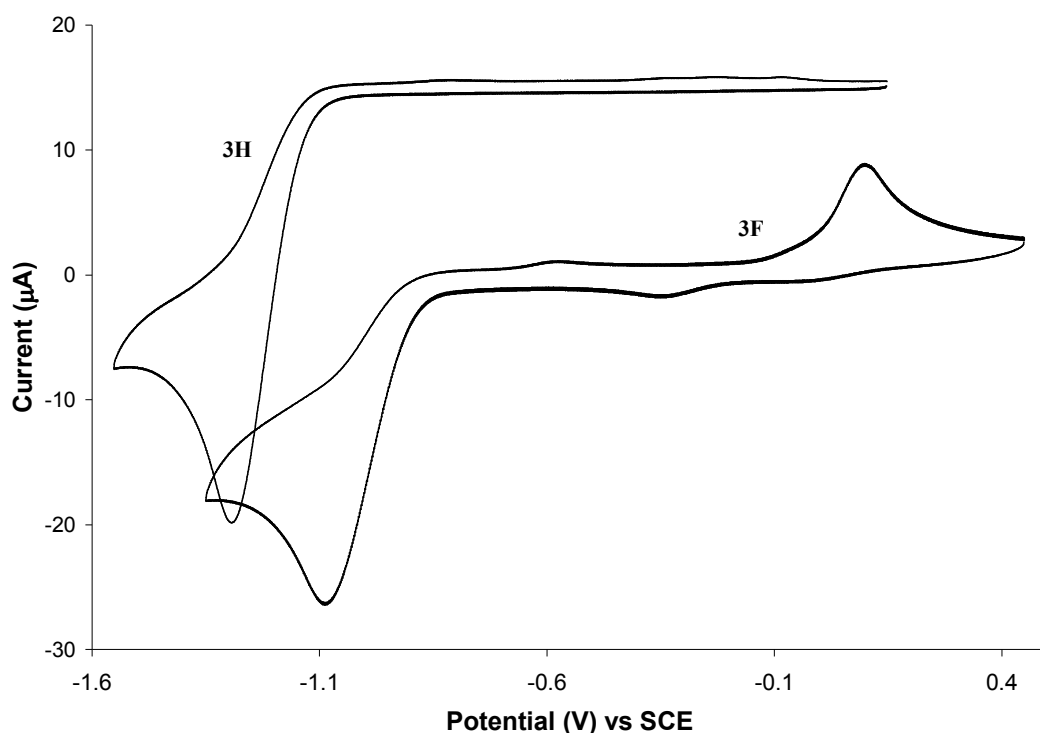
Figure 5.19: Cyclic voltammogram of the reduction of **3F** (bottom) and **3H** (top), in 0.1 M TBAPF$_6$/ CH$_2$Cl$_2$, at a scan rate of 0.1 Vs^{-1}. The CV of the **3H** is offset along the coordinate for clarity.

The reductions of the closed-ring $Co_2(CO)_6$ complexes **3bF** and **4bH** were also examined. A single bielectronic irreversible reduction peak was observed for **4bH**, which was anodically shifted by 80 mV in comparison to its open-ring isomer **4H**.

274

This can be attributed to the extended π-conjugation of the system in **4bH**, which helps to stabilise the radical anion of the $Co_2(CO)_6$ units. The subsequent anodic sweep for **4bH** displayed an oxidation peak at 0.06 V, tentatively assigned to the generation of $Co(CO)_4^-$ product.[15-17,19,24] The closed-ring isomer **3bF** was also anodically shifted (ΔE = 230 mV) in comparison to its corresponding open-ring isomer **3F**, and an oxidation peak was observed at 0.6 V in the subsequent anodic sweep, indicative of the $Co(CO)_4^-$ species. Furthermore, in contrast to **3F**, two monoelectronic reduction waves were observed for **3bF** at E_{pc} = -0.86 and -1.01 V, separated by ΔE = 175 mV, as shown in figure 5.20. The reduction peak at -1.01 V was found have a corresponding oxidation peak at -0.90 V. This result suggests that the π-conjugated backbone of the closed-ring isomer, **3bF**, facilitated stronger electronic-communication between the two $Co_2(CO)_6$ moieties,[15,20] compared to the open-ring isomer **3F**. Therefore, **3F** has the potential to act as a molecular wire, with the ability to turn the communication between the metal centres ON (closed-form) and OFF (open-form). Similar results have been reported in the literature for other dithienylethene switches substituted with metal carbonyl and phosphine ligand complexes.[21,22,25]
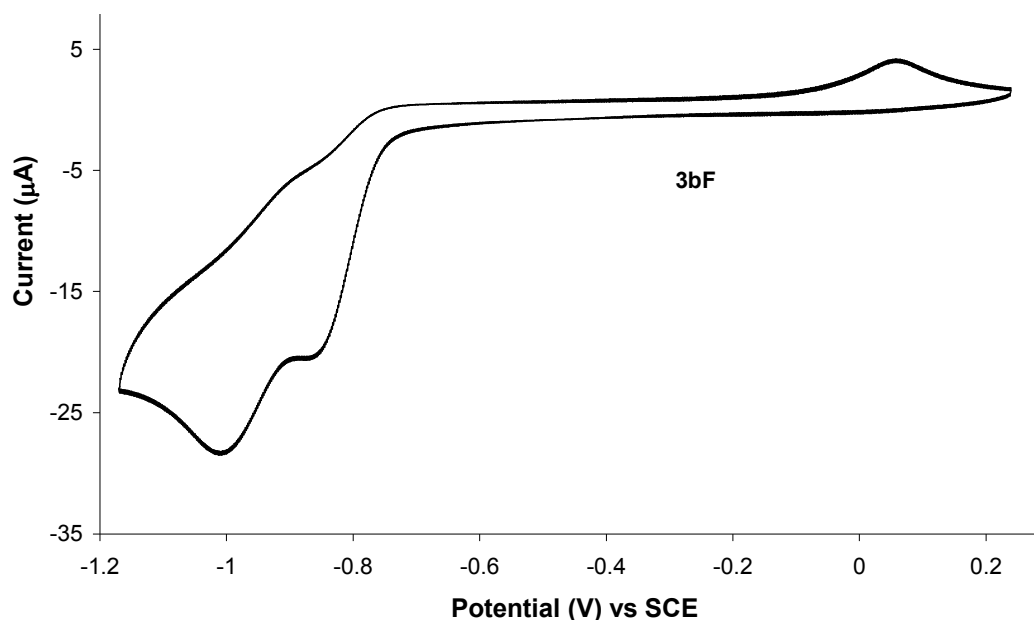
Figure 5.20: Cyclic voltammogram of the reduction process of the closed-ring $Co_2(CO)_6$ complex **3bF**, in 0.1 M $TBAPF_6/CH_2Cl_2$, at a scan rate of 0.1 Vs^{-1}.

The fact that a single bielectronic reduction wave was observed for **4bH** demonstrates that ring-closure of this complex did not increase the electronic interaction between

the metal centres. This is possibly due to the presence of the phenyl rings, thus increasing the length of the bridge between the $Co_2(CO)_6$ moieties, and hence reducing the interaction between the metal centres.[24] The presence of hydrogen atoms on the cyclopentene ring could also be a factor as hexafluoro DTE bridges have been found to facilitate stronger electronic communication between two metal centres.[21]

- **Oxidation Process**

The electrochemistry results of the thienyl-based free ligand switches described oxidative cyclisation of **1H**, **2H** and **2F**, and oxidative ring-opening of **1F**. Alkynyl $Co_2(CO)_6$ complexes are known to undergo one-electron irreversible oxidation processes, forming the corresponding cation radical $[RC_2R'Co_2(CO)_6]^{\bullet+}$. In general, oxidation of $Co_2(CO)_6$ moieties occur in the range $0.9 - 1.4$ V, and severe fouling of the electrode surface at higher oxidation potentials has been reported.[15,17,26] Therefore, this section focuses on how the oxidative processes of the $Co_2(CO)_6$ moieties influence the electrochromic behaviour of the switching units.

Table 5.4: Cyclic voltammetric data for the $Co_2(CO)_6$ complexes **3H/F**, **4H/F**, **3bF** and **4bH**, and their corresponding free ligands.

Compound	Oxidation Processes	
	E_{pa} **(V)**	E_{pc} **(V)**
1Ho	0.65^{rc}, 0.95^{rc}, 1.55^{a}	0.60^{rc}, 0.88^{rc}
3H	0.59^{rc}, 0.78^{rc}, 1.21^{a}, 1.41^{a}	0.50^{rc}, 0.70^{rc}
2Ho	0.50^{rc}, 0.82^{rc}, 1.23^{a}	0.42^{rc}, 0.75^{rc}
4H	0.55^{rc}, 0.84^{rc}, 1.23^{a}, 1.46^{a}	0.47^{rc}, 0.75^{rc}
4bH	0.52^{rc}, 0.80^{rc}, 1.37^{a}	0.42^{rc}, 0.71^{rc}
1Fo	1.71^{a}	-
1Fc	1.13^{b}	0.89^{b}
3F	1.23^{a}, 1.75^{a}	-
3bF	0.99^{b}, 1.73^{a}	0.89^{b}
2Fo	0.99^{rc}, 1.11^{rc}, 1.63^{a}	0.92^{rc}, 1.07^{rc}
4F	1.17^{a}, 1.58^{a}	-

All values listed are values of potential (V) *vs*. SCE, recorded in 0.1 M $TBAPF_6/CH_2Cl_2$, at 0.1 Vs^{-1}.
[a] indicates an irreversible oxidation process
[b] indicates a quasi-reversible oxidation process
[rc] indicates peaks assigned to ring-closed species

The results obtained from the cyclic voltammograms of the $Co_2(CO)_6$ complexes **3H/F** and **4H/F** are summarised in table 5.4. The data obtained from the CV's of the corresponding free ligand switches are listed in this table also, for comparative purposes. Oxidation processes of the $Co_2(CO)_6$ components on **3H/F** and **4H/F** were found to occur in the potential range from 0.9 to 1.71 V. Each open-ring complex displayed a single irreversible oxidation peak, representing a one-step two-electron oxidation process i.e. one-electron oxidation reaction of each of the two $Co_2(CO)_6$ units.
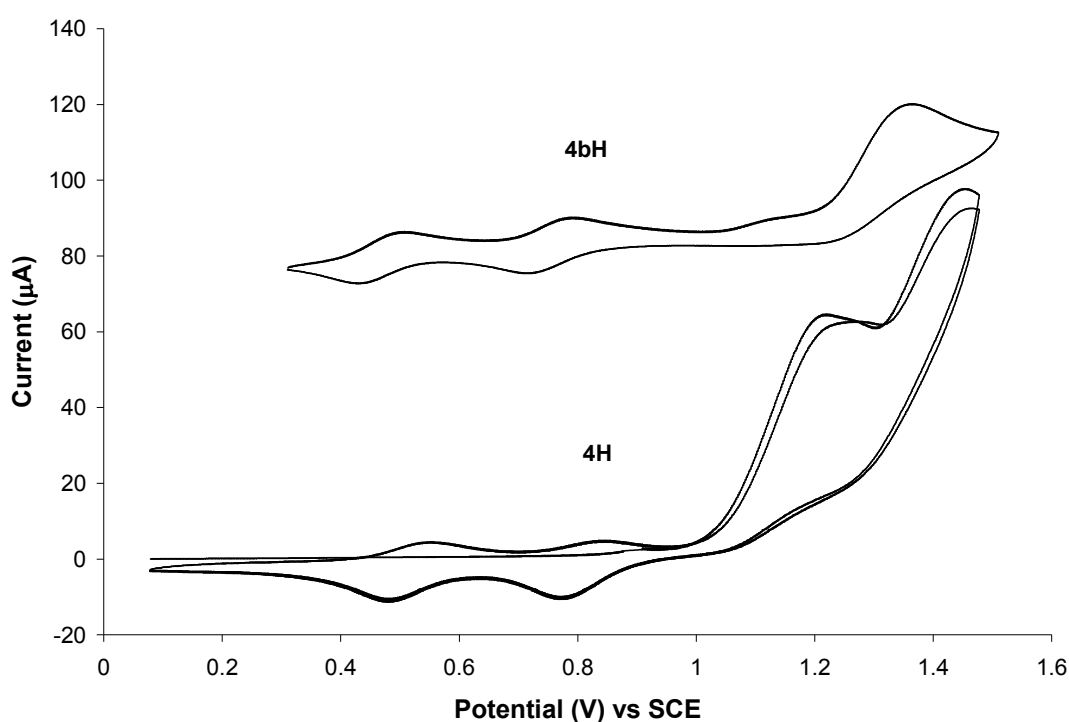
Figure 5.21: Cyclic voltammogram of the oxidation process of the open-ring isomer **4H** (bottom), and the closed-ring isomer **4bH** (top), in 0.1 M TBAPF$_6$/CH$_2$Cl$_2$, at a scan rate of 0.1 Vs^{-1}. The CV of **4bH** is offset along the coordinate for clarity.

Oxidative cyclisation was found to occur for the perhydro-derivatives **1Ho** and **2Ho**, and was also achieved for their corresponding $Co_2(CO)_6$ complexes (**3H** and **4H**, respectively). In the case of **4H**, an irreversible oxidation peak was observed at 1.23 V (*vs.* SCE), which was followed by two redox waves at $E_{1/2} = 0.51$ and 0.80 V in the subsequent cathodic and anodic cycles, indicative of the ring-closed isomer. Therefore, it can be concluded that oxidative cyclisation to the closed-ring isomer occurred for **4H**, in the same manner as described previously for the free ligand **2H**. After a number of consecutive sweeps, the CV was found to be stable, with no

significant changes observed in the oxidation waves. Following oxidation at higher potentials, a second irreversible oxidation peak was observed at 1.46 V, as shown in figure 5.21, which can be assigned to the oxidation process of the $Co_2(CO)_6$ moieties. After a number of consecutive sweeps, the oxidation peaks at 1.23 and 1.46 V decreased dramatically, indicating disintegration of the $Co_2(CO)_6$ units, resulting in fouling of the electrode.

Cyclic voltammetry was also carried out on the corresponding closed-ring $Co_2(CO)_6$ complex **4bH**. Two redox waves were observed at $E_{1/2}$ = 0.47 and 0.76 V (*vs.* SCE), indicative of the reversible formation of the monocation **4bH⁺** and dication **4bH²⁺** species, respectively. At higher potentials, an irreversible oxidation peak was observed at 1.37 V, representing the oxidation process of the $Co_2(CO)_6$ units (figure 5.21). In comparison to the open-ring isomer, the potential at which the cobalt carbonyl moieties were oxidised was cathodically shifted by 90 mV, due the stabilising effect of the extended π-conjugated system, in the closed-form, on the cationic species.

The separation between the oxidation waves of the monocation and dication species of the closed form was found to be $\Delta E \approx 280$ mV for the open and closed-ring $Co_2(CO)_6$ complexes, **4H** and **4bH** respectively. This value is similar to that recorded for the free ligand switch **1H** ($\Delta E \approx 300$ mV), therefore, the presence of the $Co_2(CO)_6$ units had little effect on the stability of the complex.

In the case of **3H**, an irreversible oxidation process of the $Co_2(CO)_6$ moieties took place at 1.21 V, followed by an oxidation process at 1.41 V, which can be attributed to a two-electron oxidation process of the thienyl units on the dithienylethene switch. The subsequent cathodic and anodic sweeps displayed two new redox waves at $E_{1/2}$ = 0.55 and 0.74 V, as shown in figure 5.22. As described previously for the free ligand **1H**, these new redox waves can be attributed to the reversible formation of the monocation and dication species of the closed-ring isomer. Hence **3H** underwent oxidative cyclisation to the closed form. The most prominent effect of the $Co_2(CO)_6$ moieties, on the electrochemical behaviour of this switch, was the anodic decrease in the potential at which the dithienylethene unit was oxidised, in comparison to the free ligand **1Ho** (ΔE = 140 mV). It would be expected that the electron-withdrawing ability of the oxidised cobalt carbonyl moieties would have the opposite effect, and shift the oxidation potential of the switch to higher values. Therefore, the fact that

oxidation of the $Co_2(CO)_6$ components and the dithienylethene switch occurred in quick succession, may suggest that intramolecular electron transfer from the oxidised cobalt carbonyl units to the switching unit occurred. Thus, a cyclisation process was induced, followed by re-oxidation of the metal carbonyls in the consecutive sweeps, and so forth. Also noted, was a decrease in the separation between the oxidation waves of the closed-ring cations, with $\Delta E = 300$ mV for the free ligand **1H**, and $\Delta E = 190$ mV for the $Co_2(CO)_6$ complex **3H**. This is indicative of a decrease in the stability of the cationic species of the closed-ring isomer due to the presence of the cobalt carbonyl moieties. Conversely, the ΔE value recorded for **4H** was found to be similar to that of its related free ligand **2H**. Therefore, the result obtained for **3H** can be ascribed to the consequence of the metal groups undergoing oxidation processes prior to the switching unit. Furthermore, after a number of consecutive sweeps, fouling of the electrode occurred due to decomposition of the $Co_2(CO)_6$ units.
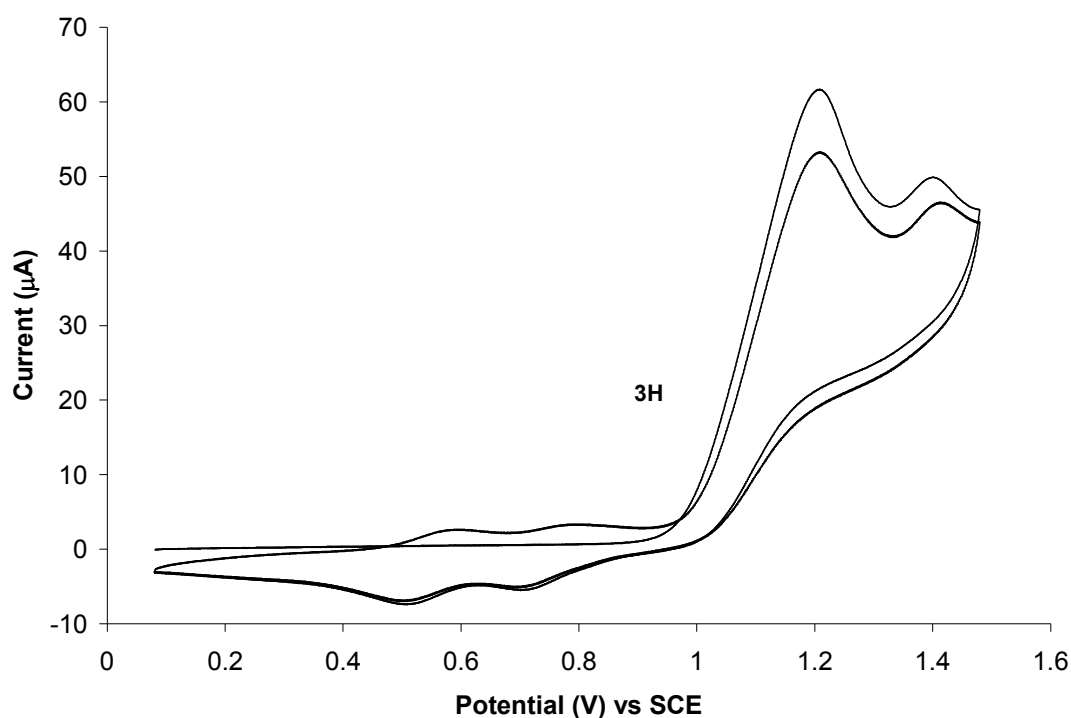
Figure 5.22: Cyclic voltammogram of the oxidation process of the $Co_2(CO)_6$ complex **3H**, in 0.1 M TBAPF$_6$/CH$_2$Cl$_2$, at a scan rate of 0.1 Vs^{-1}.

In the case of the perfluoro analogue, **3F**, the cyclic voltammogram displayed two irreversible oxidation peaks at 1.23 V and 1.75 V (*vs.* SCE), representing a two-electron oxidation process of the $Co_2(CO)_6$ moieties (i.e. one-electron oxidation of

each of the two $Co_2(CO)_6$ units), and a two-electron oxidation process of the dithienylethene unit, respectively. There was no evidence of oxidative cyclisation occurring in the subsequent sweeps (figure 5.23), which is in-keeping with the result obtained for the free ligand **1F**, in which case oxidative cycloreversion, from the closed to the open form, was observed.
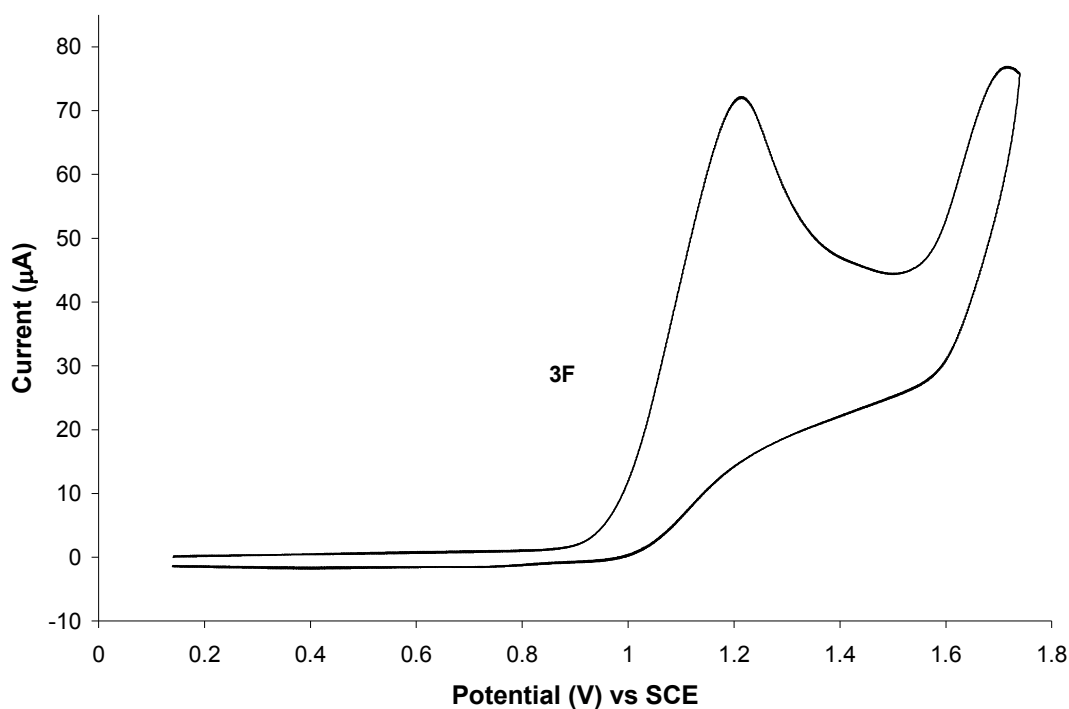
Figure 5.23: Cyclic voltammogram of the oxidation process of the open-ring $Co_2(CO)_6$ complex **3F**, in 0.1 M $TBAPF_6/CH_2Cl_2$, at a scan rate of 0.1 Vs^{-1}.

The electrochemical oxidation process of the corresponding closed-ring $Co_2(CO)_6$ complex (**3bF**) was also investigated. Following oxidation of **3bF**, a quasireversible oxidation wave was observed at $E_{1/2} = 0.94$ V ($i_{pc}/i_{pa} \approx 0.75$). This oxidation peak corresponds with the first oxidation peak of the closed-ring isomer of the free ligand **1Fc** ($E_{1/2} = 1.01$ V), as shown in figure 5.24. Therefore, the redox wave at $E_{1/2} = 0.94$ V, can be assigned to the oxidation of the closed-ring dithienylethene switch, forming the monocation species **3bF$^+$**. The fact that the oxidation wave of **3bF** is more reversible then its corresponding free ligand, indicates that the presence of the $Co_2(CO)_6$ moieties stabilises the closed-ring isomer, and hence prevents/slows down the ring-opening process. At higher potentials an irreversible oxidation wave was also observed at 1.71 V. This is attributed to oxidation of the $Co_2(CO)_6$ units. In comparison to the open-ring isomer **3F**, the oxidation process of the cobalt carbonyl

groups is anodically shifted by 480 mV. This could possibly be attributed to the fact that the first oxidation process makes the second oxidation process more difficult, hence higher potential values are required to incur oxidation of the metal centres.
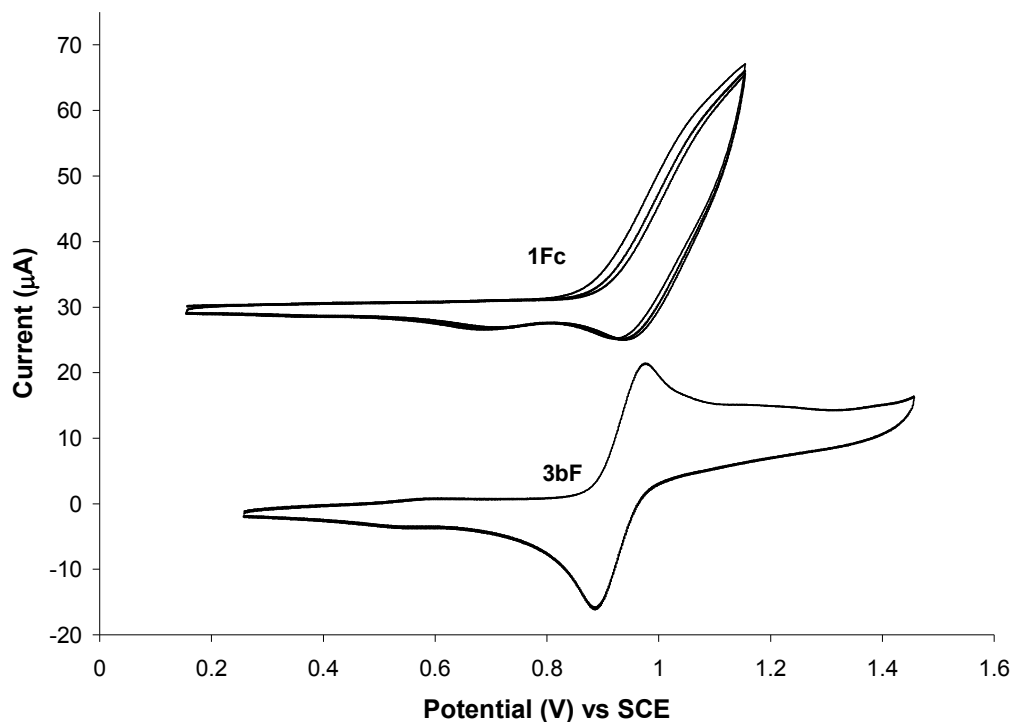
Figure 5.24: Cyclic voltammogram of the oxidation of the closed-ring $Co_2(CO)_6$ complex **3bF** (bottom), and the closed-ring isomer of the corresponding free ligand **1Fc** (top), in 0.1 M $TBAPF_6/CH_2Cl_2$, at a scan rate of 0.1 Vs^{-1}. The CV of the **1Fc** is offset along the coordinate for clarity.

In the case of the more conjugated perfluoro-derivative **4F**, an irreversible oxidation wave was observed at 1.17 V (*vs.* SCE), which is assigned to the two-electron oxidation process of the $Co_2(CO)_6$ moieties. At higher potentials, a second irreversible oxidation process was observed at 1.58 V, corresponding to the two-electron oxidation process of the dithienylethene unit. The peak at 1.58 V corresponds with the oxidation potential found for the free ligand **2Fo** (E_{pa} = 1.64 V). However, in contrast to the oxidation process of the free ligand **2Fo**, oxidative cyclisation was not observed for **4F**. This phenomenon may be explained as follows:

1) Inhibition of the cyclisation process of **4F** may be due to the order in which the dithienylethene switch and the cobalt carbonyl moieties were oxidised. In the case of **4H**, the switching unit underwent oxidation at a lower potential than the cobalt carbonyl units. In comparison, oxidation of the $Co_2(CO)_6$ components occurred before the dithienylethene switch of **4F**. Similar results have been reported for other

organometallic switches in the literature,[23] whereby the electrochromic properties of the switch were dependent on the potentials at which the metals were oxidised.

2) Although oxidation of the $Co_2(CO)_6$ moieties occurred prior to the dithienylethene unit in the case of **3H**, the results indicated that an intramolecular electron transfer process, from the metal groups to the switch, induced cyclisation. However, such a process may be inhibited for **4F** due to the presence of the phenyl rings, separating the cobalt carbonyl moieties and the switch, thus preventing electron transfer through the longer carbon chain.

3) As discussed in the previous section 5.3.2, the closed-ring cationic species of the free ligand **2F** was found to be much less stable in comparison to the perhydro analogues **1H** and **2H**. Oxidation of the $Co_2(CO)_6$ moieties increases their electron-withdrawing effect, and therefore, together with the electron-withdrawing fluorine atoms on the cyclopentene ring, it is possible that the open-ring cationic species becomes more stable than the closed-ring cations, thus preventing ring-closure.

Finally, a common effect of the $Co_2(CO)_6$ units on the electrochemical processes of the switches was observed. The CVs of the free ligand switches **1H**, **1F** and **2F** displayed redox waves at low potentials which were attributed to the generation of a new electroactive species **1Hy**, **1Fy** and **2Fy**. However, in the CVs of the corresponding metal carbonyl complexes (**3H**, **3F** and **4F**) such redox waves did not appear. Therefore, it is apparent that the presence of the $Co_2(CO)_6$ moieties inhibited the electrochemical rearrangement processes of the switches.

5.3.4 $Co_2(CO)_6$ Complexes: UV-vis/NIR Spectroelectrochemistry

The cyclic voltammetry experiments performed on the $Co_2(CO)_6$ complexes showed that oxidative cyclisation occurred for the perhydro-derivatives **3H** and **4H**, but not in the case of their corresponding perfluorinated analogues **3F** and **4F**. The oxidation of the $Co_2(CO)_6$ complexes were investigated further using UV-vis/NIR spectroelectrochemistry techniques, in 0.1 M $TBAPF_6/CH_2Cl_2$, *vs.* Ag/Ag^+. The structures of the switches discussed in this section are illustrated in figure 5.25, and the absorption bands obtained in the UV-vis/NIR spectra, following bulk electrolysis, are summarised in table 5.5. The data obtained from the corresponding free ligand switches is also presented in table 5.5 for comparative purposes.

Table 5.5: UV-vis/NIR spectroelectrochemistry data of the free ligand switches **1H/F** and **2H/F**, and their corresponding $Co_2(CO)_6$ complexes **3H/F** and **4H/F**, following oxidation processes at varying potentials.

		Free Ligand Switches			$Co_2(CO)_6$ Complexes	
	Ox (V)	λ_{abs} (nm)			Ox (V)	λ_{abs} (nm)
1Ho	Start	290, 310		**3H**	Start	274, 330, 450-670
	1.3 V	455, 566, 666			1.3V	466, 571, 671
	1.6 V	469, 575, 666, 867				
2Ho	Start	334		**4H**	Start	267, 341, 620-650
	1.4 V	471, 590(sh), 657			1.0 V	481, 576, 655, 778
					1.0.V	472, 576(sh), 655
2Hc	Start	326, 560		**4bH**	Start	262, 323, 577
	0.6 V	442, 781, > 1030			0.6 V	323, 459, 807, 1030-1620
	0.9 V	467, 590(sh), 654			0.9 V	332, 567, 661
1Fo	Start	305		**3F**	Start	275, 330, 410-630
	1.6 V	237, 345-700			1.0V	303
1Fc	Start	327, 608		**3bF**	Start	263, 358, 578, 658
	1.2V	242, 305, 442, 740-960			0.8-1.6V	300, 590
2Fo	Start	328		**4F**	Start	273, 323, 430-700
	1.8 V	613, 780-1100			1.4 V	273↓, 323↓, 430-700↓

The data was recorded in 0.1 M $TBAPF_6/CH_2Cl_2$ *vs.* Ag/Ag^+
↓ indicates decreasing of absorbance band
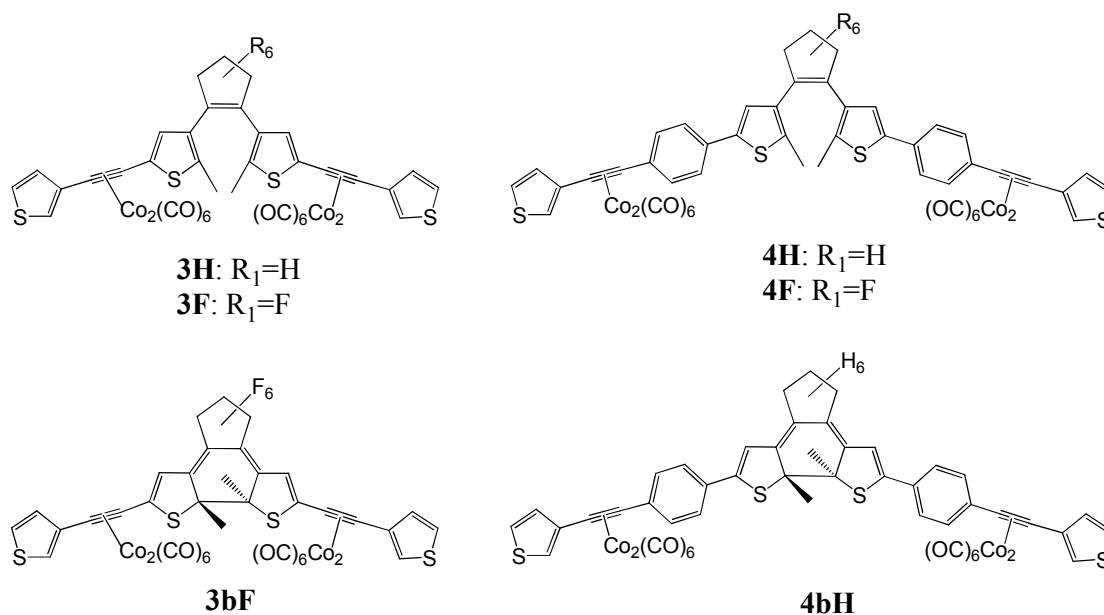
Figure 5.25: The structures of the open-ring $Co_2(CO)_6$ complexes **3H/F** and **4H/F**, and of the closed-ring $Co_2(CO)_6$ complexes **3bF** and **4bH**.

The changes observed in the UV-vis spectrum of the open-ring $Co_2(CO)_6$ complex **4H**, following oxidation processes at 1.0 V, are illustrated in figure 5.26. Bleaching of the original bands at 267 and 341 nm was observed, in conjunction with the appearance of new bands at 481, 655, 778 nm and a λ_{max} at 576 nm. Such changes are indicative of an oxidative cyclisation process of **4H**, as observed for the related free ligand switch **2H**. Therefore, these bands can be assigned to the formation of the monocation (778 nm), dication (481 and 655 nm) and the neutral (576 nm) species of the closed-form. Overtime, the absorbance bands at 481 and 655 nm increased, which is attributed to an increase in the formation of the dication species of the closed form. As the bands in the visible region began to decrease, following reduction at 0 V, the spectral features of the monocation species **4H$^+$** became more apparent, with absorption bands present at 444 and 782 nm. At the end of the experiment, the band at 267 nm did not return to its original intensity, suggesting that decomposition of the $Co_2(CO)_6$ moieties occurred under the electrochemical conditions employed here. The original absorbance at 341 nm recovered however, a band corresponding to the generation of the neutral form of the closed-ring isomer was not observed in the visible region, with a weak absorbance in the region 440 - 665 nm. Such a result can be assigned to the instability of the closed-ring cationic species over the timescale of the bulk electrolysis processes, hence resulting in ring-opening.
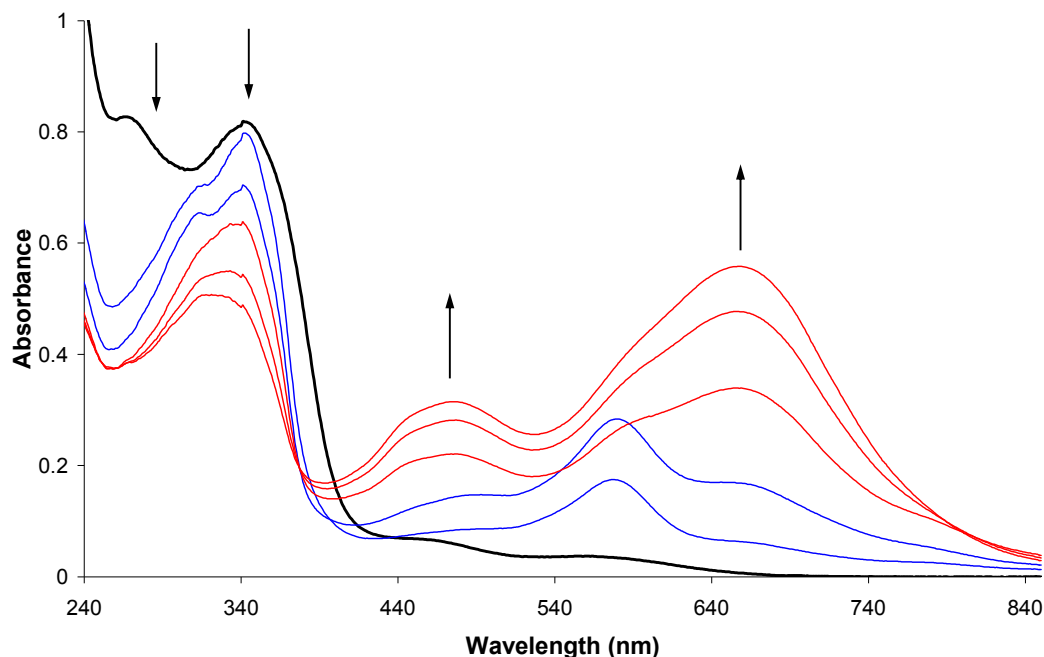
Figure 5.26: The UV-vis spectrum of the $Co_2(CO)_6$ complex **4H**, following oxidation at 1.0 V: The spectrum recorded at the start (black line); the initial increase in absorbance at 481, 655, 778 nm (blue lines); further increase in absorbance with λ_{max} = 481 and 655 nm (red lines).

Upon oxidation of the closed-ring $Co_2(CO)_6$ complex **4bH**, at 0.6 V, the band at 577 nm depleted as new bands appeared at 459 and 807 nm, with a broad absorption band in the NIR region, extending from 1030 - 1620 nm. These changes are associated with the formation of the monocation radical **4bH$^+$**. When the oxidation potential was increased to 0.9 V, the original band in the UV region at 323 nm increased and was red-shifted to 332 nm, whilst the band at 262 decreased marginally. The new bands at 459, 807 and > 1030 nm decreased, with concomitant formation of new absorbance bands at 567 and 661 nm, corresponding with the formation of the dication species **4bH^{2+}**. These changes are shown in figure 5.27, and are comparable to the results obtained for the corresponding free ligand **2Hc**. However, the absorbance at 567 was more intense then at 661 nm, suggesting that the dication species **4bH^{2+}** was too unstable to generate a significant amount. Also, the band at 567 nm is associated with the absorbance band of the closed-isomer of the free ligand, indicating that decomposition of the $Co_2(CO)_6$ moieties occurred and the free ligand was formed. Further evidence of this was found following subsequent reduction processes at 0 V, with the band at 332 nm continuing to increase in absorbance. At 0 V, a decrease in the bands in the visible region was also observed. Hence the oxidation process of **4bH** is not reversible, and appears to result in ring-opening and decomposition of the

Co$_2$(CO)$_6$ units, possibly regenerating the ring-open isomer of the free ligand **2H**. These results are similar to those obtained for the corresponding open-ring isomer **4H**.
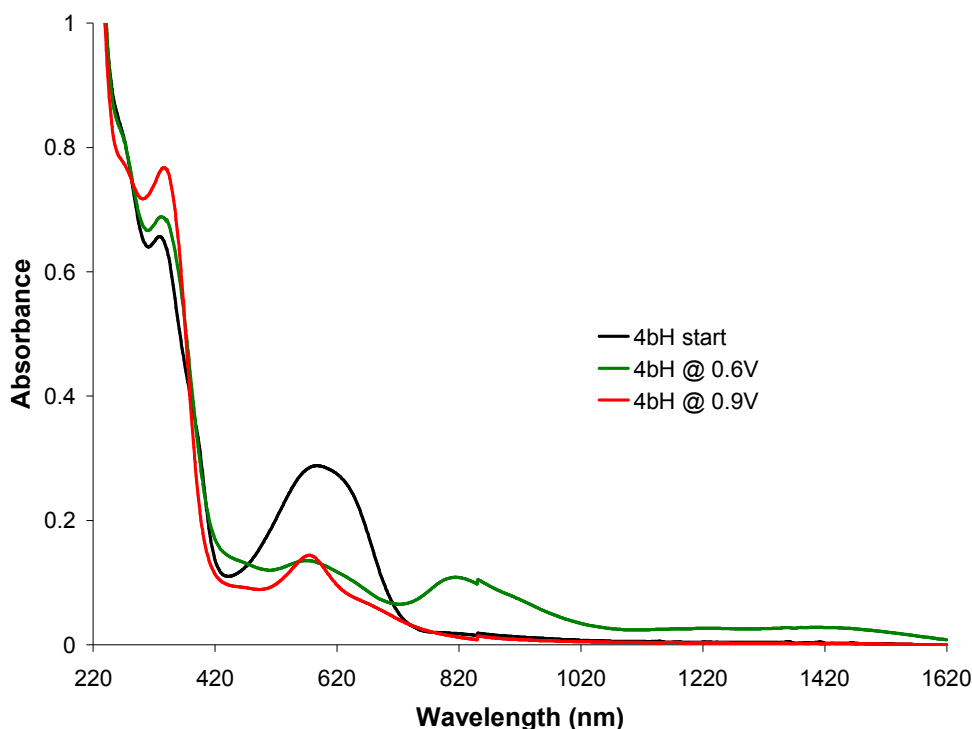
Figure 5.27: The UV-vis/NIR spectrum of the closed-ring Co$_2$(CO)$_6$ complex **4bH** (black line), following oxidation; at 0.6 V (green line), resulting in generation of the monocation species **4bH**$^+$ at 459, 807 and 1030 - 1620 nm; and at 0.9 V (red line), resulting in generation of the dication species **4bH**$^{2+}$ (660 nm) and the neutral form (567 nm).

Oxidation of **3H** at 1.3 V resulted in a decrease in the UV-vis absorption bands at 274 and 330 nm. New absorbance bands were found to grow-in in the visible region at 466, 571 and 671 nm, as shown in figure 5.28. By comparison to the results obtained for the corresponding free ligand switch **1H**, these changes can be attributed to the generation of the dication species of the closed-ring isomer. There was no evidence of the formation of the monocation, as no new bands appeared at $\lambda > 730$ nm. This could possibly be a consequence of the hypothesis proposed from the CV results of **3H**, whereby intramolecular electron transfer from the Co$_2$(CO)$_6$ moieties induced cyclisation. Such a process would lead to a two-electron oxidation of the switch, therefore generation of the monocation would not be expected. Reduction at 0 V resulted in a decrease in the bands in the visible region, and a slight increase in the bands in the UV region at 274 and 330 nm. However, these bands did not return to their initial intensity, and no new band, representative of the closed-ring isomer, was obvious in the visible region. Therefore, it can be concluded that although cyclisation to the closed-ring isomer occurs for **3H**, the cations formed during the oxidation

process were too unstable to generate the neutral closed-ring isomer. Also, decomposition of the $Co_2(CO)_6$ occurred, as evidenced by the irreversible decrease in the bands in the UV region.
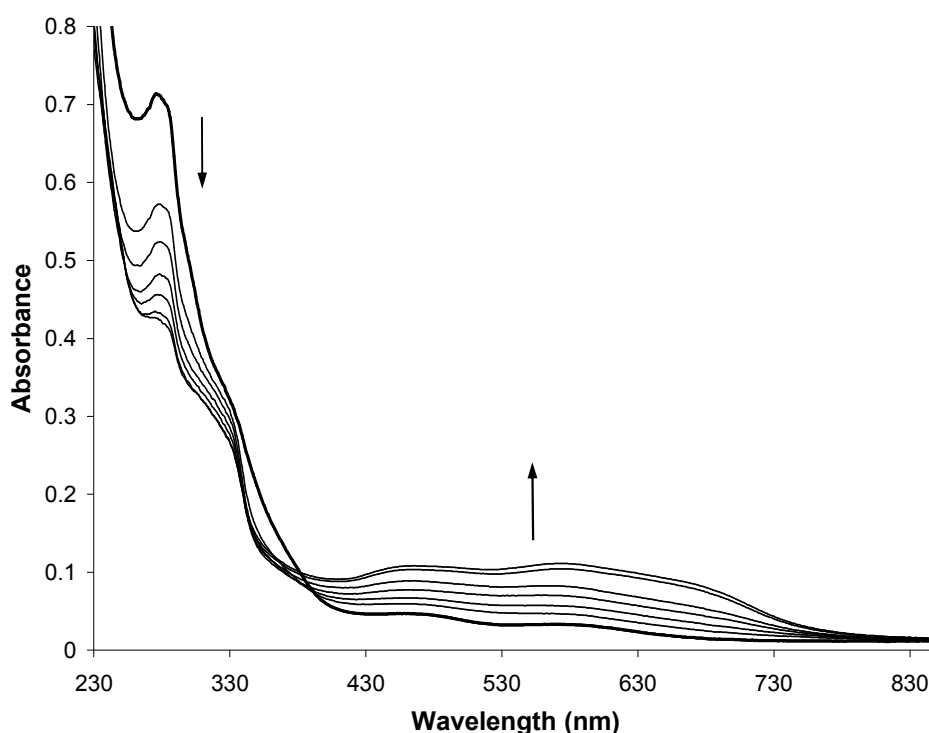
Figure 5.28: The UV-vis/NIR spectrum of the $Co_2(CO)_6$ complex **3H** (thick black line), following oxidation at 1.0 V, resulting in a decrease in the UV-region and an increase in the visible region at λ_{max} = 466, 571 and 671 nm, due to the generation of the dication species of the closed-ring isomer.

In the case of the perfluoro-derivatives, **3F** and **4F**, there was no evidence of oxidative cyclisation in the cyclic voltammetry studies. The UV-vis/NIR spectro-electrochemistry experiments confirmed this result. In the case of **3F**, the UV-vis spectrum displayed bands at 275 and 330 nm, and a low-lying absorbance band extending from approximately 410 to 630 nm. Following oxidation at 1.0 V, all of the original absorbance bands began to decrease, and a new band began to grow-in at 303 nm. This was found to be an irreversible process, with only a further increase in the band at 303 nm occurring after a potential of 0 V was applied to the solution. This result suggests that cleavage of the cobalt carbonyl moieties occurred during the oxidation processes, and the corresponding free ligand **1F** was regenerated, as demonstrated in figure 5.29. A similar result was obtained for the more-conjugated perfluoro-derivative **4F**.
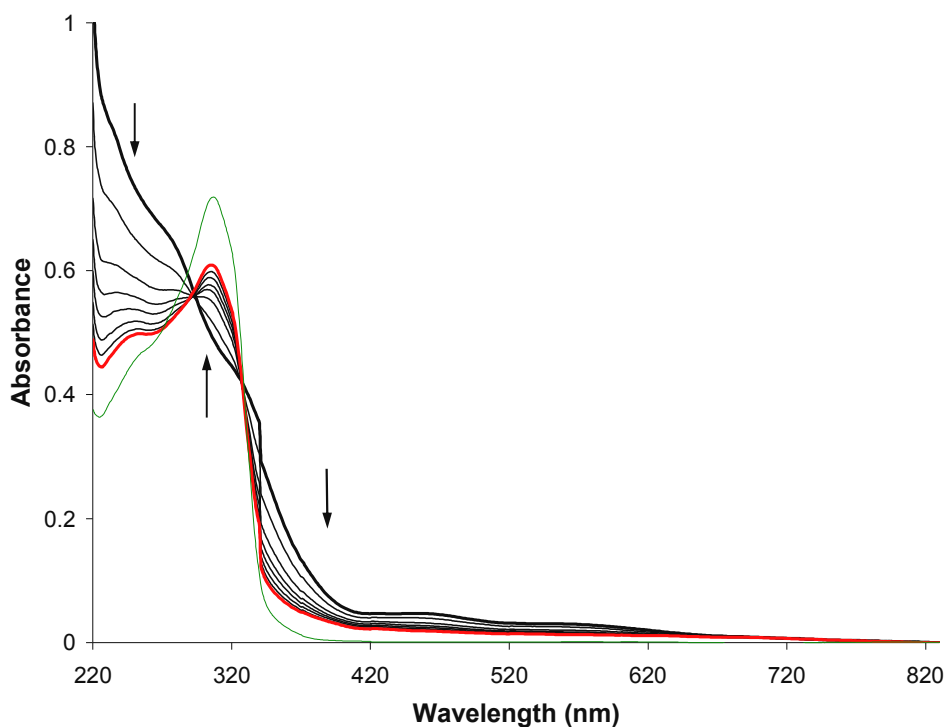
Figure 5.29: The UV-vis spectrum of the $Co_2(CO)_6$ complex **3F** (thick black line), following oxidation at 1.0 V. The final spectrum recorded at 1.0 V (red line) is similar to the absorbance spectrum of the free ligand **1F** (green line).

In the CV of the closed-ring isomer **3bF**, a quasireversible oxidation wave was observed at $E_{1/2}$ = 0.94 V. The UV-vis/NIR spectroelectrochemistry experiments showed that oxidation at 0.8 V to 1.4 V resulted in a decrease in the absorbance band in the visible region (λ_{max} = 578 and 658 nm), indicating **3bF** was undergoing a ring-opening process. However, a new band appeared to be forming underneath the absorbance band in the visible region. Also noted was a decrease in the absorbance values in the UV region, with a new band appearing at approximately 300 nm, as shown in figure 5.30. Subsequent reduction at 0 V, resulted in a further decrease in the UV region, and increase at 300 nm, which suggests that decomposition of the $Co_2(CO)_6$ moieties was taking place. In the visible region, although the absorbance band slightly decreased further, a new λ_{max} appeared to be present at 590 nm, as shown in figure 5.30. This could possibly be due to cleavage of the metal-metal bond from the alkynyl unit, thus forming the closed-ring isomer of the free ligand switch, **1F**.
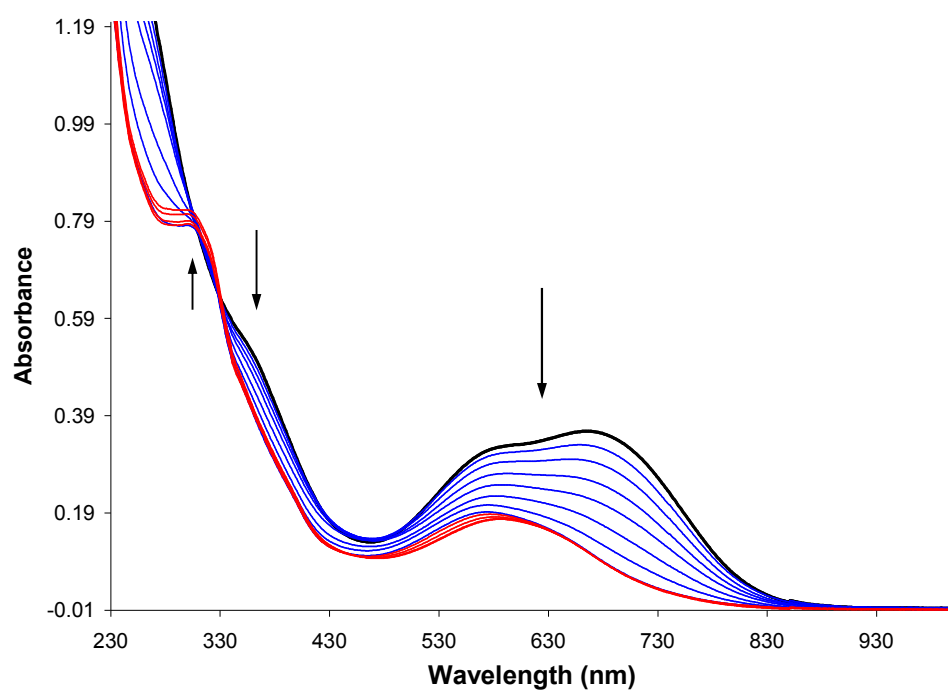
Figure 5.30: The UV-vis spectrum of the closed-ring $Co_2(CO)_6$ complex **3bF** (thick black line). Following oxidation at 0.8 to 1.6 V (blue lines) and subsequent reduction at 0 V (red lines).

5.3.5 $Co_2(CO)_6$ Complexes: IR Spectroelectrochemistry

The cyclic voltammograms have shown that the $Co_2(CO)_6$ moieties undergo irreversible oxidation processes. The results obtained from the UV-vis/NIR spectroelectrochemistry experiments have shown an irreversible decrease in the absorbance bands associated with the metal carbonyl compounds, and have indicated that cleavage of the metal-metal bond from the alkynyl unit occurs. In order to further investigate the effects of the oxidising process on the cobalt hexacarbonyl groups, IR spectroelectrochemistry experiments were carried out on the $Co_2(CO)_6$ complexes, **3H/F** and **4H/F**, in 0.1 M TBAPF$_6$/CH$_2$Cl$_2$ *vs.* Ag/Ag$^+$.

3H: R$_1$=H
3F: R$_1$=F

4H: R$_1$=H
4F: R$_1$=F

3bF

4bH
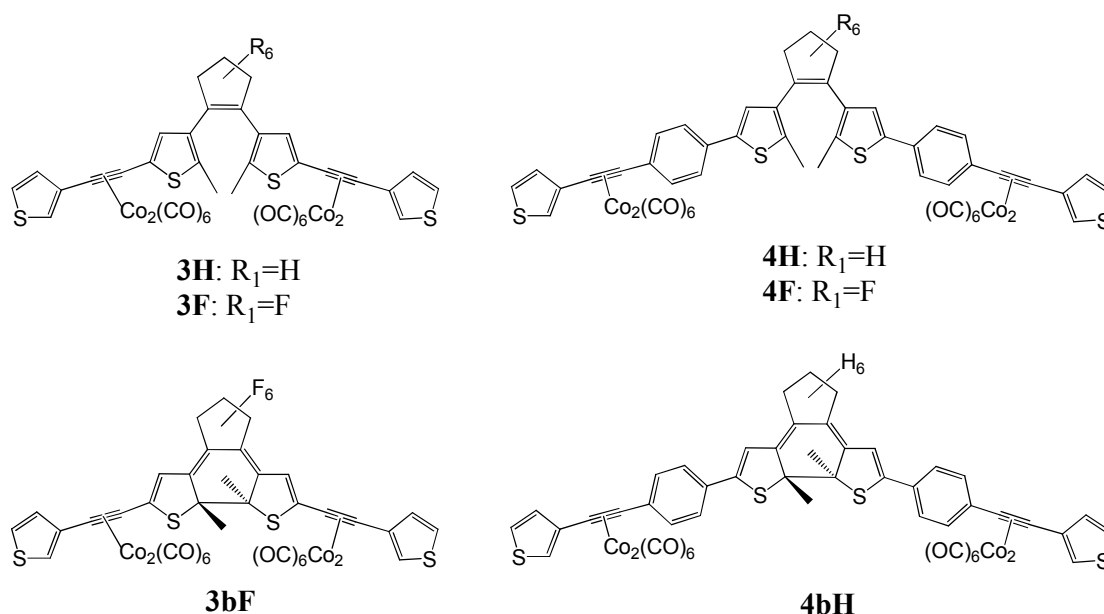
Figure 5.31: The structures of the open-ring $Co_2(CO)_6$ complexes **3H/F** and **4H/F**, and of the closed-ring $Co_2(CO)_6$ complexes **3bF** and **4bH**.

The carbonyl stretches recorded in the IR for the open-ring $Co_2(CO)_6$ complexes **3H/F** and **4H/F**, before any potentials were applied, are presented in table 5.6. Three carbonyl IR bands, in the range of 2100 - 2020 cm^{-1}, were recorded in each case. Noticeably, the IR bands for the perfluoro-derivatives were shifted to slightly higher wavenumbers due to the electron-withdrawing effect of the fluorine atoms. This effect is more pronounced for **3F**, in comparison to **4F**, which can be attributed to the presence of the phenyl-ring in **4F**, separating the $Co_2(CO)_6$ moieties from the hexafluoro-cyclopentene ring, hence reducing the effect of the fluorine atoms.

When oxidised, at approximately the same potentials at which the oxidation processes of the $Co_2(CO)_6$ moieties were observed in the CV's, depletion of the parent bands in the IR spectra was observed for each complex, and no new bands were found to appear, as shown for **3F** in figure 5.32. When the potential was set back to 0 V, bleaching of the new bands occurred and the parent bands began to grow back. However, the parent bands only returned to approximately 60% of their original absorbance values, indicating that the oxidation processes resulted in some decomposition of the complexes.
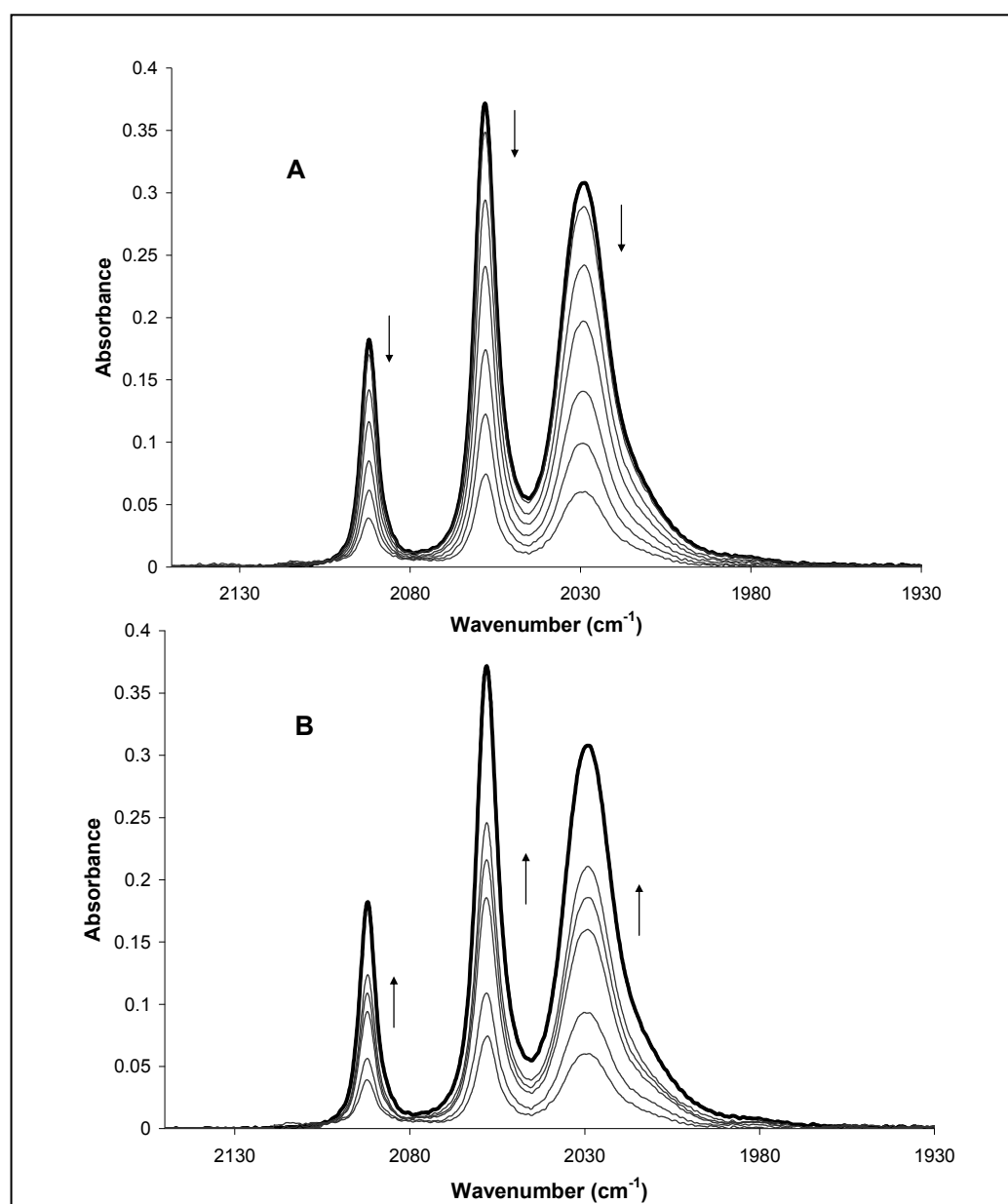
Figure 5.32: The IR spectra of the $Co_2(CO)_6$ complex **3F**, in 0.1 M TBAPF$_6$/ CH$_2$Cl$_2$, following oxidation processes (A), and subsequent reduction at 0 V (B). The parent bands recorded at the start of the experiment (i.e. before oxidation) are denoted by the thick black lines.

Table 5.6: IR spectral data of the $Co_2(CO)_6$ complexes **3H/F**, **4H/F**, **3bF** and **4bH**, before oxidation (parent bands) and during oxidation processes (new bands).

Compound	Parent Bands $\nu(CO)$ cm^{-1}	New Bands $\nu(CO)$ cm^{-1}
3H	2089, 2055, 2024	-
4H	2089, 2055, 2024	-
4bH	2090, 2055, 2026	2093, 2061, 2037 2096, 2067, 2043
3F	2092, 2058, 2028	-
3bF	2093, 2063, 2035	-
4F	2090, 2055, 2026	-

The data was recorded in 0.1 M TBAPF$_6$/CH$_2$Cl$_2$ *vs.* Ag/Ag$^+$

In the case of the closed-ring isomer **3bF**, the parent carbonyl bands recorded in the IR spectrum were present at higher wavenumbers (2093, 2063, 2035 cm^{-1}) in comparison to its open-ring form **3F** (2092, 2058 and 2028 cm^{-1}). This can be attributed to the extended conjugation of the system in the closed form, which reduces electron-density from the system, hence shifting the carbonyl bands to higher energy. Oxidation processes of **3bF** also resulted in the depletion of the parent bands in the IR, which returned to only approximately 60% of the original absorbance value recorded, following subsequent reduction at 0 V.

Conversely, in the case of the closed-ring isomer **4bH**, the IR bands were similar to the values recorded for its related open-ring form **4H**, as shown in table 5.6. This can be attributed to the presence of the phenyl-rings in **4bH**, which act as spacer groups between the cobalt carbonyl moieties and the switching unit. Hence, the influence of the conjugated closed switch on the $Co_2(CO)_6$ units is reduced, in comparison to **3bF**. On the other hand, when oxidation potentials were applied to **4bH**, new bands appeared at higher frequencies in the infra-red spectrum, as shown in figure 5.33. These changes have been assigned to the effects of the reversible oxidation processes of **4bH**, observed at potentials less than 1.0 V in the CV, representing the generation of the monocation and dication species.
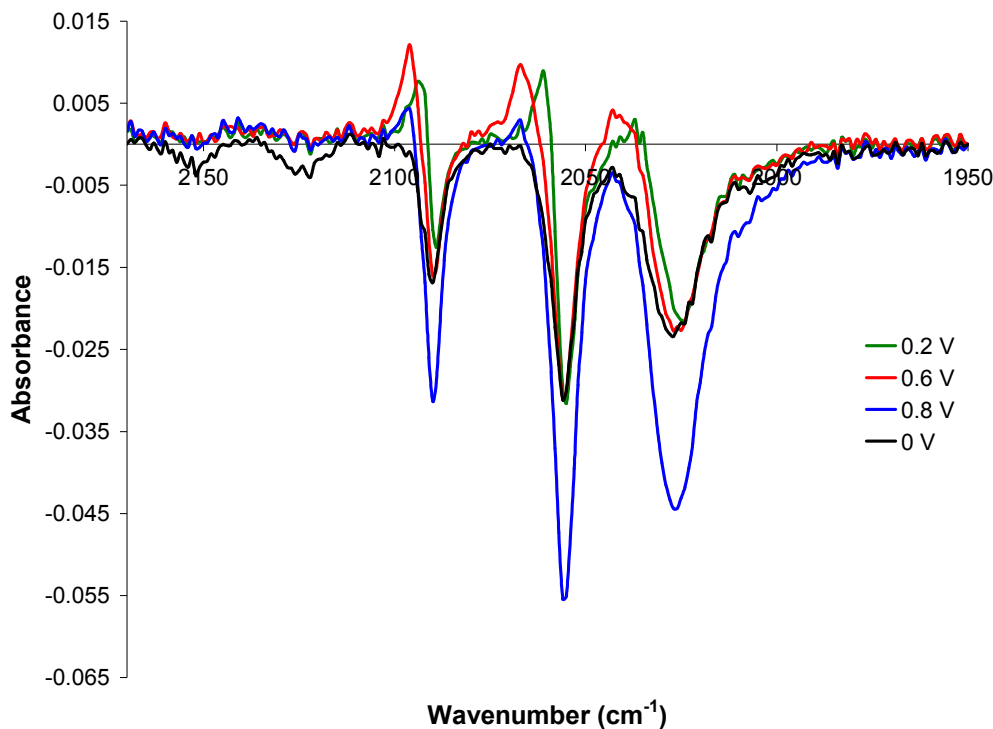
Figure 5.33: The IR difference spectra of the closed-ring $Co_2(CO)_6$ complex **4bH**, in 0.1 M TBAPF$_6$/CH$_2$Cl$_2$, during oxidation processes: At 0.2 V (green line); at 0.6 V (red line); at 0.8 V (blue line), and subsequent reduction at 0 V (black line).

Upon oxidation at 0.2 V, bleaching of the parent bands at 2090, 2055 and 2026 cm^{-1} was observed, along with the appearance of three new bands at 2093, 2061 and 2037 cm^{-1}. Such a result can be attributed to generation of the monocation species **4bH$^+$**. Removal of an electron from the complex results in a delocalised charge over the entire complex, hence removing electron-density from the $Co_2(CO)_6$ moieties, and therefore shifting the bands in the IR spectrum to higher frequencies. When the oxidation potential was increased to 0.8 V, depletion of the new bands occurred and three new bands appeared at even higher wavenumbers (2096, 2067 and 2043 cm^{-1}). These bands are tentatively assigned to the formation of the dication species **4bH^{2+}**. The electron density on the cobalt carbonyl units is further reduced following the removal of a second electron from the complex hence the carbonyl IR bands are shifted to even higher frequencies. Subsequent reduction processes led to a decrease in the new bands and regeneration of the parent IR bands, however, only to approximately 78% of the initial intensity recorded. Therefore, some decomposition of the complex also occurs for **4bH** during the oxidation processes.

5.3.6 Co₂(CO)₄dppm Complexes: Cyclic Voltammetry

Incorporating phosphine ligands onto cobalt carbonyl moieties increases the electron density on the Co-Co core, thus stabilising the metal carbonyl and facilitating reversible oxidation processes. As a result, the lifetimes of the radical anions and cations are increased, reducing the rate at which disintegration of the cobalt carbonyl moieties takes place.[15,17,18,24,26] 1,2-Bis(diphenylphosphino)methane {dppm} ligands were incorporated onto the $Co_2(CO)_6$ complexes described in the previous section, producing the corresponding $Co_2(CO)_4$dppm complexes **5H**, **5F** and **6H**. There was an insufficient amount of the fluorinated $Co_2(CO)_6$ complex **4F** to generate the corresponding tetracarbonyl complex. The redox properties of the dppm derivatives were investigated using cyclic voltammetry techniques at room temperature, in 0.1 M $TBAPF_6/CH_2Cl_2$, at a scan rate of 0.1 Vs^{-1}, and the data was calibrated against the redox couple of decamethylferrocene Fc*$^+$/Fc* ($E_{1/2}$ = -0.07 *vs.* SCE). The effects of the chelating dppm ligands on the reductive and oxidative processes of the metal carbonyl moieties, and on the electrochromic properties of the switching units, are described here. The structures of **5H**, **5F** and **6H** are illustrated in figure 5.34, and the cyclic voltammetry results of the oxidation processes are summarised in table 5.7.

5H: R=H; M₁=Co₂(CO)₄dppm
5F: R=F; M₁=Co₂(CO)₄dppm

6H: R=H; M₁=Co₂(CO)₄dppm
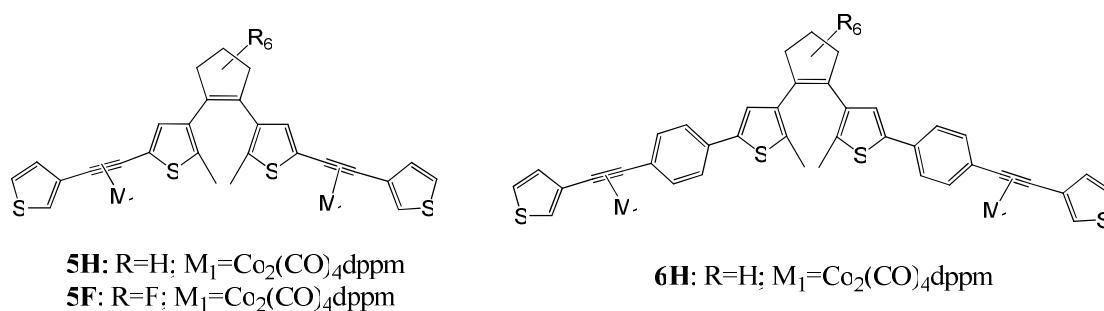
Figure 5.34: The structures of the open-ring $Co_2(CO)_4$dppm complexes **5H**, **5F** and **6H**.

- **Reduction Process**

The cyclic voltammograms of the $Co_2(CO)_6$ perhydro-derivatives **3H** and **4H** revealed single bielectronic irreversible reduction processes at -1.28 V and -1.20 V (*vs.* SCE), respectively. In the case of their corresponding $Co_2(CO)_4dppm$ complexes, **5H** and **6H** respectively, reduction processes were not found to occur within the potential limits of the CH_2Cl_2 solvent (i.e. V < -2.0 V). Such a result can be ascribed to the electron-donating ability of the dppm ligand, making the complexes more difficult to reduce and therefore more negative potentials are required to form the anionic species. This result is consistent with previous literature studies.[15,17,18,24,26]
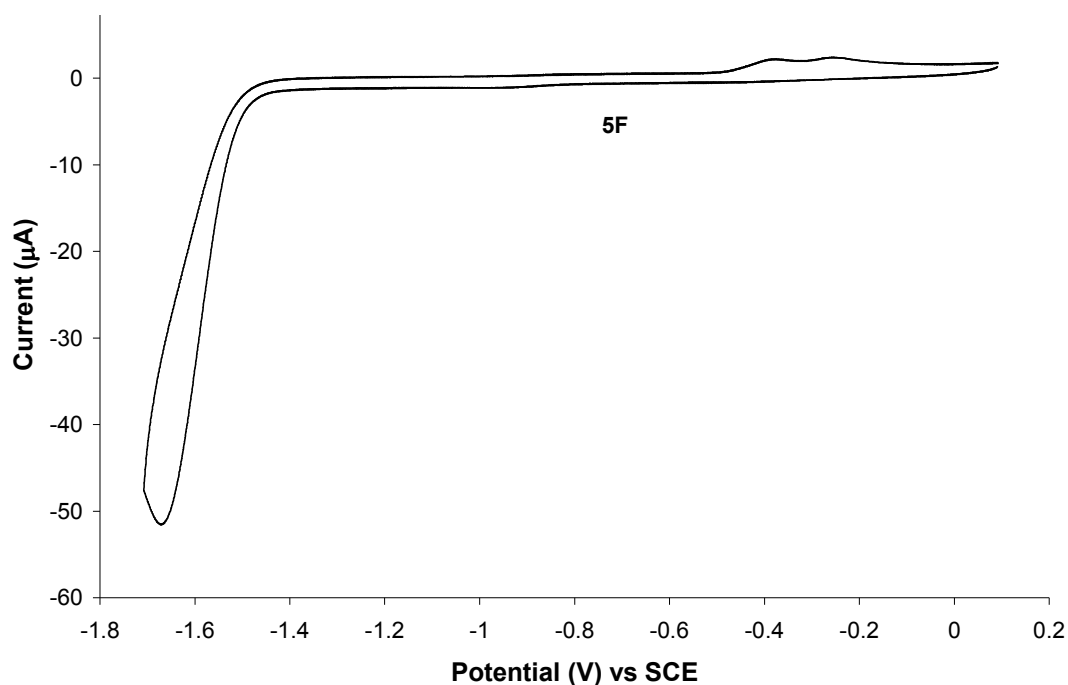
Figure 5.35: Cyclic Voltammogram of the reduction process of **5F**, in 0.1 M $TBAPF_6/CH_2Cl_2$, at a scan rate of 0.1 Vs^{-1}.

On the other hand, reduction of the $Co_2(CO)_4dppm$ moieties was observed for the perfluoro analogue, **5F**, as shown in figure 5.35. The CV of **5F** displayed a single irreversible reduction peak at -1.67 V, representing a one-step two-electron reduction process, indicating that little electronic communication exists between the two metal centres. The electron-withdrawing ability of the fluorine atoms helps to stabilise the anionic species, therefore allowing reduction processes to take place at less negative potentials in comparison to the perhydro derivatives. Although, the reduction peak of **5F**$^{2-}$ was cathodically shifted by 580 mV relative to its corresponding $Co_2(CO)_6$

complex $3F^{2-}$, as expected. Despite the tendency of phosphine ligands to impart reversibility onto the reduction processes of such cobalt carbonyl complexes, the reduction peak of **5F** was not found to be reversible under these conditions (at room temperature, at a scan rate of 0.1 Vs^{-1}). In fact the subsequent anodic sweep displayed two small oxidation peaks at -0.36 and -0.24 V, due to the formation of unknown disintegration products. Although, the relative intensities of these peaks are lower than those observed in the CV of the $Co_2(CO)_6$ complex **3F**, indicating a reduction in the rate of decomposition of **5F**, in comparison to **3F**.

- **Oxidation Process**

Introduction of electron-donating chelating phosphine ligands, onto cobalt carbonyl compounds, makes the redox centre much more electron-rich, facilitating oxidation processes at lower potentials, in comparison to their related $Co_2(CO)_6$ complexes. The extra stability on the metal centre also increases the reversibility of the electrogenerated cations. Such results have been described previously in the literature,[15,17,18,24,26] and similar effects were observed in the cyclic voltammograms of the $Co_2(CO)_4$dppm complexes **5H**, **5F** and **6H**, in comparison to the CV's of their corresponding cobalt hexacarbonyl complexes, as highlighted in table 5.7.

Table 5.7: Cyclic voltammetric data following oxidation of the $Co_2(CO)_4$dppm complexes **5H**, **5F** and **6H**, and the corresponding open-ring free ligand switches (**1Ho**, **1Fo**, **2Ho**) and $Co_2(CO)_6$ derivatives (**3H**, **3F**, **4H**).

Compound	Oxidation Potentials	
	E_{pa} (V)	E_{pc} (V)
1Ho	0.65^{rc}, 0.95^{rc}, 1.55^{a}	0.60^{rc}, 0.88^{rc}
3H	0.59^{rc}, 0.78^{rc}, 1.21^{a}, 1.41^{a}	0.50^{rc}, 0.70^{rc}
5H	0.27^{rc}, 0.59^{dppm}, 0.68^{dppm}, 1.35^{a}	0.18^{rc}, 0.50^{dppm}, 0.61^{dppm}
2Ho	0.50^{rc}, 0.82^{rc}, 1.23^{a}	0.42^{rc}, 0.75^{rc}
4H	0.55^{rc}, 0.84^{rc}, 1.23^{a}, 1.46^{a}	0.47^{rc}, 0.75^{rc}
6H	0.40^{rc}, 0.69^{dppm}, 0.96^{rc}, 1.36^{a}	0.30^{rc}, 0.51^{dppm}, 0.82^{rc}
1Fo	1.71^{a}	-
3F	1.23^{a}, 1.75^{a}	-
5F	0.65^{dppm}, 0.75^{dppm}, 1.48^{a}	0.57^{dppm}, 0.67^{dppm}

All values listed are values of potential (V) *vs*. SCE, recorded in 0.1 M TBAPF$_6$/CH$_2$Cl$_2$, at 0.1 Vs^{-1}.
[a] indicates an irreversible oxidation process
[rc] indicates peaks assigned to ring-closed species
[dppm] indicates peaks due to oxidation of the $Co_2(CO)_4$dppm moieties

The oxidation process of **6H** resulted in a quasireversible oxidation wave at $E_{1/2}$ = 0.59 V ($i_{pc}/i_{pa} \approx 0.7$), which can be attributed to a two-electron oxidation process of the $Co_2(CO)_4$dppm moieties i.e. a one-electron oxidation of each of the two $Co_2(CO)_4$dppm units. At higher potentials, an irreversible oxidation peak was observed at 1.36 V, representing a two-electron process of the dithienylethene unit. The subsequent cathodic sweep displayed two new reduction peaks at 0.82 and 0.30 V, and two corresponding new oxidation waves at 0.96 and 0.40 V (*vs.* SCE), as shown in figure 5.36. Such a result could potentially be due to an oxidative cyclisation process, with the redox waves at $E_{1/2}$ = 0.35 and 0.89 V representing the formation of the monocation and dication species of the closed form, respectively. However, the ΔE value between the two new redox waves in **6H** (ca. 690 mV) does not correspond with the ΔE values found for the closed-ring cationic species of the corresponding free ligand switch **2H** (ca. 320 mV) and $Co_2(CO)_6$ complex (ca. 280 mV). Another possibility is that the presence of the dppm redox wave at $E_{1/2}$ = 0.60 V, could be obscuring another new redox wave associated with the ring-closing process. Therefore it can be unambiguously deduced that oxidative cyclisation occurs for **6H** from the CV results. Hence, further investigations were carried out in the UV-vis spectrum in order to elucidate the oxidative processes, and the results are discussed in section 5.3.7.
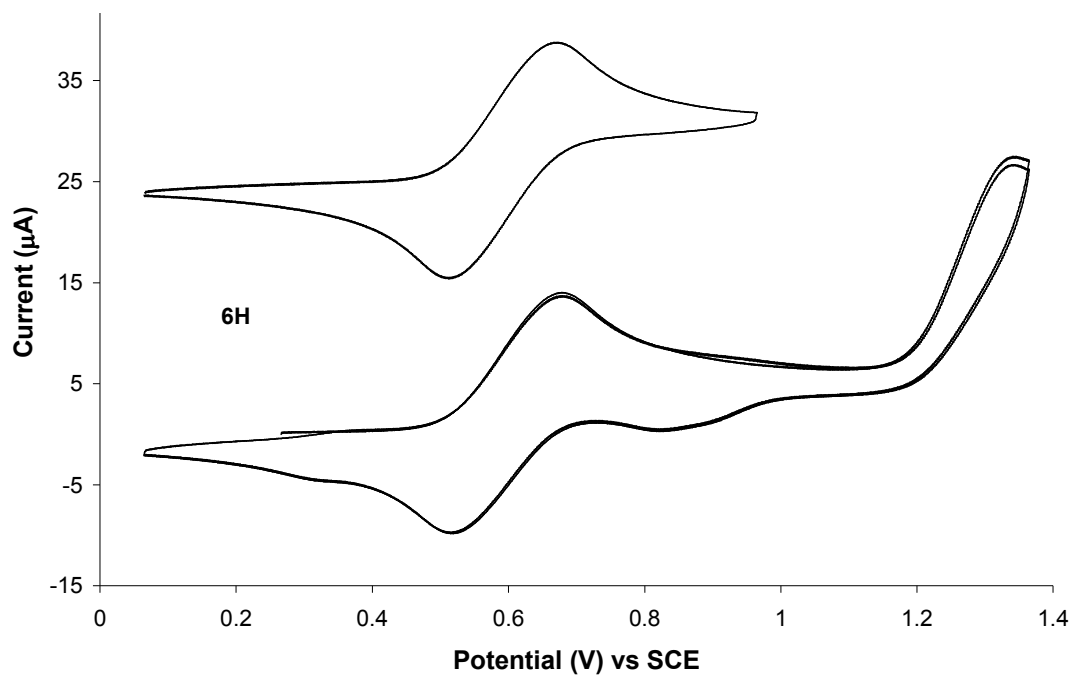
Figure 5.36: Cyclic voltammograms of the $Co_2(CO)_4$dppm complex **6H**, in 0.1 M $TBAPF_6/CH_2Cl_2$ at 0.1 Vs^{-1}, following oxidation at 0.96 V (top) and 1.37 V (bottom). The top CV is offset along the coordinate for clarity.

Oxidation of the $Co_2(CO)_4$dppm moieties on **5H** resulted in the appearance of two quasireversible monoelectronic oxidation waves at $E_{1/2}$ = 0.55 and 0.65 V (ΔE = 100 mV), indicating that some electronic communication exists between the metal centres. In the case of the longer-chain derivative **6H**, only one oxidation wave was observed, thus it appears that the shorter bridging carbon chain in **3H** promotes electronic interaction between the metal carbonyl groups. Following the first oxidation of the cobalt carbonyl moieties, a new redox wave was observed in the subsequent sweeps at $E_{1/2}$ = 0.23 V (figure 5.37). Oxidation at higher potentials (at 1.4 V) revealed an irreversible oxidation peak at 1.35 V, attributed to a two-electron oxidation process of the switching unit. In the subsequent sweeps, a new redox wave appeared in the CV at $E_{1/2}$ = 0.23 V (figure 5.37). This new redox wave corresponds to that observed following oxidation of the cobalt carbonyl moieties, as described above, although the relative intensity of the oxidation/reduction peaks increased following oxidation of the switching unit.
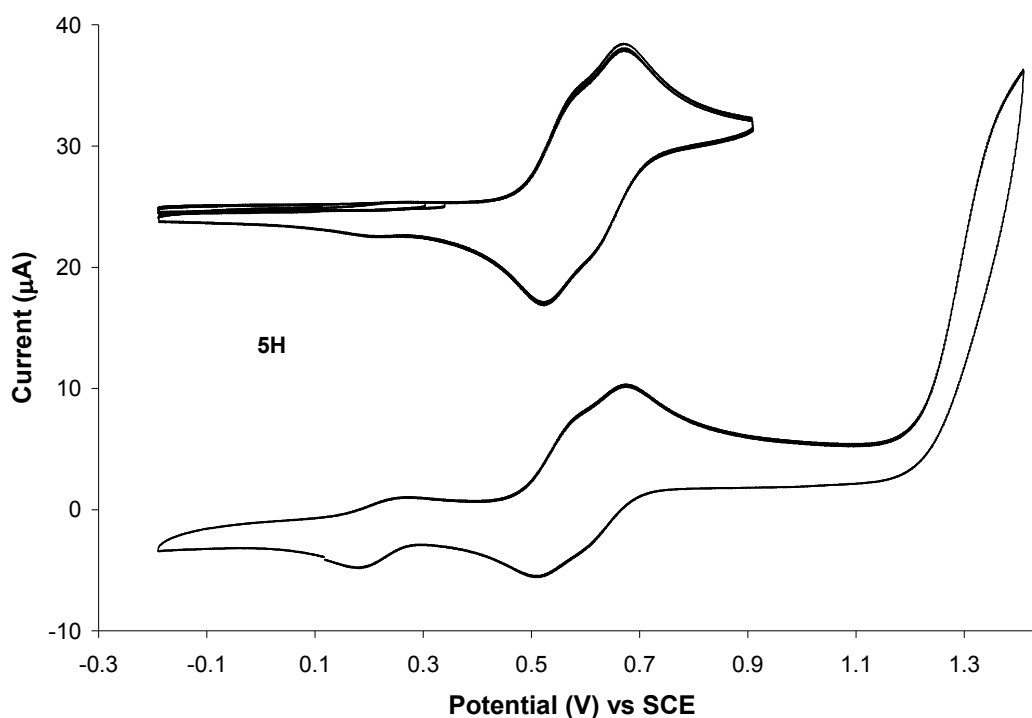
Figure 5.37: Cyclic voltammogram of the $Co_2(CO)_4$dppm complex **5H**, in 0.1 M TBAPF$_6$/CH$_2$Cl$_2$ at 0.1 Vs^{-1}, following oxidation at 0.9 V (top, sweeps 1-4) and at 1.4 V (bottom, sweeps 3-4). The top CV is offset along the coordinate for clarity.

This result suggests that cyclisation of **5H** begins following oxidation of the Co$_2$(CO)$_4$dppm moieties. The corresponding free ligand (**1H**) and Co$_2$(CO)$_6$ complex (**3H**) both underwent cyclisation reactions following oxidation of the dithienylethene unit, resulting in two new redox waves associated with the closed form. However, only one new redox wave was found for **5H**. It is possible that a second redox wave related to oxidation of the switching unit is present but its appearance is obscured by the Co$_2$(CO)$_4$dppm oxidation process. Therefore, in order to elucidate the results fully, further investigations were carried out using the UV-vis/NIR spectro-electrochemistry techniques, and the results are discussed in section 5.3.7.

In the case of the perfluoro-derivative **5F**, two closely separated quasireversible oxidation waves ($\Delta E = 100$ mV) were observed at E$_{1/2}$ = 0.61 and 0.71 V, as shown in figure 5.38. This redox process can be attributed to the oxidation of the Co$_2$(CO)$_4$dppm components, and indicates electronic interaction between the two metal centres over the dithienylethene bridge, as described previously for its perhydro-derivative **3H**. A two-electron oxidation process of the switching unit was observed at 1.48 V, with no new redox waves appearing in the consecutive sweeps. Therefore, **5F** did not undergo electrochemical ring-closing, which is consistent with the results observed for its related free ligand (**1F**) and Co$_2$(CO)$_6$ complex (**3F**).
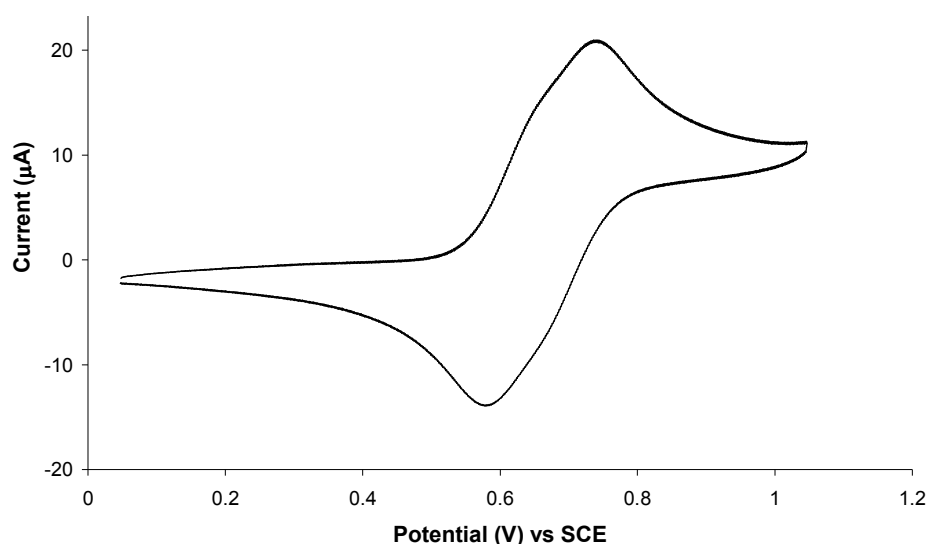
Figure 5.38: Cyclic voltammogram of the Co$_2$(CO)$_4$dppm complex **5F**, in 0.1 M TBAPF$_6$/CH$_2$Cl$_2$ at 0.1 Vs^{-1}, following oxidation at 1.1 V.

5.3.7 Co$_2$(CO)$_4$dppm Complexes: UV-vis/NIR Spectroelectrochemistry

The cyclic voltammetry experiments performed on the Co$_2$(CO)$_4$dppm complexes indicated that oxidative cyclisation occurred for the perhydro-derivatives **5H** and **6H**, but not in the case of the perfluorinated analogue **5F**. UV-vis/NIR spectro-electrochemistry techniques were employed to examine the oxidation processes of the dppm derivatives in more detail, in 0.1 M TBAPF$_6$/CH$_2$Cl$_2$ *vs.* Ag/Ag$^+$, at room temperature. The structures of the Co$_2$(CO)$_4$dppm complexes are illustrated in figure 5.39. The UV-vis/NIR spectroelectrochemistry results recorded for the tetracarbonyl dppm complexes are summarised in table 5.8, along with the data obtained from the corresponding free ligand switches and Co$_2$(CO)$_6$ complexes, for comparative purposes.

Table 5.8: UV-vis/NIR spectroelectrochemistry data of the Co$_2$(CO)$_4$dppm complexes (**5H**, **5F**, **6H**), and the corresponding free ligand switches (**1H**, **1F**, **2H**) and Co$_2$(CO)$_6$ complexes (**3H**, **3F**, **4H**), following oxidation processes at varying potentials.

Free Ligand Switches		Co$_2$(CO)$_6$ Complexes		Co$_2$(CO)$_4$dppm Complexes	
Ox	λ_{abs} (nm)	Ox	λ_{abs} (nm)	Ox	λ_{abs} (nm)
1Ho		**3H**		**5H**	
Start	290, 310	Start	274, 330, 450-670	Start	263, 346, 430-630
1.3 V	455, 566, 666	1.3V	466, 571, 671	0.8 V	432, 640
1.6 V	469, 575, 666, 867				
2Ho		**4H**		**6H**	
Start	334	Start	267, 341, 420-650	Start	276, 351, 430-630
1.4 V	471, 590(sh), 657	1.0 V	481, 576, 655, 778	1.4 V	456, 566, 771
		1.0.V	472, 576(sh), 655		
1Fo		**3F**		**5F**	
Start	305	Start	275, 330, 410-630	Start	270, 338, 430-630
1.6 V	237, 345-700	1.0V	303	1.0 V	270↓, 338↓, 430-630↓

The data was recorded in 0.1 M TBAPF$_6$/CH$_2$Cl$_2$ *vs.* Ag/Ag$^+$.
↓ indicates decreasing of absorbance band

5H: R=H; M_1=Co$_2$(CO)$_4$dppm
5F: R=F; M_1=Co$_2$(CO)$_4$dppm

6H: R=H; M_1=Co$_2$(CO)$_4$dppm
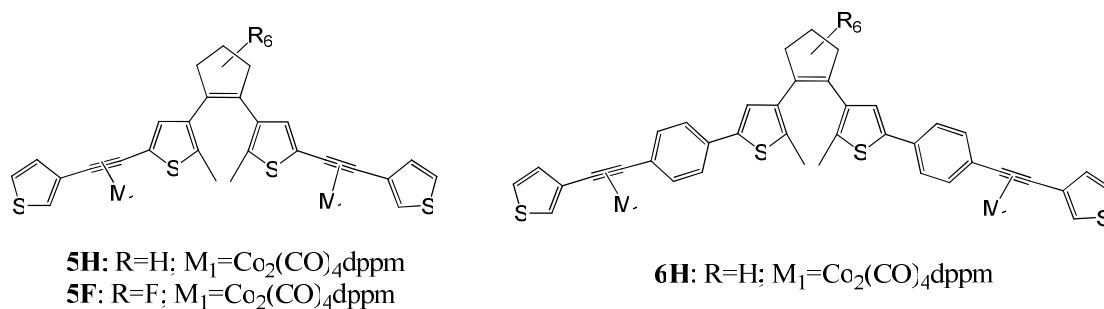
Figure 5.39: The structures of the open-ring Co$_2$(CO)$_4$dppm complexes **5H**, **5F** and **6H**.

The CV of **6H** suggested that cyclisation of the closed-ring isomer occurred following oxidation at 1.4 V. The oxidation processes were followed in the UV-vis spectrum. The original absorbance bands in the UV region at 276 and 351 decreased significantly, and new bands appeared in the visible region at 456, 566 and 771 nm, as shown in figure 5.40. These bands are associated with the formation of the monocation species of the closed-ring isomer. However, the absorbance bands were quite weak in comparison to the results recorded for the free ligand (**2H**) and Co$_2$(CO)$_6$ complex (**4H**), and as bulk electrolysis continued, they started to decrease. Subsequent reduction at 0V resulted in a slight increase in absorbance at 337 nm, and the bands in the visible region decreased, with weak bands at 456 and 771 nm remaining at the end of the experiment. Such a result suggests that a one-electron oxidation process of the open-form of **6H** undergoes cyclisation to the monocation closed-form. Therefore, the oxidation process at $E_{1/2}$ = 0.35 V in the CV of **6H** can tentatively be assigned to the generation of the closed-ring monocation radical. The fact that there was no definite evidence for the formation of the dication closed-ring species in the UV-vis spectrum, suggests that the redox wave at $E_{1/2}$ = 0.89 V, in the CV of **6H**, is not due to the dication of the closed switch. It is difficult to assign this redox wave to a particular species, and unfortunately, insufficient information was obtained from the bulk electrolysis experiments to categorically elucidate the oxidative processes observed in the CV of **6H**. However, it can be concluded that some electrogenerated ring-closing was achieved for **6H**, but to a lesser extent then previously observed for the related free ligand switch **2H** and Co$_2$(CO)$_6$ complex **4H**. Such a result could possibly be ascribed to the electron-withdrawing effect of the oxidation processes of the Co$_2$(CO)$_4$dppm moieties, occurring before the switching

unit, hence stabilising the charge on the open-ring isomer of **6H** in a localised fashion, thus hindering the cyclisation process.
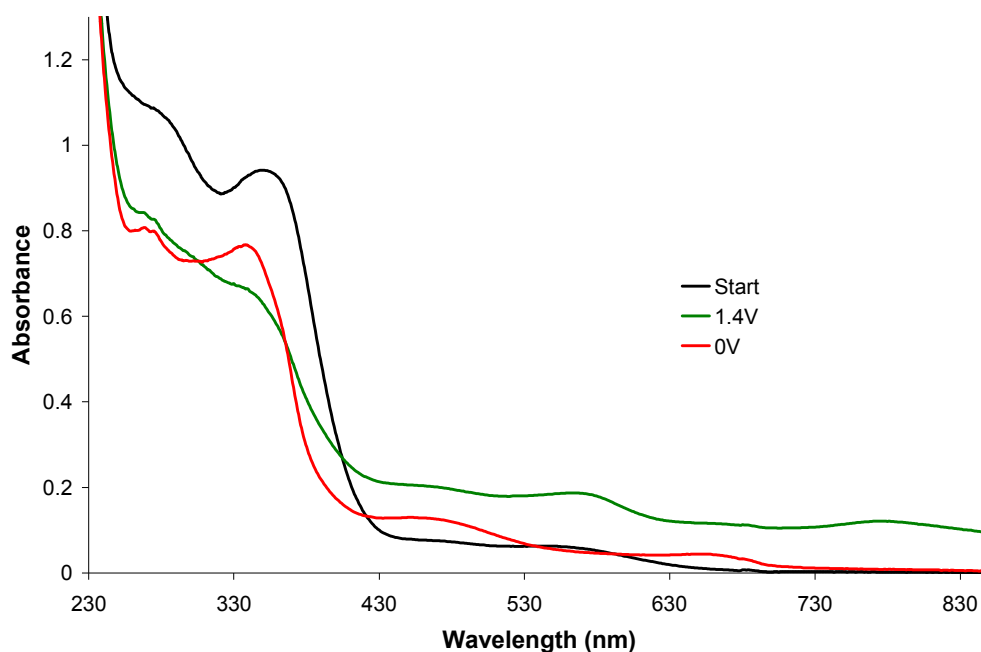
Figure 5.40: The UV-vis spectrum of the $Co_2(CO)_4$dppm complex **6H** (black line), following oxidation at 1.4 V (green line), and subsequent reduction at 0 V (red line).

When **5H** was oxidised at 0.8 V, a decrease in the bands at 263 and 346 nm was observed, accompanied by an increase in the absorbance in the visible region, with λ_{max} at 432 and 640 nm (figure 5.41). These new bands are associated with the generation of the dication species of the closed-ring isomer. Following reduction at 0V, the bands in the visible region began to decrease. An increase in the UV region at 263 and 346 nm was observed, indicating that the $Co_2(CO)_4$dppm moieties are quite stable under such conditions. Noteworthy is the fact that generation of the closed-form dication species occurred at 0.8 V, which corresponds to the potential at which the dppm units undergo oxidation processes in the CV. This suggests that oxidation of the cobalt carbonyl dppm units induces the cyclisation process, possibly via an intramolecular electron transfer mechanism, as the switching unit undergoes oxidation processes at a much higher potential (1.35 V). These results correspond well with those previously observed in the CV of **5H**, as a new redox wave ($E_{1/2}$ = 0.23 V) appeared following oxidation of the metal carbonyl groups.
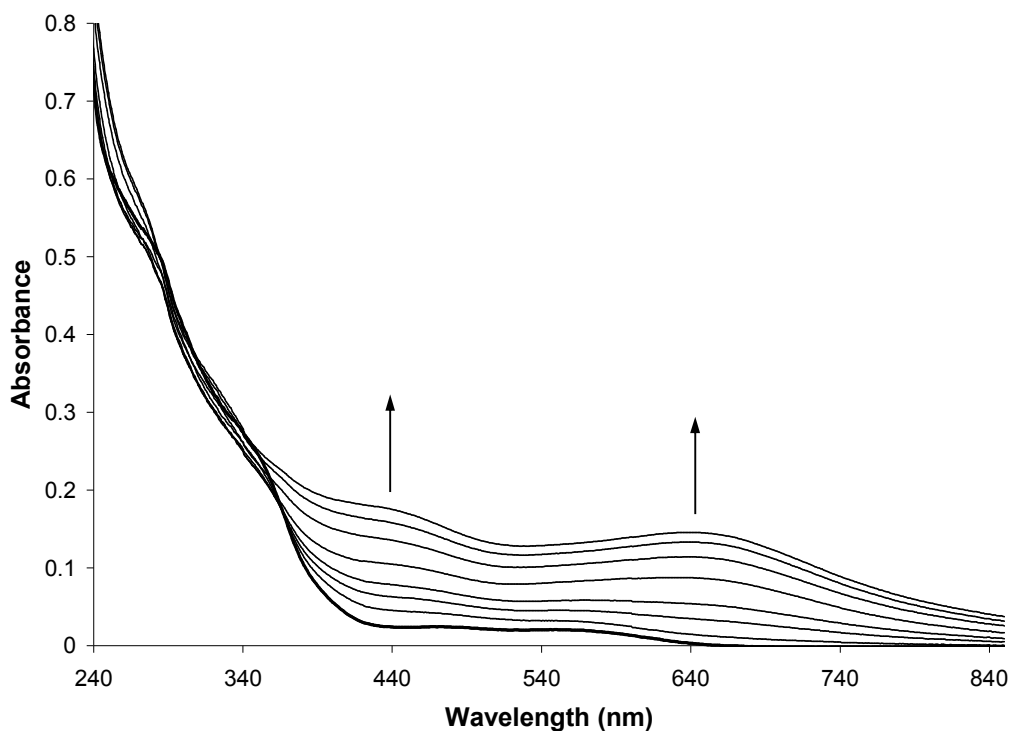
Figure 5.41: The UV-vis spectrum of the $Co_2(CO)_4dppm$ complex **5H** (thick black line). Oxidation at 0.8 V results in an increase in the visible region, due to the formation the closed-ring dication species.

The oxidation process of the perfluoro-derivative **5F** was monitored at a potential of 0.8 V initially, which was increased to 1.6 V. At both potential sets, a decrease in the original bands recorded at 270, 338 and 430-630 nm was observed, with no new bands growing-in. No changes were incurred following the subsequent reduction process at 0 V. Therefore, oxidation of **5F** resulted in some decomposition of the $Co_2(CO)_4dppm$ moieties, but did not induce cyclisation of the switching unit.

5.3.8 Co$_2$(CO)$_4$dppm Complexes: IR Spectroelectrochemistry

The cyclic voltammograms of the Co$_2$(CO)$_4$dppm complexes showed that incorporating dppm ligands, onto the metal carbonyl units, increased the stability of the oxidation processes of the cobalt carbonyl complexes, as observed from the quasi-reversible oxidation waves. However, the UV-vis/NIR spectroelectrochemistry experiments indicated that decomposition of the complexes was occurring during the oxidation processes. Therefore, IR spectroelectrochemistry experiments were carried out on these complexes (in 0.1 M TBAPF$_6$/CH$_2$Cl$_2$) in order to examine the effect of the oxidation processes on the metal carbonyl units in more detail.

5H: R=H; M$_1$=Co$_2$(CO)$_4$dppm
5F: R=F; M$_1$=Co$_2$(CO)$_4$dppm

6H: R=H; M$_1$=Co$_2$(CO)$_4$dppm
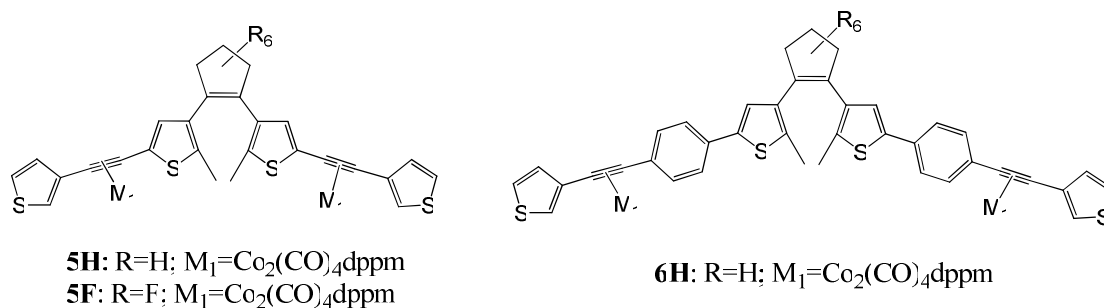
Figure 5.42: The structures of the open-ring Co$_2$(CO)$_4$dppm complexes **5H**, **5F** and **6H**.

The Co$_2$(CO)$_4$dppm complexes **5H**, **5F** and **6H** displayed three carbonyl stretches in the IR spectrum at considerably lower wavenumbers, in comparison to their related cobalt hexacarbonyl complexes. For example, the IR bands for the Co$_2$(CO)$_6$ complex **3H** were recorded at 2089, 2055 and 2024 cm^{-1}, whereas the corresponding dppm derivative **5H** displayed IR bands at 2022, 1997 and 1969 cm^{-1}. The presence of the chelating ligand increases the electron density on the metal carbonyl moiety, due to the electron donating ability of dppm onto the cobalt centres, and the fact that there are less CO molecules available for back-bonding, thereby shifting the carbonyl bands to lower frequencies. Also noted, from the data listed in table 5.9, was the shift in the tetracarbonyl IR bands of **5F** to higher frequencies, in relation to the perhydro-analogues **5H** and **6H**. This can be attributed to the electron-withdrawing effects of the fluorine atoms.

Table 5.9: The IR spectral data of the $Co_2(CO)_4$dppm complexes **5H**, **5F** and **6H**, before oxidation (parent bands) and during oxidation processes (new bands).

Compound	Parent Bands $v(CO)$ cm^{-1}	New Bands $v(CO)$ cm^{-1}
5H	2022, 1997, 1969	2065, 2043, 2022
6H	2021, 1995, 1968	2067, 2044, 2021
5F	2025, 2000, 1972	2069, 2047, 2025

The data was recorded in 0.1 M TBAPF$_6$/ CH$_2$Cl$_2$ *vs.* Ag/Ag$^+$.

The oxidation processes were found to have some intriguing effects on the IR carbonyl stretches of these $Co_2(CO)_4$dppm complexes. In the case of **5F**, bleaching of the parent bands at 2025, 2000 and 1972 cm^{-1} occurred following oxidation at 0.6 V to 0.8 V. In conjunction with these changes, two new bands began to grow-in at 2069 and 2047 cm^{-1}, as shown in figure 5.43. A further band was evident underneath the parent band at 2025 cm^{-1}, as this band did not decay at the same rate as the other parent bands at 2000 and 1972 cm^{-1}. Such a result can be attributed to the formation of the dication species. The loss of an electron from each of the two $Co_2(CO)_4$dppm moieties results in a decrease in the electron density on the metal, thus shifting the carbonyl bands to higher wavenumbers.
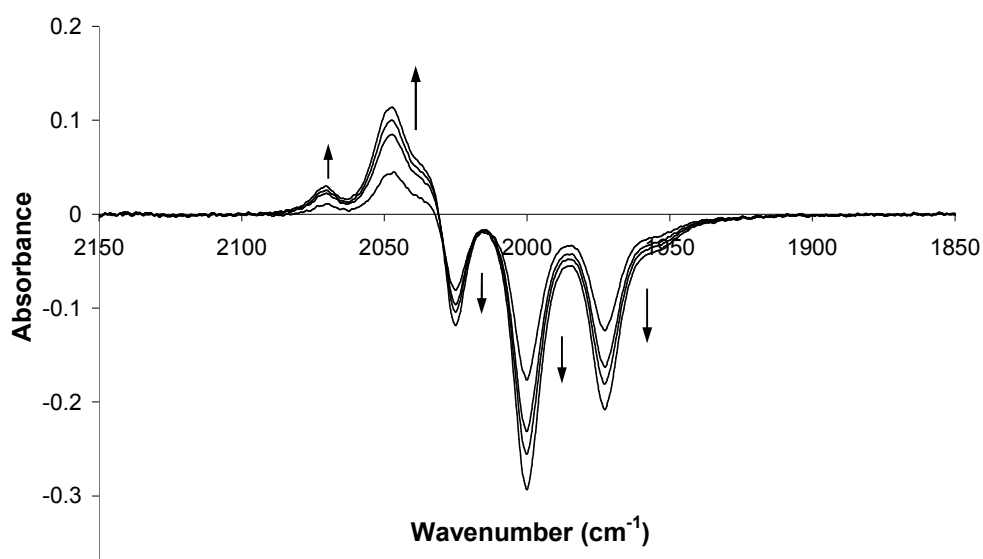
Figure 5.43: The IR difference spectra of the $Co_2(CO)_4$dppm complex **5F**, in 0.1 M TBAPF$_6$/CH$_2$Cl$_2$, during oxidation at 0.6 V. Negative bands indicate bleaching of the parent bands and the positive bands indicate formation of the monocation species.

Depletion of the new bands occurred following subsequent reduction processes at 0V, whilst the parent bands were found to recover to approximately 85% of their initial absorbance values recorded. This is a marked improvement in comparison to the percentage decomposition estimated for the $Co_2(CO)_6$ complex **3F** ($\sim$ 60%). Prolonged oxidation processes, and higher potentials, resulted in an overall decrease in the carbonyl bands in the IR spectrum. Therefore, the IR results coordinate well with the quasi-reversible oxidation process observed in the cyclic voltammogram, and the poor reversibility observed in the UV-vis/NIR spectra. Similar processes were observed for the perhydro-derivatives **5H** and **6H**, and the results are summarised in table 5.9.

5.4 Conclusion

The electrochromic properties of the thienyl-based switches were investigated and, from the cyclic voltammetry and UV-vis/NIR spectroelectrochemistry studies, it was determined that oxidative cyclisation processes, to the ring-closed isomers, were observed for **1H**, **2H** and **2F**, whereas oxidative cycloreversion, to the open-ring isomer, occurred for **1F**. The results obtained show that the direction of the oxidative switching processes (i.e. cyclisation or cycloreversion) depends on the relative stability of the open and closed-ring cation radicals. Similar results have been described previously in the literature.[1,4,5] The atoms present on the central cyclopentene units heavily influence these processes. The electron-donating ability of the hydrogen atoms provide extra electron density on the central switching unit, and hence stabilise the cation radicals of the closed-ring isomer, which is the driving force for oxidative cyclisation to occur. On the contrary, the electron-withdrawing ability of the fluorine atoms removes electron density from the central switching unit, hence efficient stabilisation of the cation radicals of the closed form is not achieved, resulting in a ring-opening process.

Incorporating phenyl rings between the dithienylethene unit and the ethynylthiophene moieties, in the case of **2H** and **2F**, were also found to influence the redox properties. In both cases, the first oxidation processes were cathodically shifted to less positive potentials with respect to their corresponding derivatives **1H** and **1F**, respectively. The presence of the electron-rich phenyl groups also provided extra stability on the cation radicals of the closed-form of **2F**, hence allowing cyclisation to the closed-ring isomer to occur. Such a result highlights how the redox properties of these switches can be tuned by altering the substituents attached to the dithienylethene unit.

Along with the redox waves associated with the open and closed isomers, the CV's of **1H**, **1F** and **2F**, also showed the appearance of redox waves at low potential values, which were assigned to the formation of unknown oxidation species (assigned as **1Hy**, **1Fy** and **2Fy**). Similar results have been described in the literature, and such species are believed to be a consequence of electrochemical rearrangement processes.[1,4]

The electrochemical properties of the cobalt carbonyl complexes were examined from two points of view. Firstly, the oxidation and reduction processes of the cobalt carbonyl moieties, and secondly, their influences on the electrochromic behaviour of the switching units.

The $Co_2(CO)_6$ complexes **3H/F** and **4H/F** underwent irreversible reduction processes followed by the decomposition of the radical anions. The substituents attached to the alkynyl units, and the atoms present on the cyclopentene ring (H *vs.* F), had a noticeable affect on the reduction potentials of the $Co_2(CO)_6$ moieties, with the potential values becoming more negative in the order of: **3F < 4F < 4H < 3H**. The fact that the reduction processes resulted in single bielectronic waves indicated that little electronic interaction existed between the two metal centres on both sides of the switching unit. Furthermore, increasing the π-conjugation of the bridging unit of **4H**, by producing the closed-ring isomer **4bH**, did not increase the electronic communication between the two cobalt carbonyl moieties. On the contrary, in the case of **3bF**, the increased π-conjugated system of the closed-ring isomer, along with a shorter carbon chain bridging unit, was found to increase the electronic communication between the metal centres, as evidenced by the presence of two monoelectronic quasireversible reduction waves in the CV, and increase the stability of the radical anions. Incorporating electron-donating dppm chelating ligands onto the cobalt carbonyl groups was found to drive the reduction processes to more negative potentials, with only the reduction process of **5F** observed below the potential limit of the solvent. The phosphine ligands were found to stabilise the radical cations, resulting in quasireversible oxidation processes for the $Co_2(CO)_4$dppm moieties, which occurred at less positive potentials in the CV's, in comparison to the cobalt hexacarbonyl units. Similar results have been reported in the literature for such cobalt carbonyl complexes.[15,17,18,24,26] Moreover, a more pronounced decrease was observed in the UV region of the absorbance spectra for the $Co_2(CO)_6$ complexes, relative to the dppm derivatives, following oxidation processes. The advantage of a shorter bridging unit was also evidenced in the CV's of the $Co_2(CO)_4$dppm complexes **5H** and **5F**, which displayed two monoelectronic waves, in contrast to the single bielectronic oxidation wave observed for the longer chain derivative **6H**. Therefore, these results highlight the ability to tune the electrochemical properties of cobalt carbonyl complexes by the introduction of phosphine ligands onto the metal. The influence of the bridging unit, on the degree of electronic communication between the cobalt

moieties, has also been emphasised, with shorter carbon chains and increased π-conjugated closed-ring systems promoting electronic interaction between the metallic centres. Therefore, the cobalt carbonyl switches described here have the potential to be used in the development of molecular wires. Switching between the open and closed isomers has the prospect to control the electronic communication properties between the ON (closed-ring) and OFF (open-ring) state, as demonstrated for **3F**.

The electrochemical properties of the cobalt carbonyl complexes were also investigated in terms of their influence on the electrochromic switching behaviour of the dithienylethene units. In the case of the perhydro-derivative, **2H**, oxidative cyclisation was also found to occur for the related $Co_2(CO)_6$ {**4H**} and $Co_2(CO)_4dppm$ {**6H**} complexes. However, the oxidation processes of the dppm derivative **6H**, monitored in the UV-vis spectrum, indicated a significant decrease in the amount of the closed-ring isomer formed, suggesting that the oxidation of the tetracarbonyl moieties, before the switching unit, reduced the stability of the cationic species produced following ring-closure. In the case of the less conjugated derivative **1H**, oxidative ring-closing was also observed for the corresponding $Co_2(CO)_6$ {**3H**} and $Co_2(CO)_4dppm$ {**5H**} complexes. However, a more prominent effect of the cobalt carbonyl moieties was observed for these complexes, which can be affiliated with the shorter carbon chain length of this perhydro switch. In the case of the $Co_2(CO)_6$ complex **3H**, the results suggested that cyclisation processes were induced following intramolecular electron transfer, from the oxidised metal carbonyl moieties, to the dithienylethene units. A similar result was apparent for the related $Co_2(CO)_4dppm$ complex **5H**. New features appeared in the CV and UV-vis/NIR spectrum of **5H**, associated with the closed-ring cation species, following oxidation of the $Co_2(CO)_4dppm$ moieties. Thus, this result suggests that the electrochemical cyclisation process of **5H** was induced by the oxidised cobalt carbonyl moieties, possibly via an intramolecular electron transfer mechanism. A similar process has been described previously by Browne et al,[4] whereby cyclisation of the dithienylethene switch was induced following intramolecular electron transfer from an oxidised methoxyphenyl group.

In contrast to the perhydro analogues, the cyclisation process of **2F** was inhibited following the introduction of $Co_2(CO)_6$ moieties onto the alkynyl units (i.e. for **4F**). This result can be attributed to the fact that the metal carbonyl units underwent

oxidation processes at much more positive potentials in comparison to the switching unit, hence providing extra stability for the subsequent formation of the open-ring radical cation species. In the case of the perfluoro-derivative **1F**, incorporating metal carbonyl moieties did not induce a cyclisation process. However, in the case of the closed-ring isomer **1Fc**, a cycloreversion process was observed, the rate of which was found to be reduced by the presence of $Co_2(CO)_6$ moieties attached to the alkynyl linkers, as shown for **3bF**. Furthermore, in all cases, the presence of the cobalt carbonyl moieties inhibited the generation of the unknown electroactive species (**1Hy**, **1Fy**, **2Fy**).

The effect of oxidation processes on the cobalt carbonyl moieties was investigated in the IR spectra. In all cases, bleaching of the parent carbonyl bands occurred, following oxidation processes. The parent bands were found to recover to their original absorbance values following subsequent reduction processes at 0 V, but not completely, due to some decomposition processes. In the case of the closed-ring $Co_2(CO)_6$ complex **4bH**, and the $Co_2(CO)_4dppm$ complexes, the carbonyl bands were found to shift to higher wavenumbers upon oxidation, and subsequent reduction indicated that the reversibility of the electrochemical processes was improved for these complexes. The increased stability of the dppm derivatives, and of the closed-ring isomer of the $Co_2(CO)_6$ complex **4bH**, highlights how the properties of the cobalt carbonyl complexes can be tuned to increase the reversibility of the system. Therefore, such complexes have the potential to utilise infra-red spectroscopy as a non-destructive read-out signal in the development of write-read-erase systems.[27,28]

5.5 Bibliography

(1) Browne, W. R.; de Jong, J. J. D.; Kudernac, T.; Walko, M.; Lucas, L. N.; Uchida, K.; van Esch, J. H.; Feringa, B. L. Oxidative Electrochemical Switching in Dithienylcyclopentenes, Part 1: Effect of Electronic Perturbation on the Efficiency and Direction of Molecular Switching. *Chem. Eur. J.* **2005**, *11*, 6414-6429.

(2) Moriyama, Y.; Matsuda, K.; Tanifuji, N.; Irie, S.; Irie, M. Electrochemical Cyclization/Cycloreversion Reactions of Diarylethenes. *Org. Lett.* **2005**, *7*, 3315-3318.

(3)   Xie, N.; Zeng, D. X.; Chen, Y. Electrochemical Switch Based on the Photoisomerization of a Diarylethene Derivative. *J Electroanal. Chem.* **2007**, *609*, 27-30.

(4) Browne, W. R.; de Jong, J. J. D.; Kudernac, T.; Walko, M.; Lucas, L. N.; Uchida, K.; van Esch, J. H.; Feringa, B. L. Oxidative Electrochemical Switching in Dithienylcyclopentenes, Part 2: Effect of Substitution and Asymmetry on the Efficiency and Direction of Molecular Switching and Redox Stability. *Chem. Eur. J.* **2005**, *11*, 6430-6441.

(5) Guirado, G.; Coudret, C.; Hliwa, M.; Launay, J. P. Understanding Electrochromic Processes Initiated by Dithienylcyclopentene Cation-Radicals. *J. Phys. Chem. B.* **2005**, *109*, 17445-17459.

(6) Peters, A.; Branda, N. R. Electrochemically Induced Ring-Closing of Photochromic 1,2-Dithienylcyclopentenes. *Chem. Commun.* **2003**, 954-955.

(7) Kowalski, K.; Winter, R. F.; Makal, A.; Pazio, A.; Wozniak, K. The Synthesis, Structure, and FTIR Spectroelectrochemistry of $W(CO)_5$ Complexes of 4-Oxo-4-(2,5-dimethylazaferrocen-1'-yl)butanoic and 5-Oxo-5-(2,5-dimethylazaferrocen-1'-yl)pentanoic Acids. *Eur. J. Inorg. Chem.* **2009**, 4069-4077.

(8) Jin, B.; Tao, F.; Liu, P. Rapid-Scan Time-Resolved FT-IR Spectroelectro-chemistry - Study on the Electron Transfer of Ferrocene-Substituted Thiophenes. *J. Electroanal. Chem.* **2008**, *624*, 179-185.

(9)   Lee, J.; Kwon, T.; Kim, E. Electropolymerization of an EDOT-Modified Diarylethene. *Tetrahedron Lett.* **2007**, *48*, 249-254.

(10) Ruiz, J.; Astruc, D. Permethylated Electron-Reservoir Sandwich Complexes as References for the Determination of Redox Potentials. Suggestion of a New Redox Scale. *C. R. Acad. Sci., Ser. IIC: Chim.* **1998**, *1*, 21-27.

(11) Tsivgoulis, G. M.; Lehn, J. M. Photoswitched and Functionalized Oligothiophenes: Synthesis and Photochemical and Electrochemical Properties. *Chem. Eur. J.* **1996**, *2*, 1399-1406.

(12) Yang, T.; Pu, S.; Fan, C.; Liu, G. Synthesis, Crystal Structure and Optoelectronic Properties of a New Unsymmetrical Photochromic Diarylethene. *Spectrochim. Acta A.* **2008**, *70*, 1065-1072.

(13) Peters, A.; Branda, N. R. Electrochromism in Photochromic Dithienylcyclopentenes. *J. Am. Chem. Soc.* **2003**, *125*, 3404-3405.

(14) Areephong, J.; Kudernac, T.; de Jong, J. J. D.; Carroll, G. T.; Pantorott, D.; Hjelm, J.; Browne, W. R.; Feringa, B. L. On/Off Photoswitching of the Electropolymerizability of Terthiophenes. *J. Am. Chem. Soc.* **2008**, *130*, 12850-12851.

(15) Arnanz, A.; Marcos, M.; Moreno, C.; Farrar, D. H.; Lough, A. J.; Yu, J. O.; Delgado, S.; González-Velasco, J. Synthesis, Structures and Comparative Electrochemical Study of 2,5-Bis(trimethylsilylethynyl)thiophene Coordinated Cobalt Carbonyl Units. *J. Organomet. Chem.* **2004**, *689*, 3218-3231.

(16) Arewgoda, M.; Rieger, P. H.; Robinson, B. H.; Simpson, J.; Visco, S. J. Paramagnetic Organo-Metallic Molecules .12. Electrochemical Studies of Reactions with Lewis-Bases Following Metal-Metal Bond Cleavage in $R_2C_2Co_2(CO)_6$ Radical Anions. *J. Am. Chem. Soc.* **1982**, *104*, 5633-5640.

(17) Marcos, M. L.; Macazaga, M. J.; Medina, R. M.; Moreno, C.; Castro, J. A.; Gomez, J. L.; Delgado, S.; González-Velasco, J. Alkynyl Cobalt Complexes. An Electrochemical Study. *Inorg. Chim. Acta* **2001**, *312*, 249-255.

(18) Medina, R. M.; Moreno, C.; Marcos, M. L.; Castro, J. A.; Benito, F.; Arnanz, A.; Delgado, S.; Gonzalez-Velasco, J.; Macazaga, M. J. Syntheses, Structures and Electrochemical Study of π-Acetylene Complexes of Cobalt. *Inorg. Chim. Acta* **2004**, *357*, 2069-2080.

(19) Osella, D.; Fiedler, J. Reinvestigation of the Electrochemical-Behavior of the $Co_2(CO)_6$(ethynylestradiol) Complex - Evidence of Efficient Recombination of the Electrogenerated Fragments. *Organometallics* **1992**, *11*, 3875-3878.

(20) Wong, W.; Lam, H.; Lee, S. Synthesis, Electrochemistry and Structural Characterization of New Dimeric Cobalt η^2-Alkyne Carbonyl Complexes. *J. of Organomet. Chem.* **2000**, *595*, 70-80.

(21) Lin, Y.; Yuan, J.; Hu, M.; Cheng, J.; Yin, J.; Jin, S.; Liu, S. H. Syntheses and Properties of Binuclear Ruthenium Vinyl Complexes with Dithienylethene Units as Multifunction Switches. *Organometallics* **2009**, *28*, 6402-6409.

(22) Motoyama, K.; Koike, T.; Akita, M. Remarkable Switching Behavior of Bimodally Stimuli-Responsive Photochromic Dithienylethenes with Redox-Active Organometallic Attachments. *Chem. Commun.* **2008**, 5812-5814.

(23)   Zhong, Y.; Vila, N.; Henderson, J. C.; Flores-Torres, S.; Abruna, H. D. Dinuclear Transition-Metal Terpyridine Complexes with a Dithienylcyclopentene Bridge Directed Toward Molecular Electronic Applications. *Inorg. Chem.* **2007***, 46*, 10470-10472.

(24)   Macazaga, M. J.; Marcos, M. L.; Moreno, C.; Benito-Lopez, F.; Gomez-González, J.; González-Velasco, J.; Medina, R. M. Syntheses, Structures and Comparative Electrochemical Study of π-Acetylene Complexes of Cobalt. *J. of Organomet. Chem.* **2006***, 691*, 138-149.

(25)   Tanaka, Y.; Inagaki, A.; Akita, M. A Photoswitchable Molecular Wire with the Dithienylethene (DTE) Linker, (dppe)(η^5-C$_5$Me$_5$)Fe-C≡C-DTE-C≡C-Fe(η^5-C$_5$Me$_5$)(dppe). *Chem. Commun.* **2007**, 1169-1171.

(26)   Arnanz, A.; Marcos, M.; Delgado, S.; González-Velasco, J.; Moreno, C. The Effect of Thiophene Ring Substitution Position on the Properties and Electrochemical Behaviour of Alkyne–dicobaltcarbonylthiophene Complexes. *J. Organomet. Chem.* **2008***, 693*, 3457-3470.

(27)   Tian, H.; Yang, S. J. Recent Progresses on Diarylethene Based Photochromic Switches. *Chem. Soc. Rev.* **2004***, 33*, 85-97.

(28)   Nakamura, S.; Yokojima, S.; Uchida, K.; Tsujioka, T.; Goldberg, A.; Murakami, A.; Shinoda, K.; Mikami, M.; Kobayashi, T.; Kobatake, S.; Matsuda, K.; Irie, M. Theoretical Investigation on Photochromic Diarylethene: A Short Review. *J. Photochem. Photobiol. A.* **2008***, 200*, 10-18.

CHAPTER 6

Electrochemistry of Ferrocenyl-based Switches and their Cobalt Carbonyl Complexes

*Chapter 6 describes the electrochromic behaviour of the perhydro- and perfluoro-switches, substituted with ethynylferrocene moieties: 1,2-Bis(5'-ethynylferrocene-2'-methylthien-3'-yl)cyclopentene {**7H**}; 1,2-Bis(5'-ethynylferrocene-2'-methylthien-3'-yl)perfluorocyclopentene {**7F**}; 1,2-Bis(5'-(4''-phenyl-ethynylferrocene)-2'-methylthien-3'-yl)-cyclopentene {**8H**}; 1,2-Bis(5'-(4''-phenyl-ethynylferrocene)-2'-methylthien-3'-yl)per-fluorocyclopentene {**8F**}. Cyclic voltammetric and UV-vis spectroelectrochemical techniques were employed to investigate the electrochemical properties of the ferrocenyl-based switches, and their corresponding $Co_2(CO)_6$ complexes {**9H**, **9F**, **10H**, **10F**, **10bF**}, and $Co_2(CO)_4dppm$ complexes {**11H**, **11F**, **12H**, **12F**}. The effects of the oxidation processes on the cobalt carbonyl moieties were examined using IR spectroelectrochemical methods.*

314

6.1 Introduction

Ferrocene is known for its exceptional electrochemical properties, due to its reversible oxidation process, with the +II state of iron oxidising to the +III state.[1] Thus, the electron-donating form of ferrocene (Fc) is oxidised to its electron-withdrawing ferrocenium ion (Fc^+). Hence, the redox-activity of ferrocene molecules can be utilised in a number of opto-electronic devices, by acting as molecular wires or switches.[2-5]

The electronic communication between ferrocene moieties, in systems containing two or more ferrocene molecules separated by a bridging unit, has been explored by cyclic voltammetry methods. For example, Thomas et al[4] investigated the electronic communication between two ferrocenyl moieties, separated by a thiophene spacer (**FTF**), as illustrated in figure 4.1. They deduced that the presence of a thiophene unit increases the electronic communication between the ferrocene moieties, in comparison to its phenylene analogues, due to the delocalisation of charge across the molecule. This was evidenced by the presence of two separate one-electron redox waves present in the cyclic voltammogram.

The ability of ferrocene molecules to undergo reversible oxidation processes can be utilised in the design of fluorescence redox-switchable molecular systems. For example, Martinez et al[5] reported a dyad (**PyFc**), consisting of a fluorescent pyrene unit and a redox-active ferrocene unit, as illustrated in figure 6.1, the fluorescence intensity of which depends on the oxidation state of the ferrocene unit. The fluorescence of the neutral form of **PyFc** was found to be weak, which was attributed to the quenching effect of the ferrocene molecule, occurring via electron transfer or energy transfer, from the electron-donating ferrocene unit, to the electron-accepting excited state of the pyrene unit. Oxidation of the ferrocene moiety was induced by both chemical and spectroelectrochemical methods. In both cases, the emission of the oxidised **PyFc$^+$** species was found to increase. This phenomenon was attributed to the formation of the ferrocenium ion Fc^+. The ferrocenium ion acts as an electron-withdrawing group, and the spectral overlap between the absorption spectrum of Fc^+ and the emission spectrum of the pyrene unit is small. Hence, energy transfer from the excited state of pyrene to the ferrocenium unit cannot take place efficiently, and so

the oxidation of the ferrocene unit to the ferrocenium ion can be considered as turning the fluorescence "ON". Spectroelectrochemical studies showed that subsequent reduction of the ferrocenium ion to, the neutral ferrocene unit, resulted in a decrease in the fluorescence intensity (i.e. turning the fluorescence "OFF"), demonstrating the reversibility of this switching process.
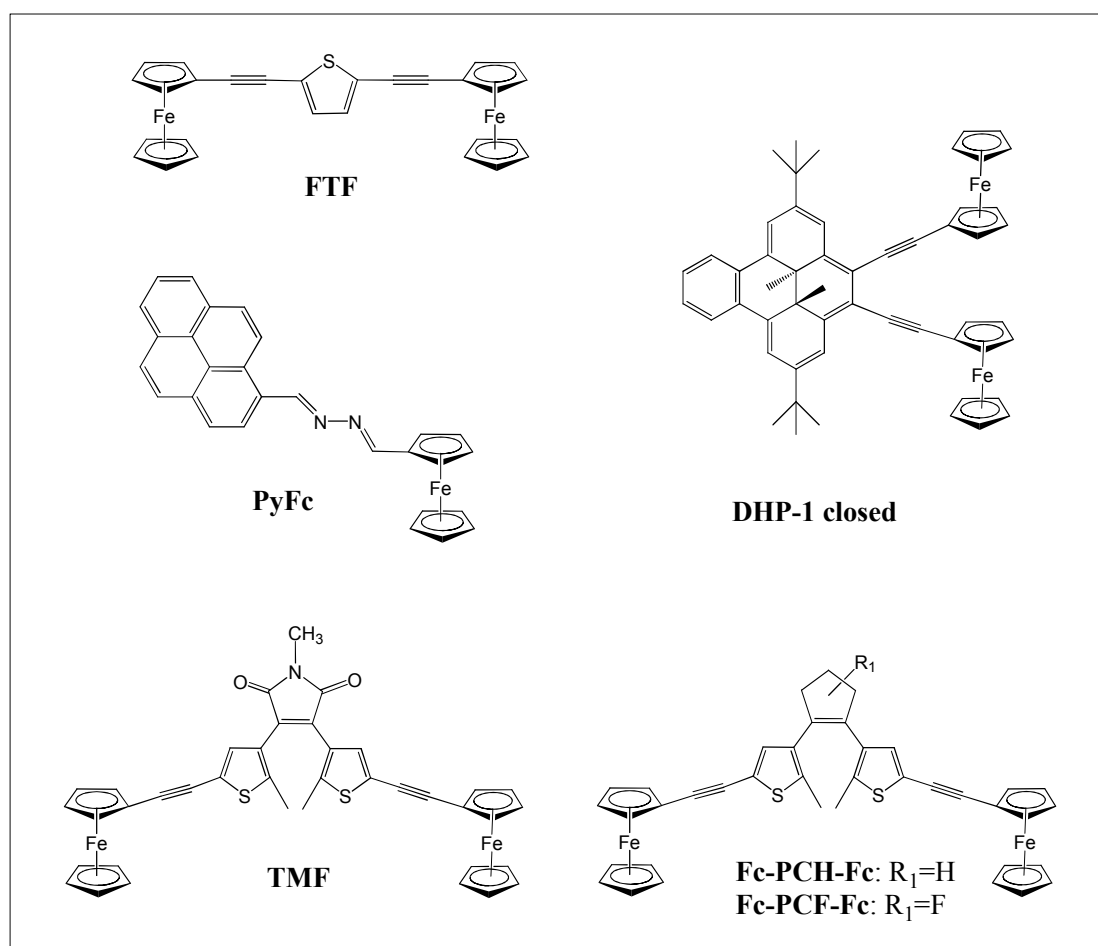
Figure 6.1: Structures of ferrocenyl-based molecules described in the literature: **FTF:**[4] **PyFc:**[5] **DHP-1 closed**;[6] **TM** and **TMF;**[7] **Fc-PCH-Fc** and **Fc-PCF-Fc.**[8]

The electrochromic properties of dithienylcyclopentene switches have been described previously in chapter 1. A number of publications[6-8] have shown that incorporating ethynylferrocene moieties onto molecular switching units affects the electrochromic properties of such switches, the structures of which are illustrated in figure 6.1. For example, Sun et al[7] described a dithienylmaleimide switch, appended with two ethynylferrocene units (**TMF**), which underwent an oxidative ring-opening process, as evidenced by cyclic voltammetry studies. Such a process could be ascribed to the electron-withdrawing ability of the oxidised ferrocenium ions.

Muratsugu et al[6] reported the electrochemical properties of a dimethyldihydropyrene switch, disubstituted with ethynylferrocene moieties (**DHP-1**). The cyclic voltammogram (CV) of the closed species (**1c**) demonstrated strong electronic communication between the two ferrocene molecules due to the presence of two separate redox waves. Conversely, only one redox wave was observed for the ferrocene moieties in the CV of the open-ring form (**1o**), with no sign of peak separation, which is consistent with the less π-conjugated structure of the open-ring isomer. However, the second oxidation scan observed in the CV of the open-form indicated that oxidative ring-closing was taking place. This theory was further supported by monitoring the chemical oxidation of the open-ring isomer in the UV-vis-NIR spectra, and they observed that the absorbance spectra of $\mathbf{1o^+}$ and $\mathbf{1o^{2+}}$ completely matched those of $\mathbf{1c^+}$ and $\mathbf{1c^{2+}}$. In fact, they deduced that the open-form of **DHP-1** was undergoing redox-assisted ring-closing following oxidation of only the ferrocene moieties.

Launay et al[8] described the electrochromic properties of dithienylcyclopentene (DTE) switches, appended with an ethynylferrocene molecule on either side, with a perhydro- and perfluoro-cyclopentene core (**Fc-PCH-Fc** and **Fc-PCF-Fc** respectively). Such switches are known to undergo oxidative ring-opening or ring-closing processes upon oxidation of the DTE core at high potentials (> 1.0 V). Following cyclic voltammetry and UV-vis spectroelectrochemical analysis of the closed-ring isomers, Launay et al observed oxidative ring-opening processes in both cases, with the perhydro-derivative undergoing a faster ring-opening process, in comparison to its perfluoro-analogue. Launay et al concluded that oxidation of the ferrocene molecules, to their electron-withdrawing ferrocenium ions, played a major role in inducing these ring-opening processes, thus allowing electrochemical isomerisation processes to occur at lower potentials, comparing to when direct oxidation of the DTE unit is required.

We also synthesised the perhydro and perfluoro-derivatives of the ferrocenyl-based dithienylcyclopentene switches (**7H** and **7F**), reported by Launay et al,[8] as described previously in chapter 2. Their electrochemical properties were investigated by cyclic voltammetry and UV-vis spectroelectrochemistry methods, and the results are detailed here. Subsequently, the effect of incorporating a phenyl-ring spacer unit between the DTE core and the ethynylferrocene moieties (**8H** and **8F**), on the electrochromic

properties, was also examined. The oxidative and reductive processes of the corresponding $Co_2(CO)_6$ (**9H**, **9F**, **10H**, **10F**) and $Co_2(CO)_4$dppm complexes (**11H**, **11F**, **12H**, **12F**) were monitored by cyclic voltammetry and UV-vis spectroelectrochemistry in order to determine if the presence of the metal carbonyls would change the electrochemical isomerisation processes of these ferrocenyl-based switches. IR spectroelectrochemical studies were also carried out. The structures of these compounds are displayed in figure 6.2.
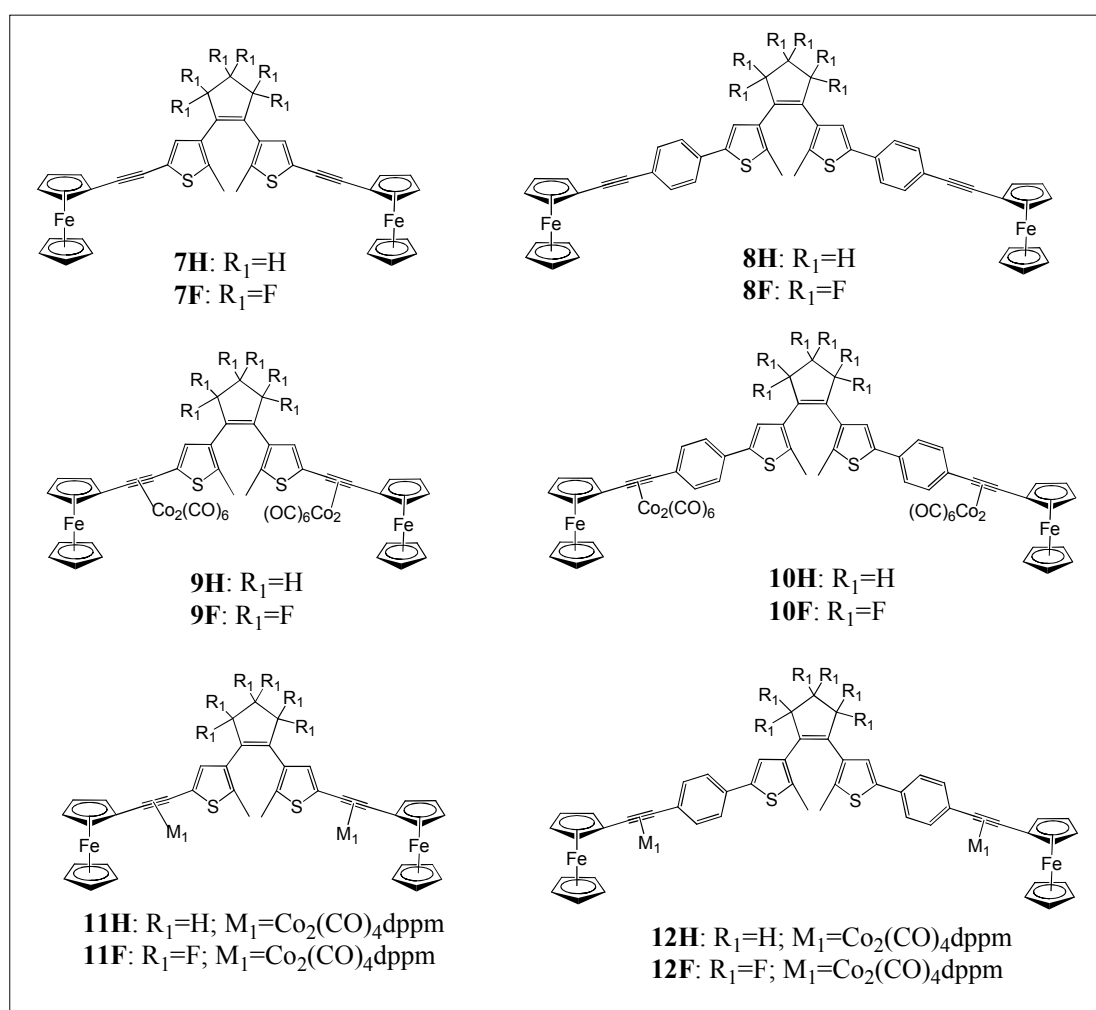
Figure 6.2: Illustrates the structures of the ferrocenyl-based dithienylperhydro- and perfluoro-cylopentene switches **7H**, **7F**, **8H** and **8F** discussed in this chapter, and the corresponding $Co_2(CO)_6$ complexes {**9H**, **9F**, **10H**, **10F, 10bF**} and $Co_2(CO)_4$dppm complexes {**11H**, **11F**, **12H**, **12F**}.

6.2 Experimental

6.2.1 General Procedures

Cyclic Voltammetry: Solutions of the compounds (~ 1 mmol) were made-up in spectroscopic grade dichloromethane, using tetrabutylammonium hexafluorophosphate (0.1 M) as the supporting electrolyte. The solutions were placed into a 10 ml two-kneck round-bottomed flask, degassed with argon and the flask was sealed. The flask was kept under an inert atmosphere throughout the experiment. A three-electrode system was set-up: glassy carbon (working electrode), a platinum wire (counter electrode) and a silver wire (reference electrode). The cyclic voltammograms were obtained at a scan rate of 0.1 Vs^{-1}, at room temperature, in the dark. The reference electrode was calibrated versus the decamethylferrocene redox couple (Fc^{*+}/Fc^*), which has a formal potential $E_{1/2}$ = -0.07V versus SCE.[9]

UV-vis/NIR Spectroelectrochemistry: An electrolyte solution was prepared using tetrabutylammonium hexafluorophosphate (0.1 M) dissolved in dichloromethane. The solutions were placed in a custom-made quartz cuvette (2 mm path length) equipped with a solvent reservoir holding a silver wire reference electrode and platinum wire counter electrode (separated from the solution using a glass tube sleeve), and a platinum gauze mesh was employed as the working electrode. Bulk electrolysis experiments were carried out in the dark at room temperature, under an atmosphere of argon. UV-vis/NIR spectra were recorded as oxidation/reduction potentials were applied, and when no further changes were observed, a potential of 0 V was applied to the system, and the resulting spectra were recorded. These experiments were typically carried out over a period of 20 to 40 minutes.

IR spectroelectrochemistry: Solutions of the cobalt carbonyl complexes were made-up in a 0.1 M tetrabutylammonium hexafluorophosphate/CH_2Cl_2 electrolyte solution. The samples were placed in an IR OTTLE cell, containing a platinum gauze mesh working electrode, a platinum counter electrode, and a silver reference electrode. Bulk electrolysis experiments were carried out by applying positive potentials to the system. The oxidation processes were monitored in the IR spectra until no further

changes were observed. Subsequently, a potential of 0V was applied and the changes in the IR spectra were recorded.

Formation of the closed-ring isomers: Solutions of the switches were made-up in deuterated acetone and placed in a sealed NMR tube. The samples were irradiated with monochromatic light at 313 nm, and monitored by ^{1}H NMR spectroscopy over time. Irradiation was continued until conversion from the open-ring to the closed-ring was complete, or before the photochemical by-products formed.

6.2.2 Materials

The dichloromethane was of spectroscopic grade and was purchased from Sigma Aldrich. The tetrabutylammonium hexafluorophosphate, decamethylferrocene and deuterated acetone were all purchased from Sigma Aldrich. The argon gas was supplied by BOC Ltd.

6.2.3 Equipment

Cyclic voltammetry and bulk electrolysis experiments were carried out using a CH Instruments Chi600a potentiostat. The electrodes used for the cyclic voltammetry experiments were a glassy carbon (working), silver wire (reference), and platinum wire (counter), all purchased from CH Instruments. UV-vis/NIR Spectroelectrochemistry experiments were carried out on a Jasco V-670 spectrophotometer, in a custom-made quartz cuvette (2 mm path-length) equipped with a solvent reservoir, which was purchased from Starna Scientific. The electrodes employed were a platinum gauze mesh (working), a silver wire (reference) and a platinum wire (counter). Infra-red spectroelectrochemistry experiments were carried out on a Perkin Elmer "Spectrum 65" FT-IR spectrometer, using an electrochemical IR OTTEL cell containing a platinum gauze working electrode, a platinum counter electrode, and a silver reference electrode, which was purchased from Specac. Photochemical experiments were carried out using a 200W Hg lamp (Oriel Instruments, model no.: 68911) containing a 313 nm filter. ^{1}H NMR spectra were recorded on a Bruker model AC 400 MHz spectrometer.

6.3 Results and Discussion

6.3.1 Ferrocenyl-based Switches: Cyclic Voltammetry

Cyclic voltammetric techniques were employed in order to investigate electrochemical induced switching, of the open and closed forms, of the ferrocenyl-based switches **7H/F** and **8H/F**. The closed-ring isomers were generated by irradiating the open forms with UV light (at 313 nm) until conversion from the open to the closed-ring was complete, or before the photochemical by-products formed, as monitored in the ^{1}H NMR. Cyclic voltammetry experiments were performed at room temperature, in 0.1 M solutions of TBAPF$_6$/CH$_2$Cl$_2$, at a scan rate of 0.1 Vs^{-1}. Decamethylferrocene was employed as a reference and the results are reported against the ferrocene redox couple Fc*$^+$/Fc* (E$_{1/2}$ = -0.07 *vs.* SCE). The structures of the open and closed switches are illustrated in figure 6.3.
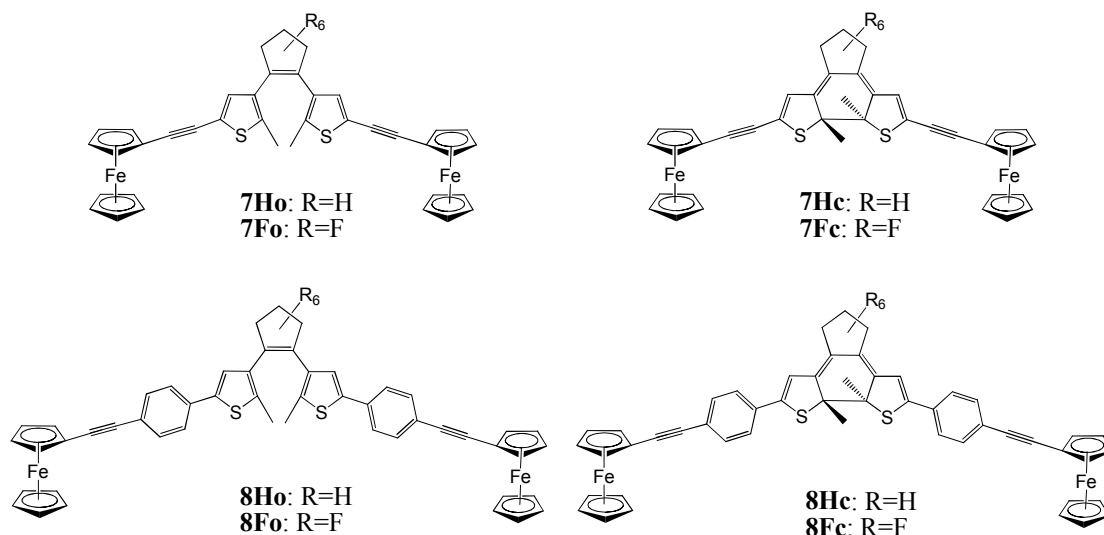
Figure 6.3: Illustrates the structures of the open and closed isomers of compounds **7H/F** and **8H/F**.

- **Reduction Process**

The reduction processes were carried out on the open and closed-ring isomers, in the potential range from 0 to -0.2 V i.e. within the potential limit of the CH_2Cl_2 solvent, and the results are summarised in table 6.1. Reduction of the open-ring isomers **7Ho**, **7Fo** and **8Ho** did not result in reduction processes at potentials greater then -2.0 V. However, in the case of the longer chain perfluoro-derivative **8F**, an irreversible reduction peak was observed at -1.85 V (*vs.* SCE), representing a two-electron reduction process, forming the dianion **8Fo^{2-}**. Such a result can be attributed to the electron-withdrawing ability of the fluorine atoms on the cyclopentene ring, which help to stabilise the LUMO (i.e. the first reduction process).[10-12] A second contributing factor is the presence of the phenyl rings, separating the dithienylethene unit from the ethynylferrocene moieties, thus reducing the influence of the electron-donating ability of the ferrocene groups, and hence allowing reduction processes to occur at less negative potentials.

Table 6.1: Redox properties, of the open and closed isomers of compounds **7H/F** and **8H/F**, following reduction processes.

Open Isomers		Closed Isomers	
	E_{pc} (V)		E_{pc} (V)
7Ho	-	**7Hc**	-1.76[a]
8Ho	-	**8Hc**	N/A
7Fo	-	**7Fc**	-1.36[a], -1.68[a]
8Fo	-1.85[a]	**8Fc**	-1.07[a], -1.40[a]

All values listed are values of potential (V) *vs.* SCE, recorded in 0.1 M TBAPF$_6$/CH$_2$Cl$_2$.
[a] indicates an irreversible reduction process.
- indicates that no reduction peaks were observed at potentials greater than -2.0 V.
N/A: the results are not available.

In the case of the closed-ring isomers of the perfluoro analogues, two reduction waves were detected below -2.0 V, representing the formation of the monoanion and dianion species. This can be attributed to the extended π-conjugation of the systems in the closed-form, which reduces the HOMO-LUMO gap, thus allowing reduction processes to occur at less negative potentials.[11,12] For example, there is a marked decrease in the reduction potential recorded for the closed-ring isomer **8Fc**, in comparison to the open-ring form **8Fo** (ΔE = 450 mV). In the CV of **7Hc**, only a single reduction peak was observed within the potential limit, assigned to the

monoanion species. Producing the closed-form of **8H** proved to be difficult, hence no reduction process was observed for **8Hc**. Noticeably, a trend emerged among the reduction potentials recorded for the closed-ring derivatives, with the potential values becoming more negative in the order of: **8Fc** < **7Fc** < **7Hc**. Such a trend can be attributed to the atoms present on the cyclopentene ring (H *vs.* F), and the effect of the substituents attached to the alkynyl units. As described previously, the electron-withdrawing fluorine atoms better stabilise the LUMO than the electron-donating hydrogen atoms, and the presence of the phenyl units in **8Fc** reduce the influence of the electron-donating ferrocene molecules. Thus **8Fc** underwent reduction at the least negative potential, and **7Hc** at the most negative value.
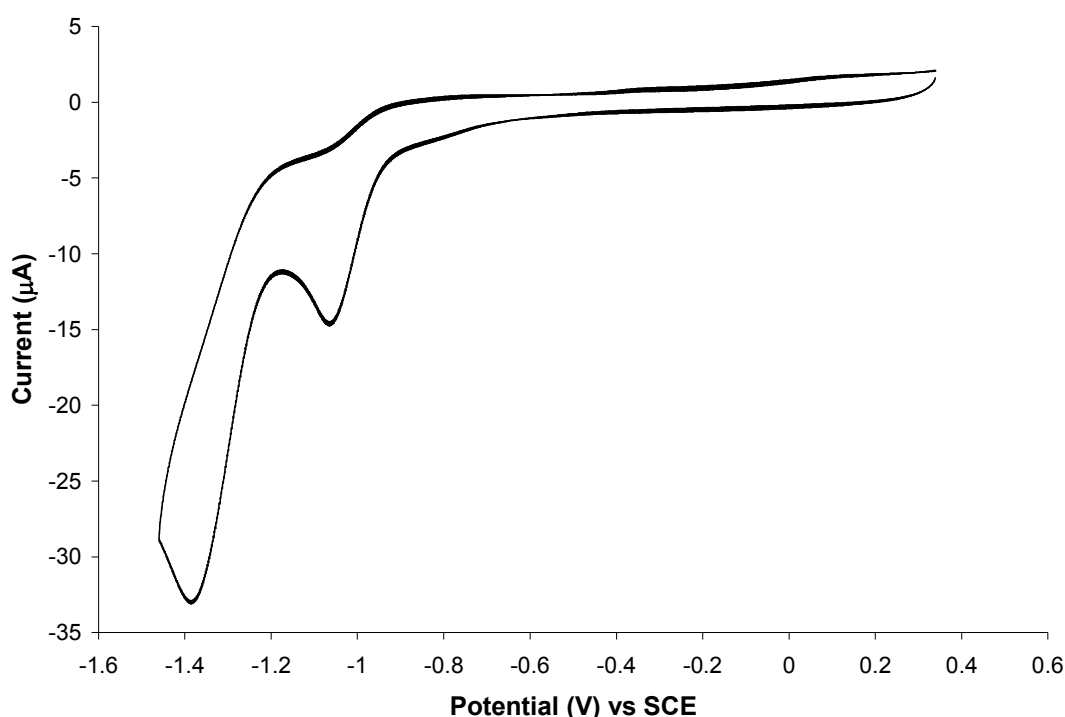
Figure 6.4: Cyclic voltammogram of the reduction process of **8Fc**, in 0.1 M TBAPF$_6$/CH$_2$Cl$_2$, at a scan rate of 0.1 Vs^{-1}.

- **Oxidation Process**

The oxidation processes of the ferrocenyl-based compounds **7H/F** and **8H/F** were investigated, in the open and closed forms, to determine if these switches underwent electrochemical cyclisation or cycloreversion processes. The oxidation potentials recorded in the CV's of these compounds are summarised in table 6.2. In each case, the ferrocenyl moieties underwent a one electron quasireversible oxidation process

$(i_{pc}/i_{pa} \approx 0.8)$, from Fe(II) to Fe(III) (as expected[1,3]), with $E_{1/2}$ values ranging from 5.7 V to 6.3 V. The CV's of the open and closed-ring isomers displayed a single bielectronic redox wave, representing a two electron process i.e. one-electron oxidation of each of the two ferrocene moieties separated by the switching unit, thus indicating that little electronic interaction exists between the two iron centres. Oxidation processes of the switching units occurred at higher potentials, and the results suggest that generation of the electron-withdrawing ferrocenium ions (Fc^+) influenced the electrochromic properties of the switches.

Table 6.2: Redox properties of **7H/F** and **8H/F**, in the open and closed forms.

	Cyclic Voltammetry Oxidation Potentials						
	Open-Ring Isomers				Closed-Ring Isomers		
	E_{pa} (V)	E_{pc} (V)	$E_{1/2}$ (V)		E_{pa} (V)	E_{pc} (V)	$E_{1/2}$ (V)
7Ho	0.68[Fc]	0.54[Fc]	0.61[Fc]	**7Hc**	0.65[Fc]	0.51[Fc]	0.58[Fc]
	0.99[rc]	0.93[rc]	0.96[rc]		0.96[rc]	0.89[rc]	0.93[rc]
	1.15[rc]	1.08[rc]	1.12[rc]		1.13[rc]	1.07[rc]	1.10[rc]
	1.50[a]						
8Ho	0.43[rc]	0.37[rc]	0.40[rc]	**8Hc**	0.44[c]	0.39[rc]	0.42[rc]
	0.68[Fc]	0.48[Fc]	0.58[Fc]		0.64[Fc]	0.51[Fc]	0.58[Fc]
	0.90[rc]	0.80[rc]	0.85[rc]		0.88[rc]	0.82[rc]	0.85[rc]
	1.32[a]						
7Fo	0.73[Fc]	0.52[Fc]	0.63[Fc]	**7Fc**	0.69[Fc]	0.57[Fc]	0.63[Fc]
	1.76[a]				1.26[rc]		
					1.37[rc]		
8Fo	0.64[Fc]	0.50[Fc]	0.57[Fc]	**8Fc**	0.66[Fc]	0.53[Fc]	0.60[Fc]
	1.05[rc]	0.98[rc]	1.02[rc]		1.06[rc]	0.98[rc]	1.02[rc]
	1.21[rc]	1.07[rc]	1.14[rc]		1.20[rc]	1.10[rc]	1.15[rc]
	1.68[a]						

All values listed are values of potential (V) *vs.* SCE, recorded in 0.1 M TBAPF$_6$/CH$_2$Cl$_2$, at 0.1 Vs^{-1}.
[a] indicates an irreversible oxidation process
[Fc] indicates peaks due to the redox couple of the ferrocene moieties
[rc] indicates peaks assigned to the ring-closed species

Electrochemical processes of the open-ring isomer **7Fo** resulted in oxidation of the ferrocene groups at $E_{1/2} = 0.63$ V, followed by an irreversible oxidation peak at 1.76 V (*vs.* SCE) due to oxidation of the dithienylethene unit. In the subsequent anodic and cathodic sweeps, no new redox waves were observed indicating that **7Fo** does not undergo oxidative cyclisation to the closed-ring isomer.
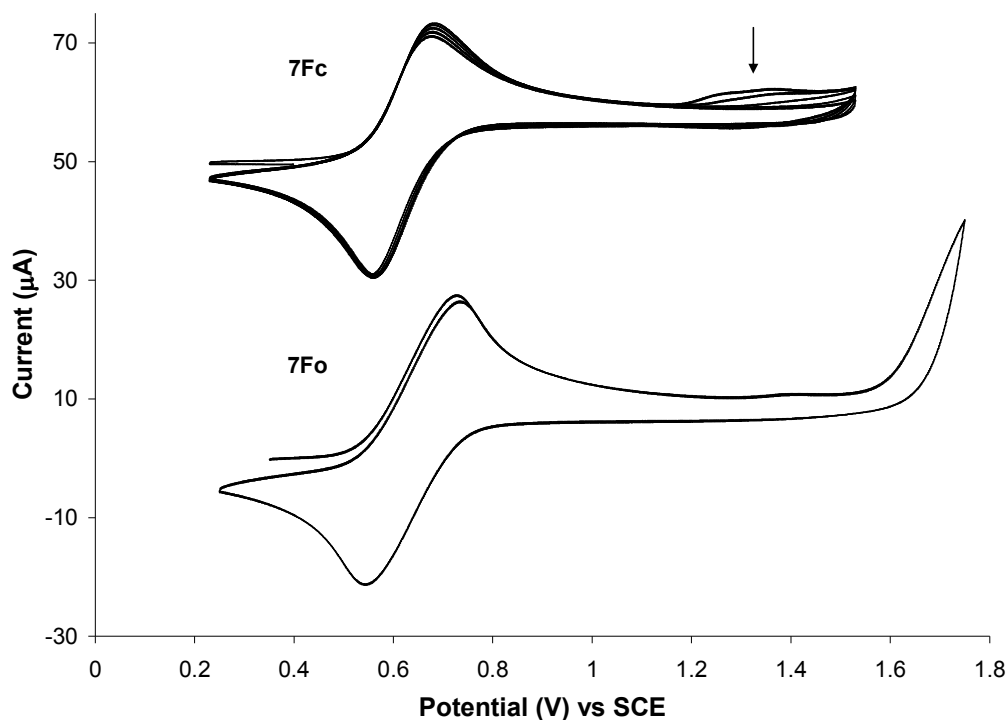
Figure 6.5 Cyclic voltammogram of **7Fo** (bottom) and **7Fc** (top), in 0.1 M TBAPF$_6$, at a scan rate of 0.1 Vs^{-1}. The CV of the closed form is offset along the coordinate for clarity.

Following oxidation of the ferrocenyl moieties at $E_{1/2}$ = 0.63 V, the CV of the corresponding closed-ring isomer **7Fc** displayed two small oxidation waves at 1.26 and 1.37 V. In the subsequent sweeps these redox waves decreased continually, as shown in figure 6.5. Such a result is indicative of an oxidative cycloreversion process. Launay et al[8] also described the occurrence of an oxidative ring-opening process for the same compound. As described previously in chapter 4, irradiation of the open-ring isomer (**7Fo**), to the closed-ring isomer (**7Fc**), is accompanied by formation of a photochemical by-product (assigned as **7Fx**). Therefore, **7Fo** was irradiated with UV light for a shorter time then that required to reach the photostationary state, to produce a small amount of the closed-ring form **7Fc**, hence why the oxidation processes of the closed-ring dithienylethene unit resulted in very small anodic peaks.

In the case of the closed-ring perhydro analogue, **7Hc**, oxidation of the ferrocene moieties was found to occur at $E_{1/2}$ = 0.58 V (*vs.* SCE). At higher potentials, two small redox waves were observed at $E_{1/2}$ = 0.93 and 1.10 V, which can be attributed to the cationic species of the closed-ring isomer. These redox processes appeared to be quite stable after twenty consecutive sweeps, at an oxidation potential of 1.25 V.

Such a result suggests that cycloreversion, to the open-ring form, does not occur for **7Hc**. It should be noted that the solution of **7Hc** contained a mixture of the open and closed form, as irradiation was stopped before all of the open-ring isomer was converted to the closed-ring isomer in order to inhibit the generation of the photochemical by-product **7Hx** (as described in chapter 4). This can explain why the oxidation processes of the closed-ring dithienylethene unit resulted in small redox waves.

Figure 6.6 Cyclic voltammogram of **7Ho** (bottom, sweep 2-3) and **7Hc** (top), in 0.1 M TBAPF$_6$, at a scan rate of 0.1 Vs^{-1}. The CV of the closed form is offset along the coordinate for clarity

In the case of the open-ring isomer, **7Ho**, oxidation of the ferrocene molecules occurred at E$_{1/2}$ = 0.61 V. Oxidation at higher potentials resulted in an irreversible peak at 1.50 V, which can be attributed to oxidation of the dithienylethene unit. In the subsequent cathodic and anodic waves two new redox waves were observed at E$_{1/2}$ = 0.96 and 1.12 V, as shown in figure 6.6, which were not present before oxidation of the dithienylethene unit took place at 1.50 V. Therefore, the results suggest that oxidation of the dithienylethene unit resulted in cyclisation to the closed-ring isomer, and hence the redox waves at E$_{1/2}$ = 0.96 and 1.12 V are a consequence of redox processes of the cationic species of the closed form.

This result is in contrast to what has been published previously for the same compound, by Launay et al.[8] They obtained identical cyclic voltammograms for the open and closed ring isomers of the perhydro-derivative, with only a single irreversible oxidation peak observed at approximately 1.44 V (*vs.* SCE), associated with the switching unit, following the ferrocene oxidation wave. They did not report any evidence of redox waves at potentials in-between these two waves. Therefore, they concluded that an extremely fast ring-opening process of the closed-ring isomer took place following the first oxidation process of the ferrocene units. It is difficult to explain why the results described here are different to those described by Launay et al. However, it should be noted that Launay et al performed their electrochemical experiments under different conditions (i.e. in 0.1 M TBAPF$_6$/acetonitrile at various scan rates). Furthermore, they described the generation of the closed-ring isomer by irradiating the open switch with UV-light until no more starting material was detected or until the photostationary state was observed, as monitored by UV-vis and ^{1}H NMR spectroscopy, but they failed to mention anything about the formation of the photochemical by-product **7Hx** during their studies.

In the case of the extended chain perhydro-derivative **8Ho**, the oxidation process of the ferrocene molecules was represented by a quasireversible two-electron oxidation wave at E$_{1/2}$ = 0.58 V, as shown in figure 6.7. An irreversible oxidation wave was observed at 1.32 V (*vs.* SCE), due to oxidation of the dithienylethene unit, and was followed by the appearance of two new redox waves at E$_{1/2}$ = 0.85 and 0.40 V, which were not present in the CV before oxidation of the switching unit occurred. After a number of consecutive sweeps, these new redox waves were found to be stable and are assigned to the cationic species of the closed-ring isomer. Hence, a cyclisation process, from the open to the closed form, occurred for **8Ho** following oxidation at 1.32 V. However, noteworthy is the sharp reduction peak in the CV of **8Ho** at 0.80 V. Such a result may be attributed to passivation of the electrode surface due to the formation of an insoluble cation species which covers the surface of the electrode.[13,14] It is possible that oxidation of the dithienylethene switch, forming the **8H^{4+}** species, makes the cation insoluble in CH$_2$Cl$_2$, thus resulting in its precipitation on the electrode surface. In the subsequent cathodic sweep, a surface confined process takes place as a result, where the precipitated **8H^{4+}** cation is reduced to the more soluble species **8H^{3+}**, thus allowing it to desorb from the surface of the electrode and return to

solution.[13] Such a process is represented by the desorption spike observed at 0.80 V, as illustrated in figure 6.7.
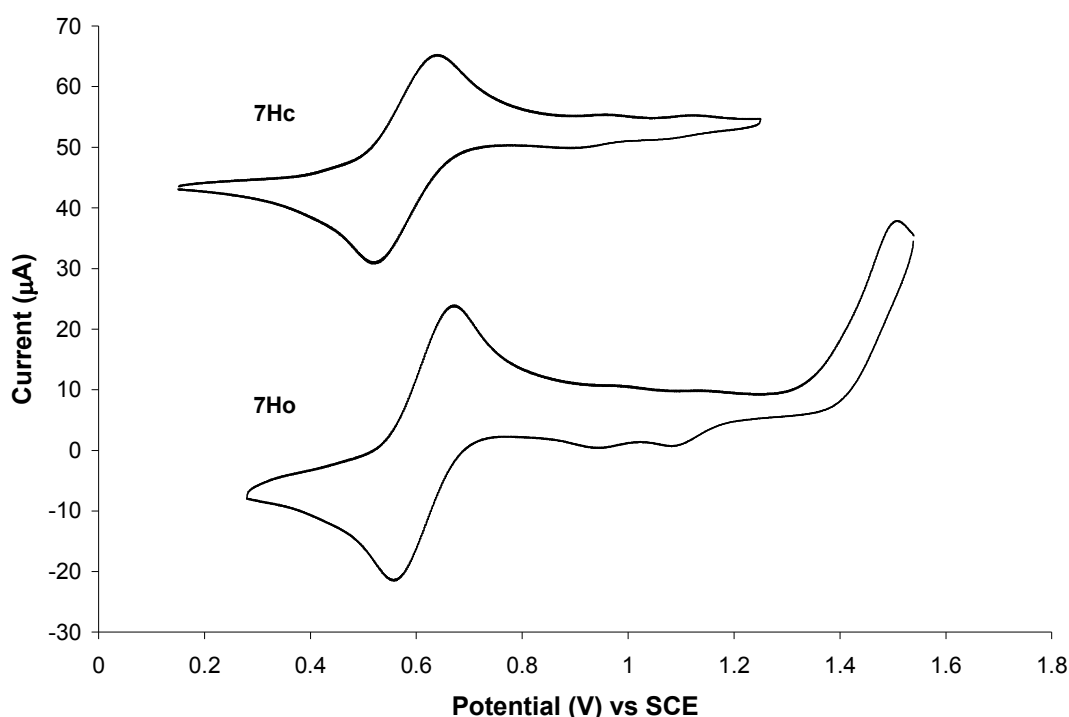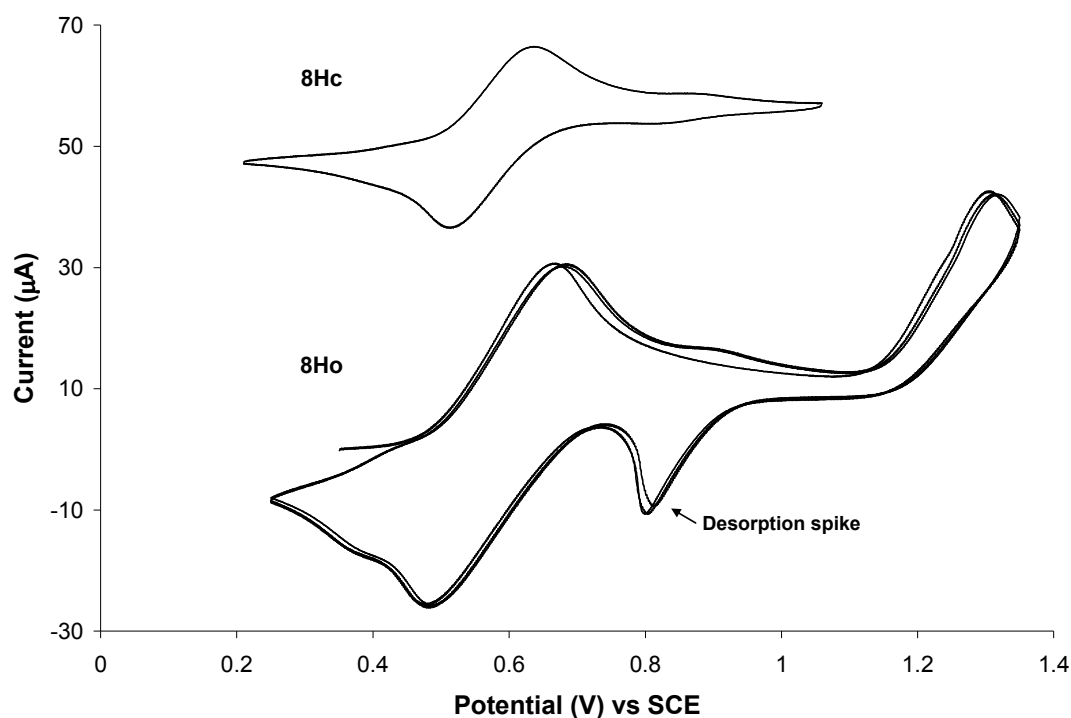

Figure 6.7 Cyclic voltammogram of **8Ho** (bottom) and **8Hc** (top), in 0.1 M TBAPF$_6$, at a scan rate of 0.1 Vs^{-1}. The CV of the closed form is offset along the coordinate for clarity.

Generation of the closed-ring isomer of **8H**, at concentrations required for electrochemical analysis (~ 1 mmol), proved to be difficult due to some decomposition processes taking place. Therefore, **8Ho** was irradiated with UV light for a shorter time then that required to reach the photostationary state, to produce a small amount of the closed-ring form, **8Hc**. The CV of this solution showed that a sufficient amount of the closed-ring isomer was produced, as oxidation waves, associated with the closed-ring switching unit, were observed at potentials lower then the first oxidation process observed for the open-ring switch (at 1.32 V). The first oxidation wave was observed at E$_{1/2}$ = 0.42, albeit small, and was obscured by the second redox wave, associated with the ferrocene moieties, at E$_{1/2}$ = 0.58 V, with a third redox wave observed at E$_{1/2}$ = 0.85 V. Therefore, the redox waves at E$_{1/2}$ = 0.415 and 0.85 V, as shown in figure 6.7, can be assigned to the monocation and dication species of the closed-ring isomer **8Hc**. The fact that these potential values are similar to those recorded for the new redox waves observed in the CV of **8Ho**,

following oxidation of the switching unit at 1.32 V, confirms that an oxidative cyclisation process occurs for **8Ho**.

The related closed-ring perfluoro analogue **8Fc**, underwent a quasireversible oxidation process at $E_{1/2}$ = 0.60 V (*vs.* SCE), due to the ferrocene molecules, followed by two redox waves at $E_{1/2}$ = 1.02 and 1.15 V, indicative of two separate one-electron oxidation processes of the closed-ring dithienylethene unit. Twenty consecutive sweeps at 1.35 V did not result in much change in the CV, indicating that the closed-ring isomer did not undergo cycloreversion to the open-ring form.
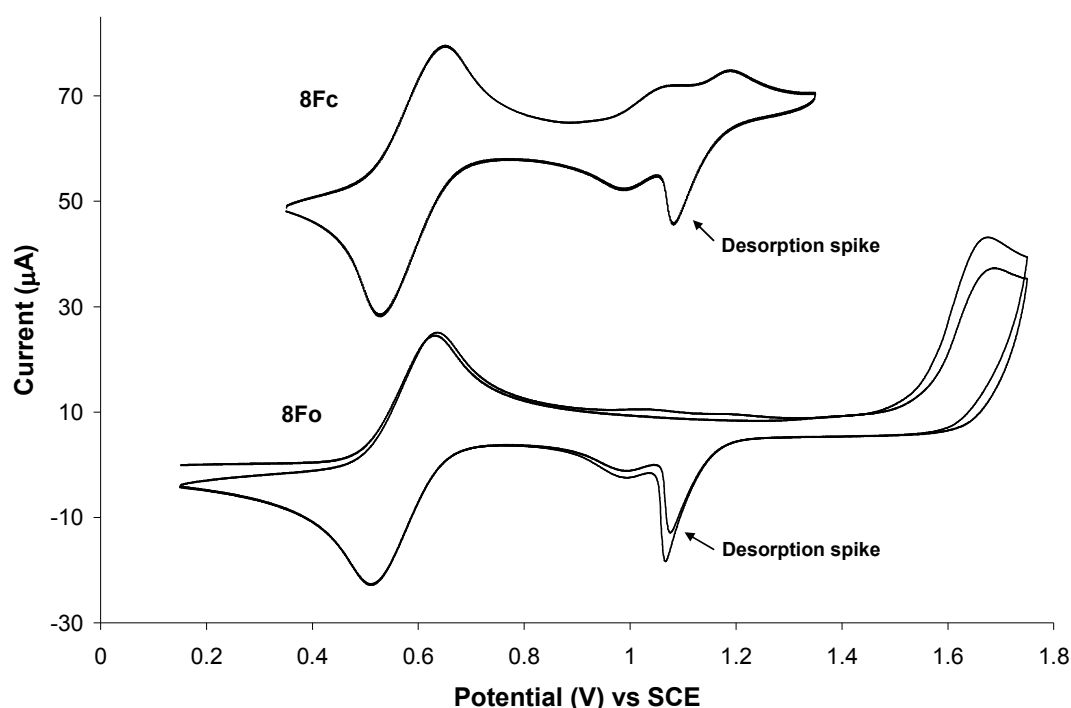
Figure 6.8 Cyclic voltammogram of **8Fo** (bottom) and **8Fc** (top), in 0.1 M TBAPF$_6$/CH$_2$Cl$_2$, at a scan rate of 0.1 Vs^{-1}. The CV of the closed form is offset along the coordinate for clarity.

Oxidation of the ferrocene molecules, on the corresponding open-ring isomer **8Fo**, occurred at $E_{1/2}$ = 0.57 V (*vs.* SCE). At higher potentials, an irreversible two-electron oxidation process of the switching unit was observed at 1.68 V. The subsequent cathodic sweep displayed two new reduction peaks at 1.07 and 0.98 V, and the following anodic sweep displayed corresponding oxidation peaks at 1.21 and 1.05 V. These redox processes were not observed in the CV before oxidation of the switching unit took place at 1.68 V, and their potential values coordinate well with the oxidation process of the closed-ring isomer **8Fc**. Therefore, it can be determined that oxidative cyclisation occurs for **8Fo**. However, a sharp desorption spike was observed in the

cathodic sweep in the CV's of both the open {**8Fo**} and closed forms {**8Fc**}, at 1.07 and 1.10 V respectively. Such a result indicates that the formation of the **8F^{4+}** cation species results in passivation of the electrode surface due to solubility issues,[13,14] which is desorbed from the electrode following reduction to the **8F^{3+}** species, as described previously for the perhydro derivative, **8H**.

Overall, the cyclic voltammetry results showed that oxidative ring-opening occurred for **7F**, whereas oxidative ring-closing occurred for **7H**, **8H** and **8F**. The electron-withdrawing fluorine atoms, and the electron-withdrawing ferrocenium ions, stabilise the cationic species of the open-ring isomer of **7F**, and together are the driving force for the electrochemical ring-opening process. On the other hand, the electron-donating hydrogen atoms on **8H** help to stabilise the cationic species of the closed-ring isomer, and the presence of the phenyl-ring spacer units, between the switch and the ferrocene moieties, help to reduce the influence of the electron-withdrawing ferrocenium ions, thus allowing oxidative cyclisation to occur. The results obtained for **7H** and **8F** further highlight the considerable effects of the substituents present on the switching unit. In the case of **7H**, oxidative cyclisation was allowed due to the electron-rich perhydro-cyclopentene ring, providing extra stability on the closed-ring cationic species. The extended chain perfluoro analogue, **8F**, was also found to undergo ring-closing via electrochemical means. This can be attributed to the presence of the electron rich phenyl rings, which provided extra stability on the cationic species of the closed-form, and also acted as spacer units, thus reducing the influence of the ferrocenium ions on the switching unit. According to literature reports,[10, 15, 16] the presence of hydrogen atoms on the cyclopentene ring are expected to promote oxidative cyclisation processes, and substituting the H atoms, with F atoms, generally results in oxidative cycloreversion. Thus the results described here highlight the resounding influence of the substituents attached to the dithienylethene unit, on the electrochromic properties of such switches.

6.3.2 Ferrocenyl-based Switches: UV-vis/NIR Spectroelectrochemistry

According to the cyclic voltammetry experiments carried out on the open and closed-ring isomers of the ferrocenyl-based switches, it was determined that oxidative cycloreversion occurred for **7F**, whereas oxidative cyclisation occurred for **7H, 8H** and **8F**.   In order to confirm these results, UV-vis/NIR spectroelectrochemical techniques were carried out on the two isomeric forms of these switches, the structures of which are illustrated in figure 6.9. The results obtained in the UV-vis/NIR spectra are summarised in table 6.3, and were assigned to the corresponding oxidation products from reference to results published in the literature.[5,8,10,17-19]
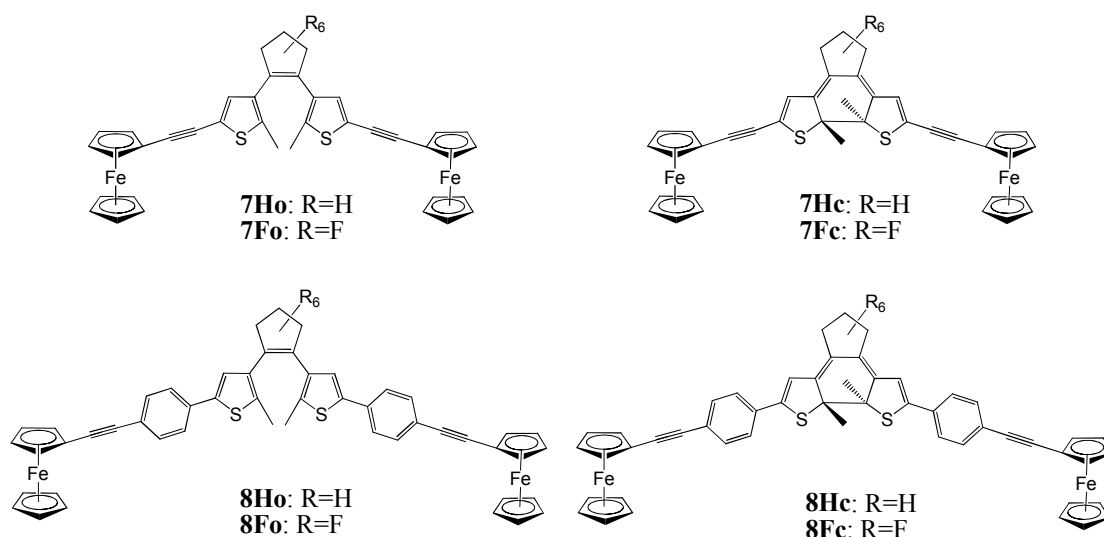
Figure 6.9: Illustrates the structures of the open and closed isomers of compounds **7H/F** and **8H/F**.

Table 6.3: UV-vis/NIR spectroelectrochemistry data of the open and closed-ring isomers of compounds **7H/F** and **8H/F**, following oxidation processes at varying potentials.

	Oxidation Potential	λ_{abs} (nm)		Oxidation Potential	λ_{abs} (nm)
7Ho	Start	260, 311, 444	**7Hc**	Start	260, 312, 548
	0.6 V	253, 409, 494 (sh), 960		0.4 V	256, 448, 959
8Ho	Start	342, 441	**8Hc**	Start	324, 560
	0.4 V	295, 424, 930		0.4 V	278, 430, 787, 940-1620
	0.8 – 1.1V	251, 441, 614, 777-1120		1.1 V	251, 281, 435, 609(sh), 647
	0.8 – 1.1V	251, 441, 646			
7Fo	Start	267, 309, 442	**7Fc**	Start	269, 313, 641
	0.6 V	267, 369, 867		0.4 V	269, 347-520, 750-1000
8Fo	Start	332, 442	**8Fc**	Start	267, 342, 619
	0.6 V	255, 317, 418, 870		0.6 V	260, 336, 423
				0.6-1.3 V	237, 317

The data was recorded in 0.1 M TBAPF$_6$/CH$_2$Cl$_2$ *vs.* Ag/Ag$^+$
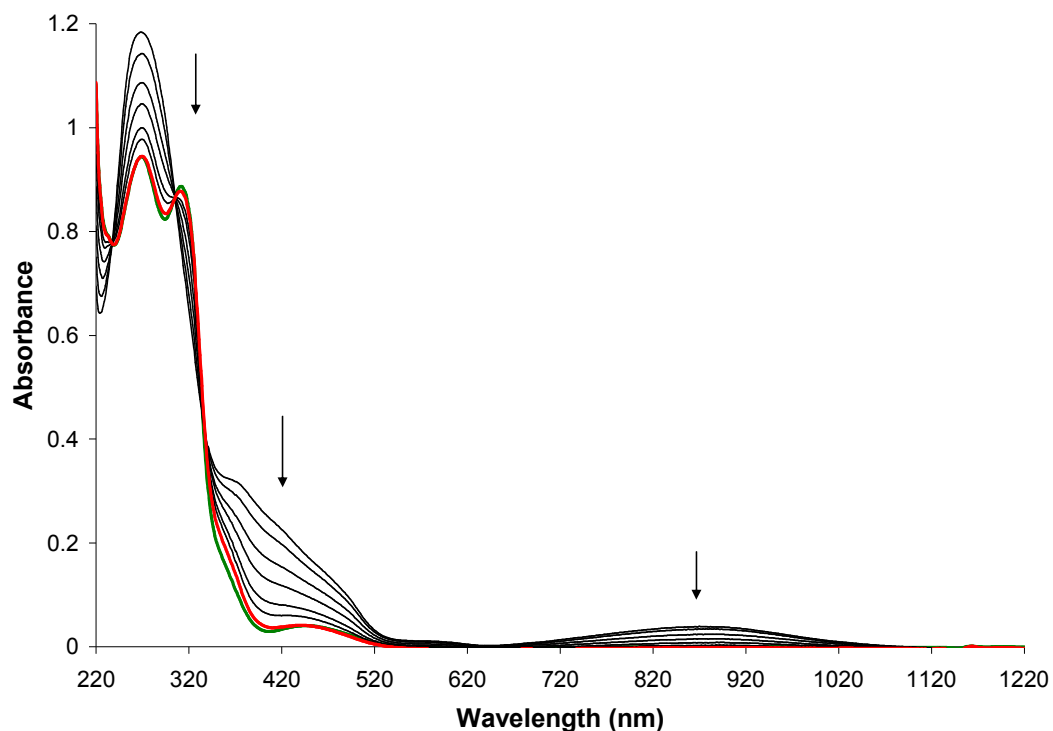
Figure 6.10: UV-vis/NIR spectra recorded during the reduction processes of the open-ring isomer **7Fo**, in 0.1 M TBAPF$_6$/CH$_2$Cl$_2$. Following oxidation at 0.6 V, subsequent reduction at 0 V resulted in a decrease in the absorbance bands associated with the oxidised ferrocene molecules (black lines), and the final spectrum recorded (red line) overlaid with the spectrum recorded at the beginning of the experiment (green line).

Oxidation of ferrocene molecules has been reported to induce changes in the UV-vis/NIR absorbance spectrum, due to the formation of the corresponding ferrocenium ions (Fc^+).[5,8,19] Applying an oxidation potential of 0.6 V, to a solution of the open-ring isomer **7Fo**, resulted in an increase in the original absorbance band at 267 nm, and the appearance of two new bands at 369 and 867 nm, in the UV-vis/NIR spectrum. These changes can be attributed to the generation of the ferrocenium ions.[5,6,20] Subsequent reduction at 0V resulted in a decrease in the new absorbance bands and the original absorbance spectrum, recorded at the start of the experiment, re-emerged (figure 6.10), demonstrating the reversible nature of the oxidation process of the ferrocene moieties.

Bulk electrolysis experiments were carried out on the closed-ring isomer **7Fc**, at 0.4 V (i.e. a potential at which the redox process of the ferrocene molecules was just beginning in the CV), and the changes recorded in the UV-vis/NIR spectra are presented in figure 6.11. The band in the visible region of the absorption spectrum at 641 nm, indicative of the conjugated closed form, began to decrease, indicating that an oxidative cycloreversion process, to the open-ring isomer, was taking place. Also noted was an increase in the original band at 269 nm, an increase in absorbance in the region 347 - 520 nm, and a low intensity absorbance in the range 750 - 1000 nm. These changes are synonymous with the formation of the ferrocenium ions.[5,6,20] Such a result suggests that oxidation of the ferrocene molecules induced a ring-opening process however it is difficult to interpret the exact mechanism involved. Oxidation of the electron-donating ferrocene molecules produces the electron-withdrawing ferrocenium ions. Electron-withdrawing substituents tend to destabilise the cationic species of the closed-ring form, thus resulting in cycloreversion to the open-ring isomer. Launay et al[8] also reported similar changes in the UV-vis spectrum of the same molecule, associated with the oxidised ferrocene units. However, in contrast to the results described here, they reported that the absorbance band associated with the closed-ring isomer (at 641 nm) was stable during oxidation processes at 0.9 V and was not found to decrease.
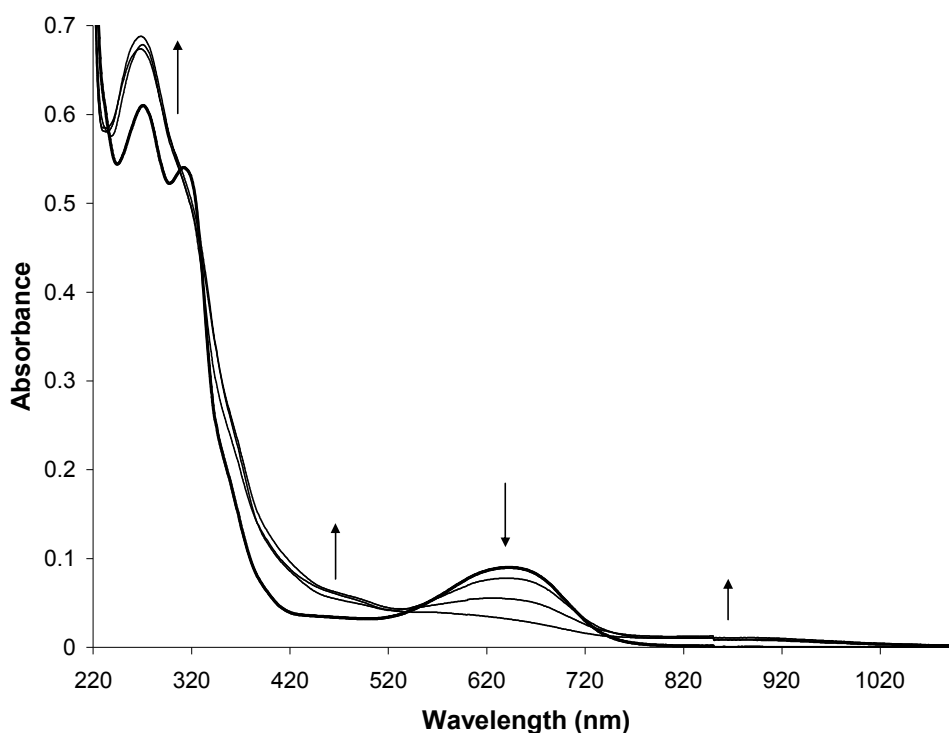
Figure 6.11: UV-vis/NIR spectra of the closed-ring isomer **7Fc** (thick black line), in 0.1 M TBAPF$_6$/CH$_2$Cl$_2$, following oxidation at 0.4 V.

The UV-vis spectrum of the closed-ring isomer, **8Hc**, displayed absorbance bands at 324 and 560 nm. Upon oxidation at 0.4 V, the original band in the visible region at 560 nm began to deplete, with strong absorbance bands appearing at 281, 430, 787 and between 940 – 1620 nm, as shown in figure 6.12. The λ_{max} at 281 and 430 nm can be assigned to the formation of the ferrocenium ions, whilst the bands at 787 and between 940-1620 nm can be assigned to the first oxidation process of the dithienylethene ring i.e. the monocation species of the closed-ring switching unit. When the oxidation potential was increased to 1.1 V, the absorbance bands at 787 and 940-1620 nm began to decrease, whilst the bands at 281 and 430 nm continued to increase, the later being red-shifted to 435 nm. Furthermore, new bands started to grow-in at 251 and 647 nm, with a shoulder at 609 nm. Such changes are indicative of the formation of the dication species of the closed-ring switching unit.[10,17,18]

Subsequent reduction at 0 V resulted in a decrease in all of the absorbance bands. The original band recorded in the UV region began to re-emerge however the λ_{max} was red-shifted to 335 nm, which is indicative of the open-ring isomer. In addition, the initial absorbance in the visible region at 560 nm did not recover. Therefore, oxidation of **8Hc** was found to generate the corresponding monocation and dication

species of the dithienylethene switch, however, a ring-opening process occurred following subsequent reduction. This can be attributed to the increased timescale at which the bulk electrolysis experiments are carried out, in comparison to the cyclic voltammetry experiments (i.e. minutes *vs.* seconds). Therefore, the cationic species of the closed-form were not stable enough to regenerate the neutral form of the closed-ring isomer within the timescale of the bulk electrolysis processes.
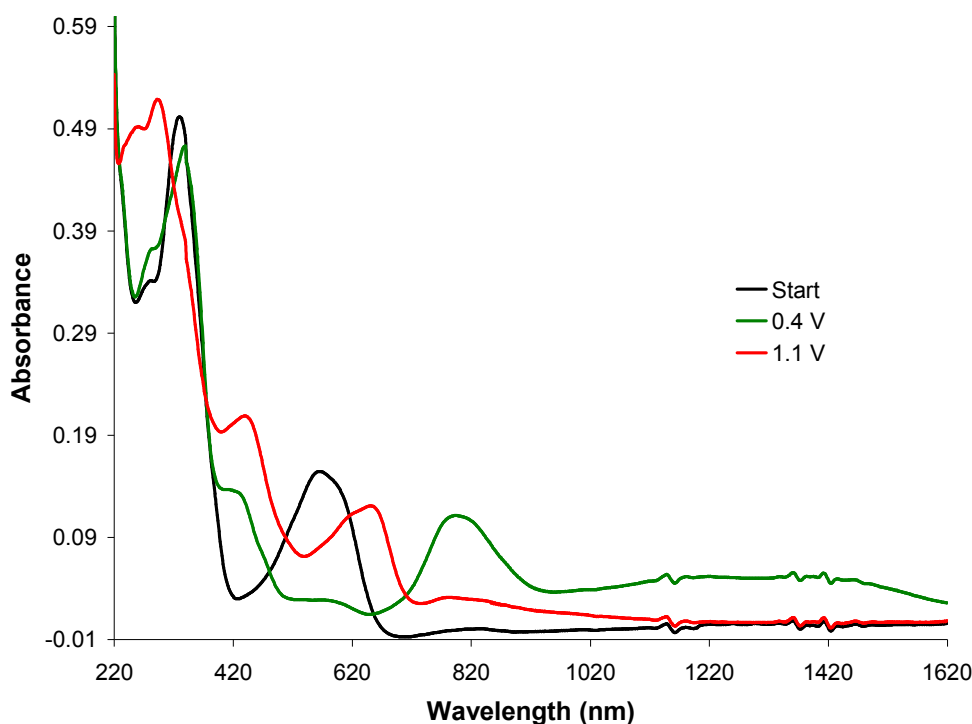
Figure 6.12: UV-vis/NIR spectra of **8Hc**, at the start (black line), and following oxidation at 0.4 V (green line) and 1.1 V (red line), in 0.1 M TBAPF$_6$/CH$_2$Cl$_2$.

In the case of the open-ring isomer, oxidation of **8Ho** at 0.4 V resulted in a decrease in the original band at 342 nm, with concomitant formation of bands at 295, 424 and 930 nm, which can be attributed to the oxidation of the ferrocene moieties to the corresponding ferrocenium ions. When higher oxidation potentials (0.8 to 1.1 V) were applied to the system, the band at 295 nm decreased and new bands appeared at 251, 441 and 646 nm, with a shoulder at 614 nm. These bands were assigned to the generation of the dication species of the closed-ring dithienylethene unit, due to the similarities with absorbance bands recorded for the closed-ring isomer, **8Hc**, during oxidation. The first few spectra recorded at this potential also displayed a broad absorbance band between 777-1120 nm, which then began to decrease as the other new bands continued to increase, as shown in figure 6.13. This phenomenon can be

attributed to the initial generation of the monocation species of the closed-ring switch, which was quickly followed by a second oxidation process, forming the dication species in a greater yield.

When reduction at 0 V was applied, the new bands began to decrease, whilst the band assigned to the monocation species, between 777-1120 nm, increased. This is due to the reduction process from the dication to the monocation species. In the consecutive spectra, the absorbance between 777-1120 nm began to decrease however reduction to the neutral form did not result at the end of the experiment. Instead, the original band in the UV region at 335 nm began to grow-back, indicating regeneration of the open-ring switch. As described previously, such a result can be attributed to the instability of the closed-ring cation species within the timescale of the bulk electrolysis experiments.
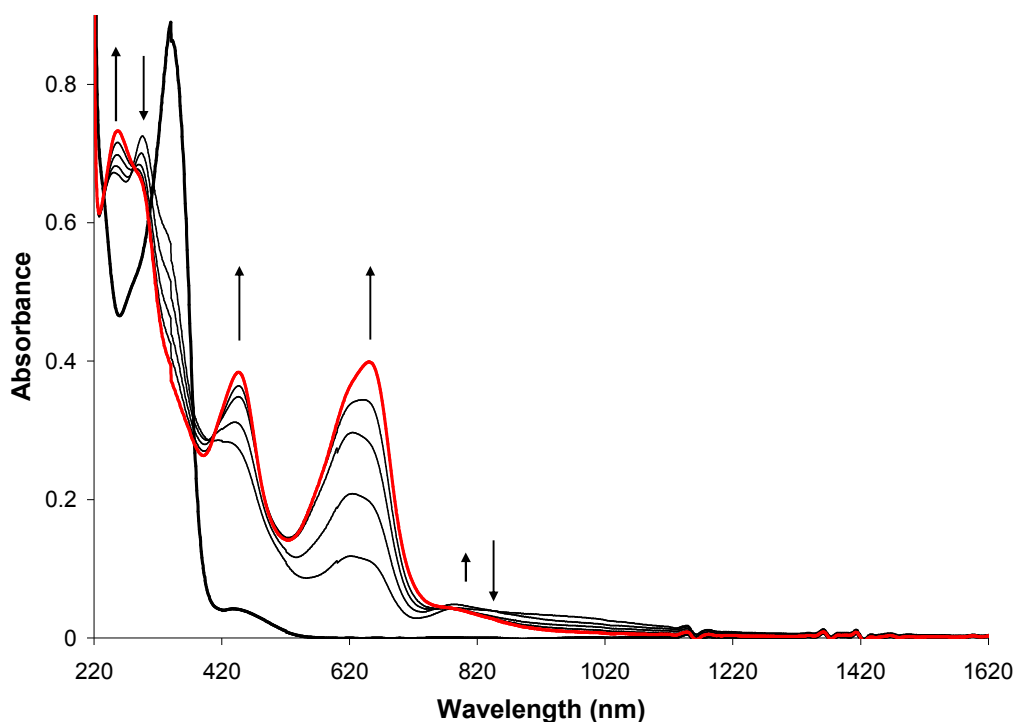
Figure 6.13: UV-vis/NIR spectra of **8Ho** at the start (thick black line), and following oxidation at 0.8 to 1.1 V (final spectrum red line), in 0.1 M TBAPF$_6$/ CH$_2$Cl$_2$.

The CVs of **7Ho** and **8Fo** showed evidence of ring-closing processes following oxidation of the switching unit. The bulk electrolysis experiments carried out for **7Ho** and **8Ho** (at 0.6 V) resulted in changes in the UV-vis/NIR spectra that can be associated with oxidation of the ferrocene units, as detailed in table 6.3 and shown for **8Fo** in figure 6.14 (inset spectrum). However, when higher potentials were applied,

corresponding to the potentials at which oxidation of the switching units was observed in the CV, spectral features associated with the formation of the closed-ring cation species were not observed in the UV-vis/NIR spectra of **7Ho** and **8Ho**.

The CV's of the corresponding closed-ring isomers **7Hc** and **8Fc**, displayed redox waves associated with the oxidation processes of the closed-ring switching units, which were found to be stable over a number of sweeps (~ 20), and there was no evidence of cycloreversion processes, back to the open forms. Thus, it would be expected for the spectroelectrochemistry experiments performed on **7Hc** and **8Fc** to show the absorbance bands of the oxidised species of the closed-forms in the UV-vis/NIR spectra. On the contrary, however, in both cases the absorbance bands in the visible region (associated with the ring-closed forms at 531 and 613 nm, respectively) were found to decrease, and only new bands associated with the oxidised ferrocene groups were observed, as shown for **8Fc** in figure 6.14.

Therefore, the UV-vis spectroelectrochemistry results, obtained for the open and closed isomers of **7H** and **8F**, indicated that their closed-ring cation species were too unstable, within the timescale of the bulk electrolysis experiments (minutes *vs.* seconds in the CV), to incur changes in the absorbance spectra. Thus, spectral features associated with the cationic species of the closed forms were not observed.
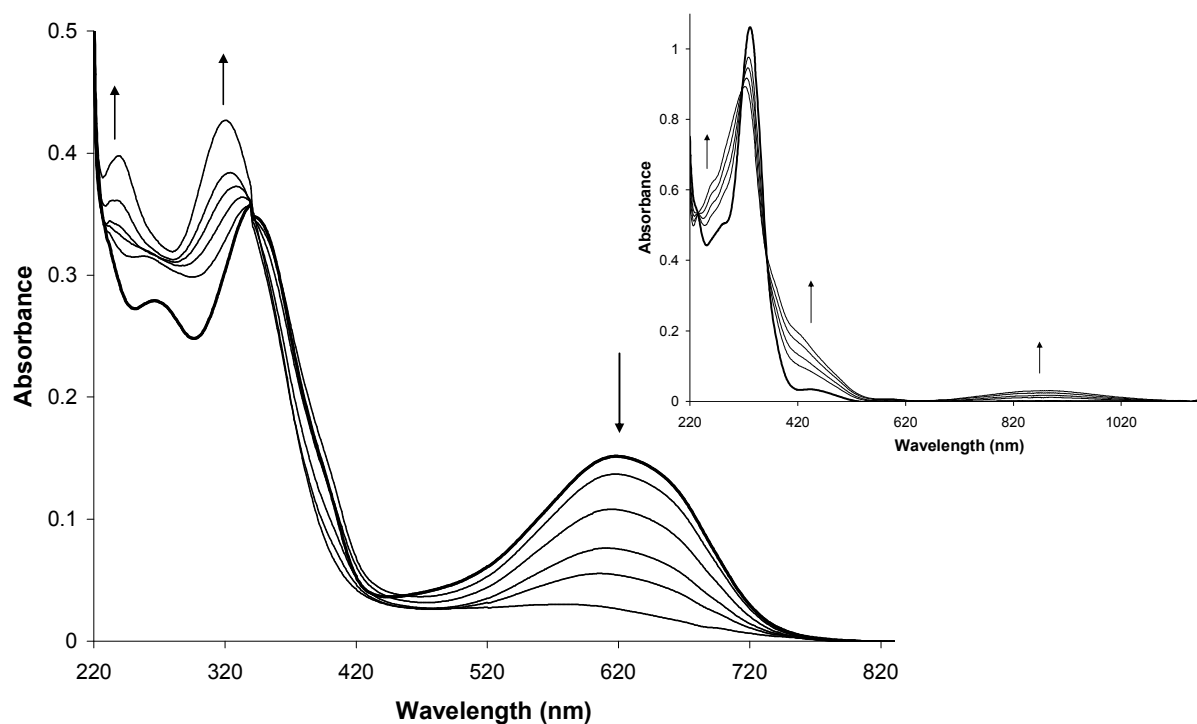
Figure 6.14: UV-vis/NIR spectra of the closed-ring isomer **8Fc** (thick black line), following oxidation at 1.2 V, in 0.1 M TBAPF$_6$/CH$_2$Cl$_2$. Inset, the UV-vis/NIR spectra of the open-ring isomer **8Fo**, following oxidation at 0.6 V.

6.3.3 Co$_2$(CO)$_6$ Complexes: Cyclic Voltammetry

A number of literature reports have described the influence of organometallic substituents on the electrochromic properties of dithienylethene switches i.e. inhibiting or inducing oxidative cyclisation/cycloreversion processes.[21-23]   In this section, the electrochemical reductive and oxidative behaviour of the open-ring Co$_2$(CO)$_6$ complexes **9H/F** and **10H/F** are discussed in terms of the redox properties found for the Co$_2$(CO)$_6$ moieties, and the effect of the cobalt carbonyl groups on the electrochromic switching behaviour of the dithienylethene units.   The cyclic voltammetry experiments were performed at room temperature, in 0.1 M solutions of TBAPF$_6$/CH$_2$Cl$_2$, at a scan rate of 0.1 Vs^{-1}.   The results were calibrated against the redox couple of decamethylferrocene Fc*$^+$/Fc* (E$_{1/2}$ = -0.07 *vs.* SCE).   The structures of the cobalt carbonyl complexes described here are illustrated in figure 6.15.
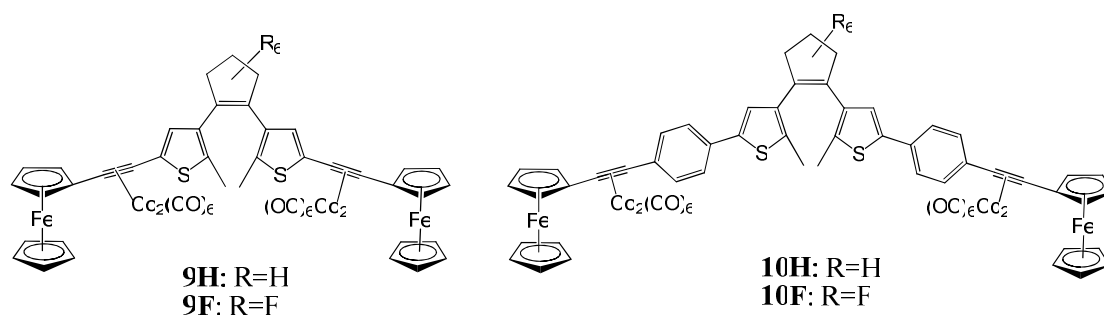
Figure 6.15: The structures of the open-ring Co$_2$(CO)$_6$ complexes **9H/F** and **10H/F**.

- **Reduction Process**

Alkynyl $Co_2(CO)_6$ complexes have been reported to undergo one-electron reduction processes to form the corresponding anion radical $[RC_2R'Co_2(CO)_6]^{\bullet-}$. Such processes are generally followed by disintegration of the cobalt carbonyl unit, due to metal-metal bond cleavage. Hence, disintegration products are formed, a number of which are electroactive, and some have been identified as $Co(CO)_4^-$, $RC_2R'Co(CO)_3$ and free alkyne.[24-28]

Similarly, reduction processes of the $Co_2(CO)_6$ switches **9H**, **9F**, **10H** and **10F** resulted in reduction peaks, in the range of -1.13 to -1.30 V (table 6.4), forming the corresponding dianion species {**9H²⁻**, **9F²⁻**, **10H²⁻** and **10F²⁻**}, due to one-electron reduction processes of each of the two $Co_2(CO)_6$ groups, substituted onto each switch. Disintegration processes of the cobalt carbonyl units were also evident for each complex, due to the appearance of new peaks in the anodic and cathodic sweeps, following the first reduction process. The potentials at which these processes took place are summarised in table 6.4. In each case, a sharp oxidation peak was observed, in the range from 0.06 to 0.08 V, with a corresponding reduction peak observed at approximately -0.40 V, which can tentatively be assigned to the formation of the $Co_2(CO)_4^-$ species, with reference to the literature.[24,26-29] Other smaller oxidation waves were observed in all the CV's and are dedicated to other unknown disintegration products.

Table 6.4: The cyclic voltammetry results of the reduction processes of **9H/F** and **10H/F**.

Compound	$Co_2(CO)_6$ Moieties		Disintegration Products	
	E_{pc} (V)	E_{pc} (V)	E_{pa} (V)	E_{pc} (V)
9H	-1.22,	-	-0.29, -0.13, 0.06	-0.40
10H	-1.17, -1.30[b]	-1.23[b]	-0.27, 0.07	-0.42
9F	-1.13,	-	-0.18, 0.08	-0.38
10F	-1.15	-	-0.23, -0.06, 0.08	-0.40

All values listed are values of potential (V) *vs.* SCE, recorded in 0.1 M TBAPF₆/CH₂Cl₂, and represent irreversible redox processes, with the exception of the values marked by [b] indicating a quasireversible process.

A single irreversible reduction peak was observed for the $Co_2(CO)_6$ complexes **9H**, **9F** and **10F**, representing a one-step two-electron reduction process, suggesting that little electronic communication existed between the two metal centres. In the case of

the perhydro-derivative **10H**, two reduction peaks were recorded at E_{pc} = -1.17 V and -1.30 V, as shown in figure 6.16. The first reduction peak, at -1.17 V, was irreversible, whereas the second process at -1.30 V was quasireversible, with a corresponding reduction peak observed at -1.23 V. The separation between the two reduction peaks was found to be ΔE = 130 mV. Such a result may be an indication of some electronic interaction existing between the two metal centres, at each end of the switch.
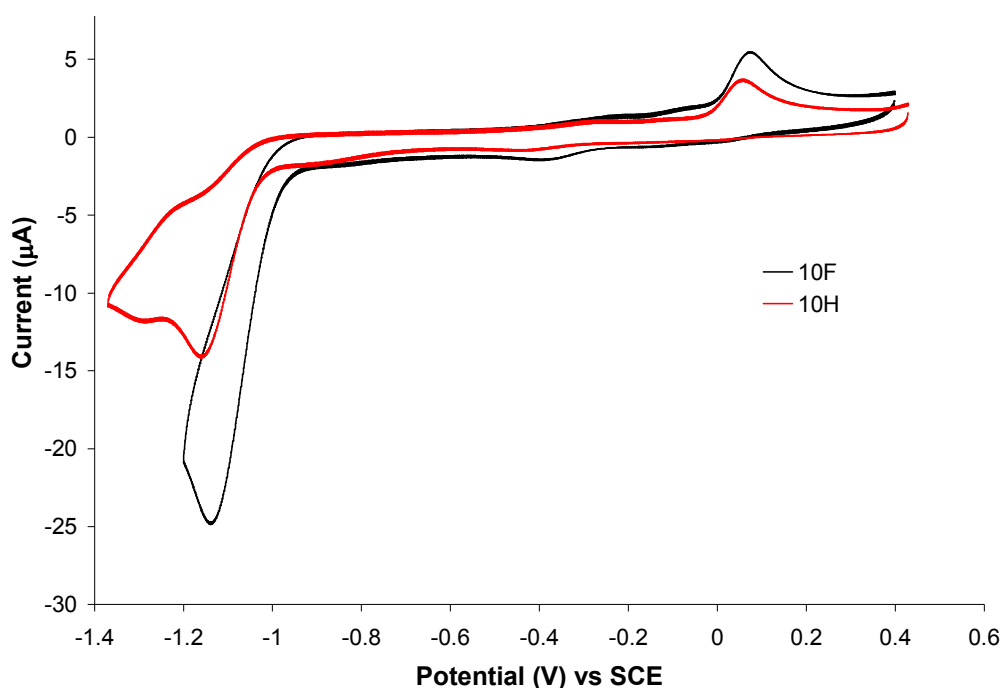
Figure 6.16: Cyclic voltammogram of the reduction process of **10H** (red line) and **10F** (black line), in 0.1 M TBAPF$_6$/CH$_2$Cl$_2$, at a scan rate of 0.1 Vs^{-1}.

Furthermore, a comparison of the potentials at which the first reduction processes take place for each of the cobalt carbonyl complexes, shows a shift towards more negative potential values in the order of: **9F** < **10F** < **10H** < **9H**. Such a trend can be attributed to the electron-withdrawing fluorine atoms, which help to stabilise the LUMO to a greater extent than the perhydro-derivatives.[10] Hence the most negative and least negative potential values were recorded for **9F** (E_{pc} = -1.13 V) and **9H** (E_{pc} = -1.22 V) respectively. The presence of the phenyl-rings between the switching unit and the Co$_2$(CO)$_6$ moieties in **10H** and **10F**, reduces the influence of the atoms on the cyclopentene ring, hence their reduction values lie in-between those of the shorter chain derivatives **9H** and **9F**.

- **Oxidation Process**

A number of literature reports have described the oxidation processes of alkynyl $Co_2(CO)_6$ complexes.[26,27,30] The cobalt hexacarbonyl moieties have been found to undergo one-electron oxidation processes, forming the corresponding cation radical $[RC_2R'Co_2(CO)_6]^{\bullet+}$, in the range of $0.9 - 1.4$ V, followed by severe fouling of the electrode surface at higher oxidation potentials. As detailed in sections 6.3.1 and 6.3.2, the electrochemistry results of the ferrocenyl-based free ligand switches described oxidative ring-opening for **7F**, and oxidative cyclisation for **7H**, **8H** and **8F**. Therefore, in this section, the effect of the oxidative processes of the $Co_2(CO)_6$ moieties, on the electrochromic behaviour of the switching units, is discussed.

Oxidation processes of the $Co_2(CO)_6$ components on **9H/F** and **10H/F** resulted in single irreversible oxidation peaks, in the potential range from 1.26 to 1.43 V, representing a one step two-electron oxidation process i.e. one-electron oxidation reaction of each of the two $Co_2(CO)_6$ units. Furthermore, for each complex, oxidation of the ferrocene molecules was represented by a single two-electron quasireversible redox wave ($i_{pc}/i_{pa} \approx 0.8$), appearing at potential values similar to those recorded for the free ligand switches ($E_{1/2}$ ranging from 0.58 V to 0.61 V). The cyclic voltammetry results obtained, following oxidation processes of the $Co_2(CO)_6$ complexes **9H/F** and **10H/F**, are summarised in table 6.5, along with the CV results of the corresponding free ligand switches, for comparative purposes.

Table 6.5: The cyclic voltammetry results of the oxidation processes of the $Co_2(CO)_6$ complexes **9H/F** and **10H/F**, and their corresponding free ligands **7H/F** and **8H/F**.

Compound	Oxidation Potentials		
	E_{pa}	E_{pc}	$E_{1/2}$
7Ho	0.68^{Fc}, 0.99^{rc}, 1.15^{rc}, 1.50^{a}	0.54^{Fc}, 0.93^{rc}, 1.08^{rc}	0.61^{Fc}
9H	0.51^{rc}, 0.66^{Fc}, 0.85^{rc}, 1.26^{a}, 1.48^{a}	0.45^{rc}, 0.54^{Fc}, 0.74^{rc}	0.60^{Fc}
8Ho	0.43^{rc}, 0.68^{Fc}, 0.90^{rc}, 1.32^{a}	0.37^{rc}, 0.48^{Fc}, 0.80^{rc}	0.58^{Fc}
10H	0.47^{rc}, 0.64^{Fc}, 0.84^{rc}, 1.28^{a}, 1.45^{a}	0.41^{rc}, 0.51^{Fc}, 0.76^{rc}	0.58^{Fc}
7Fo	0.73^{Fc}, 1.76^{a}	0.52^{Fc}	0.63^{Fc}
9F	0.67^{Fc}, 1.43^{a}, 1.66^{a}	0.49^{Fc}	0.58^{Fc}
8Fo	0.64^{Fc}, 1.05^{rc}, 1.21^{rc}, 1.68^{a}	0.50^{Fc}, 0.98^{rc}, 1.07^{rc}	0.57^{Fc}
10F	0.65^{Fc}, 0.83^{rc}, 1.37^{a}, 1.68^{a}	0.51^{Fc}, 0.78^{rc}, 0.97^{rc}	0.58^{Fc}

All values listed are values of potential (V) *vs.* SCE, recorded in 0.1 M $TBAPF_6/CH_2Cl_2$, at 0.1 Vs^{-1}..
[a] indicates an irreversible oxidation process
[Fc] indicates peaks due to the redox couple of the ferrocene moieties
[rc] indicates peaks assigned to the ring-closed species

Oxidation of **9F** resulted in a quasireversible redox wave at $E_{1/2}$ = 0.58 V, due to oxidation of the ferrocene molecules, from the Fe(II) state to the Fe(III) state. At higher potentials, an irreversible oxidation wave was observed at 1.43 V (*vs*. SCE), representing a two-electron oxidation process of the $Co_2(CO)_6$ moieties, as shown in figure 6.17. Subsequent sweeps at this potential resulted in a considerable decrease in the redox waves, which can be attributed to fouling of the electrode surface following oxidation of the cobalt carbonyl groups. A second irreversible oxidation peak was observed at 1.66 V, due to oxidation of the switching unit. There was no evidence of new redox waves in the subsequent sweeps, indicating that **9F** did not undergo oxidative cyclisation processes, which is in accordance with the result recorded for the related free ligand switch **7F**.

Figure 6.17 Cyclic voltammogram of the $Co_2(CO)_6$ complex **9F**, in 0.1 M TBAPF$_6$/CH$_2$Cl$_2$, at 0.1 Vs^{-1}, following oxidation at 1.55 V.

In the case of the longer chain perfluoro-derivative **10F**, oxidation of the ferrocene molecules, at $E_{1/2}$ = 0.58 V (*vs*. SCE), was followed by a small oxidation peak at 0.83 V and a corresponding reduction peak was observed in the return sweep at 0.78 V, as shown in figure 6.18. These peaks were not observed in the CV of the free ligand **8F**, following oxidation of the ferrocene molecules, suggesting that they are associated with the presence of the $Co_2(CO)_6$ moieties, but it is not clear what oxidation process they represent. At higher potentials, two separate irreversible oxidation peaks, each representing a two-electron process, occurred at 1.37 V and 1.68 V, allocated to the oxidation process of the $Co_2(CO)_6$ moieties and the switching unit respectively.

Following the oxidation process at 1.68 V, a small new redox wave was observed at 0.97 V, which could possibly be due to formation of the cationic species of the ring-closed isomer. However, this is not a conclusive result as in the subsequent anodic and cathodic sweeps (sweeps 3 and 4), the oxidation peaks at 1.37 and 1.68 V decreased considerably, and the reduction peak at 0.97 V disappeared, as shown in figure 6.18. In the consecutive sweeps, all the peaks in the CV decreased and became distorted, which can be attributed to severe fouling of the electrode surface following oxidation of the cobalt carbonyl units. Therefore, there was no strong evidence of oxidative cyclisation observed in the CV of **10F**.
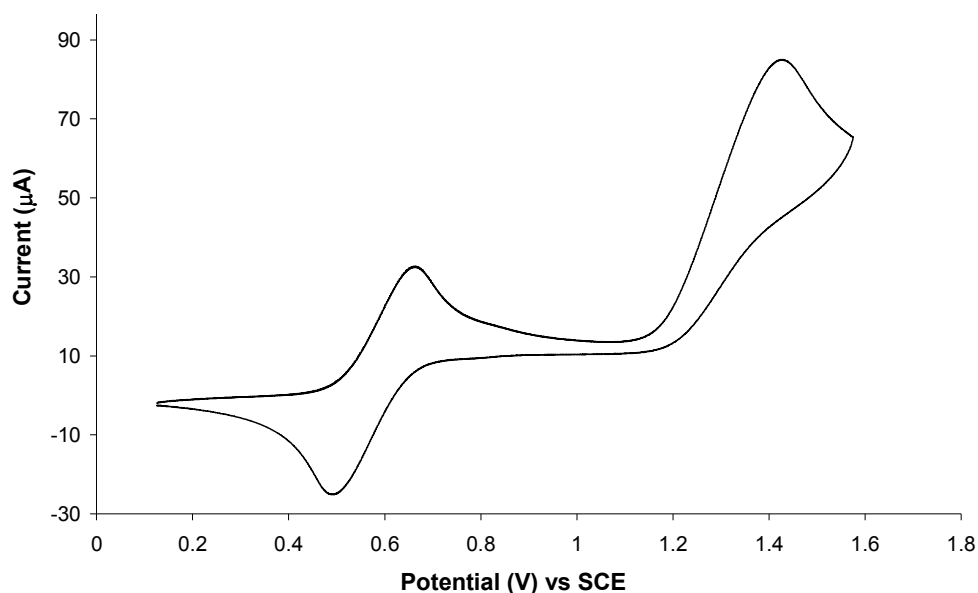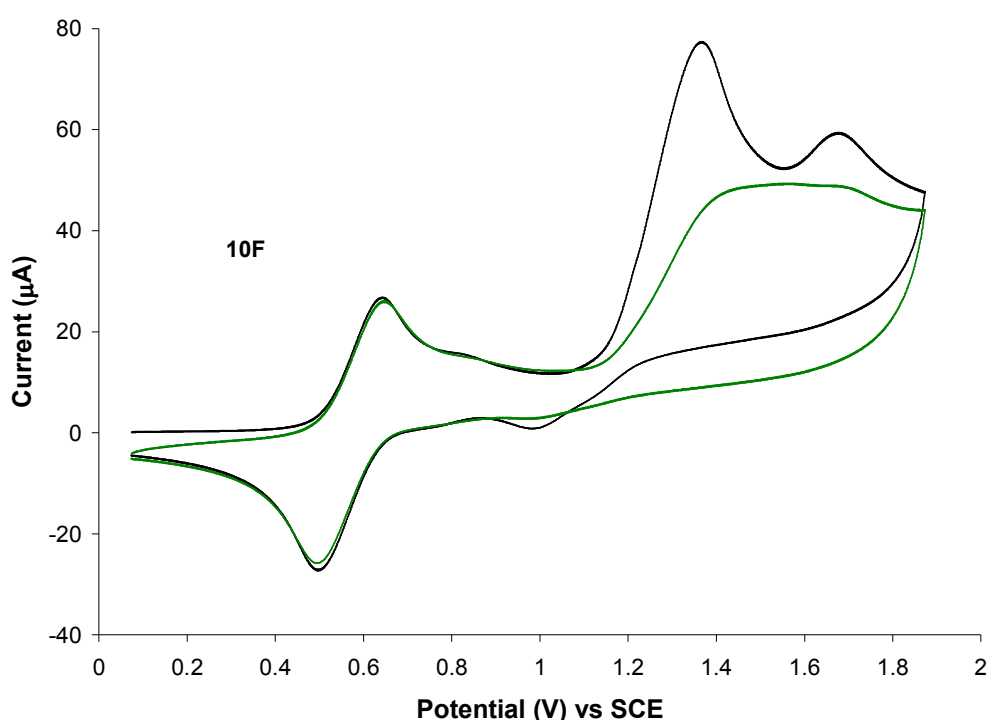

Figure 6.18 Cyclic Voltammogram of the $Co_2(CO)_6$ complex **10F**, in 0.1 M $TBAPF_6/CH_2Cl_2$, at 0.1 Vs^{-1}, following oxidation at 1.9 V. Sweeps 1 and 2 (black line) showed well defined oxidation peaks at 1.37 and 1.68 V, and a small reduction peak at 0.97 V. In the subsequent sweeps 3 and 4 (green line), these peak decreased considerably.

The CV of the corresponding $Co_2(CO)_6$ perhydro analogue **10H** showed some evidence of an oxidative cyclisation process. Following the first redox wave at $E_{1/2}$ = 0.58 V (*vs.* SCE), assigned to the formation of the ferrocenium ions, a small oxidation peak was observed at 0.84 V, and a corresponding reduction peak was found at 0.76 V in the return sweep, as shown in figure 6.19. A similar small redox wave was observed in the CV of the related fluorinated switch **10F**, as described previously, but the identity of these peaks is unknown. Oxidation of the $Co_2(CO)_6$ moieties was

found to occur at 1.28 V, and was represented by a single two-electron irreversible peak. A second irreversible wave was observed at 1.45 V, which can be assigned to a two-electron oxidation process of the switching unit. In the subsequent sweeps, the redox wave at $E_{1/2}$ = 0.80 V increased in intensity, and a very small reduction peak appeared at 0.41 V, with a corresponding oxidation wave at 0.47 V, as shown in figure 6.19. The two redox waves at $E_{1/2}$ = 0.44 and 0.80 V, coordinate well with the redox waves assigned to the cationic species of the closed-ring isomer in the CV of the free ligand **8H**. Therefore, such a result suggests that **10H** undergoes an oxidative cyclisation process. In the consecutive sweeps, however, the oxidation peaks began to decrease due to fouling of the electrode surface by the oxidised cobalt carbonyl moieties.
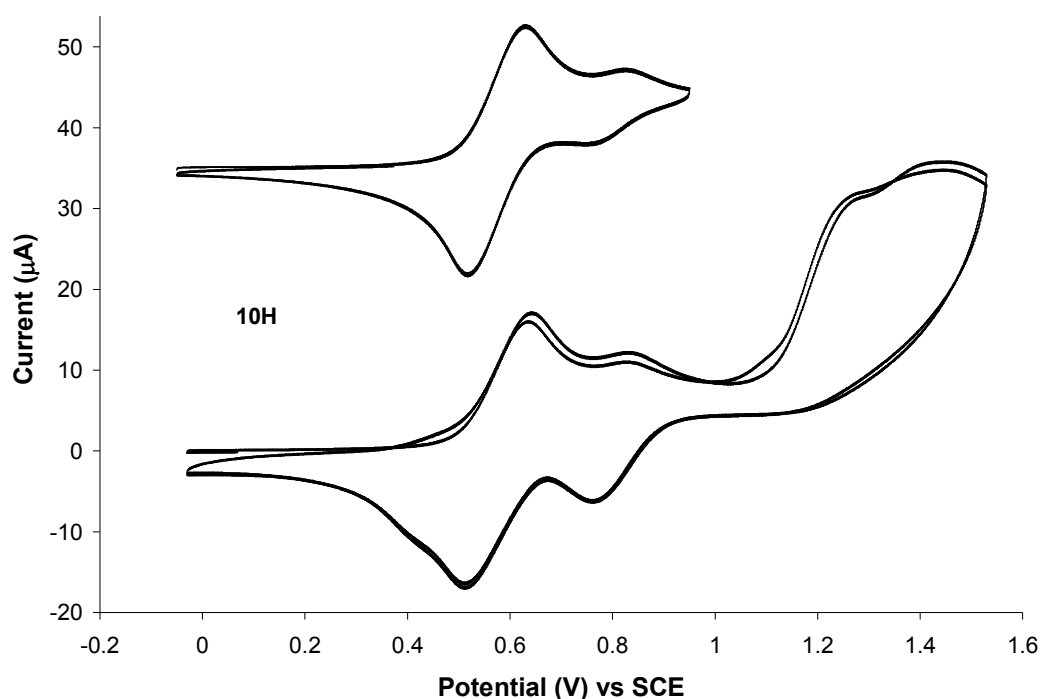
Figure 6.19 Cyclic voltammogram of the $Co_2(CO)_6$ complex **10H**, in 0.1 M TBAPF$_6$/CH$_2$Cl$_2$, at 0.1 Vs^{-1}, following oxidation at 1.55 V (bottom) and at 0.95V (top), the CV of which is offset along the coordinate for clarity.

In the case of the shorter chain perhydro-derivative **9H**, the oxidation wave of the ferrocene moieties ($E_{1/2}$ = 0.60 V) was also followed by a small oxidation peak at 0.85 V, and a related reduction peak at 0.80 V (*vs.* SCE), as already described for **10H** and **10F**. Following this, oxidation of the $Co_2(CO)_6$ groups was observed at 1.26 V, which was represented by an irreversible oxidation peak. At higher potentials, a second irreversible oxidation peak was observed at 1.48 V, which can be assigned to

oxidation of the dithienylethene unit. In the subsequent cathodic sweep, a sharp reduction peak was observed at 0.71 V, as shown in figure 6.20. This can be attributed to a desorption spike, indicating that passivation of the electrode surface occurred[13,14] following oxidation of the cobalt carbonyl moieties, and switching unit, at high potentials. Such a process was described previously for the free ligand switches **8H** and **8F**. In the second cathodic sweep, this reduction peak decreased in intensity and was anodically shifted to 0.73 V i.e. towards the potential value of the reduction peak observed following oxidation of the ferrocene units (at E_{pc} = 0.80 V). However, the intensity of this reduction peak, and the corresponding oxidation peak at 0.85 V, had increased after oxidation at 1.48 V. Furthermore, after the first oxidation process of the switching unit at 1.48 V, a new small reduction peak was observed at 0.45 V, and a corresponding oxidation peak at 0.51 V. Therefore, compared to the results obtained for **10H**, the two redox waves at $E_{1/2}$ = 0.48 and 0.79 V were tentatively assigned to the formation of the cationic species of the closed form of **9H**. However, these redox waves were obscured by the ferrocene oxidation wave which, together with the interference from passivation of the electrode surface (as evidenced by the desorption spike at 0.71 V), complicates the analysis of **9H** and therefore, it was not unambiguously deduced that **9H** underwent oxidative cyclisation.
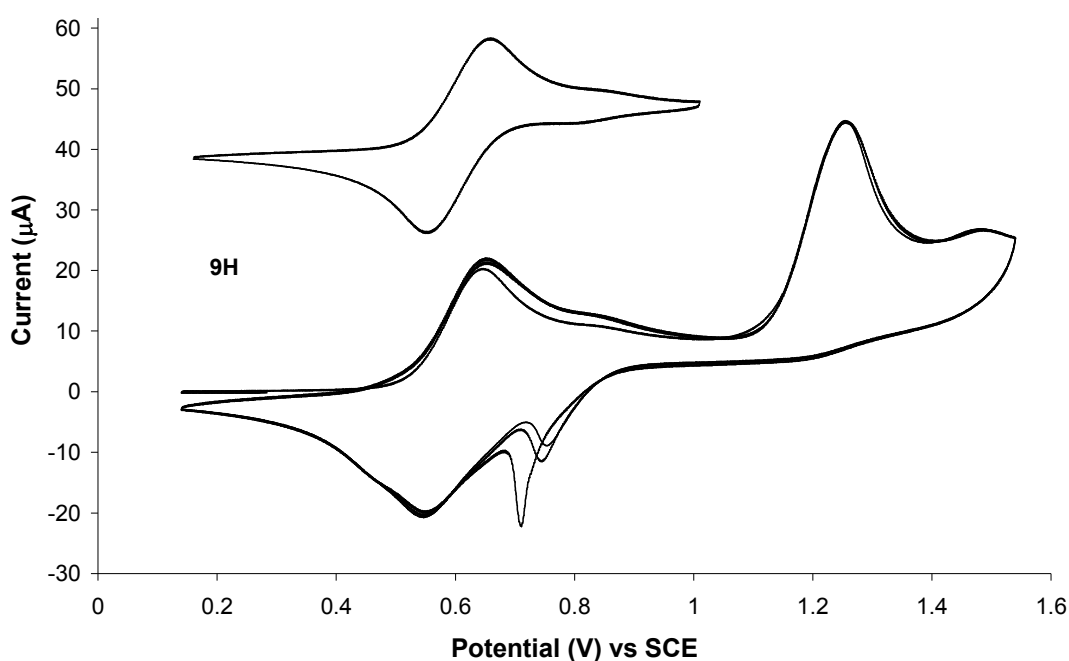
Figure 6.20 Cyclic voltammogram of the $Co_2(CO)_6$ complex **9H**, in 0.1 M TBAPF$_6$/CH$_2$Cl$_2$, at 0.1 Vs^{-1}, following oxidation at 1.55 V (bottom) and at 1.0V (top), the CV of which is offset along the coordinate for clarity.

Overall, it was found that incorporating $Co_2(CO)_6$ moieties onto the switches did not effect the direction of the electrochemical switching processes of these compounds (i.e. cyclisation/cycloreversion). However, the presence of the cobalt carbonyl moieties appeared to reduce the stability of the cationic species produced during the oxidation processes. Oxidative cyclisation was not found to occur for the perfluoro-derivative **9F**, which is in-keeping with its corresponding free ligand **7Ho**. The CV of the longer chain $Co_2(CO)_6$ complex, **10F**, did not show strong evidence of a ring-closing process, which is in contrast to the cyclisation process observed for the related free ligand **8F**. However, analysis of the CV of **10F** was difficult due to severe fouling of the electrode surface following oxidation of the cobalt carbonyl moieties. On the other hand, evidence of oxidative ring-closure was observed for the perhydro analogue, **10H**. This result is in-keeping with that observed for its free ligand **8H**, which was also found to undergo cyclisation following oxidation of the switching unit. In the case of the shorter chain $Co_2(CO)_6$ complex, **9H**, the CV showed some evidence of the formation of the closed-ring cation species. However, passivation of the electrode surface following oxidation at high potentials (> 1.2 V), and the masking of the new peaks by the ferrocene redox wave, made it difficult to analyse the CV results conclusively. Oxidative cyclisation was also observed for the corresponding free ligand **7H**.

Interestingly, there was one common entity observed in the CV's of **9H**, **10H** and **10F**, which was not observed in the CV's of their related free ligand switches. This was the small redox wave observed after the oxidation process of the ferrocene molecules, and before oxidation of the cobalt carbonyl moieties and the switching unit. The fact that this wave was not observed in the CV of **9F**, which did not show any evidence of ring-closure, together with the potential values of this oxidation/reduction process coordinating with the values observed for the closed-ring cationic species recorded in the CV's of the free ligands, suggests that this feature may be associated with the cyclisation process.

6.3.4 Co$_2$(CO)$_6$ Complexes: UV-vis/NIR Spectroelectrochemistry

The cyclic voltammograms obtained for the Co$_2$(CO)$_6$ complexes, **9H** and **10H**, showed some evidence of oxidative cyclisation processes occurring for these complexes. However, little evidence of such a process was observed in the CV of **10F**, and oxidative ring-closure was not found to occur for **9F**. In order to further investigate the electrochemical behaviour of the Co$_2$(CO)$_6$ complexes, UV-vis/NIR spectroelectrochemistry experiments were carried out, in 0.1 M TBAPF$_6$/CH$_2$Cl$_2$ versus Ag/Ag$^+$. The results obtained in the UV-vis/NIR spectra are summarised in table 6.6, and the structures of the Co$_2$(CO)$_6$ complexes are illustrated in figure 6.21.

9H: R=H
9F: R=F

10H: R=H
10F: R=F
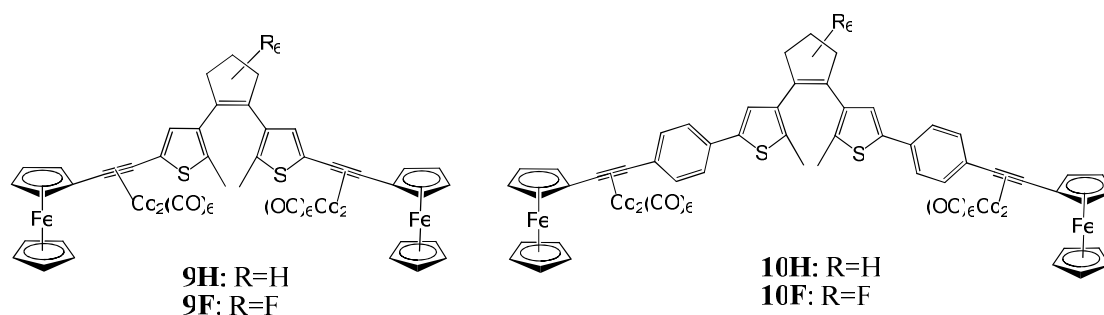
Figure 6.21: The structures of the open-ring Co$_2$(CO)$_6$ complexes **9H/F** and **10H/F**.

Table 6.6: UV-vis/NIR spectroelectrochemistry data of the Co$_2$(CO)$_6$ complexes **9H/F** and **10H/F**, following oxidation processes at varying potentials.

	Oxidation Potential	λ_{abs} (nm)
Absorbance Spectra of the Co$_2$(CO)$_6$ Complexes		
9H	Start	263, 327, 442, 568
	0.7 V	449, 931
10H	Start	274, 337, 451, 541
	1.3 V	277, 335, 447, 593, 781 (720-1200)
9F	Start	272, 328, 440, 570
	0.7V	250, 445 (380-533), 850
10F	Start	272, 337, 443, 552
	1.4 V	255, 326, 452, 850

The data was recorded in 0.1 M TBAPF$_6$/CH$_2$Cl$_2$ *vs.* Ag/Ag$^+$

Upon oxidation of **9F** at 0.7 V, an increase in the absorbance bands in the UV-vis spectrum was observed at 250 and 445 nm, along with the appearance of a low intensity absorbance band in the NIR region, extending from approximately 700 – 1200 nm, with a λ_{max} at 850 nm. These changes are shown in figure 6.22, and can be attributed to the oxidised ferrocene moieties, forming the ferrocenium ions.[5,6,20] The new absorbance bands decreased following subsequent reduction processes, although the exact spectrum recorded at the start of the experiment was not obtained, which can be ascribed to the quasireversible nature of the oxidation process of the ferrocene moieties. When higher oxidation potentials were applied to the system (above 1.0 V), the bands in the UV region began to decrease which can be assigned to the irreversible oxidation process of the $Co_2(CO)_6$ moieties. Furthermore, new spectral features were not observed in the visible/NIR regions therefore, the spectroelectrochemistry experiments verified that **9F** does not undergo oxidative cyclisation processes, which is in accordance with the results obtained in the CV experiments.
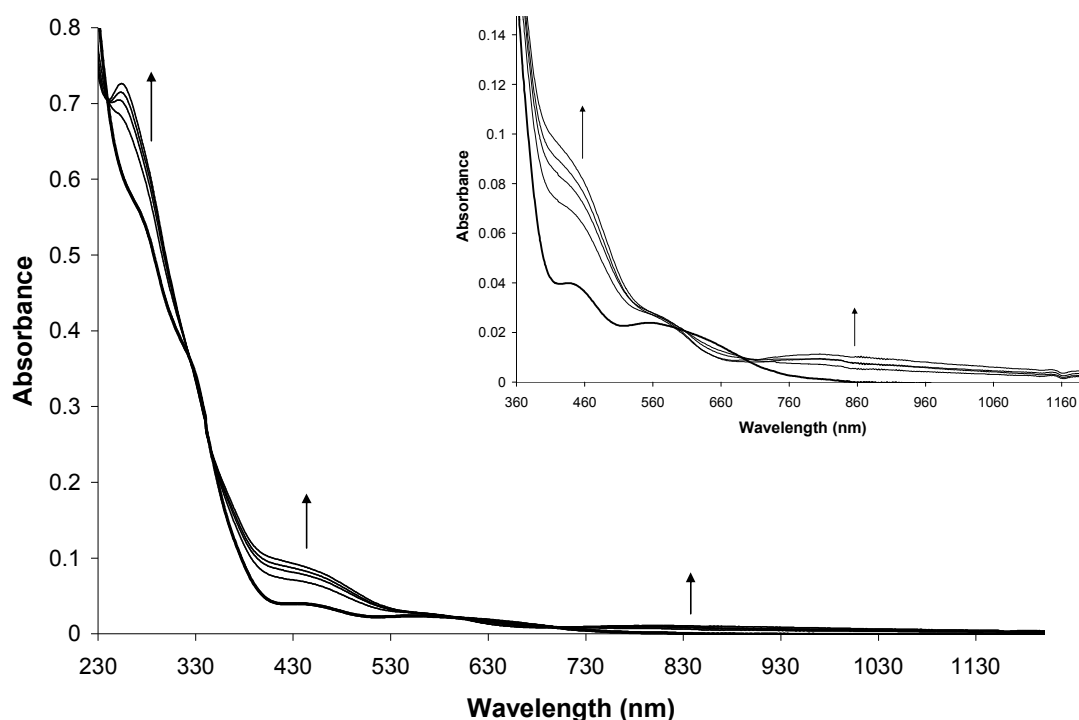
Figure 6.22: UV-vis/NIR spectrum of the $Co_2(CO)_6$ complex **9F** (thick black line), in 0.1 M TBAPF$_6$/CH$_2$Cl$_2$. Following oxidation at 0.7 V, there was an increase in the absorbance bands at 250, 445 and 850 nm. Inset, the spectrum of **9F** zoomed in between 360 and 1200 nm for clarity.

Conversely, when oxidation processes were carried out on **10H** (at 1.3 V), an initial increase in the absorbance bands was observed at 277, 335 and 447 nm, which can be

associated with the oxidation processes of the ferrocene moieties.[5,6,20] However, new absorbance features were also found to appear at 593 nm, and from 720 – 1200 nm (λ_{max} = 781 nm), as shown in figure 6.23.
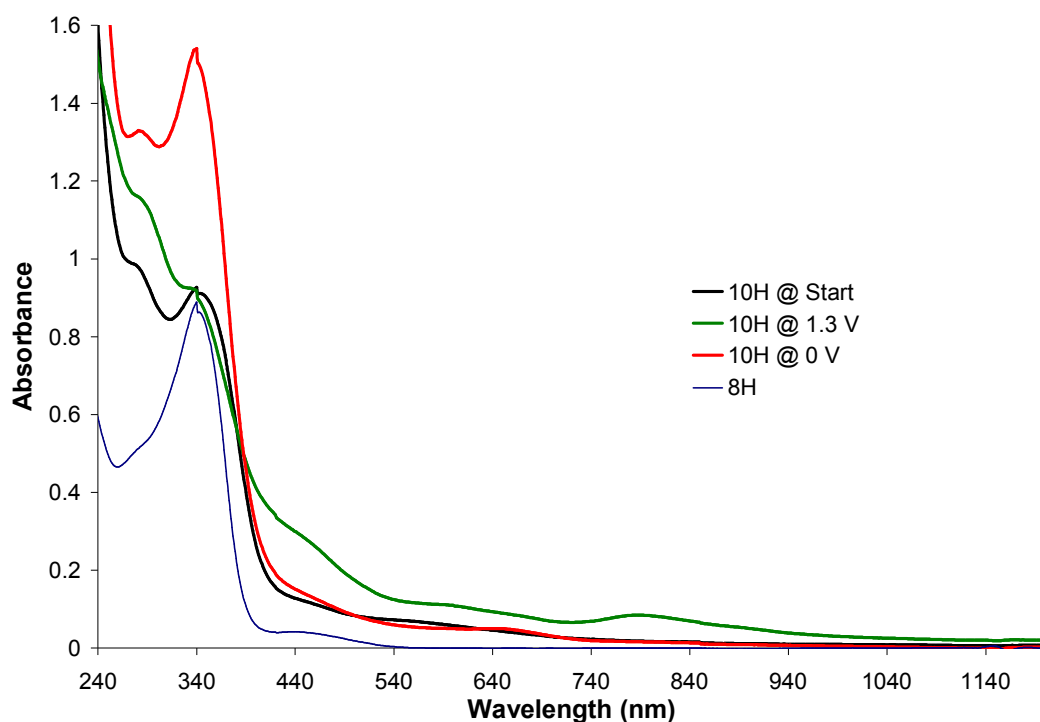
Figure 6.23: UV-vis/NIR spectra of **10H**, at the start (black line), and following oxidation at 1.3 V (green line) and reduction at 0 V (red line), in 0.1 M TBAPF$_6$/CH$_2$Cl$_2$. Also, the spectrum of the free ligand **8H** (thin blue line) is displayed for comparative purposes.

On comparing the UV-vis/NIR spectroelectrochemistry results obtained for the corresponding free ligand **8H**, and from literature reports,[10,17,31] these bands were assigned to the cationic species of the closed-ring isomer. This result is in agreement with the cyclic voltammetry results, which showed oxidation/reduction peaks associated with the closed-ring isomer. Although, in comparison to the results obtained for the **8H**, these new absorbance bands were quite weak, and began to decrease following longer oxidation times. Therefore, the results confirm that oxidative cyclisation, to the closed-ring isomer, does occur for **10H**, although the closed-ring cations are not very stable and undergo cycloreversion back to the open form under these conditions.   Reduction processes, at 0V, resulted in a decrease in the new spectral features in the visible region, with a significant increase in the absorbance bands in the UV region, to values higher than originally recorded. The final spectrum recorded showed similarities to that of **8H**, as demonstrated in figure

6.23, indicating loss of the cobalt carbonyl groups, and the formation of the free ligand.

In the UV-vis/NIR spectra of **9H** and **10F**, only spectral changes associated with the oxidised ferrocene molecules were observed, with no evidence of absorbance features associated with the closed-ring isomers in the spectra. This result is in agreement with the CV of **10F**, in which there was no strong evidence to suggest that oxidative cyclisation occurred for **10F**. However, in the case of **9H**, the CV results showed new redox waves, following the first oxidation process of the switching unit, which were tentatively assigned to the generation of the closed-ring cations. The new redox waves in the CV of **9H** were similar to those recorded in the CV of **10H**. Such changes were proven to be associated with the closed-ring cation species, as described above for **10H**, thus indicating that oxidative cyclisation occurs for **9H**. However, the bulk electrolysis experiments occur on a much longer time-scale, in comparison to the cyclic voltammetry studies (minutes *vs.* seconds respectively). Therefore it is feasible that the closed-ring cation species of **9H** were too unstable, within this time-frame, to display any spectral features in the UV-vis/NIR spectra.

6.3.5 Co$_2$(CO)$_6$ Complexes: IR Spectroelectrochemistry

The cyclic voltammograms have shown that quasireversible oxidation processes of the ferrocene molecules were found to occur prior to oxidation of the Co$_2$(CO)$_6$ moieties. Therefore, IR spectroelectrochemistry experiments were carried out on the Co$_2$(CO)$_6$ complexes **9H/F** and **10H/F** in order to investigate if the electron-withdrawing effect of the electrochemically generated ferrocenium ions would effect the carbonyl bands in the IR spectrum, and also to examine the changes in these bands when the Co$_2$(CO)$_6$ moieties undergo oxidation processes. These experiments were carried out in 0.1 M TBAPF$_6$/CH$_2$Cl$_2$ *vs.* Ag/Ag$^+$, and the structures of the Co$_2$(CO)$_6$ complexes are illustrated in figure 6.24.

9H: R=H
9F: R=F

10H: R=H
10F: R=F
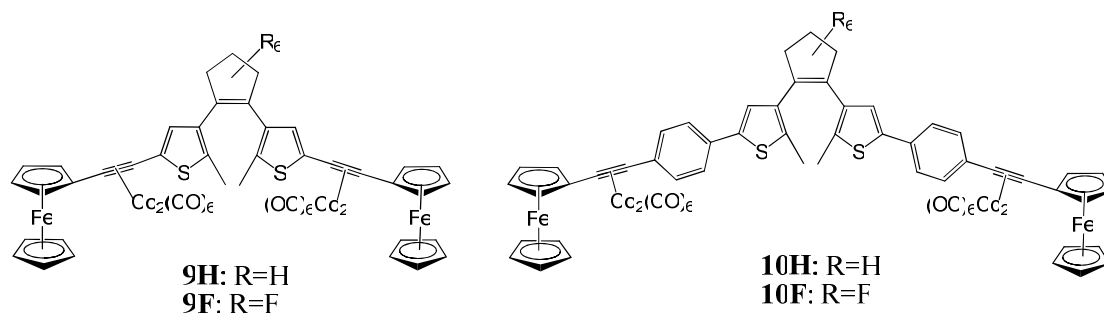
Figure 6.24: The structures of the open-ring Co$_2$(CO)$_6$ complexes **9H/F** and **10H/F**.

At the start of the experiment, three carbonyl IR bands, in the range of 2100 to 2020 cm^{-1}, were recorded for complexes **9H/F** and **10H/F**, the values of which are presented in table 6.7. The results highlight how the atoms present on the dithienylcyclopentene unit have an effect on the IR stretches of the Co$_2$(CO)$_6$ complexes, with the presence of the electron-withdrawing fluorine atoms shifting the bands to slightly higher energy wavenumbers in comparison to the perhydro analogues. Such an effect is more pronounced for **9F**, in comparison to **10F**. This can be attributed to the extended distance between the switching unit and the cobalt carbonyl moieties, by the presence of the phenyl-rings in **10F**, thus reducing the effect of the fluorine atoms on the carbonyl stretches.

Table 6.7: The IR spectral data of the $Co_2(CO)_6$ complexes **9H/F** and **10H/F**, in 0.1 M TBAPF$_6$/ CH$_2$Cl$_2$, before oxidation (parent bands) and during oxidation processes (new bands).

Compound	Start $v(CO)$ cm^{-1}	Oxidation at 0.6 V $v(CO)$ cm^{-1}
9H	2085, 2050, 2021	2098, 2065, 2039
10H	2085, 2050, 2021	2098, 2066, 2038
9F	2088, 2053, 2024	2100, 2068, 2041
10F	2086, 2051, 2022	2099, 2067, 2039

When oxidation potentials between 0.3 and 0.6 V were applied (i.e. at potentials coordinating with the beginning of the ferrocene redox processes as observed in the CV's), depletion of the parent bands in the IR spectra was observed for each complex, along with three concomitant bands appearing at higher wavenumbers. For example, oxidation of **9F** resulted in bleaching of the parent bands at 2088, 2053 and 2024 cm^{-1}, with three new bands appearing at 2100, 2068 and 2041 cm^{-1}, as shown in figure 6.25 (A). Similar results were observed for all the complexes, and the resulted are summarised in table 6.7. These new bands can be attributed to the oxidation of the ferrocene molecules. During oxidation processes, the electron-donating ferrocene molecules lose one electron, forming the corresponding electron-withdrawing ferrocenium ions, which in turn reduces the electron density on the cobalt carbonyl moieties, thus shifting the IR bands to higher frequencies.

When a potential of 0 V was applied, subsequent reduction of the ferrocenium ions occurred, thus the newly formed carbonyl bands depleted and the original bands began to grow back. Although the parent bands did not return fully, they were found to reach approximately 90 % of their original absorbance values recorded in each case, as shown for **9F** in figure 6.25 (B).

Oxidation processes at higher potentials, coordinating with the CV results at which the Co$_2$(CO)$_6$ moieties were found to undergo oxidation, resulted in a decrease in all of the cobalt carbonyl bands in the IR spectrum, with no new spectral features observed. Following, subsequent reduction at 0 V, the parent bands began to re-emerge, but they did not recover to the same absorbance values recorded at the start of the experiment.
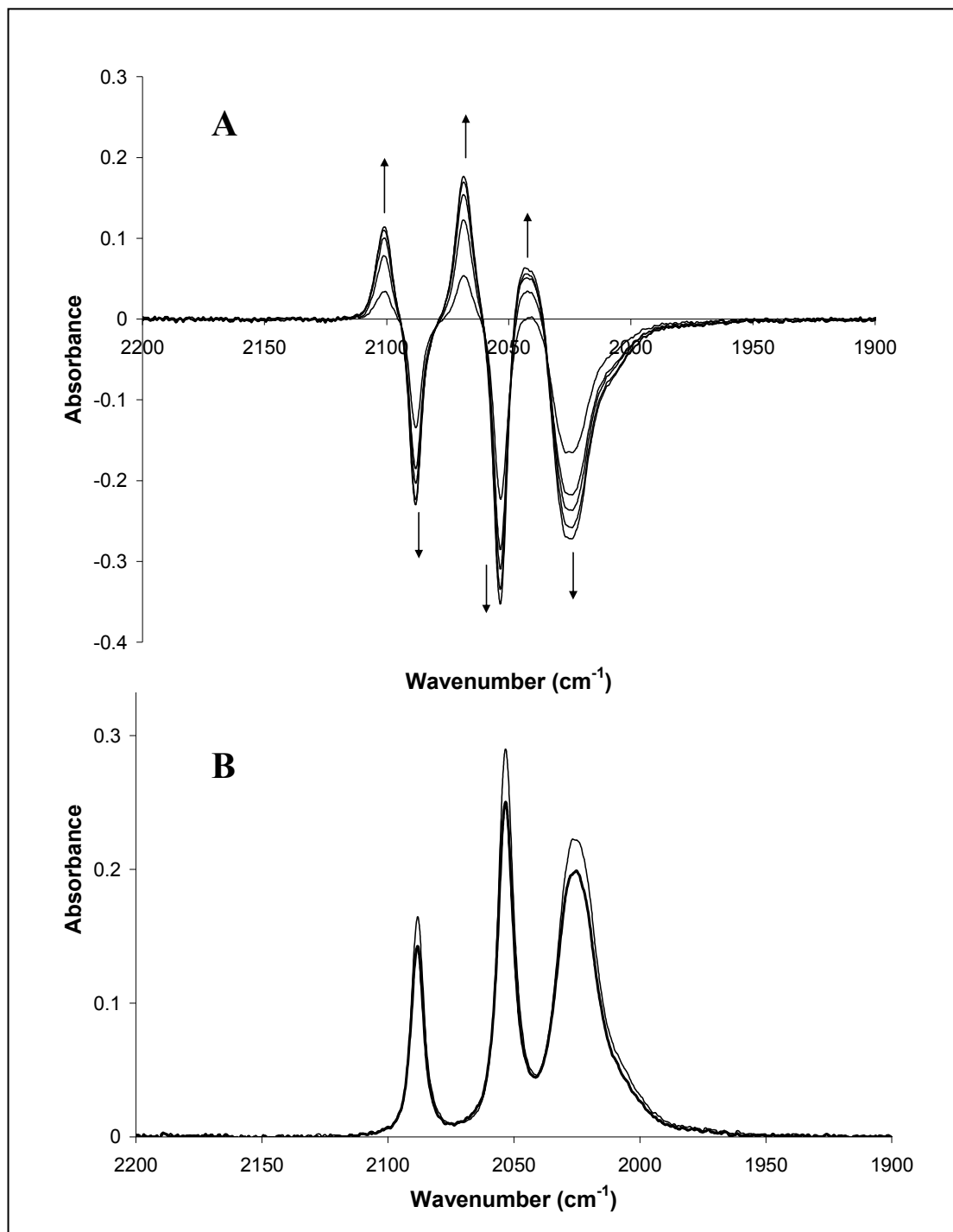
Figure 6.25: The IR spectra of the $Co_2(CO)_6$ complex **9F**, in 0.1 M TBAPF$_6$/CH$_2$Cl$_2$. (A) shows the IR difference spectrum highlighting the generation of new bands, at higher energy wavenumbers, following oxidation at 0.6 V. (B) shows the return of the parent bands, following reduction at 0 V, with the last spectrum recorded (thick black line) at ~ 90% of the absorbance value originally recorded at the start of the experiment (thin black line).

6.3.6 Co$_2$(CO)$_4$dppm Complexes: Cyclic Voltammetry

1,2-Bis(diphenylphosphino)methane {dppm} ligands were incorporated onto the Co$_2$(CO)$_6$ complexes **9H/F** and **10H/F**, described in the previous section, producing the corresponding Co$_2$(CO)$_4$dppm complexes, **11H/F** and **12H/F** respectively, the structures of which are illustrated in figure 6.26. The redox properties of the dppm derivatives were investigated using cyclic voltammetry techniques at room temperature, in 0.1 M TBAPF$_6$/CH$_2$Cl$_2$, at a scan rate of 0.1 Vs^{-1}, and the results were calibrated against the redox couple of decamethylferrocene Fc*$^+$/Fc* (E$_{1/2}$ = -0.07 *vs.* SCE). Literature reports have described how incorporating phosphine ligands, onto cobalt carbonyl groups, helps to stabilise the metal carbonyls, thus promoting reversible oxidation processes of such moieties. This effect can be attributed to the electron-donating ability of the phosphine ligands, which increases the electron density on the Co-Co core, hence, increasing the lifetimes of the radical anions and cations, and thereby reducing the rate at which disintegration processes occur.[25-27,29,30] Therefore, the influence of the chelating dppm ligands, on the reductive and oxidative processes of the metal carbonyl moieties, was investigated for compounds **11H/F** and **12H/F**.   Furthermore, the effect of the Co$_2$(CO)$_4$dppm components on the electrochromic properties of the switching units, was also examined, and the results are described here.

11H: R=H; M$_1$=Co$_2$(CO)$_4$dppm
11F: R=F; M$_1$=Co$_2$(CO)$_4$dppm

12H: R=H; M$_1$=Co$_2$(CO)$_4$dppm
12F: R=F; M$_1$=Co$_2$(CO)$_4$dppm
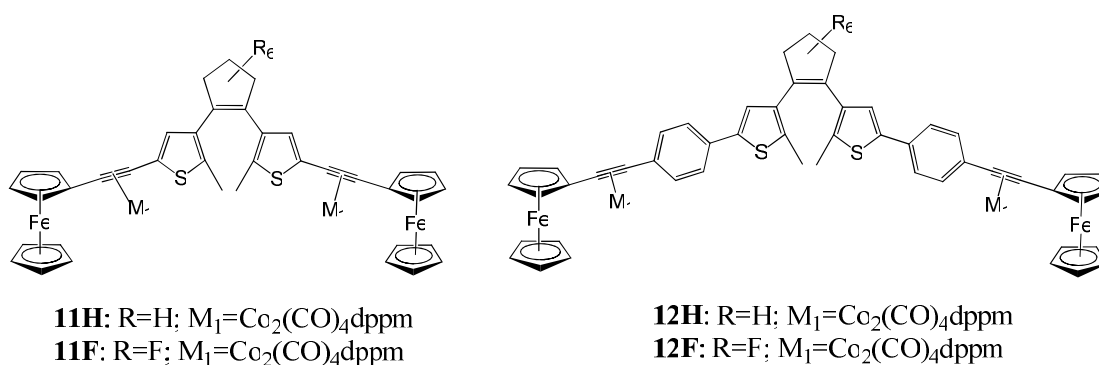
Figure 6.26: The structures of the open-ring Co$_2$(CO)$_4$dppm complexes **11H/F** and **12H/F**.

- **Reduction Process**

The first reduction processes in the CV's of the $Co_2(CO)_6$ complexes of the perhydro analogues, **9H** and **10H**, were observed at -1.17 V and -1.22 V (*vs.* SCE) respectively. Conversely, no reduction processes were observed for their corresponding $Co_2(CO)_4$dppm complexes, **11H** and **12H**, within the potential limits of the CH_2Cl_2 solvent (i.e. V < -2.0 V). This result indicates that the dppm derivatives undergo reduction process at much more negative potentials than their corresponding cobalt hexacarbonyl complexes. Similar results have been reported in the literature, and are ascribed to the electron-donating ability of the dppm ligand, making the complexes more difficult to reduce.[25-27,29,30]
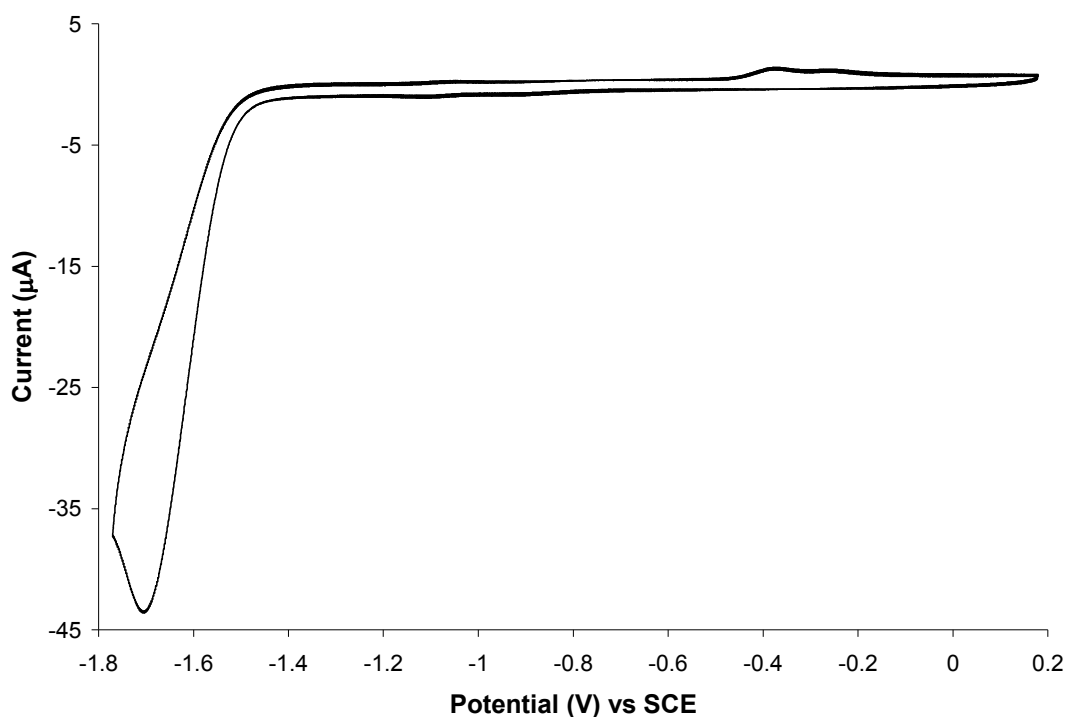
Figure 6.27: Cyclic voltammogram of the reduction process of the $Co_2(CO)_4$dppm complex **11F**, in 0.1 M TBAPF$_6$/CH$_2$Cl$_2$, at a scan rate of 0.1 Vs^{-1}.

On the other hand, reduction processes occurred for the $Co_2(CO)_4$dppm perfluoro-derivatives **11F** and **12F**, at -1.72 V and -1.74 V (*vs.* SCE) respectively, as shown for **11F** in figure 6.27. In both cases, a single irreversible bielectronic reduction peak was observed, representing a two-electron process, thus indicating that little electronic interaction existed between the two metal centres, on both sides of the switch. An

increase in the stability of the anionic species is provided by the electron-withdrawing fluorine atoms, therefore allowing reduction processes to take place at less negative potentials, in comparison to the perhydro derivatives. Having said that, the effect of the electron-rich phosphine ligands was highlighted by the considerable cathodic shift of the reduction waves of the dppm derivatives **11F** and **12F**, with respect to their $Co_2(CO)_6$ counterparts {**9F** and **10F**} i.e. $\Delta E \approx 590$ mV in both cases. Furthermore, the intensities of the oxidation peaks recorded in the subsequent anodic sweeps, at -0.24 and -0.36 V for **12F**, and at -0.21 and -0.36 V for **11F**, were found to be substantially diminished in comparison to those recorded for the cobalt hexacarbonyl complexes. These peaks are associated with disintegration products, therefore indicating that the rate of decomposition of the cobalt carbonyl moieties was significantly reduced due to the presence of the dppm ligands.

- **Oxidation Process**

As described in previous literature studies,[25-27,29,30] introducing electron-donating phosphine ligands, onto cobalt carbonyl compounds, increases the electron density on the metal centre, thus promoting more reversible oxidation processes, at lower potentials, in comparison to their related $Co_2(CO)_6$ complexes. Similar effects were observed in the CV's of the $Co_2(CO)_4$dppm complexes **11H/F** and **12H/F**, following oxidation processes, and the results are summarised in table 6.8. For comparative purposes, the oxidation potentials recorded for the corresponding free ligand ferrocenyl-based switches and $Co_2(CO)_6$ complexes are also detailed in table 6.8. The results show that incorporating dppm substituents onto the cobalt carbonyl groups reduced the potential at which the ferrocene molecules underwent oxidative processes, in comparison to the related free ligand and cobalt hexacarbonyl complexes, with $\Delta E \approx 180$ mV. Furthermore, the presence of the chelating phosphine ligands reduced the potential at which the cobalt carbonyl units underwent oxidation processes, with $E_{1/2}$ ranging from 0.86 to 0.93 V, and introduced reversibility to such processes ($i_{pc}/i_{pa} \approx 0.3$). There was no evidence of strong electronic interaction existing between the two $Co_2(CO)_4$dppm moieties as only a single bielectronic wave, representing a one-step two-electron oxidation process, was observed in the CV's of each complex.

Table 6.8: The cyclic voltammetry results following oxidation processes, of the $Co_2(CO)_4$dppm complexes **11H/F** and **12H/F**, and the corresponding open-ring free ligand switches (**7H/F** and **8H/F**) and $Co_2(CO)_6$ derivatives (**9H/F** and **10H/F**).

<div align="center">

Oxidation Processes

</div>

	E_{pa}	E_{pc}	$E_{1/2}$
7Ho	0.68^{Fc}, 0.99^{rc}, 1.15^{rc}, 1.50^{a}	0.54^{Fc}, 0.93^{rc}, 1.08^{rc}	0.61^{Fc}
9H	0.51^{rc}, 0.66^{Fc}, 0.85^{rc}, 1.26^{a}, 1.48^{a}	0.45^{rc}, 0.54^{Fc}, 0.74^{rc}	0.60^{Fc}
11H	0.19^{rc}, 0.47^{Fc}, 0.73^{rc}, 0.93^{dppm}	0.10^{rc}, 0.32^{Fc}, 0.63^{rc}, 0.78^{dppm}	0.40^{Fc}, 0.86^{dppm}
8Ho	0.43^{rc}, 0.68^{Fc}, 0.90^{rc}, 1.32^{a}	0.37^{rc}, 0.48^{Fc}, 0.80^{rc}	0.58^{Fc}
10H	0.47^{rc}, 0.64^{Fc}, 0.84^{rc}, 1.28^{a}, 1.45^{a}	0.41^{rc}, 0.51^{Fc}, 0.76^{rc}	0.58^{Fc}
12H	0.49^{Fc}, 0.64^{rc}, 1.0^{dppm}, 1.38^{a}	0.33^{Fc}, 0.62^{rc}, 0.82^{dppm}, 1.08	0.41^{Fc}, 0.91^{dppm}
7Fo	0.73^{Fc}, 1.76^{a}	0.52^{Fc}	0.63^{Fc}
9F	0.67^{Fc}, 1.43^{a}, 1.66^{a}	0.49^{Fc}	0.58^{Fc}
11F	0.49^{Fc}, 1.00^{dppm}, 1.55^{a}	0.34^{Fc}, 0.85^{dppm}	0.42^{Fc}, 0.93^{dppm}
8Fo	0.64^{Fc}, 1.05^{rc}, 1.21^{rc}, 1.68^{a}	0.50^{Fc}, 0.98^{rc}, 1.07^{rc}	0.57^{Fc}
10F	0.65^{Fc}, 0.83^{rc}, 1.37^{a}, 1.68^{a}	0.51^{Fc}, 0.78^{rc}, 0.97^{rc}	0.59^{Fc}
12F	0.45^{Fc}, 0.60^{rc}, 0.95^{dppm}, 1.48^{a}	0.36^{Fc}, 0.57^{rc}, 0.86^{dppm}, 1.13^{rc}	0.41^{Fc}, 0.91^{dppm}

All values listed are values of potential (V) *vs.* SCE, recorded in 0.1 M $TBAPF_6$/CH_2Cl_2, at 0.1 Vs^{-1}.
[a] indicates an irreversible oxidation process
[Fc] indicates peaks due to the redox couple of the ferrocene moieties
[dppm] indicates peaks due to the redox couple of the $Co_2(CO)_4$dppm moeities
[rc] indicates peaks assigned to ring-closed species
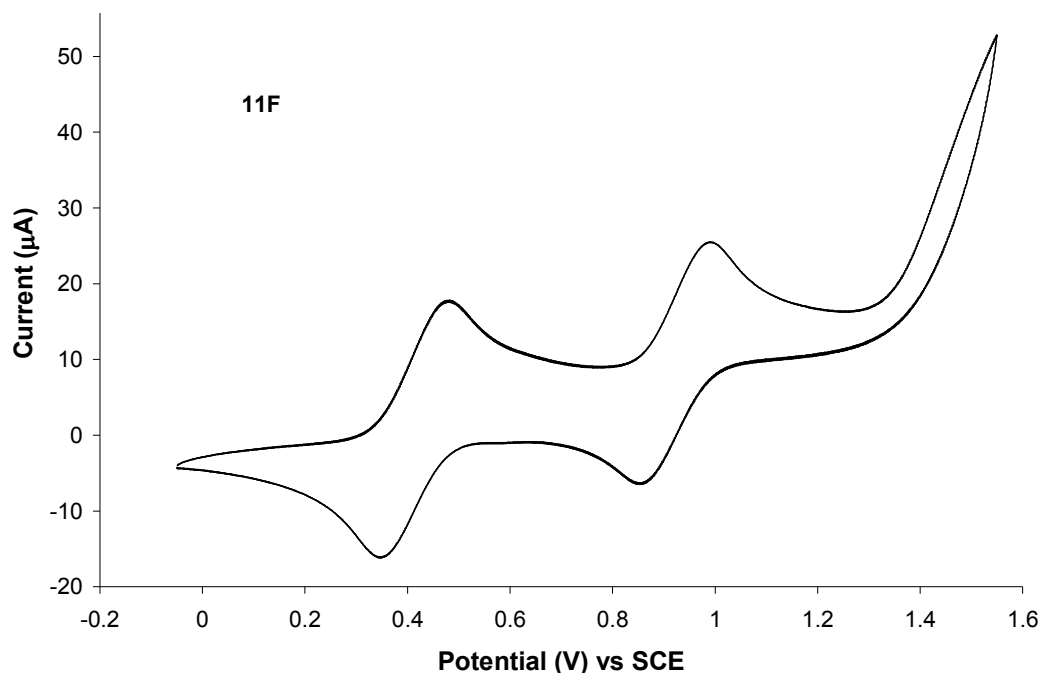
Figure 6.28: Cyclic voltammogram of the oxidation process of the $Co_2(CO)_4$dppm complex **11F**, in 0.1 M $TBAPF_6$/CH_2Cl_2, at a scan rate of 0.1 Vs^{-1}.

Oxidation of the $Co_2(CO)_4$dppm complex **11F** resulted in two quasi-reversible waves, at $E_{1/2}$ = 0.42 V and 0.93 V (*vs.* SCE), each representing a two-electron process. The first wave is associated with the oxidation processes of the two ferrocene molecules, forming the ferrocenium ions Fc^+. The second wave is assigned to a one-electron oxidation reaction of the each of the two $Co_2(CO)_4$dppm moieties. Oxidation of the switching unit was observed by an irreversible oxidation peak at 1.55 V, and no new redox waves appeared in the following cathodic and anodic sweeps, as shown in figure 6.28. Thus, **11F** was not found to undergo electrochemical cyclisation to the closed-form.
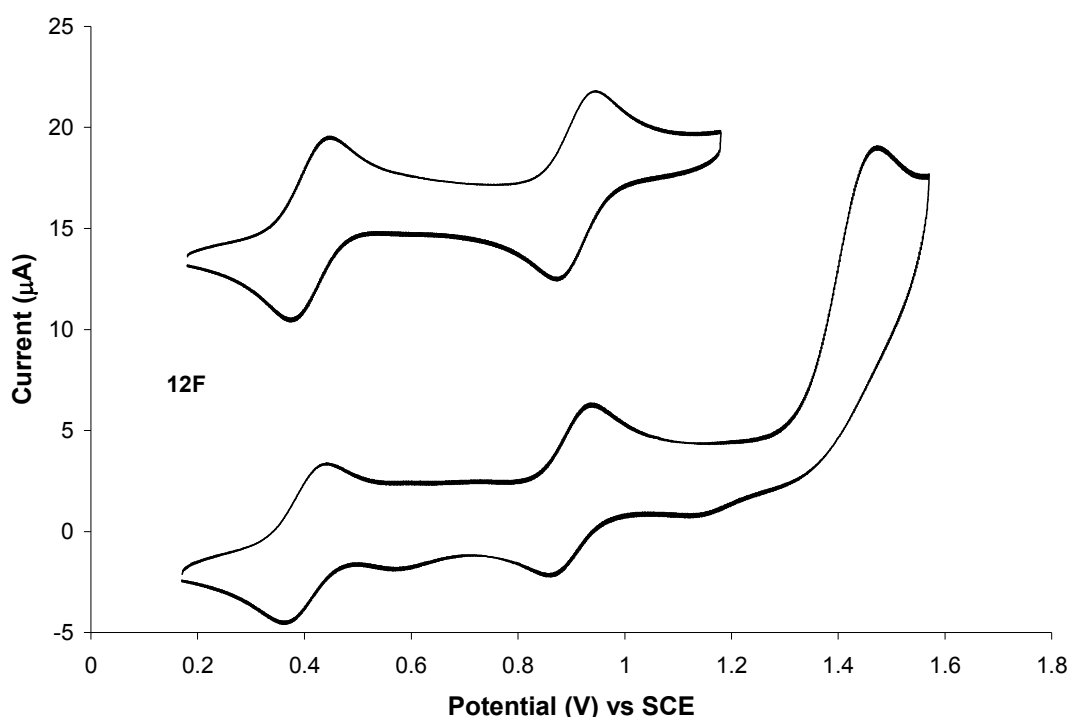
Figure 6.29 Cyclic voltammogram of the $Co_2(CO)_4$dppm complex **12F**, in 0.1 M TBAPF$_6$/CH$_2$Cl$_2$ at 0.1 Vs^{-1}, following oxidation at 1.60 V (bottom, sweep 3 and 4) and at 1.20V (top), the CV of which is offset along the coordinate for clarity.

In the case of the extended chain perfluoro analogue, **12F**, two quasi-reversible oxidation waves, due to oxidation of the ferrocene and $Co_2(CO)_4$dppm moieties, were recorded at $E_{1/2}$ = 0.41 and 0.91 V respectively. Oxidation of the switching unit occurred at 1.48 V (*vs.* SCE), and in the subsequent cathodic sweep a very small reduction peak was observed at 1.13 V. As displayed in figure 6.29, another reduction peak appeared between the two quasireversible waves at E_{pc} = 0.57 V, and a corresponding barley visible oxidation peak at 0.60 V, neither of which were present

in the CV before oxidation of the switching unit occurred at 1.48 V. Such a result may be due to the formation of the closed-ring cationic species of **12F**, however, there is not enough information from this CV to state this conclusively. All the redox waves remained quite stable following a number of consecutive sweeps ($\sim$ 10). Therefore, it is clear that incorporating the electron-donating dppm ligands onto the cobalt carbonyl moieties increased the stability this complex, in comparison to the related $Co_2(CO)_6$ complex **10F**, where severe fouling of the electrode surface occurred after one redox cycle.
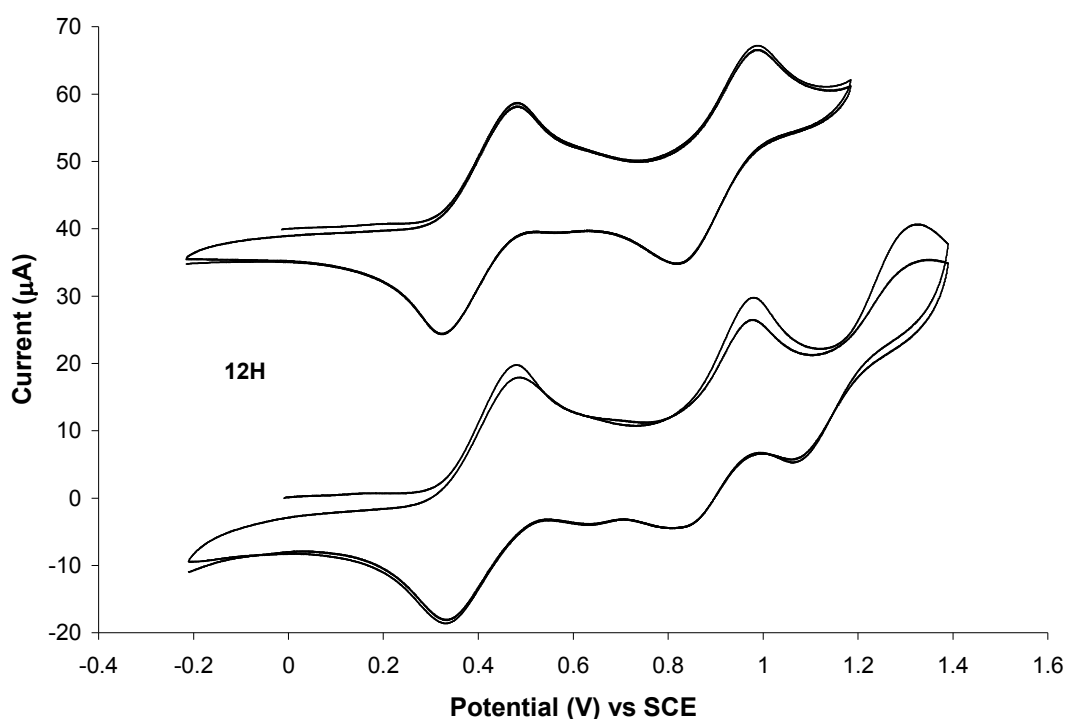
Figure 6.30 Cyclic voltammogram of the $Co_2(CO)_4$dppm complex **12H**, in 0.1 M TBAPF$_6$/CH$_2$Cl$_2$ at 0.1 Vs^{-1}, following oxidation at 1.4 V (bottom), and at 1.2 V (top), the CV of which was offset along the coordinate for clarity.

In the case of **12H**, oxidation of the ferrocene molecules occurred at $E_{1/2}$ = 0.41 V (*vs.* SCE). The $Co_2(CO)_4$dppm moieties were found to undergo a quasireversible oxidation process at $E_{1/2}$ = 0.91 V, and in the subsequent cathodic and anodic sweeps, small oxidation/reduction peaks were observed at 0.64 and 0.62 V respectively. At higher potentials, another oxidation process was recorded at 1.38 V, which can tentatively be assigned to oxidation of the switching unit. In the returning cathodic sweep, a new reduction peak was observed at 1.08 V. Furthermore, the oxidation and reduction peaks, at 0.64 and 0.62 V respectively, increased in intensity, as shown in

figure 6.30. It is difficult to determine whether the new reduction peaks at 1.08 V and 0.62 V, and oxidation peak at 0.62 V, are associated with the occurrence of an oxidative cyclisation process, as they are heavily masked by the redox waves associated with the ferrocene and $Co_2(CO)_4$dppm oxidation processes. Therefore, further investigation would be required in order to determine conclusively if **12H** undergoes electrochemically induced ring-closure.
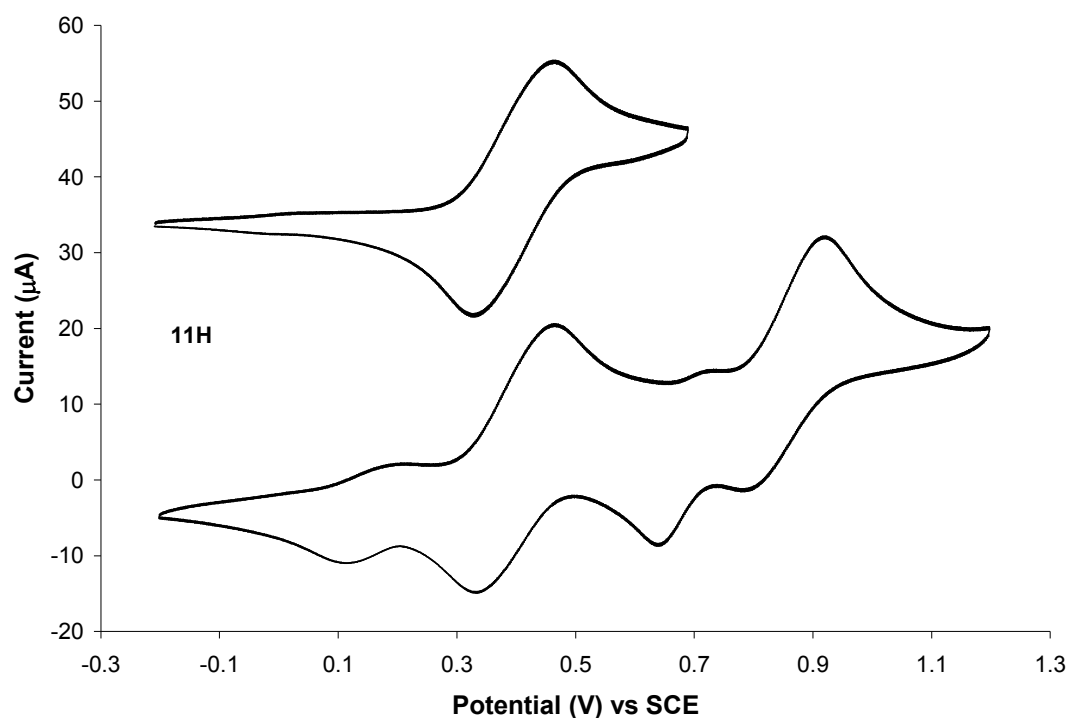
Figure 6.31 Cyclic voltammogram of the $Co_2(CO)_4$dppm complex **11H**, in 0.1 M TBAPF$_6$/CH$_2$Cl$_2$ at 0.1 Vs^{-1}, following oxidation at 1.2 V (bottom) and at 0.7 V (top), the CV of which is offset along the coordinate for clarity.

In the case of the shorter chain perhydro analogue, **11H**, strong evidence of oxidative cyclisation was observed in the CV, as shown in figure 6.31. A quasireversible redox wave, associated with the oxidation of the ferrocene molecules, was recorded at $E_{1/2} =$ 0.40 V. A second quasireversible wave was recorded at $E_{1/2} = 0.86$ V, which is assigned to the oxidation process of the $Co_2(CO)_4$dppm molecules. However, in the returning cathodic sweep two new reduction peaks appeared at 0.63 and 0.10 V, and two corresponding oxidation waves were present in the subsequent anodic cycle at 0.73 and 0.19 V respectively. These new redox waves can be attributed to the closed-ring cationic species. The fact that these redox waves appeared before oxidation of the switching unit took place indicates that the cyclisation process was induced following oxidation of the $Co_2(CO)_4$dppm moieties, possibly through an electron

transfer mechanism. The relative intensity of the new redox peaks, assigned to the closed-ring cations, indicates that a significant amount of the closed-ring isomer was formed. Further evidence of this was the absence of a large irreversible oxidation peak at higher oxidation potentials, corresponding to oxidation of the open-ring switching unit.

Overall, the cyclic voltammetry results showed that incorporating dppm ligands onto the cobalt carbonyl moieties had an interesting effect on the electrochemical properties of these switches. Firstly, oxidation processes of the ferrocene molecules occurred at lower potentials in comparison to their related free ligand and $Co_2(CO)_6$ compounds ($\Delta E \approx 180$ mV). Secondly, the oxidation peaks representing the cobalt carbonyl moieties were more reversible, and cathodically shifted (*ca.* 300 mV for the perhydro-derivatives and *ca.* 400 mV for the perfluoro analogues), when the phosphine ligands were present. Thirdly, in the case of the perfluoro-switches **11F** and **12F**, the oxidation processes of the dithienylethene units occurred at less positive potential values in comparison to their corresponding free ligands, **7F** and **8F** respectively ($\Delta E \approx 200$ mV in each case). These results are a consequence of the electron-donating ability of the dppm ligands, thus stabilising the oxidation processes of the switches and hence allowing such processes to occur at lower potential values.

In terms of the electrochromic properties of the switches, the $Co_2(CO)_4$dppm compounds on **11F** were not found to induce cyclisation processes. In the case of **12F** and **12H**, there was some evidence in the CV's to suggest that oxidative cyclisation occurred for these complexes, however, this is not a conclusive result and further investigations would be necessary to confirm this. However, for the shorter chain perhydro-derivative **11H**, the presence of the $Co_2(CO)_4$dppm moieties were found to have a considerable effect on the electrochromic behaviour of this compound. Oxidative cyclisation was found to occur for **11H**, following oxidation of the $Co_2(CO)_4$dppm moieties. Therefore, it is possible that ring-closing was induced via an electron transfer mechanism. Furthermore, the relative height of the closed-form cationic peaks indicated that a significant amount of the closed-ring isomer was produced. This result is in high contrast to the results observed for the related free ligand (**7H**) and cobalt hexacarbonyl compounds (**9H**), whereby only small oxidation/reduction peaks associated with the closed-ring cations, were observed following oxidation processes of the switching unit.

6.3.7 Co$_2$(CO)$_4$dppm Complexes: UV-vis/NIR Spectroelectrochemistry

According to the cyclic voltammetry studies of the Co$_2$(CO)$_4$dppm complexes, it appeared that **11H** underwent oxidative cyclisation processes, induced by oxidation of the cobalt carbonyl moieties, whereas there was no evidence of such processes in the case of the perfluorinated derivative **11F**. Electrochemical ring-closing was not as apparent in the CV's of **12H** and **12F**, due to the low intensity of the new redox waves observed following oxidation of the metal carbonyl groups and the switching units. In order to further investigate the oxidation processes of the dppm derivatives, UV-vis/NIR spectroelectrochemistry experiments were performed on the Co$_2$(CO)$_4$dppm complexes, in 0.1 M TBAPF$_6$/CH$_2$Cl$_2$ versus Ag/Ag$^+$. The structures of these complexes are presented in figure 6.32, and the results found in the absorbance spectra are summarised in table 6.9.

Table 6.9: UV-vis/NIR spectroelectrochemistry data of the Co$_2$(CO)$_4$dppm complexes **11H/F** and **12H/F**, following oxidation processes at varying potentials.

Absorbance Spectra of the Co$_2$(CO)$_4$dppm Complexes		
	Oxidation Potential	λ_{abs} (nm)
11H	Start	351, 498
	0.4 V	498, 720-1620
	0.8 V	441, 652,
	0 V	437, 634
12H	Start	276, 345, 495,
	0.5 V	276, 495, 750-1620
11F	Start	270, 355, 486
	0.5 V	270, 486, 750-1620
12F	Start	286, 334, 500
	0.5 V	279, 324, 500, 750-1620

The data was recorded in 0.1 M TBAPF$_6$/CH$_2$Cl$_2$ *vs.* Ag/Ag$^+$

11H: R=H; M₁=Co₂(CO)₄dppm
11F: R=F; M₁=Co₂(CO)₄dppm

12H: R=H; M₁=Co₂(CO)₄dppm
12F: R=F; M₁=Co₂(CO)₄dppm
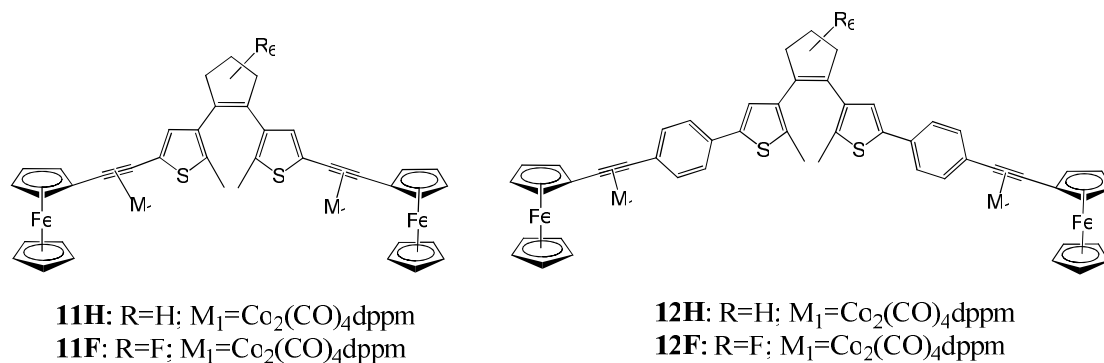
Figure 6.32: The structures of the open-ring $Co_2(CO)_4$dppm complexes **11H/F** and **12H/F**.

Oxidation of **11F**, at 0.5 V, resulted in an increase in the absorbance bands in the UV-vis spectrum at 270 and 486 nm, and a very weak absorbance extending into the NIR region, from approximately 720 – 1620 nm. These spectral changes are attributed to the oxidised ferrocene units.[5,6,20] Following oxidation processes at higher potentials (greater than 1.0 V), an overall decrease in the absorbance was observed, and subsequent reduction processes did not regenerate the original spectrum recorded. Therefore, the results showed no evidence of an oxidative cyclisation reaction for **11F**, which is in accordance with the CV, and suggest that some decomposition of the $Co_2(CO)_4$dppm moieties occurred following oxidation at potentials greater than 1.0 V.

Similar results were observed for the $Co_2(CO)_4$dppm complexes **12H** and **12F**, whereby only spectral features associated with the oxidation of the ferrocene molecules were observed in the UV-vis/NIR spectrum, during the bulk electrolysis experiments, as shown for **12H** in figure 6.33. The CV's of these complexes showed oxidation/reduction peaks, which could possibly be associated with the occurrence of an oxidative cyclisation process. However, these redox waves were very small, suggesting that if they were in fact representative of the closed-ring cation species, they may not be stable enough to be observed in the absorbance spectra, within the timescale of the bulk electrolysis experiments.
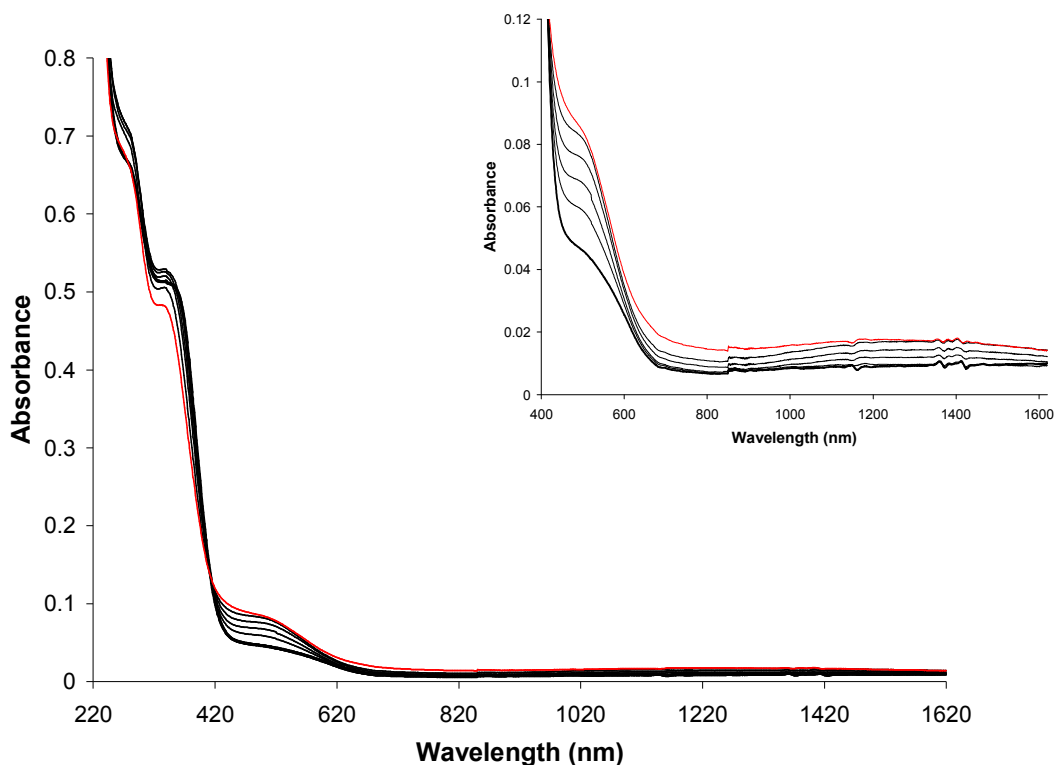
Figure 6.33: UV-vis/NIR spectrum of the $Co_2(CO)_4$dppm complex **12H** (thick black line), in 0.1 M TBAPF$_6$/CH$_2$Cl$_2$. Following oxidation at 0.5 V (black lines), there was an increase in the absorbance bands at 276, 495 and 750-1620 nm, and at 1.2 V (red line) there was no evidence of new absorption peaks associated with the closed-ring form. Inset, the spectrum of **12H** zoomed-in between 400 and 1620 nm for clarity.

In contrast to the other dppm derivatives, oxidation of **11H** was found to generate absorbance bands characteristic of the closed-ring cation species. Oxidation at 0.4 V resulted in an increase in absorbance at 498 nm, and a very weak band extending from 720 to 1620 nm, both of which can be assigned to oxidation of the ferrocene units. At a potential of 0.6 V, the band at 498 nm continued to increase, with a band at 652 nm beginning to grow-in. When the potential was increased to 0.8 V (i.e. corresponding the potential at which oxidation of the $Co_2(CO)_4$dppm moieties occurred in the CV), a significant increase was observed in the visible region of the spectrum, with λ$_{max}$ present at 441 and 652 nm, as shown in figure 6.34. With reference to the literature,[10] it can be deduced that these bands are a consequence of the formation of the dication species of the closed-ring switching unit. The fact that these absorbance features appeared at the potential value associated with the oxidation process of the cobalt carbonyl groups, indicates that the cyclisation process was induced by electron

transfer from the $Co_2(CO)_4$dppm moieties, to the dithienylethene unit, which is in accordance with the results obtained from the cyclic voltammogram of **11H**.
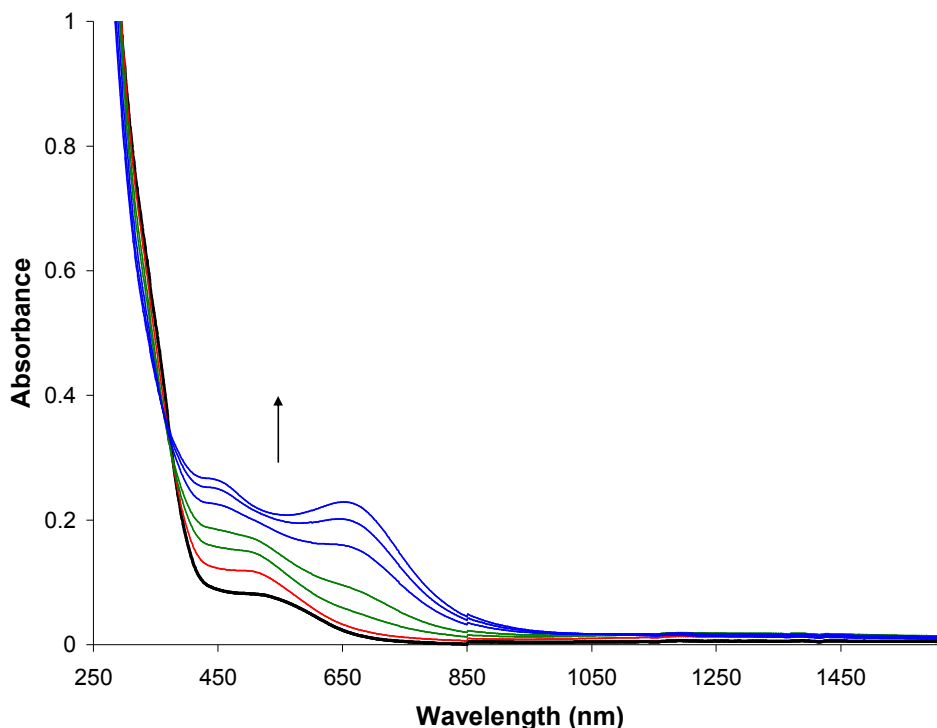
Figure 6.34: UV-vis/NIR spectra of the $Co_2(CO)_4$dppm complex **11H**, in 0.1 M TBAPF$_6$/CH$_2$Cl$_2$, at the start (black line), and following oxidation at 0.4 V (red line), 0.6 V (green lines) and 0.8 V (blue lines).

Subsequent reduction at 0 V resulted in a hypsochromic shift of these bands to 437 and 634 nm (figure 6.35), which could possibly be an indication of the formation of the neutral species of the closed form. These results show that the presence of the $Co_2(CO)_4$dppm groups have a stabilising effect on the cationic species of the closed-ring isomer, in comparison to the corresponding free ligand **7H** and $Co_2(CO)_6$ complex **9H**. When the reduction potential was decreased to -0.3 V, a decrease in the absorbance bands in the visible region was observed. However, during this process, a new absorbance band appeared, with a $\lambda_{max} = 1000$ nm, which subsequently decreased over time, as shown in figure 6.35. This spectral feature could tentatively be assigned to the reduction of the dication species of the switching unit to the monocation, or possibly to the ferrocenium ions.
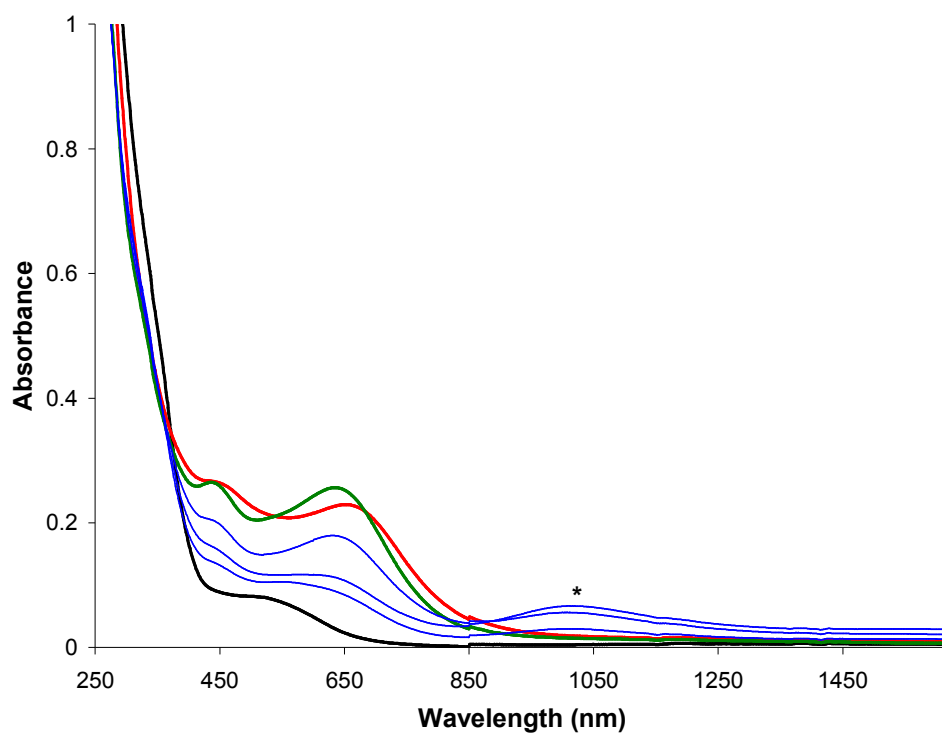
Figure 6.35: UV-vis/NIR spectra of the $Co_2(CO)_4dppm$ complex **11H**, in 0.1 M $TBAPF_6/CH_2Cl_2$, showing: the spectrum recorded at the start (black line); the final spectrum recorded after oxidation at 0.8 V (red line); the hypsochromic shift in the absorbance bands following reduction at 0 V (green line); and the decrease in the absorbance bands following reduction at -0.3 V (blue lines), with the appearance of the band at 1000 nm (*).

6.3.8 Co$_2$(CO)$_4$dppm Complexes: IR Spectroelectrochemistry

IR spectroelectrochemistry experiments were carried out on the Co$_2$(CO)$_4$dppm complexes **11H/F** and **12H/F** (in 0.1 M TBAPF$_6$/CH$_2$Cl$_2$ *vs.* Ag/Ag$^+$), the structures of which are illustrated in figure 6.36. The aim of these experiments was to examine the influence of the oxidised ferrocene molecules on the metal carbonyl groups, and to investigate the effects of the oxidation processes of the Co$_2$(CO)$_4$dppm moieties in more detail.

11H: R=H; M$_1$=Co$_2$(CO)$_4$dppm
11F: R=F; M$_1$=Co$_2$(CO)$_4$dppm

12H: R=H; M$_1$=Co$_2$(CO)$_4$dppm
12F: R=F; M$_1$=Co$_2$(CO)$_4$dppm
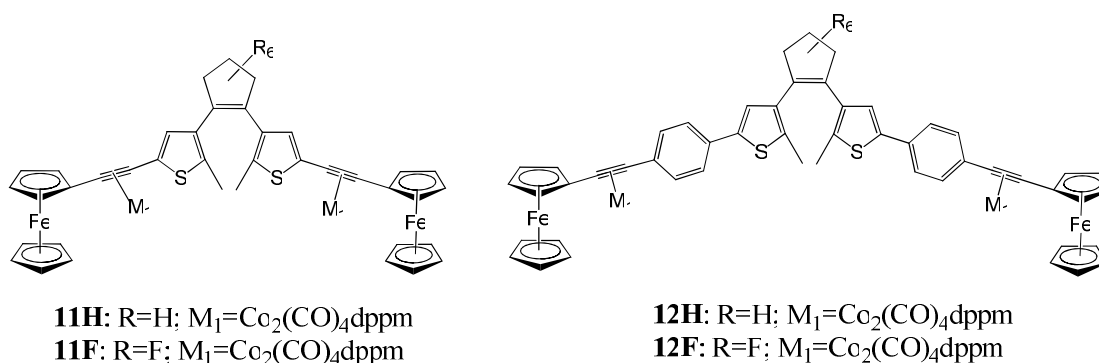
Figure 6.36: The structures of the open-ring Co$_2$(CO)$_4$dppm complexes **11H/F** and **12H/F**.

The Co$_2$(CO)$_4$dppm complexes, **11H/F** and **12H/F**, displayed three carbonyl bands in the IR spectra, in the range of 2020 to 1960 cm^{-1}, as detailed in table 6.10. In comparison to their related Co$_2$(CO)$_6$ complexes **9H/F** and **10H/F**, the carbonyl stretches recorded for the Co$_2$(CO)$_4$dppm complexes were shifted to much lower wavenumbers. For instance, the IR bands for the Co$_2$(CO)$_6$ complex **9H** displayed bands at 2085, 2050 and 2021 cm^{-1}, whereas IR bands for the corresponding dppm derivative **11H** were recorded at 2018, 1993 and 1965 cm^{-1}. This phenomenon can be attributed to the electron-donating dppm ligand, which increases the electron density on the Co-Co core. Moreover, there are less CO molecules available in the tetracarbonyl species for back-bonding, thereby shifting the carbonyl bands to lower frequencies. The IR stretching vibrations for the perfluoro-derivative, **11F**, are shifted to slightly higher wavenumbers, compared to the other complexes **11H**, **12H** and **12F**.

Table 6.10: The IR spectral data of the $Co_2(CO)_4dppm$ complexes **11H/F** and **12H/F**, in 0.1 M $TBAPF_6$/ CH_2Cl_2, at the start before oxidation , and following oxidation processes at 0.3 V and 0.8 V.

Compound	Start $v(CO)$ cm^{-1}	Oxidation at 0.3 V $v(CO)$ cm^{-1}	Oxidation at 0.8 V $v(CO)$ cm^{-1}
11H	2018, 1993, 1965	2033, 2009, 1981	2064, 2046
12H	2018, 1991, 1964	2031, 2006, 1978	2074, 2050 (sh), 2034
11F	2021, 1995, 1968	2033, 2010, 1983	2077, 2053
12F	2019, 1992, 1964	2031, 2007, 1979	2072, 2052

Oxidation processes were carried out on these complexes, firstly at potential values coordinating with the oxidation processes of the ferrocene molecules in the CV's (~ 0.3 V), and secondly at higher potentials relating to the oxidation processes of the $Co_2(CO)_4dpm$ moieties (~0.8 V). In the case of **12H**, oxidation at 0.3 V resulted in bleaching of the parent bands at 2018, 1991 and 1964 cm^{-1}, in conjunction with the appearance of three new bands at 2031, 2006 and 1978 cm^{-1}, as shown in figure 6.37. This result is associated with the oxidation processes of the ferrocene molecules at this potential. As described previously for the $Co_2(CO)_6$ complexes, the electron-withdrawing ferrocenium ions remove electron-density from the metal carbonyl groups, thus shifting their IR bands to higher energy. Similar results were found for the other $Co_2(CO)_4dppm$ complexes and the results are summarised in table 6.10.

In all cases, the new bands disappeared following subsequent reduction of the ferrocene molecules at 0 V, as the parent bands grew back to approximately 98 % of their original absorbance values. This is an improvement when compared to their $Co_2(CO)_6$ complexes, where only 90% of the parent bands re-emerged following similar processes.

Following oxidation at higher potentials, associated with the oxidation processes of the cobalt carbonyl groups, further new spectral changes were observed. After **12H** was oxidised at ~0.3 V, new bands at 2031, 2006 and 1978 cm^{-1} were generated. Increasing the potential to ~0.8 V, resulted in bleaching of these new bands and the appearance of two bands at even higher wavenumbers, 2074 and 2034 cm^{-1}, with a shoulder band at 2050 cm^{-1}, as shown in figure 6.37. Such a result can be attributed to the oxidation of the $Co_2(CO)_4dppm$ moieties. Removing an electron from the cobalt carbonyl moieties reduced the electron density on the metal, and thus the carbonyl IR

bands were shifted to higher frequencies. This effect was observed for all the dppm derivatives, and the new IR bands observed are recorded in table 6.10.

In all cases, reduction processes at 0 V resulted in depletion of all the new bands, whilst the parent bands re-appeared, but only to approximately 80% of their original intensities.
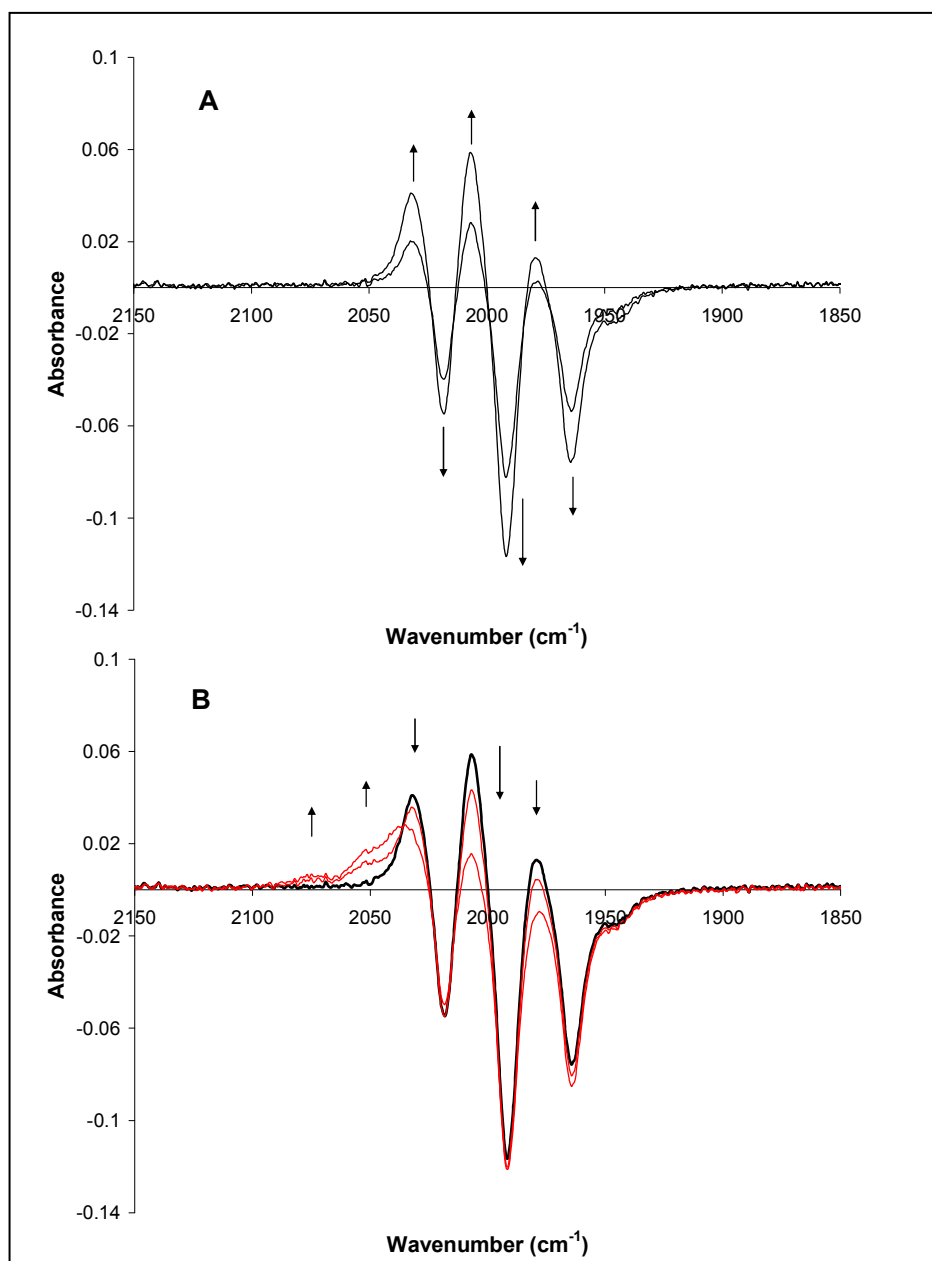
Figure 6.37: The IR difference spectra of the $Co_2(CO)_4dppm$ complex **12H**, in 0.1 M $TBAPF_6/CH_2Cl_2$. Following oxidation at 0.3 V (A), the parent bands depleted and new bands grew in at 2031, 2006 and 1978 cm^{-1}. When the oxidation potential was increased to 0.8 V (B), new bands appeared at 2074, 2050 (sh) and 2034 cm^{-1} (red lines).

6.4 Conclusion

The electrochromic properties of the ferrocenyl-based switches were investigated, and the results obtained from the cyclic voltammograms of the open and closed-ring isomers of the free ligands, **7H/F** and **8H/F**, demonstrate that it is possible to tune the electrochromic properties of dithienylethene switches by altering the substituents attached to the thienyl units, and by changing the atoms present on the central cyclopentene ring. Oxidative cycloreversion processes were observed for **7F**, whereas electrochemical ring-closing was found to occur for **7H**, **8H** and **8F**. Thus, the driving force for the ring-opening process can be assigned to the electron-withdrawing fluorine atoms and oxidised ferrocene molecules (i.e. the ferrocenium ions). Incorporating phenyl rings, between the ethynylferrocene moieties and the switching unit, was found to reduce the effects of the electron-withdrawing ferrocenium ions, and electron-donating hydrogen atoms on the cyclopentene unit provides extra stability on the closed-ring cations, thus favouring ring-closing processes.

The results obtained from the CV studies for **7F** and **8H** were verified from the UV-vis/NIR spectroelectrochemistry experiments, with efficient ring-opening processes observed for the former, and the appearance of absorbance bands in the UV-vis/NIR spectrum of the latter, associated with the closed-ring cation species. However, in the case of **7Fc**, cycloreversion processes occurred at 0.4 V, a potential at which the redox process of the ferrocene molecules began in the CV. Therefore, these results seem to suggest that the ring-opening process of **7Fc** was induced by the oxidation process of the ferrocene moieties. The absorbance spectra recorded for the open-ring isomers of **7H** and **8F** did not show any spectral changes associated with the formation of the closed-ring cations, during the oxidation processes. The bulk electrolysis experiments carried out on their closed-ring forms, **7Hc** and **8Fc**, were found to induce cycloreversion processes in both cases, an event which can tentatively be attributed to the unstable nature of the closed-ring cation species within the timescale of the bulk electrolysis experiments (minutes *vs.* seconds in the CV).

Incorporating cobalt carbonyl moieties onto the ethynylferrocene groups was found to have more pronounced influences on the electrochromic behaviour of the perhydro-

derivatives, than their corresponding perfluoro analogues. In the case of **7F**, the presence of the $Co_2(CO)_6$ {**9F**} and $Co_2(CO)_4$dppm moieties {**11F**} were not found to induce cyclisation processes for the open-ring switching unit. For the longer chain derivative **8F**, their was no strong evidence for the formation of the closed-ring cation species in the CV's of the related $Co_2(CO)_6$ {**10F**} and $Co_2(CO)_4$dppm {**12F**} complexes. The unstable nature of the oxidised hexacarbonyl moieties resulted in severe fouling of the electrode surface, and the presence of the redox waves associated with the ferrocene molecules and $Co_2(CO)_4$dppm units obscured the view of the new redox waves observed in the CV following oxidation of the dithienylethene switch. Thus, it was difficult to analyse the CV results and conclusively determine if electrochemical ring-closing occurred for these complexes. Furthermore, spectral features associated with the generation of the cation species of the closed-forms were not observed in the absorbance spectra of **10F** and **12F**, during the UV-vis/NIR spectroelectrochemistry experiments.

In the case of the perhydro-switch **8H**, introducing $Co_2(CO)_6$ moieties onto the switch {**10H**} did not prevent the oxidative cyclisation process of the switch, although the CV and UV-vis/NIR results suggested that the stability of the closed-ring cation species was reduced. In the case of the $Co_2(CO)_4$dppm complex {**12H**}, it was difficult to elucidate if electrochemical ring-closure occurred from the CV results, and moreover, cationic species of the closed-ring isomer were not observed in the UV-vis/NIR spectra during the bulk electrolysis experiments of **12H**. Therefore, the results indicate that incorporating cobalt carbonyl groups onto **8H** inhibited the electrochemical ring-closing processes of the switch. Interestingly, introducing cobalt carbonyl moieties onto the shorter chain derivative **7H**, was found to have quite a different effect on the electrochromic properties of the compound. Oxidation processes of the $Co_2(CO)_6$ complex, **9H**, resulted in new redox waves in the CV, which were tentatively assigned to the closed-ring cations. Although, the closed-ring cation species of **9H** were not stable enough to generate the corresponding absorbance bands in the UV-vis/NIR spectra during the bulk electrolysis experiments. On the other hand, the related $Co_2(CO)_4$dppm derivative {**11H**}, was found to undergo efficient oxidative cyclisation processes, as evidenced by the intense redox waves observed in the CV, together with the strong absorbance bands recorded in the UV-vis/NIR spectra, associated with the cation radicals of the closed-ring isomer. Furthermore, the results indicated that the ring-closing process was induced via an

intramolecular electron transfer mechanism, following oxidation of the $Co_2(CO)_4$dppm moieties. A similar process has been reported previously by Brown et al,[15] where an oxidative cyclisation process, of an asymmetric dithienylethene unit, was induced via electron transfer, from an oxidised methoxyphenyl substituent, to the switching unit.

The electrochemical behaviour of the cobalt carbonyl moieties was also studied. Substituting dppm ligands onto the cobalt carbonyl groups was found to influence the oxidation processes of the metal carbonyl units in the CV's. The $Co_2(CO)_6$ groups underwent irreversible oxidation processes at potentials ranging from 1.26 to 1.43 V, whereas the $Co_2(CO)_4$dppm moieties were found to undergo quasireversible processes at less positive potentials than their corresponding cobalt hexacarbonyl compounds (i.e. $E_{1/2}$ values ranging from 0.86 to 0.93 V). Such an event can be assigned to the electron-donating ability of the chelating phosphine ligands, and similar results have been reported in the literature.[25-27,29,30] The UV-vis/NIR spectroelectrochemistry experiments indicated that the metal carbonyl groups underwent some decomposition processes during oxidative processes, which was confirmed by the IR spectroelectrochemistry results. However, some intriguing changes were observed in the IR spectra of the metal carbonyls during the bulk electrolysis experiments. It was found that the redox processes of the ferrocene units shifted the carbonyl bands of the $Co_2(CO)_6$ and $Co_2(CO)_4$dppm complexes to higher wavenumbers. This process was found to be almost fully reversible for the cobalt hexacarbonyl moieties, with ~ 90% of the parent bands recovered. However, the presence of the dppm ligands increased the reversibility of the cobalt tetracarbonyl groups, with ~ 98 % recovery of the original bands in the IR. Furthermore, when potential values associated with the oxidation processes of the $Co_2(CO)_4$dppm moieties were applied, the carbonyl stretches in the IR spectra were shifted again, to even higher frequencies, with subsequent reduction processes recovering ~ 80% of the parent bands.

Overall, the results described here have demonstrated some excellent examples of how incorporating organometallic compounds, onto dithienylethene units, can allow the electrochromic properties of such switches to be tuned. Ferrocene molecules can be employed to control the electrochemical switching of such compounds, at oxidation potentials significantly lower than the high potentials normally required to oxidise the

dithienylethene unit, as shown for **7F**. A similar advantage can also be utilised by incorporating $Co_2(CO)_4$dppm groups onto the system, as shown for **11H**, whereby the presence of the cobalt tetracarbonyl moieties allowed efficient cyclisation processes to occur, at potentials less than 1.0 V. Furthermore, it has been shown how UV-vis/NIR and IR spectroscopic methods can be utilised as non-destructive readout devices for such processes. For example, the oxidative cycloreversion processes of **7F**, induced by oxidation of the ferrocene units, can be monitored by the changes observed in the UV-vis/NIR spectra due to formation of the ferrocenium ions. In the case of **11H**, electrochemical cyclisation, induced by oxidation of the $Co_2(CO)_4$dppm moieties, can be detected by the changes incurred in the IR metal carbonyl bands. Thus, the variety of results observed for all the ferrocenyl-based switches described here shows that there are a number of factors effecting the electrochemical behaviour of these compounds, and so there is much room for further development of such organometallic complexes, with the possibility of great potential towards applications in molecular devices.

6.5 Bibliography

(1) Stepnicka, P.; Trojan, L.; Kubista, J.; Ludvik, J. Internal Ferrocenylalkynes - A Comparative Electrochemical and Mass Spectrometric Study. *J. Organomet. Chem.* **2001**, *637*, 291-299.

(2) Otsuki, J.; Akasaka, T.; Araki, K. Molecular Switches for Electron and Energy Transfer Processes Based on Metal Complexes. *Coord. Chem. Rev.* **2008**, *252*, 32-56.

(3) Duffy, N. W.; Robinson, B. H.; Simpson, J. Synthesis, Structure and Electrochemistry of Ferrocenylethynylsilanes and their Complexes with Dicobalt Octacarbonyl. *J. Organomet. Chem.* **1999**, *573*, 36-46.

(4) Thomas, K. R. J.; Lin, J. T.; Wen, Y. S. Biferrocenes with Heteroaromatic Spacers: Synthesis, Structure, and Electrochemistry. *Organometallics* **2000**, *19*, 1008-1012.

(5) Martinez, R.; Ratera, I.; Tarraga, A.; Molina, P.; Veciana, J. A Simple and Robust Reversible Redox-Fluorescence Molecular Switch Based on a 1,4-Disubstituted Azine with Ferrocene and Pyrene Units. *Chem. Commun.* **2006**, 3809-3811.

(6) Muratsugu, S.; Kume, S.; Nishihara, H. Redox-Assisted Ring Closing Reaction of the Photogenerated Cyclophanediene Form of Bis(ferrocenyl)dimethyldihydro-pyrene with Interferrocene Electronic Communication Switching. *J. Am. Chem. Soc.* **2008**, *130*, 7204-+.

(7) Sun, L.; Tian, H. Dual-Controlled Dithienylmaleimide Switch Containing Ferrocene Units. *Tetrahedron Lett.* **2006**, *47*, 9227-9231.

(8) Guirado, G.; Coudret, C.; Launay, J. Electrochemical Remote Control for Dithienylethene-Ferrocene Switches. *J. Phys. Chem. C* **2007**, *111*, 2770-2776.

(9) Ruiz, J.; Astruc, D. Permethylated Electron-Reservoir Sandwich Complexes as References for the Determination of Redox Potentials. Suggestion of a New Redox Scale. *C. R. Acad. Sci., Ser. IIC: Chim.* **1998**, *1*, 21-27.

(10) Browne, W. R.; de Jong, J. J. D.; Kudernac, T.; Walko, M.; Lucas, L. N.; Uchida, K.; van Esch, J. H.; Feringa, B. L. Oxidative Electrochemical Switching in Dithienylcyclopentenes, Part 1: Effect of Electronic Perturbation on the Efficiency and Direction of Molecular Switching. *Chem. Eur. J.* **2005**, *11*, 6414-6429.

(11) Tsivgoulis, G. M.; Lehn, J. M. Photoswitched and Functionalized Oligothiophenes: Synthesis and Photochemical and Electrochemical Properties. *Chem. Eur. J.* **1996**, *2*, 1399-1406.

(12) Yang, T.; Pu, S.; Fan, C.; Liu, G. Synthesis, Crystal Structure and Optoelectronic Properties of a New Unsymmetrical Photochromic Diarylethene. *Spectrochim. Acta A.* **2008**, *70*, 1065-1072.

(13) Hurenkamp, J. H. Tuning Energy Transfer Between Chromophores: Switchable Molecular Photonic Systems. Ph.D. Thesis, Rijksuniversiteit Groningen, **2008**.

(14) Power, G.; Ritchie, I. Mixed Potentials - Experimental Illustrations of an Important Concept in Practical Electrochemistry. *J. Chem. Educ.* **1983**, *60*, 1022-1026.

(15) Browne, W. R.; de Jong, J. J. D.; Kudernac, T.; Walko, M.; Lucas, L. N.; Uchida, K.; van Esch, J. H.; Feringa, B. L. Oxidative Electrochemical Switching in Dithienylcyclopentenes, Part 2: Effect of Substitution and Asymmetry on the Efficiency and Direction of Molecular Switching and Redox Stability. *Chem. Eur. J.* **2005**, *11*, 6430-6441.

(16) Guirado, G.; Coudret, C.; Hliwa, M.; Launay, J. P. Understanding Electrochromic Processes Initiated by Dithienylcyclopentene Cation-Radicals. *J. Phys. Chem. B.* **2005**, *109*, 17445-17459.

(17) Moriyama, Y.; Matsuda, K.; Tanifuji, N.; Irie, S.; Irie, M. Electrochemical Cyclization/Cycloreversion Reactions of Diarylethenes. *Org. Lett.* **2005**, *7*, 3315-3318.

(18) Peters, A.; Branda, N. R. Electrochromism in Photochromic Dithienylcyclopentenes. *J. Am. Chem. Soc.* **2003**, *125*, 3404-3405.

(19) Das, N.; Arif, A.; Stang, P.; Sieger, M.; Sarkar, B.; Kaim, W.; Fiedler, J. Self-Assembly of Heterobimetallic Neutral Macrocycles Incorporating Ferrocene Spacer Groups: Spectroelectrochemical Analysis of the Double Two-Electron Oxidation of a Molecular Rectangle. *Inorg. Chem.* **2005**, *44*, 5798-5804.

(20) Jakob, A.; Ecorchard, P.; Linseis, M.; Winter, R. F.; Lang, H. Synthesis, Solid State Structure and Spectro-electrochemistry of Ferrocene-ethynyl Phosphine and Phosphine Oxide Transition Metal Complexes RID A-4228-2008. *J. Organomet. Chem.* **2009**, *694*, 655-666.

(21) Lin, Y.; Yuan, J.; Hu, M.; Cheng, J.; Yin, J.; Jin, S.; Liu, S. H. Syntheses and Properties of Binuclear Ruthenium Vinyl Complexes with Dithienylethene Units as Multifunction Switches. *Organometallics* **2009**, *28*, 6402-6409.

(22) Motoyama, K.; Koike, T.; Akita, M. Remarkable Switching Behavior of Bimodally Stimuli-Responsive Photochromic Dithienylethenes with Redox-Active Organometallic Attachments. *Chem. Commun.* **2008**, 5812-5814.

(23) Zhong, Y.; Vila, N.; Henderson, J. C.; Flores-Torres, S.; Abruna, H. D. Dinuclear Transition-Metal Terpyridine Complexes with a Dithienylcyclopentene Bridge Directed Toward Molecular Electronic Applications. *Inorg. Chem.* **2007**, *46*, 10470-10472.

(24) Arewgoda, M.; Rieger, P. H.; Robinson, B. H.; Simpson, J.; Visco, S. J. Paramagnetic Organometallic Molecules .12. Electrochemical Studies of Reactions with Lewis-Bases Following Metal-Metal Bond Cleavage in $R_2C_2Co_2(CO)_6$ Radical Anions. *J. Am. Chem. Soc.* **1982**, *104*, 5633-5640.

(25) Medina, R. M.; Moreno, C.; Marcos, M. L.; Castro, J. A.; Benito, F.; Arnanz, A.; Delgado, S.; Gonzalez-Velasco, J.; Macazaga, M. J. Syntheses, Structures and Electrochemical Study of π-Acetylene Complexes of Cobalt. *Inorg. Chim. Acta* **2004**, *357*, 2069-2080.

(26) Marcos, M. L.; Macazaga, M. J.; Medina, R. M.; Moreno, C.; Castro, J. A.; Gomez, J. L.; Delgado, S.; González-Velasco, J. Alkynyl Cobalt Complexes. An Electrochemical Study. *Inorg. Chim. Acta* **2001**, *312*, 249-255.

(27) Arnanz, A.; Marcos, M.; Moreno, C.; Farrar, D. H.; Lough, A. J.; Yu, J. O.; Delgado, S.; González-Velasco, J. Synthesis, Structures and Comparative Electrochemical Study of 2,5-Bis(trimethylsilylethynyl)thiophene Coordinated Cobalt Carbonyl Units. *J. Organomet. Chem.* **2004**, *689*, 3218-3231.

(28) Osella, D.; Fiedler, J. Reinvestigation of the Electrochemical-Behavior of the $Co_2(CO)_6$(ethynylestradiol) Complex - Evidence of Efficient Recombination of the Electrogenerated Fragments. *Organometallics* **1992**, *11*, 3875-3878.

(29) Macazaga, M. J.; Marcos, M. L.; Moreno, C.; Benito-Lopez, F.; Gomez-González, J.; González-Velasco, J.; Medina, R. M. Syntheses, Structures and Comparative Electrochemical Study of π-Acetylene Complexes of Cobalt. *J. Organomet. Chem.* **2006**, *691*, 138-149.

(30) Arnanz, A.; Marcos, M.; Delgado, S.; González-Velasco, J.; Moreno, C. The Effect of Thiophene Ring Substitution Position on the Properties and Electrochemical Behaviour of Alkyne–dicobaltcarbonylthiophene Complexes. *J. Organomet. Chem.* **2008**, *693*, 3457-3470.

(31) Peters, A.; Branda, N. R. Electrochemically Induced Ring-Closing of Photochromic 1,2-Dithienylcyclopentenes. *Chem. Commun.* **2003**, 954-955.

CHAPTER 7

Overall Conclusion and Future Work

Chapter seven presents a summary of the photochemical and electrochemical results obtained for the thienyl and ferrocenyl-based dithienylcyclopentene switches, and their corresponding $Co_2(CO)_6$ and $Co_2(CO)_4dppm$ complexes.   An emphasis is placed on the effects of the atoms present on the cyclopentene ring (H vs. F) and the substituents attached to the switching unit.   The potential for these switches to be utilised in a number of applications, and the need for future work in this area, is also discussed, with an overall conclusion presented at the end.

7.1 Introduction

The aim of this project was to investigate the photochemical and electrochemical properties of some dithienylethene switches in order to determine the effects of the substituents attached to the thienyl units and the atoms present on the cyclopentene ring (H *vs.* F). Dithienyl-perhydro and –perfluoro cyclopentene switches, appended with 3-ethynylthiophene and phenyl-3-ethynylthiophene substituents, were synthesised, and their cyclisation/cycloreversion processes, fatigue resistance, thermal stability, luminescent and electrochemical properties were examined. The corresponding ethynylferrocene analogues were also synthesised in order to study the effects of the organometallic substituents on the photo- and electrochemical properties of the switching units. Furthermore, novel cobalt carbonyl complexes were synthesised by incorporating $Co_2(CO)_6$ and $Co_2(CO)_4$dppm moieties onto the thienyl and ferrocenyl-based switches. Cobalt carbonyl complexes are photochemically and electrochemically active in their own right. Therefore, the aim was to investigate the effect of the photo- and electrochemical reactions of the cobalt carbonyl moieties on the ring-opening/closing processes of the switching units. The photochemical and electrochemical results were described in detail in chapters 3 and 5 respectively, for the thienyl-based switches, and in chapter 4 and 6 respectively for the ferrocenyl-based switches. In this chapter, a summary of the results observed is discussed, with an emphasis on the differences/similarities between the thienyl and ferrocenyl derivatives. A number of applications, for which the switches presented in this thesis may have potential, and a list of experiments for further research in this area is also discussed, with an overall conclusion provided in the last section.

7.2 Summary of Results

7.2.1 Photochemical Properties

- **Thienyl- and Ferrocenyl-based Free Ligand Switches**
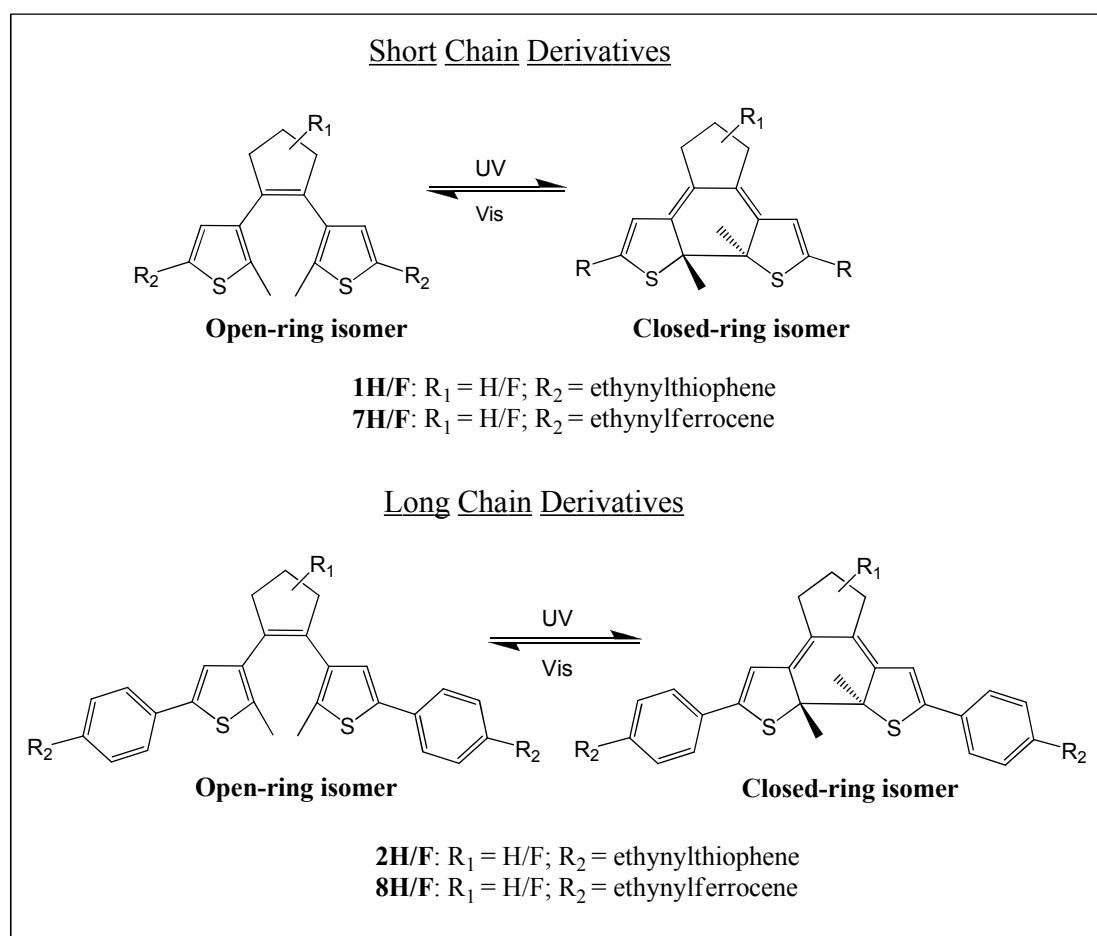
Scheme 7.1: Illustrates the cyclisation/cycloreversion processes between the open and the closed forms of the thienyl and ferrocenyl-based free ligand switches: Short chain derivatives {**1H/F** and **7H/F**} and the long chain derivatives {**2H/F** and **8H/F**} i.e. with phenyl-rings present between the switching unit and alkynyl moieties.

The following photochemical properties of the dithienylcyclopentene switches illustrated in scheme 7.1 have been investigated: Cyclisation/cycloreversion processes; fatigue resistance; thermal stability; and luminescence. The results obtained are summarised in table 7.1. The thienyl and ferrocenyl-based free ligand switches were all found to undergo cyclisation processes to the closed-ring isomers

following irradiation ($\lambda = 313$ nm), as shown in scheme 7.1. In general, the λ_{max} of the absorption band in the visible region of the UV-vis spectrum, associated with the closed form, were found to be bathochromically shifted (table 7.1) when: 1) the hydrogen atoms on the central cyclopentene ring were substituted with fluorine atoms; 2) the π-conjugation of the compounds was extended through the introduction of phenyl-rings between the dithienylethene switches and alkynyl units; 3) substituting ethynylferrocene molecules in-place of the ethynylthiophene units. An exception to this rule was found for the fluorinated ferrocene derivatives, with the λ_{max} of the shorter chain closed-ring compound **7F** ($\lambda_{max} = 641$ nm) red-shifted in comparison to the longer chain analogue **8F** ($\lambda_{max} = 621$ nm). The pronounced changes in the electronic properties of these switches, indicates good electronic communication between the central switching unit and the substituents attached to the thiophene rings on the dithienylethene unit,[1] and can be attributed to the electron-donating ability of the ferrocene moieties. These results are in-keeping with literature reports as bathochromic shifts in the λ_{max} of closed-ring isomers, due to the presence of fluorine atoms on the cyclopentene unit, and electron-donating substituents, have been reported previously by Feringa et al.[1-3]

The irradiation times required to reach the PSS of the closed-ring isomers of the thienyl-based switches appeared to decrease for the fluorinated compounds and the longer chain derivatives, with **2F** reaching the PSS in the shortest time (15 seconds). Such a straight forward trend was not as obvious for the ferrocene analogues (table 7.1), although, the longer-chain fluorinated derivative of the ferrocene switches, **8F**, was also found to undergo cyclisation in the shortest time (8 minutes). However, the efficiency of the ring-closing process was dramatically reduced for the ferrocene switches compared to the thienyl derivatives, with the PSS reached after minutes rather than seconds. Long irradiation times (hours) have been reported in the literature for similar switches appended with iron substituents,[4-6] and can be attributed to quenching of the excited state by the ferrocene units due to energy/electron transfer processes.[7-9]

Table 7.1: Summary of the photochemistry results obtained for the free ligand thienyl {**1H/F** and **2H/F**} and ferrocenyl-based {**7H/F** and **8H/F**} switches.

Cmpd	UV-vis Closed-ring[a]	Cycli-sation[a]	Cyclorev-ersion[a]	Fatigue Resistance[a]	^{1}H NMR[b]	Thermal Stability[c]
	λ_{max} (nm)	Time to reach PSS	Time taken	% degradation (5 cycles)	By-product formation	$t_{1/2}$ @ 60°C
1H	543	50 sec	7 min	10%	1Hx	1155 hr
1F	609	30 sec	1.5 min	4%	-	147 hr
2H	562	20 sec	6 min	1.5%	-	49.5 hr
2F	614	15 sec	3 min	< 1%	-	N/D
7H	548	35 min	4.5 hrs	30%*	7Hx	12 hr
7F	641	30 min	7 min	50%*	7Fx	128 hr
8H	561	40 min	7 min	50%	-	7 hr
8F	621	8 min	3 min	< 1%	-	115 hr

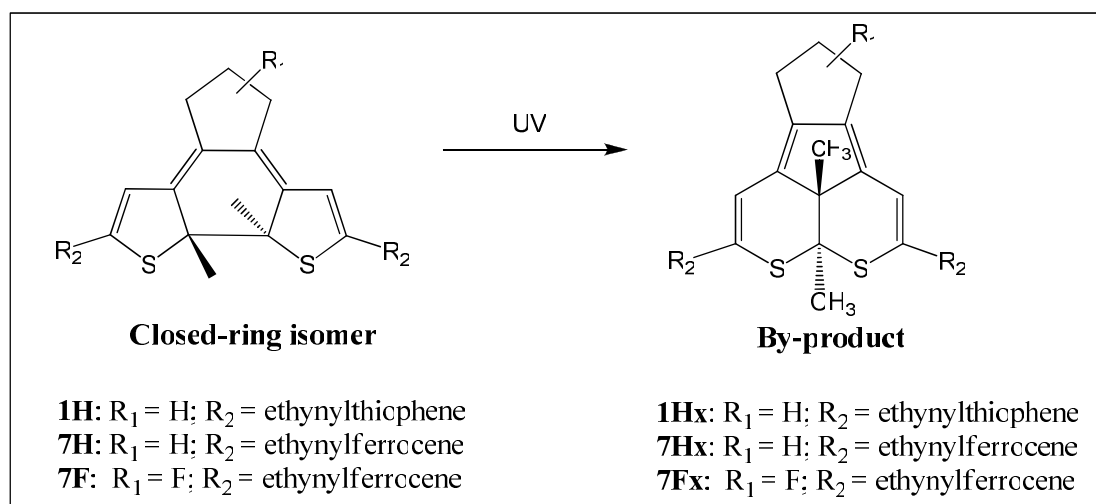[a] data recorded in THF.
[b] data recorded in deuterated acetone.
[c] data recorded in toluene.
* percentage degradation after one colouring/bleaching cycle.
- indicates no by-product formed.
N/D: no degradation

Cycloreversion processes of all the free ligand compounds were found to occur within 1.5 − 7 minutes of visible light irradiation, with the exception of **7H**, which was not found to fully return to the open-ring isomer, even after 4.5 hours of irradiation. This phenomenon can be attributed to the formation of a photostable by-product, denoted as **7Hx**, during UV irradiation processes, which was confirmed from the ^{1}H NMR studies of the cyclisation process. A similar photoproduct has been reported in a number of literature reports,[10-12] and is believed to generate from prolonged UV irradiation of the closed-ring isomer, as shown in scheme 7.2. The ^{1}H NMR spectra of **1H** and **7F** also showed evidence of the generation of a by-product during UV irradiation, denoted as **1Hx** and **7Fx**. No such by-products were observed in the ^{1}H NMR spectra of the other switches, thus indicating that extending the length of the carbon chain can inhibit such a process. Further examination of the ^{1}H NMR spectra revealed that the formation of the by-product occurs more rapidly for **7H**, followed by **7F** and then **1H**. Therefore, it is apparent that the presence of the ethynylferrocene molecules promoted the formation of such a photoproduct.

Closed-ring isomer

By-product

1H: R_1 = H; R_2 = ethynylthiophene
7H: R_1 = H; R_2 = ethynylferrocene
7F: R_1 = F; R_2 = ethynylferrocene

1Hx: R_1 = H; R_2 = ethynylthiophene
7Hx: R_1 = H; R_2 = ethynylferrocene
7Fx: R_1 = F; R_2 = ethynylferrocene

Scheme 7.2: Illustrates the formation of the photochemical by-products **1Hx**, **7Hx** and **7Fx**, following prolonged UV irradiation of the related closed-ring isomers.

The fatigue resistance experiments showed that the extended π-conjugated perfluoro-derivatives **2F** and **8F** were the most stable following five consecutive colouring/bleaching cycles, with < 1% degradation found in both cases. Increased fatigue resistance for perfluorocyclopentene switches, compared to their related H_6 derivatives, has also been reported in the literature.[1,11] However, in general, it was found that the ferrocenyl derivatives had low fatigue resistance compared to their related thiophene switches, with the order of stability found to be: **2F = 8F > 2H > 1F > 1H > 8H > 7F > 7H**. It should be noted that the % degradation was calculated from the decrease at the λ_{max} in the visible region following each cycle, therefore, although the values listed in table 7.1 indicates that **7F** degraded more so than **7H**, the degradation observed for **7H**, following the first cycloreversion process, was taken into account, as discussed in chapter 4.

The thermal stability of the closed-ring isomers were monitored at room temperature and at elevated temperatures (60, 80 and 100°C). All of the free ligand switches were found to be stable in the dark at room temperature, over a period of 10 weeks. However, at elevated temperatures, the absorbance bands in the visible region of the UV-vis spectra, associated with the closed-ring isomers, were found to decrease. The half-life ($t_{1/2}$) values were calculated and the following trend was observed, in order of decreasing stability: **2F > 1H > 1F > 7F > 8F > 2H > 7H > 8H**. In general, this trend

shows that the fluorinated switches were found to be more thermally stable than the perhydro-derivatives, and introducing ferrocene molecules, in place of the thiophene rings, reduced the thermal stability of these compounds. According to the results described in the literature, the presence of fluorine atoms on the cyclopentene ring has been found to increase the thermal stability of such switches.[1,13] However, it has also been observed that the substituents present on the thiophene units of the dithienylcyclopentene switch can have a significant influence on the stability of the closed-ring isomers, at elevated temperatures.[14-16] Thus, the results presented here are in-keeping with the literature reports. However, a mixture of cycloreversion and degradation processes were observed during the thermal stability experiments, for the thienyl and ferrocenyl switches described here, whereas only thermal ring-opening has been reported in the literature.[1,13-15,17,18]

The luminescent studies of the thienyl-based switches revealed that the shorter chain compounds {**1H** and **1F**} were non-emissive, whereas the extended chain derivatives {**2H** and **2F**} were found to fluoresce in their open-form. Cyclisation to the closed-ring form was found to quench the emission of **2H** by 51%, a phenomenon which has been well documented in the literature.[19-24] Conversely, the emission intensity of **2F** was found to marginally increase following cyclisation. A few examples of similar fluorescent behaviour have been reported in the literature.[25-27] The ferrocenyl-based switches were not found to be fluorescent, in the open- or closed-ring forms. This can be assigned to the quenching effects of the ferrocene molecules which can occur via energy/electron transfer processes.[7-9]
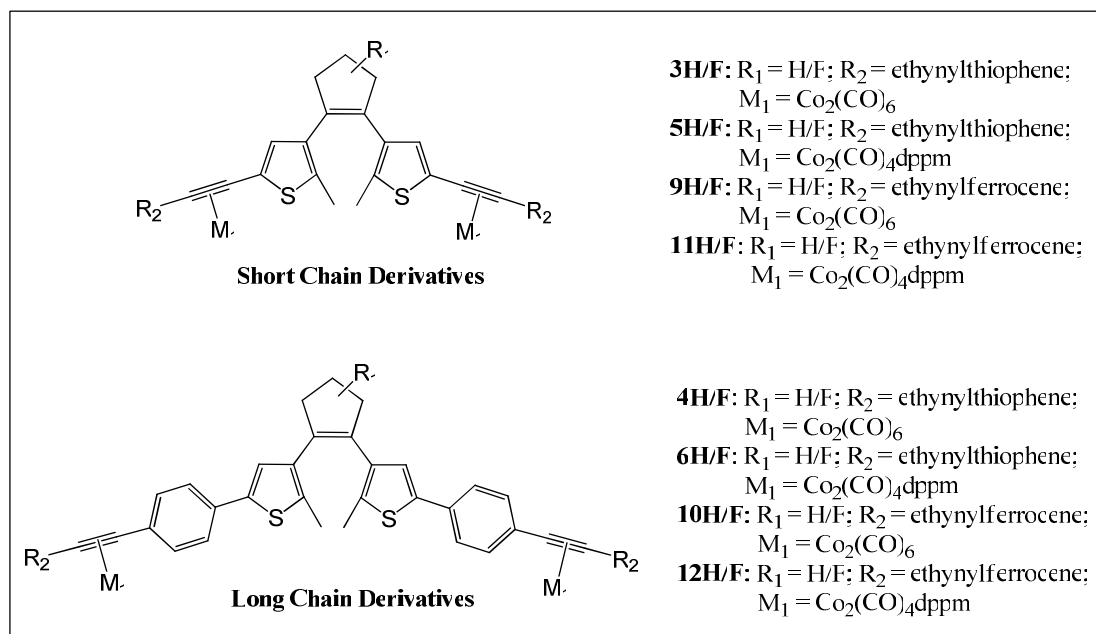
- **Cobalt Carbonyl Complexes**

Figure 7.1: Illustrates the $Co_2(CO)_6$ and $Co_2(CO)_4dppm$ complexes of the short and long chain thienyl and ferrocenyl-based switches.

Incorporating metal carbonyl complexes had considerable effects on the photocyclisation processes of the thiophene and ferrocene dithienylethene switches. Cyclisation processes were completely inhibited for the short chain ferrocenyl-based $Co_2(CO)_6$ complexes {**9H** and **9F**}, at $\lambda_{irr} = 313$ nm, however, some formation of the closed-ring isomers was observed for the thienyl-based analogues {**3H** and **3F**}. In the cases of both the thienyl and ferrocenyl switches, incorporating phenyl-rings between the dithienylethene switches and the alkynyl $Co_2(CO)_6$ units {**4H/F** and **10H/F**} allowed for cyclisation processes to occur, at $\lambda_{irr} = 313$ nm. The irradiation times required to reach the photostationary states of the cobalt carbonyl moieties were significantly increased in comparison to the free ligands, as highlighted in table 7.2. Moreover, the amount of the closed-ring isomer formed appeared to have decreased, as evidenced by the relative intensities of the absorption bands in the visible region of the UV-vis spectra of the $Co_2(CO)_6$ complexes, compared to their related free ligands.

Table 7.2: The λ_{max} observed in the visible region of the UV-vis spectra, and the time-taken to reach the PSS, following UV irradiation (at 313 and 365 nm), in THF, of the free ligand switches {**1H/F**, **2H/F**, **7H/F**, **8H/F**}, and their corresponding $Co_2(CO)_6$ {**3H/F**, **4H/F**, **9H/F**, **10H/F**} and $Co_2(CO)_4dppm$ complexes {**5H/F**, **6H**, **11H/F**, **12H/F**}.

Free Switches			$Co_2(CO)_6$ Complexes						$Co_2(CO)_4dppm$ Complexes				
	λ_{irr}=313nm				λ_{irr}=313nm		λ_{irr}=365nm				λ_{irr}=313nm		λ_{irr}=365nm
	λ_{max} (nm)	Time			λ_{max} (nm)	Time	λ_{max} (nm)	Time			λ_{max} (nm)	Time	λ_{max} (nm)	Time
1H	543	50s	**3H**		559	8m	-	-	**5H**		-	-	-	-
1F	609	20s	**3F** **3bF**		603 *661*	4m	-	-	**5F**		-	-	-	-
2H	562	30s	**4H** **4bH**		561 *584*	8m	561	9m	**6H**		563	25m	563	35m
2F	614	15s	**4F**		619	2m	619	2.5m						
7H	548	35m	**9H**		-	-	-	-	**11H**		-	-	-	-
7F	641	30m	**9F**		-	-	-	-	**11F**		-	-	-	-
8H	561	40m	**10H**		555	45m	555	55m	**12H**		552	100m	552	130m
8F	621	8m	**10F** **10bF**		621 *631*	16m	626	28m	**12F**		609	20m	626	45m

1) (-) indicates no cyclisation occurred.
2) Time in seconds (s) or minutes (m).
3) λ_{max} of **3bF**, **4bH** and **10bF** are presented in italics to indicate that these closed-ring isomers were synthesised, therefore the λ_{max} values presented were not due to irradiation at 313 nm.

Cycloreversion processes occurred for these compounds, following irradiation with visible light, however, the absorbance bands in the UV region were not found to reform completely. Thus, it was determined that during the photocyclisation processes, some decomposition of the cobalt carbonyl moieties occurred. IR studies confirmed this, as irradiation of the $Co_2(CO)_6$ complexes, in THF, resulted in a decrease in the carbonyl IR stretches. Steady-state photolysis experiments were carried out, in the presence of PPh_3, which resulted in the appearance of new IR bands at lower wavenumbers. Such a result is indicative of CO loss processes, followed by substitution reactions with PPh_3, forming a number of new photoproducts. Therefore, it is feasible that during the cyclisation processes of the $Co_2(CO)_6$ complexes, the dissociation of CO molecules occurs, followed by cleavage of the metal carbonyl moieties from the switching unit. Thus, it is possible that the solution of the cobalt carbonyl complexes at the PSS, contains the closed-ring isomer of both the free ligand

and of the $Co_2(CO)_6$ complex. In an attempt to further elucidate this result, the closed-ring $Co_2(CO)_6$ complexes **3bF**, **4bH** and **10bF** were synthesised. A comparison of the λ_{max} recorded for these closed-ring complexes, to the λ_{max} of the absorbance bands in the visible region for the free ligands, and the open-ring $Co_2(CO)_6$ complexes following UV irradiation (as presented in table 7.2), seems to support this hypothesis. Furthermore, subsequent cycloreversion processes of these cobalt carbonyl complexes were found to be more reversible for the perfluorinated switches **3F**, **4F** and **10F**, particularly in the case of the longer chain derivatives **4F** and **10F**, as the absorbance bands in the UV region of the UV-vis spectra appeared to increase back towards the initial values recorded, at the start of the experiments, to a greater extent then their corresponding perhydro analogues. Other metal carbonyl switching complexes have been reported in the literature.[5,6,26,28,29] In general it was found that the efficiency of the photocyclisation/cycloreversion processes could be tuned by incorporating different metal centres and phosphine ligands onto the metal complexes, and only one group reported evidence of decomposition of the metal carbonyl complex during the photocyclisation processes.[28]

In an attempt to stabilise the $Co_2(CO)_6$ complexes, dppm ligands were introduced onto the metal centres, producing the corresponding $Co_2(CO)_4$dppm complexes. However, in the case of the shorter chain dppm derivatives {**5H/F** and **11H/F**}, cyclisation processes were completely inhibited, at $\lambda_{irr} = 313$ nm. Conversely, ring-closing processes were observed for the extended chain analogues {**6H** and **12H/F**} at $\lambda_{irr} = 313$ nm, however, even longer irradiation times were required to reach the PSS, and the results suggested that there was a further decrease in the amount of the closed-ring isomers produced, compared to their $Co_2(CO)_6$ complexes and free ligand counterparts. Although steady-state photolysis IR studies showed that the dissociation of CO appeared to occur at a slower rate for the $Co_2(CO)_4$dppm complexes, in comparison to their $Co_2(CO)_6$ analogues, the reversibility of the cyclisation process, following ring-opening with visible light, was found to be reduced for the dppm derivatives, compared to the hexacarbonyl complexes, as evidenced by a larger decrease in the UV region of the absorbance spectra.

Furthermore, the solutions of the cobalt carbonyl moieties were irradiated at a lower energy wavelength ($\lambda = 365$ nm), in an attempt to improve the reversibility of the

photochemical processes of these metal complexes. The IR experiments showed that CO-loss processes were less efficient at 365 nm, compared to the experiments carried out at 313 nm. The UV-vis studies showed that no cyclisation processes occurred for the shorter chain derivatives at this wavelength. In the case of the longer chain analogues (with the exception of **10F** and **12F**) similar results were obtained as observed following irradiation at 313 nm, however, longer irradiation times were required to reach the photostationary state, and in the case of the $Co_2(CO)_4dppm$ analogues it appeared that the absorbance bands in the UV region did not decrease as much when irradiated at 365 nm. In the case of the $Co_2(CO)_6$ and $Co_2(CO)_4dppm$ complexes, of the phenyl-ethynylferrocene fluorinated switch, **10F** and **12F**, it appeared that conversion from the open to the closed form increased following irradiation at 365 nm, compared to 313 nm, as evidenced by the increase in the intensity of the absorbance band in the visible region of the UV-vis spectrum, associated with the closed-ring isomer.

The cobalt carbonyl complexes of the thienyl and ferrocenyl switches were all found to be non-fluorescent. However, following cyclisation of the $Co_2(CO)_6$ complex **4H**, the emission intensity was found to increase, with a further increase observed following irradiation with visible light. This result indicates that some cleavage of the $Co_2(CO)_6$ moieties occurred during UV irradiation, and the emission observed was in fact due to fluorescence of the free ligand switch **2H**. Irradiation of the corresponding $Co_2(CO)_4dppm$ complex **6H** did not induce emission, thus suggesting that cleavage of the tetracarbonyl moieties did not occur during such UV irradiation processes, which can be attributed to the stabilising effect of the dppm group. Furthermore, irradiation of the related $Co_2(CO)_6$ perflouro analogue **4F**, did not induce fluorescence, thus confirming that irradiation at 313 nm did not result in cleavage of the $Co_2(CO)_6$ moieties from the switching unit. This supports the theory that the fluorinated cobalt carbonyl switches are more stable towards irradiation at 313 nm, than their related perhydro derivatives.

The cycloreversion processes of the synthesised closed-ring $Co_2(CO)_6$ complexes **3bF**, **4bH** and **10bF** were investigated in order to determine the effects of the cobalt carbonyl moieties on the ring-opening cycle. Indeed, cycloreversion from the closed to the open form was observed for **3bF**, **4bH** and **10bF**, following irradiation with

visible light (λ > 650 nm) after 70 min, 240 min and 15 min respectively. It is clear that the efficiencies of the ring-opening processes varied greatly, and were much slower in comparison to their related free ligands **1F**, **2H** and **8F** respectively. The results suggest that the presence of the fluorine atoms on the cyclopentene-ring, and the ethynylferrocene substituents, increase the efficiency of this process, however further studies of the other $Co_2(CO)_6$ complexes would be required to conclusively determine the substituent effects on the cycloreversion process. Interestingly, the results indicated that the $Co_2(CO)_6$ moieties were also photochemically active at this low energy wavelength, due to the changes observed in the UV region of the UV-vis spectra. **3bF** was found to be the most stable during these irradiation processes, whereas **10bF** appeared to be the least stable, with evidence of some of the open-ring free ligand switch present at the end of the experiment, suggesting cleavage of the $Co_2(CO)_6$ moieties occurred at λ_{irr} > 650 nm. The stability of **4bH** was found to be somewhere in the middle of **3bF** and **10bF**. Steady-state photolysis of **4bH**, in the presence of PPh_3, resulted in CO loss reactions at λ_{irr} > 650 nm, with the appearance of new IR bands at lower wavenumbers, associated with PPh_3 substituted photoproducts. Therefore, it is clear that the closed-ring $Co_2(CO)_6$ complexes can undergo cycloreversion in-conjunction with CO dissociation processes, and the efficiency of these photochemical processes can be tuned by altering the substituents present on the dithienylethene switch. Furthermore, fluorescent studies showed that the emission intensity of **4bH** increased during cycloreversion processes, thereby providing a second method for observing the photochemical reactions of the switch and the cobalt carbonyl moieties.

7.2.2 Electrochemical Properties

The electrochromic properties of the thienyl and ferrocenyl-based free ligand switches, and cobalt carbonyl complexes, were investigated to determine the factors influencing the direction of the electrochemically-induced switching process (i.e. cyclisation/cycloreversion). Furthermore, the electrochemical behaviour of the $Co_2(CO)_6$ and $Co_2(CO)_4dppm$ moieties in the CV's were examined, and the effect of the oxidation processes on these cobalt carbonyl complexes was studied using IR spectroelectrochemistry techniques.

- **Electrochromic Properties**

Electrochemically induced cyclisation and cycloreversion processes of the thienyl and ferrocenyl-based dithienylethene switches were investigated by cyclic voltammetry and UV-vis spectroelectrochemistry techniques, and the results are summarised in table 7.3. According to literature reports, the presence of electron-withdrawing fluorine atoms on the central cyclopentene unit stabilise the oxidised open-ring form, thus oxidative cycloreversion processes are likely to occur for dithienyl-perfluoro-cyclopentene switches.[2,3,30] In-keeping with the results observed in the literature, oxidative ring-opening was observed for the closed-ring short chain perfluorinated switches, **1F** and **7F**, described here. In the case of **7F**, there was some evidence to suggest that the cycloreversion process was induced following oxidation of the ferrocene molecules. Incorporating $Co_2(CO)_6$ and $Co_2(CO)_4dppm$ moieties onto the open-ring isomers of these switches did not alter their electrochemical properties, as oxidative cyclisation process were not observed for the cobalt carbonyl derivatives. Although, the presence of $Co_2(CO)_6$ complexes on the closed form of **1F** (i.e. **3bF**) appeared to increase the reversibility of the oxidation process of the switch, and thus slow down the ring-opening reaction.

Extending the π-conjugation of the perfluorinated switches had significant effects on the electrochemical properties of **2F** and **8F**, as oxidative cyclisation processes were observed for both compounds. However, the cationic species of the closed forms were quite unstable in both cases, as observed from the UV-vis spectroelectrochemistry experiments. Incorporating cobalt carbonyl complexes onto

these switches was found to inhibit the cyclisation processes. In the case of the thienyl-based $Co_2(CO)_6$ complex, **4F**, there was no evidence of electrochemical ring-closing in the CV. New redox waves were observed in the cyclic voltammograms obtained for the ethynylferrocene $Co_2(CO)_6$ {**10F**} and $Co_2(CO)_4$dppm {**12F**} complexes, following oxidation of the switching unit, which may possibly be due to the formation of the closed-ring cations. However, the intensities of these new oxidation/reduction peaks were too weak to determine if they were a consequence of ring-closing or not. Furthermore, the formation of the closed-ring cations of these complexes were not observed in the absorption spectra during bulk electrolysis experiments.

Table 7.3: Indicates whether oxidative cyclisation (close) or oxidative cycloreversion (open) processes were observed for the open and closed-ring isomers of the thienyl and ferrocenyl free ligand switches[a]. Also, if oxidative cyclisation (close) was observed for the open-ring isomers [b] of the corresponding $Co_2(CO)_6$ and $Co_2(CO)_4$dppm complexes.

Oxidative Ring-Opening/Closing Processes					
Free Ligands[a]		$Co_2(CO)_6$ Complexes[b]		$Co_2(CO)_4$dppm Complexes[b]	
1H	Close	**3H**	Close*	**5H**	Close*
2H	Close	**4H**	Close	**6H**	Close
7H	Close	**9H**	Close (?)[c]	**11H**	Close*
8H	Close	**10H**	Close	**12H**	Close (?)[c]
1F	Open	**3F**	-	**5F**	-
2F	Close	**4F**	-		
7F	Open*	**9F**	-	**11F**	-
8F	Close	**10F**	Close (?)[c]	**12F**	Close (?)[c]

(Row labels: **Perhydro-Derivatives** for 1H–10H/12H block; **Perfluoro-Derivatives** for 1F–12F block)

- indicates that oxidative cyclisation did not occur for these open-ring isomers.
* indicates that electrochromic processes induced via an electron transfer mechanism, and not from oxidation of the switching unit.
(?)[c] The results showed some signs of oxidative cyclisation although the results were not conclusive, and further experiments are needed to confirm this.

The presence of electron-donating hydrogen atoms on the cyclopentene ring have been found to stabilise the closed-ring cations, and thus promote electrochemical cyclisation processes.[2,3,30] In the case of the perhydro-derivatives described here, oxidative cyclisation processes were observed for the long chain free ligand switches, **2H** and **8H**. Their corresponding $Co_2(CO)_6$ complexes, **4H** and **10H**, were also found

to undergo oxidative ring-closure, although the stability of the closed-ring cations produced for the ferrocene hexacarbonyl complex {**10H**} was found to be less stable compared to its free ligand derivative **8H**. Furthermore, the results obtained for the related $Co_2(CO)_4$dppm complexes, **6H** and **12H**, showed some evidence of oxidative cyclisation. However, this is not a conclusive result for **12H** as the CV results were difficult to interpret due to the presence of the redox waves associated with the ferrocene and $Co_2(CO)_4$dppm moieties, which obscured the view of the new oxidation/reduction peaks, tentatively assigned to the cationic species of the closed-ring isomer. On the other hand, the results for **6H** were easier to interpret, as the CV was not dominated by a ferrocene redox wave, and the changes observed in the UV-vis/NIR spectra during bulk electrolysis experiments, confirmed the occurrence of an electrochemical ring-closing process for **6H**. However, the stabilities of the ring-closed cations were reduced in comparison to the corresponding $Co_2(CO)_6$ complex {**4H**} and free ligand {**2H**}.

Oxidation processes of the short chain perhydro switches, **1H** and **7H**, resulted in cyclisation to the closed-ring forms. However, the cationic species of the closed-ring isomers were found to be more stable for **1H**, in comparison to its ferrocene-derivative **7H**, as evidenced by the UV-vis spectroelectrochemistry results. This is most likely due to the effect of the electron-withdrawing ferrocenium ions on **7H**. In the case of the related $Co_2(CO)_6$ complexes, **3H** and **9H**, there was evidence of oxidative ring-closure in the CV's of both, but in the absorbance spectra of **3H** only. Furthermore, there was some evidence in the CV of **3H** to suggest that the ring-closing process was possibly induced following oxidation of the $Co_2(CO)_6$ moieties. Oxidative cyclisation was also observed for the $Co_2(CO)_4$dppm complexes of both the thiophene {**5H**} and ferrocene {**11H**} switches. The presence of the dppm ligands, on the cobalt centres, appeared to stabilise the closed-ring cations in both cases, compared to their $Co_2(CO)_6$ complexes. Furthermore, there was strong evidence that the cyclisation process was induced following oxidation of the $Co_2(CO)_4$dppm moieties, particularly in the case of the ferrocene derivative **11H**. It is probable that an intramolecular electron transfer process took place, from the oxidised cobalt carbonyl groups, to the switching unit, as such a process was observed previously by Browne at al,[3] involving a methoxyphenyl group.

- **Electrochemical Behaviour of the Cobalt Carbonyl Moieties**

The reduction processes of the $Co_2(CO)_6$ complexes resulted in irreversible reduction processes of the cobalt carbonyl moieties, followed by some decomposition of the radical anions in all cases. Similar results have been reported in the literature.[31-35] The potential values at which the reduction processes occurred were influenced by substituents attached to the alkynyl units and the atoms present on the cyclopentene ring. Overall, it was found that the short chain perfluorinated switches were reduced at the least negative potential values, and the short chain perhydro derivatives underwent reduction at the most negative potentials. Reduction of the longer chain analogues occurred at potential values in between those of the short chain perfluoro and perhydro switches, as the presence phenyl-ring spacer units reduced the effect of the cyclopentene ring atoms (H *vs.* F), on the $Co_2(CO)_6$ moieties. In all cases a single reduction peak was observed, indicating that little electronic communication existed between the two metal centres on either side of the switch. Substituting the thiophene rings with ferrocene molecules was not found to affect the reductive behaviour of the metal carbonyl complexes, with the exception of **10H**. Reduction of **10H** resulted in two reduction peaks. This could possibly be an indication of electronic communication existing between the two $Co_2(CO)_6$ moieties, separated by the dithienylethene bridging unit.[34,36] This result can be attributed to the influence of the ferrocene groups, as only a single irreversible reduction peak was observed for the corresponding thiophene derivative, **4H**.

The extended π-conjugation in the closed-ring isomer was found to increase the electronic communication between the $Co_2(CO)_6$ moieties[34,36] for the short chain switch **3bF**, with two separate reduction peaks observed, in contrast to the single reduction peak recorded for the open-ring isomer **3F**. Similar results have been recorded in the literature for closed-ring dithienylethene switches appended with metal carbonyl and phosphine ligand complexes.[5,6,28] However, extending the π-conjugation of the longer chain $Co_2(CO)_6$ perhydro switch, **4H**, was not found to increase the electronic interaction between the two metal centres, as only one irreversible reduction peak was observed in the CV of the closed-form **4bH**.

Incorporating chelating phosphine ligands onto the cobalt carbonyl moieties, producing the corresponding $Co_2(CO)_4dppm$ complexes, was found to shift the reduction processes to more negative potentials and the oxidation processes to less

positive potentials, compared to the hexacarbonyl moieties, due to the electron-donating effect of the dppm ligands. Furthermore, the extra electron-density on the Co-Co core stabilises the metal carbonyl and facilitates reversible oxidation processes. Thus, irreversible oxidation processes were observed for the $Co_2(CO)_6$ moieties, whereas quasi-reversible waves, at less positive potentials, were observed for the dppm derivatives. These results are in agreement with the results reported in the literature for other cobalt carbonyl complexes substituted with phosphine ligands.[32-34,37,38] Furthermore, in the case of the short chain thiophene derivatives, **5H** and **5F**, two monoelectronic redox waves were observed in the CV, indicating that the $Co_2(CO)_4$dppm moieties on either side of the switch were interacting electronically.[32,34,37] On the other hand, only single redox waves were observed for the longer chain analogue **6H**, and for all the ferrocene tetracarbonyl complexes.

IR spectroelectrochemistry experiments showed that the oxidation processes of the cobalt carbonyl switching complexes had significant effects on the carbonyl stretches in the IR spectra. Oxidation of the ferrocene units was found to shift the carbonyl IR bands to higher wavenumbers. This was attributed to the effect of the electron-withdrawing ferrocenium ions, removing electron density from the cobalt carbonyl centres. When potentials were applied, corresponding to the oxidation process of the $Co_2(CO)_6$ moieties, for both the thienyl and ferrocenyl-based complexes, the carbonyl bands were found to decrease, with no new bands appearing in the IR. Conversely, oxidation of the $Co_2(CO)_4$dppm moieties resulted in a shift in the carbonyl IR bands to higher wavenumbers, for both the thienyl and ferrocenyl-based derivatives. Furthermore, the reversible oxidation processes of the closed-ring $Co_2(CO)_6$ switch **4bH**, was also found to induce changes in the carbonyl IR peaks. Oxidation to the monocation and dication species of the closed-ring switch, at potentials less than 1.0 V, was found to shift the carbonyl IR bands to higher wavenumbers. Therefore, the results described here demonstrate how the oxidation processes of the cobalt carbonyl switches can be monitored by changes in the carbonyl vibrational stretches in the IR spectra. However, some decomposition of the cobalt carbonyl moieties was observed during these oxidation processes. Although, the IR results showed that the oxidation processes of the $Co_2(CO)_4$dppm moieties were more reversible than the $Co_2(CO)_6$ units. Thus, the presence of the dppm ligands helps to stabilise the cobalt carbonyl groups, which is consistent with the results observed in the CV.

7.3 Applications

The photochemical and electrochemical behaviour of the thienyl and ferrocenyl based-switches described here, and their cobalt carbonyl derivatives, have shown promising features which may be utilised towards the development of a number of applications:

1) Write-Read-Erase Memory Devices

A number of the free ligand dithienylethene switches, described in this report, have demonstrated photochemical and electrochemical properties suitable for the development of write-read-erase memory devices.[10,39,40] Cyclisation processes can be induced either photochemically or electrochemically (write), followed by cycloreversion back to the open form by photo- or electro-chemical means (erase). The information may be read-out in a non-destructive manner, by monitoring the first reversible oxidation process of the closed-form, at a potential where the open-form is electrochemically inert.[41] Fluorescence discrimination between the open and closed forms is a common non-destructive read-out method described for such switches.[20,21,42] However, the majority of the switches reported here were found to be non-emissive, with the exception of **2H** and **2F**, in which case the excitation wavelengths used to induce fluorescence was found to influence the ratio of the two isomers i.e. resulted in ring-closing in each case. Furthermore, the emission intensity of **2F** was not found to change much between the open and closed forms. Therefore, the fluorescent properties of **2H** and **2F** were not found to be useful in terms of a non-destructive read-out method. The advantage of amalgamating cobalt carbonyl moieties and dithienylethene switches into the same system is the potential to use the pronounced infra-red spectral changes of the carbonyl stretches, incurred during oxidation processes, as a non-destructive readout signal in the development of such read-write-erase systems. Although, fatigue resistance and thermal stability are very important properties for the development of memory devices, therefore, in order to utilise the cobalt carbonyl complexes for such applications, further research would be required to improve their stability.

2) Molecular Wires

Organometallic complexes, separated by a dithienylethene switch as a bridging unit, can be used as molecular wires due to the ability of the two metal centres to communicate electronically through the bridging group.[6,28,43] Switching between the open and closed-ring forms, can switch the molecular wires between the "ON" (closed-form) and "OFF" (open-form) states. The electrochemical properties of the cobalt carbonyl complexes presented here have shown some potential towards the development of such molecular wires, eg. the open and closed forms of **3F**. However, there are some limitations to the use of such organometallic switches as molecular wires, due to some decomposition of the cobalt carbonyl moieties following photo- and electro-chemical processes. However, the results have shown that the stability of the cobalt carbonyl complexes, towards photo and electro-chemical processes, can be manipulated by altering the substituents attached to the dithienylethene switch i.e. by substituting fluorine atoms in place of hydrogen atoms on the cyclopentene ring, and incorporating dppm ligands onto the cobalt carbonyl moieties.

3) Carbon-Monoxide Releasing Molecules (CORMs)

The potential use of carbon monoxide in therapeutic applications has been established.[44-47] Carbon monoxide releasing molecules (CORMs) have been identified as viable sources of CO, in which CO can be released in a controllable and tuneable rate, at specific sites, and a number of literature reports have investigated the use of transition metal carbonyl complexes for the development of CORMs.[48-51] The results obtained for the closed-ring isomers of the $Co_2(CO)_6$ complexes described in this report (**3bF**, **4bH** and **10bF**) have shown potential towards the development of CORMs. Photolysing these complexes with low energy visible light ($\lambda > 650$ nm), was found to result in CO loss reactions, as evidenced by the steady-state IR studies, along with cycloreversion processes, back to the open-form. The photochemical reactivity of the cobalt carbonyl moieties varied for each switching complex, as **3bF** was found to be the most stable whereas some cleavage of the metal carbonyl units was evident for **10bF**. Thus, it is possible that the rate of CO loss could be controlled by the substituents attached to the switching unit. Furthermore, dithienylethene switches are known to show fluorescence discrimination between the open and closed

forms.[20,23,25-27,52]   Thus, irradiating the closed-ring isomers at 650 nm could induce CO loss, along with a cycloreversion process back to the open form, thereby inducing or quenching the fluorescence of the switch.   Further research into similar $Co_2(CO)_6$ switches, with highly fluorescent substituents attached, could lead to the development of CORMs for therapeutic purposes, with a controlled rate of CO release monitored via fluorescent changes of the switching unit i.e. the dithienylethene unit may act as a fluorescent probe.
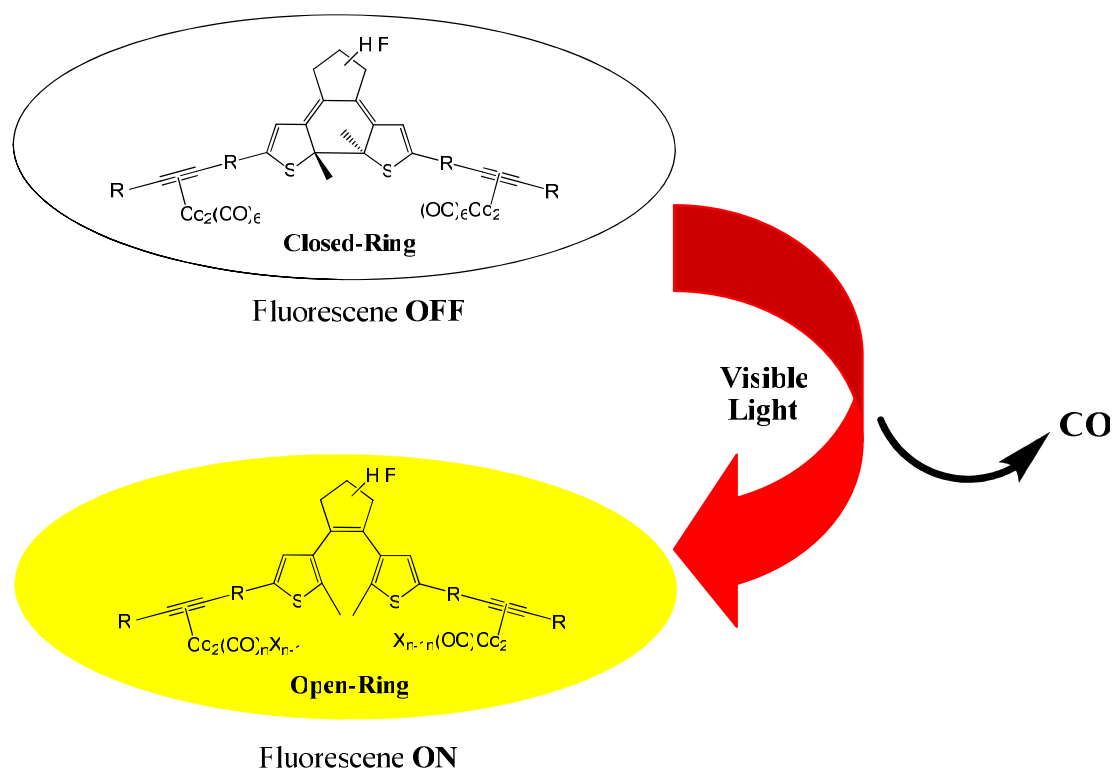
Scheme 7.3: A representation of how a cobalt carbonyl dithienylethene complex may be utilised as a carbon monoxide releasing molecule, whilst monitoring the release of CO by the change in the fluorescence properties of the switching unit, following irradiation at $\lambda = 650$ nm. "X" represents a substituent which takes the place of a CO molecule, following CO release.

7.4 Future Work

In order to advance our understanding of the photochemical and electrochemical properties of the dithienylethene switches, and their cobalt carbonyl complexes, reported in this thesis, there are a number of experiments that could be completed:

- **Synthesis**

1) Synthesise and fully characterise the closed-ring isomers of the $Co_2(CO)_6$ and $Co_2(CO)_4$dppm complexes of all the thienyl and ferrocenyl-based switches, as already described for **3bF**, **4bH** and **10bF**.

- **Photochemistry**

2) Record the absorbance spectra of the "synthesised" closed-ring cobalt carbonyl complexes, and compare the λ_{max} values in the visible region with those recorded for the open-ring cobalt carbonyl complexes following UV irradiation.

3) Investigate the cycloreversion processes of the closed-ring cobalt carbonyl complexes in order to determine the substituent effects on the efficiency of the ring-opening process.

4) Perform theoretical calculations for the cobalt carbonyl complexes, in order to determine the relative energy levels of the intraligand and MLCT singlet and triplet states, in an attempt to elucidate the mechanisms involved in the ring-closing process of these metal complexes.

5) Perform the photochemical studies of the cobalt carbonyl complexes in different solvents in order to examine the effects of different solvents on the photochemical activity of the switching unit and the cobalt carbonyl moieties.

6) Investigate if the ferrocene-based switches will fluoresce when the emission studies are performed at low temperature.

- **Electrochemistry**

7) Perform the cyclic voltammetry experiments of the dithienylethene switches, and their $Co_2(CO)_6$ and $Co_2(CO)_4dppm$ complexes, at various scan rates, different solvents and lower temperatures, as it has been shown in the literature that varying the conditions of these experiments can increase the reversibility the oxidation/reduction processes.[31,32,34,35,37]

8) Investigate the oxidation processes of the closed-ring cobalt carbonyl complexes, by CV and UV-vis/NIR spectroelectrochemistry, in order to help elucidate the electrochromic properties of the open-ring cobalt carbonyl complexes.

9) Investigate the oxidation/reduction processes of the closed-ring cobalt carbonyl complexes, by cyclic voltammetry, to examine the extent of electronic communication between the two metal centres across the π-conjugated backbone of the dithienylethene bridging unit.

10) Examine the effect on the emission properties of the ferrocenyl-based switches, following oxidation of the ferrocene molecules.

7.5 Overall Conclusion

Overall, it was determined that the photochemical properties of these dithienylcyclopentene switches, in relation to their cyclisation/cycloreversion processes, fatigue resistance and thermal stability, can be improved by substituting fluorine atoms in place of hydrogen atoms on the central cyclopentene unit, and increasing the π-conjugation of the system, through the presence of phenyl-rings between the switching unit and alkynyl moieties, as evidenced for **2F** and **8F**. Furthermore, replacing the ferrocene substituents on **8F**, with thiophene substituents, significantly improved the photochemical properties of these switches. Therefore, **2F** was found to be the most suitable candidate for the development of memory devices. Incorporating $Co_2(CO)_6$ and $Co_2(CO)_4$dppm moieties onto the switches resulted in a decrease in the efficiency of the cyclisation and cycloreversion processes, with complete inhibition of the ring-closing process in some cases, and decomposition of the cobalt carbonyl moieties. However, the ability to tune the properties of the cobalt carbonyl complexes was highlighted, as once again it was found that fluorinated cyclopentene rings, and the presence of phenyl-ring spacer groups, improved the efficiency and reversibility of the photochromic processes, with the most promising results obtained for the $Co_2(CO)_6$ complexes **4F** and **10F**.

In terms of the electrochromic switching behaviour of the dithienylethene switches, it has been established that the direction of the switching process (i.e. cyclisation/cycloreversion) is heavily influenced by the atoms present on the cyclopentene ring (H *vs.* F) and the substituents attached to thienyl rings of the dithienylethene unit. This can be attributed to their ability to stabilise the cation species of either the open-ring or closed-ring forms. The presence of the fluorine atoms on the central cyclopentene unit have been found to promote oxidative cycloreversion processes, due to their electron-withdrawing nature (as described for **1F** and **7F**). On the other hand, the electron-donating ability of the hexahydro-cyclopentene ring has been found to be the driving force for oxidative cyclisation processes to occur (as described for **1H**, **2H**, **7H** and **8H**). With regards to the substituents attached to dithienylethene units, a number of factors have been found to

affect the efficiency or direction of the electrochemical switching processes. The stability of the closed-ring cation species were found to be increased by: 1) the presence of the electron-rich phenyl-ring substituents, which allowed oxidative cyclisation to occur for the fluorinated switches (**2F** and **8F**), and increased the stability of the closed-ring cations for the perhydro derivatives (**2H** and **8H**), in comparison to the shorter chain analogues (**1H** and **7H**); 2) the presence of the $Co_2(CO)_4dppm$ moieties increased the stability of the closed-ring isomer of **11H**, in comparison to its corresponding $Co_2(CO)_6$ complex and free ligand, and **5H** in comparison to its hexacarbonyl derivative **3H**. Other factors have been established which appeared to reduce the stability of the closed-ring cation species: 1) the presence of the ferrocene molecules (eg. for **7H** and **8H**), as they undergo oxidation, forming the electron-withdrawing ferrocenium ions, before oxidation of the switching unit occurs; 2) the presence of the $Co_2(CO)_6$ moieties reduced the stability of the closed-ring cations eg. for **3H**, **7H**, **10H** and **10F**, and inhibited cyclisation for **4F**; 3) the presence of the $Co_2(CO)_4dppm$ moieties were found to reduce the stability of the closed-ring cations for the longer chain compounds eg. for **6H**, **12H** and **12F**. Furthermore, the ability to utilise the substituents attached to the dithienylethene unit, as a "remote control" to induce ring-opening/closing processes, at lower potentials than that required to oxidise the switching units, has been established. From the results described here, it appeared that oxidation of the ferrocene molecules on **7Fc** induced a cycloreversion process, and oxidation of the $Co_2(CO)_4dppm$ moieties on **11H** and **5H** resulted in ring-closing. This phenomenon is tentatively attributed to an intramolecular electron transfer mechanism, from the oxidised substituents, to the dithienylethene unit.

Overall, the factors influencing the photochromic and electrochromic switching properties of the thienyl and ferrocenyl-based dithienylethene switches have been described here in detail. The ability to tune these properties by altering the atoms present on the cyclopentene ring, the substituents attached to the dithienylethene unit, and the introduction of organometallic compounds onto the switch has been highlighted. Incorporating cobalt carbonyl moieties onto the switches was found to have a considerable effect on these properties. The effects were not necessarily found to be advantageous, in relation to the photochemical cyclisation processes of the switching unit, due to the tendency of the cobalt carbonyl moieties to undergo

decomposition following UV irradiation. However, the presence of the cobalt carbonyl units was found to increase the efficiency and alter the direction of the electrochromic switching processes, in some cases. Furthermore, the ability to increase the stability of these complexes, by altering the substituents attached to the switching unit and on the metal centre, has been demonstrated here. Also, literature reports have shown that varying the conditions of the photo- and electro-chemical experiments can increase the stability of such metal complexes.[31,32,34,35,37,53,54] Hence, further investigations could improve the stability of such cobalt carbonyl switches, and thus increase their suitability towards the development of future applications, such as those mentioned in the previous section. Therefore, in conclusion, this thesis has presented a comprehensive study on novel cobalt carbonyl dithienylethene switches which has led to some very interesting results, and further research into this area has exciting prospects for the future!

7.6 Bibliography

(1) de Jong, J. J. D.; Lucas, L. N.; Hania, R.; Pugzlys, A.; Kellogg, R. M.; Feringa, B. L.; Duppen, K.; van Esch, J. H. Photochromic Properties of Perhydro- and Perfluorodithienylcyclopentene Molecular Switches. *Eur. J. Org. Chem.* **2003**, 1887-1893.

(2) Browne, W. R.; de Jong, J. J. D.; Kudernac, T.; Walko, M.; Lucas, L. N.; Uchida, K.; van Esch, J. H.; Feringa, B. L. Oxidative Electrochemical Switching in Dithienylcyclopentenes, Part 1: Effect of Electronic Perturbation on the Efficiency and Direction of Molecular Switching. *Chem. Eur. J.* **2005**, *11*, 6414-6429.

(3) Browne, W. R.; de Jong, J. J. D.; Kudernac, T.; Walko, M.; Lucas, L. N.; Uchida, K.; van Esch, J. H.; Feringa, B. L. Oxidative Electrochemical Switching in Dithienylcyclopentenes, Part 2: Effect of Substitution and Asymmetry on the Efficiency and Direction of Molecular Switching and Redox Stability. *Chem. Eur. J.* **2005**, *11*, 6430-6441.

(4) Zhong, Y.; Vila, N.; Henderson, J. C.; Abruna, H. D. Transition-Metal Tris-bipyridines Containing Three Dithienylcyclopentenes: Synthesis, Photochromic, and Electrochromic Properties. *Inorg. Chem.* **2009**, *48*, 7080-7085.

(5) Motoyama, K.; Koike, T.; Akita, M. Remarkable Switching Behavior of Bimodally Stimuli-Responsive Photochromic Dithienylethenes with Redox-Active Organometallic Attachments. *Chem. Commun.* **2008**, 5812-5814.

(6) Tanaka, Y.; Inagaki, A.; Akita, M. A Photoswitchable Molecular Wire with the Dithienylethene (DTE) Linker, (dppe)(η^5-C$_5$Me$_5$)Fe-C≡C-DTE-C≡C-Fe(η^5-C$_5$Me$_5$)(dppe). *Chem. Commun.* **2007**, 1169-1171.

(7) Fery-Forgues, S.; Delavaux-Nicot, B. Ferrocene and Ferrocenyl Derivatives in Luminescent Systems. *J. Photochem. Photobiol. A.* **2000**, *132*, 137-159.

(8) Herkstroeter, W. G. Triplet Energies of Azulene, Beta-Carotene, and Ferrocene. *J. Am. Chem. Soc.* **1975**, *97*, 4161-4167.

(9) Martinez, R.; Ratera, I.; Tarraga, A.; Molina, P.; Veciana, J. A Simple and Robust Reversible Redox-Fluorescence Molecular Switch Based on a 1,4-Disubstituted Azine with Ferrocene and Pyrene Units. *Chem. Commun.* **2006**, 3809-3811.

(10) Irie, M. Diarylethenes for Memories and Switches. *Chem. Rev.* **2000**, *100*, 1685-1716.

(11) Peters, A.; Branda, N. R. Limited Photochromism in Covalently Linked Double 1,2-Dithienylethenes. *Adv. Mater. Opt. Electron.* **2000**, *10*, 245-249.

(12) Irie, M.; Lifka, T.; Uchida, K.; Kobatake, S.; Shindo, Y. Fatigue Resistant Properties of Photochromic Dithienylethenes: By-Product Formation. *Chem. Commun.* **1999**, 747-748.

(13) Lucas, L. N. Dithienylcyclopentene Optical Switches Towards Photoresponsive Supramolecular Materials, Ph.D. Thesis, Rijksuniversiteit Groningen, **2001**.

(14) Lucas, L. N.; de Jong, J. J. D.; van Esch, J. H.; Kellogg, R. M.; Feringa, B. L. Syntheses of Dithienylcyclopentene Optical Molecular Switches. *E. J. Org. Chem.* **2003**, 155-166.

(15) Lucas, L. N.; van Esch, J.; Kellogg, R. M.; Feringa, B. L. A New Class of Photochromic 1,2-Diarylethenes; Synthesis and Switching Properties of Bis(3-thienyl)cyclopentenes. *Chem. Commun.* **1998**, 2313-2314.

(16) Morimitsu, K.; Shibata, K.; Kobatake, S.; Irie, M. Dithienylethenes with a Novel Photochromic Performance. *J. Org. Chem.* **2002**, *67*, 4574-4578.

(17) Irie, M.; Sakemura, K.; Okinaka, M.; Uchida, K. Photochromism of Dithienylethenes with Electron-Donating Substituents. *J. Org. Chem.* **1995**, *60*, 8305-8309.

(18) Uchida, K.; Matsuoka, T.; Kobatake, S.; Yamaguchi, T.; Irie, M. Substituent Effect on the Photochromic Reactivity of Bis(2-thienyl)perfluorocyclopentenes. *Tetrahedron* **2001**, *57*, 4559-4565.

(19) Pu, S.; Li, M.; Fan, C.; Liu, G.; Shen, L. Synthesis and the Optoelectronic Properties of Diarylethene Derivatives having Benzothiophene and n-Alkyl Thiophene Units. *J. Mol. Struct.* **2009**, *919*, 100-111.

(20) Xiao, S.; Yi, T.; Zhou, Y.; Zhao, Q.; Li, F.; Huang, C. Multi-State Molecular Switches Based on Dithienylperfluorocyclopentene and Imidazo [4,5-f] [1,10] Phenanthroline. *Tetrahedron* **2006**, *62*, 10072-10078.

(21) Yang, T.; Pu, S.; Fan, C.; Liu, G. Synthesis, Crystal Structure and Optoelectronic Properties of a New Unsymmetrical Photochromic Diarylethene. *Spectrochim. Acta A.* **2008**, *70*, 1065-1072.

(22) Pu, S.; Miao, W.; Cui, S.; Liu, G.; Liu, W. The Synthesis of Novel Photochromic Diarylethenes Bearing a Biphenyl Moiety and the Effects of Substitution on their Properties. *Dyes Pigments* **2010**, *87*, 257-267.

(23) Zheng, H.; Zhou, W.; Yuan, M.; Yin, X.; Zuo, Z.; Ouyang, C.; Liu, H.; Li, Y.; Zhu, D. Optic and Proton Dual-Control of the Fluorescence of Rhodamine Based on Photochromic Diarylethene: Mimicking the Performance of an Integrated Logic Gate. *Tetrahedron Lett.* **2009**, *50*, 1588-1592.

(24) Jukes, R. T. F.; Adamo, V.; Hartl, F.; Belser, P.; De Cola, L. Photochromic Dithienylethene Derivatives Containing Ru(II) or Os(II) Metal Units. Sensitized Photocyclization from a Triplet State. *Inorg. Chem.* **2004**, *43*, 2779-2792.

(25) Jeong, Y.; Yang, S. I.; Kim, E.; Ahn, K. Development of Highly Fluorescent Photochromic Material with High Fatigue Resistance. *Tetrahedron* **2006***, 62*, 5855-5861.

(26) Fernandez-Acebes, A.; Lehn, J. M. Optical Switching and Fluorescence Modulation Properties of Photochromic Metal Complexes Derived from Dithienylethene Ligands. *Chem. Eur. J.* **1999***, 5*, 3285-3292.

(27) Kim, M.; Kawai, T.; Irie, M. Fluorescence Modulation in Photochromic Amorphous Diarylethenes. *Opt. Mater.* **2003***, 21*, 271-274.

(28) Lin, Y.; Yuan, J.; Hu, M.; Cheng, J.; Yin, J.; Jin, S.; Liu, S. H. Syntheses and Properties of Binuclear Ruthenium Vinyl Complexes with Dithienylethene Units as Multifunction Switches. *Organometallics* **2009***, 28*, 6402-6409.

(29) Yam, V. W. W.; Ko, C. C.; Zhu, N. Y. Photochromic and Luminescence Switching Properties of a Versatile Diarylethene-Containing 1,10-Phenanthroline Ligand and its Rhenium(I) Complex. *J. Am. Chem. Soc.* **2004***, 126*, 12734-12735.

(30) Guirado, G.; Coudret, C.; Hliwa, M.; Launay, J. P. Understanding Electrochromic Processes Initiated by Dithienylcyclopentene Cation-Radicals. *J. Phys. Chem. B.* **2005***, 109*, 17445-17459.

(31) Arewgoda, M.; Rieger, P. H.; Robinson, B. H.; Simpson, J.; Visco, S. J. Paramagnetic Organometallic Molecules .12. Electrochemical Studies of Reactions with Lewis-Bases Following Metal-Metal Bond Cleavage in $R_2C_2Co_2(CO)_6$ Radical Anions. *J. Am. Chem. Soc.* **1982***, 104*, 5633-5640.

(32) Medina, R. M.; Moreno, C.; Marcos, M. L.; Castro, J. A.; Benito, F.; Arnanz, A.; Delgado, S.; Gonzalez-Velasco, J.; Macazaga, M. J. Syntheses, Structures and Electrochemical Study of π-Acetylene Complexes of Cobalt. *Inorg. Chim. Acta* **2004***, 357*, 2069-2080.

(33) Marcos, M. L.; Macazaga, M. J.; Medina, R. M.; Moreno, C.; Castro, J. A.; Gomez, J. L.; Delgado, S.; González-Velasco, J. Alkynyl Cobalt Complexes. An Electrochemical Study. *Inorg. Chim. Acta* **2001***, 312*, 249-255.

(34) Arnanz, A.; Marcos, M.; Moreno, C.; Farrar, D. H.; Lough, A. J.; Yu, J. O.; Delgado, S.; González-Velasco, J. Synthesis, Structures and Comparative Electrochemical Study of 2,5-Bis(trimethylsilylethynyl)thiophene Coordinated Cobalt Carbonyl Units. *J. Organomet. Chem.* **2004***, 689*, 3218-3231.

(35) Osella, D.; Fiedler, J. Reinvestigation of the Electrochemical-Behavior of the $Co_2(CO)_6$(ethynylestradiol) Complex - Evidence of Efficient Recombination of the Electrogenerated Fragments. *Organometallics* **1992***, 11*, 3875-3878.

(36) Wong, W.; Lam, H.; Lee, S. Synthesis, Electrochemistry and Structural Characterization of New Dimeric Cobalt η^2-Alkyne Carbonyl Complexes. *J. Organomet. Chem.* **2000***, 595*, 70-80.
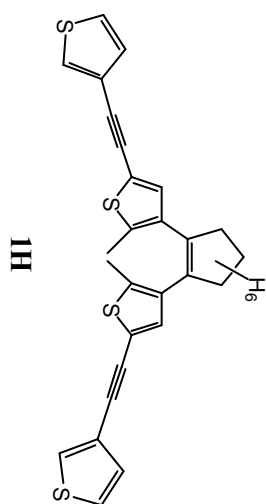
(37) Macazaga, M. J.; Marcos, M. L.; Moreno, C.; Benito-Lopez, F.; Gomez-González, J.; González-Velasco, J.; Medina, R. M. Syntheses, Structures and Comparative Electrochemical Study of π-Acetylene Complexes of Cobalt. *J.Organomet. Chem.* **2006***, 691*, 138-149.

(38) Arnanz, A.; Marcos, M.; Delgado, S.; González-Velasco, J.; Moreno, C. The Effect of Thiophene Ring Substitution Position on the Properties and Electrochemical Behaviour of Alkyne–dicobaltcarbonylthiophene Complexes. *J. Organomet. Chem.* **2008***, 693*, 3457-3470.

(39) Tian, H.; Yang, S. J. Recent Progresses on Diarylethene Based Photochromic Switches. *Chem. Soc. Rev.* **2004***, 33*, 85-97.

(40) Matsuda, K.; Irie, M. Diarylethene as a Photoswitching Unit. *J. Photochem. Photobiol. C.* **2004***, 5*, 169-182.

(41) Areephong, J.; Browne, W. R.; Katsonis, N.; Feringa, B. L. Photo- and Electro-chromism of Diarylethene Modified ITO Electrodes - Towards Molecular Based Read-Write-Erase Information Storage. *Chem. Commun.* **2006**, 3930-3932.

(42) Pu, S.; Liu, G.; Li, G.; Wang, R.; Yang, T. Synthesis, Crystal Structure and its Optical and Electrochemical Properties of a New Unsymmetrical Diarylethene. *J. Mol. Struct.* **2007***, 833*, 23-29.

(43) Fraysse, S.; Coudret, C.; Launay, J. P. Synthesis and Properties of Dinuclear Complexes with a Photochromic Bridge: An Intervalence Electron Transfer Switching "On" and "Off". *Eur. J. Inorg. Chem.* **2000**, 1581-1590.

(44) Alberto, R.; Motterlini, R. Chemistry and Biological Activities of CO-Releasing Molecules (CORMs) and Transition Metal Complexes. *Dalton Trans.* **2007**, 1651-1660.

(45) Mann, B. E.; Motterlini, R. CO and NO in Medicine. *Chem. Commun.* **2007**, 4197-4208.

(46) Ryter, S. W.; Choi, A. M. Therapeutic Applications of Carbon Monoxide in Lung Disease. *Curr. Opin. Pharmacol.* **2006***, 6*, 257-262.

(47) Ryter, S. W.; Alam, J.; Choi, A. M. K. Heme Oxygenase-1/Carbon Monoxide: From Basic Science to Therapeutic Applications. *Physiol. Rev.* **2006***, 86*, 583-650.

(48) Atkin, A. J.; Williams, S.; Sawle, P.; Motterlini, R.; Lynam, J. M.; Fairlamb, I. J. S. μ_2-Alkyne Dicobalt(0)hexacarbonyl Complexes as Carbon Monoxide-Releasing Molecules (CO-RMs): Probing the Release Mechanism. *Dalton Trans.* **2009**, 3653-3656.

(49) Kretschmer, R.; Gessner, G.; Gorls, H.; Heinemann, S. H.; Westerhausen, M. Dicarbonyl-bis(cysteamine)iron(II) A Light Induced Carbon Monoxide Releasing Molecule Based on Iron (CORM-S1). *J. Inorg. Biochem.* **2011***, 105*, 6-9.

(50) Zhang, W.; Atkin, A. J.; Thatcher, R. J.; Whitwood, A. C.; Fairlamb, I. J. S.; Lynam, J. M. Diversity and Design of Metal-Based Carbon Monoxide-Releasing Molecules (CO-RMs) in Aqueous Systems: Revealing the Essential Trends. *Dalton Trans.* **2009**, 4351-4358.

(51) Zhang, W.; Whitwood, A. C.; Fairlamb, I. J. S.; Lynam, J. M. Group 6 Carbon Monoxide-Releasing Metal Complexes with Biologically-Compatible Leaving Groups. *Inorg. Chem.* **2010**, *49*, 8941-8952.

(52) Pu, S. Z.; Yang, T. S.; Li, G. Z.; Xu, J. K.; Chen, B. Substituent Position Effect on the Optoelectronic Properties of Photochromic Diarylethenes. *Tetrahedron Lett.* **2006**, *47*, 3167-3171.

(53) M. Draper, S.; Long, C.; M. Myers, B. The Photochemistry of (μ_2-$RC_2H)Co_2(CO)_6$ Species (R=H or C6H5), Important Intermediates in the Pauson–Khand Reaction. *J. Organomet. Chem.* **1999**, *588*, 195-199.

(54) Marhenke, J.; Massick, S. M.; Ford, P. C. Time-Resolved Infrared Study of Reactive Species Produced by Flash Photolysis of the Hydroformylation Catalyst Precursor $Co_2(CO)_6(PMePh_2)_2$. *Inorg. Chim. Acta.* **2007**, *360*, 825-836.

APPENDIX

408

8.0
1.79
7.5
2.00
2.00
2.00
7.0

6.5

6.0

5.5

5.0

4.5

4.0

3.5
4.10
3.0

2.5

2.00
6.16
2.0 ppm

7.903
7.898
7.895
7.656
7.649
7.644
7.636
7.253
7.250
7.240
7.237
7.135

1H

H₆

H₂O

d⁶-DMSO

2.792
2.774
2.755

2.061
2.046
2.027
2.008
1.989
1.970

7.821
7.818
7.814
7.811
7.634
7.626
7.621
7.614
7.366
7.363
7.354
7.351
7.248

3H

H$_2$O

CH$_3$ &
Cyclopentene
H$_6$ protons
under acetone
& H$_2$O peaks

d^6- acetone

| 8.0 | 7.5 | 7.0 | 6.5 | 6.0 | 5.5 | 5.0 | 4.5 | 4.0 | 3.5 | 3.0 | 2.5 | ppm |

1.92 2.08 2.00 2.07
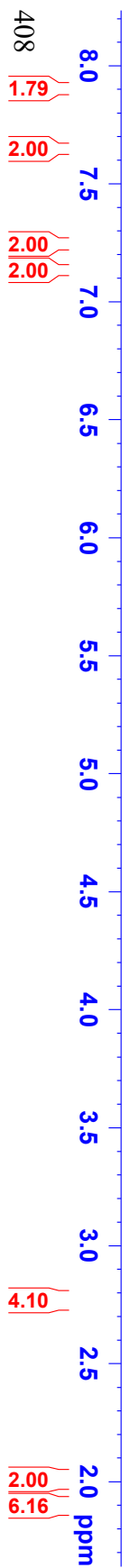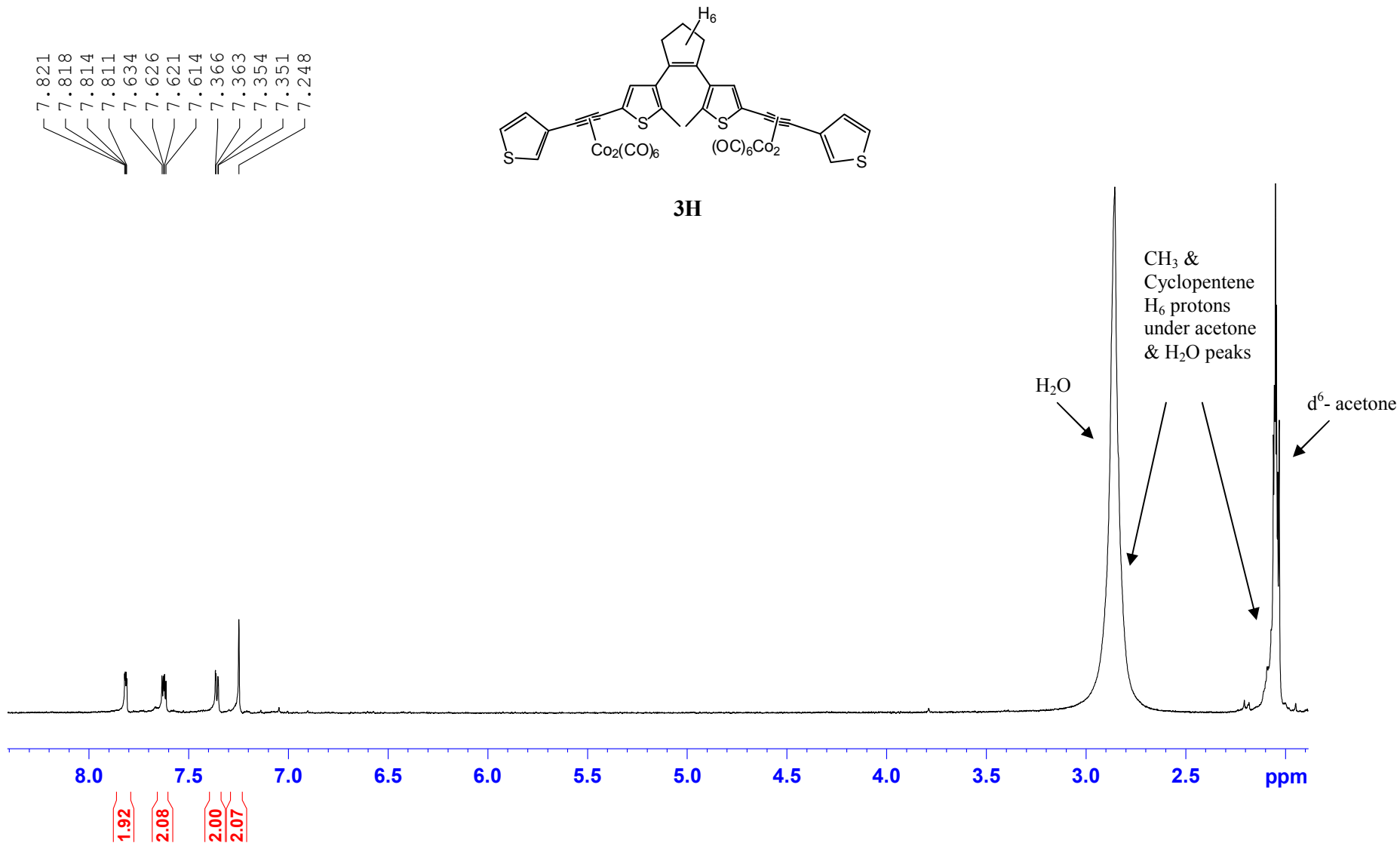
5H in d^6-acetone

7.393
7.356
7.347
7.345
7.335
7.326
7.295
7.286
7.283
7.273
7.260
7.233
7.219
7.206
7.193
7.155
7.148
6.816

5H
M$_1$ = Co$_2$(CO)$_4$dppm
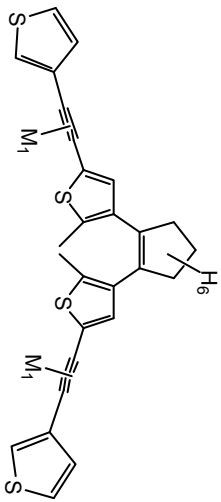
3.659
3.641
3.624
3.418
3.407
3.395
3.383

Diethyl Ether

H$_2$O

d^6 - acetone

2.685
2.673
2.660

2.057
2.053
2.049
2.046
2.042
2.031
1.835

48.95
2.06
3.85
4.00
6.00

7.5 7.0 6.5 6.0 5.5 5.0 4.5 4.0 3.5 3.0 2.5 2.0 ppm

7.977
7.974
7.970
7.967
7.679
7.672
7.667
7.660
7.398
7.309
7.289
7.286
7.277
7.274

1F

H$_2$O

d^6- DMSO

1.968

8.0   7.5   7.0   6.5   6.0   5.5   5.0   4.5   4.0   3.5   3.0   2.5   ppm

1.87   2.06   2.08   2.06   6.00

411
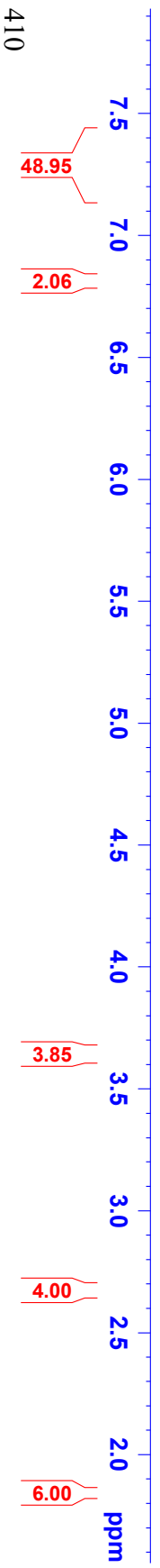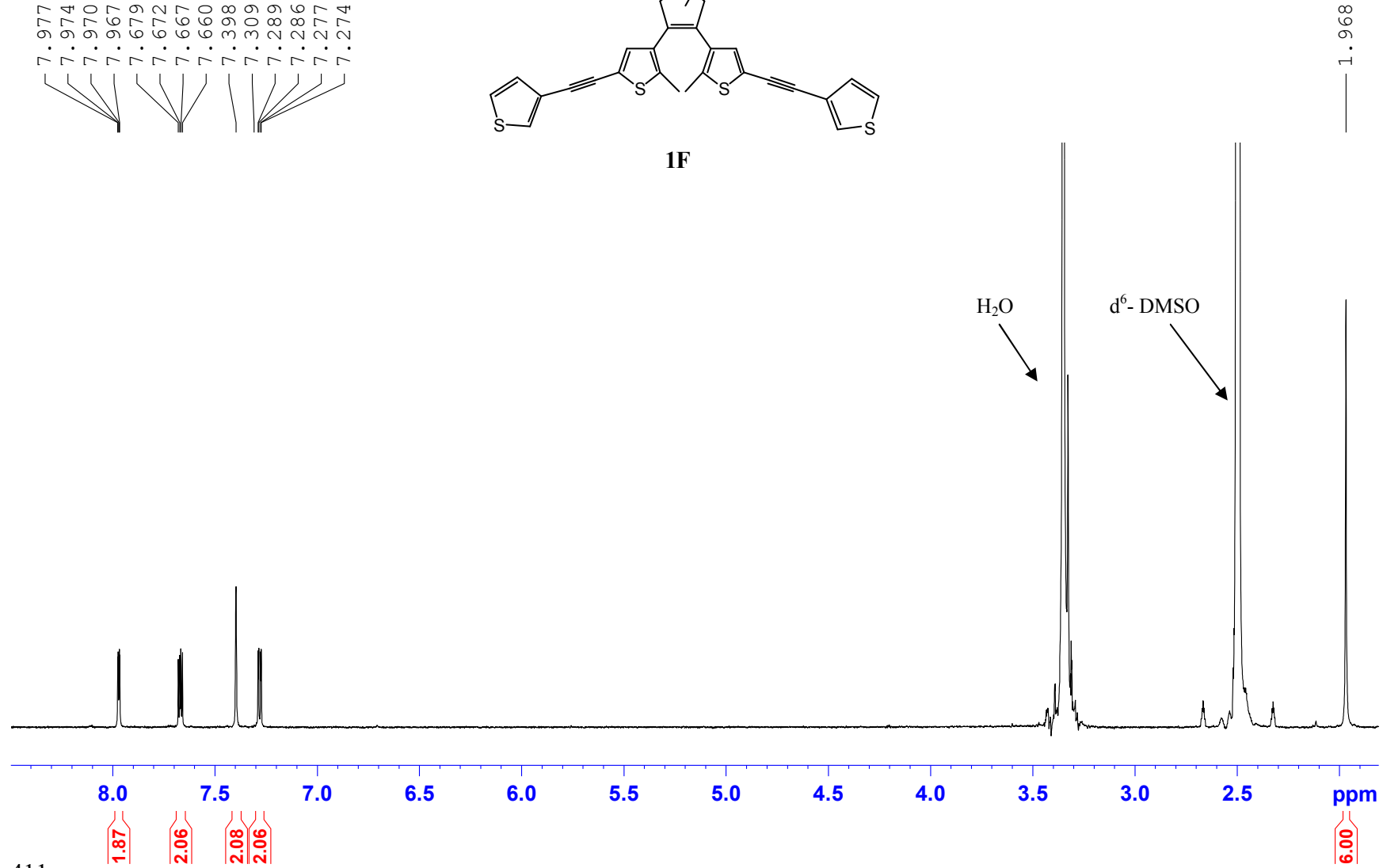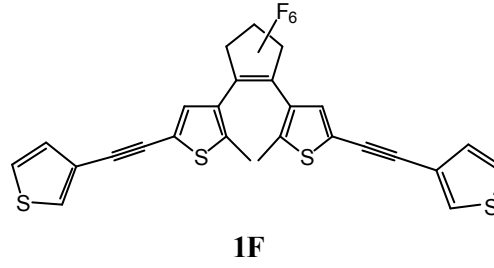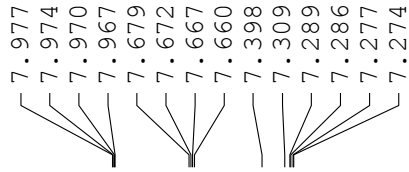
3F in d⁶-acetone

7.847
7.844
7.840
7.837
7.666
7.659
7.654
7.646
7.508
7.370
7.366
7.357
7.354

2.078
2.050

H₂O

d⁶- acetone

3F

2.00 2.13 2.00 1.92

6.16

8.5 8.0 7.5 7.0 6.5 6.0 5.5 5.0 4.5 4.0 3.5 3.0 2.5 2.0 ppm

412

413
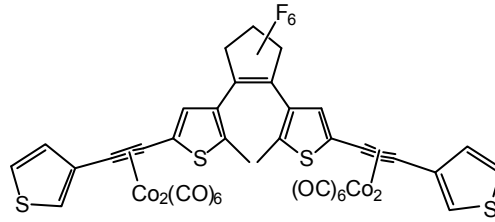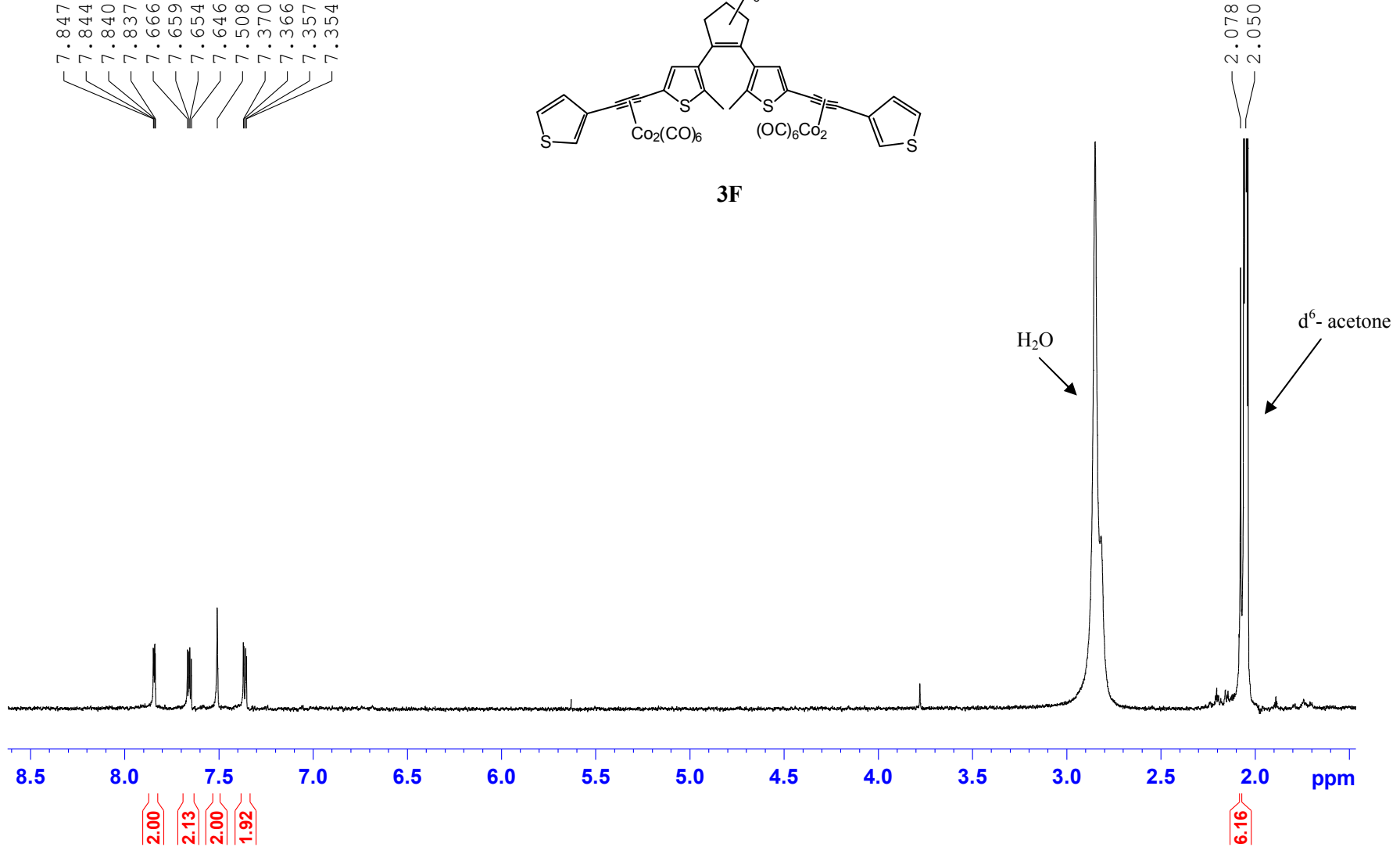
5F in d⁶-acetone

7.337
7.329
7.323
7.297
7.288
7.279
7.272
7.247
7.227
7.206
7.187
7.143
7.133
7.041

5F

$M_1 = Co_2(CO)_4dppm$
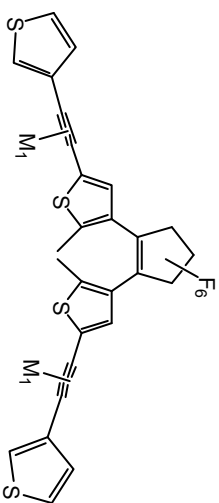
3.776
3.746
3.714
3.687
3.668
3.650
3.641
3.614
3.581

DCM

H_2O

d⁶ - acetone

1.896
1.891
1.885
1.866

45.96
1.88
4.05
6.05
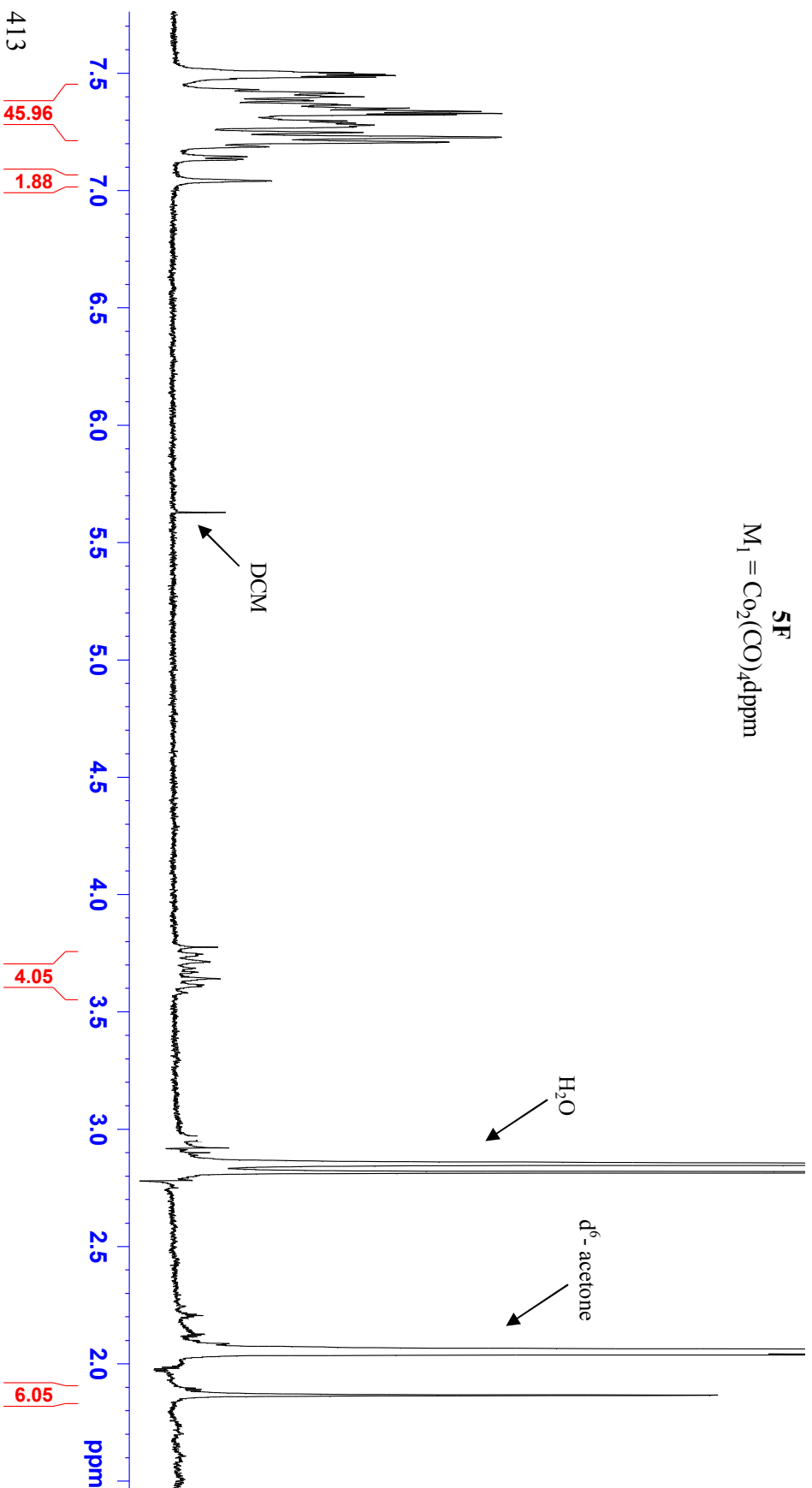
2H in d⁶-DMSO

7.902
7.899
7.670
7.662
7.657
7.650
7.603
7.587
7.582
7.524
7.503
7.412
7.281
7.278
7.268
7.265

H₂O
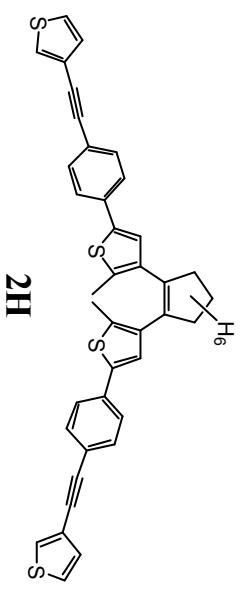
d⁶ - DMSO

2.868
2.850
2.831

2.070
2.051
2.032
2.013
1.919

2H

1.77
2.02
4.17
4.03
2.00
1.97
3.87
2.09
6.13

8.0   7.5   7.0   6.5   6.0   5.5   5.0   4.5   4.0   3.5   3.0   2.5   2.0   ppm

4H in d⁶-acetone

7.671
7.668
7.562
7.542
7.528
7.517
7.507
7.497
7.217

5.492

H₆

4H

Co₂(CO)₆   (OC)₆Co₂

2.896
2.786
2.768
2.749
2.676
2.642
2.308
2.076
1.998
1.980
1.957
1.942

d⁶- acetone

H₂O

CH₃ &
Cyclopentene
protons under
acetone peak

DCM

7.5   7.0   6.5   6.0   5.5   5.0   4.5   4.0   3.5   3.0   2.5   ppm

1.81 10.35 4.00   4.03

415

6H in d⁶-acetone

7.440
7.433
7.428
7.420
7.346
7.340
7.307
7.287
7.274
7.238
7.221
7.167
7.149
7.133
7.025
7.014

2.891
2.874
3.606
3.580
3.554

2.114
2.090
2.032

H₆

6H

$M_1 = Co_2(CO)_4dppm$

Cyclopentene
protons under
acetone &
H₂O peak

H₂O

d⁶- acetone

54.05

2.05

3.96

5.90

7.5   7.0   6.5   6.0   5.5   5.0   4.5   4.0   3.5   3.0   2.5   ppm

416

7.541
7.520
7.318
7.259
7.216
7.208

1.975

2F

CDCl$_3$

DCM

Ethyl acetate

Diethyl Ether

7.5 7.0 6.5 6.0 5.5 5.0 4.5 4.0 3.5 3.0 2.5 ppm

10.10 4.08 1.95 6.00

4F in d^6-acetone

7.799
7.693
7.672
7.659
7.648
7.638
7.628
7.347

2.807

2.062
2.057
2.051

F$_6$

Co$_2$(CO)$_6$ **4F**   (OC)$_6$Co$_2$

d^6-acetone

H$_2$O

CH$_3$ protons
under acetone
peak

DCM

7.5 7.0 6.5 6.0 5.5 5.0 4.5 4.0 3.5 3.0 2.5 ppm

1.88
10.20
3.94

418

7H in CDCl$_3$

7.26

6.872

H$_6$

7H

4.602

4.302

2.803

2.160

1.987

CDCl$_3$

7.5 7.0 6.5 6.0 5.5 5.0 4.5 4.0 3.5 3.0 2.5 2.0 ppm

2.03

4.05

14.13

4.00

2.02

5.95

419

9H in d^6- acetone

7.471

4.579
4.575
4.570
4.516
4.511
4.507
4.276
4.245

2.145
2.085

H$_2$O

d^6-acetone

9H

2.00

4.57
4.50

10.51

2.02
6.27

7.5   7.0   6.5   6.0   5.5   5.0   4.5   4.0   3.5   3.0   2.5   2.0   ppm

11H in d^6-acetone

7.385
7.347
7.326
7.316
7.311
7.285
7.266
7.247
7.195
7.176
7.158
7.015

4.418
4.413
4.352
4.347
4.343
4.105

3.699
3.673
3.636
3.629
3.620
3.603

2.800
2.778
2.759

2.211
2.205
2.200
2.086

11H

M_1 = Co$_2$(CO)$_4$dppm

H$_2$O

Diethyl
Ether

CH$_3$ &
Cyclo-
pentene H$_6$
protons
under
acetone &
H$_2$O peaks

d^6-acetone

7.5 7.0 6.5 6.0 5.5 5.0 4.5 4.0 3.5 3.0 2.5 2.0 ppm

40.50   2.04   3.90 4.15   10.00   7.34

421

7.26
7.154
4.521
4.356
1.961

7F

F₆
Fe
Fe

CDCl₃
DCM

7.5 7.0 6.5 6.0 5.5 5.0 4.5 4.0 3.5 3.0 2.5 ppm

1.96 4.00 14.13 6.06

422

9F

7.738

4.587
4.545
4.281
4.270

2.151

H$_2$O

d^6-acetone

| 8.0 | 7.5 | 7.0 | 6.5 | 6.0 | 5.5 | 5.0 | 4.5 | 4.0 | 3.5 | 3.0 | 2.5 | 2.0 | ppm |

2.00

4.03
4.11

9.90

6.10

423

11F in d⁶-acetone

11F
$M_1 = Co_2(CO)_4dppm$

7.407
7.396
7.380
7.353
7.336
7.318
7.286
7.268
7.250
7.216
7.191
7.173
7.156

4.419
4.373
4.369
4.364
4.079
3.813
3.785
3.775
3.753
3.730
3.686
3.658
3.646
3.631

H_2O

d^6-acetone

1.999
1.973

42.56

8.04

10.00

3.92

5.93

8H in CDCl₃

7.440

7.061

CDCl₃

Fe

8H

H₆

S

S

Fe

4.521
4.506
4.502
4.497
4.244

2.883
2.866
2.848
2.828
2.581
2.572

2.128
2.110
2.090
2.071
2.017
1.999
1.980

8.09
2.10
4.00
14.30
4.02
2.01
6.12

10H in d^6-acetone

7.989
7.969
7.773
7.752
7.399

H$_6$

Fe
Co$_2$(CO)$_6$
(OC)$_6$Co$_2$
Fe

10H

4.594
4.528
4.255

2.934
2.915
2.897

d^6-acetone

H$_2$O

CH$_3$ &
Cyclopentene
protons under
acetone peak

8.0 7.5 7.0 6.5 6.0 5.5 5.0 4.5 4.0 3.5 3.0 2.5 ppm

4.49 4.27 2.00 4.10 4.34 10.57 4.15

426

12H in d⁶-acetone

7.715
7.695
7.612
7.591
7.384
7.337
7.321
7.307
7.294
7.282
7.264
7.247
7.228
7.208
7.178
7.159
7.140

12H

$M_1 = Co_2(CO)_4dppm$

M_1

Fe

M_1

Fe

S

S

H_6

4.319

3.938

3.581
3.555
3.528

H_2O

2.942
2.924
2.905

2.081

d⁶-acetone peak

CH_3 & Cyclopentene protons under acetone peak

3.86
4.26

42.35

8.13

9.81

4.14

3.91

8.0 7.5 7.0 6.5 6.0 5.5 5.0 4.5 4.0 3.5 3.0 2.5 ppm

10F in d⁶-acetone

8.054
8.049
8.037
8.033
7.894
7.889
7.872
7.666

4.610
4.606
4.601
4.545
4.540
4.536
4.262

H2O

2.113

d⁶-acetone

10F

4.11
4.02
1.98

3.92
3.99
9.94

6.00

12F in CDCl$_3$

7.502
7.343
7.26
7.154

4.327
3.974
3.237
2.016

12F

M$_1$ = Co$_2$(CO)$_4$dppm

CDCl$_3$

DCM

Diethyl
Ether

7.5 7.0 6.5 6.0 5.5 5.0 4.5 4.0 3.5 3.0 2.5 ppm

3.90 4.09 42.39 8.15 10.10 4.00 6.17

Excited State Dynamics and Activation Parameters of Remarkably Slow Photoinduced CO Loss from (η^6-Benzene)Cr(CO)$_3$ in *n*-Heptane Solution: A DFT and Picosecond-Time-Resolved Infrared Study

Ian P. Clark,[†] Michael W. George,[‡] Gregory M. Greetham,[†] Emma C. Harvey,[§] Conor Long,*,[§] Jennifer C. Manton,[§] and Mary T. Pryce[§]

School of Chemical Sciences, Dublin City University, Dublin 9, Ireland, Central Laser Facility, Science and Technology Facilities Council, Rutherford Appleton Laboratory, Harwell Science and Innovation Campus, Didcot, OX11 0QX, United Kingdom, and School of Chemistry, University of Nottingham, Nottingham, NG7 2RD, United Kingdom

This text redacted due to 3rd party copyright
This text redacted due to 3rd party copyright
This text redacted due to 3rd party copyright
This text redacted due to 3rd party copyright
This text redacted due to 3rd party copyright
This text redacted due to 3rd party copyright
This text redacted due to 3rd party copyright
This text redacted due to 3rd party copyright
This text redacted due to 3rd party copyright
This text redacted due to 3rd party copyright
This text redacted due to 3rd party copyright
This text redacted due to 3rd party copyright
This text redacted due to 3rd party copyright
This text redacted due to 3rd party copyright
This text redacted due to 3rd party copyright
This text redacted due to 3rd party copyright
This text redacted due to 3rd party copyright
This text redacted due to 3rd party copyright
This text redacted due to 3rd party copyright

Photochemistry of (η^6-Arene)Cr(CO)$_3$ (Arene = Methylbenzoate, Naphthalene, or Phenanthrene) in *n*-Heptane Solution: Population of Two Excited States Following 400 nm Excitation As Detected by Picosecond Time-Resolved Infrared Spectroscopy

Ian P. Clark,[‡] Michael W. George,[§] Gregory M. Greetham,[‡] Emma C. Harvey,[†] Conor Long,[†,*] Jennifer C. Manton,[†] and Mary T. Pryce[†]

[†]School of Chemical Sciences, Dublin City University, Dublin 9, Ireland

[‡]Central Laser Facility, Science & Technology Facilities Council, Rutherford Appleton Laboratory, Harwell Science and Innovation Campus, Didcot, OX11 0QX, United Kingdom

[§]School of Chemistry, University of Nottingham, Nottingham, NG7 2RD, United Kingdom

S *Supporting Information*